

H. Yamaguchi

Fluid Mechanics
and its Applications

Engineering Fluid Mechanics

 Springer

Engineering Fluid Mechanics

FLUID MECHANICS AND ITS APPLICATIONS

Volume 85

Series Editor: R. MOREAU

MADYLAM

Ecole Nationale Supérieure d'Hydraulique de Grenoble

Boîte Postale 95

38402 Saint Martin d'Hères Cedex, France

Aims and Scope of the Series

The purpose of this series is to focus on subjects in which fluid mechanics plays a fundamental role.

As well as the more traditional applications of aeronautics, hydraulics, heat and mass transfer etc., books will be published dealing with topics which are currently in a state of rapid development, such as turbulence, suspensions and multiphase fluids, super and hypersonic flows and numerical modeling techniques.

It is a widely held view that it is the interdisciplinary subjects that will receive intense scientific attention, bringing them to the forefront of technological advancement. Fluids have the ability to transport matter and its properties as well as to transmit force, therefore fluid mechanics is a subject that is particularly open to cross fertilization with other sciences and disciplines of engineering. The subject of fluid mechanics will be highly relevant in domains such as chemical, metallurgical, biological and ecological engineering. This series is particularly open to such new multidisciplinary domains.

The median level of presentation is the first year graduate student. Some texts are monographs defining the current state of a field; others are accessible to final year undergraduates; but essentially the emphasis is on readability and clarity.

For a list of related mechanics titles, see final pages.

Engineering Fluid Mechanics

by

H. Yamaguchi

*Doshisha University,
Kyo-Tanabeshi,
Kyoto, Japan*



Springer

Library of Congress Control Number: 2007943475

ISBN 978-1-4020-6741-9 (HB)
ISBN 978-1-4020-6742-6 (e-book)

Published by Springer,
P.O. Box 17, 3300 AA Dordrecht, The Netherlands.

www.springer.com

Printed on acid-free paper

All Rights Reserved

© 2008 Springer Science+Business Media B.V.

No part of this work may be reproduced, stored in a retrieval system, or transmitted in any form or by any means, electronic, mechanical, photocopying, microfilming, recording or otherwise, without written permission from the Publisher, with the exception of any material supplied specifically for the purpose of being entered and executed on a computer system, for exclusive use by the purchaser of the work.

Credits

Chapter 4 Part of data plot in Fig. 4.22; adapted with permission from Nikann Kogyo Shinnbunnsya, Ref. (T. Nishiyama, Fig. 6.17 in “Fluid Dynamics(I)”, Nikkan Kogyo Shinnbunnsya Tokyo, 1989. ISBN 4-526-00515-0 C3053). Fig. 4.41(a) and (b), and Fig. 4.42; courtesy of Teral Kyokuto Inc. (permission given with written form by personal communication).

Chapter 6 Fig. 6.2; adapted with permission from Forsch. Ing.-Wes., Ref. (P.L. Silveston, Fig. 5 in “Warmedurchgang in waagerechten Flüssigkeitsschichten”, Part I, Forsch. Ing.-Wes., No. 24, 29–32 and 56–69, 1958). Fig. 6.8; adapted with permission from Cambridge University Press, Ref. (E. Achenbach, J. Fluid Mech., Fig. 8 in “Influence of Surface Roughness on the Cross-flow Around a Circular Cylinder”, 46, 1971 and Fig. 6 in “Experiments on the Flow Past Spheres at Very high Reynolds Number”, 54, 1972). Fig. 6.11; adapted with permission from VDI-VERLAG G.M.B.H., Ref. (J. Nikuradse, Fig. 9 in “Stromungsgesetze in rauhen Rohren”, Forsch. Arb. Ing.-Wes., No. 361, 1933).

Chapter 7 Fig. 7.9; adapted with permission from Elsevier, Ref. (R.R. Huilgol and N. Phan-Thien, Fig. 49.5 in “Fluid Mechanics of Viscoelasticity”, Elsevier Science B.V., 1997. ISBN 0-444-82661-0). Fig. 7.10; adapted with permission from John Wiley & Sons, Ref. (H. Munstedt, Fig. 8 in “Dependence of the Elongational Behavior of Polystyrene Melts on Molecular Weight and Molecular Weight Distribution, J. Rheol., 37, 1993).

Chapter 8 Fig. 8.1(c); courtesy of Ferro Tech. Corp. (permission given with written form by personal communication). Fig. 8.2(a) and (b); courtesy of Taihokohzai Co. Ltd. (permission given with written form by personal communication). Fig. 8.10; adapted with permission from Elsevier, Ref. (L. Schwab, U. Hildebrandt and K. Stierstadt, Fig. 3 in “Magnetic Benerd Convection”, J. Magn. Magn. Mater., 39(1–2), 1983).

Preface

This book is intended for advanced engineering students in university or college and could serve as a reference for practical engineers. In recent years the development of fluid machineries has required a wider range of study in order to achieve a new level of developmental and conceptual progress. The field of fluid engineering is quite diverse in the sense that so many variations of flow exist in fluid machinery or an installation, whose characteristics are wholly dependent upon the flow field which is determined by the function of the machine setting itself. One who is studying fluid engineering, for the purpose of gaining a working knowledge of fluid machineries and their relevant installations, must understand not only the type of fluids used in practice, but also the fundamental flow problems associated with actual fluid machineries. Hence, the intended purpose of this book is to provide the fundamental and physical aspects of fluid mechanics and to develop engineering practice for fluid machineries.

The subject of fluid engineering is most often approached at the senior undergraduate or postgraduate level of study. At this stage, the student or practical engineer is assumed to already have a basic mathematical background of vector and tensor analysis with a fair understanding of elementary fluid mechanics, such as Bernoulli equation, potential flow, and Poiseuille flow. The information in this book is organized by subject matter in such a way that students can understand basic theory and progressively deepen their level of knowledge, following the order of presentation. In each section chapter exercises are provided, and problems are also given so as to enable students to understand the theoretical implications and to apply them to engineering problems. Suggestions of further readings and relevant references are listed at the end of each chapter for students eager to delve more deeply into various topics. The SI units system has been provided at the end of the introduction. Exercises and problems are worked out by SI Units throughout this text.

Chapter 1 concerns the fundamentals of continuum mechanics. The chapter involves a description of the nature of continuum, and the basis of kinematic fluid flow. Mathematical treatments necessary for describing quantities of fluid motion, which lay the groundwork for proceeding chapters, are also dealt with at this stage.

Chapter 2 encompasses the general conservation laws of fluid flow, involving mass, linear momentum, angular momentum and energy conservation. These will allow us to provide constitutive equations (relations) for the (unconstituted) conservation equations; thus, a closed system of equations, namely the governing equations of a specified fluid flow, can be obtained. Newtonian fluid, non-Newtonian fluid, viscoelastic fluid, and magnetic fluid are developed in later chapters.

Chapters 3 and 4 provide the basic theory for fluid engineering in an inviscid flow, from which hydrostatics, potential flows and incompressible flows are derived for practical use in Chapter 3. Thermodynamics equations are also introduced for analysis in this chapter. Specific engineering terms and concepts are defined in the proceeding chapters when appropriate. The importance in derivation of the Bernoulli equation is considered from the view of applying the equation to various engineering problems.

In consideration of engineering applications, Chapter 4 deals with fundamental methods to characterize turbomachines, and provides definitions of efficiencies. The concept of efficiencies is largely based on energy transfer and conversion. This chapter in particular explicates the basic treatments of hydraulic machineries, which are widely used in engineering practice. Although there are a large variety of hydraulic machineries available, each serving its needs and purposes, the treatment for these fluid machineries in this chapter is oriented more towards the turbomachineries in general rather than the specific type.

Chapter 5 is concerned with basic theory for compressible flow. In particular, unidirectional steady state flow process is considered. Fanno and Rayleigh processes in compressible flows are treated in more detail in view of wider applications to engineering practice. Shock waves are also touched on in this chapter.

Chapter 6 focuses on Newtonian flow. Viscosity, the most important concept in fluid mechanics is brought into the discussion, which leads us to the derivation of Navier-Stokes equations. Viscous flows are the objective in this chapter. Basic flows in many engineering applications are introduced, in which boundary layer theories are more thoroughly examined.

Chapter 7 explores some of the more advanced topics in fluid engineering so that the student wishing to further develop their interest in research fields or gain perspective for their future careers may glean some insight from these discussions. This chapter concerns non-Newtonian fluid flow in particular, which cannot be characterized in the same way as Newtonian fluids. The topic chiefly discussed here is polymeric fluid in light of more advanced applications, involving not only non-Newtonian viscosity, but also elasticity in regard to the rheological properties of fluids. Some constitutive equations of viscoelastic fluids are introduced in this chapter, for

the purpose of applying them to numerical work.

In the final chapter, Chapter 8, ferrohydrodynamics is introduced along side recent developments in magnetic fluids. The fundamental treatment of magnetic fluids is based on the modeling of suspensions of magnetic grains, whose scale is in the order of 10nm. The novel idea of suspension through the process of magnetization is introduced in deriving a closure system of ferrohydrodynamics equations. Some engineering applications of magnetic fluids are outlined.

There are four appendixes in which further details have been included. The appendixes are arranged in such a way that readers can, when necessary, refer to basic mathematical treatments and extend their understanding on a specific subject in the main text. Tables of physical properties are also provided as reference for readers requiring data for solving problems in the text or for more practical designing works. References are provided at the end of each chapter, some of which are to be regarded as suggestions for further reading and others as cited sources.

Finally the author wishes to acknowledge his indebtedness to Ms. Jacobs, associated editor of SPRINGER, for her encouragement in the publication of this book. The author also wish to express his appreciation to Professor Mingjun Li, Dr. Xin-Rong Zhang, Mr. Takuya Kuwahara, Mr. Yuta Ito, Mr. Minoru Masuda and postgraduate students from the fluid engineering laboratory in Doshisha University for their useful suggestions and assistance after reading parts of the manuscript. And thanks also to Professor Sigemitsu Shuchi and Ms. Cleito Feugas for offering amendments and proofing the manuscript.

Kyoto, Japan

Hiroshi Yamaguchi

Contents

Introduction.....	1
1. Fundamentals in Continuum Mechanics	5
1.1 Dynamics of Fluid Motion.....	5
1.2 Dynamics in Rotating Reference Frame	16
1.3 Material Objectivity and Convective Derivatives.....	19
1.4 Displacement Gradient and Relative Strain	22
1.5 Reynolds' Transport Theorem.....	23
1.6 Forces on Volume Element	26
Exercise.....	30
Problems	38
Nomenclature.....	40
Bibliography	41
2. Conservation Equations in Continuum Mechanics	43
2.1 Mass Conservation.....	43
2.2 Linear Momentum Conservation	44
2.3 Angular Momentum Conservation.....	47
2.4 Energy Conservation.....	52
2.5 Thermodynamic Relations	56
Exercise.....	62
Problems	69
Nomenclature.....	70
Bibliography	71
3. Fluid Static and Interfaces	73
3.1 Fluid Static	73
3.2 Fluid-fluid Interfaces	87
Exercise.....	90
Problems	110
Nomenclature.....	112
Bibliography	113

4. Perfect Flow	115
4.1 Potential and Inviscid Flows.....	115
Exercise	129
Problems	173
4.2 General Theories of Turbomachinery	180
4.2.1 Moment of Momentum Theory.....	183
4.2.2 Airfoil Theory	188
4.2.3 Efficiency and Similarity Rules of Turbomachinery.....	194
4.2.4 Cavitation.....	203
Exercise	208
Problems	218
Nomenclature.....	220
Bibliography	222
 5. Compressible Flow	 225
5.1 Speed of Sound and Mach Number	225
5.2 Isentropic Flow	230
5.3 Fanno and Rayleigh Lines	241
5.4 Normal Shock Waves.....	246
5.5 Oblique Shock Wave.....	251
Exercise	255
Problems	271
Nomenclature.....	276
Bibliography	277
 6. Newtonian Flow	 279
6.1 Navier-Stokes Equation	282
Problems	285
6.2 Similitude and Nondimensionalization.....	286
Exercise	295
Problems	298
6.3 Basic Flows Derived from Navier-Stokes Equation.....	298
6.3.1 Unidirectional Flow in a Gap Space	299
6.3.2 Lubrication Theory.....	306
6.3.3 Flow Around a Sphere.....	312
Problems	318
6.4 Flow Through Pipe	319
6.4.1 Entrance Flow	320
6.4.2 Fully Developed Flow in Pipe	322
6.4.3 Transient Hagen-Poiseuille Flow in Pipe.....	330

Exercise	334
Problems	339
6.5 Laminar Boundary Layer Theory	340
6.5.1 Flow over a Flat Plate	340
6.5.2 Integral Analysis of Boundary Layer Equation.....	346
6.5.3 Boundary Layer Separation.....	350
6.5.4 Integral Relation for Thermal Energy	353
Exercise.....	355
Problems	362
6.6 Turbulent Flow.....	364
6.6.1 Turbulence Models.....	370
6.6.2 Turbulent Heat Transfer	381
Exercise.....	385
Problems	390
Nomenclature.....	391
Bibliography	394
 7. Non-Newtonian Fluid and Flow.....	 399
7.1 Non-Newtonian Fluids and Generalized Newtonian Fluid Flow	 400
7.1.1 Rheological Classifications	400
7.1.2 Generalized Newtonian Fluid Flows.....	406
Exercise.....	408
Problems	415
7.2 Standard Flow and Material Functions	417
7.2.1 Simple Shear Flow	418
7.2.2 Shearfree Flow	421
7.2.3 Oscillatory Rheometric Flow	424
7.2.4 Viscometric Flow in Rheometry	428
Exercise.....	437
Problems	445
7.3 Viscoelastic Fluid and Flow.....	447
7.3.1 Linear Viscoelastic Rheological Equations.....	448
7.3.2 Linear and Nonlinear Viscoelastic Models	456
7.3.3 Viscoelastic Models to Standard Flow and Application to Some Engineering Flow Problems.....	 465
7.3.3.1 UCM, CRM and Giesekus Equations.....	465
7.3.3.2 Unidirectional Basic Flow Problems.....	472
Exercise.....	478
Problems	489
Nomenclature.....	491
Bibliography	493

8. Magnetic Fluid and Flow	497
8.1 Thermophysical Properties	498
Exercise	504
Problems	506
8.2 Ferrohydrodynamic Equations	507
Exercise	516
Problems	519
8.3 Basic Flows and Applications.....	520
8.3.1 Generalized Bernoulli Equation.....	521
8.3.2 Hydrostatics	522
8.3.3 Thermoconvective Phenomena	527
Exercise	532
Problems	537
Nomenclature.....	538
Bibliography	540
 Appendix.....	 543
 Index	 561

Introduction

Since the beginning of human civilization, communities have consistently been established at locations that feature a viable source of flowing water. Throughout history, people have continuously attempted to manipulate the natural flow of water, in order to affect an improvement in such areas as agricultural stability, living environment, and transportation. Indeed, even sensitivity to air currents and cloud flow has been important to the development of civilization's ability to adapt, and adapt to, the natural environment. Along with a reliable source of water, weather prediction and awareness of seasonal changes have been critical to basic social structures like farming, animal husbandry, and housing.

As understanding of the natural world has grown, and modern technologies have emerged, we have become increasingly reliant on the fundamental principles of fluid flow. Humanity has come to depend upon the development and design of modern transport, like cars and aircraft, which are rooted in an essential understanding and knowledge of fluid flows. Not only are fluid flows critical for solving aerodynamics problems, but also for a plethora of engineering problems concerning energy conservation and transmission. Time and again, methodological engineering, and even bio-medical studies, have proven the universally accepted tenant that understanding fluid flow is critical to the development of applied knowledge. Furthermore, it is clear that they are all, in the end, derived from the field of fluid engineering, which is key to opening the mental door to various forms of inspiration.

Topics covered in fluid engineering are quite diverse. However, the theoretical background of fluid engineering is based upon fluid mechanics (or hydrodynamics), which assumes that all basic equations relating to the conservation law, i.e. mass, linear momentum, angular momentum and energy, are derived from the concept of continuum mechanics. From the common definition of a fluid, avoiding complicated discussions on fluid characteristics, it is seen that both the gaseous and liquid phases of matter can customarily be qualified as fluids. In dealing with the mechanics of fluid flow, a continuum concept has to be introduced before commencing discussion on the kinematics of fluid. We can treat fluids as continuum if they are homogeneous, uniform and of macroscopic volume, in which only

bulk properties are interested by taking mean molecules, atoms and aggregations of the like, which consist of the fluid.

When deriving governing fluid mechanics equations, particularly for fluids of low molecular weight, for instance water or air, the Navier-Stokes equation can be obtained directly through Newton's law of viscosity. These have been called Newtonian fluids in consideration of their conservation of linear momentum. Based on the Navier-Stokes equation together with continuity and energy equations, all the practical equations and formula in fluid engineering dealing with conventional hydraulic and air machineries can be satisfactorily obtained. Moreover, decades of experiments and engineering practices have demonstrated the dependability of this theory.

However, there exist fluids, which do not necessarily obey Newton's law of viscosity, and those fluids, so-called non-Newtonian fluids, include polymeric fluids – polymer solutions, polymer melts and multi-phase systems, and electro-magnetic fluids – magnetic fluids, plasmas, and so forth. All basic equations of the conservation law derived from continuum mechanics can still be upheld, but in each case for non-Newtonian fluid the relationship between the internal stress and the applied strain, namely the constitutive equation (or relation) must be specified, instead of Newton's law of viscosity. Due to growing interest in industrial applications, flows of non-Newtonian polymeric fluids and magnetic fluids are introduced in this book as advanced topics in fluid engineering, which may serve to catalyze interest in very challenging subjects for readers who wish to further extend their knowledge.

In science and engineering, when converting from absolute to engineering unit and vice versa, some confusion occasionally arises. In 1960, the metric system of units (Système International d'Unités or more commonly known as the S.I. system) was introduced to overcome this problem. The S.I. system, is dimensionally consistent as it uses the absolute M.K.S system (M for Meter [m]; K for Kilogram [kg]; and S for Second [s]). Other fundamental units include the Ampere [A] for electric current; mol [mol] for molecular weight; and Candela [Cd] for brightness of light. It also includes the two supplementary units radian [rad] for angle and steradian [st rad] for solid angle, as well as degrees Kelvin [K] for temperature. With the S.I. system the units for heat, work and energy are the same (i.e. Joule [J], which is defined as the work done when a force of 1N is displaced through 1m along its direction). This is one of the advantages of the S.I. system.

Furthermore, it is noted that in the S.I. system of units, some of the units are named after scientists, such as Newton [N] for force; Kelvin [K] for temperature; Stokes [St] for dynamic viscosity; Poise [P] for kinematic viscosity; Watt [W] for power; Pascal [Pa] for pressure; Hertz [Hz] for

frequency; Joule [J] for energy; Coulomb [C] for electric charge; Ampere [A] for electric current; and Tesla [T] for magnetic flux density. These units, and combinations thereof, are the fundamental units of the S.I. system. The typically combined units frequently used in fluid engineering are listed in Table 1.1. Throughout this book, the numerical examples and problems are given in the S.I. system of units.

Table 1 Named-combined unit

Unit	Abbreviation	Combined relation
Ampere	A	$1 \text{ A} = 1 \text{ C/s}$
Gauss	G	$1 \text{ G} = 10^4 \text{ T}$
Hertz	Hz	$1 \text{ Hz} = 1 \text{ Cycle/s}$
Joule	J	$1 \text{ J} = 1 \text{ N} \cdot \text{m}$
Newton	N	$1 \text{ N} = 1 \text{ Kg} \cdot \text{m/s}^2$
Oersted	Oe	$(1000/4\pi) \text{ A/m}$
Pascal	Pa	$1 \text{ Pa} = 1 \text{ N/m}^2$
Poise	P	$1 \text{ dyns/cm}^2 = 0.1 \text{ Pa} \cdot \text{s}$
Stokes	St	$1 \text{ St} = 1 \text{ cm}^2/\text{s} = 10^4 \text{ m}^2/\text{s}$
Tesla	T	$1 \text{ T} = \text{N/A} \cdot \text{m}$
Watt	W	$1 \text{ W} = 1 \text{ J/s}$
Non-S.I. system of units		C ;electric charge, Coulomb

1. Fundamentals in Continuum Mechanics

Certain concepts and definitions are basic to the study of continuum mechanics, and they should be thoroughly understood at the outset. Below, a description of the motion of flow is given in three dimensional space with respect to the reference frame or relative to the rotational frame. Dynamics involves the frequent use of derivatives of scalars, vectors and tensors. Velocity and acceleration are the time derivatives, which are important kinematic parameters necessary to set an equation of motion in Newtonian mechanics, on which continuum mechanics is based. Also given are forces connected with space derivatives in regard to displacement gradient and relative strain, which are other important aspects of continuum mechanics. In this chapter, definitions of stress tensors and strain tensors are also provided, and will be developed in more detail in the chapters to follow.

1.1 Dynamics of Fluid Motion

When we deal with fluid motion, in many fluid engineering cases the dynamics of a molecule, or the molecular structure of the fluid body, does not explicitly come into effect. At the scale of molecular motion, properties of the fluid body, such as density, are typically subject to extreme variation with respect to the instantaneous distance of the frame. While, for the motion of fluid flow, the macro-motion with the scale of flow channel or external object takes place, thus we may apply the “continuum hypothesis”, with which the fluid body has a continuous structure in the instantaneous frame of space, as schematically indicated in Fig. 1.1. In Fig. 1.1, let us denote L_m as the small scale (molecular scale), which can be taken as the mean free path of the molecule; L_l as the large scale, which can be the characteristic length of the geometric configuration of fluid motion. Moreover, there may exist an intermediate length scale L_i , where a certain effect of a molecule or the molecular structure retains the properties of fluid. In order to quantify the effect of the scale in the properties of fluid, and consequently to the dynamics of fluid motion, we will take the ratio between the actual characteristic length of flow geometry, typically L_l , and

the mean free path of the molecules (the correlation length of the molecules) L_m , such that we get the following formula where Γ is called the Knudsen number.

$$\Gamma = \frac{L_m}{L_l} \quad (1.1.1)$$

“Continuum Mechanics” in a general sense, and “Fluid Mechanics” in particular, is normally valid when $\Gamma \ll 1$, where the continuum hypothesis can be assured. Henceforth we shall make two assumptions: first, that in every case, the flow of fluid has a small Knudsen Number, with which the scale of momentum of flow is far longer than the correlation length of the molecules; and second, that the fluid body has a continuous structure.

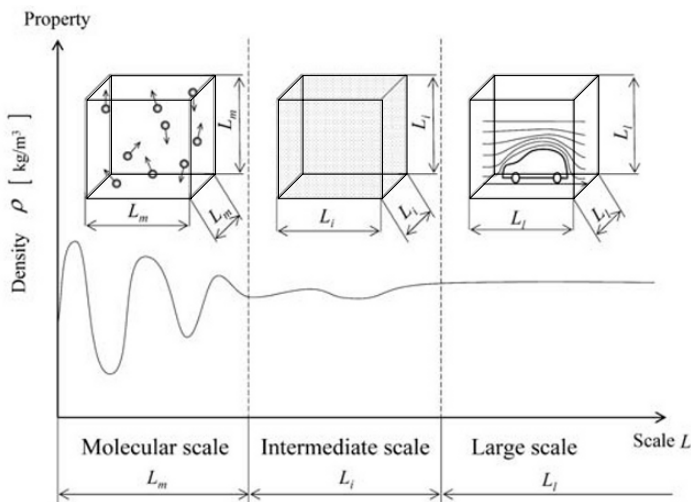


Fig. 1.1 Property variation with scale (as typically seen with properties such as density ρ)

It is interesting to mention, although we will not deal with the problem in this text, that there is a field of study that deals with small scaled flow phenomena in continuum mechanics. These phenomena have been dubbed fluid flows in a micro-channel, or micro-fluid-mechanics as it is more commonly referred to. The reader may wish to refer to a more detailed description provided by Kim and Kavila, 1991, and Tabeling, 2005.

The motion of a fluid can be perfectly determined, when the velocity at every point of the space is occupied by fluid motion. Therefore, to express the velocity with independent variables, there are two distinct methods, the so-called Eulerian and Lagrangian specifications.

One method is to trace the motion of a particle in space with time. In particular, a particle in fluid is called “fluid particle”, which is a subdivision of the fluid around a specific point \mathbf{x} . This method is called Lagrangian specification. The position vector of the fluid particle, considering a motion relative to a given frame of reference at time t , can be expressed as

$$\mathbf{x} = \mathbf{x}(\mathbf{x}_0, t) \quad (1.1.2)$$

where \mathbf{x}_0 and t are independent parameters, and \mathbf{x}_0 is the original position at $t = 0$, $\mathbf{x}_0 = \mathbf{x}(\mathbf{x}_0, 0)$. The velocity \mathbf{u} and acceleration \mathbf{a} at time t can be written similarly as

$$\mathbf{u} = \mathbf{u}(\mathbf{x}_0, t) = \frac{\partial \mathbf{x}}{\partial t} \quad (1.1.3)$$

$$\mathbf{a} = \mathbf{a}(\mathbf{x}_0, t) = \frac{\partial \mathbf{u}}{\partial t} \quad (1.1.4)$$

As seen in Fig. 1.2(a), Lagrangian specification describes the motion of a body of mass (fluid particle) and its variation of flow state along the particle path.

Another method is to give the spatial distribution of flow state as a function of spatial coordinates \mathbf{x} ($\mathbf{x} = (x, y, z)$; x, y, z are Euler variables) and time t , where \mathbf{x} and t are independent variables. This method is called Eulerian specification, and describes the variation of flow state in a position \mathbf{x} (position vector in spatial coordinates \mathbf{x}) at a given time t , not describing the behavior of each particle, see Fig. 1.2(b). In the Eulerian specification the velocity \mathbf{u} can be expressed as

$$\mathbf{u} = \mathbf{u}(\mathbf{x}, t) \quad (1.1.5)$$

The expression of the acceleration \mathbf{a} in an Eulerian specification is given by differentiation following the motion of a fluid particle and the rate of change of the velocity of that particle with respect to time

$$\mathbf{a} = \lim_{\Delta t \rightarrow 0} \frac{\mathbf{u}(\mathbf{x} + \Delta \mathbf{x}, t + \Delta t) - \mathbf{u}(\mathbf{x}, t)}{\Delta t} = \frac{\partial \mathbf{u}}{\partial t} + \lim_{\Delta t \rightarrow 0} \left(\frac{\Delta \mathbf{x}}{\Delta t} \cdot \nabla \mathbf{u} \right) \quad (1.1.6)$$

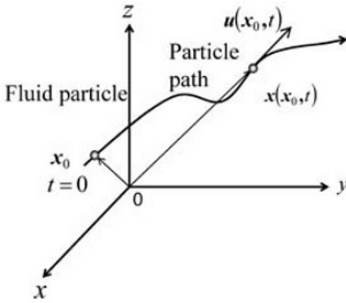
Particularly in fluid mechanics, \mathbf{a} in Eq. (1.1.6) is called the material derivative or substantial derivative, and is often expressed as

$$\mathbf{a} = \frac{D\mathbf{u}}{Dt} = \left(\frac{\partial}{\partial t} + \mathbf{u} \cdot \nabla \right) \mathbf{u} \quad (1.1.7)$$

In general, the rate of change over time of material parameter A , where A can be a scalar, vector or tensor associated with the (material) point at time t , can be expressed by the material derivative (the differential operator D/Dt is also called Lagrangian derivative) as

$$\frac{DA(\mathbf{x}_0, t)}{Dt} = \frac{\partial}{\partial t} A(\mathbf{x}, t) + (\mathbf{u} \cdot \nabla) A(\mathbf{x}, t) \quad (1.1.8)$$

(a) Lagrangian specification



(b) Eulerian specification

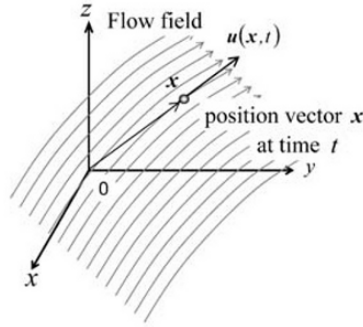


Fig. 1.2 Description of fluid motion

The derivative defined in Eq. (1.1.7) can be further written, using vector identities (see section of Appendix B-5), as follows

$$\frac{D\mathbf{u}}{Dt} = \frac{\partial \mathbf{u}}{\partial t} + \nabla \left(\frac{1}{2} |\mathbf{u}|^2 \right) - \mathbf{u} \times (\nabla \times \mathbf{u}) \quad (1.1.9)$$

The term $(\mathbf{u} \cdot \nabla) \mathbf{u}$ or $(\mathbf{u} \cdot \nabla) A$, operating in Eqs. (1.1.7) and (1.1.8) respectively, are called the convective term, which express the fact that, for time independent flow $\partial/\partial t = 0$, the fluid properties, such \mathbf{u} or A , depend only upon the spatial coordinates \mathbf{x} . Namely, the changes in fluid properties are due to the changing spatial position of a given fluid particle as it flows. The terms $\partial \mathbf{u} / \partial t$, $\partial A / \partial t$ are the Eulerian time derivatives evaluated at a position \mathbf{x} .

Having established the conceptual and mathematical representation of the kinematic description of motion, we will now consider the decomposition of motion. This will be done in order to establish the concept and mathematical description of that rate. An important concept in a motion of continuum is to know how the deformation can be expressed from the velocity field $\mathbf{u} = \mathbf{u}(\mathbf{x}, t)$.

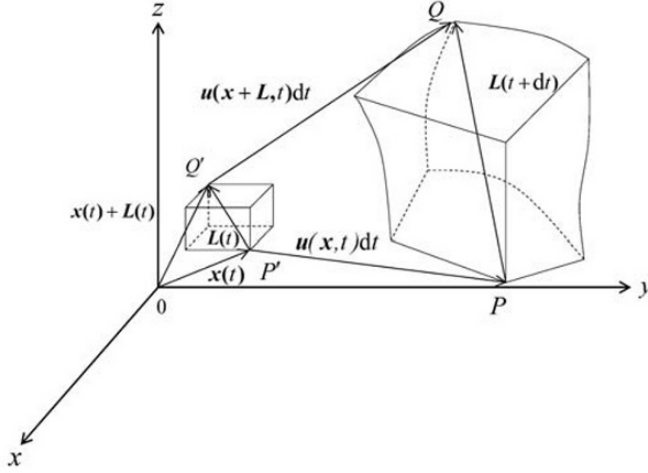


Fig. 1.3 Material line L change

Let us consider the configuration of an infinitesimal element $L(t)$ of a straight material line. It undergoes translation, rotation, and stretching, as a result of the nonuniform velocity field of $\mathbf{u} = d\mathbf{x}/dt$. As time elapses, the material line element $L(t)$ moves to the new positions P and Q , where $L(t)$ becomes $L(t + dt)$. From the figure in Fig. 1.3, it is clear that

$$\begin{aligned} L(t + dt) &= [\{\mathbf{x}(t) + L(t)\} + \mathbf{u}(\mathbf{x} + L, t)dt] - [\mathbf{x}(t) + \mathbf{u}(\mathbf{x}, t)dt] \\ &= L(t) + \mathbf{u}(\mathbf{x} + L, t)dt - \mathbf{u}(\mathbf{x}, t)dt \end{aligned} \quad (1.1.10)$$

so that, the changing rate of $L(t)$ as $t \rightarrow t + dt$ can be written as

$$\frac{L(t + dt) - L(t)}{dt} = \mathbf{u}(\mathbf{x} + L, t) - \mathbf{u}(\mathbf{x}, t) = L \frac{\partial \mathbf{u}(\mathbf{x}, t)}{\partial L} + \dots \quad (1.1.11)$$

where the right hand side of Eq. (1.1.11) is a Taylor series expansion for $\mathbf{u}(\mathbf{x}, t)$ around $L(t)$. Equation (1.1.11) can be further modified as

$$\frac{\left\{ \frac{\mathbf{L}(t+dt) - \mathbf{L}(t)}{dt} \right\}}{\mathbf{L}(t)} \approx \frac{\partial \mathbf{u}(\mathbf{x}, t)}{\partial \mathbf{L}(t)} \quad (1.1.12)$$

Let us denote $\Delta \mathbf{X} = \mathbf{L}(t + \Delta t) - \mathbf{L}(t)$ and $\mathbf{L}(t) = \Delta \mathbf{x}$, since we are taking $\mathbf{L}(t)$ as an infinitesimal line element, so that we have

$$\frac{\mathbf{L}(t + \Delta t) - \mathbf{L}(t)}{\mathbf{L}(t)} = \frac{\Delta \mathbf{X}}{\Delta \mathbf{x}} \left(= \frac{\partial \mathbf{X}}{\partial \mathbf{x}} = \mathbf{E} \right) \quad (1.1.13)$$

and

$$\frac{\partial \mathbf{u}(\mathbf{x}, t)}{\partial \mathbf{L}(t)} = \lim_{\Delta \mathbf{x} \rightarrow 0} \frac{\Delta \mathbf{u}}{\Delta \mathbf{x}} \left(= \frac{\partial \mathbf{u}}{\partial \mathbf{x}} = \nabla \mathbf{u} \right) \quad (1.1.14)$$

where \mathbf{E} is called the displacement gradient tensor and $\nabla \mathbf{u}$ is called the velocity gradient tensor. Using the notation defined in Eqs. (1.1.13) and (1.1.14). Thus, the change rate of material line element $\mathbf{L}(t)$, which is given by Eq. (1.1.11), will be written by the formula

$$\begin{aligned} \Delta \mathbf{x} \cdot \nabla \mathbf{u} &= \Delta \mathbf{x} \cdot \left\{ \frac{1}{2} (\nabla \mathbf{u} + \nabla \mathbf{u}^T) + \frac{1}{2} (\nabla \mathbf{u} - \nabla \mathbf{u}^T) \right\} \\ &= \Delta \mathbf{x} \cdot (\mathbf{e} + \boldsymbol{\omega}) \end{aligned} \quad (1.1.15)$$

where superscript T denotes the transpose of tensor. It is noted here that in expanding Eq. (1.1.15) the velocity gradient tensor $\nabla \mathbf{u}$, arbitrary second order tensor is decomposed into symmetric and skew-symmetric (or anti-symmetric) parts. We now define the rate of strain (or the rate of deformation) tensor, as the symmetric part of the velocity gradient tensor

$$\mathbf{e} = \frac{1}{2} (\nabla \mathbf{u} + \nabla \mathbf{u}^T) \quad (1.1.16)$$

and the vorticity (or spin) tensor, as the skew-symmetric part of the velocity gradient tensor

$$\boldsymbol{\omega} = \frac{1}{2} (\nabla \mathbf{u} - \nabla \mathbf{u}^T) \quad (1.1.17)$$

Thus, the change rate of $\mathbf{L}(t)$ due to translation $\mathbf{u}(\mathbf{x}, t)$ can be straining $\Delta \mathbf{x} \cdot \mathbf{e}$ and rotation $\Delta \mathbf{x} \cdot \boldsymbol{\omega}$. Consequently the velocity gradient tensor can be written by

$$\nabla \mathbf{u} = \mathbf{e} + \boldsymbol{\omega} \quad (1.1.18)$$

In order to gain more physical insight for tensors \mathbf{e} and $\boldsymbol{\omega}$ in continuum mechanics, we will examine \mathbf{e} in the first place. Referring Eq. (1.1.16), \mathbf{e} can be written by the Cartesian suffix convention for three values, $i = 1, 2$ and 3 , or $j = 1, 2$ and 3 , which correspond to x , y and z respectively as follows

$$\mathbf{e} = \hat{\mathbf{e}}_i \hat{\mathbf{e}}_j e_{ij} = \hat{\mathbf{e}}_i \hat{\mathbf{e}}_j \frac{1}{2} \left(\frac{\partial u_i}{\partial x_j} + \frac{\partial u_j}{\partial x_i} \right) \quad (1.1.19)$$

where $\hat{\mathbf{e}}_i \hat{\mathbf{e}}_j$ is the unit dyad (see Appendix B-1), and the components of the rate of strain tensor e_{ij} is presented by

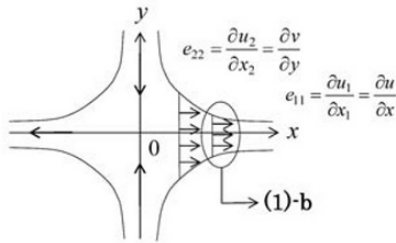
$$e_{ij} = \begin{bmatrix} \frac{\partial u_1}{\partial x_1} & \frac{1}{2} \left(\frac{\partial u_1}{\partial x_2} + \frac{\partial u_2}{\partial x_1} \right) & \frac{1}{2} \left(\frac{\partial u_1}{\partial x_3} + \frac{\partial u_3}{\partial x_1} \right) \\ \frac{1}{2} \left(\frac{\partial u_2}{\partial x_1} + \frac{\partial u_1}{\partial x_2} \right) & \frac{\partial u_2}{\partial x_2} & \frac{1}{2} \left(\frac{\partial u_2}{\partial x_3} + \frac{\partial u_3}{\partial x_2} \right) \\ \frac{1}{2} \left(\frac{\partial u_3}{\partial x_1} + \frac{\partial u_1}{\partial x_3} \right) & \frac{1}{2} \left(\frac{\partial u_3}{\partial x_2} + \frac{\partial u_2}{\partial x_3} \right) & \frac{\partial u_3}{\partial x_3} \end{bmatrix} = \begin{bmatrix} e_{11} & e_{12} & e_{13} \\ e_{21} & e_{22} & e_{23} \\ e_{31} & e_{32} & e_{33} \end{bmatrix} \quad (1.1.20)$$

It is easily known from Eq. (1.1.20) that e_{ij} is the symmetric and has 6 independent components, i.e. $e_{11}, e_{22}, e_{33}, e_{12} = e_{21}, e_{23} = e_{32}$ and $e_{31} = e_{13}$. The orthogonal components e_{11} , e_{22} , and e_{33} are the rate of elongational strain, due to a local deformation of fluid in stretching or contraction in x , y , and z axis respectively. In addition the off-orthogonal components e_{12} , e_{23} , and e_{31} (as well as e_{21} , e_{32} , and e_{13}) are, on the other hand, due to a local deformation of fluid in shearing in the plane of $x-y$, $y-z$, and $z-x$ respectively. Figure 1.4 gives an idea of the deformation rate occurring in fluid in $x-y$ plane. Figure 1.4 (1)-a shows the simple elongational (or extensional) flow field as one of typical stretching and contraction of flow, where the rate of elongational strain appears. Furthermore, in order to make the point clear, in Fig. 1.4 (1)-b the stretching of a fluid element in the elongational flow field is indicated. Similarly in Fig. 1.4 (2)-a the diagram shows the simple shear flow field, where the shear strain takes place and (2)-b a sketch of the shear field is displayed, where a fluid element is sheared in the flow direction.

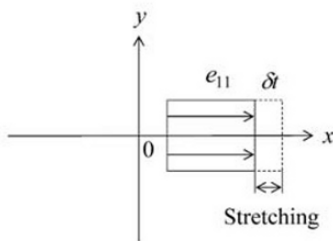
The symmetry of the tensor \mathbf{e} guarantees that there will always be three mutual orthogonal orientations of $\hat{\mathbf{p}} = \partial \mathbf{X} / \partial \mathbf{x}$, for each of which the corresponding rate of deformation is either elongation or contraction, that is the principal rates of deformation, to which we can assign $e'_1 = e_{11}$, $e'_2 = e_{22}$ and $e'_3 = e_{33}$. The summations of e'_1 , e'_2 and e'_3 are invariant for coordinate transformation, which give the proportional rate of increase of an infinitesimal material volume

$$\nabla \cdot \mathbf{u} = \text{div } \mathbf{u} = e'_1 + e'_2 + e'_3 \quad (1.1.21)$$

(1)-a Simple elongational
(or extensional) flow field

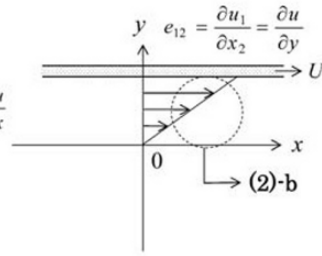


(1)-b

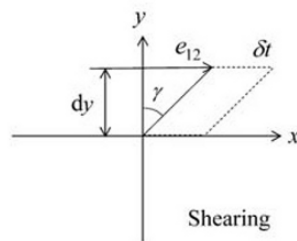


Stretching

(2)-a Simple shear flow field



(2)-b



Shearing

Fig. 1.4 Local deformation of fluid

This quantity defined in Eq. (1.1.21) is called the divergence of the velocity field of $\mathbf{u}(\mathbf{x}, t)$. Furthermore, a definition that is independent from a coordinates system can be given by

$$\begin{aligned}
 \operatorname{div} \mathbf{u} &= \frac{1}{\delta V} \frac{D(\delta V)}{Dt} = \frac{1}{\delta V} \int_S \hat{\mathbf{n}} \cdot \mathbf{u} dS \\
 &= \frac{1}{\delta V} \int_V \nabla \cdot \mathbf{u} dV
 \end{aligned} \tag{1.1.22}$$

Equation (1.1.22) is called the Euler's relation, which implies the physical rate of change over time of the volume of moving fluid particles per unit volume. It is noted that to write the volume integral $\int_V \nabla \cdot \mathbf{u} dV$ from the surface integral $\int_S \hat{\mathbf{n}} \cdot \mathbf{u} dS$ the Gauss' divergence theorem is applied.

The skew-symmetric part $\boldsymbol{\omega}$ given by Eq. (1.1.17) of the velocity gradient tensor $\nabla \mathbf{u}$ can be similarly written by the Cartesian suffix convention as

$$\boldsymbol{\omega} = \hat{\mathbf{e}}_i \hat{\mathbf{e}}_j \omega_{ij} = \hat{\mathbf{e}}_i \hat{\mathbf{e}}_j \frac{1}{2} \left(\frac{\partial u_i}{\partial x_j} - \frac{\partial u_j}{\partial x_i} \right) \tag{1.1.23}$$

and ω_{ij} can be further written in matrix form

$$\begin{aligned}
 \omega_{ij} &= \frac{1}{2} \begin{bmatrix} 0 & \left(\frac{\partial u_1}{\partial x_2} - \frac{\partial u_2}{\partial x_1} \right) & \left(\frac{\partial u_1}{\partial x_3} - \frac{\partial u_3}{\partial x_1} \right) \\ \left(\frac{\partial u_2}{\partial x_1} - \frac{\partial u_1}{\partial x_2} \right) & 0 & \left(\frac{\partial u_2}{\partial x_3} - \frac{\partial u_3}{\partial x_2} \right) \\ \left(\frac{\partial u_3}{\partial x_1} - \frac{\partial u_1}{\partial x_3} \right) & \left(\frac{\partial u_3}{\partial x_2} - \frac{\partial u_2}{\partial x_3} \right) & 0 \end{bmatrix} \\
 &= \frac{1}{2} \begin{bmatrix} 0 & \omega_{12} & \omega_{13} \\ \omega_{21} & 0 & \omega_{23} \\ \omega_{31} & \omega_{32} & 0 \end{bmatrix}
 \end{aligned} \tag{1.1.24}$$

Components, which appear in Eq. (1.1.23), as the components of $\boldsymbol{\omega} = \nabla \times \mathbf{u}$, are related with the following formula

$$\begin{aligned}
 \nabla \times \mathbf{u} &= \hat{\mathbf{e}}_1 \left(\frac{\partial u_3}{\partial x_2} - \frac{\partial u_2}{\partial x_3} \right) + \hat{\mathbf{e}}_2 \left(\frac{\partial u_1}{\partial x_3} - \frac{\partial u_3}{\partial x_1} \right) + \hat{\mathbf{e}}_3 \left(\frac{\partial u_2}{\partial x_1} - \frac{\partial u_1}{\partial x_2} \right) \\
 &= \hat{\mathbf{e}}_1 \omega_1 + \hat{\mathbf{e}}_2 \omega_2 + \hat{\mathbf{e}}_3 \omega_3
 \end{aligned} \tag{1.1.25}$$

It may be useful to consider $\boldsymbol{\omega} = \nabla \times \mathbf{u}$ in a little more detail for the sake of coupling equations in the following chapters. The nature of $\nabla \times \mathbf{u}$ can be examined by introducing the alternator or alternating unit tensor $\boldsymbol{\varepsilon} = \hat{\mathbf{e}}_i \hat{\mathbf{e}}_j \hat{\mathbf{e}}_k \varepsilon_{ijk}$ as follows

$$\begin{aligned}
 \nabla \times \mathbf{u} &= \varepsilon_{ijk} \hat{\mathbf{e}}_i \frac{\partial u_k}{\partial x_j} \\
 &= \varepsilon_{1jk} \hat{\mathbf{e}}_1 \frac{\partial u_k}{\partial x_j} + \varepsilon_{2jk} \hat{\mathbf{e}}_2 \frac{\partial u_k}{\partial x_j} + \varepsilon_{3jk} \hat{\mathbf{e}}_3 \frac{\partial u_k}{\partial x_j} \\
 &= \hat{\mathbf{e}}_1 \left(\frac{\partial u_3}{\partial x_2} - \frac{\partial u_2}{\partial x_3} \right) + \hat{\mathbf{e}}_2 \left(\frac{\partial u_1}{\partial x_3} - \frac{\partial u_3}{\partial x_1} \right) + \hat{\mathbf{e}}_3 \left(\frac{\partial u_2}{\partial x_1} - \frac{\partial u_1}{\partial x_2} \right) \\
 &= \hat{\mathbf{e}}_1 \omega_1 + \hat{\mathbf{e}}_2 \omega_2 + \hat{\mathbf{e}}_3 \omega_3
 \end{aligned} \tag{1.1.26}$$

Thus, in comparison with (1.1.23) and (1.1.25), a vector $\boldsymbol{\omega}$ (in this case $\nabla \times \mathbf{u}$) with components ω_1 , ω_2 and ω_3 can be reduced from a general second order tensor \mathbf{S} (in the present case $\partial u_i / \partial x_j$, $\partial \mathbf{u} / \partial \mathbf{x}$, $\nabla \mathbf{u}$ or $\text{grad } \mathbf{u}$), whose components of skew-symmetric part (in this case $\boldsymbol{\omega}$) are written by

$$\boldsymbol{\omega} = \frac{1}{2} \begin{bmatrix} 0 & -\omega_3 & \omega_2 \\ \omega_3 & 0 & -\omega_1 \\ -\omega_2 & \omega_1 & 0 \end{bmatrix} \tag{1.1.27}$$

Note that the vector $\boldsymbol{\omega} = (\omega_1, \omega_2, \omega_3)$ is called the pseudovector of the tensor \mathbf{S} or simply the vector of tensor \mathbf{S} . See Exercise 1.4.

By employing the alternator $\boldsymbol{\varepsilon}$, the vector $\boldsymbol{\omega}$ may be found from \mathbf{S} , more specifically from the skew-symmetric part \mathbf{S}_a of \mathbf{S} , denoting $\mathbf{S}_a = \boldsymbol{\omega} / 2$ while the symmetric part \mathbf{S}_s of \mathbf{S} may be expressed by $\mathbf{S}_s = \mathbf{e} / 2$. The following relationships are particularly useful;

$$\boldsymbol{\omega} = -\boldsymbol{\varepsilon} \cdot \mathbf{S} \tag{1.1.28}$$

$$\mathbf{S}_a = \frac{1}{2} \boldsymbol{\varepsilon} \cdot \boldsymbol{\omega} \tag{1.1.29}$$

Note that from Eqs. (1.1.28) and (1.1.29) the pseudovector $\boldsymbol{\omega}$ is zero, $\boldsymbol{\omega} = 0$, if a second order tensor \mathbf{S} is symmetric $\mathbf{S}_a = 0$, and vice versa.

For the sake of clarity and convenience, the unit tensor \mathbf{I} and the alternator $\boldsymbol{\varepsilon}$ are defined below. \mathbf{I} is defined such that

$$\mathbf{I} = \hat{\mathbf{e}}_i \hat{\mathbf{e}}_j \delta_{ij} \quad (1.1.30)$$

where δ_{ij} is the Kronecker delta and $\hat{\mathbf{e}}_i \hat{\mathbf{e}}_j$ is the unit dyad. δ_{ij} is defined as

$$\delta_{ij} = \begin{cases} 1 & \text{if } i = j \\ 0 & \text{if } i \neq j \end{cases} \quad (1.1.31)$$

$\boldsymbol{\varepsilon}$ is similarly defined by

$$\boldsymbol{\varepsilon} = \hat{\mathbf{e}}_i \hat{\mathbf{e}}_j \hat{\mathbf{e}}_k \varepsilon_{ijk} \quad (1.1.32)$$

where ε_{ijk} is the Eddington notation and $\hat{\mathbf{e}}_i \hat{\mathbf{e}}_j \hat{\mathbf{e}}_k$ is the unit polyadic. Thus, the alternator is a polyadic. ε_{ijk} is defined in the following manner

$$\varepsilon_{ijk} = \begin{cases} +1 & \text{if } ijk = 123, 231, \text{ or } 312 \\ -1 & \text{if } ijk = 321, 132, \text{ or } 213 \\ 0 & \text{if } i = j, i = k, \text{ or } j = k \end{cases} \quad (1.1.33)$$

It is useful for $\boldsymbol{\varepsilon}$ to be alternatively expressed with the form

$$\boldsymbol{\varepsilon} = (\hat{\mathbf{e}}_1 \hat{\mathbf{e}}_2 \hat{\mathbf{e}}_3 + \hat{\mathbf{e}}_2 \hat{\mathbf{e}}_3 \hat{\mathbf{e}}_1 + \hat{\mathbf{e}}_3 \hat{\mathbf{e}}_1 \hat{\mathbf{e}}_2 - \hat{\mathbf{e}}_1 \hat{\mathbf{e}}_3 \hat{\mathbf{e}}_2 - \hat{\mathbf{e}}_2 \hat{\mathbf{e}}_1 \hat{\mathbf{e}}_3 - \hat{\mathbf{e}}_3 \hat{\mathbf{e}}_2 \hat{\mathbf{e}}_1) \quad (1.1.34)$$

After giving mathematical formalities for the tensor $\boldsymbol{\omega}$, we will see how $\boldsymbol{\omega}$ may cause a local deformation in the flow field $\mathbf{u}(\mathbf{x}, t)$. The deformation due to $\boldsymbol{\omega}$ can be examined from Eq. (1.1.11) as

$$\Delta \mathbf{X} = \mathbf{L}(t + dt) - \mathbf{L}(t) \approx \left[\mathbf{L} \cdot \left(\frac{\partial \mathbf{u}}{\partial \mathbf{L}} \right)_a \right] dt \quad (1.1.35)$$

Note that $(\partial \mathbf{u} / \partial \mathbf{L})_a$ is a skew-symmetric part of the velocity gradient tensor. It is further noted that by taking an infinitesimal time duration $dt \approx \delta t$ and on infinitesimal line element $\mathbf{L} = \Delta \mathbf{x} \approx \delta \mathbf{x}$, we can obtain the deformation in x - y plane, for example

$$\begin{aligned} \Delta \mathbf{X} &= [\delta \mathbf{x} \cdot \boldsymbol{\omega}] \delta t = \frac{1}{2} (\delta x, \delta y, 0) \begin{bmatrix} 0 & -\omega_3 & 0 \\ \omega_3 & 0 & 0 \\ 0 & 0 & 0 \end{bmatrix} \delta t \hat{\mathbf{e}}_3 \\ &= \left(\frac{1}{2} \delta y \omega_3 - \frac{1}{2} \delta x \omega_3 \right) \delta t \hat{\mathbf{e}}_3 \end{aligned} \quad (1.1.36)$$

The implication of Eq. (1.1.36) is, in the $x-y$ plane, that as indicated in Fig. 1.5, the fluid element $\delta x - \delta y$ is rotated around the z axis with its angular velocity $\Omega_3 = \omega_3/2$. Thus, as easily speculated from Fig. 1.5, the vorticity tensor $\boldsymbol{\omega}$ represents a rigid body rotation of fluid element with angular velocity $\boldsymbol{\Omega} = \boldsymbol{\omega}/2$. The pseudovector of the velocity gradient tensor, i.e. $\boldsymbol{\omega} = \nabla \times \mathbf{u} = -\boldsymbol{\varepsilon} : \nabla \mathbf{u}$, is called the vorticity vector. The vorticity vector $\boldsymbol{\omega}$ is an important flow parameter in fluid mechanics.

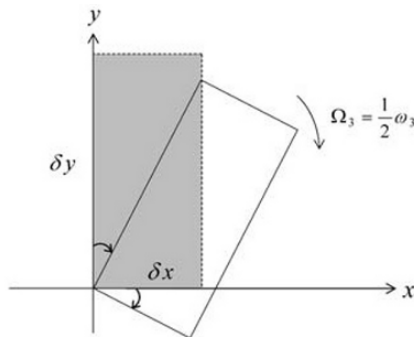


Fig. 1.5 Rigid body rotation of fluid element $\delta x - \delta y$

1.2 Dynamics in Rotating Reference Frame

In consideration of kinematics let us explore the relationship between an inertial and a rotating reference frame. For brevity, let the rotating reference frame be rotated with a constant angular velocity $\boldsymbol{\Omega}$ with respect to the inertial reference frame, supposing no translation of the rotating reference frame to the inertial reference frame, see Fig. 1.6. It is noted that we adopt a right-handed orthogonal coordinates system, where $\boldsymbol{\Omega} > 0$ is an angular velocity vector, which rotates to the direction of a right-handed screw. The position vectors \mathbf{x}_0 and \mathbf{x}_r of a material point \mathbf{x} in the inertial frame and rotating frame respectively are related as

$$\mathbf{x}_r = \mathbf{Q} \cdot \mathbf{x}_0 \quad (1.2.1)$$

where \mathbf{Q} is a rotation tensor, which is an orthogonal tensor with a relation of $\mathbf{Q}^T \cdot \mathbf{Q} = \mathbf{I}$, and $\mathbf{Q}^T = \mathbf{Q}^{-1}$ (where \mathbf{Q} is a unitary matrix); \mathbf{Q}^{-1}

denotes the inverse of the tensor \mathbf{Q} and \mathbf{Q}^T denotes the transpose of the tensor \mathbf{Q} .

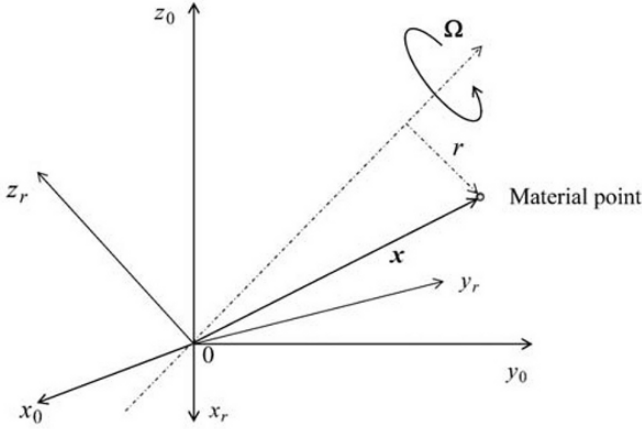


Fig. 1.6 Rotating reference frame with inertial reference frame

In order to correlate two frames kinematically, we shall consider a velocity and acceleration at the material point. To start with, apply D/Dt , the material derivative, to Eq. (1.2.1) to obtain the relative velocity \mathbf{u}_r

$$\begin{aligned} \mathbf{u}_r &= \frac{D\mathbf{x}_r}{Dt} = \frac{D\mathbf{Q}}{Dt} \cdot \mathbf{x}_0 + \mathbf{Q} \cdot \frac{D\mathbf{x}_0}{Dt} \\ &= \frac{D\mathbf{Q}}{Dt} \cdot \mathbf{Q}^{-1} \cdot \mathbf{x}_r + \mathbf{Q} \cdot \frac{D\mathbf{x}_0}{Dt} \end{aligned} \quad (1.2.2)$$

Equation (1.2.2) can be further written with the velocity \mathbf{u}_0 in the inertial frame, letting $D\mathbf{x}_0/Dt = \mathbf{u}_0$ by

$$\mathbf{u}_r = -\boldsymbol{\Omega} \times \mathbf{x}_r + \mathbf{Q} \cdot \mathbf{u}_0 \quad (1.2.3)$$

Here we used tensor calculus (for relative position vector \mathbf{x}_r , see Problem 1-1) as

$$\boldsymbol{\Omega} \times \mathbf{x}_r = -\frac{D\mathbf{Q}}{Dt} \cdot \mathbf{Q}^T \cdot \mathbf{x}_r = -\frac{D\mathbf{Q}}{Dt} \cdot \mathbf{Q}^{-1} \cdot \mathbf{x}_r \quad (1.2.4)$$

It is noted that $\mathbf{\Omega}$ is the pseudovector of the skew-symmetric tensor $(D\mathbf{Q}/Dt) \cdot \mathbf{Q}^T$ in the same manner explained for the vorticity vector $\boldsymbol{\omega}$ previously. Next, by taking the material derivative again to Eq. (1.2.3), we can obtain the relative acceleration \mathbf{a}_r of the material point \mathbf{x} as follows

$$\begin{aligned} \mathbf{a}_r &= \frac{D\mathbf{u}_r}{Dt} \\ &= -\mathbf{\Omega} \times \mathbf{u}_r + \frac{D\mathbf{Q}}{Dt} \cdot \mathbf{Q}^{-1} \cdot \mathbf{u}_r + \frac{D\mathbf{Q}}{Dt} \cdot \mathbf{Q}^{-1} \cdot (\mathbf{\Omega} \times \mathbf{x}_r) + \mathbf{Q} \cdot \mathbf{a}_0 \end{aligned} \quad (1.2.5)$$

Consequently from Eq. (1.1.4), we can obtain the acceleration vector \mathbf{a}_0 , i.e. the acceleration of the inertial frame, by relating Eq. (1.2.5) in the rotating frame as

$$\mathbf{a}_0 = \mathbf{a}_r + 2\mathbf{\Omega} \times \mathbf{u}_r + \mathbf{\Omega} \times (\mathbf{\Omega} \times \mathbf{x}_r) \quad (1.2.6)$$

where it is derived when an inertial frame is instantaneously coincident with the rotating frame, as $\mathbf{Q} = \mathbf{I}$. In Eq. (1.2.6), the first term in the right hand side of the equation is the rectilinear acceleration, the second is the Corioli's acceleration, and the third is the centripetal acceleration. With identical vectors, it is easy to show that the third term of Eq. (1.2.6), i.e. the centripetal acceleration can be reduced to the potential form as

$$\mathbf{\Omega} \times (\mathbf{\Omega} \times \mathbf{x}_r) = -\nabla \left(\frac{1}{2} |\mathbf{\Omega} \times \mathbf{x}_r|^2 \right) = -\nabla \left(\frac{1}{2} \Omega^2 r^2 \right) \quad (1.2.7)$$

so that, defining a potential function ϕ , and setting $\phi = \Omega^2 r^2 / 2$, where r simply denotes distance from the axis of rotation, the centripetal acceleration can be expressed as

$$\mathbf{\Omega} \times (\mathbf{\Omega} \times \mathbf{x}_r) = -\nabla \phi \quad (1.2.8)$$

It may be worthwhile to note that the operation to reduce the relation (1.2.6) can be simply understood by a vector algebra for a fluid particle rotating at a constant angular velocity $\mathbf{\Omega}$ along an axis of rotation in the inertial reference frame at a material point \mathbf{x}

$$\mathbf{x}_0 = \mathbf{x}_r \quad (1.2.9)$$

and

$$\mathbf{u}_0 = \mathbf{u}_r + \mathbf{\Omega} \times \mathbf{x}_r \quad (1.2.10)$$

Equation (1.2.9) refers to the instantaneous moment, when $\mathbf{Q} = \mathbf{I}$, and Eq. (1.2.10) implies the relative velocity of the fluid particle rotating to the

inertial frame. Thus, taking the time derivative to Eq. (1.2.10), as we have similarly done to Eq. (1.2.3), we can obtain the acceleration of the fluid particle relative to the inertial frame as

$$\mathbf{a}_0 = \frac{D\mathbf{u}_0}{Dt} = \frac{d\mathbf{u}_r}{dt} + 2\boldsymbol{\Omega} \times \mathbf{u}_r + \boldsymbol{\Omega} \times (\boldsymbol{\Omega} \times \mathbf{x}_r) \quad (1.2.11)$$

which is exactly the same form as Eq. (1.2.6). The relation given by Eq. (1.2.11) can again be written, using the potential ϕ

$$\mathbf{a}_0 = \mathbf{a}_r + 2\boldsymbol{\Omega} \times \mathbf{u}_r - \nabla \phi \quad (1.2.12)$$

where $\phi = \Omega^2 r^2 / 2$.

1.3 Material Objectivity and Convective Derivatives

On the microstructure level material elements may be affected by strong electromagnetic field or strong inertial forces; however, on the continuum level the physical characteristic of a material, such as demonstrated by the Hooke's law (the relationship between the extension and the force can be regarded as a physical property of spring itself), is independent of the motion of the observer. This concept is called "the material objectivity" or "the principle of frame invariance". Particularly in dealing with the relationship between a deformation and a stress in continuum, so-called constitutive equation, this concept is of some importance.

In order to satisfy the principle of frame invariance, the following linear transformation by \mathbf{E} (see \mathbf{Q} and \mathbf{E} in Eqs. (1.2.1) and (1.3.4) for equivalence) must be satisfied for any arbitrary vectors (say a velocity vector $\mathbf{u}(\mathbf{x}, t)$) and second order tensor (say a stress tensor $\mathbf{T}(\mathbf{x}, t)$) in the Cartesian reference frame. This can be set in the inertial reference frame in such a way that

$$\mathbf{u}_r = \mathbf{Q} \cdot \mathbf{u}_0 \quad \text{to} \quad \mathbf{u} = \mathbf{E} \cdot \mathbf{u}' \quad (1.3.1)$$

$$\mathbf{T}_r = \mathbf{Q} \cdot \mathbf{T}_0 \cdot \mathbf{Q}^T \quad \text{to} \quad \mathbf{T} = \mathbf{E} \cdot \mathbf{T}' \cdot \mathbf{E}^T \quad (1.3.2)$$

where the suffix r denotes the rotating reference frame. Note that scalar properties (such temperature, density, etc.) are always frame invariant.

Now we will direct our attention to how the time derivative of vectors and tensors are affected in order for the principle of frame invariance to be satisfied. We will consider this problem with respect to the transformation

of a material line element as displayed in Fig. 1.3, where the material line element $\mathbf{L}(t) = \Delta \mathbf{x}$ (in the material reference frame) is transformed to $\mathbf{L}(t + dt)$ (in the new space frame), noting that $\mathbf{L}(t + dt) - \mathbf{L}(t) = \Delta \mathbf{X}$ and defining the displacement gradient tensors as

$$\lim_{\Delta x \rightarrow 0} \frac{\Delta \mathbf{X}}{\Delta \mathbf{x}} \approx \frac{\partial \mathbf{X}}{\partial \mathbf{x}} = \mathbf{E} \quad (1.3.3)$$

so that Eq. (1.3.3) can be further written as

$$\Delta \mathbf{X} \approx \mathbf{E} \cdot \Delta \mathbf{x} \quad (1.3.4)$$

and

$$\Delta \mathbf{x} \approx \mathbf{E}^{-1} \cdot \Delta \mathbf{X} \quad (1.3.5)$$

Eventually \mathbf{E} is a linear transformation tensor, and in order to verify the principle of frame invariance we will transform a tensor \mathbf{T}' (in the material reference frame) to \mathbf{T} (in the new space frame). This transformation can be written

$$\mathbf{T} = \mathbf{E} \cdot \mathbf{T}' \cdot \mathbf{E}^T \quad (1.3.6)$$

and the reverse transformation is defined by

$$\mathbf{T}' = \mathbf{E}^{-1} \cdot \mathbf{T} \cdot (\mathbf{E}^{-1})^T \quad (1.3.7)$$

Thus, the material derivative of \mathbf{T}' in Eq. (1.3.7) will be

$$\frac{D\mathbf{T}'}{Dt} = \dot{\mathbf{E}}^{-1} \cdot \mathbf{T} \cdot (\mathbf{E}^{-1})^T + \mathbf{E}^{-1} \cdot \dot{\mathbf{T}} \cdot (\mathbf{E}^{-1})^T + \mathbf{E}^{-1} \cdot \mathbf{T} \cdot (\dot{\mathbf{E}}^{-1})^T \quad (1.3.8)$$

denoting the material derivative, i.e. $D\mathbf{T}'/Dt = \dot{\mathbf{T}}'$. Equation (1.3.8) can be further reduced to the form

$$\begin{aligned} \dot{\mathbf{T}}' &= \mathbf{E}^{-1} \cdot \dot{\mathbf{T}} \cdot (\mathbf{E}^{-1})^T - \mathbf{E}^{-1} \cdot (\nabla \mathbf{u} \cdot \mathbf{T}) \cdot (\mathbf{E}^{-1})^T - \mathbf{E}^{-1} \cdot (\mathbf{T} \cdot \nabla \mathbf{u}^T) \cdot (\mathbf{E}^{-1})^T \\ &= \mathbf{E}^{-1} \cdot (\dot{\mathbf{T}} - \nabla \mathbf{u} \cdot \mathbf{T} - \mathbf{T} \cdot \nabla \mathbf{u}^T) \cdot (\mathbf{E}^{-1})^T \end{aligned} \quad (1.3.9)$$

It is noted that to derive Eq. (1.3.9) we have used the relations $\dot{\mathbf{E}}^{-1} = -\mathbf{E}^{-1} \cdot \dot{\mathbf{E}} \cdot \mathbf{E}^{-1}$ and $\nabla \mathbf{u} = \partial \mathbf{u} / \partial \mathbf{x} = \dot{\mathbf{E}} \cdot \mathbf{E}^{-1}$. The relations are obtained from Eq. (1.3.4) for the velocity \mathbf{u} as

$$\mathbf{u} = \frac{d\mathbf{X}}{dt} = \dot{\mathbf{E}} \cdot \Delta \mathbf{x} \quad (1.3.10)$$

and

$$\nabla \mathbf{u} = \frac{\partial \mathbf{u}}{\partial \mathbf{X}} = \dot{\mathbf{E}} \cdot \frac{\partial \mathbf{x}}{\partial \mathbf{X}} = \dot{\mathbf{E}} \cdot \mathbf{E}^{-1} \quad (1.3.11)$$

Consequently, the tensor $(\dot{\mathbf{T}} - \nabla \mathbf{u} \cdot \mathbf{T} - \mathbf{T} \cdot \nabla \mathbf{u}^T)$ is linearly transformed by a material line element of \mathbf{E}^{-1} , and we denote Eq. (1.3.9) as

$$\dot{\mathbf{T}}' = \mathbf{E}^{-1} \cdot \overset{\nabla}{\mathbf{T}} \cdot (\mathbf{E}^{-1})^T \quad (1.3.12)$$

where $\overset{\nabla}{\mathbf{T}}$ is called the upper convective derivative, which is defined as follows

$$\begin{aligned} \overset{\nabla}{\mathbf{T}} &= \frac{D\mathbf{T}}{Dt} - \nabla \mathbf{u} \cdot \mathbf{T} - \mathbf{T} \cdot \nabla \mathbf{u}^T \\ &= \dot{\mathbf{T}} - \nabla \mathbf{u} \cdot \mathbf{T} - \mathbf{T} \cdot \nabla \mathbf{u}^T \end{aligned} \quad (1.3.13)$$

In the upper convective derivative, the base vectors are “contravariant” base vectors. That is, the base coordinate vectors are parallel to material lines, which are deformed (stretched and rotated) with a material line.

In a similar manner, with “covariant” base vectors, that are normal to material planes, where in a deformation each base vector rotates to remain normal and stretches so that its length remains proportional to the area of the material plane to which it is normal, we have the lower convective derivative defined by

$$\overset{\Delta}{\mathbf{T}} = \dot{\mathbf{T}} + \nabla \mathbf{u}^T \cdot \mathbf{T} + \mathbf{T} \cdot \nabla \mathbf{u} \quad (1.3.14)$$

If we extend further, we will see that when material lines are in a deformation with rotational coordinates, we can define the derivative in the following manner

$$\overset{\circ}{\mathbf{T}} = \dot{\mathbf{T}} - \boldsymbol{\omega} \cdot \mathbf{T} + \mathbf{T} \cdot \boldsymbol{\omega} \quad (1.3.15a)$$

or alternatively

$$\overset{\circ}{\mathbf{T}} = \dot{\mathbf{T}} - \frac{1}{2}(\boldsymbol{\omega} \cdot \mathbf{T} - \mathbf{T} \cdot \boldsymbol{\omega}) \quad (1.3.15b)$$

where $\boldsymbol{\omega}$ is the spin tensor and the derivative $\overset{\circ}{\mathbf{T}}$ is called the corotational derivative (a) or the Jaumann derivative (b). The corotational (Jaumann) derivative can be gotten from the upper convective derivative directly by setting $\nabla \mathbf{u} = \mathbf{e} + \boldsymbol{\omega} = 0 + \boldsymbol{\omega}$, and using $\boldsymbol{\omega} = -\boldsymbol{\omega}^T$.

The three derivatives, Eqs. (1.3.13), (1.3.14) and (1.3.15), can satisfy the principle of frame invariance, and this can be easily demonstrated to meet the condition in Eq. (1.3.2) for the rotation tensor \mathbf{Q} to give

$$\begin{aligned}
 & \frac{D\mathbf{T}'}{Dt'} - \nabla \mathbf{u}' \cdot \mathbf{T}' - \mathbf{T}' \cdot (\nabla \mathbf{u}')^T \\
 &= \frac{D}{Dt} (\mathbf{Q} \cdot \mathbf{T} \cdot \mathbf{Q}^T) - (\mathbf{Q} \cdot \nabla \mathbf{u} \cdot \mathbf{Q}^T + \boldsymbol{\Omega}) \cdot \mathbf{Q} \cdot \mathbf{T} \cdot \mathbf{Q}^T \\
 & \quad - \mathbf{Q} \cdot \mathbf{T} \cdot \mathbf{Q}^T \cdot (\mathbf{Q} \cdot \nabla \mathbf{u}^T \cdot \mathbf{Q}^T + \boldsymbol{\Omega}^T) \\
 &= \mathbf{Q} \cdot \left(\frac{D\mathbf{T}}{Dt} - \nabla \mathbf{u} \cdot \mathbf{T} - \mathbf{T} \cdot \nabla \mathbf{u}^T \right) \cdot \mathbf{Q}^T
 \end{aligned} \tag{1.3.16}$$

So, $\overset{\nabla}{\mathbf{T}}$ meets the sufficient condition for the principle of frame invariance. Observe that in deriving Eq. (1.3.16), the following relation was used

$$\boldsymbol{\Omega} = \dot{\mathbf{Q}} \cdot \mathbf{Q}^T = -\mathbf{Q} \cdot \dot{\mathbf{Q}}^T = -\boldsymbol{\Omega}^T \tag{1.3.17}$$

since we have $\mathbf{Q} \cdot \mathbf{Q}^T = \mathbf{I}$, where \mathbf{Q} is the unitary matrix, which is written by $\dot{\mathbf{Q}} \cdot \mathbf{Q}^T = -\mathbf{Q} \cdot \dot{\mathbf{Q}}^T$. It is further noted that the velocity gradient tensor $\nabla \mathbf{u}$ itself does not satisfies the principle of frame invariance as it is shown that

$$\begin{aligned}
 \nabla \mathbf{u}' &= \mathbf{Q} \cdot \nabla \mathbf{u} \cdot \mathbf{Q}^T + \dot{\mathbf{Q}} \cdot \mathbf{Q}^T \\
 &= \mathbf{Q} \cdot \nabla \mathbf{u} \cdot \mathbf{Q}^T + \boldsymbol{\Omega}
 \end{aligned} \tag{1.3.18}$$

1.4 Displacement Gradient and Relative Strain

The displacement gradient tensor \mathbf{E} , defined in Eqs. (1.1.13) and (1.3.3), is not generally symmetric and contains both deformation and rotation of a material line. Thus, \mathbf{E} itself is not a quantity of the frame invariance and one may have to exclude the effect of rotation of a material line, particularly when a constitutive equation is considered. In order to define finite strain tensors, which are free from rotation, we can simply take the square of the length of $\Delta \mathbf{x}$ or $\Delta \mathbf{X}$, for the material lines before and after deformation respectively (see Fig. 1.3), such that

$$ds^2 = \Delta \mathbf{x}^T \cdot \Delta \mathbf{x} = (\mathbf{E}^{-1} \cdot \Delta \mathbf{X})^T \cdot (\mathbf{E}^{-1} \cdot \Delta \mathbf{X}) = d\mathbf{X}^T \cdot (\mathbf{E} \cdot \mathbf{E}^T)^{-1} \cdot d\mathbf{X} \tag{1.4.1}$$

$$dS^2 = \Delta \mathbf{X}^T \cdot \Delta \mathbf{X} = (\mathbf{E} \cdot \Delta \mathbf{x})^T \cdot (\mathbf{E} \cdot \Delta \mathbf{x}) = d\mathbf{x}^T \cdot (\mathbf{E}^T \cdot \mathbf{E}) \cdot d\mathbf{x} \tag{1.4.2}$$

Equations (1.4.1) and (1.4.2) contain metric tensors, $(\mathbf{E} \cdot \mathbf{E}^T)^{-1}$ and $(\mathbf{E}^T \cdot \mathbf{E})$ respectively.

Hereafter we define strain tensors, one of which is called the Cauchy strain tensor \mathbf{C} defined by

$$\mathbf{C} = \mathbf{E}^T \cdot \mathbf{E} \quad (1.4.3)$$

and the other is called the Finger strain tensor defined by

$$\mathbf{C}^{-1} = \mathbf{E}^{-1} \cdot \mathbf{E}^{-1T} \quad (1.4.4)$$

These two tensors are both positive symmetric, and describe the deformation from t to $t + \Delta t$ of a material line, which are free from rotation. Considering the character of two tensors, \mathbf{C} and \mathbf{C}^{-1} , we can define two closely related relative strain tensors as follows

$$\boldsymbol{\gamma}^R = \mathbf{I} - \mathbf{C} \quad (1.4.5)$$

$$\boldsymbol{\gamma}_R = \mathbf{C}^{-1} - \mathbf{I} \quad (1.4.6)$$

These two relative strain tensors are very useful and are often used in deriving integral constitutive equations for viscoelastic fluids.

1.5 Reynolds' Transport Theorem

In deriving conservation equations of flow, it is particularly important to consider the volume integral $I = \int_{V(t)} F(\mathbf{x}, t) dV$, of which material derivative is defined as DI/Dt . $V = V(t)$ is a closed volume of fluid particles, or otherwise known as a material volume (element) consisting of a representative material line, and $F(\mathbf{x}, t)$ is any scalar, vector, or tensor function. Reynolds' transport theorem concerns the rate of change of any volume integral, i.e. DI/Dt .

Before proceeding further, it may be useful to consider the change of a material volume dV_0 from coordinates $\boldsymbol{\xi}$ at time t_0 to coordinates \mathbf{x} at time t , where $\boldsymbol{\xi}$ is the material coordinates, and they are Cartesian coordinates, $\boldsymbol{\xi} = (\xi_1, \xi_2, \xi_3)$. Also let the volume element dV_0 be $d\xi_1, d\xi_2, d\xi_3$ of an elementary parallelepiped, as sketched in Fig. 1.7. Due to the fluid motion, this parallelepiped dV_0 is moved to some neighborhood of the Cartesian point $\mathbf{x} = \mathbf{x}(\boldsymbol{\xi}, t)$ at time t , with the volume element of dV ,

whose sides are dx_1 , dx_2 and dx_3 , i.e. $dV = dx_1 dx_2 dx_3$. The change of coordinates $\mathbf{x} = (x_1, x_2, x_3)$ must be given to the corresponding coordinates $\boldsymbol{\xi} = (\xi_1, \xi_2, \xi_3)$ by

$$x_i = x_i(\xi_1, \xi_2, \xi_3) \quad (1.5.1)$$

The sides dx_1 , dx_2 and dx_3 of the volume element can be given by chain rule as

$$dx_i = \frac{\partial x_i}{\partial \xi_j} d\xi_j \quad \text{for } i = 1, 2, 3 \quad (1.5.2)$$

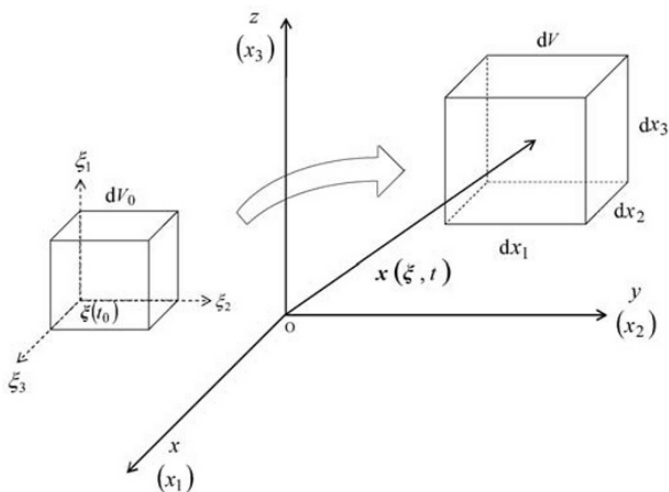


Fig. 1.7 Change of material volume at time t

The resultant volume element dV can be calculated by the box product $[\]$ of vectors' $d\mathbf{x}_1$, $d\mathbf{x}_2$, and $d\mathbf{x}_3$ three sides, representing material line elements of dV

$$\begin{aligned} dV &= [d\mathbf{x}_1 d\mathbf{x}_2 d\mathbf{x}_3] = d\mathbf{x}_1 \cdot (d\mathbf{x}_2 \times d\mathbf{x}_3) \\ &= J d\xi_1 d\xi_2 d\xi_3 \end{aligned} \quad (1.5.3)$$

where J is called the Jacobian of the transformation of the variables, and is defined as

$$J = \frac{\partial (x_1, x_2, x_3)}{\partial (\xi_1, \xi_2, \xi_3)} = \epsilon_{ijk} \frac{\partial x_1}{\partial \xi_i} \frac{\partial x_2}{\partial \xi_j} \frac{\partial x_3}{\partial \xi_k} = \begin{vmatrix} \frac{\partial x_1}{\partial \xi_1} & \frac{\partial x_1}{\partial \xi_2} & \frac{\partial x_1}{\partial \xi_3} \\ \frac{\partial x_2}{\partial \xi_1} & \frac{\partial x_2}{\partial \xi_2} & \frac{\partial x_2}{\partial \xi_3} \\ \frac{\partial x_3}{\partial \xi_1} & \frac{\partial x_3}{\partial \xi_2} & \frac{\partial x_3}{\partial \xi_3} \end{vmatrix} \quad (1.5.4)$$

From the relation given by Eq. (1.5.3), J is the ratio of a material volume element to its initial volume as

$$J = \frac{dV}{dV_0} \quad (1.5.5)$$

and $dV = JdV_0$. This is called the dilatation.

In consideration of the dilatation, the time derivative (the material derivative) of the volume integral $I = \int_{V(t)} F(\mathbf{x}, t) dV$ can be written (by means of the Lagrangian description)

$$\begin{aligned} \frac{DI}{Dt} &= \frac{D}{Dt} \int_{V(t)} F(\mathbf{x}, t) dV = \frac{D}{Dt} \int_{V_0} F[\mathbf{x}(\xi, t), t] J dV_0 \\ &= \int_{V_0} \left(\frac{DF}{Dt} J + F \frac{DJ}{Dt} \right) dV_0 \end{aligned} \quad (1.5.6)$$

Using the definition of the divergence in Eq. (1.1.22), we can obtain the dilatation's relative rate of change along a path line of a fluid particle as follows

$$\text{div} \mathbf{u} = \frac{1}{dV} \frac{D(dV)}{Dt} = \frac{1}{JdV_0} \frac{D(JdV_0)}{Dt} = \frac{1}{J} \frac{DJ}{Dt} \quad (1.5.7)$$

Thus, from Eqs. (1.5.6) and (1.5.7) we can obtain the following relationship

$$\frac{DI}{Dt} = \int_{V_0} \left\{ \frac{DF}{Dt} + F(\nabla \cdot \mathbf{u}) \right\} J dV_0 = \int_V \left\{ \frac{DF}{Dt} + F(\nabla \cdot \mathbf{u}) \right\} dV \quad (1.5.8)$$

The formula (1.5.8) is called the Reynolds' transport theorem, and can be further extended into a number of different forms, using the definition of the material derivative given by Eq. (1.1.7) as

$$\frac{DI}{Dt} = \int_V \left\{ \frac{\partial F}{\partial t} + \nabla \cdot (F\mathbf{u}) \right\} dV \quad (1.5.9)$$

$$= \int_V \frac{\partial F}{\partial t} dV + \int_S \hat{\mathbf{n}} \cdot F\mathbf{u} dS \quad (1.5.10)$$

It should be noted that the Gauss' divergence theorem was applied in order to write the surface integral $\int_S \sim dS$ from the volume integral $\int_V \sim dV$.

The physical picture of the Reynolds' transport theorem is that the rate of change of the integral of F in Lagrangian description is the sum of the integral of the rate of change at a point, and the net flow of F over the control volume surface in Eulerian description.

1.6 Forces on Volume Element

There are two kinds of forces acting on a volume element of a continuum medium. The volume element taken in a flow field is called the control volume in Eulerian description and equivalently called the fluid particle in Lagrangian description. In both cases, as depicted in Fig. 1.8, "Body forces" as one of the two kinds, can be regarded as reaching the medium and acting over the entire volume. Body forces, which are represented by a symbol \mathbf{g} , are due to long-range forces, such as gravitation (with the gravitational acceleration \mathbf{g}) or electromagnetic forces, etc. They are usually independent from a deformation of the volume element and are caused by an external field of source.

"Surface forces", of another kind, are to be regarded as acting upon the surface of each part of the volume element. The origins of surface forces are chiefly due to two short-range forces, viscous and elastic forces, those have strong dependence on a deformation of the volume element. The surface forces have molecular origin in the vicinity of the surface, and act on internal forces through the surface. Surface forces may also be generated by an externally applied field, such as electromagnetic field, through surface coupling. We shall see detailed descriptions of body forces and surface forces in later chapters, such as Chapter 7 and Chapter 8. However, at present we will treat the surface forces, with reference to stresses, that can be represented by a stress tensor. We follow to define a general stress tensor in a continuum medium, in this chapter, through Cauchy's fundamental theorem for stress.

Stress is a vector quantity defined as a force per unit area. Let $\Delta \mathbf{F}$ be a force exerted across an area dS , on which the unit outward normal vector $\hat{\mathbf{n}}$ is acting by the material. From Cauchy's theorem, the stress vector at the point a of ΔS located by a position vector \mathbf{x} at time t can be defined by

$$\lim_{\Delta S \rightarrow 0} \frac{\Delta \mathbf{F}}{\Delta S} = \frac{d\mathbf{F}}{dS} = \mathbf{t}_{(n)}(\mathbf{x}, t) \quad (1.6.1)$$

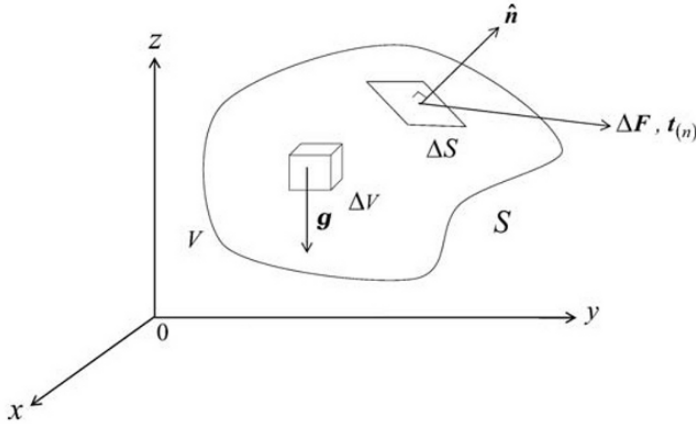


Fig. 1.8 Body and surface forces

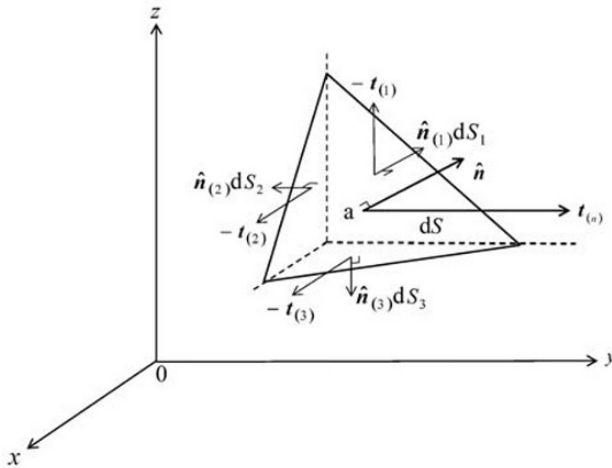


Fig. 1.9 Stresses on surface elements

In order to give an insight to the nature of the stress $\mathbf{t}_{(n)}$ at point a , we consider an elementary tetrahedron of the body as schematically displayed in Fig. 1.9, where the front surface dS has a normal unit vector of $\hat{\mathbf{n}}$. As elucidated in Fig. 1.9, the small tetrahedron has three of its faces, where the surface elements are $dS_1 = \hat{\mathbf{n}}_{(1)}dS_1$, $dS_2 = \hat{\mathbf{n}}_{(2)}dS_2$ and $dS_3 = \hat{\mathbf{n}}_{(3)}dS_3$, denoting $\hat{\mathbf{n}}_{(i)}$ the normal unit vector and dS_i the area of each element. We may further indicate the stress vectors over each of three faces, by $\mathbf{t}_{(i)}$ for 1, 2, 3 and n . Since the surface of the tetrahedron is closed, owing that four faces $i = 1, 2, 3$ and n bind the tetrahedron, we apply the principle of local equilibrium to the stress forces, subjecting to infinitesimal tetrahedron, so that

$$\mathbf{t}_{(n)}dS - (\mathbf{t}_{(1)}dS_1 + \mathbf{t}_{(2)}dS_2 + \mathbf{t}_{(3)}dS_3) = 0 \quad (1.6.2)$$

Then, in the limit of $dS_i \rightarrow 0$, we can write the components of the surface element in such a way that

$$(\hat{\mathbf{n}}_{(1)}dS_1, \hat{\mathbf{n}}_{(2)}dS_2, \hat{\mathbf{n}}_{(3)}dS_3) = (\hat{\mathbf{n}}_{(1)}, \hat{\mathbf{n}}_{(2)}, \hat{\mathbf{n}}_{(3)})dS \quad (1.6.3)$$

since $dS = dS_1 = dS_2 = dS_3$ can certainly be true. Thus Eq. (1.6.2) becomes

$$\mathbf{t}_{(n)} = \hat{\mathbf{n}} \cdot (\hat{\mathbf{n}}_{(1)}\mathbf{t}_{(1)} + \hat{\mathbf{n}}_{(2)}\mathbf{t}_{(2)} + \hat{\mathbf{n}}_{(3)}\mathbf{t}_{(3)}) \quad (1.6.4)$$

The expression in the parenthesis is a dyadic and each term in the parenthesis has three components, that is

$$\hat{\mathbf{n}}_{(1)}\mathbf{t}_{(1)} = \begin{pmatrix} T_{11} \\ T_{12} \\ T_{13} \end{pmatrix} \hat{\mathbf{e}}_1 \hat{\mathbf{e}}_j, \quad \hat{\mathbf{n}}_{(2)}\mathbf{t}_{(2)} = \begin{pmatrix} T_{21} \\ T_{22} \\ T_{23} \end{pmatrix} \hat{\mathbf{e}}_2 \hat{\mathbf{e}}_j, \quad \hat{\mathbf{n}}_{(3)}\mathbf{t}_{(3)} = \begin{pmatrix} T_{31} \\ T_{32} \\ T_{33} \end{pmatrix} \hat{\mathbf{e}}_3 \hat{\mathbf{e}}_j \quad (1.6.5)$$

where $\hat{\mathbf{n}}_{(i)}\mathbf{t}_{(i)}$ shows the vector components of $\mathbf{t}_{(i)}$ on the surface of $\hat{\mathbf{n}}_{(i)}dS_{(i)}$ facing $\hat{\mathbf{n}}_{(i)}$ direction, and so on.

Using the dyadic notation, Eq. (1.6.5) can be written as

$$\begin{aligned} \mathbf{T} &= \begin{pmatrix} T_{11} & T_{12} & T_{13} \\ T_{21} & T_{22} & T_{23} \\ T_{31} & T_{32} & T_{33} \end{pmatrix} \hat{\mathbf{e}}_i \hat{\mathbf{e}}_j \\ &= T_{ij} \hat{\mathbf{e}}_i \hat{\mathbf{e}}_j \end{aligned} \quad (1.6.6)$$

where \mathbf{T} is called the stress tensor, which has components of a second order matrix. Therefore, Eq. (1.6.4) can be written alternatively with the stress \mathbf{T} by

$$t_j = n_i T_{ij} \quad (1.6.7)$$

or

$$\mathbf{t}_{(n)} = \hat{\mathbf{n}} \cdot \mathbf{T} \quad (1.6.8)$$

The expression of Eq. (1.6.6) is called Cauchy's stress formula. It can be verified by some tensor calculus that $\hat{\mathbf{n}} \cdot \mathbf{T} = \mathbf{T}^T \cdot \hat{\mathbf{n}}$, where \mathbf{T}^T is the transpose of \mathbf{T} . It is, however, only true that when the tensor \mathbf{T} is symmetric, the relationship of $\hat{\mathbf{n}} \cdot \mathbf{T} = \mathbf{T}^T \cdot \hat{\mathbf{n}}$ can be held.

The diagonal components T_{11} , T_{22} and T_{33} of the stress tensor \mathbf{T} are called the normal stresses and the off-diagonal components T_{12} , T_{21} , T_{31} , T_{13} , T_{23} and T_{32} are called the shear stresses.

When continuum medium is at rest, implying that fluid velocity is identically zero at any given time, any stress acting upon a volume element is called hydrostatic stress, except for very specific cases in non-Newtonian fluids or electromagnetic medium, which will be introduced in the later chapters. The hydrostatic stress is a normal stress, which is independent of the orientation. The hydrostatic stress can be expressed by denoting $-p$ as

$$n_i T_{ij} = -p n_j \quad (1.6.9)$$

and this expression yields the following relationship as

$$T_{ij} = -p \delta_{ij} \quad (1.6.10)$$

or alternatively

$$\mathbf{T} = -p \mathbf{I} \quad (1.6.11)$$

where \mathbf{I} is the unit tensor. p in Eqs. (1.6.10) and (1.6.11) can be identified as the thermodynamic pressure in a compressive fluid under assumption that the fluid is in equilibrium even when the fluid is in motion. However, in incompressible limit, p can be treated as an independent dynamic variable, retaining p as a pressure. Including the hydrostatic stress, the stress tensor may be written as

$$T_{ij} = -p \delta_{ij} + \tau_{ij} \quad (1.6.12)$$

or alternatively

$$\mathbf{T} = -p\mathbf{I} + \boldsymbol{\tau} \quad (1.6.13)$$

The stress tensor $\boldsymbol{\tau}$, which is often termed as deviatoric stress tensor, may include various contributions, depending upon the physical character of the continuum medium, such as compressibility, viscoelastic nature, and external (such as electromagnetic) field effects, likewise for p mentioned above. A general expression of the total stress \mathbf{T} may be expressed by

$$T_{ij} = -p^* \delta_{ij} + \tau_{ij}^* \quad (1.6.14)$$

where p^* and τ_{ij}^* are the extended pressure and stress tensor respectively. The mean of T_{ij} is defined as

$$T_m = \frac{1}{3} T_{ii} = -p^* + \frac{1}{3} \tau_{ii}^* \quad (1.6.15)$$

and the deviatoric stress τ_{ij} is defined as

$$\tau_{ij} = T_{ij} - T_m \delta_{ij} \quad (1.6.16)$$

In viscous, incompressible Newtonian fluid, i.e. $\tau_{ii}^* = 0$ and $p^* = p$, the mean stress is equal to the pressure p as

$$T_m = -p \quad (1.6.17)$$

This fluid is sometimes called the perfect fluid.

Exercise

Exercise 1.1 Dyadic Product $\nabla \mathbf{u}$

$\nabla \mathbf{u}$ is called the gradient of vector \mathbf{u} and is sometimes written $\partial \mathbf{u} / \partial \mathbf{x}$ or $\text{grad } \mathbf{u}$. $\nabla \mathbf{u}$ is the second order tensor in the Cartesian coordinates system. Show $\nabla \mathbf{u}$ as the dyadic product, using suffix notation of tensor with unit dyads $\hat{\mathbf{e}}_i \hat{\mathbf{e}}_j$.

Ans.

$$\nabla \mathbf{u} = \left(\hat{\mathbf{e}}_i \frac{\partial}{\partial x_i} \right) (\hat{\mathbf{e}}_j u_j) = \hat{\mathbf{e}}_i \hat{\mathbf{e}}_j \frac{\partial u_j}{\partial x_i} \quad (1)$$

Equation (1) shows that $\nabla \mathbf{u}$ is a second order tensor whose ij components are $\partial u_j / \partial u_i$.

Exercise 1.2 Convective Term

In Eq. (1.1.7), the term $(\mathbf{u} \cdot \nabla) \mathbf{u} = \mathbf{u} \cdot \nabla \mathbf{u}$ is called the convective term in fluid mechanics. Using the vector identities in Appendix B-5 (B.5-6), reduce Eq. (1.1.9).

$$\nabla(\mathbf{u} \cdot \mathbf{v}) = \mathbf{u} \cdot \nabla \mathbf{v} + \mathbf{v} \cdot \nabla \mathbf{u} + \mathbf{u} \times (\nabla \times \mathbf{v}) + \mathbf{v} \times (\nabla \times \mathbf{u}) \quad (1)$$

Ans.

Set $\mathbf{v} = \mathbf{u}$, which gives

$$\mathbf{u} \cdot \nabla \mathbf{u} = \frac{1}{2} \nabla |\mathbf{u}|^2 - \mathbf{u} \times (\nabla \times \mathbf{u}) \quad (2)$$

When the vorticity vector $\boldsymbol{\omega} = \nabla \times \mathbf{u}$, Eq. (2) becomes

$$\mathbf{u} \cdot \nabla \mathbf{u} = \nabla \left(\frac{1}{2} |\mathbf{u}|^2 \right) - \mathbf{u} \times \boldsymbol{\omega} \quad (3)$$

If the velocity field \mathbf{u} is irrotational, i.e. $\boldsymbol{\omega} = \nabla \times \mathbf{u} = 0$, \mathbf{u} has a scalar potential ϕ such that

$$\mathbf{u} = -\nabla \phi \quad (4)$$

and with the scalar potential the convective term will be written

$$\mathbf{u} \cdot \nabla \mathbf{u} = \nabla \left(\frac{1}{2} |\nabla \phi|^2 \right) \quad (5)$$

Exercise 1.3 Euler's Relation

Proof the Euler Relation given by Eq. (1.1.22)

$$\frac{DJ}{Dt} = J \nabla \cdot \mathbf{u} \quad (1)$$

where

$$J = \varepsilon_{ijk} \frac{\partial x_1}{\partial \zeta_i} \frac{\partial x_2}{\partial \zeta_j} \frac{\partial x_3}{\partial \zeta_k} = \begin{vmatrix} \frac{\partial x_1}{\partial \zeta_1} & \frac{\partial x_1}{\partial \zeta_2} & \frac{\partial x_1}{\partial \zeta_3} \\ \frac{\partial x_2}{\partial \zeta_1} & \frac{\partial x_2}{\partial \zeta_2} & \frac{\partial x_2}{\partial \zeta_3} \\ \frac{\partial x_3}{\partial \zeta_1} & \frac{\partial x_3}{\partial \zeta_2} & \frac{\partial x_3}{\partial \zeta_3} \end{vmatrix} \quad (2)$$

Ans.

We firstly write the following relation, for the velocity gradient

$$\frac{D}{Dt} \frac{\partial x_i}{\partial \zeta_j} = \frac{\partial}{\partial \zeta_j} \frac{Dx_i}{Dt} = \frac{\partial u_i}{\partial \zeta_j} \quad (3)$$

With this relation, we are able to set an expression of the time change of the Jacobian as follows

$$\frac{DJ}{Dt} = \varepsilon_{ijk} \frac{\partial u_1}{\partial \zeta_i} \frac{\partial x_2}{\partial \zeta_j} \frac{\partial x_3}{\partial \zeta_k} + \varepsilon_{ijk} \frac{\partial x_1}{\partial \zeta_i} \frac{\partial u_2}{\partial \zeta_j} \frac{\partial x_3}{\partial \zeta_k} + \varepsilon_{ijk} \frac{\partial x_1}{\partial \zeta_i} \frac{\partial x_2}{\partial \zeta_j} \frac{\partial u_3}{\partial \zeta_k} \quad (4)$$

While Eq. (3) may be formulated by chain rule

$$\frac{\partial u_i}{\partial \zeta_j} = \frac{\partial x_k}{\partial \zeta_j} \frac{\partial u_i}{\partial x_k} = \frac{\partial u_i}{\partial x_1} \frac{\partial x_1}{\partial \zeta_j} + \frac{\partial u_i}{\partial x_2} \frac{\partial x_2}{\partial \zeta_j} + \frac{\partial u_i}{\partial x_3} \frac{\partial x_3}{\partial \zeta_j} \quad (5)$$

Thus, finally Eq. (4) can be reduced to give the required form

$$\begin{aligned} \frac{DJ}{Dt} &= \varepsilon_{ijk} \frac{\partial u_1}{\partial x_1} \frac{\partial x_1}{\partial \zeta_i} \frac{\partial x_2}{\partial \zeta_j} \frac{\partial x_3}{\partial \zeta_k} + \varepsilon_{ijk} \frac{\partial x_1}{\partial \zeta_i} \frac{\partial u_2}{\partial x_1} \frac{\partial x_2}{\partial \zeta_j} \frac{\partial x_3}{\partial \zeta_k} + \varepsilon_{ijk} \frac{\partial x_1}{\partial \zeta_i} \frac{\partial x_2}{\partial \zeta_j} \frac{\partial u_3}{\partial x_1} \frac{\partial x_3}{\partial \zeta_k} \\ &= \varepsilon_{ijk} \frac{\partial u_1}{\partial x_1} \frac{\partial x_1}{\partial \zeta_i} \frac{\partial x_2}{\partial \zeta_j} \frac{\partial x_3}{\partial \zeta_k} + \varepsilon_{ijk} \frac{\partial u_1}{\partial x_2} \frac{\partial x_2}{\partial \zeta_i} \frac{\partial x_2}{\partial \zeta_j} \frac{\partial x_3}{\partial \zeta_k} + \varepsilon_{ijk} \frac{\partial u_1}{\partial x_3} \frac{\partial x_3}{\partial \zeta_i} \frac{\partial x_2}{\partial \zeta_j} \frac{\partial x_3}{\partial \zeta_k} \\ &\quad + \varepsilon_{ijk} \frac{\partial u_2}{\partial x_1} \frac{\partial x_1}{\partial \zeta_i} \frac{\partial x_2}{\partial \zeta_j} \frac{\partial x_3}{\partial \zeta_k} + \varepsilon_{ijk} \frac{\partial u_2}{\partial x_2} \frac{\partial x_1}{\partial \zeta_i} \frac{\partial x_2}{\partial \zeta_j} \frac{\partial x_3}{\partial \zeta_k} + \varepsilon_{ijk} \frac{\partial u_2}{\partial x_3} \frac{\partial x_3}{\partial \zeta_i} \frac{\partial x_2}{\partial \zeta_j} \frac{\partial x_3}{\partial \zeta_k} \\ &\quad + \varepsilon_{ijk} \frac{\partial u_3}{\partial x_1} \frac{\partial x_1}{\partial \zeta_i} \frac{\partial x_2}{\partial \zeta_j} \frac{\partial x_3}{\partial \zeta_k} + \varepsilon_{ijk} \frac{\partial u_3}{\partial x_2} \frac{\partial x_1}{\partial \zeta_i} \frac{\partial x_2}{\partial \zeta_j} \frac{\partial x_3}{\partial \zeta_k} + \varepsilon_{ijk} \frac{\partial u_3}{\partial x_3} \frac{\partial x_3}{\partial \zeta_i} \frac{\partial x_2}{\partial \zeta_j} \frac{\partial x_3}{\partial \zeta_k} \\ &= J \frac{\partial u_1}{\partial x_1} + J \frac{\partial u_2}{\partial x_2} + J \frac{\partial u_3}{\partial x_3} \\ &= J \nabla \cdot \mathbf{u} \end{aligned} \quad (6)$$

Exercise 1.4 Pseudovector

If $\boldsymbol{\omega}$ is a pseudovector of a second order tensor \mathbf{S} , examine the nature of $\boldsymbol{\omega}$ in consideration of Eq. (1.1.28).

$$\boldsymbol{\omega} = -\boldsymbol{\varepsilon} \cdot \mathbf{S} \quad (1)$$

Ans.

Decompose \mathbf{S} into the symmetric part and skew-symmetric part as

$$\begin{aligned} \mathbf{S} &= \frac{1}{2}(\mathbf{S} + \mathbf{S}^T) + \frac{1}{2}(\mathbf{S} - \mathbf{S}^T) \\ &= \mathbf{S}_s + \mathbf{S}_a \end{aligned} \quad (2)$$

where the skew-symmetric part is written by components

$$\begin{aligned} \mathbf{S}_a &= \frac{1}{2} \begin{bmatrix} 0 & s_{12} - s_{21} & s_{13} - s_{31} \\ s_{21} - s_{12} & 0 & s_{23} - s_{32} \\ s_{31} - s_{13} & s_{32} - s_{23} & 0 \end{bmatrix} \\ &= \frac{1}{2} \begin{bmatrix} 0 & \omega_3 & -\omega_2 \\ -\omega_3 & 0 & \omega_1 \\ \omega_2 & -\omega_1 & 0 \end{bmatrix} \end{aligned} \quad (3)$$

Namely vector $\boldsymbol{\omega}$ is expressed with components ω_1 , ω_2 and ω_3 as

$$\boldsymbol{\omega} = \hat{\mathbf{e}}_1 \omega_1 + \hat{\mathbf{e}}_2 \omega_2 + \hat{\mathbf{e}}_3 \omega_3 \quad (4)$$

where $\boldsymbol{\omega}$ is obtained by $-\boldsymbol{\varepsilon} \cdot \mathbf{S}$ (see Eq. (1.1.26) for example), this implies that components of the skew-symmetric part of the second order tensor are composed of components of the pseudovector. If \mathbf{S} is assumed to be a velocity gradient $\nabla \mathbf{u}$, the vorticity vector $\boldsymbol{\omega}$ is derived from components of the spin tensor, which is the skew-symmetric part of the tensor $\nabla \mathbf{u}$.

Exercise 1.5 Material Objectivity

The upper convective Maxwell model constitutive equation (a linear viscoelastic model, in Chapter 7) can be written by

$$\boldsymbol{\tau} + \lambda \overset{\nabla}{\boldsymbol{\tau}} = 2\eta_0 \mathbf{e} \quad (1)$$

where $\boldsymbol{\tau}$ is a second order tensor, λ and η_0 are constant and \mathbf{e} is the rate of deformation tensor (see Eq. (1.1.16)). Show that Eq. (1) satisfy the material objectivity.

Ans.

The material objectivity has to be met by the linear transformation for tensor \mathbf{A} as follows

$$\mathbf{A} = \mathbf{Q}(t) \cdot \mathbf{A}' \cdot \mathbf{Q}(t)^T \quad (2)$$

where $\mathbf{Q}(t)$ is a rotation tensor, defined in Eq. (1.2.1). Therefore, the constitutive Equation of Eq. (1) has to be invariant by the transformation of Eq. (2), that is

$$\boldsymbol{\tau}' + \lambda \overset{\nabla}{\boldsymbol{\tau}'} = 2\eta_0 \mathbf{e}' \quad (3)$$

where

$$\boldsymbol{\tau}' = \mathbf{Q} \cdot \boldsymbol{\tau} \cdot \mathbf{Q}^T \quad (4)$$

$$\overset{\nabla}{\boldsymbol{\tau}'} = \mathbf{Q} \cdot \overset{\nabla}{\boldsymbol{\tau}} \cdot \mathbf{Q}^T \quad (5)$$

and

$$\mathbf{e}' = \mathbf{Q} \cdot \mathbf{e} \cdot \mathbf{Q}^T \quad (6)$$

knowing that scalar constants are frame invariants.

In order to verify the invariance of Eq. (1), take the transformation to the model equation

$$\mathbf{Q} \cdot \left(\boldsymbol{\tau} + \lambda \overset{\nabla}{\boldsymbol{\tau}} = 2\eta_0 \mathbf{e} \right) \cdot \mathbf{Q}^T \quad (7)$$

Since Eq. (7) is linear, we can write

$$(\mathbf{Q} \cdot \boldsymbol{\tau} \cdot \mathbf{Q}^T) + \lambda \left(\mathbf{Q} \cdot \overset{\nabla}{\boldsymbol{\tau}} \cdot \mathbf{Q}^T \right) = 2\eta_0 (\mathbf{Q} \cdot \mathbf{e} \cdot \mathbf{Q}^T) \quad (8)$$

Thus we can recover the given equation by knowing Eqs. (4), (5) and (6)

$$\boldsymbol{\tau}' + \lambda \overset{\nabla}{\boldsymbol{\tau}'} = 2\eta_0 \mathbf{e}' \quad (9)$$

In deriving Eq. (9), we used the principal of frame invariance (the material objectivity) for the upper convective derivative given in Eq. (1.3.16).

Exercise 1.6 Reynolds' Transport Theorem

Give a physical picture of the Reynolds' transport theorem, considering the rate of change of a certain quantity F of matter moving through a control volume, as depicted in Fig. 1.10,

Ans.

Consider a control volume of region **A**, which contains a quantity of matter at some time t , indicated by the solid line. At some time later time $t + \Delta t$, the boundary of the system has a new physical location as shown by the dotted line, at which the control volume occupies regions **B** and **A** minus **C**. The increment of the matter is written

$$\Delta m = \{m_A(t + \Delta t) - m_C(t + \Delta t) + m_B(t + \Delta t)\} - m_A(t) \quad (1)$$

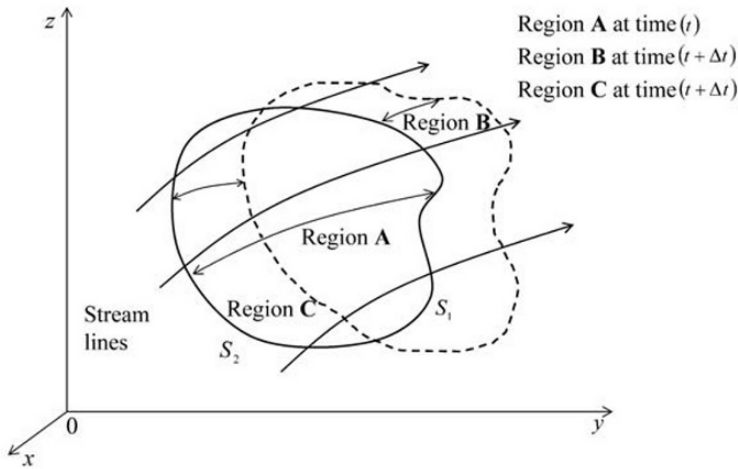


Fig. 1.10 System of moving control volume and fixed control volume

Taking differentiation to Eq. (1) with respect to time Δt and after rearrangement, we can write

$$\frac{\Delta m}{\Delta t} = \frac{m_A(t + \Delta t) - m_A(t)}{\Delta t} + \frac{m_B(t + \Delta t) - m_C(t + \Delta t)}{\Delta t} \quad (2)$$

The rate of change of m is calculated by taking the limit of Eq. (2) as $\Delta t \rightarrow 0$. The first term on the right hand side of Eq. (2) thus becomes

$$\lim_{\Delta t \rightarrow 0} \frac{m_A(t + \Delta t) - m_A(t)}{\Delta t} = \frac{\partial}{\partial t} m_A = \dot{m}_A = \frac{\partial}{\partial t} \int_V F dV \quad (3)$$

Since region A is fixed in the coordinates, we can write

$$\frac{\partial}{\partial t} \int_V F dV = \int_V \frac{\partial F}{\partial t} dV \quad (4)$$

In a similar manner as the second term becomes

$$\lim_{\Delta t \rightarrow 0} \frac{m_B(t + \Delta t) - m_C(t + \Delta t)}{\Delta t} = \dot{m}_B - \dot{m}_C \quad (5)$$

where \dot{m}_B is the rate of change of m through surface area S_1 from control volume (region A), and which is expressed by surface integral

$$\dot{m}_B = \int_{S_1} F \mathbf{u} \cdot d\mathbf{S} \quad (6)$$

where $F\mathbf{u}$ is the flux of F (F is transported through the surface of the control volume by stream of flow with velocity \mathbf{u}).

Similarly \dot{m}_C is expressed

$$\dot{m}_C = - \int_{S_2} F \mathbf{u} \cdot d\mathbf{S} \quad (7)$$

where the minus sign means the inward to the surface of the control volume. With Eqs. (6) and (7), Equation (5) becomes

$$\dot{m}_B - \dot{m}_C = \int_S F \mathbf{u} \cdot d\mathbf{S} \quad (8)$$

Therefore, the rate of change of m is altogether written

$$\lim_{\Delta t \rightarrow 0} \frac{\Delta m}{\Delta t} = \frac{D}{Dt} \int_V F dV = \int_V \frac{\partial F}{\partial t} dV + \int_S F \mathbf{u} \cdot d\mathbf{S} \quad (9)$$

This is a Lagrangian-to-Eulerian description of the rate of change of an extensive integral quantity given by Eq. (1.5.10).

Exercise 1.7 Principal Axes of Stress

The pressure p defined in Eq. (1.6.17) is the mean of the normal stresses, that is, one third of the trace of the total stress tensor \mathbf{T} . It appears that p is meant to be the mean of the principal stresses. Give the definition of the principal stresses and its direction of the principal axis.

Ans.

When the direction of a stress vector $\mathbf{t}_{(n)}$ is equal to that of an unit normal vector $\hat{\mathbf{n}}$, if $\mathbf{t}_{(n)}$ is derived from a stress tensor \mathbf{T} by Cauchy's stress formula, the direction of $\hat{\mathbf{n}}$ is called the direction of the principal axes of stress and the stresses are the principal stresses.

Thus, in case of $\hat{\mathbf{n}}$ being parallel with the principal axes, we can write

$$\mathbf{t}_{(n)} = \hat{\mathbf{n}} \cdot \mathbf{T} = \lambda \hat{\mathbf{n}} \quad (1)$$

where λ is a scalar quantity. Equation (1) gives a relationship written as

$$\hat{\mathbf{n}} \cdot (\mathbf{T} - \lambda \mathbf{I}) = 0 \quad (2)$$

and Eq. (2) has to satisfy

$$|\mathbf{T} - \lambda \mathbf{I}| = 0 \quad (3)$$

for the condition of $\hat{\mathbf{n}} \neq 0$. Equation (3) is called the characteristic equation of stress tensor \mathbf{T} . Roots of Eq. (3) give eigenvalues, which are the principal stresses for the principal axes.

The perfect fluid given by Eq. (1.6.17) is an isotropic fluid in a sense that a simple direct stress acting in it does not produce a shearing deformation. In the functional relation between stress and deformation must be independent of the orientation of the coordinates system.

The component form of Eq. (3) is written by

$$\begin{vmatrix} T_{11} - \lambda & T_{12} & T_{13} \\ T_{21} & T_{22} - \lambda & T_{23} \\ T_{31} & T_{32} & T_{33} - \lambda \end{vmatrix} = 0 \quad (4)$$

with which we have a third order polynomial equation for λ as follows

$$\lambda^3 - I_1 \lambda^2 + I_2 \lambda - I_3 = 0 \quad (5)$$

Since λ is independent of choice of the coordinates system, the coefficients of I_1, I_2 and I_3 in Eq. (5) are also independent of the choice of the coordinates. Therefore, I_1, I_2 and I_3 are frame invariants. Equation (5) is also true for other tensors such as the rate of deformation tensor, which is discussed in more detail in Chapter 7, I_1, I_2 and I_3 are respectively given by

$$I_1 = t_r \mathbf{T} \quad (6)$$

$$I_2 = \frac{1}{2} \left[(t_r \mathbf{T})^2 - \mathbf{T} : \mathbf{T} \right] = \frac{1}{2} \left[(t_r \mathbf{T})^2 - t_r (\mathbf{T}^2) \right] \quad (7)$$

if \mathbf{T} is symmetric, i.e. $t_r (\mathbf{T}^2) = \mathbf{T} : \mathbf{T}$,
and

$$I_3 = \det \mathbf{T} \quad (8)$$

Note that if σ_1, σ_2 and σ_3 are the principal stresses, I_1, I_2 and I_3 are respectively given by

$$I_1 = \sigma_{ii} = \sum_m^3 \sigma_m = \sigma_1 + \sigma_2 + \sigma_3 \quad (9)$$

$$I_2 = \frac{1}{2} (\sigma_{ii} \sigma_{jj} - \sigma_{ij} \sigma_{ji}) = (\sigma_1 \sigma_2 + \sigma_2 \sigma_3 + \sigma_3 \sigma_1) \quad (10)$$

and

$$I_3 = \det \sigma_{ij} = \sigma_1 \sigma_2 \sigma_3 \quad (11)$$

Problems

1-1. Show that $\dot{\mathbf{Q}} \cdot \mathbf{Q}^T$ is a skew-symmetric tensor, and whose pseudovector is Ω .

$$\text{Ans.} \left[\begin{array}{l} \mathbf{Q} \cdot \mathbf{Q}^T = \mathbf{I}, \dot{\mathbf{Q}} \cdot \mathbf{Q}^T + \mathbf{Q} \cdot \dot{\mathbf{Q}}^T = 0 \\ \text{so that } \dot{\mathbf{Q}} \cdot \mathbf{Q}^T = -\mathbf{Q} \cdot \dot{\mathbf{Q}}^T = -(\dot{\mathbf{Q}} \cdot \mathbf{Q}^T)^T \\ \mathbf{r}(t) = \mathbf{Q}(t) \cdot \mathbf{r}_0 \quad (\text{rigid rotation } \Omega \text{ for fixed } \mathbf{r}_0) \\ \dot{\mathbf{r}} = \dot{\mathbf{Q}} \cdot \mathbf{r}_0 = \dot{\mathbf{Q}} \cdot \mathbf{Q}^{-1} \cdot \mathbf{r} = (\dot{\mathbf{Q}} \cdot \mathbf{Q}^T) \cdot \mathbf{r} = \Omega \times \mathbf{r} \\ \text{where } \dot{\mathbf{r}} = \mathbf{u} = \Omega \times \mathbf{r} \end{array} \right]$$

- 1-2. If \mathbf{Q} is a rotation tensor, show that \mathbf{Q} is a unitary matrix, which satisfies $\mathbf{Q}^T = \mathbf{Q}^{-1}$. Consider the two dimensional axis rotation by θ where the frame is transferred $x' - y'$ to $x - y$.

$$\text{Ans.} \left[\begin{array}{l} \begin{pmatrix} x \\ y \end{pmatrix} = \begin{pmatrix} \cos \theta & \sin \theta \\ -\sin \theta & \cos \theta \end{pmatrix} \begin{pmatrix} x' \\ y' \end{pmatrix} \\ \mathbf{x} = \mathbf{Q} \cdot \mathbf{x}' \\ \therefore \mathbf{Q}^T = \mathbf{Q}^{-1} \end{array} \right]$$

- 1-3. Proof for Cartesian vectors \mathbf{u} and \mathbf{v} , that

$$\nabla \times (\mathbf{u} \times \mathbf{v}) = \mathbf{v} \cdot \nabla \mathbf{u} - \mathbf{u} \cdot \nabla \mathbf{v} + \mathbf{u}(\nabla \cdot \mathbf{v}) - \mathbf{v}(\nabla \cdot \mathbf{u})$$

$$\text{Ans.} \left[\begin{array}{l} \varepsilon_{ijk} \frac{\partial}{\partial x_j} (\varepsilon_{klm} u_l v_m) = \varepsilon_{ijk} \varepsilon_{klm} \frac{\partial}{\partial x_j} (u_l v_m) = \varepsilon_{kij} \varepsilon_{klm} \frac{\partial}{\partial x_j} (u_l v_m) \\ = (\delta_{il} \delta_{jm} - \delta_{im} \delta_{jl}) \left\{ \left(\frac{\partial}{\partial x_j} u_l \right) v_m + u_l \frac{\partial}{\partial x_j} v_m \right\} \\ = \left(\frac{\partial}{\partial x_j} u_i \right) v_j + u_i \frac{\partial}{\partial x_j} v_j - \left(\frac{\partial}{\partial x_j} u_j \right) v_i - u_j \frac{\partial}{\partial x_j} v_i \\ = \left(v_i \frac{\partial}{\partial x_j} \right) u_j - \left(u_j \frac{\partial}{\partial x_j} \right) v_i + u_i \left(\frac{\partial}{\partial x_j} v_j \right) - v_i \left(\frac{\partial}{\partial x_j} u_j \right) \end{array} \right]$$

- 1-4. When a scalar function $p(\mathbf{x}, t)$ differs from a material surface, but $p(\mathbf{x}, t)$ moves with a velocity \mathbf{v} different from the stream velocity \mathbf{u} , show that

$$(\mathbf{u} - \mathbf{v}) \cdot \hat{\mathbf{n}} = \frac{\left(\frac{dp}{dt} \right)}{|\nabla p|}$$

$$\text{Ans.} \left[\begin{array}{l} \text{If } p(\mathbf{x}, t) \text{ is the material surface,} \\ \frac{dp}{dt} = \frac{\partial p}{\partial t} + \mathbf{w} \cdot \nabla p, \\ \text{but move with relative velocity } \mathbf{w} = \mathbf{u} - \mathbf{v}, \\ \text{and not with material point } \frac{\partial p}{\partial t} = 0 \\ \frac{dp}{dt} = (\mathbf{u} - \mathbf{v}) \cdot \nabla p = (\mathbf{u} - \mathbf{v}) \cdot \hat{\mathbf{n}} |\nabla p| \end{array} \right]$$

1-5. Verify that the Finger tensor defined in Eq. (1.4.4), i.e. $\mathbf{C}^{-1} = \mathbf{E}^{-1} \cdot \mathbf{E}^{-1T}$ is symmetric. Consider \mathbf{E}^{-1} in the Cartesian coordinates system.

$$Ans. \left[\begin{array}{l} \mathbf{C}^{-1} = \mathbf{E}^{-1} \cdot \mathbf{E}^{-1T} \\ \mathbf{E}^{-1} = \frac{\partial x_i}{\partial X_j} = \begin{pmatrix} \frac{\partial x_1}{\partial X_1} & \frac{\partial x_1}{\partial X_2} & \frac{\partial x_1}{\partial X_3} \\ \frac{\partial x_2}{\partial X_1} & \frac{\partial x_2}{\partial X_2} & \frac{\partial x_2}{\partial X_3} \\ \frac{\partial x_3}{\partial X_1} & \frac{\partial x_3}{\partial X_2} & \frac{\partial x_3}{\partial X_3} \end{pmatrix}, \quad \mathbf{E}^{-1T} = \frac{\partial x_j}{\partial X_i} = \begin{pmatrix} \frac{\partial x_1}{\partial X_1} & \frac{\partial x_2}{\partial X_1} & \frac{\partial x_3}{\partial X_1} \\ \frac{\partial x_1}{\partial X_2} & \frac{\partial x_2}{\partial X_2} & \frac{\partial x_3}{\partial X_2} \\ \frac{\partial x_1}{\partial X_3} & \frac{\partial x_2}{\partial X_3} & \frac{\partial x_3}{\partial X_3} \end{pmatrix} \\ C_{ij}^{-1} = E_{ik}^{-1} E_{kj}^{-1T} = \frac{\partial x_i}{\partial X_k} \frac{\partial x_j}{\partial X_k} \end{array} \right]$$

1-6. Obtain components T_{xx} , T_{xy} and T_{xz} of tensor \mathbf{T} .

$$Ans. \left[\begin{array}{l} T_{xx} = \mathbf{i} \cdot \mathbf{T} \cdot \mathbf{i} \\ T_{xy} = \mathbf{i} \cdot \mathbf{T} \cdot \mathbf{j} \\ T_{xz} = \mathbf{i} \cdot \mathbf{T} \cdot \mathbf{k} \end{array} \right]$$

1-7. Show that the velocity gradient tensor $\nabla \mathbf{u}$ does not satisfy the principle of frame invariance.

$$Ans. \left[\begin{array}{l} \mathbf{x}_r = \mathbf{Q} \cdot \mathbf{x}_0 \left(\mathbf{x}_0 = \mathbf{Q}^T \cdot \mathbf{x}_r, \text{ and } \frac{\partial \mathbf{x}_0}{\partial \mathbf{x}_r} = \mathbf{Q}^T \right) \\ \mathbf{u}_r = \mathbf{Q} \cdot \mathbf{u}_0 + \dot{\mathbf{Q}} \cdot \mathbf{x}_0 \\ \nabla \mathbf{u}_r = \mathbf{Q} \cdot \frac{\partial \mathbf{u}_0}{\partial \mathbf{x}_0} \cdot \frac{\partial \mathbf{x}_0}{\partial \mathbf{x}_r} + \dot{\mathbf{Q}} \cdot \frac{\partial \mathbf{x}_0}{\partial \mathbf{x}_r} \\ = \mathbf{Q} \cdot \nabla \mathbf{u}_0 \cdot \mathbf{Q}^T + \dot{\mathbf{Q}} \cdot \mathbf{Q}^T \\ = \mathbf{Q} \cdot \nabla \mathbf{u}_0 \cdot \mathbf{Q}^T + \Omega \\ \nabla \mathbf{u}^* = \mathbf{Q} \cdot \nabla \mathbf{u} \cdot \mathbf{Q}^T + \Omega \text{ is not linear transformation of } \mathbf{Q}. \end{array} \right]$$

Nomenclature

- A : material parameter
- \mathbf{a} : acceleration
- \mathbf{C} : Cauchy strain tensor
- \mathbf{C}^{-1} : Finger tensor
- \mathbf{E} : displacement gradient tensor
- \mathbf{e} : rate of strain tensor
- $\hat{\mathbf{e}}_i$: unit base vector $(\mathbf{i}, \mathbf{j}, \mathbf{k})$

$\hat{\mathbf{e}}_i \hat{\mathbf{e}}_j$: unit dyad
\mathbf{F}	: force
\mathbf{g}	: body force
\mathbf{g}	: gravitation acceleration
\mathbf{I}	: unit tensor
J	: Jacobian
\mathbf{L}	: material line element
L_i	: Intermediate scale
L_l	: large scale
L_m	: molecular scale
$\hat{\mathbf{n}}$: unit normal vector
p	: pressure
\mathbf{Q}	: rotation tensor
\mathbf{S}	: general second order tensor
S	: surface area
\mathbf{T}	: total stress tensor
$\mathbf{t}_{(n)}$: stress vector
t	: time
\mathbf{u}	: velocity
\mathbf{x}	: position vector in vector space
Γ	: Knudsen number
δ_{ij}	: Kronecker delta
ε	: (polyadic) alternator
ε_{ijk}	: Eddington notation
λ	: eigenvalue
ϕ	: scalar potential
Ω	: angular velocity
ω	: spin tensor
ω	: vorticity vector

Bibliography

The content in this chapter is standard matter and treated in almost all texts. The mathematical methods in accounting Cartesian vectors and tensors are found in

1. A. Rutherford, *Vectors, Tensors, and the Basic Equations of Fluid Mechanics*, Prentice-Hall, Inc., Englewood Cliffs, NJ, 1962.

2. F. B. Hildebrand, *Advanced Calculus for Applications* (2nd Edition), Prentice-Hall, Inc., Englewood Cliffs, NJ, 1976.
3. R. B. Bird, C. F. Curtiss, R. C. Armstrong and O. Hassanger, *Dynamics of Polymeric Liquids* (2nd Edition), John Wiley & Sons, A Wiley-Interscience Publication, New York, Vol. 1 and Vol. 2, 1987. Appendices are useful.
4. G. B. Arfken and H. J. Weber, *Mathematical Methods for Physicists* (6th Edition), Elsevier, Academic Press, Amsterdam, 2005.

Some interesting topics on microhydrodynamics are found in

5. S. Kim and S. J. Karrila, *Microhydrodynamics, Principles and Selected Applications*, Butterworth-Heinemann, a division of Reed Publishing (U.S.A.) Inc., Oxford, London, 1991.
6. P. Tabeling, *Introduction to Microfluidics*, Oxford University Press Inc., New York, 2005.

2. Conservation Equations in Continuum Mechanics

Sir Isaac Newton was the first to correctly state the basic laws governing the motion of a particle and to demonstrate their validity. The dynamics of continuum uses the concept of a particle, called the fluid particle, which follows Newton's second law of motion. In continuum mechanics, they are written in the form of conservation equations. In this chapter, the basic forms of conservation laws are introduced to mass, linear momentum, angular momentum and energy. One of which is Cauchy's equation, which is equivalent to Newton's second law of motion. These conservation equations are unconstituted; however, later chapters looking at specific types of fluid flow will consider constituted equations as well.

2.1 Mass Conservation

Let us begin to consider the flow system of a continuum medium, which consists of fluid particles. A fluid particle, that moves with a velocity \mathbf{u} and has the density $\rho(\mathbf{x}, t)$ at position $\mathbf{x} = \mathbf{x}(\mathbf{x}_0, t)$, is a representative object of the medium, having the mass of finite volume V . The mass of the fluid particle can be obtained, see Fig. 2.1, using volume integral by

$$m = \int_V \rho dV \quad (2.1.1)$$

If we postulate that there are no sources or sinks in the medium, the mass of the fluid particle does not change in position and time, i.e. the mass is conserved in space and time as follows

$$\frac{Dm}{Dt} = \frac{D}{Dt} \int_V \rho dV = 0 \quad (2.1.2)$$

By setting F as $F = \rho$ in the Reynolds' transport theorem given by Eq. (1.5.8), we have

$$\int_V \left[\frac{D\rho}{Dt} + \rho(\nabla \cdot \mathbf{u}) \right] dV = 0 \quad (2.1.3)$$

Since the volume of the fluid particle is arbitrary, the volume integral in Eq. (2.1.3) can be made to vanish in an identical manner from the fluid system of the continuum, which gives

$$\frac{D\rho}{Dt} + \rho(\nabla \cdot \mathbf{u}) = 0 \quad (2.1.4)$$

Equation (2.1.4) can be further expanded, using the definition of the material derivative of Eq. (1.1.7) to give

$$\frac{\partial \rho}{\partial t} + \nabla \cdot \rho \mathbf{u} = 0 \quad (2.1.5)$$

Equations (2.1.4) and (2.1.5) are both called the equation of continuity (or the continuity equation). Considering the nature of derivation and for the sake of distinguishing between the two, Eq. (2.1.4) is often called the non-conservation form of the continuity equation, and Eq. (2.1.5) is called the conservation form of the continuity equation. $\rho \mathbf{u}$ in Eq. (2.1.5) is identified as the mass flux.

If the medium of continuum is incompressible, the density ρ of each material point \mathbf{x} is kept constant with respect to time t . This will lead Eq. (2.1.4) to a form, setting $D\rho/Dt = 0$, as follows

$$\nabla \cdot \mathbf{u} = 0 \quad (2.1.6)$$

The flow field described by Eq. (2.1.6) is called the solenoidal velocity field. When, in fact, the flow of a medium is incompressible, the flow is an isotropic flow, in which pressure change does not affect its density.

2.2 Linear Momentum Conservation

Studying the dynamics of flow in a continuous medium requires the forces acting on a fluid particle and the acceleration of the fluid particle to be in an inertial frame of reference. The law that governs the dynamic motion of continuum medium is given by the conservation of linear momentum. Note that “linear” is understood as the motion of a particle in the direction of the acceleration, and is used in order to distinguish it from the “angular” momentum. Below we have shown two kinds of forces seen when in dealing with the motion of a continuum medium. As previously

described in Section 1.6, they are surface forces, representatively written as $\mathbf{t}_{(n)}dS$ for a surface element $\mathbf{n}dS$, and body forces, similarly expressed $\rho\mathbf{g}dV$ for a volume element dV . The linear momentum at a position of $\mathbf{x} = \mathbf{x}(x_0, t)$ can be written $\rho\mathbf{u}dV$ for a volume element inside the finite volume of the fluid particle.

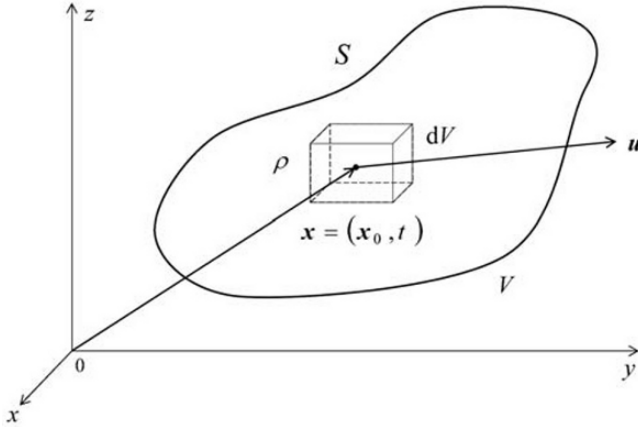


Fig. 2.1 A fluid particle moving with velocity \mathbf{u}

The volume element, the density of which is ρ , is in motion with a velocity of \mathbf{u} , as shown in Fig. 2.2. The conservation of the linear momentum of the fluid particle can be written

$$\frac{D}{Dt} \int_V \rho \mathbf{u} dV = \int_S \mathbf{t}_{(n)} dS + \int_V \rho \mathbf{g} dV \quad (2.2.1)$$

where the left hand side of Eq. (2.2.1) represents the change of linear momentum, and the first term of the right hand side of Eq. (2.2.1) corresponds to the net surface force and the second term signifies the net body force acting on the fluid particle. This is an integral form of the equation of motion, derived from the principle of the conservation of linear momentum. The equation of (2.2.1) can be changed by considering Cauchy's stress formula given by Eq. (1.6.8) and can be reduced into the volume integral form, using Gauss' divergence theorem. After applying Reynolds' transport theorem from Eq. (1.5.8) to the change of linear momentum, specifically setting $\mathbf{F} = \rho\mathbf{u}$ in Eq. (2.2.1), we can obtain the conservation of linear momentum in volume integral form

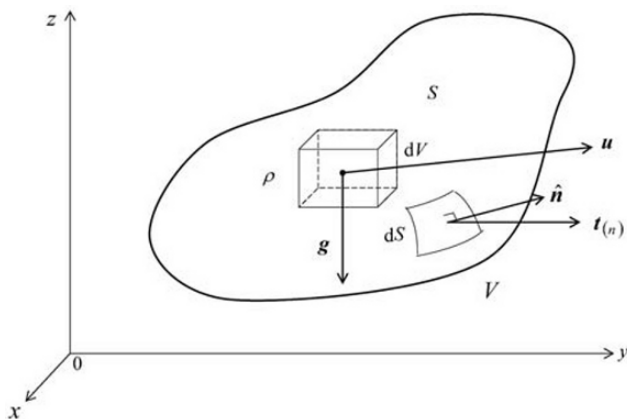


Fig. 2.2 Force acting on a fluid

$$\int_V \left\{ \frac{D(\rho \mathbf{u})}{Dt} + \rho \mathbf{u} (\nabla \cdot \mathbf{u}) \right\} dV = \int_V \nabla \cdot \mathbf{T} dV + \int_V \rho \mathbf{g} dV \quad (2.2.2)$$

However, since the volume V of the fluid particle is arbitrary, this equation is only satisfied if

$$\frac{D(\rho \mathbf{u})}{Dt} + \rho \mathbf{u} (\nabla \cdot \mathbf{u}) = \nabla \cdot \mathbf{T} + \rho \mathbf{g} \quad (2.2.3)$$

which can alternatively be expressed

$$\frac{\partial \rho \mathbf{u}}{\partial t} + \nabla \cdot (\rho \mathbf{u} \mathbf{u}) = \nabla \cdot \mathbf{T} + \rho \mathbf{g} \quad (2.2.4)$$

Considering the continuity equation, Eq. (2.2.4), where $\rho \mathbf{u} \mathbf{u}$ is called the linear momentum flux, can be re-arranged as Eq. (2.1.5)

$$\rho \frac{D\mathbf{u}}{Dt} + \mathbf{u} \left(\frac{\partial \rho}{\partial t} + \rho \nabla \cdot \mathbf{u} \right) = \nabla \cdot \mathbf{T} + \rho \mathbf{g} \quad (2.2.5)$$

and thus

$$\rho \frac{D\mathbf{u}}{Dt} = \nabla \cdot \mathbf{T} + \rho \mathbf{g} \quad (2.2.6)$$

The Eq. (2.2.6) is called Cauchy's equation of motion. The equation is valid for any continuum when the stress tensor \mathbf{T} and the body force $\rho \mathbf{g}$

are specified. It should be noted that the body force of gravity furnishes an example of \mathbf{g} for problems we consider in the text. Equation (2.2.6) can be further reduced to a form, using the definition of the substantial derivative given by Eq. (1.1.7) as follows

$$\rho \left(\frac{\partial \mathbf{u}}{\partial t} + \mathbf{u} \cdot \nabla \mathbf{u} \right) = \nabla \cdot \mathbf{T} + \rho \mathbf{g} \quad (2.2.7)$$

Again considering the nature of derivation, and to clearly distinguish between Eqs. (2.2.4) and (2.2.7), Eq. (2.2.4) is often called the conservation form of the linear momentum and Eq. (2.2.7) the non-conservation form of the linear momentum.

If the continuum is incompressible, i.e. $\nabla \cdot \mathbf{u} = 0$, and we take the rotation, i.e. $\nabla \times ()$, of each of the terms in Eq. (2.2.7), we can then obtain

$$\rho \frac{\partial \boldsymbol{\omega}}{\partial t} + \rho \mathbf{u} \cdot \nabla \boldsymbol{\omega} - \rho \boldsymbol{\omega} \cdot \nabla \mathbf{u} = \nabla \times (\nabla \cdot \mathbf{T}) \quad (2.2.8)$$

Equation (2.2.8) is called the vorticity transport equation. The advantage of using Eq. (2.2.8) is that the gravitational acceleration \mathbf{g} , where $\mathbf{g} = -g\hat{\mathbf{e}}_z$, can be eliminated in the same way, if the force can be identified as a potential force, such that $p = p^* - \rho \mathbf{g} \cdot \mathbf{x}$, with the pressure gradient $\nabla p^* = \nabla p - \rho \mathbf{g}$. As a result of this reduction, Eq. (2.2.8) may be expressed in the following form

$$\rho \frac{\partial \boldsymbol{\omega}}{\partial t} + \rho \mathbf{u} \cdot \nabla \boldsymbol{\omega} - \rho \boldsymbol{\omega} \cdot \nabla \mathbf{u} = \nabla \times (\nabla \cdot \boldsymbol{\tau}) \quad (2.2.9)$$

where $\boldsymbol{\tau}$ is the deviatoric stress tensor, as introduced in Eq. (1.6.13). Equation (2.2.9) is particularly useful when a velocity field is described by a stream function. In this case, the system of flow can be expressed with a component of the vorticity vector normal to the flow plane and the stream function. The terms appearing in the left hand side of Eqs. (2.2.8) and (2.2.9) in kinematics of $\boldsymbol{\omega}$ are respectively the transient term, the convective term and the straining term.

2.3 Angular Momentum Conservation

Some continuum while in motion are strongly effected by an external field. As such, the angular momentum per unit mass does not simply equate to the moments of the linear momentum per unit mass. This is particularly

true when there are other torques, which are not part of the moments of force, appearing in the linear momentum equation. Such material of continuum is called polar material. Within the frame of the continuum mechanic, speaking in general terms, we will derive a conservation equation of angular momentum. Before proceeding to the polar fluid, we will examine non-polar fluid in great detail, so that its properties and character are clearly understood.

We shall designate $\mathbf{x} \times \rho \mathbf{u} dV$ as the angular momentum of a volume element in a fluid particle while $\mathbf{x} \times \rho \mathbf{g} dV$ and $\mathbf{x} \times \mathbf{t}_{(n)} dS$ are torques due to body force and surface force respectively. Next, applying the conservation law to these forces, it suggests that the net change of the angular momentum is equal to the net torque acting upon the fluid particle, see Fig. 2.3. The conservation equation of the angular momentum can be thus written as follows

$$\frac{D}{Dt} \int_V (\mathbf{x} \times \rho \mathbf{u}) dV = \int_V (\mathbf{x} \times \rho \mathbf{g}) dV + \int_S (\mathbf{x} \times \mathbf{t}_{(n)}) dS \quad (2.3.1)$$

With the aid of the Reynolds' transport theorem of Eq. (1.5.8) and the continuity equation of Eq. (2.1.5), setting $\mathbf{F} = \mathbf{x} \times \mathbf{u}$ and using the relation $\mathbf{u} \times \mathbf{u} = 0$ and $D(\mathbf{x} \times \mathbf{u})/Dt = \mathbf{x} \times d\mathbf{u}/dt$, we have

$$\int_V \rho \left(\mathbf{x} \times \frac{d\mathbf{u}}{dt} \right) dV = \int_V \rho (\mathbf{x} \times \mathbf{g}) dV + \int_S (\mathbf{x} \times \mathbf{t}_{(n)}) dS \quad (2.3.2)$$

The second term of the right hand side of Eq. (2.3.2) can be further reduced to the following forms, using Cauchy's stress formula given by Eq. (1.6.8).

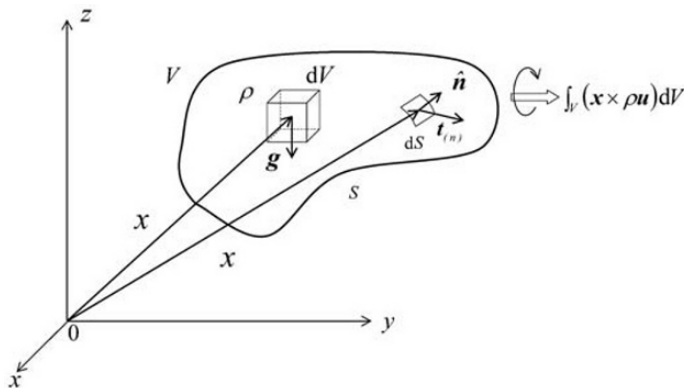


Fig. 2.3 Torques due to body force and surface force

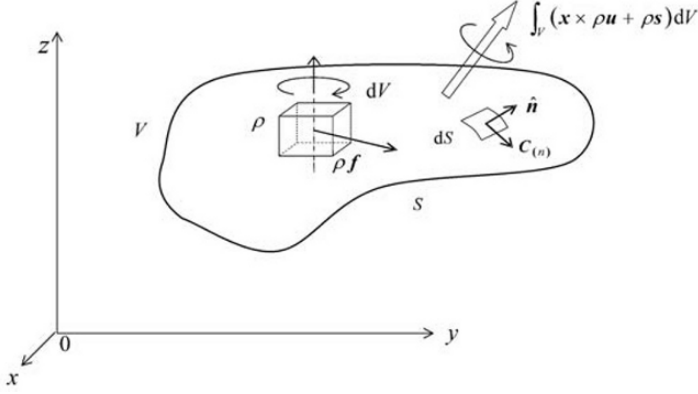


Fig. 2.4 Body couple and surface couple

$$\begin{aligned} \int_S (\mathbf{x} \times \mathbf{t}_{(n)}) dS &= - \int_S (\hat{\mathbf{n}} \cdot \mathbf{T}) \times \mathbf{x} dS = - \int_S \hat{\mathbf{n}} \cdot (\mathbf{T} \times \mathbf{x}) dS \\ &= - \int_V \nabla \cdot (\mathbf{T} \times \mathbf{x}) dV \end{aligned} \quad (2.3.3)$$

Here, we used the polyadic alternator $\hat{\mathbf{e}}_i \times \hat{\mathbf{e}}_j = \varepsilon_{ijk} \hat{\mathbf{e}}_k$ and the Gauss' divergence theorem, shown as

$$\int_S \varepsilon_{ijk} x_j t_{kl} n_l dS = \int_V \frac{\partial \{ \varepsilon_{ijk} (x_j T_{lk}) \}}{\partial x_l} dV \quad (2.3.4)$$

Furthermore, it will be shown that the i th component of $\nabla \cdot (\mathbf{T} \times \mathbf{x})$, i.e. $\partial \{ \varepsilon_{ijk} (x_j T_{lk}) \} / \partial x_l$, can be expressed by the following relations

$$\frac{\partial \{ \varepsilon_{ijk} (x_j T_{lk}) \}}{\partial x_l} = -\varepsilon_{ijk} x_j \frac{\partial T_{lk}}{\partial x_l} - \varepsilon_{ijk} T_{jk} = -\mathbf{x} \times (\nabla \cdot \mathbf{T}) - \mathbf{A} \quad (2.3.5)$$

where we used $\partial x_j / \partial x_l = \delta_{jl}$. The vector \mathbf{A} in Eq. (2.3.5) is a pseudovector, which has these components of the skew-symmetric part of the stress tensor \mathbf{T} , which is demonstrated here as

$$\mathbf{A} = \hat{\mathbf{e}}_1 (T_{23} - T_{32}) + \hat{\mathbf{e}}_2 (T_{31} - T_{13}) + \hat{\mathbf{e}}_3 (T_{12} - T_{21}) = \hat{\mathbf{e}}_1 A_1 + \hat{\mathbf{e}}_2 A_2 + \hat{\mathbf{e}}_3 A_3 \quad (2.3.6)$$

where the components of \mathbf{A} are derived from the matrix

$$\mathbf{T}_a = \frac{1}{2} \begin{bmatrix} 0 & A_3 & -A_2 \\ -A_3 & 0 & A_1 \\ A_2 & A_1 & 0 \end{bmatrix} \quad (2.3.7)$$

where \mathbf{T}_a is the skew-symmetric part of the tensor \mathbf{T} derived from the following relationship

$$\mathbf{T} = \frac{1}{2}(\mathbf{T} + \mathbf{T}^T) + \frac{1}{2}(\mathbf{T} - \mathbf{T}^T) = \mathbf{T}_s + \mathbf{T}_a \quad (2.3.8)$$

where \mathbf{T}_s is the symmetric part of the tensor \mathbf{T} .

Equation (2.3.6) implies the fact that \mathbf{A} is the vector of the tensor \mathbf{T} , indicating that \mathbf{A} can be obtained from the tensor \mathbf{T} and conversely \mathbf{T}_a can be found from the pseudovector \mathbf{A} as follows

$$\mathbf{A} = -\boldsymbol{\varepsilon} : \mathbf{T} \quad (2.3.9)$$

and

$$\mathbf{T}_a = \frac{1}{2} \boldsymbol{\varepsilon} \cdot \mathbf{A} \quad (2.3.10)$$

Employing Eqs. (2.3.3) and (2.3.5) to the integral equation of Eq. (2.3.2), we have the resultant integral equation

$$\int_V \mathbf{x} \times \left(\rho \frac{D\mathbf{u}}{Dt} - \rho \mathbf{g} - \nabla \cdot \mathbf{T} \right) dV = \int_V \mathbf{A} dV \quad (2.3.11)$$

The volume integral vanishes identically since the volume is arbitrary, so that

$$\mathbf{x} \times \left(\rho \frac{D\mathbf{u}}{Dt} - \rho \mathbf{g} - \nabla \cdot \mathbf{T} \right) = \mathbf{A} \quad (2.3.12)$$

The left hand side vanishes identically by Cauchy's equation of motion (see given by Eq. (2.2.6)), the conservation law of linear momentum, consequently, we reach the conclusion that $\mathbf{A} = 0$. This implies from Eq. (2.3.10), that the skew-symmetric part of the stress tensor \mathbf{T} vanishes, so that the stress is written

$$\mathbf{T} = \mathbf{T}_s \text{ or } T_{ij} = T_{ji} \quad (2.3.13)$$

Considering the angular momentum of the linear momentum equation (Cauchy's equation of motion), for a non-polar fluid it can be concluded that the stress tensor is symmetric. If, in other words, the stress tensor of a continuum medium in motion is symmetric, the angular momentum of a linear momentum equation is always conserved so that the motion of fluid can only be determined by the linear momentum equation.

In treating a polar fluid, however, an angular momentum due to a long-range force may be exerted on a fluid particle, and likewise for the body force per unit mass from distant surroundings. As displayed schematically in Fig. 2.4, for example, the extra angular momentum we introduce to a polar fluid may be a body couple $\rho \mathbf{f}$ in addition to the body torque $\mathbf{x} \times \rho \mathbf{g}$, i.e. \mathbf{f} per unit mass. In similar fashion, a surface couple $\mathbf{C}_{(n)}$ per unit surface may also be introduced to the surface of a fluid particle, as a surface traction couple, due to a short-range force, and likewise for the surface torque $\mathbf{x} \times \mathbf{t}_{(n)}$. The total angular momentum \mathbf{L} of a fluid particle is considered in a certain way that \mathbf{L} may consist of the sum of the moment of linear momentum $\mathbf{x} \times \rho \mathbf{u}$ per unit mass and an internal angular momentum (or intrinsic angular momentum \mathbf{s}) per unit mass, which accounts for the local spin field of a material element. Thus, in consideration of the balance of total angular momentum, we have

$$\begin{aligned} \frac{D\mathbf{L}}{Dt} &= \frac{D}{Dt} \int_V (\mathbf{x} \times \rho \mathbf{u} + \rho \mathbf{s}) dV \\ &= \int_V (\mathbf{x} \times \rho \mathbf{g} + \rho \mathbf{f}) dV + \int_S (\mathbf{x} \times \mathbf{t}_{(n)} + \mathbf{C}_{(n)}) dS \end{aligned} \quad (2.3.14)$$

In Eq. (2.3.14), $\mathbf{t}_{(n)}$ can be given by Cauchy's stress formula, as seen earlier in Eq. (1.6.8), i.e. $\mathbf{t}_{(n)} = \hat{\mathbf{n}} \cdot \mathbf{T}$. Analogously, $\mathbf{C}_{(n)}$ can also be found by a similar expression given below, since $\mathbf{C}_{(n)}$ arises from diffusive transport of internal angular momentum where \mathbf{c} is called the couple stress tensor.

$$\mathbf{C}_{(n)} = \hat{\mathbf{n}} \cdot \mathbf{c} \quad (2.3.15)$$

Introducing Eqs. (1.6.8) and (2.3.15) to Eq. (2.3.14) yields, after tensor calculus likewise deriving Eq. (2.3.5), we have

$$\begin{aligned} &\frac{D}{Dt} \int_V \rho (\mathbf{x} \times \mathbf{u} + \mathbf{s}) dV \\ &= \int_V \{ \rho \mathbf{f} + \mathbf{x} \times \rho \mathbf{g} + \nabla \cdot \mathbf{c} + \mathbf{x} \times (\nabla \cdot \mathbf{T}) \} dV \end{aligned} \quad (2.3.16)$$

Applying the Reynolds' transport theorem and the continuity equation to the left hand side of Eq. (2.3.16), and vanishing the volume integration due to an arbitrary volume, we have

$$\rho \frac{D}{Dt}(\mathbf{x} \times \mathbf{u} + \mathbf{s}) = \rho \mathbf{f} + \mathbf{x} \times \rho \mathbf{g} + \nabla \cdot \mathbf{c} + \mathbf{x} \times (\nabla \cdot \mathbf{T}) + \mathbf{A} \quad (2.3.17)$$

Equation (2.3.17) is an equation of the total angular momentum of general form for polar fluids. In order to exploit the conservation of angular momentum, Eq. (2.3.17) can be further reduced to simpler form with the following procedure. That is, first taking the vector product of \mathbf{x} to Cauchy's equation of motion, we can obtain

$$\mathbf{x} \times \rho \frac{D\mathbf{u}}{Dt} = \mathbf{x} \times \rho \mathbf{g} + \mathbf{x} \times \nabla \cdot \mathbf{T} \quad (2.3.18)$$

and then using the relationship $\mathbf{x} \times D\mathbf{u}/Dt = D(\mathbf{x} \times \mathbf{u})/Dt$, Eq. (2.3.17) can be reduced to the following expression after subtracting Eq. (2.3.18) from (2.3.17) as follows

$$\rho \frac{Ds}{Dt} = \rho \mathbf{f} + \nabla \cdot \mathbf{c} + \mathbf{A} \quad (2.3.19)$$

This is a resultant equation for the internal angular momentum for a polar fluid.

In the case of a polar fluid, the skew-symmetric part of the stress tensor \mathbf{T}_a from Eq. (2.3.10) would be generated by an effect of the body couple $\rho \mathbf{f}$ and the diffusion of the surface couple $\nabla \cdot \mathbf{c}$ to the net change of the internal angular momentum $\rho(Ds/Dt)$. Equation (2.3.19) is a non-conservation form. The conservation form of the equation for the internal angular momentum can be reduced to the following form, after the mass conservation is taken in account, so as to yield the following, where $\rho \mathbf{us}$ is called the spin flux.

$$\frac{\partial \rho \mathbf{s}}{\partial t} + \nabla \cdot (\rho \mathbf{us}) = \rho \mathbf{f} + \nabla \cdot \mathbf{c} + \mathbf{A} \quad (2.3.20)$$

2.4 Energy Conservation

The energy conservation of a continuum medium can be considered from the first law of thermodynamics, when the law is applied to the thermodynamic

system of a particle. The first law of thermodynamics in a dynamic system implies the conservation of thermal energy and work, which means that

$$d(k + u) = \delta Q - \delta W \quad (2.4.1)$$

where δW and δQ are the work done by the system, and the heat supplied to the system respectively. k and u in Eq. (2.4.1) are the kinetic energy and the internal energy of the system respectively. When the system is at equilibrium, Eq. (2.4.1) can be written with a unit of power by

$$\begin{aligned} \frac{d(k + u)}{dt} &= \frac{\delta Q}{\delta t} - \frac{\delta W}{\delta t} \\ &= \dot{Q} - \dot{W} \end{aligned} \quad (2.4.2)$$

where \dot{W} and \dot{Q} are the work output by the system and the heat input to the system respectively.

In consideration of the first law of thermodynamics as applied to a system of a certain fluid particle as depicted in Fig. 2.5, we may be able to obtain the work output \dot{W} in the first place, taking a dot product to the forces of the fluid particle as follows

$$\dot{W} = \int_S \mathbf{t}_{(n)} \cdot \mathbf{u} dS + \int_V \rho \mathbf{g} \cdot \mathbf{u} dV \quad (2.4.3)$$

The first term of the right hand side is the work output by a surface force and the second term is the work output by a body force. While applying a dot product of \mathbf{u} to Cauchy's equation of motion from Eq. (2.2.6), we can have the following expression

$$\begin{aligned} \rho \frac{D}{Dt} \left(\frac{\mathbf{u}^2}{2} \right) &= (\nabla \cdot \mathbf{T}) \cdot \mathbf{u} + \rho \mathbf{g} \cdot \mathbf{u} \\ &= \nabla \cdot (\mathbf{T} \cdot \mathbf{u}) - \mathbf{T} : \nabla \mathbf{u} + \rho \mathbf{g} \cdot \mathbf{u} \end{aligned} \quad (2.4.4)$$

Equation (2.4.4) can also be written by a volume integral form as

$$\begin{aligned} \frac{D}{Dt} \int_V \frac{1}{2} \rho (\mathbf{u} \cdot \mathbf{u}) dV + \int_V \mathbf{T} : \nabla \mathbf{u} dV \\ = \int_V \nabla \cdot (\mathbf{T} \cdot \mathbf{u}) dV + \int_V \rho \mathbf{g} \cdot \mathbf{u} dV \end{aligned} \quad (2.4.5)$$

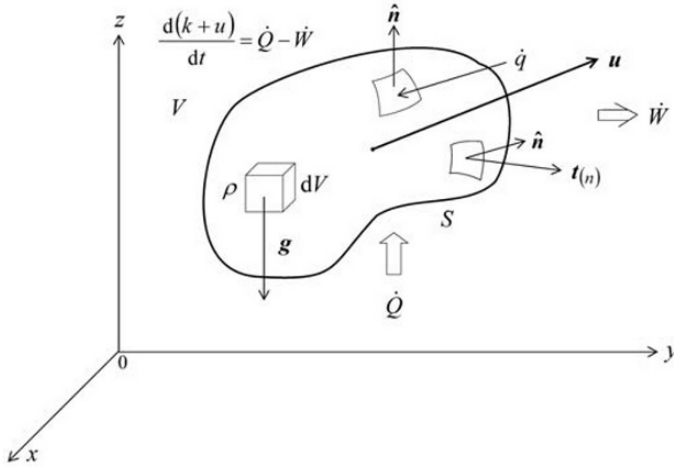


Fig. 2.5 The first law of thermodynamics to a fluid particle

Denoting Cauchy's stress formula from Eq. (1.6.8), i.e. $\mathbf{t}_{(n)} = \hat{\mathbf{n}} \cdot \mathbf{T}$ and applying Gauss' divergence theorem to the surface integral in Eq. (2.4.3), we can write the work output \dot{W} as

$$\dot{W} = \int_V \nabla \cdot (\mathbf{T} \cdot \mathbf{u}) dV + \int_V \rho \mathbf{g} \cdot \mathbf{u} dV \quad (2.4.6)$$

Thus, equating the right hand side of Eq. (2.4.5) with Eq. (2.4.6), we can newly express the work output \dot{W} as

$$\dot{W} = \frac{D}{Dt} \int_V \frac{1}{2} \rho (\mathbf{u} \cdot \mathbf{u}) dV + \int_V \mathbf{T} : \nabla \mathbf{u} dV \quad (2.4.7)$$

Equation (2.4.7) indicates that the work output of a system of a fluid particle can be divided into two parts; the change of kinetic energy and the rate at which the internal stresses do work.

Let us examine further the scenario where \mathbf{T} is not symmetric. Denoting again $\mathbf{T} = (\mathbf{T}_a + \mathbf{T}_s)$ in Eq. (2.3.8), and $\nabla \mathbf{u} = \mathbf{e} + \boldsymbol{\omega}$ in Eq. (1.1.18), the work output due to the internal stress can be written as

$$\begin{aligned} \mathbf{T} : \nabla \mathbf{u} &= (\mathbf{T}_s + \mathbf{T}_a) : (\mathbf{e} + \boldsymbol{\omega}) \\ &= \mathbf{T}_s : \mathbf{e} + \mathbf{T}_a : \boldsymbol{\omega} \end{aligned} \quad (2.4.8)$$

Thus, we have decomposed $\nabla \mathbf{u}$ into the symmetric and skew-symmetric parts so that other products vanish identically. Let us further consider the second term of Eq. (2.4.8) from Eq. (1.1.29) for the spin tensor

$$\boldsymbol{\omega} = \hat{\mathbf{e}}_i \hat{\mathbf{e}}_j \frac{1}{2} \left(\frac{\partial u_i}{\partial x_j} - \frac{\partial u_j}{\partial x_i} \right) = \frac{1}{2} \boldsymbol{\varepsilon} \cdot \boldsymbol{\omega} \quad (2.4.9)$$

Furthermore, \mathbf{T}_a as given by Eq. (2.3.10), utilizing these identities, we can reduce the term to

$$\begin{aligned} \mathbf{T}_a : \boldsymbol{\omega} &= \left(\frac{1}{2} \boldsymbol{\varepsilon} \cdot \mathbf{A} \right) : \left(\frac{1}{2} \boldsymbol{\varepsilon} \cdot \boldsymbol{\omega} \right) \\ &= \frac{1}{4} \varepsilon_{ijk} \varepsilon_{ijp} \omega_k A_p \\ &= \frac{1}{2} \delta_{kp} \omega_k A_p \\ &= \frac{1}{2} \boldsymbol{\omega} \cdot \mathbf{A} \end{aligned} \quad (2.4.10)$$

As a result, Eq. (2.4.10) indicates that the skew-symmetric part of the stress tensor does produce an output work, owing to the vorticity. However, as easily demonstrated when the stress is symmetric, the work output due to the internal stress is simply shown by the deformation as

$$\mathbf{T} : \nabla \mathbf{u} = \mathbf{T}_s : \mathbf{e} \quad (2.4.11)$$

The heat input of the system of a fluid particle is conceived to consist of heat transferred to the system through the surface and heat generated in the system, so that \dot{Q} can be written as

$$\dot{Q} = - \int_S \dot{\mathbf{q}} \cdot d\mathbf{S} + \int_V \rho b dV \quad (2.4.12)$$

Here, \mathbf{q} is the heat flux vector; the negative sign is assigned toward the surface, i.e. opposite to the surface direction $\hat{\mathbf{n}}$. Moreover, b is the amount of heat generated per unit mass in the system. Equation (2.4.12) can be converted into a volume integral by applying Gauss' divergence theorem as follows

$$\dot{Q} = \int_V (-\nabla \cdot \mathbf{q} + \rho b) dV \quad (2.4.13)$$

The total change of the system energy expressed with k and u in Eq. (2.4.2) can be written as

$$\frac{d(k+u)}{dt} = \frac{D}{Dt} \int_V \left(\frac{1}{2} \rho (\mathbf{u} \cdot \mathbf{u}) + \rho u \right) dV \quad (2.4.14)$$

As we can see, u is the internal energy per unit mass. The energy possessed by the system may include spin energy if the continuum has an internal structure and field energy derived from an externally imposed field, depending upon the circumstance and property of the continuum in motion. Generally speaking, within the continuum mechanics we write the energy equation of a fluid, by substituting Eqs. (2.4.7) and (2.4.13) together with Eq. (2.4.14) into Eq. (2.4.2), we can obtain the equation of the energy conservation as

$$\frac{D}{Dt} \int_V \rho u dV = \int_V (\mathbf{T} : \nabla \mathbf{u} - \nabla \cdot \mathbf{q} + \rho b) dV \quad (2.4.15)$$

Note that the power \dot{W} is chosen as to the work input to the system in Eq. (2.4.15), where the sign of plus is assigned. After vanishing the volume integral from both sides of equation (2.4.15) for an arbitrary volume and with Reynolds' transport theorem to the right hand side of Eq. (2.4.15), we can obtain the resultant equation to yield

$$\frac{\partial \rho}{\partial t} + \nabla \cdot (\rho \mathbf{u}) = - \nabla \cdot \mathbf{q} + \mathbf{T} : \nabla \mathbf{u} + \rho b \quad (2.4.16)$$

This is the conservation equation of energy, which is called the Neumann energy equation in the conservation form. The equation can also be reduced to the non-conservation form, as practiced previously by considering the equation of mass continuity, which yield the form

$$\rho \frac{Du}{Dt} = - \nabla \cdot \mathbf{q} + \mathbf{T} : \nabla \mathbf{u} + \rho b \quad (2.4.17)$$

The Neumann energy equation given by Eq. (2.4.16) or (2.4.17) is an expression derived from the first law of thermodynamics. The equations contain thermodynamic properties, such as u and ρ , so that the equations can be further expanded thermodynamically in order to define the state of continuum undergoing thermal process.

2.5 Thermodynamic Relations

The state of a thermodynamic system can be determined by its thermodynamic properties, which are connected by its relationship to the general term

$$f(p, v, T) = 0 \quad (2.5.1)$$

As such, p is the thermodynamic pressure, or simply the pressure, v is the specific volume $v = 1/\rho$ and T is the absolute temperature. Equation (2.5.1) is called the equation of state, where its functional form depends upon the state of the thermodynamic properties of the substance contained in the system. Any one of the three variables in Eq. (2.5.1) can be expressed as a function of the other two by solving Eq. (2.5.1). This means that the thermodynamic state is completely determined by two remaining thermodynamic properties. An important concept to note here is the state of equilibrium, which we can determine through the thermodynamic state from Eq. (2.5.1). The state of equilibrium is that property which does not vary over time when the external conditions remain unchanged.

In some situations, when a continuum is in motion with chemical reaction, a relaxation process or in a large temperature gradient, that is a process that results in the inability of the system to reach the state of equilibrium in the time available, some processes have to be considered by the states of non-equilibrium. However, the majority of processes in engineering fluid mechanics are in the state of equilibrium, and the system undergoes the reversible process where the process is connected only between those initial and final states which are states of equilibrium.

As introduced in Eq. (2.4.1), the first law of thermodynamics in a dynamic system of a continuum, the internal energy u can be regarded as independent of the kinematics of the motion of flow in the limit of the equilibrium thermodynamics (thermodynamics) as follows

$$du = \delta Q - \delta W \quad (2.5.2)$$

The first law of thermodynamics, demonstrated by Eq. (2.5.2), gives the conservation of energy in quantity, but does not have any information on the quality of the energy. The work done by the system δW and the heat supplied to the system δQ are not thermodynamic properties, which cannot be determined by being given two equilibrium states between a transformation process. However, δW may be determined by a known reversible process of work transfer, considering p and v at two given equilibrium points of states as follows

$$\delta W = p dv \quad (2.5.3)$$

It is the δQ that can not be determined by any other known thermodynamic properties, but only by the thermodynamic property s , the entropy. The second law of thermodynamics gives a corollary that there exists a

thermodynamic property of a system such that a change in its value from state 1 to 2 is equal to

$$\begin{aligned}\int_1^2 \frac{\delta Q}{T} &= s_2 - s_1 \\ &= \Delta s\end{aligned}\tag{2.5.4}$$

For any reversible process, δQ can be written by the change (the differentiation) of the entropy as

$$\delta Q = T ds\tag{2.5.5}$$

Thus, Eq. (2.5.2) can be written with Eqs. (2.5.3) and (2.5.5) as follows

$$du = T ds - p dv\tag{2.5.6}$$

or

$$du = T ds - p d\left(\frac{1}{\rho}\right)\tag{2.5.7}$$

Obtaining a new thermodynamic property s , we have the following thermodynamic relationship between the thermodynamic properties of p, v, T, s :

$$\left(\frac{\partial T}{\partial v}\right)_s = -\left(\frac{\partial p}{\partial s}\right)_v\tag{2.5.8}$$

$$\left(\frac{\partial T}{\partial p}\right)_s = \left(\frac{\partial v}{\partial s}\right)_p\tag{2.5.9}$$

$$\left(\frac{\partial p}{\partial T}\right)_v = \left(\frac{\partial s}{\partial v}\right)_T\tag{2.5.10}$$

$$\left(\frac{\partial v}{\partial T}\right)_p = -\left(\frac{\partial s}{\partial p}\right)_T\tag{2.5.11}$$

Equations (2.5.8) to (2.5.11) are called the Maxwell equations, which form the basis for obtaining further important thermodynamic relationships which may be utilized for evaluation of thermal properties of continuum substance.

Among others, an important thermal property is the specific heat, which is a quantity that gives the heat supplied to the system when the temperature difference is given, so that

$$\delta Q = c dT \quad (2.5.12)$$

where c is the specific heat. Substituting Eq. (2.5.12) to the first law of thermodynamics Eq. (2.5.2) and denoting $\delta W = p dv$ from Eq. (2.5.3), we have the following relationships;

$$c dT = du + p dv \quad (2.5.13)$$

or

$$c dT = dh - v dp \quad (2.5.14)$$

Such that h is defined as

$$\begin{aligned} h &= u + p v \\ &= u + p \left(\frac{1}{\rho} \right) \end{aligned} \quad (2.5.15)$$

In Eq. (2.5.15) h is the enthalpy per unit mass, which is a specific energy function. From Eqs. (2.5.13) and (2.5.14), therefore, we can obtain two kinds of specific heat:

$$c_v = \left(\frac{\partial u}{\partial T} \right)_v \quad (2.5.16)$$

and

$$c_p = \left(\frac{\partial h}{\partial T} \right)_p \quad (2.5.17)$$

c_v denotes the specific heat evaluated at constant volume (constant density) and c_p denotes the specific heat evaluated at constant pressure.

Considering the thermodynamic relations, we are now in position to expand the Neumann energy equation of Eq. (2.4.17) by decomposing the total stress tensor \mathbf{T} into $\boldsymbol{\tau}$ and p as described in Eq. (1.6.13). Denoting that p in Eq. (1.6.13) is regarded as the thermodynamic pressure in the state of equilibrium, so that Eq. (2.4.17) becomes

$$\rho \frac{Du}{Dt} = -\nabla \cdot \mathbf{q} - p \nabla \cdot \mathbf{u} + \boldsymbol{\tau} : \nabla \mathbf{u} + \rho b \quad (2.5.18)$$

Since Du in Eq. (2.5.18) can be regarded as the total differentiation by the two thermodynamic properties v and T , it then yields

$$Du = \left(\frac{\partial u}{\partial v} \right)_T dv + \left(\frac{\partial u}{\partial T} \right)_v dT \quad (2.5.19)$$

From Eq. (2.5.6), we can write Eq. (2.5.19) as

$$\frac{Du}{Dt} = \left(-p + T \left(\frac{\partial s}{\partial v} \right)_T \right) \frac{Dv}{Dt} + \left(\frac{\partial u}{\partial T} \right)_v \frac{DT}{Dt} \quad (2.5.20)$$

$(\partial s / \partial v)_T$ is obtained from the Maxwell equation of Eq. (2.5.10). The material derivative of v in Eq. (2.5.20) in a limit of $\delta v = 1/\rho$ can be written as follows

$$\frac{Dv}{Dt} = \frac{D \left(\frac{1}{\rho} \right)}{Dt} = -\frac{1}{\rho^2} \frac{D\rho}{Dt} = \frac{1}{\rho} \nabla \cdot \mathbf{u} \quad (2.5.21)$$

Thus, using Eqs. (2.5.20) and (2.5.21), Eq. (2.5.18) can be rewritten as

$$\rho c_v \frac{DT}{Dt} = -\nabla \cdot \mathbf{q} + \boldsymbol{\tau} : \nabla \mathbf{u} - T \left(\frac{\partial p}{\partial T} \right)_v \nabla \cdot \mathbf{u} + \rho b \quad (2.5.22)$$

Here, the term $(\partial u / \partial T)_v$ was replaced by the specific heat c_v given by Eq. (2.5.16). With a similar manipulation, using the enthalpy h defined in Eq. (2.5.15), i.e. $u = h - pv$, into Eq. (2.5.18), we can obtain the following expressions for the conservation equation of energy as follows;

$$\rho c_p \frac{DT}{Dt} = -\nabla \cdot \mathbf{q} + \boldsymbol{\tau} : \nabla \mathbf{u} + \left[\frac{\partial \ln(1/\rho)}{\partial \ln T} \right]_p \frac{Dp}{Dt} + \rho b \quad (2.5.23)$$

and

$$\rho c_p \frac{DT}{Dt} = -\nabla \cdot \mathbf{q} + \boldsymbol{\tau} : \nabla \mathbf{u} + \beta_T T \frac{Dp}{Dt} + \rho b \quad (2.5.24)$$

We can now see that the term $(\partial h / \partial T)_p$ was replaced by the specific heat c_p defined by Eq. (2.5.17). In Eq. (2.5.24), β_T is the coefficient of thermal expansion, which is made apparent by

$$\beta_T = -\frac{1}{\rho} \left(\frac{\partial \rho}{\partial T} \right)_p \quad (2.5.25)$$

Note that for an ideal gas $\beta_T = 1/T$ and for a liquid, β_T is usually smaller than $1/T$. The enthalpy change dh is also written by using the quantity β_T , and it can be thus derived from the thermodynamics relationship;

$$dh = c_p dT + (1 - \beta_T T) \frac{dp}{\rho} \quad (2.5.26)$$

In the case of an incompressible flow, i.e. $\nabla \cdot \mathbf{u} = 0$, or if the pressure variation is supposed to be small enough that the term Dp/Dt in Eq. (2.5.23) can be disregarded, which is really limited to nearly incompressible material, the conservation equation of energy will become

$$\rho c_p \frac{DT}{Dt} = -\nabla \cdot \mathbf{q} + \boldsymbol{\tau} : \nabla \mathbf{u} + \rho b \quad (2.5.27)$$

It should be kept in mind that in a compressible flow or a nearly incompressible flow of continuum, the specific heat is c_p . In most practice flows of nearly incompressible materials, it is satisfactory to say that $c_p \approx c_v$.

Considering Eq. (2.4.12), the heat transfer \mathbf{q} to a fluid particle is considered to be carried out by heat conduction through the surface. In this case \mathbf{q} is given by Fourier's law;

$$\mathbf{q} = -k_c \nabla T \quad (2.5.28)$$

Here, k_c is the thermal conductivity, noting that $\hat{\mathbf{n}}$ is directed toward the surface in Eq. (2.4.12). It is further to be noted that Eq. (2.5.28) stands for homogeneous and non-diffusing mixtures. Thus, using Eqs. (2.5.28), (2.5.27) is written

$$\rho c_p \frac{DT}{Dt} = \nabla \cdot (k_c \nabla T) + \boldsymbol{\tau} : \nabla \mathbf{u} + \rho b \quad (2.5.29)$$

Moreover, for a constant k_c , Eq. (2.5.29) can be further simplified:

$$\frac{DT}{Dt} = k_c \nabla^2 T + \left(\frac{1}{\rho c_p} \right) \boldsymbol{\tau} : \nabla \mathbf{u} + \frac{b}{c_p} \quad (2.5.30)$$

where, $k_\alpha = k_c / \rho c_p$ is called the thermal diffusivity. Equation (2.5.30) gives an equation for the temperature field of the flow.

Exercise

Exercise 2.1 Mass Conservation

Consider a steady state flow in a branching channel, entering inlet section 1 and leaving sections 2 and 3 with mean velocity vectors \mathbf{u}_1 , \mathbf{u}_2 and \mathbf{u}_3 respectively, normal to the cross sectional area (surface element) of A_1 , A_2 and A_3 as shown in Fig. 2.6. Write the continuity equation of the system. If outlet section 3 is blocked, what will the continuity equation be?

Ans.

Using the continuity equation of (2.1.5) for the steady state, i.e. $\partial/\partial t = 0$, the integral equation may be recovered by Gauss's divergence theorem

$$\int_V \nabla \cdot \rho \mathbf{u} dV = \int_S \rho \mathbf{u} \cdot d\mathbf{S} = 0 \quad (1)$$

Applying Eq. (1) to the current system gives

$$-\int_{A_1} \rho_1 u_1 dS + \int_{A_2} \rho_2 u_2 dS + \int_{A_3} \rho_3 u_3 dS + \int_S \rho \mathbf{u} \cdot d\mathbf{S} = 0 \quad (2)$$

Since at the channel surface there is a relationship of $\mathbf{u} \perp d\mathbf{S}$, which is to say that there will be no flow across the wall, the last term of Eq. (2) vanishes. So that

$$\rho_1 A_1 u_1 = \rho_2 A_2 u_2 + \rho_3 A_3 u_3 \quad (3)$$

This is the continuity equation of the system. If $u_3 = 0$, Eq. (3) becomes

$$\rho_1 A_1 u_1 = \rho_2 A_2 u_2 \quad (4)$$

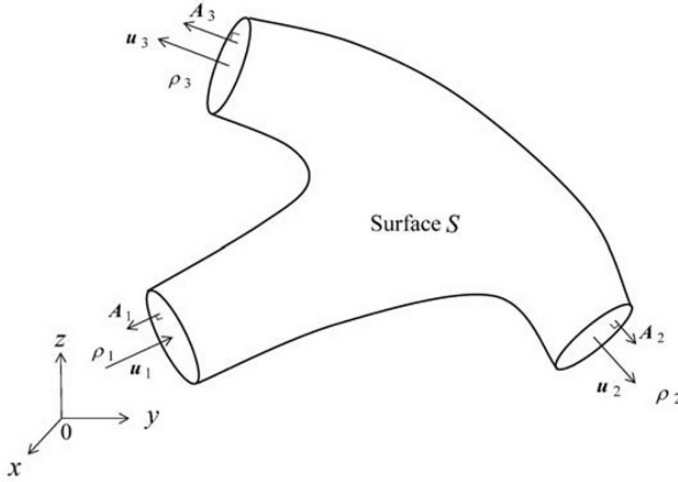


Fig. 2.6 Flow in branching channel

and

$$\dot{m}_1 = \dot{m}_2 \quad (5)$$

Equation (5) indicates that the mass flow rate \dot{m} is conserved from the inlet to the outlet of the channel.

Exercise 2.2 Conservation of Linear Momentum

A steady state flow is passing through a section of a channel as shown in Fig. 2.7. The forces \mathbf{F}_1 and \mathbf{F}_2 acting on the control volume (the channel volume) are due to the surface force and body force respectively. Assuming the inlet's mean velocity \mathbf{u}_1 and outlet's mean velocity \mathbf{u}_2 are respectively parallel to the surface element A_1 and A_2 , write a linear momentum equation of this system.

Ans.

For steady state of flow, the conservation equation of linear momentum can be written by referring to Eq. (2.2.4) as follows

$$\nabla \cdot \rho \mathbf{u} \mathbf{u} = \nabla \cdot \mathbf{T} + \rho \mathbf{g} \quad (1)$$

Using the volume integral in the equation and applying Gauss's divergence theorem we have

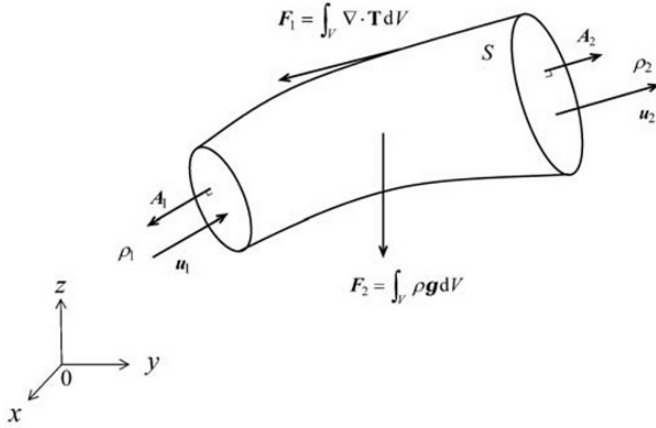


Fig. 2.7 Forces acting on a section of channel

$$\int_S (\rho \mathbf{u}) \mathbf{u} \cdot d\mathbf{S} = \int_V \nabla \cdot \mathbf{T} dV + \int_V \rho \mathbf{g} dV = \mathbf{F}_1 + \mathbf{F}_2 \quad (2)$$

The left hand side of Eq. (2) is calculated as follows when applied to the system

$$\begin{aligned} \int_{A_1} (\rho \mathbf{u}) \mathbf{u} \cdot d\mathbf{S} + \int_{A_2} (\rho \mathbf{u}) \mathbf{u} \cdot d\mathbf{S} + \int_S (\rho \mathbf{u}) \mathbf{u} \cdot d\mathbf{S} \\ = -(\rho_1 u_1 A_1) \mathbf{u}_1 + (\rho_2 u_2 A_2) \mathbf{u}_2 \end{aligned} \quad (3)$$

The integral over the channel wall becomes null due to no cross flow through the wall. Therefore, Eq. (2) can be reduced to the form

$$\dot{m}_2 \mathbf{u}_2 - \dot{m}_1 \mathbf{u}_1 = \mathbf{F}_1 + \mathbf{F}_2 \quad (4)$$

With the continuity equation from Exercise 2.1, i.e. $\dot{m} = \dot{m}_1 = \dot{m}_2$, we can derive the conservation equation of linear momentum for this system as follows

$$\dot{m}(\mathbf{u}_2 - \mathbf{u}_1) = \mathbf{F}_1 + \mathbf{F}_2 \quad (5)$$

Equation (5) is nothing but Newton's second law of motion, stating the change of momentum is equal to the sum of forces applied to the system.

Exercise 2.3 Torque on Control Volume

When considering non-polar fluid, the conservation equation of the angular momentum given by Eq. (2.3.1) can be alternatively expressed by the general form

$$\frac{DL}{Dt} = N \quad (1)$$

where \mathbf{L} is the net angular momentum acting on a control volume (in the Eulerian description) and N is defined as the net torque exerted on the system. Verify the steady torque N_z around the z axis due to the change of \mathbf{L} , where \mathbf{L} is obtained from

$$\mathbf{L} = \int_V (\mathbf{x} \times \rho \mathbf{u}) dV \quad (2)$$

See Fig. 2.8 for the flow configuration.

Ans.

With the aid of Reynolds' transport theorem, to the left hand side of Eq. (1) we have

$$\frac{D}{Dt} \int_V (\mathbf{x} \times \rho \mathbf{u}) dV = \int_V \frac{\partial (\mathbf{x} \times \rho \mathbf{u})}{\partial t} dV + \int_S \hat{\mathbf{n}} \cdot (\mathbf{x} \times \rho \mathbf{u}) \mathbf{u} dS \quad (3)$$

Additionally, for a steady state, i.e. $\partial/\partial t = 0$, Eq. (3) will be

$$\frac{DL}{Dt} = \int_S (\mathbf{x} \times \mathbf{u})(\rho \mathbf{u}) \cdot \hat{\mathbf{n}} dS \quad (4)$$

Equation (4) can be integrated, as depicted schematically in Fig. 2.8, to give the surface of the control volume;

$$\begin{aligned} & \int_S (\mathbf{x} \times \mathbf{u})(\rho \mathbf{u}) \cdot \hat{\mathbf{n}} dS \\ &= \int_{A_1} (\mathbf{x}_1 \times \mathbf{u}_1)(\rho_1 \mathbf{u}_1) \cdot \hat{\mathbf{n}} dS + \int_{A_2} (\mathbf{x}_2 \times \mathbf{u}_2)(\rho_2 \mathbf{u}_2) \cdot \hat{\mathbf{n}} dS + \int_S (\mathbf{x} \times \mathbf{u})(\rho \mathbf{u}) \cdot \hat{\mathbf{n}} dS \quad (5) \end{aligned}$$

Since there would not be any cross flow through the channel wall, the last term of Eq. (5) vanishes and we have

$$\begin{aligned} \frac{DL}{Dt} &= -\rho_1 u_1 A_1 (\mathbf{x}_1 \times \mathbf{u}_1) + \rho_2 u_2 A_2 (\mathbf{x}_2 \times \mathbf{u}_2) \\ &= -\dot{m}_1 (\mathbf{x}_1 \times \mathbf{u}_1) + \dot{m}_2 (\mathbf{x}_2 \times \mathbf{u}_2) \quad (6) \end{aligned}$$

Therefore the change of angular momentum around the z axis can be obtained by applying the dot product of \hat{e}_z to Eq. (6), which is

$$\frac{DL_z}{Dt} = \dot{m}_2(r_2 u_{2t}) - \dot{m}_1(r_1 u_{1t}) \quad (7)$$

Note that u_{2t} and u_{1t} are the tangential components of the velocity vector \mathbf{u}_1 and \mathbf{u}_2 respectively, perpendicular to the z axis. Considering the equation of continuity, i.e. $\dot{m} = \dot{m}_1 = \dot{m}_2$, we can finally derive the torque N_z , which is given by the following formula;

$$N_z = \dot{m}(r_2 u_{2t} - r_1 u_{1t}) \quad (8)$$

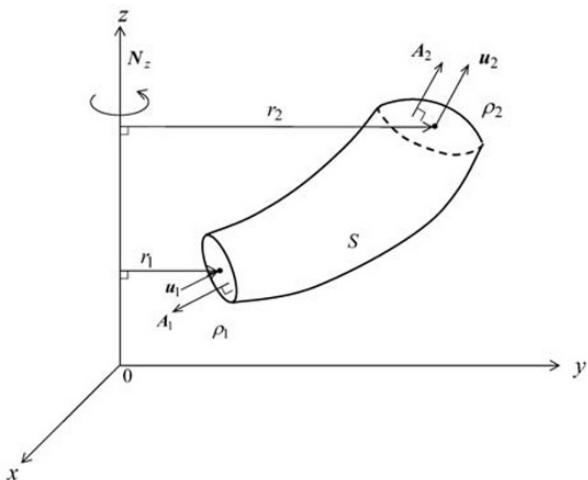


Fig. 2.8 Torque exerted on control volume

From the perspective of engineering application, torque is a very important parameter to characterize rotating machineries, particularly for the rotors of turbomachines in fluid engineering. Equation (8) is often referred to as Euler's pump or turbine equation, which will be studied in more detail for turbomachines in a few sections of Chapter 4.

Exercise 2.4 Energy Conservation of a System

Consider a control volume as a thermodynamic system, where a perfect fluid enters from section 1 and leaves from section 2. Velocities \mathbf{u}_1 and \mathbf{u}_2 at each section are parallel to the surface elements A_1 and A_2 respectively,

as shown in Fig. 2.9. If we assume that the system gives mechanical work \dot{W}_m to the surrounding, besides its work input \dot{W}_s to the system, the first law of thermodynamics in the system may be applied to the system by writing the conservation of energy as follows

$$\frac{D}{Dt}(k + u) = (\dot{Q} + \dot{W}_s) - \dot{W}_m \quad (1)$$

Derive an expression of an energy conservation equation at a steady state for the system in Fig. 2.9. Note that the minus sign of the mechanical work done \dot{W}_m by the system is meant to be toward the outside (surrounding) of the system and the plus sign of \dot{Q} is heat transferred to the system from the outside (the surrounding).

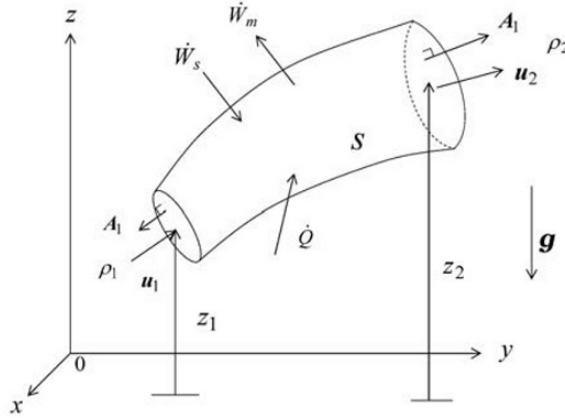


Fig. 2.9 Energy conservation of a system

Ans.

We shall derive an expression for the energy balance to the heat input and the mechanical work by writing

$$\dot{Q} - \dot{W}_m = \frac{D}{Dt}(k + u) - \dot{W}_s \quad (2)$$

The right hand side of Eq. (2) can be expanded in consideration of Eqs. (2.4.3) and (2.4.14) as follows

$$\frac{D}{Dt}(k+u) - \dot{W}_s = \frac{D}{Dt} \left[\int_V \left\{ \frac{1}{2} \rho (\mathbf{u} \cdot \mathbf{u}) + \rho u \right\} dV \right] - \left(\int_S \mathbf{t}_{(n)} \cdot \mathbf{u} dS + \int_V \rho \mathbf{g} \cdot \mathbf{u} dV \right) \quad (3)$$

Furthermore, for the stress vector $\mathbf{t}_{(n)}$, Cauchy's stress formula of Eq. (1.6.8) can be applied as

$$\mathbf{t}_{(n)} = \hat{\mathbf{n}} \cdot \mathbf{T} = \hat{\mathbf{n}} \cdot (-p \mathbf{I}) \quad (4)$$

Note that the flow is assumed to be a perfect fluid as given by Eq. (1.6.11). Substituting Eq. (4) into (3) and applying Reynolds' transport theorem to the first term of right hand side of Eq. (3) with the condition $\partial/\partial t = 0$ yields

$$\begin{aligned} \dot{Q} - \dot{W}_m &= \int_S \left\{ \frac{1}{2} \rho \mathbf{u} (\mathbf{u} \cdot \mathbf{u}) + \rho u \right\} \cdot \hat{\mathbf{n}} dS \\ &\quad - \left\{ \int_S \rho \mathbf{u} \cdot \frac{-p}{\rho} \cdot \hat{\mathbf{n}} dS + \int_S \rho \mathbf{u} \cdot (-g\mathbf{z}) \cdot \hat{\mathbf{n}} dS \right\} \end{aligned} \quad (5)$$

Here, the volume integration of Eq. (3) was transformed into the surface integral by Gauss's divergence theorem, and it is noted that the gravitational acceleration \mathbf{g} is given by the potential $\mathbf{g} = -\nabla g\mathbf{z}$. Carrying over the surface integral of Eq. (5) to the control volume, noting that there would not be any cross flow through the wall of the control volume, but only through the inlet and outlet sections, as depicted Fig. 2.9, we can obtain

$$\begin{aligned} \dot{Q} - \dot{W}_m &= \left(\frac{1}{2} \rho_2 u_2 A_2 u_2^2 - \frac{1}{2} \rho_1 u_1 A_1 u_1^2 \right) + (\rho_2 u_2 A_2 u_{\otimes} - \rho_1 u_1 A_1 u_{\ominus}) \\ &\quad + \left(\rho_2 u_2 A_2 \frac{p_2}{\rho_2} - \rho_1 u_1 A_1 \frac{p_1}{\rho_1} \right) + (\rho_2 u_2 A_2 g z_2 - \rho_1 u_1 A_1 g z_1) \\ &= \dot{m} \left[\frac{1}{2} (u_2^2 - u_1^2) + \left(\frac{p_2}{\rho_2} - \frac{p_1}{\rho_1} \right) + g(z_2 - z_1) + (u_{\otimes} - u_{\ominus}) \right] \end{aligned} \quad (6)$$

Here, notations of u_{\otimes} and u_{\ominus} are the internal energy per unit mass at the outlet and inlet respectively (in order to distinguish between the velocity components and the internal energy). In deriving Eq. (6), the equation of continuity is used by setting $\dot{m} = \dot{m}_1 = \dot{m}_2$.

Problems

- 2-1. Give some examples, in which the equation of continuity given by Eq. (2.1.5) does not follow; provide reasons as well.

Ans. [Chemical reactions in the flow process, etc.]

- 2-2. In incompressible irrotational flow, the velocity field is entirely described by a scalar function of $\phi(\mathbf{x})$, by solving the Laplace's equation $\nabla^2 \phi = 0$. Give proof of this problem.

Ans. $\left[\begin{array}{l} \nabla \cdot \mathbf{u} \text{ and } \nabla \times \mathbf{u} = 0, \mathbf{u} = \nabla \phi \text{ since } \nabla \times \nabla \phi = 0, \\ \text{So that } \nabla^2 \phi = 0 \end{array} \right]$

- 2-3. Write the non-conservation form of the linear momentum given by Eq. (2.2.7), in Cartesian coordinates system, using x, y, z as coordinates and $\mathbf{u} = u(u_x, u_y, u_z)$, $\mathbf{T} = T_{xx}, T_{xy}, \dots$, $\mathbf{g} = (g_x, g_y, g_z)$, and p .

Ans. [See Appendix B-7]

- 2-4. Write the vorticity transport equation given by Eq. (2.2.9) on a two-dimensional plane (the $x-y$ plane), setting $\boldsymbol{\omega} = \omega_z \hat{\mathbf{e}}_z$. Use notations similar to those of Problem 2-3.

Ans. $\left[\begin{array}{l} \rho \frac{D\omega_z}{Dt} + \rho \left[u_x \frac{\partial \omega_z}{\partial x} + u_y \frac{\partial \omega_z}{\partial y} \right] \\ = \frac{\partial}{\partial x} \left(\frac{\partial \tau_{xy}}{\partial x} + \frac{\partial \tau_{yy}}{\partial y} \right) - \frac{\partial}{\partial y} \left(\frac{\partial \tau_{xx}}{\partial x} + \frac{\partial \tau_{yx}}{\partial y} \right) \end{array} \right]$

- 2-5. If the stress tensor \mathbf{T} has the skew-symmetric part, what care has to be taken in order to analyze the flow system?

Ans. $\left[\begin{array}{l} \text{Angular momentum equation} \\ \text{has to be included to the} \\ \text{system of equations.} \end{array} \right]$

2-6. Obtain a form to calculate the power from Eq. (8) in Exercise 2.3.

$$Ans. \left[\begin{array}{l} \text{Assume } u_{2t} = r_2 \omega, u_{1t} = r_1 \omega, \\ \text{in which } \omega \text{ is the angular velocity} \\ \text{of the flow rotation around } z \\ \text{axis. } P = N_z \omega = \dot{m} (r_2^2 - r_1^2) \omega^2 \end{array} \right]$$

2-7. In the energy conservation equation, Eq. (2.5.29), if the stress is symmetric, write a two-dimensional equation using the Cartesian coordinates system (the $x-y$ plane) assuming the thermal conductivity is constant, and ignore the internal heat generation.

$$Ans. \left[\begin{array}{l} \text{See Appendix B - 9} \\ \text{for } \frac{\partial}{\partial t} = 0 \text{ and use} \\ \boldsymbol{\tau} : \nabla \mathbf{u} = \tau_{xx} \left(\frac{\partial u_x}{\partial x} \right) + \tau_{xy} \left(\frac{\partial u_x}{\partial y} \right) + \tau_{yx} \left(\frac{\partial u_y}{\partial x} \right) + \tau_{yy} \left(\frac{\partial u_y}{\partial y} \right) \end{array} \right]$$

Nomenclature

\mathbf{A}	: pseudovector
A_1, A_2, A_3	: components of pseudovector
$C_{(n)}$: diffusive transport of internal angular momentum
\mathbf{c}	: couple stress tensor
c_p	: specific heat evaluated at constant pressure
c_v	: specific heat evaluated at constant volume
\mathbf{g}	: body force
\mathbf{g}	: gravitational acceleration
h	: specific enthalpy
k	: specific kinetic energy
k_c	: thermal conductivity
k_α	: thermal diffusivity
\mathbf{L}	: external angular momentum
m	: mass
\dot{m}	: mass flow rate
$\hat{\mathbf{n}}$: unit normal (surface direction) vector
p	: thermodynamic pressure

\dot{Q}	: heat input
\mathbf{q}	: heat flux vector
s	: specific entropy
$d\mathbf{S}, A$: surface element and surface areas
\mathbf{T}	: total stress tensor
\mathbf{T}_a	: skew-symmetric part of the tensor
\mathbf{T}_s	: symmetric part of the tensor
T	: absolute temperature
t	: time
$\mathbf{t}_{(n)}$: stress vector
\mathbf{u}	: velocity vector
u	: specific internal energy and x -directional velocity component
V	: finite volume of fluid particle or control volume
v	: specific volume ($1/\rho$)
\dot{W}	: work output
β_T	: coefficient of thermal expansion
ρ	: density
$\boldsymbol{\tau}$: deviatoric stress
$\boldsymbol{\omega}$: vorticity
ω	: angular velocity

Bibliography

Conservation laws in continuum mechanics are found in almost all texts. To a detailed extent, angular momentum conservation and energy conservation are found in the following texts listed below.

1. A. Rutherford, *Vectors, Tensors, and the Basic Equation of Fluid Mechanics*, Prentice-Hall, Inc., Englewood Cliffs, NJ, 1962.
2. R. E. Rosensweig, *Ferrohydrodynamics*, Cambridge University Press, Cambridge, MA, 1985. Republished from Dover Publications, Inc., 1997.
3. S. M. Richardson, *Fluid Mechanics*, Hemisphere Publishing Corporation, New York, 1989.

3. Fluid Static and Interfaces

Now we will look at how the four general conservation laws we developed in previous chapters can be applied to a great many important engineering problems when we constitute the system of equations. For many physical flows in engineering problems, the assumptions of frictionless or inviscid and incompressible flows allow us to create a reasonably accurate model representing practical situations.

For the sake of aiding understanding of how to apply the laws we have just developed in closed systems, we will begin to consider a number of simpler but still very useful models demonstrated in practical cases.

Fluid static is the simplest case in fluid engineering where the fluid is at the static state in equilibrium, where the concept of pressure is of particular importance.

When fluids considered as continuum medium do not involve relative motion between any parts of the fluid, the state of fluid motion is in static equilibrium. Without the presence of velocity gradients in static equilibrium, the only stress present is the hydrostatic stress, except for in very specific cases involving non-Newtonian fluids or electromagnetic medium. The isotropic pressure, which acts normal to the surface of any orientation of a fluid particle in static equilibrium, is the hydrostatic pressure, which is identical to the thermodynamic pressure, as verified in Section 2.5.

Fluid static or hydrostatics deals with the mechanics of fluid in static equilibrium. Fluids in static equilibrium may have common boundaries, where two single phases are in contact. The pressure discontinuity across the interface occurs due to surface tension, having the curvature of the interface. This chapter also deals with a basic interfacial phenomenon, which is often encountered in engineering applications.

3.1 Fluid Static

Let us consider linear momentum conservation with a fluid particle rotating in an inertial reference frame. From Cauchy's equation of motion,

given in Eq. (2.2.6), and the acceleration of the fluid particle relative to the inertial reference frame, given in Eq. (1.2.12), we can write

$$\rho(\mathbf{a}_r + 2\Omega \times \mathbf{u}_r - \nabla \phi) = \nabla \cdot \mathbf{T} + \rho \mathbf{g} \quad (3.1.1)$$

Here \mathbf{a}_r is the relative acceleration and \mathbf{u}_r is the relative velocity to the inertial reference frame. Since in static equilibrium there is no relative motion of fluid particles, \mathbf{u}_r can be set identically at zero. The total stress tensor \mathbf{T} can be only written in term of the hydrostatic pressure p , which is given in Eq. (1.6.11), and the body force \mathbf{g} can be regarded as the force due to gravity \mathbf{g} . Thus, Eq. (3.1.1) can be written as

$$\rho(\mathbf{a}_r - \nabla \phi) = -\nabla p + \rho \mathbf{g} \quad (3.1.2)$$

Thus, $-\nabla \phi$ represents the centripetal acceleration and ϕ is $\phi = (\Omega^2 r^2 / 2)$, in which Ω is the angular velocity and r is the radius of rotation. Equation (3.1.2) is the hydrostatic equation, which relates pressure distribution to acceleration, body force and density.

In applications of hydrostatics, the body force is due to the gravity and its direction is toward the center of Earth, where we can take the coordinate z for the positive direction opposite to the gravity as shown in Fig. 3.1. In an inertial reference frame, supposing there would not be rigid-body rotational acceleration, i.e. $\Omega = 0$ so that $-\nabla \phi = 0$ and $\mathbf{a}_r = 0$, Eq. (3.1.2) can thus be written by the following ordinary differential equation as

$$\frac{dp}{dz} = -\rho g \quad (3.1.3)$$

It is noted that dp is positive when dz is negative, so that the pressure increases when z decreases, as depicted in Fig. 3.1.

With incompressible flows, we can assume the density ρ in Eq. (3.1.3) to be constant. The variation of the pressure p in the z -direction can be obtained by the integrating Eq. (3.1.3) with respect to z as follows

$$p - p_0 = -\rho g z \quad (3.1.4)$$

where p_0 is the reference pressure at $z = 0$. By converting pressure to equate to the height of a liquid column, Eq. (3.1.4) can be written as

$$\frac{p}{\rho g} + z = \frac{p_0}{\rho g} = \text{const.} \quad (3.1.5)$$

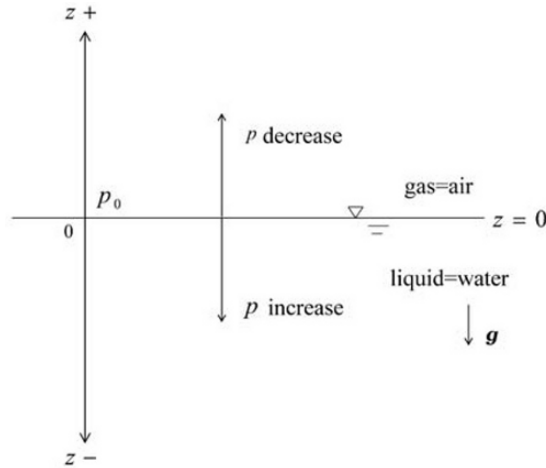


Fig. 3.1 Coordinate z and pressure p

The quantity $p_0/\rho g$ that appeared in Eq. (3.1.5) is referred to as the piezometric head. Using columns of liquid, pressures are measured by manometers. Figure 3.2 shows a U-tube manometer, which may be used to measure pressure p_1 in a pipe or a vessel containing a fluid of density ρ_1 . The tube contains a liquid of greater density ρ_2 than that of the metered fluid. The datum line, from which the liquid columns levels of z_1 and z_2 are measured, is located at $z = 0$ as shown in Fig. 3.2. p_a the atmospheric pressure acts on the liquid column level of z_2 side, so that in static equilibrium of the balance of pressure at the datum line can be written as

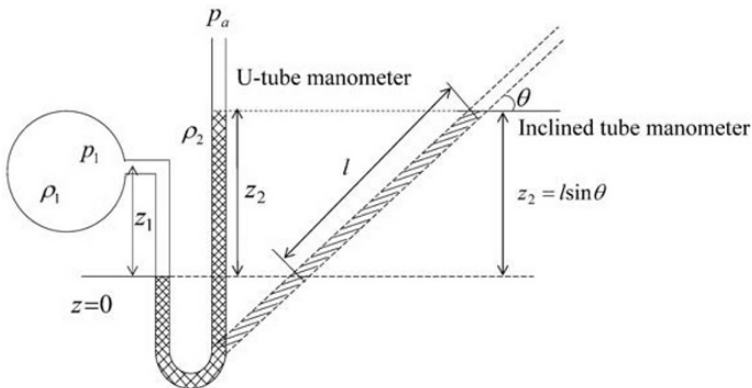


Fig. 3.2 U-tube manometer and inclined tube manometer

$$p_1 + \rho_1 g z_1 = p_a + \rho_2 g z_2 \quad (3.1.6)$$

and solving for p_1

$$p_1 = (\rho_2 g z_2 - \rho_1 g z_1) + p_a \quad (3.1.7)$$

Thus, according to Eq. (3.1.7), the absolute pressure p_1 can be measured by reading the scales of z_1 and z_2 . The read pressure $(\rho_2 g z_2 - \rho_1 g z_1)$ is referred to as a gauge pressure. It is mentioned that at the vacuum, p_1 and ρ_1 will be set zero, with which z_2 becomes a negative reading to the datum line, metering z_2 as $p_a / \rho_2 g$. For the standard atmospheric pressure, z_2 is measured via a 760 mm liquid column of mercury; this implies that $p_a = 1013 \text{ [mmbar]} = 1.013 \times 10^5 \text{ [N/m}^2\text{]}$. For measuring gas pressure, ρ_1 is much smaller than ρ_2 , and Eq. (3.1.7) is simply written where

$$p_1 = \rho_2 g z_2 + p_a \quad (3.1.8)$$

If the gauge pressure $(\rho_2 g z_2)$ is too small to be read on the scale of z_2 , the liquid column can be inclined, as shown in Fig. 3.2 by the hatched lines. This arrangement of a manometer is referred to as the inclined tube manometer, with which the reading of scale l on the tube is taken to give $z_1 = l \sin \theta$. The inclined tube enables the reading of the scale l to be recorded with greater sensitivity.

In engineering design of vessels, dams, water-gate and etc., there are necessities for calculations of the overall magnitudes and representative location of forces that act on a submerged plane or curved surface. In the application of the hydrostatic equation in such engineering problem, we shall consider forces on submerged surfaces. As shown in Fig. 3.3, force \mathbf{F} acting on a surface, submerged in a liquid may be obtained by integrating the pressure $-p$ (the negative sign of p indicates the direction toward the surface element, while the surface force acts toward the direction to a unit normal vector $\hat{\mathbf{n}}$ is positive) over the surface as follows

$$\mathbf{F} = \int_S -p d\mathbf{S} \quad (3.1.9)$$

and

$$\mathbf{F} = \int_S -p \hat{\mathbf{n}} dS \quad (3.1.10)$$

Next let us write the unit normal vector in terms of direction cosines as

$$\hat{n} = \cos \alpha \hat{e}_1 + \cos \beta \hat{e}_2 + \cos \gamma \hat{e}_3 = l_i \hat{e}_i \quad (3.1.11)$$

After considering Eq. (3.1.11), thus Eq. (3.1.10) becomes

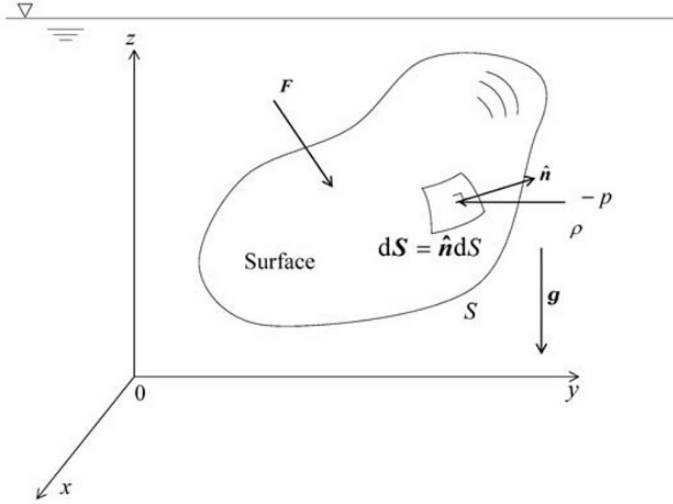


Fig. 3.3 Forces on submerged surface

$$\begin{aligned} \mathbf{F} &= \int_S -p l_i dS \hat{e}_i = \int_{S_1} -p dS_1 \hat{e}_1 + \int_{S_2} -p dS_2 \hat{e}_2 + \int_{S_3} -p dS_3 \hat{e}_3 \\ &= F_1 \hat{e}_1 + F_2 \hat{e}_2 + F_3 \hat{e}_3 \end{aligned} \quad (3.1.12)$$

and

$$|\mathbf{F}| = \sqrt{F_1^2 + F_2^2 + F_3^2} \quad (3.1.13)$$

where dS_1 , dS_2 and dS_3 are the projections of the elementary area $d\mathbf{S}$ on 2–3 ($y-z$), 1–3 ($x-z$) and 1–2 ($x-y$) plane, respectively. Equations. (3.1.12) and (3.1.13) indicate that the overall magnitude of a force on a curved surface is the vector sum of forces projected on each projection plane.

Consider a simple case, where a flat plate is submerged in a liquid to the depth of h_1 and h_2 from the liquid level. Since the object is flat, we can take the projection plane for the same direction of \hat{n} , and we can think of that the plane as being placed with a constant angle α to the level of the liquid, as depicted in Fig. 3.4. Hence, for convenience, a local coordinate y

along the plate surface is taken from a datum coordinate x at the liquid level. The hydrostatic pressure p on the plate surface at the depth $-h$ from the liquid level will be easily calculated by Eq. (3.1.4) as

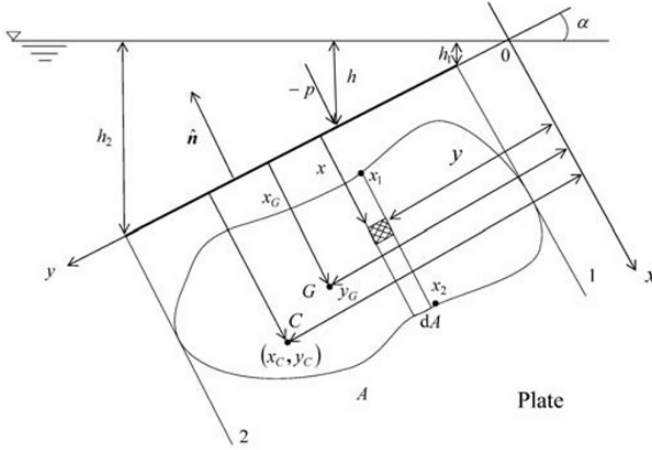


Fig. 3.4 Submerged plate

$$p = -\rho g(-h) \quad (3.1.14)$$

Here, only the gauge pressure is considered. Thus, the overall force acting to the plate is

$$\begin{aligned} \mathbf{F} &= - \int_A \rho g h \cdot \hat{\mathbf{n}} dA \\ &= -\rho g \int_A h \cdot \hat{\mathbf{n}} dA \\ &= -\rho g \left(\int_A h dA \right) \hat{\mathbf{n}} \end{aligned} \quad (3.1.15)$$

The integral $\int_A h dA$ can be calculated with the local coordinates $x-y$, referring to Fig. 3.4 as follows

$$\int_A h dA = \int_1^2 y \sin \alpha dA = \sin \alpha \cdot \int_1^2 y dA = \sin \alpha \cdot y_G A \quad (3.1.16)$$

Here, y_G is referred to as the centroid, $dA = \int_{x_1}^{x_2} dy$ is the surface element across the plate, and A is the total surface area of the plate. Note that x_G

(x directional centroid) is rather irrelevant since p varies with respect to h (and consequently to y). Therefore, Eq. (3.1.15) becomes either

$$\mathbf{F} = -\rho g \sin \alpha \cdot y_G A \cdot \hat{\mathbf{n}} \quad (3.1.17)$$

or

$$\mathbf{F} = -\rho g h_G \cdot A \hat{\mathbf{n}} \quad (3.1.18)$$

From Eq. (3.1.18), it may be stated that the overall force exerted by a liquid on a static equilibrium is the product of the surface area and the pressure p_G at the centroid, $p_G = \rho g h_G$.

The representative point on the plate, where the overall force \mathbf{F} acts on the surface, is not at the centroid point, but is referred to as the center of pressure $C(\mathbf{x}_C)$ as shown in Fig. 3.4. The local coordinates $\mathbf{x}_C = (x_C, y_C)$ of the center of pressure C are obtained by the concept that the moment balance in the static equilibrium also been halted, as follows

$$\mathbf{x}_C \times \mathbf{F} = \int_A \mathbf{x} \times (-p \hat{\mathbf{n}}) dA \quad (3.1.19)$$

\mathbf{F} is given by Eq. (3.1.10). With reference to Fig. 3.4, \mathbf{x}_C with the local coordinates (x_C, y_C) can be obtained from \mathbf{x}_C of Eq. (3.1.19) where

$$x_C F = \int_A x dF \quad \text{and} \quad y_C F = \int_A y dF \quad (3.1.20)$$

Here, F is $|\mathbf{F}|$ and $dF = \rho g h dA = \rho g y \sin \alpha dA$. Thus, with Eq. (3.1.17), x_C and y_C can be calculated to give

$$x_C = \frac{1}{A y_G} \int_A x y dA \quad \text{and} \quad y_C = \frac{1}{A y_G} \int_A y^2 dA \quad (3.1.21)$$

The integrations in Eq. (3.1.21), $\int_A x y dA = I_{xy}$ and $\int_A y^2 dA = I_x$, are called the product of the surface area A and the second moment of the surface area A (or, alternatively, the product of inertia and the moment of inertia of the surface area A) about x axis respectively. In addition, with some algebra for the surface A , I_{xy} and I_x are expressed with respect to the centroid axis parallel to the x and y axes in Fig. 3.4 as follows

$$I_{xy} = I'_{xy} + A x_G y_G \quad \text{and} \quad I_x = I'_x + A y_G^2 \quad (3.1.22)$$

where I'_{xy} and I'_x are those at the centroid axis. Thus, using the relationship, Eq. (3.1.21) can be further written for x_C and y_C where

$$x_C = x_G + \frac{I'_{xy}}{Ay_G} \quad \text{and} \quad y_C = y_G + \frac{I'_x}{Ay_G} \quad (3.1.23)$$

In case, for a more simple geometric plate, such as when the plate area is symmetric about any one of the centroid axis, I'_{xy} becomes zero, so that the center of pressure is expressed as

$$\mathbf{x}_C = \left(x_G, y_G + \frac{I'_x}{Ay_G} \right) \quad (3.1.24)$$

This indicates that the overall force acting on the submerged plate is at a deeper point y_C than the position of the centroid y_G of the plate. In application of further geometric cases of plate, Table 3.1 lists some of representative I'_x .

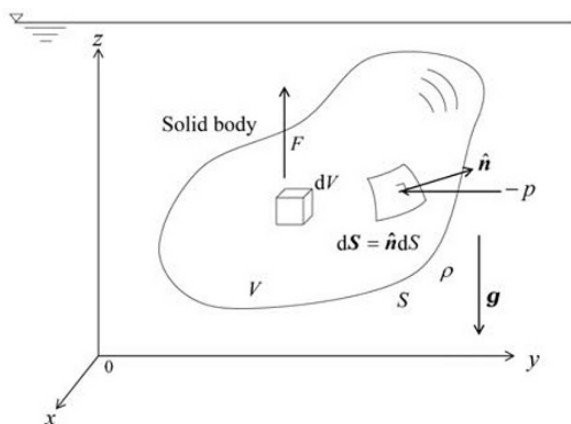
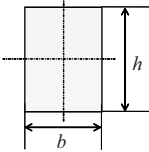
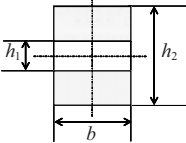
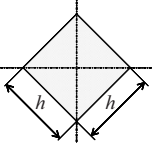
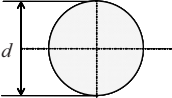
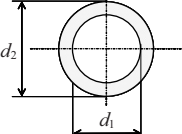
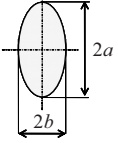
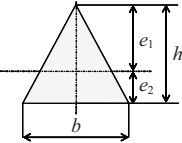


Fig. 3.5 Buoyant force on submerged body

With the same manner, in case of a curved surface, the overall force on a surface can be obtained as the vector sum of each projected plate, as verified in Eq. (3.1.12), see Exercise 3.4.

With the extension of forces on submerged surface, we will now consider the force acting on the surface of a solid body immersed in a fluid, as shown schematically in Fig. 3.5. With the same manner as considered in Eq. (3.1.9), we take a surface integral over the body where

Table 3.1 List of some representative I'_x

Sectional	Section area	Second moment of surface area
	bh	$\frac{bh^3}{12}$
	$b(h_2 - h_1)$	$\frac{1}{12}b(h_2^3 - h_1^3)$
	h^2	$\frac{h^4}{12}$
	$\frac{1}{4}\pi d^2$	$\frac{1}{64}\pi d^4$
	$\frac{\pi(d_2^2 - d_1^2)}{4}$	$\frac{1}{64}\pi(d_2^4 - d_1^4)$
	πab	$\frac{\pi a^3 b}{4}$
	$\frac{1}{2}bh$	$\frac{1}{36}bh^3$ $e_1 = 2h/3$ $e_3 = h/3$

$$\mathbf{F} = \int_{S(\text{closed})} -p d\mathbf{S} \quad (3.1.25)$$

$$= \int_{S(\text{closed})} -p \hat{\mathbf{n}} dS \quad (3.1.26)$$

$$= \int_V -\nabla p dV \quad (3.1.27)$$

where Eq. (3.1.27) is obtained from Eq. (3.1.26) by applying the Gauss' divergence theorem. Noting in the hydrodynamic equation given in Eq. (3.1.2), an inertial reference frame without a rigid body rotation, one can write ∇p as

$$\nabla p = \rho \mathbf{g} \quad (3.1.28)$$

so that Eq. (3.1.27) becomes

$$\mathbf{F} = - \int_V \rho \mathbf{g} dV \quad (3.1.29)$$

The gravity acceleration \mathbf{g} is supposed to be negative for z direction, i.e.

$$\mathbf{g} = -g \hat{\mathbf{e}}_z$$

Thus, Eq. (3.1.29) can be straightforwardly written in the simple form

$$\begin{aligned} \mathbf{F} &= \rho g \int_V dV \hat{\mathbf{e}}_z \\ &= \rho g V \hat{\mathbf{e}}_z \end{aligned} \quad (3.1.30)$$

Equation (3.1.30) is well-known principle of Archimedes, saying that due to the vertical force F , the weight of an immersed body in a liquid will be reduced by an amount equal to the weigh of the displaced liquid $\rho g V$, and the force is called the buoyant force.

Opposite to the situation of the buoyant force, there is a case when a pressurized fluid (usually a gas) is contained in a vessel, called a pressure vessel, where the force on the inner wall of the vessel is exerted by the inner pressure, as depicted in Fig. 3.6. Certainly without a body force $\rho \mathbf{g}$, the overall force acting on the inner wall of enclosure is zero from an analogy of Eq. (3.1.27), where ∇p is zero everywhere in the enclosure. However, let us examine a partial force on a surface of the enclosure S_1 , which is cut by an arbitrary plane A , where the plane A has an unit normal vector $\hat{\mathbf{n}}_A$, and, for brevity's sake, let us take the local Cartesian coordinates

system x, y, z , i.e. $\hat{n}_A = \hat{e}_z$ as shown in Fig. 3.6. The partial force F_{S_1} on the surface S_1 is calculated with the following formula

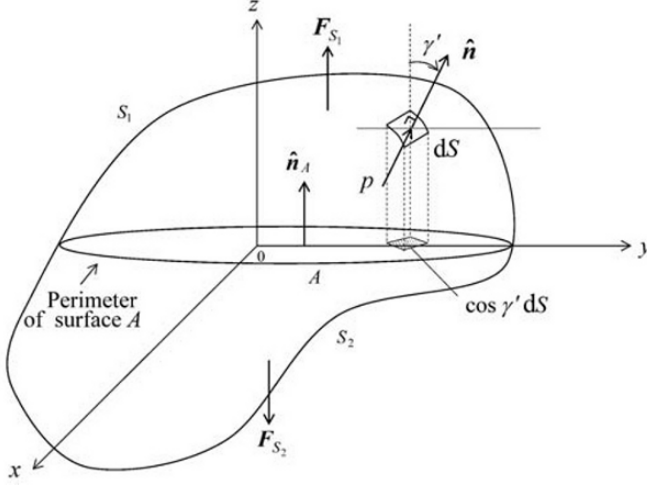


Fig. 3.6 Inner pressure on enclosed surface

$$F_{S_1} = \int_{S_1} p \hat{n} dS \quad (3.1.31)$$

Denoting $\hat{n} = \cos \alpha' \hat{e}_x + \cos \beta' \hat{e}_y + \cos \gamma' \hat{e}_z$, where $\cos \alpha'$, $\cos \beta'$ and $\cos \gamma'$ are directional cosines in the local coordinates system, which yields

$$\begin{aligned} F_{S_1} &= p \left(\int_{S_1} \cos \alpha' dS \hat{e}_x + \int_{S_1} \cos \beta' dS \hat{e}_y + \int_{S_1} \cos \gamma' dS \hat{e}_z \right) \\ &= p \int_{S_1} \cos \gamma' dS \hat{e}_z \end{aligned} \quad (3.1.32)$$

since the integrals of α' and β' involve $0 \leq \alpha' \leq \pi$ and $0 \leq \beta' \leq \pi$ respectively, while γ' is $0 \leq \gamma' \leq \pi/2$ for S_1 surface, i.e.

$$\int_{S_1} \cos \alpha' dS = \int_{S_1} \left\{ \int_0^\pi \cos \alpha' d\alpha' \right\} dS_\alpha = 0 \quad (3.1.33a)$$

$$\int_{S_1} \cos\beta' dS = \int_{S_1} \left\{ \int_0^\pi \cos\beta' d\beta' \right\} dS_\beta = 0 \quad (3.1.33b)$$

$$\int_{S_1} \cos\gamma' dS = \int_{S_1} \left\{ \int_0^{\pi/2} \cos\gamma' d\gamma' \right\} dS_\gamma \neq 0 \quad (3.1.33c)$$

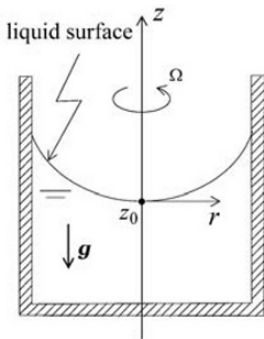
where $dS_\alpha = f(r, \beta, \gamma)$, $dS_\beta = f(r, \alpha, \gamma)$, and $dS_\gamma = f(r, \alpha, \beta)$, thus only \hat{e}_z term survives. In Eq. (3.1.33c), $\cos\gamma' ds$ is a surface element on the plane A , which gives

$$\mathbf{F}_{S_1} = pA\hat{e}_z = pA\hat{n}_z \quad (3.1.34)$$

Equation (3.1.34) indicates that the partial force on an arbitrary inner surface S_1 , which is cut by an arbitrary plane A , is equivalent to the force pA acting on the plane A toward the direction of normal to the plane A . Similarly for S_2 surface, $\mathbf{F}_{S_2} = -pA\hat{e}_z$ would be expected, which balanced as $\mathbf{F}_{S_1} = -\mathbf{F}_{S_2}$, since the overall force on the inner surface is zero. Usually for a pressure vessel, \mathbf{F}_{S_1} force is sustained by a wall thickness of the perimeter of the plane A .

A fluid is still in static equilibrium when the fluid is rotated and accelerated in an inertial frame, where each fluid particle in a fluid rotates and accelerated as if the fluid is a rigid body. From Eq. (3.1.2) the generalized hydrostatic equation can be expressed in the accelerating reference frame as

(a)



(b)

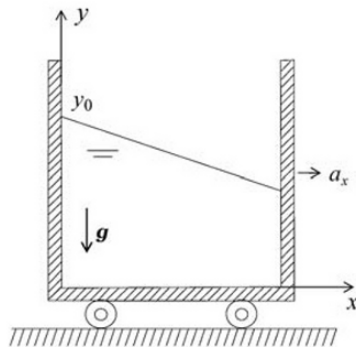


Fig. 3.7 Liquid in accelerating reference frame

$$\nabla p = \rho(-\mathbf{a}_r + \nabla \phi) + \rho \mathbf{g} \quad (3.1.35)$$

where $\phi = \Omega^2 r^2/2$ and \mathbf{a}_r are the relative acceleration of a fluid to the inertial reference frame. This is D'Alembert's principle, where the reversed accelerating force in the inertial reference frame can be included as a body force in dealing with a problem of hydrostatics in an accelerating reference frame.

In order to illustrate the physical meaning of Eq. (3.1.35), let us consider a situation of a liquid contained in a rotating container, such as shown in Fig. 3.7(a), assuming that the liquid reaches static equilibrium with respect to the container and the rotating reference frame $r-z$. As seen in Fig. 3.7(a), the free surface of the liquid will be curved since the centrifugal force is acting on a fluid particle, pushing the liquid toward the wall of the container. The configuration of the static state is called the forced vortex. In the rotating reference frame $r-z$, the pressure distribution in the liquid is a function of r and z so that the differential equation to give the pressure distribution is of the total differentiation of p as follows

$$dp = \frac{\partial p}{\partial r} dr + \frac{\partial p}{\partial z} dz \quad (3.1.36)$$

The partial differentiations of Eq. (3.1.36) are given in Eq. (3.1.35), regarding the fact that there is no relative acceleration, i.e. setting $\mathbf{a}_r = 0$

$$\frac{\partial p}{\partial r} = \rho r \Omega^2 \quad (3.1.37)$$

and

$$\frac{\partial p}{\partial z} = -\rho g \quad (3.1.38)$$

Thus, Eq. (3.1.36) becomes

$$dp = \rho r \Omega^2 dr - \rho g dz \quad (3.1.39)$$

We can now integrate Eq. (3.1.39) between any two points (r_0, z_0) and (r, z) to obtain

$$\begin{aligned}
 p - p_0 &= \frac{1}{2} \rho \Omega^2 (r^2 - r_0^2) - \rho g (z - z_0) \\
 &= \frac{1}{2} \rho r^2 \Omega^2 - \rho g (z - z_0)
 \end{aligned} \tag{3.1.40}$$

where we have set $r_0 = 0$ at the center of rotation. In Eq. (3.1.40), we can see that pressure varies with the square of the radius and a large pressure difference $p - p_0$ that is created inside the forced vortex. This is the working principle of a centrifugal pump, where a low pressure liquid is fed into the center of the rotation, and expelled toward the radius with a higher pressure. The surface of the forced vortex can be calculated by setting $p = p_0$, where at the liquid surface pressure is the same as the surrounding pressure (atmospheric pressure p_a for example if the surface tension is neglected). Thus, from Eq. (3.1.40), we can obtain the surface profile

$$z - z_0 = \frac{\Omega^2 r^2}{2g} \tag{3.1.41}$$

It is easily seen from Eq. (3.1.41), that the free surface is a paraboloid of revolution.

In the same manner, let us consider another situation, as shown in Fig. 3.7(b), where a fluid in a tank is in static equilibrium relative to the reference frame, which linearly accelerates toward x direction with an acceleration component a_x . Similar to Eq. (3.1.36), we have

$$dp = \frac{\partial p}{\partial x} dx + \frac{\partial p}{\partial y} dy \tag{3.1.42}$$

in which $\partial p / \partial x$ and $\partial p / \partial y$ are given in Eq. (3.1.35) as follows

$$\frac{\partial p}{\partial x} = -\rho a_x \tag{3.1.43}$$

and

$$\frac{\partial p}{\partial y} = -\rho g \tag{3.1.44}$$

Thus, Eq. (3.1.42) becomes, to obtain p in a differential form

$$dp = -\rho a_x dx - \rho g dy \quad (3.1.45)$$

We can integrate Eq. (3.1.45) between any two points (x_0, y_0) and (x, y) to give

$$\begin{aligned} p - p_0 &= -\rho a_x (x - x_0) - \rho g (y - y_0) \\ &= -\rho a_x x - \rho g (y - y_0) \end{aligned} \quad (3.1.46)$$

where we set $x_0 = 0$ at the lower left corner of the tank, as shown in Fig. 3.7(b). With the same thought as considered in Eq. (3.1.41), we can obtain the shape of the free surface of the liquid as follows

$$y = -\frac{a_x}{g} x + y_0 \quad (3.1.47)$$

Thus, as verified by Eq. (3.1.47) and sketched in Fig. 3.7(b), the free surface declines linearly toward the direction of the acceleration.

3.2 Fluid-fluid Interfaces

In treating mechanics on the interface of two immiscible fluids, A and B, the boundary condition is such that

$$\mathbf{u}_A \cdot \hat{\mathbf{n}} = \mathbf{u}_B \cdot \hat{\mathbf{n}} \quad (3.2.1)$$

As such, the interface moves with the same velocities \mathbf{u}_A and \mathbf{u}_B at the interface of fluid A and fluid B respectively. $\hat{\mathbf{n}}$ denotes the unit normal to the interface directed from A to B, as shown in Fig. 3.8. A balance of forces, including inertial and body forces, may be expressed as follows

$$\rho'(-\mathbf{a} + \mathbf{g}) + \hat{\mathbf{n}} \cdot (\mathbf{T}_A - \mathbf{T}_B) + \sigma \left(\frac{1}{R_I} + \frac{1}{R_{II}} \right) \cdot \hat{\mathbf{n}} + \nabla_n \sigma = 0 \quad (3.2.2)$$

ρ' is the interface density, σ is the surface tension, $\nabla_n \sigma$ is the gradient of σ normal to the interface, \mathbf{a} is the acceleration, and \mathbf{g} is the gravity acceleration (the body force) for the mass of ρ' . \mathbf{T}_A and \mathbf{T}_B are respectively the total stress tensor expressed in Eq. (1.6.11), and R_I and R_{II} are the principal radii of curvature of the interface between fluid A and B. It is mentioned here that the third term in Eq. (3.2.2) is called the Young-Laplace relationship. Note that R_I and R_{II} are positive when the corresponding center of curvature is in fluid A, and vice versa.

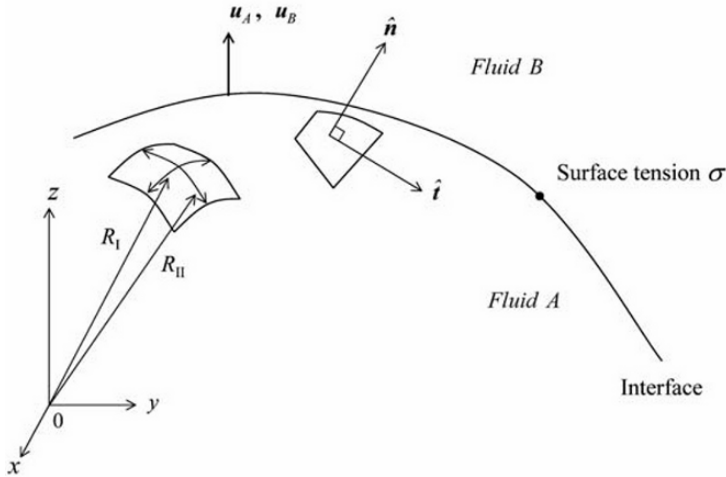


Fig. 3.8 Interface of two immiscible fluid

Equation (3.2.2) is rather general, such that the $\nabla_n \sigma$ term may become important with regard to a film with surfactants, temperature gradients and when the total stress tensor may include effects from an electromagnetic field, and likewise for Eq. (1.6.14). However, without losing generality, we can just assume that those effects and terms included in Eq. (3.2.2) can be neglected, further denoting that the surface density ρ' is negligible. So under that assumption, Eq. (3.2.2) can be simply written as

$$\hat{n} \cdot (-p_A \mathbf{I} + \boldsymbol{\tau}_A) - \hat{n} \cdot (-p_B \mathbf{I} + \boldsymbol{\tau}_B) + \sigma \left(\frac{1}{R_I} + \frac{1}{R_{II}} \right) \cdot \hat{n} = 0 \quad (3.2.3)$$

Equation (3.2.3) gives important stress conditions at the interface, by decomposing Eq. (3.2.3) to \hat{n} - direction and \hat{t} - direction, where \hat{t} is the unit tangent to the interface. For \hat{n} - the direction of the interface, we can write

$$\hat{n} \cdot \left\{ \hat{n} \cdot (-p_A \mathbf{I} + \boldsymbol{\tau}_A) - \hat{n} \cdot (-p_B \mathbf{I} + \boldsymbol{\tau}_B) + \sigma \left(\frac{1}{R_I} + \frac{1}{R_{II}} \right) \cdot \hat{n} \right\} = 0$$

So that

$$p_B - p_A + (\boldsymbol{\tau}_A)_{nn} - (\boldsymbol{\tau}_B)_{nn} + \sigma \left(\frac{1}{R_I} + \frac{1}{R_{II}} \right) = 0 \quad (3.2.4)$$

Equation (3.2.4) is referred to as the normal stress interface condition. A pressure discontinuity occurs if the normal components of $\boldsymbol{\tau}_A$ and $\boldsymbol{\tau}_B$ to the interfacial surface (denoting nn -suffix) and surface tension are present.

For $\hat{\mathbf{t}}$ – direction of the interface, we can write

$$\hat{\mathbf{t}} \cdot \left\{ \hat{\mathbf{n}} \cdot (-p_A \mathbf{I} + \boldsymbol{\tau}_A) - \hat{\mathbf{n}} \cdot (-p_B \mathbf{I} + \boldsymbol{\tau}_B) + \sigma \left(\frac{1}{R_I} + \frac{1}{R_{II}} \right) \cdot \hat{\mathbf{n}} \right\} = 0$$

So that we have

$$(\boldsymbol{\tau}_A)_{nt} - (\boldsymbol{\tau}_B)_{nt} = 0 \quad (3.2.5)$$

Equation (3.2.5) implies that the tangential shear stresses of fluid A and fluid B, denoting the nt -suffix, are the same at the interface.

In an application of Eq. (3.2.3), let us consider a specific example of a bubble in a liquid, as depicted in Fig. 3.9. Denoting that the bubble is in static equilibrium, where the pressure p_A of the bubble and p_B of the surrounding liquid are acting on the spherical surface, and the force due to the pressure difference is balanced with the surface tension of the two fluids. We examine the force F_S as illustrated in Fig. 3.9, due to the inner pressure, acting on the enclosed surface. From Eq. (3.1.34), F_S is straightforwardly calculated for a sphere as follows

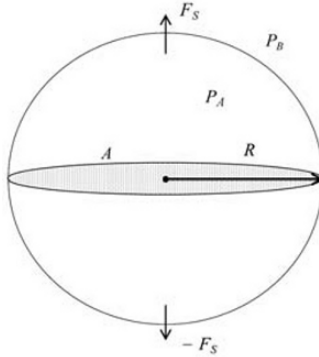


Fig. 3.9 Bubble in static equilibrium

$$F_S = (p_A - p_B) \cdot \pi R^2 \quad (3.2.6)$$

Considering that $p_A > p_B$. This force F_S is aligned normal to the plane A , i.e. the force F_S is supported at the perimeter of the circle area A due to the force by the surface tension, which keeps both halves of the sphere together. Thus, F_S is equal to the force by the surface tension

$$F_s = 2\pi R\sigma \quad (3.2.7)$$

Equating Eqs. (3.2.7) and (3.2.6), we can obtain a relationship, that is

$$p_A - p_B = \frac{2\sigma}{R} \quad (3.2.8)$$

Now let us examine the resultant equation of Eq. (3.2.8) from the point of view of the interfacial force balance at equilibrium. According to the equation of stress at the interface, Eq. (3.2.3) can be rewritten, assuming that the bubble is in static equilibrium and implying that there is no motion in either fluid A or B , i.e. $\tau_A = \tau_B = 0$, with the condition of $R_I = R_{II} = R$ for spherical configuration, by

$$\hat{n} \cdot (p_A - p_B) = \hat{n} \cdot \frac{2\sigma}{R}$$

so that it can be reduced to

$$p_A - p_B = \frac{2\sigma}{R} \quad (3.2.9)$$

This gives us the same result as Eq. (3.2.8).

Exercise

Exercise 3.1 Micromanometer

Two identical reservoirs, whose cross-sectional area is A , are connected with a U-tube of cross-sectional area a , as shown in Fig. 3.10. In the U-tube a heavy liquid of the density ρ_3 is used as a base liquid, with which the measurement reading of the liquid level takes place. In the reservoir tanks, there is a lighter immiscible liquid with density ρ_2 , which occupies the remaining portion of the U-tube. Using this arrangement we can measure the pressure p in a vessel, whose density is ρ_1 . Assuming one end of the reservoir tank is opened to the surrounding, such as the atmosphere p_a with the density of ρ_0 , show the measurement method of this manometer.

Ans.

There is a relationship of volume equality between the reading z of liquid ρ_3 and the level difference Δh of liquid ρ_2

$$az = \Delta h A \quad (1)$$

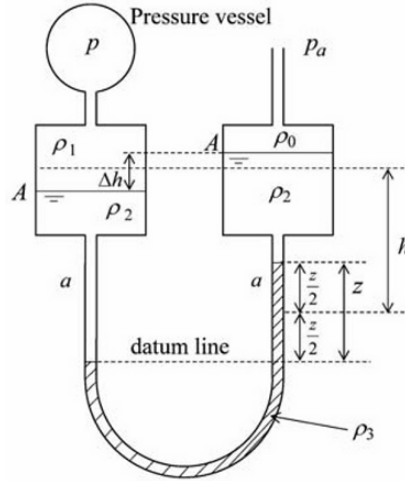


Fig. 3.10 Micromanometer

Taking the datum line at the lowest level of the manometric liquid ρ_3 and the mean level difference as h , we have the pressure balance equation as follows

$$p + \rho_1 g \Delta h + \rho_2 g \left(h - \frac{\Delta h}{2} + \frac{z}{2} \right) = p_a + \rho_2 g \left(h + \frac{\Delta h}{2} - \frac{z}{2} \right) + \rho_3 g z \quad (2)$$

Using the relationship given by Eq. (1), Eq. (2) can be reduced to

$$p - p_a = \left[\frac{a}{A} (\rho_2 - \rho_1) + (\rho_3 - \rho_2) \right] g z \quad (3)$$

Thus, by reading a scale of z , measurement of the pressure p can be achieved. Particularly with this manometer, small pressure differences $(p - p_a)$ are accurately measurable by choosing the density difference $(\rho_2 - \rho_1)$ and $(\rho_3 - \rho_2)$ smaller, as well as keeping (a/A) small. A manometer with this arrangement is called micromanometer.

Exercise 3.2 Hydrostatic Paradox

Obtain overall force F exerted by a liquid column in the static equilibrium for cases (a), (b), (c), and (d) in Fig. 3.11.

Ans.

For all cases, we try to obtain the pressure on the bottom surface A . From the hydrostatic equation Eq. (3.1.2) without \mathbf{a}_r and ϕ , in which no linear acceleration and no rotation of fluid are conditioned, we have

$$\nabla p = \rho \mathbf{g} \quad (1)$$

Since the body force term $\rho \mathbf{g}$ can be written by a potential function $\phi = -\rho g z$ under the earth's gravity field, Eq. (1) becomes

$$\nabla \Phi = 0 \quad (2)$$

Bearing in mind $\Phi = p + \phi$. Consider the integral of Φ from point 0 to 1 as

$$\int_0^1 d\Phi = \int_0^1 \nabla \Phi \cdot d\mathbf{r} = 0 \quad (3)$$

This also yields

$$\begin{aligned} \int_0^1 d\Phi &= \int_0^1 d(p + \phi) = [p + \phi]_0^1 = (p_1 + \phi_1) - (-p_a + \phi_0) \\ &= (p_1 + p_a) + (\phi_1 - \phi_0) \end{aligned} \quad (4)$$

Thus, from Eqs. (3) and (4), we know

$$p_1 = -p_a - (\phi_1 - \phi_0) \quad (5)$$

p_1 in Eq. (5) is independent from the path line of the integral, and only determined by the difference between the relative points 0 and 1. Resulting from Eq. (5):

$$\begin{aligned} p_1 &= -p_a + \rho g z_1 - \rho g z_0 \\ &= -p_a + \rho g (z_1 - z_0) \\ &= -p_a - \rho g h \end{aligned} \quad (6)$$

Thus, the overall force \mathbf{F} is

$$\begin{aligned} \mathbf{F} &= \int_A -p \hat{n} dS \\ &= -(p_a + \rho g h) A \hat{\mathbf{e}}_z \end{aligned} \quad (7)$$

By the same token, for the gauge pressure force F_G we can write

$$F_G = \rho g h A (-\hat{e}_z) \quad (8)$$

The overall force F acting on the surface A is the same for (a–d). This is called the hydrostatic paradox. Equation (8) is equivalent to Eq. (3.1.18), in which h_G is set as $h_G = h$ since the area A is horizontal. Equation (6) can also be proven by the Bernoulli equation, setting the velocity head at zero.

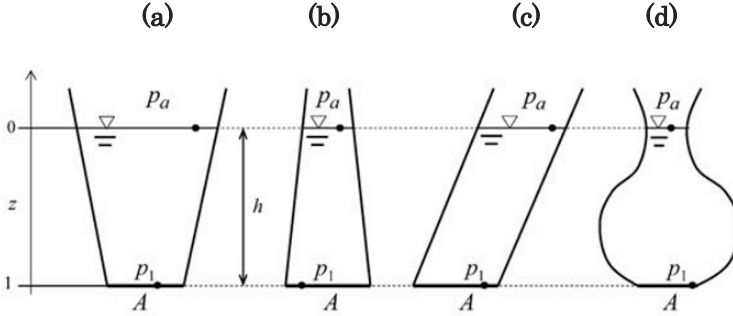


Fig. 3.11 Hydrostatic paradox

Exercise 3.3 Pressure at High Altitude

Estimate the pressure at 10000m above the sea level, assuming;

(i) linearly varying temperatures

$$T = -az + T_0 \quad (1)$$

and

(ii) polytropic changes

$$p \left(\frac{1}{\rho} \right)^n = \text{const.} \quad (2)$$

We may use the ideal gas law for the equation of the state of air

$$p \left(\frac{1}{\rho} \right) = RT \quad (3)$$

Considering the specific gas constant $R = 287 \text{ J/kg} \cdot \text{K}$. For Eqs. (1) and (2) the constants are the lapse rate $a = 0.650 \times 10^{-2} \text{ K/m}$, the standard temperature at sea level which is $T_0 = 288 \text{ K}$, the polytropic constant for air is $n = 1.235$ and the standard atmospheric pressure is $p_a = 1.013 \times 10^5 \text{ N/m}^2$.

Ans.

For case (i) and (ii), the hydrostatic equation Eq. (3.1.3) can be applied, referring to Fig. 3.1 for z increasing as follows

$$\frac{dp}{dz} = -\rho g \quad (4)$$

(i) From the equation of state given by Eq. (3), the density is expressed as

$$\rho = \frac{P}{RT} \quad (5)$$

Since the temperature T in Eq. (5) varies linearly for increasing altitude z as shown in Eq. (1), the density is represented as

$$\rho = \frac{P}{R(-az + T_0)} \quad (6)$$

The density variation of Eq. (6) is then substituted into the hydrodynamic equation of Eq. (4), which gives

$$\frac{dp}{p} = -\frac{g}{R} \frac{1}{(-az + T_0)} dz \quad (7)$$

This can be integrated to give a solution for p_1 as follows

$$\int \frac{dp}{p} = -\frac{g}{R} \int \frac{1}{(-az + T_0)} dz \quad (8)$$

Thus we can calculate

$$\begin{aligned} p_1 &= p_a \left(\frac{T_0 - az}{T_0} \right)^{g/aR} \\ &= 1.013 \times 10^5 \left(\frac{288 - 0.650 \times 10^{-2} \times 10000}{288} \right)^{\frac{9.81}{0.650 \times 10^{-2} \times 287}} \\ &= 0.264 \times 10^5 \text{ N/m}^2 \end{aligned} \quad (9)$$

(ii) Applying the polytropic atmospheric change given by Eq. (2), the relation between pressure and density at any altitude can be written as

$$\rho = \rho_0 \left(\frac{p}{p_a} \right)^{\frac{1}{n}} \quad (10)$$

The density variation of Eq. (10) is then substituted into the hydrostatic equation of Eq. (4), which gives

$$\frac{dp}{p^{\frac{1}{n}}} = - \left(\frac{1}{p_a} \right)^{\frac{1}{n}} \rho_0 g dz \quad (11)$$

This can be integrated to give a solution for p_1 as follows

$$\int \frac{dp}{p^{\frac{1}{n}}} = - \left(\frac{1}{p_a} \right)^{\frac{1}{n}} \rho_0 g \int dz \quad (12)$$

Hence, we can calculate

$$\begin{aligned} p_1 &= p_a \left(1 - \frac{n-1}{n} \frac{\rho_0 g}{p_0} z \right)^{\frac{n}{n-1}} \\ &= p_a \left(1 - \frac{n-1}{n} \frac{g}{RT_0} z \right)^{\frac{n}{n-1}} \\ &= 1.013 \times 10^5 \left(1 - \frac{1.235-1}{1.235} \frac{9.81}{287 \times 288} \times 10000 \right)^{\frac{1.235}{1.235-1}} \\ &= 0.264 \times 10^5 \text{ N/m}^2 \end{aligned} \quad (13)$$

It is further thought that, from p_1 expressed in Eq. (13), the density at z is easily obtained by Eq. (10) as

$$\rho = \rho_0 \left(1 - \frac{n-1}{n} \frac{g z}{RT_0} \right)^{\frac{1}{n-1}} \quad (14)$$

With the equation of state given by Eq. (3), the temperature variation can be calculated as follows

$$\begin{aligned}
 T &= T_0 \left[1 - \left(\frac{n-1}{n} \frac{g}{RT_0} \right) z \right] \\
 &= - \left(\frac{n-1}{n} \frac{g}{R} \right) z + T_0
 \end{aligned} \tag{15}$$

Equation (15) indicates that the temperature variation for an elevation z is linear and the lapse rate can be calculated by those values given for n , R , T_0 , yielding

$$a = \frac{n-1}{n} \frac{g}{R} = 0.650 \times 10^{-2} \text{ K/m} \tag{16}$$

In the troposphere (the nearest earth atmosphere to sea level), the pressure variation is linear at an average rate of 0.65°C per 100 m to a distance of 1000 m in the polar region to 14000 m in the equatorial region. According to the calculation shown above, an airplane flying with an altitude of 10000 m may experience 0.26 degrees of atmospheric pressure with a temperature of -50°C .

Exercise 3.4 Forces on Tank Wall

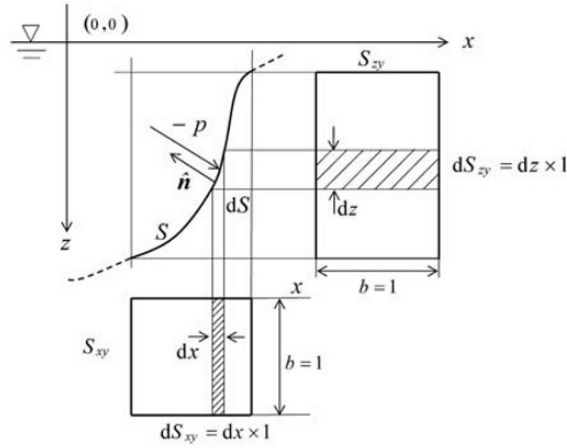
Find the forces on the tank walls, as shown in Fig. 3.12, for a portion of a vessel filled with a liquid. Also determine the center of pressure in each case. Consider first the general wall shape with unit depth as depicted in Fig. 3.12(a), then calculate the specific configuration as shown in Fig. 3.12(b). In the case of Fig. 3.12(b), the shape of the tank walls is expressed by following relation, provide the answer.

$$z = \frac{d_1}{a^2} x^2; \quad 0 \leq x \leq a \quad \text{and} \quad 0 \leq z \leq d_1$$

Ans.

Let us consider a general approach in the $x-z$ plane for an arbitrary curved surface, as schematically shown in Fig. 3.12(a). The force acting on the wall element dS is found to be

(a)



(b)

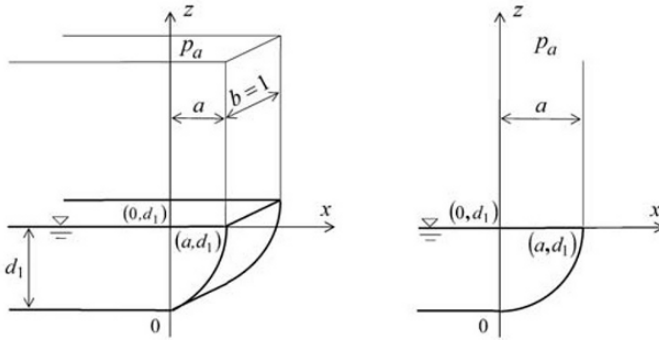


Fig. 3.12 Pressure on curved walls

$$\begin{aligned}
 dF &= -p \hat{n} dS \\
 &= -p(\cos \alpha \hat{e}_x + \cos \beta \hat{e}_z) dS \\
 &= -p dS_{zy} \hat{e}_x - p dS_{xy} \hat{e}_z \\
 &= -p dz \hat{e}_x - p dx \hat{e}_z \\
 &= dF_x \hat{e}_x + dF_z \hat{e}_z
 \end{aligned} \tag{1}$$

$\cos \alpha$ and $\cos \beta$ are the direction cosines for \hat{n} . Thus, the force acting on the surface area S is calculated by integrating Eq. (1) as

$$\begin{aligned}\mathbf{F} &= \int dF_x \hat{\mathbf{e}}_x + \int dF_z \hat{\mathbf{e}}_z \\ &= F_x \hat{\mathbf{e}}_x + F_z \hat{\mathbf{e}}_z\end{aligned}\quad (2)$$

The force \mathbf{F} has two components $F_x = \int -pdz$ and $F_z = \int -pdx$ in the direction of x and z respectively. The magnitude of \mathbf{F} and the action angle α (the inclination of this force to the horizontal plane) are

$$|\mathbf{F}| = \sqrt{F_x^2 + F_z^2} \quad \text{and} \quad \alpha = \tan^{-1} \left| \frac{F_z}{F_x} \right| \quad (3)$$

Setting $p = -\rho g z$, the gauge pressure of \mathbf{F}_x and \mathbf{F}_z can be calculated as follows:

$$F_x = \rho g \int z dz = \rho g z_G S_{zy} \quad (4)$$

$$F_z = \rho g \int z dx = \rho g V \quad (5)$$

z_G is the centroid of the projected area S_{zy} , and V is the volume of liquid contained vertically on the surfaces.

The center of pressure \mathbf{x}_C can be directly obtained by the moment balance equation given by Eq. (3.1.19) as repeatedly written by

$$\mathbf{x}_C \times \mathbf{F} = \int_S \mathbf{x} \times (-p \hat{\mathbf{n}}) dS \quad (6)$$

$\mathbf{x}_C = x_C \hat{\mathbf{e}}_x + z_C \hat{\mathbf{e}}_z$. Substituting Eqs. (1) and (2) into Eq. (6), we can obtain the coordinates of the center of \mathbf{x}_C as

$$x_C = \frac{\int_S x(-p dx)}{F_z} \quad (7)$$

$$z_C = \frac{\int_S z(-p dz)}{F_x} \quad (8)$$

Again considering $p = -\rho g z$ together with Eqs. (4) and (5), we can get \mathbf{x}_C as

$$x_C = \frac{\rho g \int x \cdot z dx}{\rho g V} = \frac{I_{xz}}{V} \quad (9)$$

$$z_C = \frac{\rho g \int z \cdot z dx}{\rho g z_G S_{zy}} = \frac{I_z}{z_G S_{zy}} \quad (10)$$

Now we can consider the problems for Fig. 3.12(b), knowing the general relations of Eqs. (1–10). Denote p as the gauge pressure, based on the level of liquid, i.e. $p = -\rho g z$. Note that the surrounding pressure p_a is atmospheric and the force acting on the inner surface of the tank wall is subject to liquid pressure. Also, denoting that the surface dS_{zy} is negative and dS_{xy} is positive, the force on the wall is thus calculated as follows, according to Eqs. (4) and (5)

$$\begin{aligned} F_x &= \rho g \int_0^{d_1} z dz \cdot b = \rho g \left[\frac{1}{2} z^2 \right]_0^{d_1} \cdot b = \frac{1}{2} \rho g d_1^2 \cdot b \\ &= \rho g \left(\frac{d_1}{2} \right) (d_1) \times 1 \\ & (= \rho g z_G S_{zy}) \end{aligned} \quad (11)$$

$$\begin{aligned} F_z &= \rho g \int_0^a z dx \cdot b = \rho g \int_0^a \left(\frac{d_1}{a^2} x^2 \right) dx \cdot b \\ &= \frac{1}{3} \rho g a d_1 \\ & (= \rho g V) \end{aligned} \quad (12)$$

$$F = \sqrt{F_x^2 + F_z^2} \quad \text{and} \quad \alpha = \tan^{-1} \left| \frac{F_z}{F_x} \right| \quad (13)$$

For the center of pressure x_C , we can calculate x_C and z_C from Eqs. (9) and (10) as follows

$$x_C = \frac{\int_0^a xz dx}{V} = \frac{1}{V} \int_0^a x \left(\frac{d_1}{a^2} x^2 \right) dx = \frac{3}{4} a \quad (14)$$

and

$$z_C = \frac{\int_0^{d_1} z^2 dz}{z_G S_{zy}} = \frac{\frac{1}{3} d_1^3}{\frac{1}{2} d_1^2} = \frac{2}{3} d_1 \quad (15)$$

Consequently, the horizontal forces of F_x are all the same in any wall shape, so that the overall force F , the action angle α and the center of pressure x_C are determined by F_z , which is similarly the volume of liquid contained vertically on the surface of the walls.

In obtaining forces and the center of pressure for a required geometry, one must not be too anxious about the centroid and the moment of inertia or the product of inertia, but simply carry on the integration for Eqs. (4), (5), (7) and (8) to get the results for the required geometry.

Exercise 3.5 Stability of Floating Objects

Discuss the criteria of stable floatation for a cylindrical object with a sliding weight inside, if the body is tilted slightly in the horizontal direction as shown in Fig. 3.13 (a). Consider the following: (i) when the weight is at the bottom; and (ii) when the weight is slid forward to the top of the cylinder. Let W be the representative weight of the floating object, and let D be the diameter of the cylinder. Use α ($\alpha \ll 1$) as the tilt angle and ρ as the density of the liquid.

Ans.

We first consider that the floating object is in equilibrium vertically before tilting, so that the floating object is vertically stable and $W = F$, where F is the buoyant force acting at C and W is the total weight represented by the weight at the center of gravity G . Let l be the length of the cylinder of the submerged portion, and let a be the distance of G from the liquid level as shown in Fig. 3.13(a).

With a small tilt angle α , the equilibrium may be stable or unstable, depending upon the resultant body couple due to tilting. If the body couple

at the axis of rotation O acts in a direction such as to restore the object to its original position, the object is considered to be stable. Contrarily, if the couple is in the opposite direction and acts to increase the tilt angle, the object in this case is unstable. It is quite reasonable to assume for the small tilt angle that the position of the center of gravity G remains unchanged with respect to the object, i.e. along the center line of the cylinder, while the center of buoyancy C takes a new position, as shown in Fig. 3.13(b). Draw a vertical line from the new center of buoyancy C' so that it intersects the center line of the cylinder at a point M , called the “metacenter.” The stability of the object thus wholly depends upon the direction of the couple force due to F and W at new position after tilting. In effect, restoring the couple in the tilt position will stabilize the equilibrium if M lies above G , i.e. the positive couple. On the other hand the equilibrium will be unstable if M lies below G , i.e. the negative couple.

Now let us calculate \overline{MG} , called the metacentric height, and examine the conditions to determine whether \overline{MG} may be negative or positive. Suppose, with reference to Fig. 3.13(b), that the center of buoyancy is shifted from the position C to C' after tilting. The resultant torque (due to the buoyant force F after tilting) should be the sum of the original torque (due to the buoyant force F before tilting) and the contribution of the buoyancy torque from the elementary prismatic volume around the axis of rotation O as shown in Fig. 3.13(b) due to tilting as follows

$$Fb_2 = -Fb_1 + M_0 \quad (1)$$

Fb_2 is the resultant torque about the axis of rotation O , $-Fb_1$ is the original torque and M_0 is the torque due to an additional buoyant force caused by the volume of the displaced fluid. The sign of the torque is negative to increase the tilting and positive to restore the floating object to its original position, as shown in Fig. 3.13. b_1 and b_2 are the normal distances to the buoyant force vector F before and after tilting respectively. From Eq. (1) we have

$$M_0 = F(b_1 + b_2) \quad (2)$$

$(b_1 + b_2)$ can be further written as

$$b_1 + b_2 = \overline{MC} \cdot \sin \alpha \approx \overline{MC} \alpha = (\overline{MG} + \overline{GC}) \alpha \quad (3)$$

so that we have

$$M_0 = F(\overline{MG} + \overline{GC}) \alpha \quad (4)$$

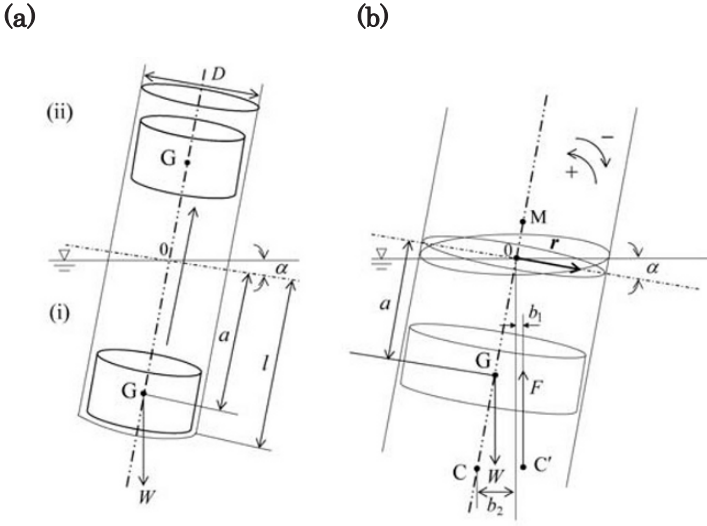


Fig. 3.13 Stability of a tilted object

M_0 in Eq. (4) is the net torque due to the buoyant force in the elementary prismatic volume, the specific value of which can be obtained by carrying out following integral

$$M_0 = 2 \int_V \mathbf{r} \times \rho \mathbf{g} dV \quad (5)$$

Note that dV is the volume element at the position of \mathbf{r} from 0. Since the tilting angle α is small, $\mathbf{r} \perp \mathbf{g}$ can be true, thus Eq. (5) becomes

$$M_0 = 2 \int_{r,\theta} r \rho g r^2 \alpha d\theta dr \quad (6)$$

$dV \approx r^2 \alpha d\theta dr$, and

$$\begin{aligned} M_0 &= 2 \rho g \alpha \int_{-\frac{\pi}{2}}^{\frac{\pi}{2}} \left\{ \int_0^R r^3 dr \right\} d\theta \\ &= \rho g \alpha \left(\frac{R^4}{2} \pi \right) \\ &= \rho g \alpha \left(\frac{D^4}{32} \pi \right) \end{aligned} \quad (7)$$

$I = (D^4/32)\pi$ is the second moment of surface area at the cross section of the cylinder. F is balanced with W at equilibrium before tilting, and F can be estimated by

$$F = \rho g V_e \quad (8)$$

V_e is the displaced volume at equilibrium before tilting. Now it is desirable to derive an expression for \overline{MG} , using Eqs. (4), (7) and (8). Thus we have

$$\begin{aligned} \overline{MG} &= \frac{M_0}{F_\alpha} - \overline{GC} \\ &= \frac{\rho g \alpha \cdot I}{\rho g V_e \cdot \alpha} - \overline{GC} \\ &= \frac{I}{V_e} - \overline{GC} \end{aligned} \quad (9)$$

The couple force τ_c about 0 is written as

$$\tau_c = W \overline{MG} \sin \alpha \approx W \cdot \overline{MG} \cdot \alpha \quad (10)$$

And it follows that

$$\begin{aligned} \tau_c &= W \cdot \overline{MG} \cdot \alpha \\ &= F \cdot \overline{MG} \cdot \alpha \end{aligned} \quad (11)$$

Therefore, for the stability of the floating object we have the general criteria:

- if $\overline{MG} > 0$, $\tau_c > 0$ thus stable,
- if $\overline{MG} < 0$, $\tau_c < 0$ thus unstable
- if $\overline{MG} = 0$, $\tau_c = 0$ this is meta stable.

For the stability of the floating object in Fig. 3.13(a), we have the following parameters

$$V_e = \pi \left(\frac{D}{2} \right)^2 l \quad (12)$$

We can also get

$$\overline{GC} = a - \frac{l}{2} \quad (13)$$

Therefore, from Eq. (9), \overline{MG} will be calculated by the following formula

$$\overline{MG} = \frac{D^2}{8l} - \left(a - \frac{l}{2} \right) \quad (14)$$

It is mentioned that l in Eq. (14) can be eliminated from the equilibrium condition before tilting using following relation

$$W = \pi \left(\frac{D}{2} \right)^2 l \rho g \quad (15)$$

And that is

$$l = \frac{4W}{\rho g \pi D^2} \quad (16)$$

From Eqs. (14–16), the stability is given by examining the sign of \overline{MG} as the weight is slid upward

$$a < \frac{D^2}{8l} + \frac{l}{2}; \quad \text{stable}$$

$$a = \frac{D^2}{8l} + \frac{l}{2}; \quad \text{meta stable}$$

$$a > \frac{D^2}{8l} + \frac{l}{2}; \quad \text{unstable}$$

Exercise 3.6 Measurement of Surface Tension

A plate with the dimension of Height \times Width \times Depth ($a \times b \times c$) and density ρ_p is submerged in a liquid B at the interface between the air and the liquid, as shown in Fig. 3.14. The density of the liquid B is ρ_B and that of air is ρ_A . The height of the submerged part of the plate is h_B from which the plate is pulled up from the liquid B . Determine the surface tension σ without knowing ρ_A and ρ_B in advance; however, the contact angle θ is known.

Ans.

Set the datum force F_0 before submerging the plate to the liquid B . F_0 is the force to hold the plate in the air; i.e.

$$\begin{aligned}
 F_0 &= g\rho_P bca - g\rho_A bca \\
 &= gbc(\rho_P - \rho_A)(h_A + h_B)
 \end{aligned}
 \tag{1}$$

The second term on the right hand side of Eq. (1) is the net force exerted by the air, otherwise known as the buoyant force. The force balance when the plate is submerged in liquid B is given by

$$F + F_A + F_B + F_\sigma + W = 0 \tag{2}$$

F is the lift force, F_A is the net force exerted by the air, F_B is the buoyant force of liquid B , F_σ is the net force due to surface tension and W is the weight of the plate. Accordingly, these forces are:

$$F_A = -\rho_A gh_A bc \tag{3}$$

$$F_B = -\rho_B gh_B bc \tag{4}$$

$$F_\sigma = -\sigma[2(b+c)]\cos\theta \tag{5}$$

$$\begin{aligned}
 W &= -\rho_P gabc \\
 &= -\rho_P g(h_A + h_B)bc
 \end{aligned}
 \tag{6}$$

Thus, from Eqs. (3–6), Eq. (2) gives F as

$$F = gbc\{h_A(\rho_P + \rho_A) + h_B(\rho_P + \rho_B)\} + \sigma(2bc)\cos\theta \tag{7}$$

Using F_0 in Eqs. (1–7), we have following relationship

$$\sigma = \frac{1}{2(b+c)\cos\theta} \{(F - F_0) - gbch_B(\rho_A - \rho_B)\} \tag{8}$$

Thus, when the plate is pulled up to position, and when the bottom of the plate is just lined up with the level of the liquid h_B , i.e. $h_B = 0$, we can obtain the surface tension σ , measuring F at $h_B = 0$

$$\sigma = \frac{1}{2(b+c)\cos\theta} (F - F_0) \tag{9}$$

The contact angle θ must be measured while the plate is submerged. The technique to measure the surface tension is called the Wilhelmy plate method.

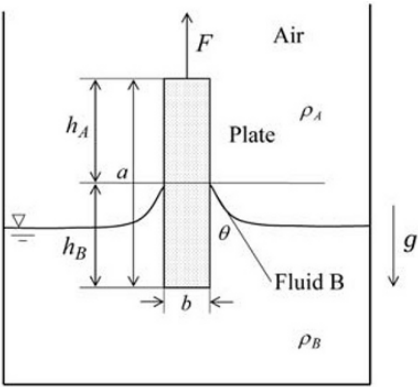


Fig. 3.14 The Wilhelmy plate

Exercise 3.7 Pressure vessels

Obtain wall stress of (a) a Spherical tank and (b) a Cylindrical tank, as shown in Fig. 3.15.

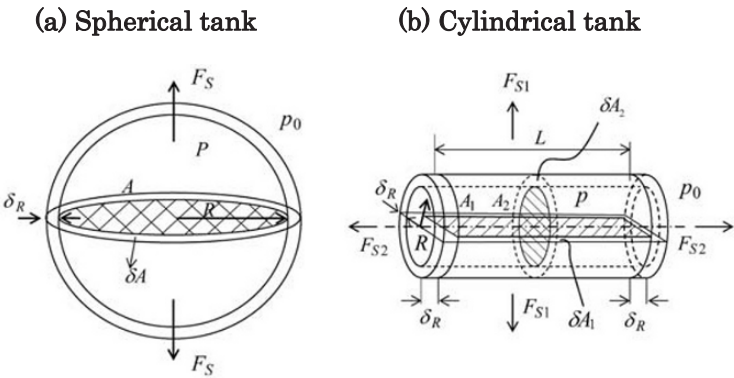


Fig. 3.15 Pressure vessels

Ans.

(i) The configuration of the spherical tank is spherically symmetric, so that force F_S , which keeps both halves of the sphere apart, is supported by the cross-sectional area of wall δA . From Eq. (3.1.34), F_S is obtained by

$$F_S = (p - p_0)A = (p - p_0)\pi R^2 \quad (1)$$

Thus the stress of the wall τ_W is

$$\tau_W = \frac{F_S}{\delta A} = \frac{(p - p_0)\pi R^2}{2\pi R \delta_R + \pi \delta_R^2} \quad (2)$$

If $\delta_R \ll R$, the stress τ_W can be calculated by

$$\tau_W = \frac{(p - p_0)R}{2\delta_R} \quad (3)$$

(ii) In the case of the cylindrical tank, there are two principle forces acting on the wall. One is the radial force F_{S1} , and another is the axial force F_{S2} , both of which keep the halves of the tank apart in each direction. Again from Eq. (3.1.34), the radial force F_{S1} is

$$F_{S1} = (p - p_0)A_1 = (p - p_0)2RL \quad (4)$$

Thus, the stress of the wall τ_{W1} due to F_{S1} force can be obtained from

$$\tau_{W1} = \frac{F_{S1}}{\delta_{A2}} = \frac{(p - p_0)2RL}{2(2R + 2\delta_R)\delta_R + 2(\delta_R \times L)} \quad (5)$$

If $\delta_R \ll R$, the stress τ_{W1} will become approximately

$$\tau_{W1} = \frac{(p - p_0)RL}{(2R + L)\delta_R} \quad (6)$$

Similarly, the stress of the wall τ_{W2} due to the F_{S2} force will be

$$\tau_{W2} = \frac{F_{S2}}{\delta_{A2}} = \frac{(p - p_0)\pi R^2}{2\pi R \delta_R + \pi \delta_R^2} \quad (7)$$

If $\delta_R \ll R$, the τ_{W2} becomes approximately

$$\tau_{W2} = \frac{(p - p_0)R}{2\delta_R} \quad (8)$$

Eventually it will be the same as the spherical tank case in axial direction.

Exercise 3.8 Oil Feeding Reservoir

The cylindrical container shown in Fig. 3.16 is rotated with the shaft about its centerline. Lubrication oil, whose density is ρ with height h , is enclosed in the container before rotation. What is the rotational speed necessary for the oil to reach the diameter D at the upper wall of the container? Also, obtain the pressure p_A at the lower corner of the container at point A, when it is rotated at that speed. Note that the container is opened for atmospheric pressure p_a .

Ans.

From Eq. (3.1.41), the profile of the free surface is given by

$$z - z_0 = \frac{\Omega^2 r^2}{2g} \quad (1)$$

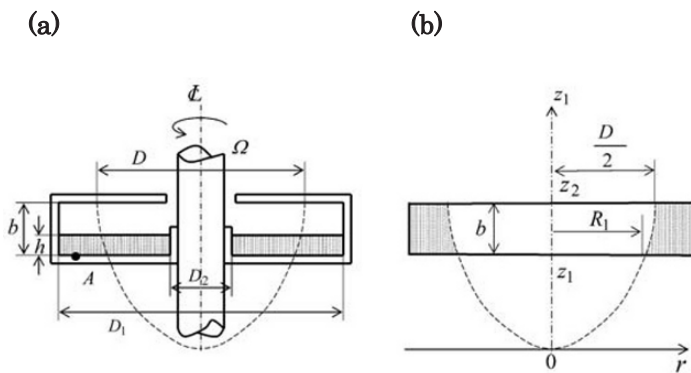


Fig. 3.16 Oil feeding reservoir

z_0 is the datum level, Ω is the angular velocity of the rotation and r is the radius. Setting $z_0 = 0$, a portion of the free surface is a paraboloid of revolution. Denote z_1 and z_2 as points on the lower wall and the upper

wall of the container respectively from the level $z_0 = 0$. From Eq. (1), z_1 and z_2 are thus given by the following formula

$$z_2 = \frac{\Omega^2}{2g} \left(\frac{D}{2} \right)^2 \quad (2)$$

$$z_1 = z_2 - b \quad (3)$$

From Eqs. (2) and (3), the radius of the free surface R_1 at the level of z_1 is easily obtained from

$$R_1^2 = \left(\frac{D}{2} \right)^2 - \frac{2g}{\Omega^2} b \quad (4)$$

Knowing radii $D/2$ and R_1 , we can obtain the volume of oil V contained after rotation from

$$V = \pi \left\{ \left(\frac{D}{2} \right)^2 - R_1^2 \right\} \frac{b}{2} + \pi \left\{ \left(\frac{D_1}{2} \right)^2 - \left(\frac{D}{2} \right)^2 \right\} b \quad (5)$$

This is further written in terms of the known parameters as

$$V = \pi \left[\left(\frac{2g}{\Omega^2} \right) \frac{b^2}{2} + \left\{ \left(\frac{D_1}{2} \right)^2 - \left(\frac{D}{2} \right)^2 \right\} b \right] \quad (6)$$

The oil volume contained at the original state before the rotation, is given by

$$V = \pi \left\{ \left(\frac{D_1}{2} \right)^2 - \left(\frac{D_2}{2} \right)^2 \right\} h \quad (7)$$

From equating Eqs. (6) and (7), we can obtain the required Ω as

$$\Omega = \sqrt{\frac{gb^2}{\left\{ \left(\frac{D_1}{2} \right)^2 - \left(\frac{D_2}{2} \right)^2 \right\} h - \left\{ \left(\frac{D_1}{2} \right)^2 - \left(\frac{D}{2} \right)^2 \right\} b}} \quad (8)$$

To find the pressure at point A as indicated in Fig. 3.16, we use Eq. (3.1.40)

$$p_A = \frac{1}{2} \rho \Omega^2 \left\{ \left(\frac{D_1}{2} \right)^2 - R_1^2 \right\} - \rho g z_1 + p_a \quad (9)$$

Also, by Eqs. (1), (2), (3) and (4), we can calculate p_A as

$$p_A = \frac{1}{2} \rho \left\{ \left(\frac{D_1}{2} \right)^2 - 2 \left(\frac{D}{2} \right)^2 \right\} \frac{gb^2}{\left\{ \left(\frac{D_1}{2} \right)^2 - \left(\frac{D_2}{2} \right)^2 \right\} h - \left\{ \left(\frac{D_1}{2} \right)^2 - \left(\frac{D}{2} \right)^2 \right\} b} + 2\rho g b + p_a \quad (10)$$

This is an example of an oil feeding reservoir for lubricating and cooling a vertical shaft bearing. Installing an oil feed tube at point A, oil is fed to the bearing part with pressure p_A when the shaft is rotated with angular velocity Ω .

Problems

- 3-1. Obtain the pressure if a U-tube manometer, which is installed at the pipe centerline, of a horizontal oil transportation pipe and reads 200 mmHg. The oil in the manometer is depressed 150 mm below the pipe centerline. The density ρ_0 of the oil is $0.80 \times 10^3 \text{ kg/m}^3$ and the density ρ_m of the mercury is $13.6 \times 10^3 \text{ kg/m}^3$.

Ans. $[25.5 \times 10^3 \text{ N/m}^2 \text{ gauge}]$

- 3-2. Calculate the atmospheric pressure, temperature, and density at an altitude of 15 km, in such a case as the troposphere being 11 km high. The pressure and temperature at sea level are 101.3 kN/m^2 and 15°C respectively. The polytropic index $n = 1.235$ is equal in the troposphere and it is assumed that the stratosphere is isothermal. Note that the stratosphere is the second layer of atmosphere after the troposphere, and is extended over 11km above.

$$\text{Ans. } \begin{bmatrix} 0.120 \times 10^5 \text{ N/m}^2 \\ 216.5 \text{ K} \\ 0.1933 \text{ kg/m}^3 \end{bmatrix}$$

- 3-3. A circular observation window of 0.5 m in diameter is installed in an inclined tank wall at 60° to the horizontal level. The water is 5 m deep above the center of the window. Determine the resultant hydrostatic pressure force on the window and the center of pressure.

$$\text{Ans. } \begin{bmatrix} 9.63 \times 10^3 \text{ N} \\ 2.71 \times 10^{-3} \text{ m below the center of the window.} \end{bmatrix}$$

- 3-4. A barge is loaded with coal such that the center of gravity of the barge with the loaded coal is at the waterline, as shown in Fig. 3.17. Discuss the stability of the barge.

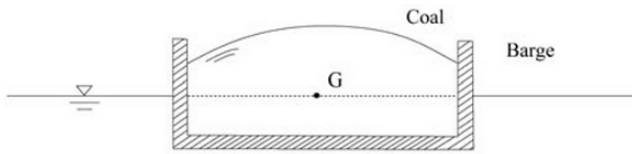


Fig. 3.17 Loaded barge

- 3-5. There is an air bubble 1.0×10^{-3} m in diameter in the water. Knowing the surface tension $\sigma = 72.8 \times 10^{-3}$ N/m (water-air interface), estimate the pressure inside of the bubble. The depth of the water where the bubble is found is 10m below the water level. Also, calculate the diameter where the bubble is raised to a depth of 5m below the water level.

$$\text{Ans. } \begin{bmatrix} 1.997 \times 10^5 \text{ N/m}^2 \text{ abs.} \\ 1.099 \times 10^{-3} \text{ m} \end{bmatrix}$$

- 3-6. Utilizing a U-tube, an accelerometer is made to measure the acceleration of a train, as shown in Fig. 3.18. The meter is mounted in the vehicle so that the legs are vertical, and the tube is filled with a liquid of ρ . Measuring the level difference Δh between the legs, determine the acceleration a_x of the vehicle. The distance between the legs is L .

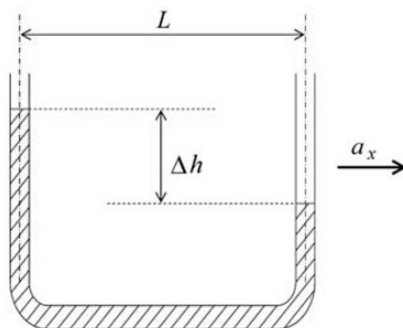


Fig. 3.18 U-tube accelerometer

$$Ans. \left[\left(\frac{\Delta h}{L} \right) g \right]$$

Nomenclature

A, a	: area
\mathbf{a}	: acceleration vector
\mathbf{a}_r	: relative acceleration
a, b, d, l	: length (scale)
C	: center of pressure
D, d	: diameter
\mathbf{F}	: force vector
G	: center of gravity
\mathbf{g}	: body force
\mathbf{g}	: gravity acceleration
h	: height or length
I	: I_x second moment of surface area I_{xy} product of surface area
$\hat{\mathbf{n}}$: unit normal vector
p	: thermodynamic pressure
p_0	: reference pressure
p_a	: atmospheric pressure

R, r	: specific gas constant (R) or radius
S	: area
T	: temperature
\mathbf{T}	: total stress tensor
t	: time
$\hat{\mathbf{t}}$: unit tangential vector
\mathbf{u}	: velocity vector
V	: finite volume
x_C	: center of pressure (x direction)
x_G	: x directional centroid
y_C	: center of pressure (y direction)
y_G	: y directional centroid
x, y, z	: Cartesian coordinates system
r, θ, ϕ	: spherical coordinates system
α, β, γ	
and α', β', γ'	: angle
ρ	: density
σ	: surface tension
τ_c	: couple force
ϕ	: scalar potential
Ω	: angular velocity

Bibliography

Basic problems in hydrostatics and fluid transport are treated to a greater extent in the following sources.

1. E.J. Shaughnessy, I.M. Katz and J.P. Schaffer, *Introduction to Fluid Mechanics*, Oxford University Press, Inc., Oxford, 2005.
2. D.N. Roy, *Applied Fluid Mechanics*, Ellis Horwood Limited, 1988.
3. W.P. Graebel, *Engineering Fluid Mechanics*, Taylor & Francis Publishers, Abigdon, 2001.
4. M.C. Potter, D.C. Wiggert and M. Hondzo, *Mechanics of Fluids* (2nd edition), Prentice-Hall, Inc., Englewood Cliffs, NJ, 1997.

4. Perfect Flow

In this chapter, we will look at the simplest form of constitutive equations for fluids having no viscous stress. To expand our range of applications further, we will then extend the concept of inviscid flow to include potential flow and unidirectional incompressible flow.

Within a frame work of inviscid flow many useful formulae for turbomachineries will be examined in this chapter. Other examples which are widely observed in fluid engineering are to be treated with the concept of inviscid flow, and correspond with viscous flow at large Reynolds numbers. A fluid with no viscous stress is often referred to as a perfect fluid, and the constitutive equation takes the simplest form as follows

$$T_{ij} = -p\delta_{ij} \quad (4.1)$$

A detailed discussion regarding the constitutive equation of Eq. (4.1) will be given in the following section. Presently, however, please note that when we substitute Eq. (4.1) into Eq. (2.2.7) we can obtain

$$\rho \left(\frac{\partial \mathbf{u}}{\partial t} + \mathbf{u} \cdot \nabla \mathbf{u} \right) = -\nabla p + \rho \mathbf{g} \quad (4.2)$$

Here, the body force $\rho \mathbf{g}$ is treated as the gravitational force (per unit volume). This equation is called the Euler equation, and is valid for inviscid flows in general. In many engineering problems, the Euler equation is solved or reduced into a more convenient form with the continuity equation of Eq. (2.1.5).

4.1 Potential and Inviscid Flows

When flows are far from solid surface, which is often observed outside the boundary layer, the effects of viscosity are usually very small and it is assumed that flows are frictionless and irrotational. These flows are known as potential flows. If the flow is irrotational, the velocity field can be written as follows, with reference to Eq. (1.1.26)

$$\nabla \times \mathbf{u} = 0 \quad (4.1.1)$$

Additionally, with a vector identity, it immediately follows that there exists a velocity potential ϕ , such that the velocity \mathbf{u} can be defined as

$$\mathbf{u} = -\nabla \phi \quad (4.1.2)$$

Furthermore, if we impose the condition of a steady incompressible flow to the potential flow, from the continuity equation Eq. (2.1.6) the velocity potential ϕ satisfies Laplace's equation as follows

$$-\nabla \cdot (\nabla \phi) = 0 \quad (4.1.3)$$

and

$$\nabla^2 \phi = 0 \quad (4.1.4)$$

As such ϕ serves a harmonic function. If we further confine our consideration here to two dimensional steady incompressible flows, we can introduce another important scalar function, the stream function ψ . ψ is defined in such a way that the velocity components ($u_1, u_2 = u, v$) of \mathbf{u} in Cartesian coordinates ($x_1, x_2 \equiv x, y$) are given by the following relations to satisfy the continuity equation of Eq. (2.1.6)

$$u = \frac{\partial \psi}{\partial y} \quad \text{and} \quad v = -\frac{\partial \psi}{\partial x} \quad (4.1.5)$$

Besides which, we have the condition of irrotational flow, given by Eq. (4.1.1) in two dimensional space written as

$$\frac{\partial v}{\partial x} - \frac{\partial u}{\partial y} = 0 \quad (4.1.6)$$

Substituting u and v of Eq. (4.1.5) into Eq. (4.1.6) again satisfies Laplace's equation, yielding the condition that ψ is also harmonic as follows

$$\nabla^2 \psi = 0 \quad (4.1.7)$$

Note that the stream function ψ can be defined for any two dimensional flow, or flow in two dimensional symmetric plane, regardless of whether the flow is irrotational or not. This holds true as long as the flow is steady incompressible.

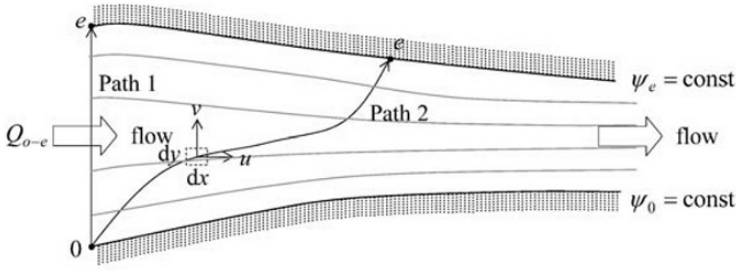


Fig. 4.1 Stream function

Two important concepts arise from the stream function. First, the lines of constant stream function ψ are the streamlines. Second, the difference between the numerical values of two stream functions, such as $\psi_e - \psi_0$ in Fig. 4.1, is equal to the flow rate Q_{e-0} intersecting the two lines. This is derived from following the formula

$$Q_{e-0} = - \int_0^e (v dx - u dy) = \int_0^e \left(\frac{\partial \psi}{\partial x} dx + \frac{\partial \psi}{\partial y} dy \right) = \int_0^e d\psi = \psi_e - \psi_0 \quad (4.1.8)$$

The integral Eq. (4.1.8) is independent of the path, as shown in Fig. 4.1 for path 1 and path 2. Furthermore, Eq. (4.1.8) yields the result for a closed path c that

$$\oint_c d\psi = 0 \quad (4.1.9)$$

Equations (4.1.4) and (4.1.7) are valid in any coordinates system, and it has to be notified that Eqs. (4.1.2) and (4.1.5) yield the following relationships

$$u = \frac{\partial \phi}{\partial x} = \frac{\partial \psi}{\partial y}, \quad v = \frac{\partial \phi}{\partial y} = -\frac{\partial \psi}{\partial x} \quad (4.1.10)$$

Similarly, for instance with the polar coordinates r and θ , and the corresponding velocity components u_r and u_θ respectively, we can write the fundamental relationships as follows

$$u_r = \frac{\partial \phi}{\partial r} = \frac{1}{r} \frac{\partial \psi}{\partial \theta}, \quad u_\theta = \frac{1}{r} \frac{\partial \phi}{\partial \theta} = -\frac{\partial \psi}{\partial r} \quad (4.1.11)$$

The relationships, such as given by Eqs. (4.1.10) or (4.1.11) are called the Cauchy-Riemann conditions. An important result from the fact that ϕ and ψ are harmonic, which satisfy the Cauchy-Riemann conditions, is that lines of ϕ and ψ are mutually orthogonal, as indicated in Fig. 4.2.

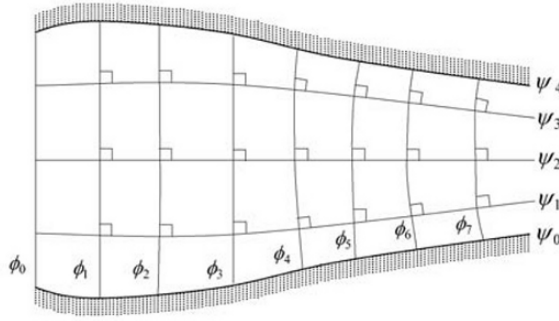


Fig. 4.2 Stream function ψ and velocity potential ϕ

Considering the fact that ϕ and ψ satisfy the Cauchy-Riemann conditions, a complex function $W(z)$, called the complex potential, is defined in such a way that

$$W(z) = \phi + i\psi \quad (4.1.12)$$

Here, $i = \sqrt{-1}$ and $z = x + iy$. We consider ϕ and ψ to be functions of z , the complex variable, instead of x and y . The physical flow can be presented with a complex number z in a space, called z -plane. $W(z)$ is an analytic function, where ϕ and ψ are conjugate functions, which satisfies $\nabla^2\phi = \nabla^2\psi = 0$.

Differentiating $W(z)$ with respect to z gives the following relationship

$$\frac{dW}{dz} = u - iv = w \quad (4.1.13)$$

where w is the complex velocity. The conjugate functions ϕ and ψ satisfy Laplace's equation, which is linear. We may be, therefore, able to superimpose solutions ϕ and ψ for different flows to obtain the new values of ϕ and ψ . In other words, we can superimpose the flows to determine a new $W(z)$. This is often put into practice with such that a source, sink, or potential vortex, or doublet is superimposed onto a uniform flow.

There are typical complex potentials $W_i(z)$ of some basic flows listed below:

$$W_0(z) = U_\infty z, \quad (4.1.14)$$

U_∞ ; real constant. The flow is uniform flow field; (Fig. 4.3(a))

$$W_1(z) = \frac{q}{2\pi} \ln z, \quad (4.1.15)$$

q ; real constant. The flow is source ($q > 0$) and sink ($q < 0$);
(Fig. 4.3(b))

$$W_2(z) = i \frac{\Gamma}{2\pi} \ln z, \quad (4.1.16)$$

Γ ; circulation, real constant. The flow is potential vortex;
(Fig. 4.3(c))

$$W_3(z) = \frac{m}{z}, \quad (4.1.17)$$

m ; doublet strength, real constant. The flow is doublet;
(Fig. 4.3(d))

$$W_4(z) = W_0(z) + W_3(z) = U_\infty z + \frac{m}{z} = U_\infty \left(z + \frac{a^2}{z} \right) \quad (4.1.18)$$

U_∞ , m and a ; real constants. The flow is flow past a circular
cylinder; (Fig. 4.3(e))

There are more complex flow fields to be generated by combination of those complex potential $W_i(z)$. Some schematics are displayed in Fig. 4.3(a–e), which are respectively corresponded to Eqs. (4.1.14–4.1.18).

With a mathematical technique, called a conformal mapping, a simple flow pattern can be transformed into a more complex one, such as flow past around a rotating cylinder to airfoils and etc. One of the most known mapping function is

$$z = \zeta + \frac{a^2}{\zeta} \quad (4.1.19)$$

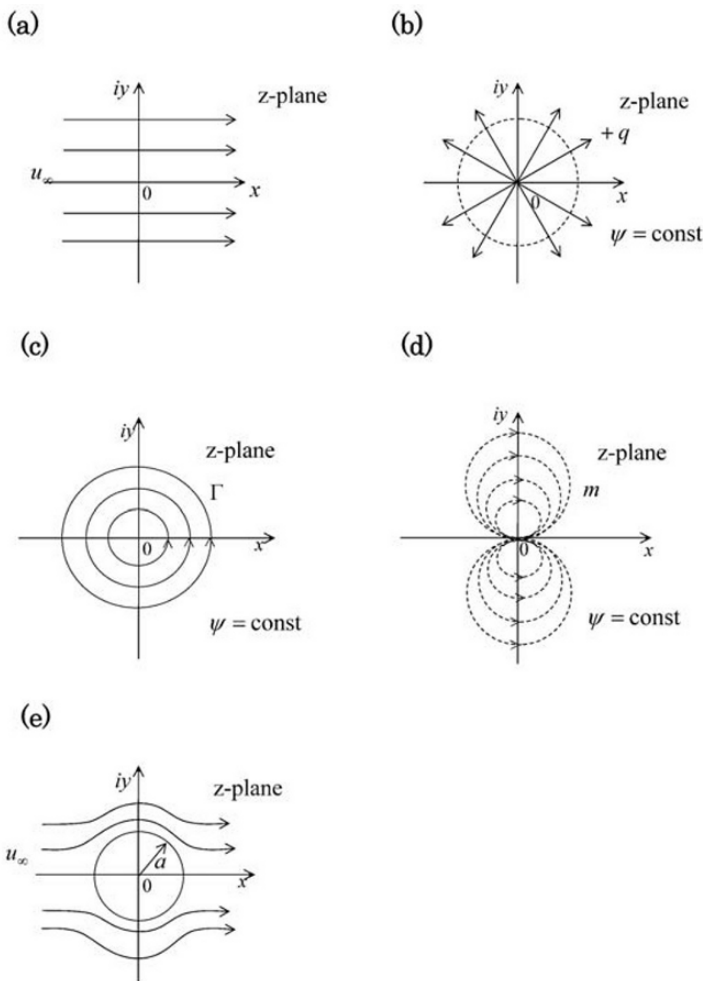


Fig. 4.3 Flow patterns with $W_i(z)$

Note that $\zeta = \eta(x, y) + i\xi(x, y)$ and a is positive real constant. The mapping function given by Eq. (4.1.19) is the Joukowski transformation, which transforms $W_4(z)$ of Eq. (4.1.18) into a flow on airfoil, for example. In general, a mapping function $\zeta = f(z)$ transforms a basic flow in z -plane to $\eta - \xi$ plane, where the orthogonality of ϕ and ψ is preserved.

When we consider an inviscid flow, lifting the irrotational condition, the Navier-Stokes equation reduces to the Euler equation given by Eq.

(4.2). The Euler equation is often used to investigate compressible flow at high speed, where viscous and turbulent effects are important only in a limited region near solid surfaces. With modern computers, flows over an aircraft may be simulated using Euler equations with which flows do not stick to walls and slip is allowed at the solid boundaries. Such flow simulations with the aid of computational fluid dynamics (CFD) are being done on a research basis, and we shall not go too deeply into this field of study, though these compressible flows will be treated in later chapters in this text.

Considering the Euler equation, we now look into the most important theorem in engineering fluid mechanics, Bernoulli's theorem. The Euler equation of Eq. (4.2) can be written in general vector form, using vector identity in the convective term as follows

$$\rho \left(\frac{\partial \mathbf{u}}{\partial t} + \nabla \frac{1}{2} |\mathbf{u}|^2 - \mathbf{u} \times \nabla \times \mathbf{u} \right) = -\nabla p + \rho \mathbf{g} \quad (4.1.20)$$

and

$$\frac{\partial \mathbf{u}}{\partial t} + \nabla \frac{1}{2} |\mathbf{u}|^2 - \mathbf{u} \times \boldsymbol{\omega} = -\frac{1}{\rho} \nabla p - \nabla \Phi \quad (4.1.21)$$

The gravitational force $\rho \mathbf{g}$ is assumed here as a conservation force and is written by a scalar potential Φ as

$$\rho \mathbf{g} = -\rho \nabla \Phi \quad (4.1.22)$$

The first integral of the equation can be obtained by integrating Eq. (4.1.21) between two arbitrary points along a path l , letting $d\mathbf{l}$ be a line element of length along the path l . We then have

$$\int_1^2 \frac{\partial \mathbf{u}}{\partial t} \cdot d\mathbf{l} + \int_1^2 \left(\frac{1}{2} |\mathbf{u}|^2 \right) \cdot d\mathbf{l} + \int_1^2 \frac{1}{\rho} \nabla p \cdot d\mathbf{l} + \int_1^2 \frac{\partial \Phi}{\partial t} \cdot d\mathbf{l} = \int_1^2 \mathbf{u} \times \boldsymbol{\omega} \cdot d\mathbf{l} \quad (4.1.23)$$

The third term on the left side of Eq. (4.1.23) contains thermodynamics properties, ρ and p , and if we assume that the flow along l is isentropic, then the relationship between ρ and p is

$$p = f(\rho) \quad (4.1.24)$$

From Eq. (4.1.24), the integral can be replaced by the function

$$\int \frac{\partial P(\rho)}{\partial t} \cdot d\mathbf{l} = \int \frac{1}{\rho} \nabla p \cdot d\mathbf{l} \quad (4.1.25)$$

The function $P(\rho)$ is called the pressure function. On the right side of Eq. (4.1.23), the integral of $\mathbf{u} \times \boldsymbol{\omega}$ along l will become null, if we take the path l either along a stream line or a vortex line. This occurs because \mathbf{u} and $\boldsymbol{\omega}$ are mutually perpendicular and there are no components of either vector along the path l . Therefore, if the flow is steady, i.e. $\partial \mathbf{u} / \partial t = 0$, the integral Eq. (4.1.23) yields the following formula, where the integral is carried out either along a stream line or a vortex line to give

$$\frac{1}{2} |\mathbf{u}_1|^2 + P_1 + \Phi_1 = \frac{1}{2} |\mathbf{u}_2|^2 + P_2 + \Phi_2 \quad (4.1.26)$$

This is the basic form of the Bernoulli equation. The first term (in both sides of Eq. (4.1.26) shows the kinetic energy per unit mass, the second term is the pressure potential per unit mass, and the third term represents the external force (body force) due to potential energy per unit mass. Namely, the Bernoulli equation contains three kinds of energy, and total of which are conserved. The Bernoulli equation is valid for either along a stream line or a vortex line with inviscid, isentropic and steady flows. When we take a surface with constant value of either a stream line or a vortex line, Eq. (4.1.26) can be reduced to the form

$$\frac{1}{2} |\mathbf{u}|^2 + P + \Phi = \text{const.} \quad (4.1.27)$$

This surface is often called the Bernoulli's surface, if we choose the Bernoulli's surface as a stream tube, as depicted in Fig. 4.4. We can include the mass continuity with the Bernoulli equation. Often such one dimensional flow equations are used in many engineering problems. From the continuity equation of Eq. (2.1.5), assuming a steady flow, a volume integral to an element of the stream tube, ①–② in Fig. 4.4, gives

$$\int_V \nabla \cdot \rho \mathbf{u} dV = 0 \quad (4.1.28)$$

Moreover, by the Gauss's divergence theorem, it becomes

$$\int_A \rho \mathbf{u} \cdot d\mathbf{S} = 0 \quad (4.1.29)$$

Additionally, over the entire surface of the stream tube we have

$$\int_{A_1} \rho \mathbf{u} \cdot d\mathbf{S}_1 + \int_{A_2} \rho \mathbf{u} \cdot d\mathbf{S}_2 + \int_{A_3} \rho \mathbf{u} \cdot d\mathbf{S}_3 = 0 \quad (4.1.30)$$

Since there is no flow across the surface of the stream tube of the Bernoulli's surface, the third term of Eq. (4.1.30) is zero.

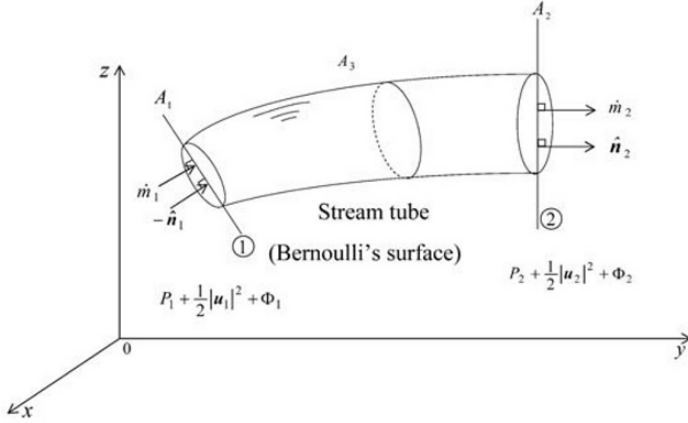


Fig. 4.4 Bernoulli's theorem

$$\int_{A_1} \rho \mathbf{u} \cdot d\mathbf{S}_1 = - \int_{A_2} \rho \mathbf{u} \cdot d\mathbf{S}_2 \quad (4.1.31)$$

If we take an outward surface positive and at ① and ② namely at the inlet and outlet respectively, $\mathbf{n}_1 \perp d\mathbf{S}_1$ and $\mathbf{n}_2 \perp d\mathbf{S}_2$ are assumed, we resultantly derive the mass continuity as follows

$$\rho_1 u_1 A_1 = \rho_2 u_2 A_2 \quad (4.1.32)$$

and

$$\dot{m} = \rho u A = \text{const.} \quad (4.1.33)$$

\dot{m} is the mass flow rate, which is conserved at any position along the stream tube, see also Exercise 2.1. The set of equations, Eqs. (4.1.27) and (4.1.33), are often used to solve engineering problems, that is, the Bernoulli equation together with the mass continuity may be used or reduced to appropriate forms under various flow situations.

If a flow is irrotational, the velocity field has a scalar potential, similar to Eq. (4.1.2) as

$$\mathbf{u} = \nabla \phi \quad (4.1.34)$$

Furthermore, if we assume a time dependent inviscid flow, we can obtain a more general form of the Bernoulli equation from Eq. (4.1.23) in the same manner

$$\frac{\partial \phi}{\partial t} + \frac{1}{2} |\mathbf{u}|^2 + P + \Phi = f(t) \quad (4.1.35)$$

Equation (4.1.35) is often called the pressure equation and has more broad application in time dependent inviscid flows (for perfect flow).

In many engineering applications of hydraulics, flows are to be steady incompressible and the body force (external force) is gravitational, so that P and Φ can be written as

$$P = \frac{P}{\rho} \text{ and } \Phi = gz \quad (4.1.36)$$

g is the gravitational acceleration, and z is the coordinate from a datum level in the gravity field. So Eq. (4.1.35) can be written together with the continuity equation as follows

$$Q = uA = \text{const.} \quad (4.1.37)$$

and

$$\frac{1}{2} \rho u^2 + p + \rho g z = \text{const.} \quad (4.1.38)$$

Q is the volume flow rate. In hydraulics, Eq. (4.1.38) is often called the Bernoulli equation (energy per unit volume). We may also express Eq. (4.1.38) in another form

$$\frac{u^2}{2g} + \frac{p}{\rho g} + z = \text{const.} = H \quad (4.1.39)$$

The Bernoulli equation of (4.1.39) is a form with a unit called head [m], and it states that the sum total of velocity head, pressure head and potential head remains constant along a stream tube (Fig. 4.4) for steady, incompressible and inviscid flow. The sum total of these three types of head is also called the total head H [m].

The Bernoulli equation can be further extended in the rotating reference frame, such as often encountered in turbo machineries. The acceleration of a fluid particle, which implies the stream tube between ① and ②, relative to the inertial reference frame, is derived in Eq. (1.2.12). Using the first integral of the Euler equation in the rotating reference frame, the formula may be written

$$\begin{aligned} & \int_1^2 \frac{\partial \mathbf{u}_r}{\partial t} \cdot d\mathbf{l} + \int_1^2 \left(\frac{1}{2} |\mathbf{u}_r|^2 \right) \cdot d\mathbf{l} - \int_1^2 \frac{\partial}{\partial t} \left(\frac{1}{2} \Omega^2 r^2 \right) \cdot d\mathbf{l} \\ & + \int_1^2 \frac{1}{\rho} \nabla p \cdot d\mathbf{l} + \int_1^2 \frac{\partial \Phi}{\partial t} \cdot d\mathbf{l} = \int_1^2 \mathbf{u}_r \times \boldsymbol{\omega}_r \cdot d\mathbf{l} - 2 \int_1^2 \mathbf{u}_r \times \boldsymbol{\Omega} \cdot d\mathbf{l} \end{aligned} \quad (4.1.40)$$

In hydraulic turbo machineries, the gravitational body force (the potential head) and the Coriolis force can be ignored compared to other dominant forces, so that the integral Eq. (4.1.40) along a stream line yields the following form, assuming the flow is steady and incompressible

$$\frac{p}{\rho g} + \frac{w^2}{2g} - \frac{u^2}{2g} = \text{const.} \quad (4.1.41)$$

w is the relative velocity in a rotating reference frame and u is the rotating speed of the stream tube to the inertial reference frame, i.e.

$$u = \Omega_z r \quad (4.1.42)$$

Through Eqs. (4.1.40–4.1.42) r is the radius of the stream tube from the axis of rotation. A detailed schematic is displayed in Fig. 4.5. It is mentioned here that it is sometimes convenient (or rather conventional) to draw a diagram to obtain the absolute velocity c at both end ① or ② in designing turbo machineries. The vector sum of these velocity diagrams, as shown in Fig. 4.5, is called the velocity diagram, which is explained in more detail in later chapters.

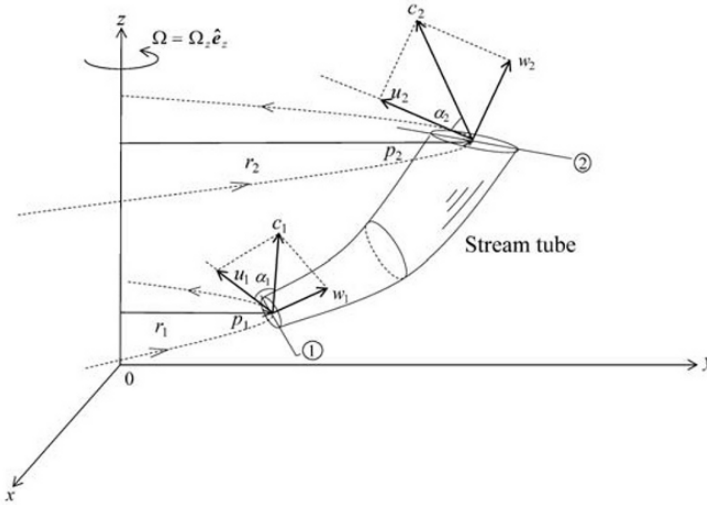


Fig. 4.5 Kinematic configuration of rotating stream tube

In engineering applications of fluid mechanics, one is often interested in estimating the overall force acting on a device in a region of space, where fluid enters and leaves. By extending a volume element, with which basic governing equations of fluid motion were derived in the previous chapter, we can identify the region of interest in fluid flow as a control

volume. A control volume may be fixed in space, or be moved with deformation in a turbo machinery, and it is recognized that the basic laws of dynamics can be applied directly to the control volume. The same holds true for the fluid particle concept. The conservation of linear momentum of the fluid particle given by Eq. (2.2.1), thus, directly applies to a control volume as follows

$$\frac{D}{Dt} \int_V \rho \mathbf{u} dV = \sum_i \mathbf{f}_i \quad (4.1.43)$$

\mathbf{f}_i represents the various forces acting on the control volume. Equation (4.1.43) is a form of Newton's second law of motion. In classical dynamics, Newton's second law is always the starting point. The inertia term of Eq. (4.1.43) can be written in an integral form over the control volume, which is fixed in space, according to Eq. (2.2.4)

$$\frac{\partial}{\partial t} \int_V \rho \mathbf{u} dV + \int_S \rho \mathbf{u} (\mathbf{u} \cdot \hat{\mathbf{n}}) dS = \sum_i \mathbf{f}_i \quad (4.1.44)$$

The second term on the left side of Eq. (4.1.42) is the net momentum flux across the control surface, and $(\mathbf{u} \cdot \hat{\mathbf{n}}) dS$ is simply the volume flux for each surface element $\hat{\mathbf{n}} dS$.

Equation (4.1.44) can be applied to a control volume, of a portion of stream tube or equivalently a device which has an entrance and an exit across which the flow may be uniform, as depicted in Fig. 4.6. Note that Fig. 4.6(a) is a stream tube when the forces $\sum_i \mathbf{f}_i$ are applied, and Fig. 4.6(b) is a more specific example of a configuration of single-suction pump treated as one control volume. The flow is rotated in the pump by axial shaft rotation of Ω and the flow velocity at the outlet \mathbf{u}_2 is 90° diverted from inlet \mathbf{u}_1 to discharge at higher pressure. Assuming the flow is steady, Eq. (4.1.44) can be considerably simplified as

$$\int_{A_1} \rho_1 \mathbf{u}_1 (\mathbf{u}_1 \cdot \hat{\mathbf{n}}) dS + \int_{A_2} \rho_2 \mathbf{u}_2 (\mathbf{u}_2 \cdot \hat{\mathbf{n}}) dS = \sum_i \mathbf{f}_i \quad (4.1.45)$$

and

$$-(\rho_1 u_1 A_1) \mathbf{u}_1 + (\rho_2 u_2 A_2) \mathbf{u}_2 = \sum_i \mathbf{f}_i \quad (4.1.46)$$

At the entrance, $\mathbf{u}_1 \cdot \hat{\mathbf{n}} = -u_1$, since the surface element $\hat{\mathbf{n}} dS$ faces inward and at the exit, $\mathbf{u}_2 \cdot \hat{\mathbf{n}} = u_2$. Thus, with the mass continuity by Eqs. (4.1.33), (4.1.46) can be written

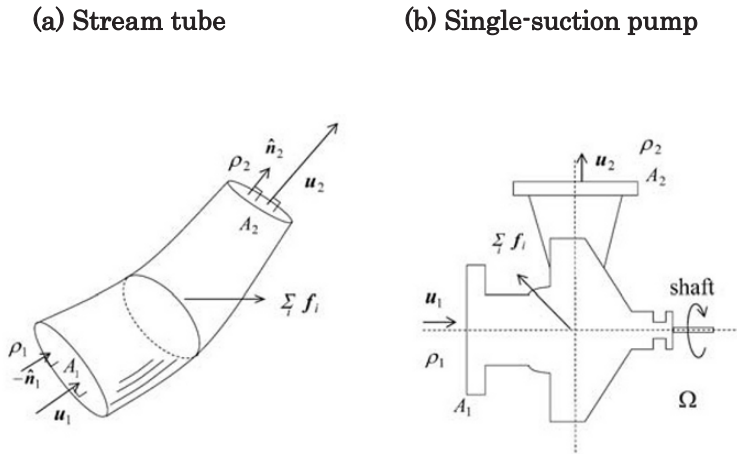


Fig. 4.6 Forces on control volume

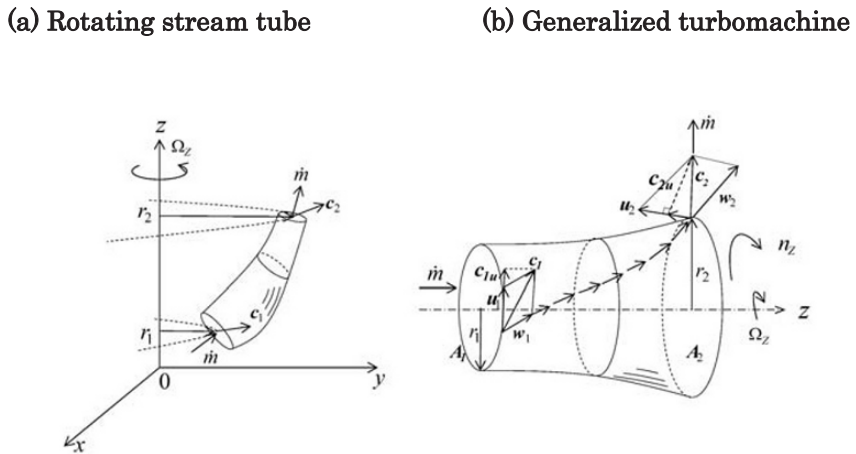


Fig. 4.7 Moment of momentum on control volume

$$\dot{m}(\mathbf{u}_2 - \mathbf{u}_1) = \sum_i \mathbf{f}_i \quad (4.1.47)$$

Note that Eq. (4.1.47) is a vector equation, with which Bernoulli equation of Eq. (4.1.26) and the mass continuity equation of Eq. (4.1.32) are valid. Forces \mathbf{f}_i , acting upon a control volume, can be a gravitational force (body force), a pressure (surface force), etc, and the sum of which is the net force that alters the flow directions \mathbf{u}_1 and \mathbf{u}_2 resultantly.

Knowing the linear momentum equation given by Eq. (4.1.47) of a control volume, we may be able to derive a moment-of-momentum equation for a control volume directly from the conservation of angular momentum for a non-polar fluid, i.e. the pseudovector \mathbf{A} is identically zero. Similar to Eq. (4.1.43), the linear momentum equation, we can write a moment-of-momentum equation (to be more exact, the angular momentum of linear momentum equation), according to Eq. (2.3.1)

$$\frac{D}{Dt} \int_V (\mathbf{x} \times \rho \mathbf{u}) dV = \sum_i \mathbf{n}_i \quad (4.1.48)$$

\mathbf{n}_i represents the torques (due to various forces) acting on a control volume. We can apply the Reynolds' transport theorem of Eq. (1.5.10–4.1.48) so that we can write

$$\int_V \frac{\partial(\mathbf{x} \times \rho \mathbf{u})}{\partial t} dV + \int_S \mathbf{x} \times \rho \mathbf{u} \cdot (\mathbf{u} \cdot \hat{\mathbf{n}}) dS = \sum_i \mathbf{n}_i \quad (4.1.49)$$

In the same manner that we derived the linear momentum equation of Eq. (4.1.47), assuming the flow is steady, Eq. (4.1.49) is written in a considerably simple form for a portion of stream tube, as shown Fig. 4.7(a) rotating around an axis of z with an angular velocity Ω_z , as follows

$$\dot{m}(\mathbf{r}_2 \times \mathbf{c}_2 - \mathbf{r}_1 \times \mathbf{c}_1) = \sum_i \mathbf{n}_i \quad (4.1.50)$$

\mathbf{r}_1 and \mathbf{r}_2 are position vectors of inlet and exit of the rotating stream tube respectively, and \mathbf{c}_1 and \mathbf{c}_2 are corresponding absolute velocities at inlet and exit respectively. Equation (4.1.50) is the moment-of-momentum equation for a control volume. It can be applied to the control volume enclosing the rotor of a generalized turbomachine, with reference to Fig. 4.7(b), as follows

$$\dot{m}(r_2 c_{2u} - r_1 c_{1u}) = n_z \quad (4.1.51)$$

c_{1u} and c_{2u} are the circumferential absolute velocities of entering and leaving flow from the rotating control volume (turbomachine) respectively and n_z is the net torque, acting on the control volume. Note that \mathbf{u}_1 and \mathbf{u}_2 are the circumferential velocity of rotating control volume in Fig. 4.7(b), where in the diagram the direction of \mathbf{u}_2 is rather toward the paper surface, but is deliberately oriented in a different direction for the sake of clarity. Equation (4.1.49) is directly obtained from Eq. (4.1.48), because we know that $\mathbf{r}_1 \perp \mathbf{c}_1$ and $\mathbf{r}_2 \perp \mathbf{c}_2$ are the inlet and outlet conditions. In Fig. 4.7(b), it is further noted that \mathbf{w}_1 and \mathbf{w}_2 are relative velocities, \mathbf{u}_1 and \mathbf{u}_2 are circumferential velocities (often referred to as the blade speed) respectively at inlet and exit of the rotating control volume (turbomachine). The rate of energy P_w , at which the control volume (turbomachine) does work on the fluid, is expressed by

$$P_w = n_z \cdot \Omega_z \quad (4.1.52)$$

and

$$P_w = \dot{m}(u_2 c_{2u} - u_1 c_{1u}) \quad (4.1.53)$$

The Eq. (4.1.53) is sometimes referred to as Euler's pump or turbine equation as well, depending on $P_w > 0$ or $P_w < 0$ respectively. See also Exercise 2.3.

Exercise

Exercise 4.1.1 Measurement of Flow Velocity by a Pitot Tube with Mach Correction

A velocity-measuring instrument called a Pitot tube, as show in Fig. 4.8, named after its inventor, Henri de Pitot (1695–1771), consists of the stagnation hole at the front of the tube measuring p_0 while the static holes on the side sense p_∞ . The velocity can be measured, knowing the pressure difference ($p_0 - p_\infty$), by a differential such as U-tube manometer, as depicted in Fig. 4.8. Explain the measurement principle, and discuss if the flow is not incompressible.

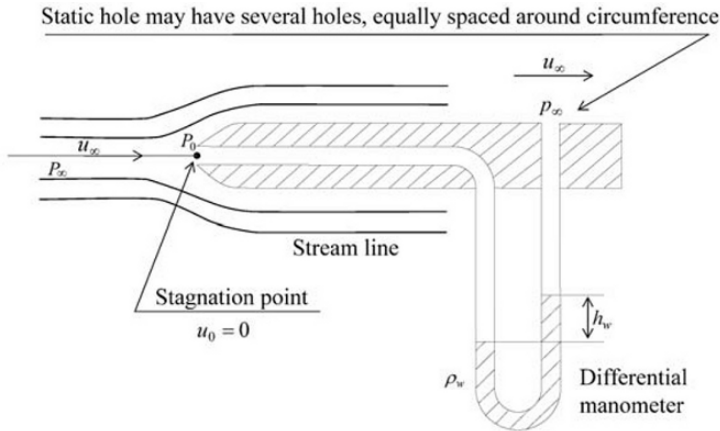


Fig. 4.8 Pitot tube

Ans.

Consider the Bernoulli equation of Eq. (4.1.38), which holds true at any point along the stream line of the flow. At the front of the tube (in fact any body immersed in a free stream), there is a stagnation point, at which the flow is diverted down stream and the velocity is zero. On the other hand in the upstream and downstream of the free stream, particularly close to a static hole (more strictly at a point along the stream line diverted from the stagnation point), the static pressure is p_∞ with the velocity of u_∞ . Thus, the Bernoulli equation will be

$$p_0 = \frac{1}{2} \rho u_\infty^2 + p_\infty \quad (1)$$

The gravitational potential (pressure head) is ignored due to small potential difference between the stagnation hole and the static hole. It is noted that p_0 is sometimes called the stagnation pressure and $\rho u_\infty^2 / 2$ is called the dynamic pressure. From Eq. (1), u_∞ can be obtained by

$$u_\infty = \sqrt{\frac{2(p_0 - p_\infty)}{\rho}} \quad (2)$$

A differential manometer placed across the output of these values registers the pressure difference $\Delta p = (p_0 - p_\infty)$, which is measured such that

$$\Delta p = \rho_w h_w g \quad (3)$$

ρ_w is the density of the liquid column and h_w is the reading for the column difference. Therefore, knowing ρ , the density of the fluid in priori, we can obtain the fluid velocity u_∞ by Eq. (2), measuring Δp by a differential manometer. In order to obtain accurate measurement, the position of the static holes is recommended as $6d$ apart from the stagnation hole, where d is the diameter of the tube and $d/2$ is the diameter of the stagnation hole.

A substantial error may occur if the tube is yawed with an angle facing the flow direction. Care must be taken in determining whether the direction of u_∞ is parallel to the axis of the tube, checking that Δp reading always remains at maximum with respect to the flow direction. Also when the velocity of a compressible flow becomes higher, a correction of compressibility becomes necessary. Although further details of the compressible flow analysis are given in the later chapter, we will consider here the correction of compressibility, commonly called the Mach correction of the Pitot tube.

This is done by considering the energy equation of the compressible flow with reference to Eq. (5.2.9), so we have

$$\frac{k}{k-1} \frac{p_0}{\rho_0} = \frac{1}{2} u_\infty^2 + \frac{k}{k-1} \frac{p_\infty}{\rho_\infty} \quad (4)$$

Equation (4) is the one dimensional steady compressible energy equation (ignoring gravitational potential), which is equivalent to Eq. (1), and where k is the specific heat ratio of the flow defined by $k = c_p / c_v$. From Eq. (4) with the definition of the Mach number M , i.e. $M = u_\infty / a$, where a is the sound speed, Eq. (4) can be rewritten as follows, with reference to Eq. (5.2.15)

$$\frac{p_0}{p_\infty} = \left(1 + \frac{k-1}{2} M^2 \right)^{\frac{k}{k-1}} \quad (5)$$

The right hand side of Eq. (5) can be expanded with binomial expansion

$$\frac{p_0}{p_\infty} = 1 + \frac{k}{2} M^2 \left(1 + \frac{1}{4} M^2 + \frac{2-k}{24} M^4 + \dots \right) \quad (6)$$

Thus, we have

$$p_0 = p_\infty + \frac{k}{2} \frac{u_\infty^2}{a^2} p_\infty \left(1 + \frac{1}{4} M^2 + \frac{2-k}{24} M^4 + \dots \right) \quad (7)$$

Since the required sound speed is defined as $a = \sqrt{kp_\infty / \rho_\infty}$, we can write Eq. (7) as

$$p_0 - p_\infty = \frac{\rho_\infty u_\infty^2}{2} \left(1 + \frac{1}{4} M^2 + \frac{2-k}{24} M^4 + \dots \right) \quad (8)$$

Therefore, the required speed u_∞ is written as

$$u_\infty = \varepsilon_M \sqrt{\frac{2(p_0 - p_\infty)}{\rho_\infty}} \quad (9)$$

ε_M is the correction coefficient ($\alpha_c = 1 + 1/4 M^2 + (2-k)/24 M^4 + \dots$ is called the compressibility factor, see more detail in Exercise 5.1) defined by

$$\varepsilon_M = 1 / \left(1 + \frac{1}{4} M^2 + \frac{2-k}{24} M^4 + \dots \right)^{\frac{1}{2}} = \alpha_c^{-\frac{1}{2}} \quad (10)$$

Based on Eq. (9), if the Mach number is $M=0.2$, for taking an ideal gas with $k=1.4$, ε_M will be $\varepsilon_M=0.995$ and only a 0.5% error in the measurement may occur due to the compressibility. Consequently when the flow velocity does not exceed $M=0.2$ (or if one allows some margin of error to $\varepsilon_M=0.97(3\%)$ when the Mach number is approximately $M=0.3$), the flow can be treated as incompressible and the velocity of which can be measured with Eq. (2) directly derived from the Bernoulli equation.

In supersonic flows, static holes will give a fair approximation of the static pressure upstream of the shock, provided that those static holes are placed at least $10d$ (diameter of the Pitot tube) downstream of the stagnation hole. For reference, see Shapiro (1953) and Bean (1971).

Exercise 4.1.2 Measurement of Volumetric Flow Rate by an Orifice Meter

Consider a steady state flow through a restrictive orifice plate with area A_0 mounted in a circular tube with area A_1 , as shown in Fig. 4.9. Downstream

of the orifice hole, the stream lines tend to converge to form a minimal flow area A_c , termed as the vena contracta. Static pressure taps are located before and after the orifice plate. One upstream tap is located in the undisturbed flow region, recommended at distance d before the plate, and another one is located in the vicinity of the vena contracta, recommended at distance $d/2$ after the plate, where d can be chosen as the diameter of the tube i.e. $d = d_1$. Assuming the flow is inviscid and incompressible, show the method of finding the flow rate Q in the tube by measuring the pressure difference. Also give some other examples to measure the flow rate other than the orifice meter.

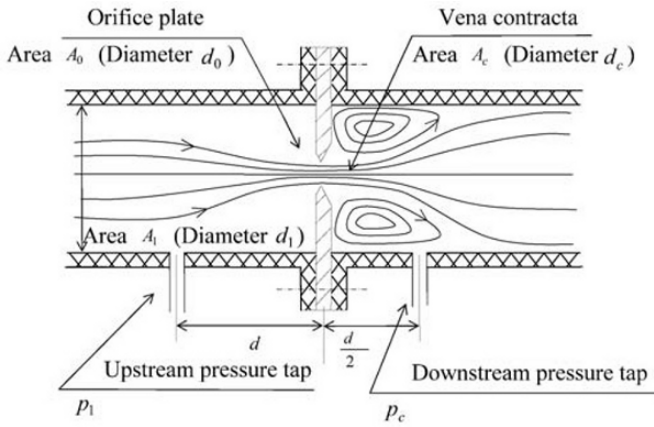


Fig. 4.9 Orifice meter

Ans.

The continuity equation Eq. (4.1.33) and the Bernoulli equation Eq. (4.1.38) are used to estimate the flow rate.

$$\dot{m} = \rho Q = \rho u_1 A_1 = \rho u_c A_c \quad (1)$$

And

$$\frac{1}{2} \rho u_1^2 + p_1 = \frac{1}{2} \rho u_c^2 + p_c \quad (2)$$

ρ is the density (constant) of the fluid, u_1 is the velocity at the position of

the upstream static tap which measures p_1 , and u_c is the velocity at the position of the vena contracta where the static pressure to be measured by the downstream tap is assumed to be p_c . The gravitational potential (pressure head) is ignored due to the fact that the distance between the static pressure taps is small enough and the tube is usually placed in a horizontal position. Combining Eqs. (1) and (2), and solving for u_c yields

$$u_c = \sqrt{\frac{2(p_1 - p_c)}{\rho \{1 - (A_c/A_1)^2\}}} \quad (3)$$

The ideal flow rate Q_i is

$$Q_i = u_c A_c \quad (4)$$

In realistic measurements, however, the exact measurements of p_c and A_c are difficult. Furthermore, they are also changed with viscous effects, or more specifically, with a changing Reynolds number. So it is convenient, in consideration of realistic flow measurement that A_c be replaced by introducing a correction factor C_c as follows

$$A'_c = C_c A_0 \quad (5)$$

C_c is termed the contraction coefficient. In a similar way, u_c may also be corrected by introducing a velocity coefficient C_v , since u_c in Eq. (3) includes A_c

$$u'_c = C_v \sqrt{\frac{2(p_1 - p_c)}{\rho \{1 - (C_c A_0/A_1)^2\}}} \quad (6)$$

Combining Eqs. (5) and (6), the actual flow rate Q is given by the relation

$$Q = \frac{C_v C_c A_0}{\sqrt{1 - (C_c A_0/A_1)^2}} \sqrt{\frac{2(p_1 - p_c)}{\rho}} \quad (7)$$

Conventionally the recommended correlation for flow rate Q through an orifice meter is

$$Q = K_f A_0 \sqrt{\frac{2}{\rho} (p_1 - p_c)} \quad (8)$$

K_f is the flow coefficient defined as

$$K_f = \frac{C_d}{\sqrt{1 - C_c^2 \beta^4}} \quad (9)$$

In Eq. (9), $C_d = C_v \cdot C_c$ is termed the discharge coefficient and $\beta = \sqrt{A_0/A_1} = d/d_0$ is the diameter ratio. The experimental values of K_f and C_d are primarily affected by the Reynolds number Re , β , other geometric effects such as the shape of the restrictive orifice, and the location of the static pressure taps. Namely for K_f , we can write

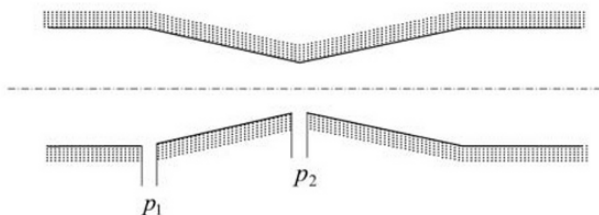
$$K_f = f(Re, \beta, \text{geometric effects}) \quad (10)$$

There are also compressibility effects to be considered, particularly in compressible fluids, when the throat Mach number is greater than about $M = 0.2$, as previously practiced in Exercise 4.1.1.

In regard to flow rate measurement instruments, as demonstrated here, an element of constriction is inserted into the fluid stream, where the pressure difference across the constriction is measured so as to give an estimate of the volumetric flow rate. These flow meters are known as Bernoulli obstruction flow meters, and other examples beside the orifice meter are the Venturi tube and the choked nozzle, as illustrated in Fig. 4.10 (a) and (b). The Venturi tube is designed to give the discharge coefficient nearly unity, while with the orifice meter a large flow distortion would occur and resultant has a fairly low discharge coefficient, sometimes in the area of 0.6. One advantage of the orifice meter is that it is quite inexpensive to make and install while the Venturi tube is the opposite. The flow nozzle has a character in between the two. Note that the downstream static pressure tap is positioned at the throat of the Venturi tube measuring the pressure $p_c = p_2$. At the same time, with the choked nozzle positioned downstream, the static pressure tap is placed near the nozzle exits to read $p_c = p_2$.

Apart from measuring flow rate the Venturi tube is often used as an aspirator, or suction pump. For such a use a small tube is attached to the side near the throat, where the reduced pressure draws fluid at usually slow rate. These devices are frequently seen in fluid engineering as well as chemical plants.

(a) Venturi tube (or Venturi meter)



(b) Flow nozzle

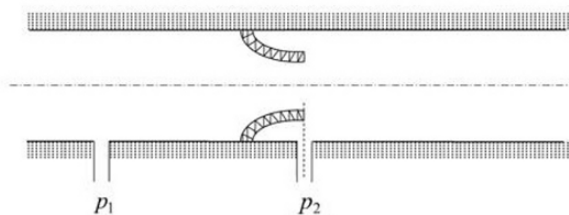


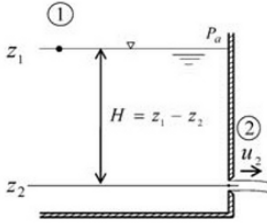
Fig. 4.10 Venturi tube and flow nozzle

Exercise 4.1.3 Tab-orifice and Measurement of Volumetric Flow by a Weir

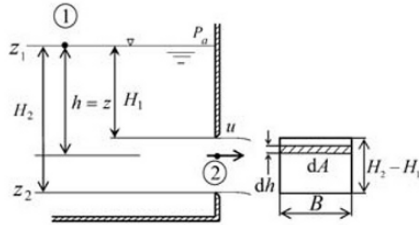
(i) A small orifice (tank-orifice) is installed at the side of a large tank, and through the orifice a liquid is discharged, as show in Fig. 4.11(a). The orifice is located at a position z_2 from a datum level, while H is the distance of the orifice from the liquid level, and the position of the liquid level is z_1 from a datum level.

Assuming that the liquid level of the tank is constant and the opening area of the orifice is so small that the vena contracta is negligible, determine the velocity of the free jet from the orifice where the surrounding pressure is atmospheric.

(a) Tank-orifice



(b) Open tank



(c) V-notch weir

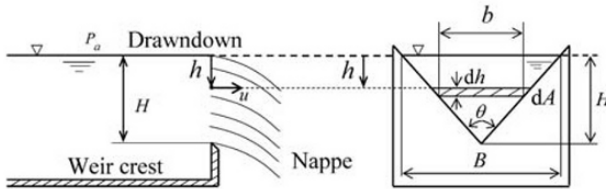


Fig. 4.11 Tank-orifice and Sharp-crested weir

(ii) A rectangular opening (large orifice) is found at the side of a large tank, as shown in Fig. 4.11(b). The dimensions of the open tank are $B \times (H_2 - H_1)$, for which the upper edge of the orifice is located at H_1 from the liquid level and the lower edge is at H_2 from the liquid level. Estimate the overall discharge of a liquid from the open tank where the surrounding pressure is atmospheric, assuming that the liquid level of the tank is kept constant.

(iii) In a measurement of high volumetric flow rate of a liquid, a weir is often utilized. Also, a weir is the most common means of measuring overall discharge in an open channel. There are basically two types of weir (for metering discharge), both of which have an obstruction placed in an open channel that leads the flow through an opening or aperture designed to measure the discharge. A sharp-crested weir is a type of weir which has a vertical plate placed normal to the flow, consisting of a sharp-edge crest. This is typical in rectangular sharp-crested weir or V-notch weir, so that the nappe behaves like a free jet, as shown in Fig. 4.11(c). A broad-crested

weir is another type of weir, which has some elevation above the channel bottom to reduce the flow level. The elevation is long enough so that the level on the elevation becomes parallel to the upstream level of the channel. Knowing a mean velocity on the elevation, the volumetric flow rate of the discharged liquid through the weir may be obtained, measuring the actual height of the liquid on the elevation, see Problem 4.1-3.

For a typical volumetric flow rate measurement, in this exercise show a method to measure the discharge of a liquid in the case of a V-notch weir as shown in Fig. 4.11(c).

Ans.

The gravitational potential head (pressure) causes flow through the tank-orifice, open tank and weir. In order to tackle the problems, application of the mass continuity and Bernoulli equations are essential.

(i) Applying the Bernoulli equation of Eq. (4.1.38) between point ① and ②, denoting that the velocity u_1 on the surface is zero and pressures at points ① and ② are both atmospheric p_a , it follows that

$$\frac{1}{2}\rho u_1^2 + p_a + \rho g z_1 = \frac{1}{2}\rho u_2^2 + p_a + \rho g z_2 \quad (1)$$

Setting $u_1 = 0$ and denoting ρ the density of fluid being constant, we have

$$u_2 = \sqrt{2g(z_1 - z_2)} = \sqrt{2gH} \quad (2)$$

The velocity of efflux is equal to velocity of free fall from the surface of the tank. This relation is called Torricelli's theorem.

(ii) This is an example of a large orifice discharge. We can assume that the discharge flow at the orifice is ideal so that the vena contracta can be neglected, and that the discharge velocity at the orifice is horizontal. Uniform flow exists across the width at the position h from the liquid level. We first apply the Bernoulli equation along the representative stream line at ① the liquid level, where the descendent velocity of the liquid surface is assumed to be zero, and to a point at ② $z = h$ in the orifice plane. It follows that the velocity u at $z = h$ is

$$u = \sqrt{2gh} \quad (3)$$

This is the Torricelli's theorem in the previous problem (i). Let us take an infinite area dA on the orifice plane, as shown in Fig. 4.11(b), where $dA = B dh$. The ideal discharge is given as

$$Q = \int_{H_1}^{H_2} u dA = B \int_{H_1}^{H_2} \sqrt{2gh} dh = \frac{2}{3} B \sqrt{2g} \left(H_2^{3/2} - H_1^{3/2} \right) \quad (4)$$

In actual experimental situations, there would be contraction at the orifice so that for real flow a discharge coefficient C_d must be considered, and Eq. (4) can be expressed as follows

$$Q = C_d \frac{2}{3} B \sqrt{2g} \left(H_2^{3/2} - H_1^{3/2} \right) \quad (5)$$

(iii) The use of a V-notch weir is an accurate way of measuring large volumetric flow rate in many engineering applications. However, in actual flows there exists a nappe at the weir, as indicated in Fig. 4.11(c), although large lateral contractions are not usually present because of the presence of the side walls. In the same manner as considered in (ii) for tank orifice, we can define an idealized flow situation, first of all, assuming that the nappe does not exist and the level of liquid surface at the weir is the same as that upstream. Again the flow velocity in the V-notch plane at $z = h$ from the liquid level is thought to be one obtained by the Torricelli's theorem

$$u = \sqrt{2gh} \quad (6)$$

Denoting the infinite area dA at $z = h$ in the V-notch plane as $dA = b dh$, where $b/B = (H - h)/H$, the ideal discharge is given by

$$Q = \int_0^H u dA = \int_0^H \sqrt{2gh} \frac{B(H - h)}{H} dh \quad (7)$$

The integration of Eq. (7) will give the following formula

$$Q = \frac{4}{15} \sqrt{2g} B H^{5/2} \quad (8)$$

Since $\tan(\theta/2) = B/2H$, we can write Eq. (8) as

$$Q = \frac{8}{15} \sqrt{2g} \tan\left(\frac{\theta}{2}\right) H^{5/2} \quad (9)$$

In actual experimental situations, there would be nappe at the V-notch plane so that, similar to the large orifice, we will introduce the discharge coefficient C_d , and it follows that

$$Q = C_d \frac{8}{15} \sqrt{2g} \tan\left(\frac{\theta}{2}\right) H^{5/2} \quad (10)$$

In engineering applications, the θ range would be $22^\circ \leq \theta \leq 120^\circ$ where $C_d \approx 0.6$. For accurate measurement of discharge, meticulous calibration is required for C_d .

Exercise 4.1.4 Sudden Expansions, Contractions, Bend and Flow Through Rotating Blades

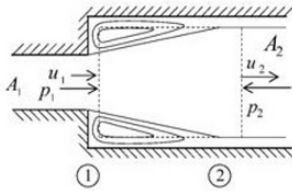
In pipelines there are regions, where the pipe cross-sectional area changes abruptly, as often seen at pipe joints. In long pipelines, total pressure loss (head loss) is mostly caused by viscous loss along the pipelines, where losses due to hydrodynamic effects, such as flow separations and secondary circulations (vortices) in these abruptly changed cross-sectional area, bends or other plumbing (piping) parts, are normally small. Those losses due to hydrodynamic effects are known as minor losses. However, in a short pipe system, minor losses, are not to be neglected.

(i) Find an expression for the pressure loss (head loss) in a sudden expansion in a pipeline, as shown in Fig. 4.12(a). Denoting that a pipe of cross-sectional area A_1 of ① is connected to the sudden expansion part of cross-sectional area A_2 of ②. The pressure at joint ① is p_1 and one at a downstream region of fully developed flow is p_2 . Assume uniform flow enters the sudden expansion part ① with a velocity u_1 , and leaves the region at ② with u_2 . The fluid density is ρ .

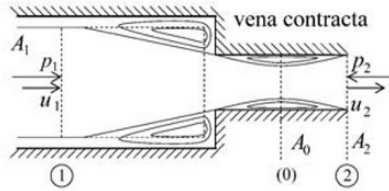
(ii) Similar to (i), find an expression for the pressure loss (head loss) in a sudden contraction in a pipeline, as shown in Fig. 4.12(b). Consider that in the sudden contraction part the vena contract occurs so that the exit's condition is taken at region ② when the flow reaches fully developed uniform velocity, where the pressure and velocity is p_2 and u_2 respectively.

(iii) There are many elements, which cause pressure loss (head loss) beside frictional pressure loss (viscous loss) in pipelines. These are minor losses. Explain a method to measure the minor loss in an experiment or to determine one from a numerical simulation result, taking an example of a 90° bend in a flow channel as shown in Fig. 4.12(c).

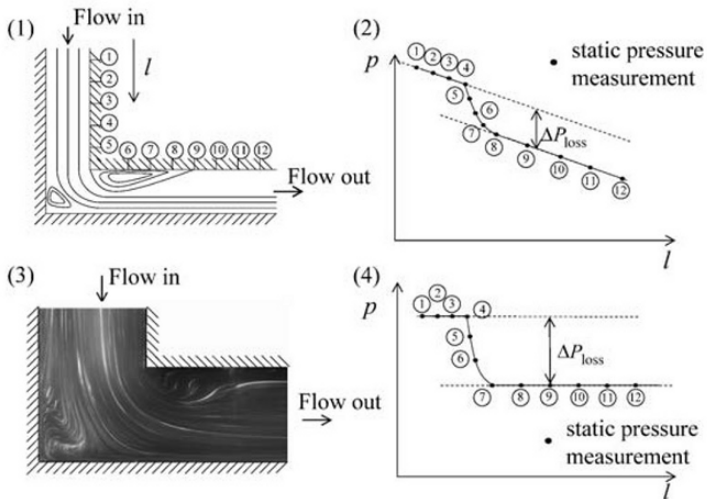
(a) Sudden expansion



(b) Sudden contraction



(c) 90° bend



(d) Flow through rotating blade

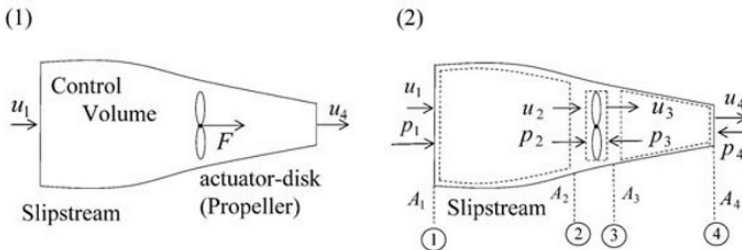


Fig. 4.12 Sudden expansion, contraction, bend and flow through rotating blade

(iv) The thrust force exerted by a rotating blade is a major concern for driving marine vessels (screw), pumping air (fan), flying planes (propeller), wind-driven power generators (wind turbine) and so on. The theory of the thrust force by a rotating blade is originally due to W.J.R. Rankine, and developed by R. E. Froude, and it is known as the actuator-disk theory. The theory applies to a rotating blade to produce the thrust force by a given power, bearing in mind that it can be replaced by a stationary disk which provides a pressure rise across, as depicted in Fig. 4.12(d)(1) and (2). Taking appropriate control volume for the system, find an expression for the thrust force F and associated power to a propeller and estimate the efficiency. Assume that the propeller is a thin actuator-disk so that both side of the propeller A_2 and A_3 are the same in area. Assume further that the incoming and exiting flows are uniform with velocities u_1 and u_4 respectively, as depicted in Fig. 4.12(d)(2). The control volume is assumed to be formed between side boundaries, called the slipstream, as shown in Fig. 4.12(d)(1) and (2). The fluid density is ρ .

Ans.

(i) The pressure loss can be determined with the mass continuity, the integrated momentum and Bernoulli equation for the control volume in Fig. 4.12(a). The set of equations are respectively:

$$\rho u_1 A_1 = \rho u_2 A_2 \quad (1)$$

$$\rho Q(u_2 - u_1) = (p_1 - p_2) A_2 \quad (2)$$

$$\frac{1}{2} \rho u_1^2 + p_1 + \rho g z = \frac{1}{2} \rho u_2^2 + p_2 + \rho g z + \rho g h_l \quad (3)$$

$Q = u_1 A_1 = u_2 A_2$ the volume flow rate and z are levels of the reference point ① and ②, which are the same. From Eqs. (1)–(3), solving for the head loss h_l , we have

$$h_l = \frac{u_1^2}{2g} \left(1 - \frac{A_1}{A_2} \right)^2 \quad (4)$$

Further, by definition of the correction factor ξ , Eq. (4) can be written by

$$h_l = \frac{u_1^2}{2g} \xi \left(1 - \frac{A_1}{A_2} \right)^2 \quad (5)$$

Alternately, to the head loss h_l by defining the pressure loss coefficient ζ

$$h_l = \zeta \frac{(u_1 - u_2)^2}{2g} = \zeta \left(\frac{u_1^2}{2g} \right) \quad (6)$$

In Eqs. (5) and (6) we used a relationship between the area ratio (A_1/A_2) and ζ as

$$\zeta = \xi \left(1 - \frac{A_1}{A_2} \right)^2 \quad (7)$$

Note that ξ is defined as the correction factor which is normally near unity.

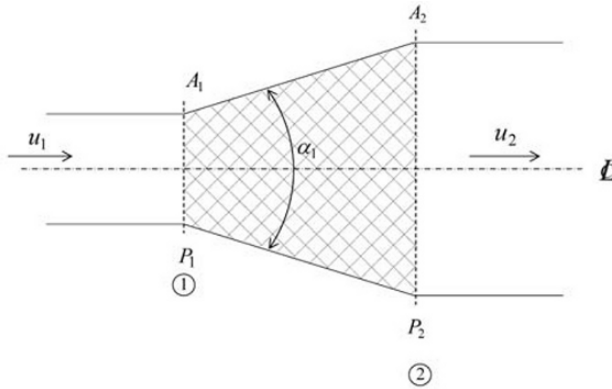


Fig. 4.13 Conical diffuser

(ii) In contracting flow, a flow separation at the entrance of the outlet pipe occurs, where the flow is accelerated to the point of vena contracta (0), and decelerated from (0) to ② in which the flow is fully developed. In the same manner as question (i), we can arrive at the head loss ①–② as follows

$$h_l = \zeta \left(\frac{u_2^2}{2g} \right) = \zeta \left(1 - \frac{A_2}{A_1} \right)^2 \frac{u_2^2}{2g} \quad (8)$$

In general, major head loss occurs in decelerating flow, while in accelerating flow the head loss is rather small. Thus, taking the control volume between (0)–(2), we may be able to write the head loss h_s as follows

$$h_s = \frac{(u_0 - u_2)^2}{2g} = \left(\frac{1}{C_c} - 1 \right)^2 \frac{u_2^2}{2g} \quad (9)$$

C_c is the contraction coefficient defined by $C_c = A_0/A_2$.

Equation (8) covers overall head loss between ① and ②, in which Eq. (9) dominates the head loss, thus consequently taking the following relation

$$h_l \approx h_s \quad \text{and} \quad \zeta \approx \left(\frac{1}{C_c} - 1 \right)^2 \quad (10)$$

So that we have for ①–②

$$h_l = \left(\frac{1}{C_c} - 1 \right)^2 \frac{u_2^2}{2g} \quad (11)$$

In calculating Eq. (11), we have the following well-known expression of C_c (ref. D.N. Roy, 1988)

$$C_c = \frac{1}{1 + 0.707(1 - A_2/A_1)^{1/2}} \quad (12)$$

C_c is the same as the contraction coefficient of the orifice plate. For flows from a large reservoir through a pipe (i.e. $A_2/A_1 \approx 0$), ζ may be $\zeta \approx 0.5$. The loss can be minimized by rounding the corner of the entrance pipe, shaping the Bell-mouth, which yields $\zeta \approx 0.05$ in practical engineering problems.

With the similar treatment as above, we can extend our problem to the cases of effuser or diffuser. The head loss in a diffuser is greater than an effuser in the same contraction ratio A_1/A_2 . In a conical diffuser for a divergence angle α as indicated in Fig. 4.13, the correction factor ξ given by Eq. (12) in question (i) takes the values 1.1 to 1.2 for α being between 60° and 70° , and drops until it reaches approximately 1.0–1.05 at $\alpha = 180^\circ$. In the diffuser, the diffuser efficiency η_d of the pressure recovery is defined as

$$\eta_d = \frac{\text{Actual pressure recovery}}{\text{Theoretical pressure recovery}} \quad (13)$$

$$= \frac{p_2 - p_1}{p_{2th} - p_1} = 1 - \frac{h_l}{(u_1^2 - u_2^2)/2g}$$

Additionally, using ξ defined by Eq. (14) in question (i), we have

$$\eta_d = 1 - \xi \left(\frac{1 - A_1/A_2}{1 + A_1/A_2} \right) \quad (14)$$

(iii) Imagine that the pressure (the static wall pressure) distribution along the wall is known, either by experimental measurement or numerical result. We can then plot the pressure data for locations of pressure taps as shown ①–⑫ in Fig. 4.12(c)(1) (or for wall points in numerical results). In the case of a long channel, there would be a strong pressure gradient in upstream and downstream regions due to viscous (frictional) losses as indicated in Fig. 4.12(c)(2). As seen in Fig. 4.12(c)(2), at locations ①–④ and locations ⑧–⑫, the pressure gradients in the fully developed regions are almost the same, which is unaffected by the minor loss due to the bend in locations ④–⑧. The minor loss is the pressure drop caused by the flow configuration in the bend, usually by flow separation and local circulation at local points ④–⑧. The minor loss Δp_{loss} is the difference between the two parallel lines of fully developed flow regions, i.e. between lines of locations ①–④ and locations ⑧–⑫.

On the other hand, in the case of relatively short channel, the viscous losses at upstream and downstream regions, before and after the bend, are small, yielding the trend that the pressure gradients of the regions are almost null. Namely, the lines of pressure distribution at locations ①–④ and locations ⑦–⑫ are almost horizontal, keeping their values almost constant in the two regions. The pressure loss Δp_{loss} due to the bend in a short channel (as typically seen in such channels as shown in Fig. 4.12 (c)(3)) is representatively displayed in Fig. 4.12(c)(4). As demonstrated, the pressure loss Δp_{loss} can be simply determined as a pressure difference between any two arbitrary points between the upstream and downstream (fully developed) flow regions. Figure 4.12(c)(3) is a typical flow configuration in a 90° bend in a short channel.

The pressure loss coefficient ζ at this bend is often defined as

$$\zeta = \frac{\Delta p_{\text{loss}}}{\frac{1}{2} \rho u^2} \quad (15)$$

where u is the average flow velocity. ζ is usually a function of the Reynolds number and geometric parameters.

(iv) The thrust force F given by the pressure is the net force acting on the control volume in Fig. 4.12(d)(1). Thus, the integrated momentum equation applied to the large control volume gives

$$F = \rho Q(u_4 - u_1) \quad (16)$$

Q is the volumetric flow rate propelled by the propeller when a control volume as indicated in Fig. 4.12(d)(2) is drawn in the vicinity of the propeller such that $u_2 = u_3$. Thus, the momentum equation would give F by the following form

$$F = A(p_3 - p_2) \quad (17)$$

When we assume no energy loss or gain due to viscous effects between points ① and ④, and there is no area change between ② and ③, we can write the conditions as follows

$$A = A_2 = A_3 \quad (18)$$

$$u = u_2 = u_3 \quad (19)$$

The Bernoulli equations of the points between ① and ② and ③–④ are written

$$p_1 + \frac{1}{2} \rho u_1^2 = p_2 + \frac{1}{2} \rho u_2^2 \quad (20)$$

$$p_3 + \frac{1}{2} \rho u_3^2 = p_4 + \frac{1}{2} \rho u_4^2 \quad (21)$$

The potential head is the same at all points. Using the fact that the pressure is the same all around the control volume, we can recognize that

$$p_1 = p_4 = p_{\text{atm}} \quad (22)$$

p_{atm} is the surrounding pressure. From Eqs. (20), (21) and (22), we have

$$\frac{1}{2} \rho (u_1^2 - u_4^2) = p_2 - p_3 \quad (23)$$

With Eqs. (16), (17) and (23), we have the relation

$$\frac{1}{2} \rho A (u_1^2 - u_4^2) = \rho A v (u_1 - u_4) \quad (24)$$

Thus, consequently we can obtain v as

$$v = \frac{1}{2} (u_1 + u_4) \quad (25)$$

v is the flow velocity through the propeller. Equation (25) shows that the flow velocity through the propeller is the average of the upstream and downstream velocity.

The power W_{fluid} required to propel the fluid between points ① and ④, i.e. to produce the fluid motion, not considering losses, will be

$$W_{\text{fluid}} = \frac{1}{2} \rho Q (u_4^2 - u_1^2) \quad (26)$$

A moving propeller attached to a vessel (ship or aircraft moving with velocity v) requires the power W_{prop} given by

$$\begin{aligned} W_{\text{prop}} &= F u_1 \\ &= \rho Q u_1 (u_4 - u_1) \end{aligned} \quad (27)$$

The theoretical propeller efficiency η_p is then given by the following expression, from Eqs. (26) and (27)

$$\begin{aligned} \eta_p &= \frac{W_{\text{prop}}}{W_{\text{fluid}}} = \frac{2u_1}{u_4 + u_1} \\ &= \frac{u_1}{v} \end{aligned} \quad (28)$$

The maximum efficiency of a propeller can be obtained by designating the condition that W_{prop} becomes maximum. So that, eliminating u_4 using Eq. (25) from Eq. (27) and differentiating Eq. (27) with respect to v , while keeping u_1 constant, we have

$$v = \frac{1}{2} u_1 \quad (29)$$

Therefore, the maximum efficiency of a propeller is ideally obtained by

$$\begin{aligned} \eta_{P_{\max}} &= \frac{W_{\text{prop}}}{W_{\text{fluid}}} = \frac{-\frac{1}{2} \rho Q u_1^2}{-\frac{1}{4} \rho Q u_1^2} \\ &= 50\% \end{aligned} \quad (30)$$



Fig. 4.14 Wind turbine

Similarly the maximum efficiency, that a wind turbine as depicted in Fig. 4.14 can attain, can be found, using the same control volume as treated in Fig. 4.12(d), while reversing the wind direction from ④ to ①. In the same manner as the propeller, W_{fluid} is calculated by differentiating with respect to v , while keeping u_4 constant, so that we have

$$v = \frac{4}{3} u_4 \quad (31)$$

The maximum efficiency of a wind turbine is ideally estimated by

$$\eta_{T_{\max}} = \frac{W_{\text{fluid}}}{W_{\text{turb}}} = \frac{\frac{8}{27} \rho Q u_4^2}{\frac{1}{2} \rho Q u_4^2} = 59.3\% \quad (32)$$

In actual cases for both propeller and wind turbine, the efficiency is less than the ideal situation as obtained in Eqs. (30) and (32), due to viscous loss and the complex flow configuration through the rotor. There would be a strong swirl component of velocity. However, the expressions of Eqs. (30) and (32) would give the maximum attainable efficiency, which may provide a target design.

Exercise 4.1.5 The Rayleigh-Plesset Equation

There is a spherical bubble in a perfect, incompressible liquid of infinite extent. The bubble growth is due to a pressure variation at a distance from the bubble. Referring to Fig. 4.15, the radius of the bubble at any time $t > 0$ is $R = R(t)$, and r is the radius to any point in the liquid, where the origin o of coordinates is at the bubble center, which is at rest in the inertial reference frame. Derive an equation of motion for a spherical bubble in a liquid for given external pressure $p(t)$, which varies with time, with a condition that the pressure at the bubble surface is $p(R)$.

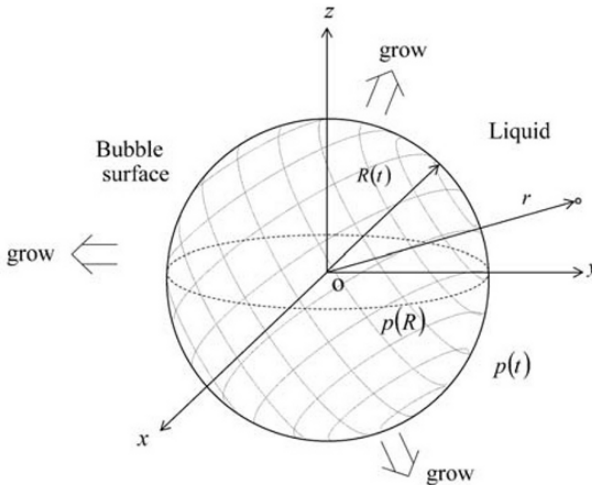


Fig. 4.15 Growing bubble

Ans.

Let us assume that the flow is irrotational, so that the velocity field is written in terms of the velocity potential ϕ given by Eq. (4.1.2). With spherical symmetry the surface velocity of the growing bubble is the radial velocity u of the fluid flow, and it is a function of r , so that the velocity potential $\phi = \phi(r)$ satisfies the Laplace equation

$$\nabla^2 \phi(r) = 0 \quad (1)$$

For the spherical coordinates system with spherical symmetry, we have

$$\frac{1}{r^2} \frac{d}{dr} \left(r^2 \frac{d\phi}{dr} \right) = 0 \quad (2)$$

The integration of Eq. (2) will give the general solution as

$$\phi(r) = -\frac{m}{r} + c \quad (3)$$

where m and c are constants. With Eq. (3), the radial velocity u is thus given as follows

$$u = \left(\nabla \phi \right)_r = \frac{d\phi}{dr} = \frac{m}{r^2} \quad (4)$$

With the boundary condition at the bubble surface, we may write

$$u = \frac{dR}{dt} = \dot{R} \quad \text{at } r = R \quad (5)$$

Thus, that we can write Eq. (4) as

$$\dot{R} = \frac{m}{R^2} \quad \text{and} \quad m = R^2 \dot{R} \quad (6)$$

Using m of Eq. (6) into Eq. (3) and setting c in Eq. (3) to zero, we can obtain an expression of ϕ as

$$\phi(r) = -\frac{R^2 \dot{R}}{r} \quad (7)$$

Equation (7) satisfies the problem condition that is

$$u = 0 \quad \text{for } r = \infty \quad (8)$$

and

$$u = \infty \quad \text{for } r = 0 \quad (9)$$

Knowing the velocity field as the velocity potential, we can apply the pressure equation if Eq. (4.1.35), ignoring the gravitational potential, to write

$$-\frac{d\phi}{dt} + \frac{1}{2}(\nabla\phi)^2 + \frac{p(r)}{\rho} = \frac{p(t)}{\rho} \quad (10)$$

$p(r)$ is the static pressure at r . With Eqs. (4) and (6) we can write the time variation of ϕ as

$$(\nabla\phi)^2 = \frac{R^4 \dot{R}^2}{r^4} \quad (11)$$

and

$$\frac{\partial\phi}{\partial t} = \frac{1}{r} (2R\dot{R}^2 + R^2\ddot{R}) \quad (12)$$

Eqs. (11) and (12) are to be applied to the bubble surface, i.e. $r = R$, and with that the following expressions are obtained by

$$(\nabla\phi)^2 = \dot{R}^2 \quad (13)$$

further

$$\frac{d\phi}{dt} = 2\dot{R}^2 + R\ddot{R} \quad (14)$$

Substituting Eqs. (13) and (14) into Eq. (10), at the bubble surface, i.e. $r = R$, we can finally obtain the equation of motion for the bubble radius to write

$$\frac{p(R) - p(t)}{\rho} = \frac{3}{2}\dot{R}^2 + R\ddot{R} \quad (15)$$

which can alternatively be expressed

$$\frac{p(R) - p(t)}{\rho} = \frac{1}{2\dot{R}R^2} \frac{d}{dt} (R^3 \dot{R}^2) \quad (16)$$

Equations (15) and (16) are referred to as the Rayleigh-Plesset equation, which can be used to estimate the growth and collapse of a vapor bubble for known pressure change $p(t)$. In the Rayleigh-Plesset equation, $p(R)$ is often assumed from the surface tension effect on the bubble surface as follows

$$p(R) = p_v - \frac{2\sigma}{R} \quad (17)$$

Note that p_v is the vapor pressure of the bubble at a given temperature and σ is the surface tension of a vapor-liquid interface.

Exercise 4.1.6 Kelvin's Circulation Theorem and Lift on Airfoil

For a steady barotropic flow of a perfect fluid, show that the circulation around any closed material curve is invariant. Explain how the lift of an airfoil is generated when the potential flow starts up around the airfoil.

Note that the motion of the fluid is called barotropic if the density and pressure are directly related. The simple relation between p and ρ is such that

$$\nabla P(\rho) = \nabla \int \frac{dp}{\rho}$$

where P is the pressure function. The fluid itself is called piezotropic when the pressure and density are directly related. Thus all piezotropic fluid flows are barotropic.

Ans.

The Euler Eq. (4.2) can be written in terms of the pressure function (4.1.25) and a body force potential (gravitational potential function) (4.1.22) as follows

$$\begin{aligned} \frac{D\mathbf{u}}{Dt} &= -\frac{1}{\rho} \nabla p + \mathbf{g} \\ &= -\nabla(P(\rho) + \Phi) \end{aligned} \quad (1)$$

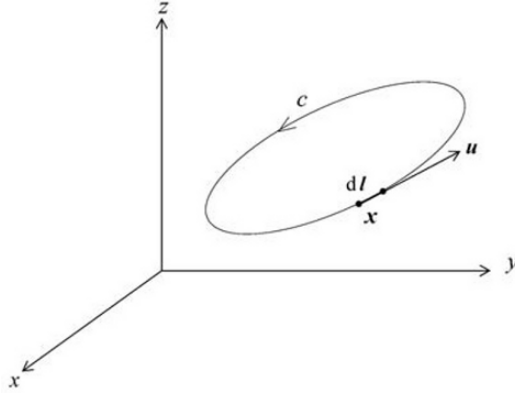
where

$$\mathbf{g} = -\nabla \Phi \quad (2)$$

and

$$P(\rho) = \int \frac{dp}{\rho} \quad (3)$$

The left hand side of Eq. (1) is the material derivative and the acceleration of the flow is expressed by

Fig. 4.16 Circulation around c

$$\mathbf{a} = \frac{D\mathbf{u}}{Dt} \quad (4)$$

Let us consider the circulation around any material closed curve c and examine the time derivative of the circulation as follows

$$\frac{D}{Dt} \int_c \mathbf{u} \cdot d\mathbf{l} = \int_c \frac{D\mathbf{u}}{Dt} \cdot d\mathbf{l} + \int_c \mathbf{u} \cdot d\left(\frac{D\mathbf{l}}{Dt}\right) \quad (5)$$

Denote the coordinate of a point on c be \mathbf{x} and the line element $d\mathbf{l} = d\mathbf{x}$, which moves with flow, so that Eq. (5) becomes

$$\begin{aligned} \frac{D}{Dt} \int_c \mathbf{u} \cdot d\mathbf{l} &= \int_c \mathbf{a} \cdot d\mathbf{x} + \int_c \mathbf{u} \cdot d\left(\frac{D\mathbf{x}}{Dt}\right) \\ &= \int_c \mathbf{a} \cdot d\mathbf{x} + \int_c \mathbf{u} \cdot d\mathbf{u} \end{aligned} \quad (6)$$

Thus

$$\frac{D}{Dt} \int_c \mathbf{u} \cdot d\mathbf{l} = \int_c \mathbf{a} \cdot d\mathbf{x} + \int_c d\left(\frac{1}{2}|\mathbf{u}|^2\right) \quad (7)$$

The second integral of Eq. (7) vanishes identically due to the cyclic integral of the total differentiation being zero. For the barotropic flow, the first integral also vanishes. This is because from Eqs. (1) and (4), that is

$$\begin{aligned}
 \int_c \mathbf{a} \cdot d\mathbf{x} &= - \int_c \nabla(P + \Phi) \cdot d\mathbf{x} \\
 &= - \int_c d(P + \Phi) \\
 &= 0
 \end{aligned}
 \tag{8}$$

Therefore

$$\frac{D}{Dt} \int_c \mathbf{u} \cdot d\mathbf{l} = \frac{D\Gamma}{Dt} = 0
 \tag{9}$$

It follows that the circulation Γ is kept constant, i.e.

$$\Gamma = \text{const.}
 \tag{10}$$

This is Kelvin's circulation theorem, Kelvin (1869). It states that, for steady barotropic flow, in a continuous motion of the perfect fluid under the conservation force, the circulation around any material closed curve, that is moving with the flow, is kept constant. It is mentioned that there are conditions, in which the motion of a viscous fluid at a very large Reynolds number may be approximated to that of a perfect fluid. It is useful to consider the inviscid limit in many engineering problems such an airfoil, as mentioned in the proceeding problems.

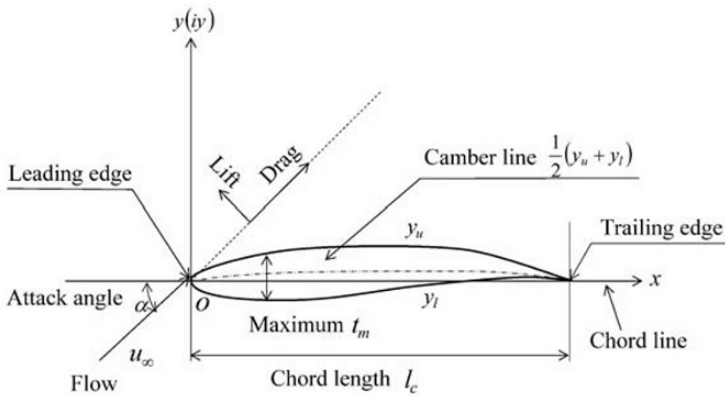


Fig. 4.17 Airfoil nomenclature

Figure 4.17 shows a schematic of an airfoil (aerofoil) and its nomenclatures in common use. Note that the schematic of the airfoil in Fig. 4.17 is drawn thick and exaggerated for the sake of clarity. The camber line is the mean profile. The shape of an airfoil is designed in many ways to meet engineering demands, but they are usually well rounded at the leading

edge and sharp at the trailing edge. When the ratio of the maximum thickness to the chord length (t_m/l_c) and the ratio of the maximum camber to the chord length are small, we consider the airfoil is thin.

The lift force and drag force are exerted by an airfoil, and they are normal to each other in the direction of flow as shown in Fig. 4.17. The angle α between the approaching free stream and the chord line is called the attack angle. The attack angle is usually supposed to be small.

Now for the question of the lift as the flow starts up, we consider the potential flow of a perfect fluid with no circulation immediately after the startup. The stagnation point S_p is observed on the airfoil in the vicinity of the trailing edge as shown in Fig. 4.18(a). This phenomenon will be treated in the next problem in detail; at this moment the velocity and the pressure are infinite at the trailing edge, where the sharp bend flow persists around the trailing edge. In real situations, soon after the start-up, the stagnation point S_p moves to the trailing edge, and at the same time a small vortex, due to the flow separation, is formed and after a few moments it is shed and lost downstream. The vortex generated after the startup is called the starting vortex as depicted in Fig. 4.18(b) and (c).

In order to discuss the lift on an airfoil, we must look at the circulation around the airfoil. The airfoil circulation has recently been studied in more detail and is considered to be an important factor. However before proceeding further, it is interesting to develop a deeper insight into how the circulation is generated phenomenologically. Figure 4.18(d) is a schematic expressing how circulation around an airfoil is generated when the flow is starting up. By Kelvin's circulation theorem the total circulation Γ in a flow domain bounded by a closed curve c must be constant and kept at zero, since the flow is in a quiescent state at the beginning. After the starting vortex is created, the circulation in a closed curve c_2 has a value, say $+\Gamma_2 (\neq 0)$, since inside the curve there is a starting vortex. The total circulation in the fluid must be constant in time $\Gamma = 0$, and hence $-\Gamma_1$, which is the circulation in a closed curve c_1 and must exist to cancel Γ_2 , is equal but of opposite sign to the starting vortex Γ_2 as shown in Fig. 4.18(d). Thus, we have a relationship

$$\begin{aligned} |-\Gamma_1| &= |+\Gamma_2| \\ \Gamma &= \Gamma_1 - \Gamma_2 = 0 \end{aligned} \quad (11)$$

What is happening about the airfoil is that a group of so-called bounding vortex is being formed around the region of the airfoil hypothetically to produce $-\Gamma_1$ in the closed curve c_1 . It should be mentioned, not to con-

tradict the irrotational flow assumption, that owing to the Stokes integral theorem

$$-\Gamma_1 = \int_{c_1} \mathbf{u} \cdot d\mathbf{l} = \int_S \nabla \times \mathbf{u} \cdot d\mathbf{S} \quad (12)$$

Thus, the distribution of vorticity $\nabla \times \mathbf{u} = \boldsymbol{\omega}$ on the airfoil surface must be considered. The starting vortex falls far behind after some time, and the airfoil gets lift L due to Γ_1 . The derivation of the lift on an airfoil will be described in the proceeding paragraph. A large closed curve c , including the airfoil and the starting vortex, always gives zero circulation $\Gamma = 0$ altogether, even as time elapses. With the same analogy, a vortex appears when the flow is stopped, which is called a stopping vortex. The stopping vortex is generated about the airfoil to encounter $-\Gamma_1$ and is released from the airfoil, keeping the total circulation zero, i.e. $\Gamma = -\Gamma_1 + \Gamma_2 = 0$. Those two vortices, namely the starting vortex and stopping vortex, are shed as a pair after the flow is stopped. Isn't it interesting? There would be vortices all over the place in this world, if only the perfect fluid existed.

The circulation around an airfoil $-\Gamma_1$ is therefore determined by shifting the stagnation point S_p to the trailing edge. The flow leaves the airfoil with a finite velocity at the trailing edge without bending around the edge, where the pressure difference at the edge between upper and lower surface of the airfoil becomes zero. The condition to determine $-\Gamma_1$ around the airfoil is justified by shifting S_p to the trailing edge. This is called the Kutta condition, and the sequence of this phenomenon is also called the Kutta-Joukowski hypothesis. The Kutta-Joukowski hypothesis simply states that infinite velocities are not admissible in real flow situations.

The origin of the lift of a body placed in a potential flow can be derived from a thought that the force $\mathbf{F} = (F_x, F_y)$ acting on the body is the net force due to pressure on the body, which is given by

$$\mathbf{F} = - \int_{c_0} P d\mathbf{S} \quad (13)$$

c_0 is the closed curve of the body surface and $d\mathbf{S}$ is the surface element on the body, i.e. $d\mathbf{S} = \hat{\mathbf{n}} dS$; $\hat{\mathbf{n}}$ is the unit normal vector facing outward on the body surface. The components F_x and F_y are written by

$$F_x = - \int_{c_0} P n_x dS = - \int_{c_0} P \frac{dy}{dS} dS = - \int_{c_0} P dy \quad (14)$$

and

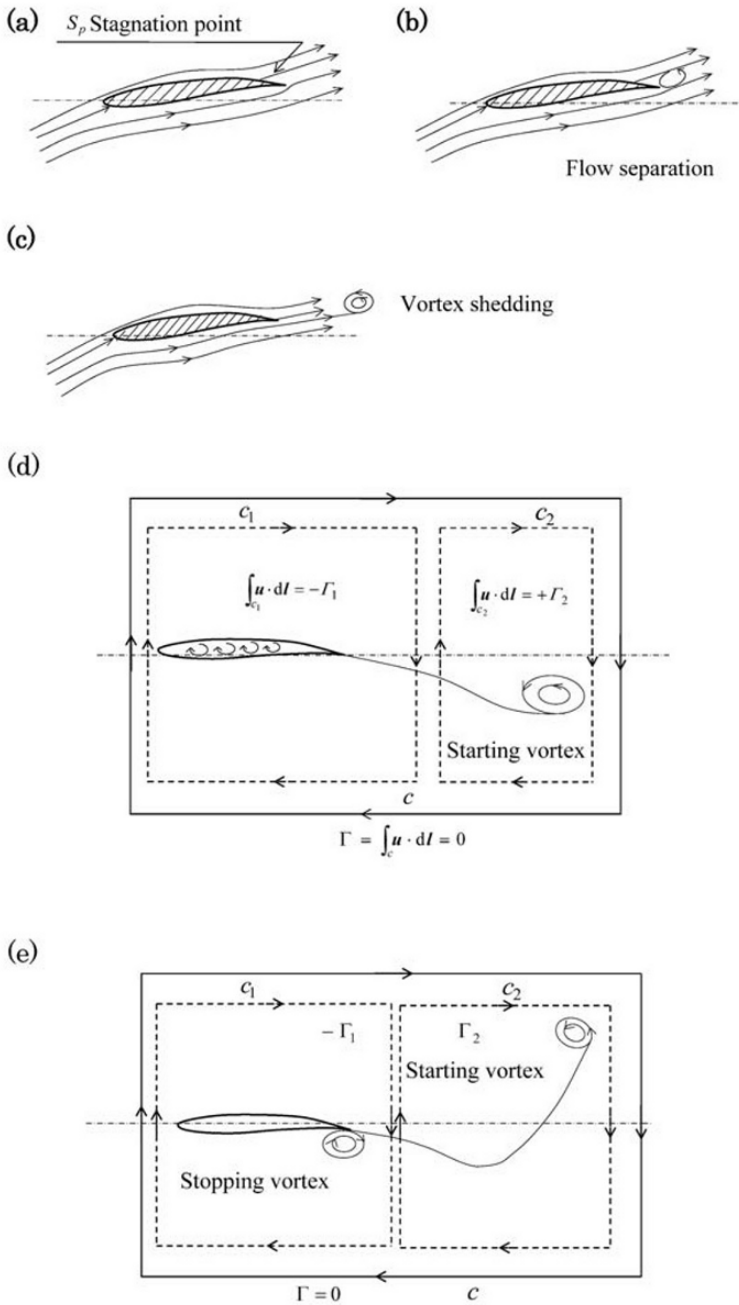


Fig. 4.18 Starting up flow around an airfoil

$$F_y = - \int_{c_0} P n_y dS = - \int_{c_0} P \frac{dx}{dS} dS = - \int_{c_0} P dx \quad (15)$$

Thus, \mathbf{F} is expressed by the complex expression

$$\begin{aligned} \mathbf{F} = F_x - iF_y &= -i \int_{c_0} P(dx - idy) \\ &= -i \int_{c_0} P \overline{dz} \end{aligned} \quad (16)$$

$\overline{dz} = dx - idy$ is the conjugate of $dz = dx + idy$. From Eq. (1) for the steady barotropic flow, we have (with reference to Eq. (4.1.21))

$$\nabla \frac{1}{2} |\mathbf{u}|^2 - \mathbf{u} \times \boldsymbol{\omega} = -\nabla(P + \Phi) \quad (17)$$

Considering the potential flow, i.e. $\boldsymbol{\omega} = \nabla \times \mathbf{u} = 0$ irrotational, the pressure P of Eq. (17) is substituted into Eq. (16), which gives

$$\mathbf{F} = F_x - iF_y = i\rho \int_{c_0} \left[\frac{1}{2} \left| \frac{dW}{dz} \right|^2 + \Phi \right] \overline{dz} \quad (18)$$

\mathbf{u} in Eq. (17) was expressed by the complex potential $W(z)$

$$\mathbf{u} = u - iv = \frac{dW}{dz} \quad (19)$$

Hence

$$|\mathbf{u}|^2 = \left| \frac{dW}{dz} \right|^2 \quad (20)$$

Assuming that there would not be external body force, i.e. $\Phi = 0$, Eq. (18) becomes

$$F_x - iF_y = \frac{i\rho}{2} \int_{c_0} \left| \frac{dW}{dz} \right|^2 \overline{dz} \quad (21)$$

In the potential flow, the body surface itself is the stream line, i.e. the closed curve c_0 is the line of $\psi = \text{Const.}$, so that

$$\int_{c_0} \left| \frac{dW}{dz} \right|^2 \overline{dz} = \int_{c_0} \frac{dW}{dz} \frac{\overline{dW}}{\overline{dz}} \overline{dz} = \int_{c_0} \left(\frac{dW}{dz} \right)^2 dz \quad (22)$$

Further, since $W(z)$ is the analytic function, the integration $\int_{c_0} \sim dz$ can be performed with an arbitrary closed curve, say c_1 , around the body, which is expressed as

$$F_x - iF_y = \frac{i\rho}{2} \int_{c_1} \left(\frac{dW}{dz} \right)^2 dz \quad (23)$$

Equation (23) is known as Blasius' first theorem, Blasius (1910). In a similar manner, the moment M_0 about the origin of the normal stress exerted on the body is

$$\begin{aligned} M_0 &= \int_{c_0} P(xdx + ydy) = -\frac{1}{4} \rho \int_{c_0} \frac{dW}{dz} \frac{\overline{dW}}{d\bar{z}} d(z \cdot \bar{z}) \\ &= -\frac{1}{2} \rho \operatorname{Re} \left[\int_{c_1} \left(\frac{dW}{dz} \right)^2 z dz \right] \end{aligned} \quad (24)$$

Re indicates the real part of the complex number. Equation (24) is also known as Blasius' second theorem, Blasius (1910).

The Blasius theorem can be applied to any steady irrotational flow in surrounding the body. The complex function dW/dz may be expanded for z with a sufficiently large order as

$$\frac{dW}{dz} = U_\infty e^{-i\alpha} + \frac{A}{z} + \frac{B}{z^2} + \dots \quad (25)$$

U_∞ is the approaching free stream and α is the attack angle. dW/dz gives the complex velocity in the z -plane with the velocity potential $W(z)$ being

$$W(z) = U_0 e^{-i\alpha} z + A \ln z - \frac{B}{z} + \dots \quad (26)$$

The second term in Eq. (26) is the complex potential due to circulation Γ_1 so that we have

$$\left(\frac{dW}{dz} \right)^2 = (U_\infty^2) e^{-2i\alpha} - i \left(\frac{\Gamma_1 U_\infty}{\pi z} \right) e^{-i\alpha} - \left(\frac{\Gamma_1 - 8\pi^2 B U_\infty}{4\pi^2 z^2} \right) e^{-i\alpha} + \dots \quad (27)$$

From Blasius' first theorem we can obtain the force \mathbf{F} acting on the body:

$$\begin{aligned}
 \mathbf{F} = F_x - iF_y &= \frac{1}{2} \rho i \left[2\pi i \left(-i \frac{\Gamma_1 U_\infty e^{-i\alpha}}{\pi z} \right) \right] \\
 &= \rho i \Gamma_1 U_\infty e^{-i\alpha}
 \end{aligned} \tag{28}$$

Equation (28) is the Kutta-Joukowski theorem, stating that the net force on the body is directed perpendicular to U_∞ and

$$F_y = L = -\rho U_\infty \Gamma_1 \tag{29}$$

Thus, the lift L is generated due to Γ_1 , which may be dependent upon the velocity field around the airfoil. It should be mentioned that there would be no force acting on the body (airfoil), where there would not be source $q = 0$ (Eq. (4.1.15)) on the solid wall, for the direction parallel to U_∞ , i.e.

$$F_x = D = 0 \tag{30}$$

This is the D'Alembert paradox, stating that there would be no drag force acting upon a body placed in a potential flow. Drag force is produced by surface friction in the boundary layer, which will be discussed in the proceeding chapters.

In the same manner, Blasius' second theorem gives the moment M_0 by substituting Eq. (27) into Eq. (24). See Problem 4.1-9.

Exercise 4.1.7 Joukowski Airfoil

Two dimensional airfoils are necessary for the preliminary design of airplane wings, propeller blades, wind turbines and so forth. In those engineering airfoil applications the lift force is the prime aim for an airplane to support its own weight against gravity or for the one blade of a rotating propeller or wind turbine to exert the torque. A body placed in the potential flow may not experience the drag force, but has indeed the lift force, which is the major concern in this exercise. The simplest airfoil among many is the Joukowski airfoil, which can be obtained from the flow around a circular cylinder by a conformal transformation known as the Joukowski transformation as introduced in Eq. (4.1.19).

Examine shapes of the Joukowski airfoil and give the lift and moment.

Ans.

From Riemann's conformal mapping theorem, there exists an analytical function that an outside domain of an arbitrary body expressed by a

closed surface in the ζ -plane can be conformally transformed to the z -plane as the outside domain of a circle. The transformation from ζ to z is

$$z = C_0\zeta + \frac{C_1}{\zeta} + \frac{C_2}{\zeta^2} + \dots + \frac{C_n}{\zeta^n} + \dots \quad (1)$$

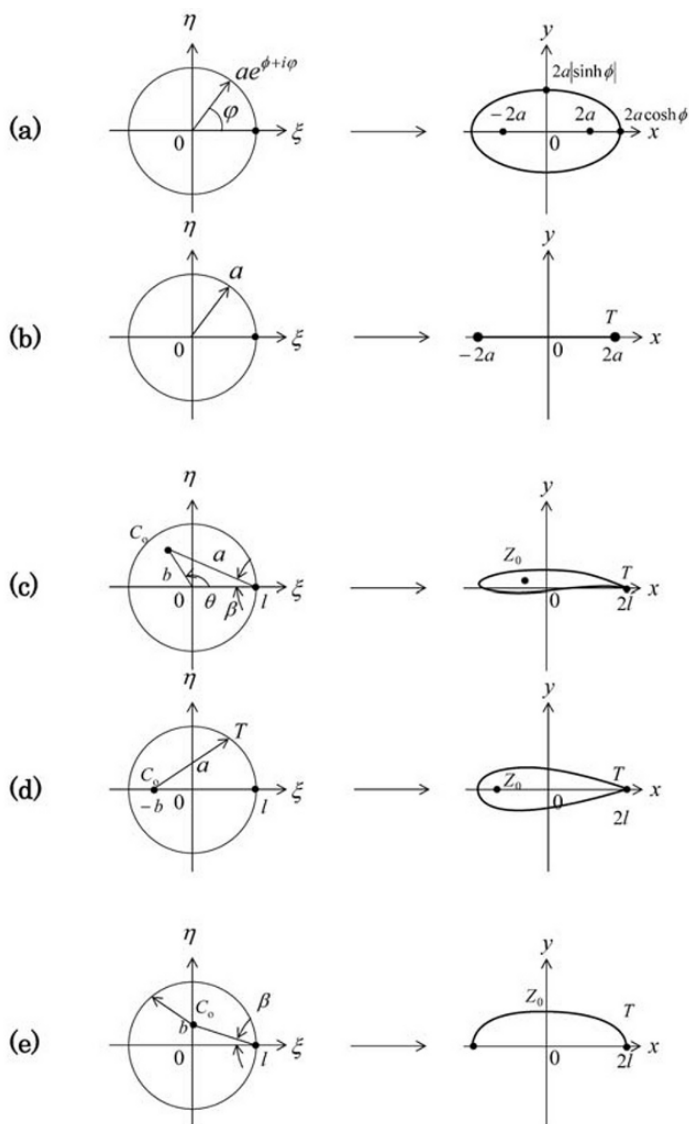


Fig. 4.19 Joukowski transformation

Equation (1) is the Laurent polynomial expansion, where complex constants $C_0, C_1, C_2 \dots C_n$ are chosen to give an appropriate airfoil shape. The Joukowski transformation is such that

$$z = \zeta + \frac{a^2}{\zeta} \quad (2)$$

$\zeta = \eta(x, y) + i\xi(x, y)$, $z = x + iy$ and a is a positive real constant. Equation (2) gives the Joukowski airfoil shape, depending upon the choice of the circle in the ζ -plane. Figure 4.19(a)–(e) are various cases of airfoil shapes.

Let us denote a circle in the ζ -plane as $R = ae^\phi$. The singularity of the transformation is a point, which is obtained from the relationship

$$\frac{d\zeta}{dz} = 1 - \frac{a^2}{z^2} = 0 \quad (3)$$

This gives us $z = \pm a$. In an airfoil, $z = a$ is chosen at the trailing edge. Now let us set a circle in the ζ -plane by writing ζ as

$$\zeta = ae^{\phi+i\varphi} \quad (4)$$

ϕ and φ are real constants. The transformation of Eq. (2) thus provides us with

$$z = a \left\{ e^{\phi+i\varphi} + e^{-(\phi+i\varphi)} \right\} \quad (5)$$

And in the z -plane after eliminating φ , Eq. (5) affords us

$$\frac{x^2}{(2a \cosh \phi)^2} + \frac{y^2}{(2a \sinh \phi)^2} = 1 \quad (6)$$

For constant ϕ , Eq. (6) supplies an equation of an ellipse with semi-major axis $2a \cosh \phi$, semi-minor axis $2a |\sinh \phi|$ and foci $x = \pm 2a$, $y = 0$, as shown in Fig. 4.19(a). Therefore, $R = |\zeta| = ae^\phi = \text{Constant}$; a circle with the center at the origin of the ζ -plane, will be transformed as an ellipse in the z -plane. Setting $\phi = 0$, the ellipse is degenerated into a segment of line on x axis, whose length is $4a$, as shown in Fig. 4.19(b). Shifting the center of circle in the ζ -plane to a point C_o will give

$$\zeta - C_o = ae^{\phi+i\varphi} \quad (7)$$

Particularly in order to set the singularity at the trailing edge, we may be able to choose C_o as

$$C_o = be^{i(\pi-\theta)} = be^{-i\theta} \quad (8)$$

Further, we can set for a as

$$a = (l^2 + b^2 - 2lb\cos\theta)^{\frac{1}{2}} \quad (9)$$

When Eq. (7) is transformed to the z -plane by the Joukowski transformation of Eq. (2), the shape that appears in the z -plane is called the Joukowski airfoil, as shown in Fig. 4.19(c). Particularly if C_o is placed on the real axis, such that $C_o = -b$ in the ζ -plane, it becomes a symmetric Joukowski airfoil. Furthermore, when C_o is placed on the imaginary axis, such that $C_o = bi$ in the ζ -plane, the airfoil shape may become a circular arc airfoil. The Joukowski airfoils in (c)–(e) are to be obtained by implicit function as follows:

(c)

$$\zeta = z + \frac{a^2}{z} \quad (10)$$

(d)

$$\frac{\zeta - na}{\zeta + na} = \left(\frac{z - a}{z + a} \right)^n \quad (11)$$

(e)

$$\zeta = C_0 z + \frac{C_1}{z} + \frac{C_2}{z^2} + \frac{C_3}{z^3} + \dots \quad (12)$$

The most typically used airfoil type in engineering application is found in (c), which also gives the general flow configuration of a uniform stream over a cylinder. As seen in Fig. 4.19(c), the Joukowski airfoil has a cusp at the trailing edge so that there would be strength problems in actual usage. Since the Joukowski transformation, Eq. (2) can be equivalently rewritten by the following expression:

$$\frac{z - 2a}{z + 2a} = \left(\frac{\zeta - a}{\zeta + a} \right)^2 \quad (13)$$

The power of 2 in Eq. (13) can be replaced by the integer n , expanding the general form, which gives the following expression:

$$\frac{z - na}{z + na} = \left(\frac{\zeta - a}{\zeta + a} \right)^n \quad (14)$$

Equation (14) is called the Kàrmàn-Trefftz transformation and the airfoil generated by the transformation from the cylinder (a circle in the ζ -plane) is referred to as the Kàrmàn-Trefftz airfoils, see Fig.4.20(a). More general transformation can be derived directly from Eq. (1), taking the terms up to n , i.e.

$$z = C_0\zeta + \frac{C_1}{\zeta} + \frac{C_2}{\zeta^2} + \cdots + \frac{C_n}{\zeta^n} \quad (15)$$

The airfoil design based on Eq. (15) is referred to as the Mises airfoil, see Fig.4.20(b). These airfoils, based on the transformation by Eqs. (14) and (15), are flexible in design because of choices of the singularity points that are located in the appropriate positions, so that optimum design of an airfoil will be possible and be able to meet various engineering demands.

(a) Kàrmàn-Trefftz airfoil



(b) Mises airfoil



Fig. 4.20 Other airfoil shapes

Referring to Fig. 4.19(c), the cylinder (a circle in ζ -plane) is mapped into the z -plane by the Joukowski airfoil; at the same time, a flow around the cylinder in ζ -plane can also be mapped into the flow in the z -plane by the Joukowski transformation. This expresses flow around the Joukowski airfoil. In order to verify the flow field through rigorous efforts, we can write the complex potential $W(\zeta)$ in the following manner.

The flow field described by $W(\zeta)$ about the cylinder, whose center is placed at C_o , with the approaching free stream velocity U_∞ at an attack

angle α , as shown in Fig. 4.21(a). This is identically taken from Fig. 4.19(c), and can be expressed by the expression:

$$W(\zeta) = -U_\infty \left[(\zeta - be^{i\theta})e^{-i\alpha} + \frac{a^2 e^{i\alpha}}{(\zeta - be^{i\theta})} \right] \quad (16)$$

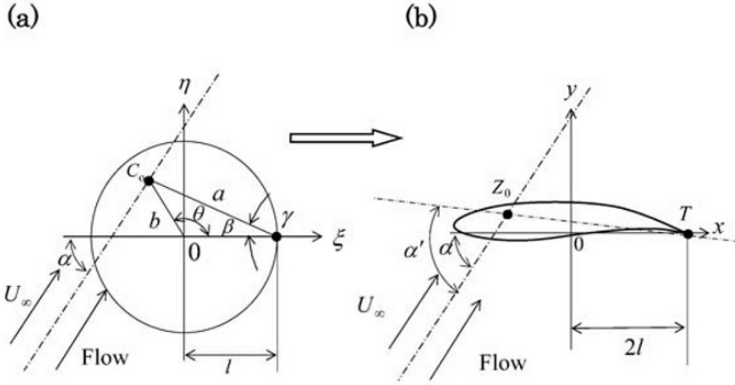


Fig. 4.21 Lift and moment on Joukowski airfoil

The point where $\zeta = l$ transforms into $z = 2l$ is at the trailing edge of the airfoil. However, $W(\zeta)$ in Eq. (16) has infinite velocity at the trailing edge; as a result, the singularity at the trailing edge must be removed from the Kutta-Joukowski hypothesis (Kutta condition) by adding a circulation. This is done by introducing the potential vortex given by Eq. (4.1.16) into Eq. (16), so that the singularity is removed at the trailing edge and the velocity at the trailing edge can become finite. The new complex potential W will be

$$W(\zeta) = -U_\infty \left\{ e^{-i\alpha} (\zeta - be^{i\theta}) + \frac{a^2 e^{i\alpha}}{\zeta - be^{i\theta}} \right\} + i \frac{\Gamma}{2\pi} \ln \left(\frac{\zeta - be^{i\theta}}{a} \right) \quad (17)$$

With $W(\zeta)$ in Eq. (17), the velocity at the trailing edge of the airfoil is given by

$$\frac{dW}{dz} = \frac{dW}{d\zeta} \frac{d\zeta}{dz} \quad \text{for } \zeta = l \text{ and } \zeta = 2l \quad (18)$$

and

$$\frac{dz}{d\zeta} = 1 - \frac{l^2}{\zeta^2} = 0 \quad (19)$$

Therefore, for dW/dz to be finite at the trailing edge, $dW/d\zeta$ must be zero, and this condition (Kutta Condition) determines the value of Γ . From Eq. (17), we have

$$\frac{dW}{d\zeta} = -U_\infty \left[e^{-i\alpha} - \frac{a^2 e^{i\alpha}}{(\zeta - be^{i\theta})^2} \right] + i \frac{\Gamma}{2\pi} \frac{1}{(\zeta - be^{i\theta})} = 0 \quad (20)$$

From the geometry of Fig. 4.21, we have

$$(\zeta - be^{i\theta}) = \zeta - l + ae^{i(-\beta)} \quad (21)$$

and for $\zeta = l$, Γ is obtained from Eq. (20) as follows

$$\Gamma = -4\pi a U_\infty \sin(\beta + \alpha) \quad (22)$$

The lift of an airfoil can be given by the Kutta-Joukowski theorem with the Blasius' first theorem, see Eq. (29) in Exercise 4.1.6

$$L = -\rho U_\infty \Gamma \quad (23)$$

where the lift L is perpendicular to the approaching free stream. Therefore, the lift is

$$L = 4a\pi\rho U_\infty^2 \sin(\beta + \alpha) \quad (24)$$

In order to examine the performance characteristics of an airfoil, the lift coefficient C_L is often used, where C_L is defined as a unit of length of the airfoil. This in turn refers to the chord length l_c or width of the airfoil, such that

$$C_L = \frac{L/l_c}{1/2\rho U_\infty^2} \quad (25)$$

It is now desired to estimate C_L of Joukowski airfoil where, taking $l_c \approx 4a$, we have

$$C_L = 2\pi \sin(\beta + \alpha) \quad (26)$$

Small $\beta + \alpha = \alpha'$; α' is often referred to as the absolute attack angle, which is greater than the apparent attack angle α , where we have

$$C_L \approx 2\pi\alpha' \quad (27)$$

In Fig. 4.22, some comparisons with the measurement of C_L and C_D are displayed, where C_D is similarly defined by

$$C_D = \frac{D/l_c}{1/2\rho U_\infty^2} \quad (28)$$

As observed in Fig. 4.22 (note that in an analytical symmetric case, $\alpha = \alpha'$ is also displayed with dotted line (b)), C_L increases with α' and then drops all of sudden, where the stall of airfoil occurs at α'_s . At the stall a flow separation (the viscous boundary layer separation) from the surface of an airfoil occurs and the circulation is lost, causing sharp drop of the lift. However, as seen in Fig. 4.22, the analytical estimate by Eq. (27) will give reasonable account for the (real) experimental measurement before reaching the stall angle α'_s . The drag of the potential flow is identically zero, as seen in Exercise 4.1.6, except in the experiment where the viscous friction causes the drag (due to the boundary layer), and the drag sharply increases after the stall angle α'_s caused by the flow separation.

The moment M_0 comes to the center of the origin in z -plane, whose value is to be obtained from Blasius' second theorem, as in Eq. (24) in Exercise 4.1.6

$$\begin{aligned} M_0 &= -\frac{1}{2}\rho\text{Re}\left\{\int_{c_1}\left(\frac{dW}{dz}\right)^2 z dz\right\} \\ &= -\frac{1}{2}\rho\text{Re}\left\{\int_{c_1}\left(\frac{dW}{d\zeta}\right)^2\left(\frac{d\zeta}{dz}\right)z d\zeta\right\} \end{aligned} \quad (29)$$

and with Eqs. (20) and (21), M_0 is expressed by

$$M_0 = 2\pi\rho U_\infty^2 l^2 \sin\{2(\gamma - \alpha)\} - \rho U_\infty \Gamma b \cos(\delta - \alpha) \quad (30)$$

where γ and δ are defined as

$$C_o = Z_0 = b e^{i(\pi - \theta)}, \quad \delta = \pi - \theta \quad (31)$$

and

$$a^2 = l^2 e^{2i\gamma} \quad (32)$$

Thus, the moment M at the point Z_0 in the airfoil, which implies the shifted center of the cylinder C_o in ζ -plane, is

$$\begin{aligned}
 M &= M_0 - Ll \cos(\delta - \alpha) \\
 &= 2\pi\rho U_\infty^2 l^2 \sin 2(\gamma - \alpha)
 \end{aligned}
 \tag{33}$$

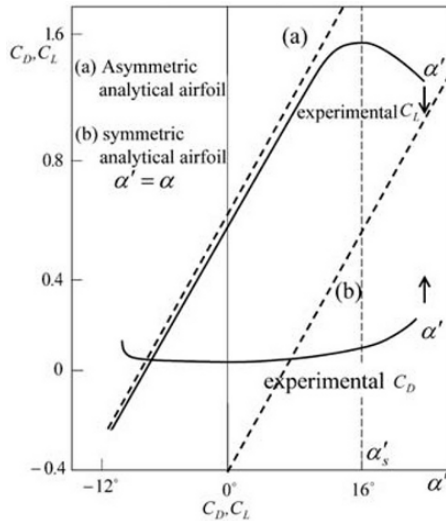


Fig. 4.22 Some comparison of C_L and C_D with experiment (Experimental data replotted after Nishiyama, 1989)

The moment coefficient C_M is similarly defined as following

$$C_M = \frac{M/l_c^2}{\frac{1}{2}\rho U_\infty^2} = 4\pi \sin 2(\gamma - \alpha)
 \tag{34}$$

where $l_c = l$ was taken tacitly.

Exercise 4.1.8 Forces on Deflectors

A liquid of an absolute velocity is deflected by a deflector to an angle of α forward and downward, as illustrated in Fig. 4.23. The surrounding pressure is kept constant by the atmospheric everywhere, and the pressure in liquid entering the deflector is the same as that in the liquid deflecting at the deflection point. The jet is free-jet, the column of which is kept constant without laterally spreading. The body force due to the gravity is small and can be neglected. The viscous force is also small and neglected everywhere. The deflection of the jet is confined in the two dimensional plane, as seen in Fig. 4.23.

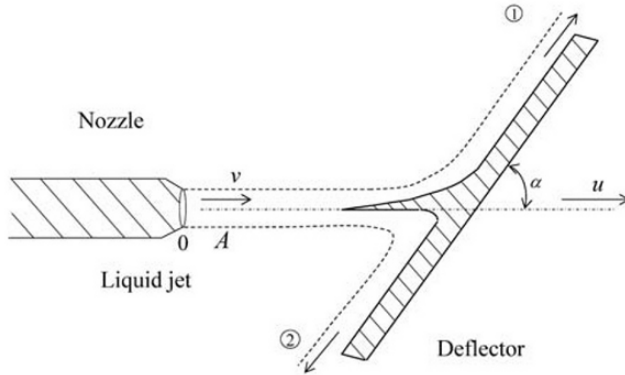


Fig. 4.23 Liquid jet at deflector

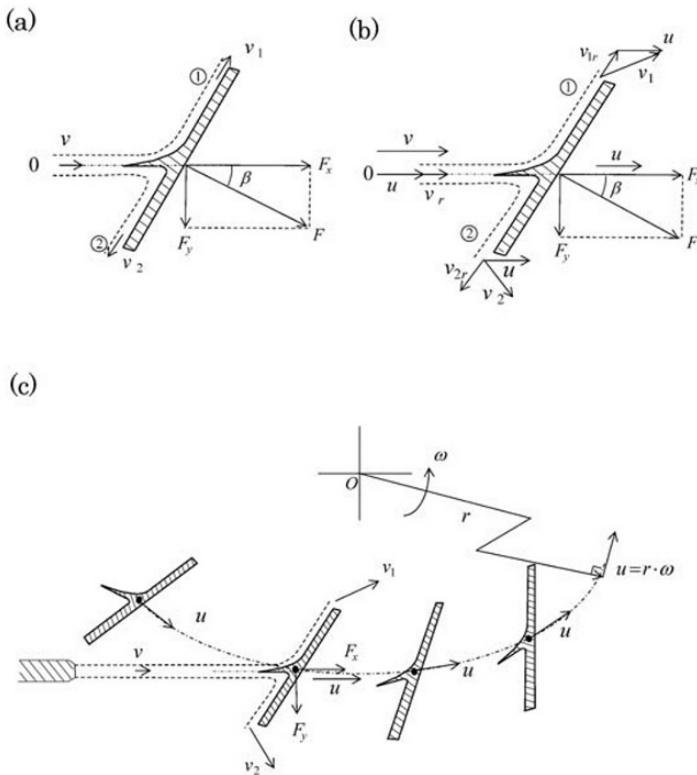


Fig. 4.24 Case study of liquid jet at deflector

The area of the entering liquid jet is A , and $1/3$ of the flow rate of the entering liquid jet is deflected downward (to the direction ②). Examine the following cases:

- (i) Determine the force acting on the deflector and the direction of the force when the deflector is stationary in the inertial reference frame.
- (ii) Determine the force acting on the deflector, and the direction of the force and the power of the deflector, when the deflector is moved to the direction of the liquid jet with an absolute velocity u in the inertial reference frame.
- (iii) Determine the physical parameters, if a series of deflectors (a cascade) are in action. Also describe a certain type of turbomachinery if the theory is applied in engineering practice, and estimate the kinetic energy given to run the machinery.

Note that the density of the liquid is ρ , which it is kept constant throughout the process.

Ans.

The exercise is the application of the integral form of the momentum equation over the control volume, which appears to preclude an integral part of analysis for turbomachines, such as turbines, pumps, compressors, and so forth.

- (i) Let us consider the control volume on the deflector as illustrated in Fig. 4.24(a), defining the exiting velocities v_1 and v_2 from upward ① and downward ② flow respectively. Denote that the forces acting on the control volume are f_x and f_y in x direction and y direction respectively, where the entering direction of the liquid jet is in x direction. From Eq. (4.1.47), the forces are

$$\dot{m}_1(v_1 \cos \alpha - v) + \dot{m}_2(-v_2 \cos \alpha - v) = f_x \quad (1)$$

$$\dot{m}_1(v_1 \sin \alpha - 0) + \dot{m}_2(-v_2 \sin \alpha - 0) = f_y \quad (2)$$

where for the mass flow rate \dot{m}_1 and \dot{m}_2 , we have given conditions

$$\dot{m}_1 = \rho \frac{2}{3} Q = \rho \frac{2}{3} (vA) \quad (3)$$

$$\dot{m}_2 = \rho \frac{1}{3} Q = \rho \frac{1}{3} (vA) \quad (4)$$

Bernoulli equation gives us a clue that the magnitude of v_1 , v_2 and v are all equal, because from 0 to ① and 0 to ② in the control volume, we can write Bernoulli equations as

$$\frac{1}{2}\rho v^2 + p_{\text{atm}} + \rho g z_0 = \frac{1}{2}\rho v_1^2 + p_{\text{atm}} + \rho g z_0 \quad (5)$$

$$\frac{1}{2}\rho v^2 + p_{\text{atm}} + \rho g z_0 = \frac{1}{2}\rho v_2^2 + p_{\text{atm}} + \rho g z_0 \quad (6)$$

where p_{atm} is the surrounding pressure and the gravitational effect $\rho g z_0$ is to be neglected. Thus, from Eqs. (1) to (4), we have

$$f_x = \rho v^2 A \left(\frac{1}{3} \cos \alpha - 1 \right) \quad (7)$$

$$f_y = \frac{1}{3} \rho v^2 A \sin \alpha \quad (8)$$

where f_x and f_y are the forces acting on the control volume (to liquid flow). Therefore, the forces acting upon the deflection are to be considered as the reaction forces

$$F_x = -f_x = \rho v^2 A \left(1 - \frac{1}{3} \cos \alpha \right) \quad (9)$$

$$F_y = -f_y = -\frac{1}{3} \rho v^2 A \sin \alpha \quad (10)$$

The direction of the resultant forces is thus

$$\beta = \tan^{-1} \frac{|F_y|}{|F_x|} = \tan^{-1} \left| \frac{1/3 \sin \alpha}{(1 - 1/3 \cos \alpha)} \right| \quad (11)$$

and its magnitude is

$$F = \sqrt{F_x^2 + F_y^2} = \frac{1}{3} \rho v^2 A \sqrt{10 + 6 \cos \alpha} \quad (12)$$

(ii) The deflector is moved with the liquid jet with the relative velocity v_r as

$$v_r = v - u \quad (13)$$

so that the mass flow rate relative to the deflector must be changed accordingly by

$$\dot{m}_{1r} = \rho \frac{2}{3} Q_r = \rho \frac{2}{3} (v_r A) \quad (14)$$

$$\dot{m}_{2r} = \rho \frac{1}{3} Q_r = \rho \frac{1}{3} (v_r A) \quad (15)$$

The Eqs. (1), (2), (5) and (6) will be solved for f_x and f_y , with Eqs. (14) and (15), using the relative (moving) frame locked onto the deflector by replacing v by v_r . We can thus obtain, by a heuristic argument, which the forces are written by

$$F_x = \rho(v-u)^2 A \left(1 - \frac{1}{3} \cos \alpha\right) \quad (16)$$

$$F_y = -\frac{1}{3} \rho(v-u)^2 A \sin \alpha \quad (17)$$

$$\beta = \tan^{-1} \frac{|F_y|}{|F_x|} = \tan^{-1} \left| \frac{1/3 \sin \alpha}{(1 - 1/3 \cos \alpha)} \right| \quad (18)$$

and

$$F = \sqrt{F_x^2 + F_y^2} = \frac{1}{3} \rho(v-u)^2 A \sqrt{10 + 6 \cos \alpha} \quad (19)$$

The kinetic energy W_s given to the deflector is thus expressed as follows

$$W_s = F_x \cdot u = \rho(v-u)^2 u A \left(1 - \frac{1}{3} \cos \alpha\right) \quad (20)$$

(iii) For a series of deflectors, the actual force on a deflector is zero before and after the liquid jet strikes the deflector. The situations considered are analogous to an impulse turbine, such as a Pelton wheel (refer for further exercises in Section 4.2). In order to examine the problem, we will idealize the situations that the jet (the discharge from a nozzle) is deflected with an angle of α on average, where the jet strikes the deflector and is deflected with the relative velocity v_r to the deflector, as discussed in the previous

problem (ii), i.e. $v_r = v - u$ according to Eq. (13). That said, the mass flow rate continuously striking the deflector, one after another, is defined in Eqs. (3) and (4) on average. Therefore, we solve for f_x and f_y with Eqs. (1), (2), (5) and (6) by replacing v with v_r , but we can consider the discharge Q with Eqs. (3) and (4). Resultantly, then, we have a force acting upon a deflector on average

$$F_x = \rho v(v-u)A\left(1 - \frac{1}{3}\cos\alpha\right) \quad (21)$$

$$F_y = -\frac{1}{3}\rho v(v-u)A\sin\alpha \quad (22)$$

$$\beta = \tan^{-1}\left|\frac{F_y}{F_x}\right| = \tan^{-1}\left|\frac{1/3\sin\alpha}{\left(1 - 1/3\cos\alpha\right)}\right| \quad (23)$$

and

$$F = \sqrt{F_x^2 + F_y^2} = \frac{1}{3}\rho(v-u)vA\sqrt{10 + 6\cos\alpha} \quad (24)$$

The kinetic energy W_d given to run the deflectors with the absolute speed u in the direction of the discharge (the direction of liquid jet) is thus given by

$$W_d = F_x \cdot u = \rho v(v-u)uA\left(1 - \frac{1}{3}\cos\alpha\right) \quad (25)$$

where $u = r \cdot \omega$ and r is the radius to which each deflector rotates with the angular velocity ω , which is analogous to the Pelton wheel.

Problems

4.1-1 In the potential flow, examine the flow field when one source of strength q and one sink of strength $-q$ are spaced equidistant $\pm a$ from the origin in the x -axis in an uniform flow U_∞ (as shown in Fig. 4.25). The complex potential $W(z)$ will be given by following formula

$$\begin{aligned}
 W(z) &= \phi + i\psi \\
 &= \left\{ -U_{\infty}x - \frac{q}{4\pi} \ln \frac{(x+a)^2 + y^2}{(x-a)^2 + y^2} \right\} \\
 &\quad + i \left[-U_{\infty}y - \frac{q}{2\pi} \left\{ \tan^{-1} \left(\frac{y}{x+a} \right) - \tan^{-1} \left(\frac{y}{x-a} \right) \right\} \right] \\
 &= \left[-U_{\infty}x - \frac{q}{2\pi} \ln r_1 + \frac{q}{2\pi} \ln r_2 \right] + i \left[-U_{\infty}y - \frac{q}{2\pi} \theta_1 + \frac{q}{2\pi} \theta_2 \right]
 \end{aligned}$$

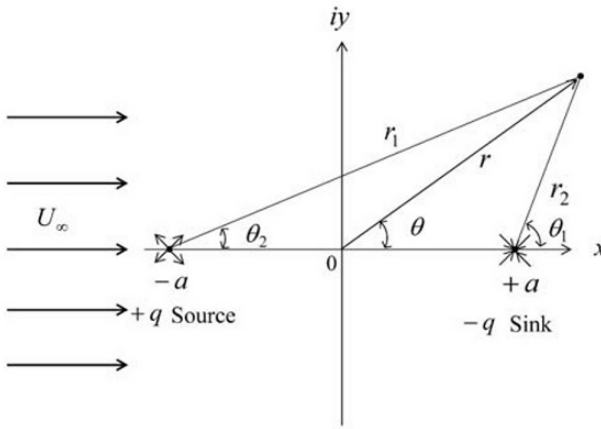


Fig. 4.25 One potential flow with source and sink

Ans. [The Rankine ovoid (oval)]

4.1-2 Siphons are used to discharge liquid from a reservoir as a simple and inexpensive way of pumping, as illustrated in Fig. 4.26. Find the elevation z_3 and the static pressure at the highest point ②, and discuss the function of the siphon, denoting that the discharge flow rate is Q and the level of point ② is known as z_2 (given) and the pipe has a uniform cross sectional area A . Neglect the effect of friction and assume that the area of the reservoir tank is large enough, compared to the siphon cross-sectional area, to disregard the kinetic energy at suction ① compared to the other kinetic energies. The surrounding pressure is the atmospheric p_a and the density of the liquid is ρ .

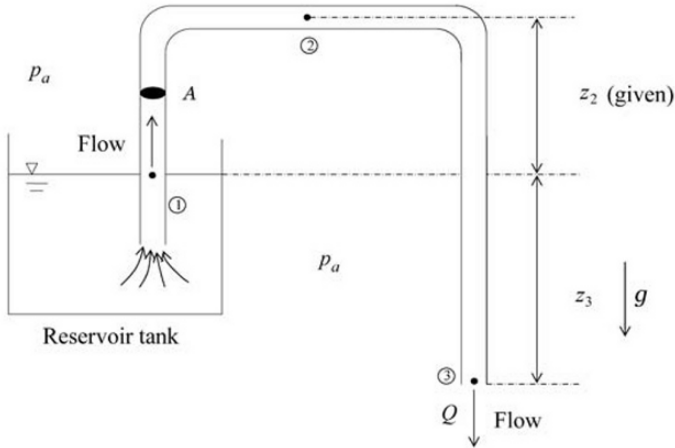


Fig. 4.26 Siphon

$$\text{Ans. } \left[\begin{array}{l} z_3 = \frac{(Q/A)^2}{2g} \\ P_2 = -\rho g(z_2 + z_3) \\ P_2 \geq P_{\text{sat}} \text{ (Vapor pressure)} \end{array} \right]$$

4.1-3 In open channels, such as broad shallow rivers and irrigation canals, the flow rate can be measured by a simple mean, the so-called broad-crested weir as illustrated in Fig. 4.27. The weir is usually raised from the channel bed by a concrete crest with a height of z_0 , letting the width of the crest to be b . The upstream crest should be well rounded to minimize a loss due to flow separation. When z_0 is sufficient to choke the flow and the crest is long enough so that the over flow streams are in parallel to the crest surface.

For the choked flow, a critical flow condition exists, and condition y may be $y = 3/2 y_c$, in which the flow is tranquil. Assuming that the kinetic energy at point ① is neglected, i.e. $v_1 = 0$, and Bernoulli equation from ① to ② can be applied, determine the velocity v_2 at point ②, and then estimate the flow rate Q by considering y as the measuring parameter.

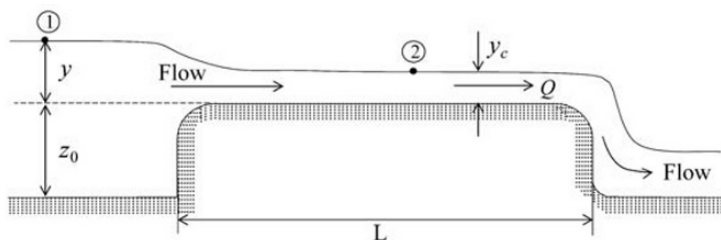


Fig. 4.27 Broad-crested wire

$$\text{Ans. } \left[v_2 = \sqrt{2g(y - y_c)} , \quad Q = \frac{2}{3} \sqrt{\frac{2}{3}} g b y^{\frac{3}{2}} \right]$$

4.1-4 A nozzle is discharging a liquid of density ρ into the atmospheric pressure p_a , as illustrated in Fig. 4.28. Find the pressure at point ① and calculate the force F_{x1} of the fluid acting on the nozzle in parts ①–②. The liquid can be treated as a high velocity jet to give discharge to a Pelton wheel or in fire fighting. The force, in this problem, is that fire fighters must hold the nozzle.

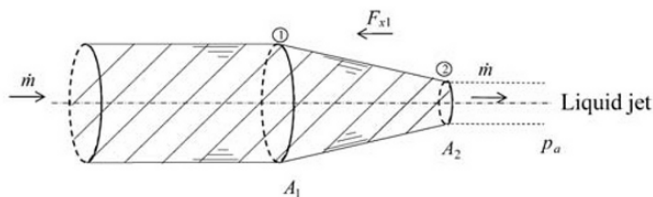


Fig. 4.28 Nozzle

$$\text{Ans. } \left[p_1 = \frac{\dot{m}^2}{2\rho} \left(\frac{1}{A_2^2} - \frac{1}{A_1^2} \right) \right. \\ \left. F_{x1} = \frac{\dot{m}^2}{2\rho} \frac{1}{A_1} \left(\frac{A_1}{A_2} - 1 \right)^2 \right]$$

4.1-5 The liquid jet is discharged from a nozzle of the cross sectional area A_2 with the discharge mass flow rate of \dot{m} . Calculate the force F

of the liquid jet acting on the deflector as a function of the inclined angle α , as illustrated in Fig. 4.29, and compare the divided mass from rate of \dot{m}_1 and \dot{m}_2 . Discuss the difference between the force F_{x1} (the force acting on the nozzle, Problem 4.1-4), and the force F_x (the x component of force acting on the deflector). Assume the liquid is a perfect fluid and the column of the jet is kept constant without the vena contracta.

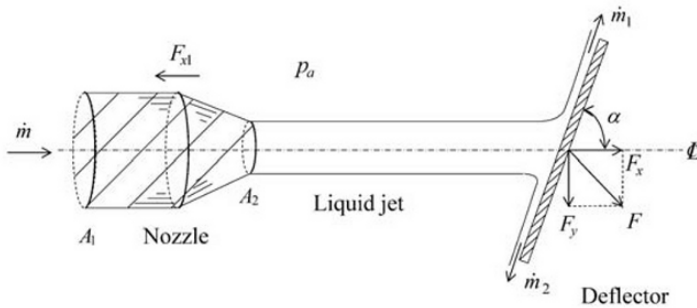


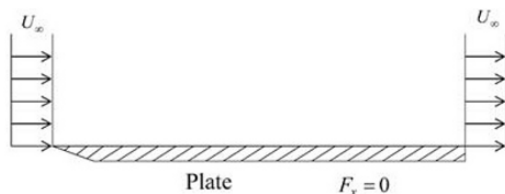
Fig. 4.29 Deflector

$$\text{Ans. } \left[F_x = \frac{\dot{m}^2}{\rho A_2} \sin^2 \alpha, \dot{m}_1 = \frac{\dot{m}}{2} (1 + \cos \alpha), \dot{m}_2 = \frac{\dot{m}}{2} (1 - \cos \alpha) \right]$$

- 4.1-6 In treating a drag force acting on a flat plate, there would not be any drag force on the plate if the fluid flowing on the plate is a perfect fluid. This is due to the reason that there is no viscosity, so that the flow over the plate is kept constant at the approaching velocity U_∞ ; namely, the flow slips (the slip condition) on the plate and there would not be any momentum change of the fluid, thus the drag force F_x is null, as depicted in Fig. 4.30(a). However, in a more realistic situation, fluid has a viscosity and the velocity at the surface of the plate is kept at zero; a no-slip condition. Consequently, the velocity on the plate has a distribution to the perpendicular direction (y -direction) against the flow direction (x -direction), which is called the boundary layer. Due to the boundary layer, there would be a momentum change in the control volume (1-2-3-4), including the boundary layer, as illustrated in Fig. 4.30(b). Determine the overall

drag force, and the drag coefficient of the plate, assuming that the velocity profile at the trailing edge is linear within the boundary layer, whose thickness is h . Consider the flow is steady with the density ρ and tackle the problem by applying Eq. (4.1.44) for the control volume, as indicated in Fig. 4.30(b).

(a)



(b)

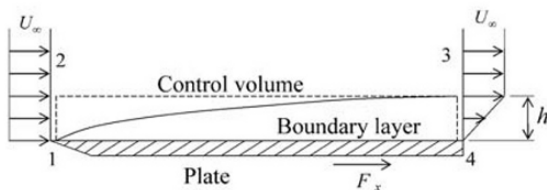


Fig. 4.30 Drag force on a plate

$$Ans. \left[D = F_x = \frac{\rho U_\infty^2 h}{6}, C_D = \frac{1}{3} \right]$$

*Problem 4.1-8 is helpful to think of this problem

*More details in the boundary layer theory

4.1-7 Draw a Kàrmàn-Trefftz airfoil (wing) and a Mises airfoil (wing), as respectively given by Eqs. (14) and (15) in Exercise 4.1.7, with appropriate constants. Illustrating with a computer will be helpful.

4.1-8 Give an idea to measure a drag force on an airfoil, the velocity profile in downstream is measured as $u = u(y)$, as illustrated in Fig. 4.31.

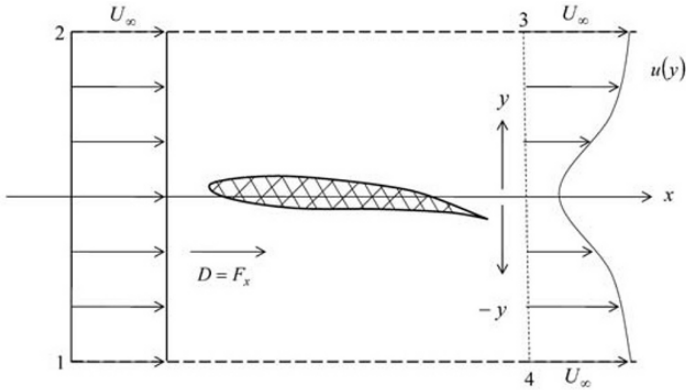


Fig. 4.31 Drag on an airfoil

$$Ans. \left[D = F_x = \int_{1 \rightarrow 2 \rightarrow 3 \rightarrow 4} \rho u (U_\infty - u) dS \right]$$

- 4.1-9 With the same manner as the Blasius' first theorem, obtain the moment M_0 from the Blasius' second theorem by substituting Eq. (27) into Eq. (24) in Exercise 4.1.6.

$$Ans. \left[M_0 = \pi \rho \text{Im} (2U_\infty e^{-i\alpha} B) \right]$$

- 4.1-10 A sprinkler, as illustrated in Fig. 4.32, discharges water (the density is ρ) at the volumetric flow rate of Q from each nozzle, whose opening area is A . Determine the rotational velocity (the angular velocity) of the sprinkler and the torque to hold the sprinkler stationary. Ignore mechanical loss and air resistance.

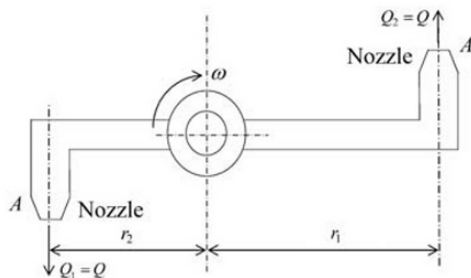
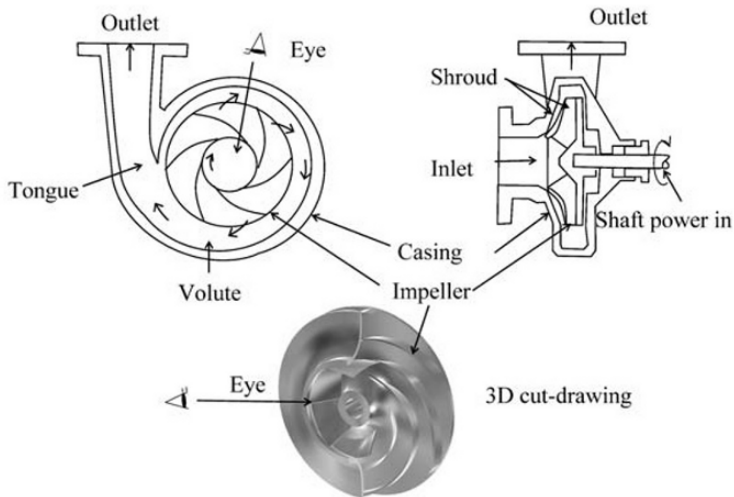
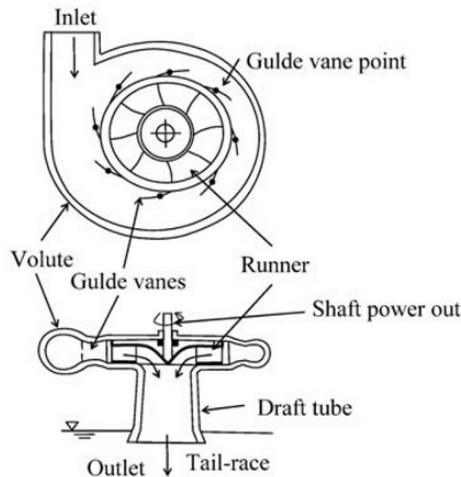


Fig. 4.32 Sprinkler

$$Ans. \left[\begin{array}{l} T_r = \rho Q_1 r_1 v_{1u} + \rho Q_2 r_2 v_{2u} = 0 \\ Q_1 = Q_2 = Q \\ v_{1u} = w_1 - u_1 = \frac{Q}{A} - r_1 \omega, \quad v_{2u} = w_2 - u_2 = \frac{Q}{A} - r_2 \omega \\ \therefore \omega = \left(\frac{r_1 + r_2}{r_1^2 + r_2^2} \right) \frac{Q}{A} \quad \therefore T_0 = \rho \frac{Q^2}{A} (r_1 + r_2) \end{array} \right]$$

4.2 General Theories of Turbomachinery

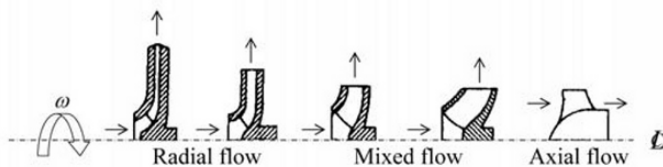
Turbomachines are the devices in which mechanical energy is transferred either to, or from, a continuously flowing fluid by means of the dynamic action of rotating propellers or vanes. Generally speaking, two main categories of turbomachine are identified. A turbopump (including fans and compressors) adds energy to a system to increase the fluid pressure (or head) with the result of an enthalpy increase in the fluid. A turbine (including wind, hydraulic, steam and gas turbines) extracts energy from a system to produce power by expanding fluid to a lower pressure (or head) with the result of an enthalpy decrease in the fluid. More often, the energy transferred to those of turbomachines is mechanical work that is converted to or from electric power. In Fig. 4.33(a) a single-suction pump; (b) a single-stage reaction turbine, are schematically displayed.

(a) Single-suction pump**(b) Single-stage reaction turbine; Francis turbine****Fig. 4.33 Radial-flow turbopump and turbine nomenclature**

The chief objective of this section is to study the general theories of turbomachinery based on the fluid mechanics and thermodynamics. The majority of content in this section is devoted to pumps that are typical example of turbomachineries. A fundamental treatment of compressible flows is also studied in applications of fans and gas turbines. Dimensional

analysis and performance laws, probably the widest comprehension of the general behavior of all turbomachines, are presented prior to the discussions on more general treatment of the similitude and dimensional analysis in later chapter. Methods of analyzing the detailed flow process and the performance characteristics differ largely, depending upon the geometrical configuration of the turbomachines, and in this text no detailed behavior of individual types in actual operation is considered, but more general theories are investigated.

(a) Pump



(b) Hydraulic turbine

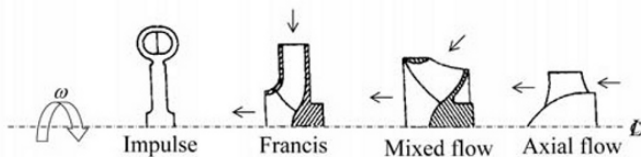


Fig. 4.34 Various types of rotors (impeller vane) in turbomachine

In order to achieve the energy conversion between vanes and fluid, it is very necessary for both vanes and fluid to gain force in a rotational direction. For fluid passing through vanes, the change of velocity component in rotational direction occurs by force, so that the torque or the magnitude of energy conversion can be readily estimated by Euler's pump (or turbine) law verified in Eqs. (4.1.51) and (4.1.53). We need to know, however, the flow fields at inlet and outlet to the vanes to obtain the energy conversion *a priori*. For a turbomachine with a greater number of vanes and with larger contact between the vane surface and the fluid flow, the moment of momentum theory (the Euler's pump or turbine law) would be more appropriate to apply. On the other hand, when the number of vanes are less and have smaller contact surface area with fluid flow, the airfoil theory may be more appropriate to apply. Both approaches are useful for designing

turbomachines, particularly for radial and mixed flow turbomachines with the moment of the momentum theory, and for axial flow turbomachine with the airfoil theory. Figure 4.34 shows the typical geometric configurations of turbomachines based on the flow direction through the machines.

4.2.1 Moment of Momentum Theory

Figure 4.35 shows schematics for an idealized radial flow pump impeller, in which (a) is a control volume from the frontal view together with its meridian cross section. In an idealized impeller, the thickness of each vane is to be neglected so that, as seen in Fig. 4.35(a), the flow enters to the control volume radially, along vanes with a relative velocity w_1 , and thus leaves with a relative velocity w_2 , while in the meridian plane the axial flow is diverted into a radial direction as the impeller rotates with an angular velocity ω .

The representative geometry of the impeller is that r_1 is the inlet radius, r_2 the outlet radius, b_1 and b_2 the width of the impeller at inlet and outlet respectively. The velocity diagram at the inlet with suffix 1 and the outlet with suffix 2 is illustrated in Fig. 4.35(b). u is the circumferential velocity, i.e. $u = r\omega$, and c is the absolute velocity to the inertial reference frame. It is worth mentioning that the image of the flow configuration in Fig. 4.35(b) is derived from the general concept of turbomachine, as displayed in Figs. 4.5, 4.6 and 4.7. The angle β is vane angle, through which the flow enters and leaves the impeller in the control volume with relative velocity w_1 and w_2 respectively. The radial and circumferential component of c are respectively denoted by c_m and c_u at locations of 1 and 2. α is the angle between the absolute velocity vector c and the circumferential velocity vector u at locations 1 and 2.

According to the theory of the moment of momentum and the Euler's pump (or turbine) equation, the shaft torque T_r and power P_w transmitted to a fluid from an impeller can be conventionally written as

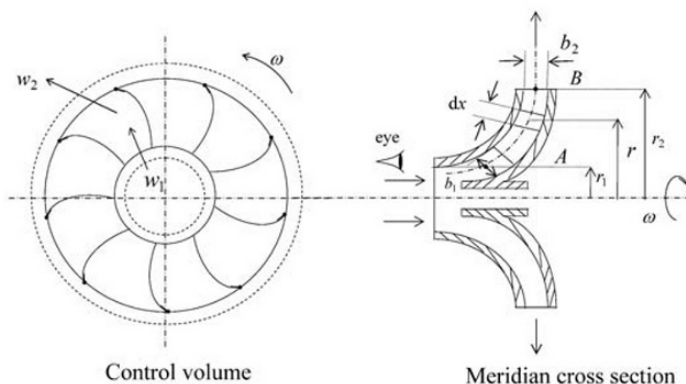
$$\begin{aligned} T_r &= \dot{m}(r_2 c_{2u} - r_1 c_{1u}) \\ &= \rho Q(r_2 c_2 \cos \alpha_2 - r_1 c_1 \cos \alpha_1) \end{aligned} \quad (4.2.1)$$

and

$$\begin{aligned} P_w &= T_r \cdot \omega \\ &= \rho Q(u_2 c_{2u} - u_1 c_{1u}) \end{aligned} \quad (4.2.2)$$

where n_z and Ω_z are conventionally replaced by notions of T_r and ω that are the torque and angular velocity respectively in Eqs. (4.1.51) and (4.1.53). It is noted again that in the case of T_r and $P_w > 0$, for the pump, and in the case of T_r and $P_w < 0$, for the turbine.

(a) Impeller



(b) Velocity diagrams at control surface

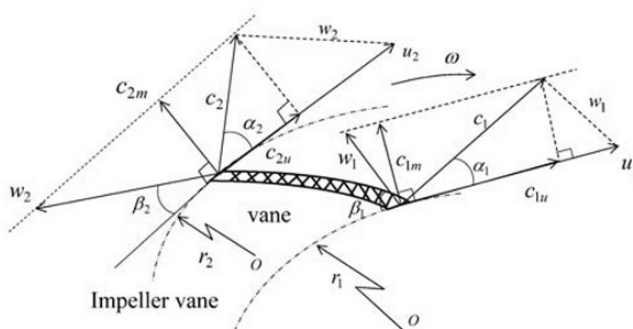


Fig. 4.35 Idealized radial flow pump

Noting that the fluid is a perfect fluid, which is satisfactorily justified for actual turbomachines through which flows have large Reynolds number and can be regarded as the inviscid flow. The theoretical power transmission of L_{th} per unit mass, neglecting energy loss, is expressed as

$$L_{th} = \frac{P_w}{\rho Q} = u_2 c_{2u} - u_1 c_{1u} \quad (4.2.3)$$

L_{th} is often called the theoretical specific energy, and furthermore the theoretical pressure head (Euler head) that rises across pump H_{th} is written as

$$H_{th} = \frac{L_{th}}{g} = \frac{1}{g} (u_2 c_{2u} - u_1 c_{1u}) \quad (4.2.4)$$

With the aid of the velocity diagram at points 1 and 2 in Fig. 4.35(b), we have

$$\begin{aligned} w^2 &= u^2 + c^2 - 2uc \cos \alpha \\ &= u^2 + c^2 - 2uc_u \end{aligned} \quad (4.2.5)$$

Combining Eqs. (4.2.5) and (4.2.4), we can reduce H_{th} to write

$$\begin{aligned} H_{th} &= \frac{u_2^2 - u_1^2}{2g} + \frac{w_1^2 - w_2^2}{2g} + \frac{c_2^2 - c_1^2}{2g} \\ &= \frac{c_2^2 - c_1^2}{2g} + \frac{1}{2g} [(u_2^2 - u_1^2) - (w_2^2 - w_1^2)] \end{aligned} \quad (4.2.6)$$

When we consider the equation given in Eq. (4.1.41) where the rotating reference frame at points 1 and 2, we can write Eq. (4.2.6) as follows

$$H_{th} = \frac{c_2^2 - c_1^2}{2g} + \frac{p_2 - p_1}{\rho g} \quad (4.2.7)$$

Equation (4.2.7) indicates that for a pump, i.e. $H_{th} \geq 0$, the energy given by rotating the impeller to a fluid results in the rise of kinetic energy (the first term of Eq. (4.2.7)) and the pressure rises (the second term of Eq. (4.2.7)). Similarly for turbines, it becomes the opposite, i.e. $H_{th} \leq 0$. The actual delivered head H , measured as the head difference between the inlet and outlet flanges of the pumps, as sometime called the manometric head, is less than the theoretical head H_{th} , due to a loss in head h_l , as this can be written as

$$H = H_{th} - h_l \quad (4.2.8)$$

For hydraulic turbines, the impeller can be regarded as a runner and water flows in opposite direction to the pump. For example, in the Francis turbines, the fluid power input to the turbine would be given as

$$P_w = \rho g Q H_{(t)\text{th}} \quad (4.2.9)$$

in which $H_{(t)\text{th}}$ is the theoretical head drop across the turbine. The actual head drop $H_{(t)}$ may be

$$H_{(t)} = H_{(t)\text{th}} + h_l \quad (4.2.10)$$

where the loss of head h_l will be added to the theoretical head $H_{(t)\text{th}}$.

Returning to the pump as our representative objective, the maximum theoretical head H_{th} in Eq. (4.2.4) can be achieved if c_{1u} becomes zero. This is the case when the inlet flows to an impeller and meets a condition, $\beta_1 = \pi/2$, i.e. $\alpha_1 = 0$ in Fig. 4.35(b), and namely this is the case when the flow has no swirling motion at the inlet and enters to an impeller along vanes normal to rotational direction. So that ideally we have

$$H_{\text{th}\infty} = \frac{1}{g} u_2 c_{2u} \quad (4.2.11)$$

and from the velocity diagram at 2 in Fig. 4.35(b), we have

$$\begin{aligned} H_{\text{th}\infty} &= \frac{1}{g} u_2^2 - \frac{1}{g} u_2 c_{2m} \cot \beta_2 \\ &= \frac{\omega^2 r_2^2}{g} - \frac{\omega \cot \beta_2}{2\pi b_2 g} Q \\ &= -\varepsilon_1 Q + \varepsilon_2 \end{aligned} \quad (4.2.12)$$

where ε_1 and ε_2 are kept constant when geometric parameters and the rotational speed are fixed. It should be noted that in deriving Eq. (4.2.12) the following relations are used

$$c_{2u} = c_2 \cos \alpha_2 = u_2 - c_{2m} \cot \beta_2 \quad (4.2.13a)$$

$$c_{2m} = \frac{Q}{2\pi r_2 b_2} \quad (4.2.13b)$$

$$u_2 = r_2 \omega \quad (4.2.14)$$

Equation (4.2.13b) is obtained by applying the mass continuity equation to the outlet (point 2) of the impeller. In an actual design of a radial flow turbomachine, there are vanes of finite thickness (conventionally 6~8 vanes in a pump impeller and 15~17 vanes in a turbine runner), and particularly

in a pump where there is a slip of flow at the outlet of an impeller, as illustrated in Fig. 4.36(a). As shown in Fig. 4.36(a), the relative velocity w_2 with the vane angle β_2 would be shifted to w'_2 and β'_2 respectively. This is largely caused by the fact that the flow is affected through the impeller of a pump, as illustrated in Fig. 4.36(b), due to the circulatory flow which is induced to have a rotation opposite to that of the impeller and thus modifies the outlet velocity diagram from an ideal pump. Therefore, there becomes a decelerating flow where the flow is quite uneven between the vanes. As a result, we have the difference from $H_{th\infty}$ to be written as

$$H_{th\infty} - H'_{th\infty} = \frac{1}{g} u_2 (c_{2u} - c'_{2u}) \quad (4.2.15)$$

and

$$H_{th\infty} - H'_{th\infty} = P_c H'_{th\infty} \quad (4.2.16)$$

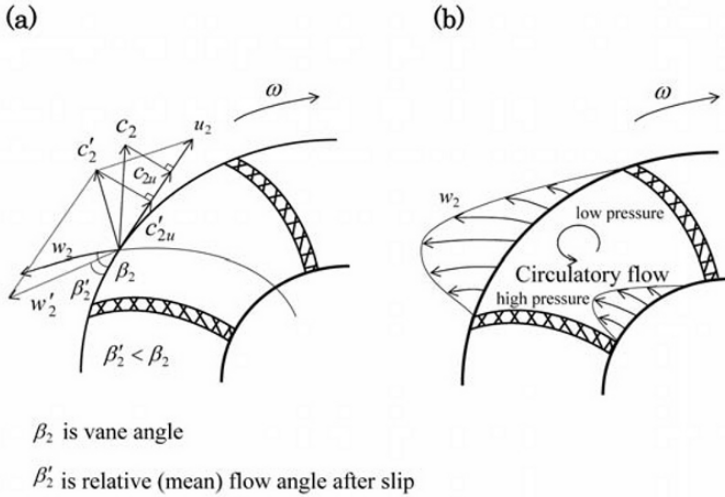


Fig. 4.36 Slip flow at outlet of impeller

Equation (4.2.16) compares the relative head difference between the ideal head $H_{th\infty}$ and the actual (after considering slip) head $H'_{th\infty}$, giving the ratio between the tangential components of absolute velocity corresponding to the angles β_2 and β'_2 respectively. This is indicated in Fig. 4.36(a). Equation (4.2.16) can be further reduced to a formula

$$\sigma_s = \frac{c'_{2u}}{c_{2u}} = \frac{1}{P_c + 1} \quad (4.2.17)$$

where σ_s is called a slip factor, and P_c is a correlation constant obtained by experience in an actual pump design. P_c may be written, as a result of many attempts in predicting the amount of slip from impellers, Pfleiderer(1961)

$$P_c = q_c \frac{r_2^2}{s_c I_s} \quad (4.2.18)$$

Note that in Eq. (4.2.18), q_c is an experimental constant and usually given by the following correlational formula for a radial flow impeller (10–30% lower value for pumps with outlet guide vanes)

$$q_c = (0.55 \sim 0.68) + 0.6 \sin \beta_2 \quad (4.2.19)$$

and for impeller vanes with a three dimensional curved surface

$$q_c = (1.0 \sim 1.2) \left(1 + \sin \beta_2 \right) \left(\frac{r_1}{r_2} \right) \quad (4.2.19)$$

In Eq. (4.2.18), I_s is the first moment of an area for the axis of rotation along the center line of the meridian cross-section, as shown in Fig. 4.35(a) and defined for the radial flow pump as

$$I_s = \int_{r_1}^{r_2} r dr = \frac{1}{2} (r_2^2 - r_1^2) \quad (4.2.20)$$

s_c is the number of vanes in an impeller, where for pump

$$s_c \approx 6 \sim 8 \quad (4.2.21)$$

The information given from the slip factor given in Eq. (4.2.17) is of vital importance, particularly to the compressor designer, where accurate knowledge of it appears to preclude the possibility of achieving a higher energy conversion rate between the impeller and fluid.

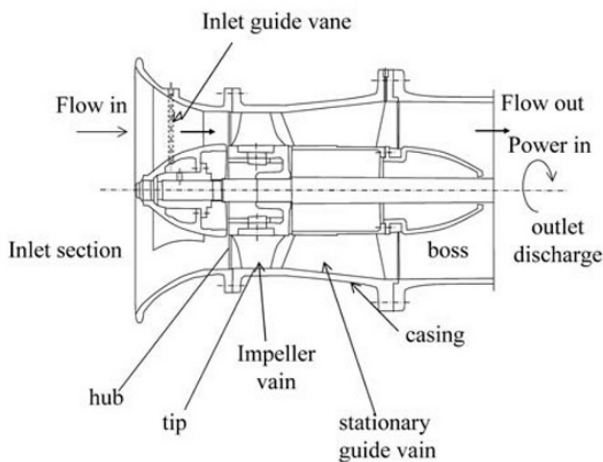
4.2.2 Airfoil Theory

As mentioned in the previous section, the airfoil theory is more appropriate to apply for designing turbomachines, whose numbers of vanes are smaller

and with a less contact surface area than with fluid flow. This is often encountered in axial flow turbomachines, where the flow to and from a turbomachine is in the axial direction of the rotation (shaft rotation), as illustrated in Fig. 4.37(a) and (b). In order to figure out the axial flow turbomachine, (a) schematics of an axial flow pump and (b) an axial flow turbine (Kaplan turbine) are displayed in Fig. 4.37. Usually in the actual axial flow turbomachines, there are inlet guide vanes (which are not regarded as part of a control volume in the case of a pump. It usually functions in directing flow away from the axial direction), rotor vanes (impeller vane in pump and runner in turbine) and stationary guide vanes in pumps. In axial flow turbomachines, a number of identical vanes, which are equally spaced and paralleled to one another, are arranged so that they form a cascade geometry. For the axial flow turbomachines of a high hub-tip ratio, radial velocities are negligible and, to a close approximation, the flow may be regarded as two dimensional. To obtain a truly two dimensional flow, however, there would require a cascade of infinite extent so that there would not be any flow interaction between each neighboring vane. In Fig. 4.38(a), the control volume of an impeller vane is illustrated, and with it the energy input through the shaft rotation is converted into flow energy.

The flow approaches the cascade, as illustrates in Fig. 4.38(b), with an absolute velocity c_1 at an angle α_1 and leaves downstream of the cascade with the absolute velocity c_2 at an angle α_2 . It is denoted that in the following analysis the flow is assumed to be incompressible ($M \leq 0.3$) and steady in the control volume with the rotational speed u . The assumption of the steady flow is valid for an isolated cascade, where for the control volume the number of vanes is low. The velocity diagrams at the inlet and the outlet can be composed as shown in Fig. 4.38(b). The absolute velocities c_1 and c_2 are obtained by the vector sum of the rotational speed u and the relative velocity w at the inlet and outlet respectively. In the airfoil theory, approaching the axial flow turbomachines, the averaged velocities to a representative airfoil are composed by taking the averaged velocity diagram with reference to Fig. 4.38(c), where \bar{w} and \bar{c} are the average relative velocity and absolute velocity respectively with the average angle is $\bar{\alpha}$ and $\bar{\beta}$. In Fig. 4.38(c), \bar{c} is composed with u and the arithmetic mean of w_1 and w_2 , whose circumferential component is $\bar{w} = (w_{1u} + w_{2u})/2$.

(a) Axial flow turbomachines ; axial flow pump



(b) Axial flow turbine; Kaplan turbine

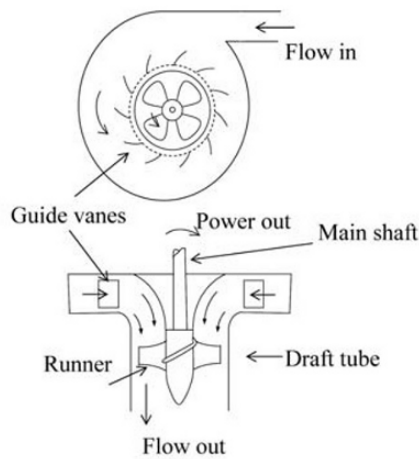
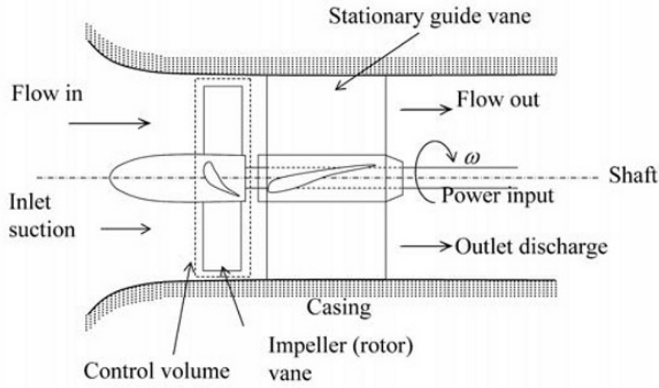
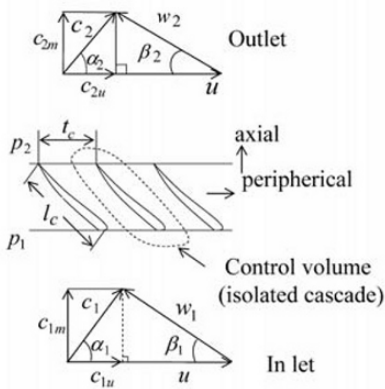


Fig. 4.37 Axial flow turbomachines and their nomenclature

(a) Impeller vane, axisymmetric arrangement



(b) Inlet outlet velocity



(c) Velocity diagram for average velocity and force

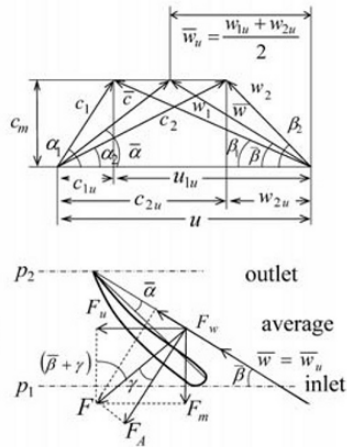


Fig. 4.38 Idealized axial flow pump

The theoretical pressure head rise H_{th} in the case of a pump (or pressure head drop in case of turbine) across the cascade low can then be calculated based on the forces acting upon a representative airfoil in the isolated cascade as illustrated in a lower diagram in Fig. 4.38(c). Setting $F_A = L$ (lift force) and $F_w = D$ (drag force) on the airfoil for the average attack angle $\bar{\alpha}$ with reference to Fig. 4.38(c), we can write, following the definitions of Eqs. (25) and (28) in Exercise 4.1.7

$$F_A = C_L \frac{1}{2} \rho \bar{w}^2 l_c \quad (4.2.22)$$

$$F_w = C_D \frac{1}{2} \rho \bar{w}^2 l_c \quad (4.2.23)$$

where C_L and C_D are the lift and drag coefficient per unit length of the airfoil respectively and l_c is the cord length of the airfoil. Denoting F as the resultant force by F_w and F_A , and F is decomposed in the peripherical direction and the axial direction written as F_u and F_w respectively, as indicated in Fig. 4.38(c) with a representative angle γ . So that, we have

$$\begin{aligned} F_u &= F \cos \left\{ \frac{\pi}{2} - (\bar{\beta} \pm \gamma) \right\} \\ &= F \sin(\bar{\beta} \pm \gamma) \end{aligned} \quad (4.2.24)$$

and furthermore

$$\begin{aligned} F_u &= F_A \sin \bar{\beta} - F_w \cos \bar{\beta} \\ &= F_A (\sin \bar{\beta} \pm \gamma \cos \bar{\beta}) \end{aligned} \quad (4.2.25)$$

where $-\gamma$ is a turbine, $+\gamma$ is a pump (or fan) and together are given as

$$\frac{F_w}{F_A} = \frac{C_D}{C_L} = \tan \gamma \equiv \gamma \quad (4.2.26)$$

It is now desired to derive an expression for the theoretical pressure head H_{th} to characterize the turbomachine. This can be achieved directly by considering the work transfer in energy balance. Taking an annulus element (vane element) between r and $r + dr$, as indicated in Fig. 4.39, the work transfer $d\bar{W}_p$ between the fluid and the annulus element can be written, from Eq. (4.2.25), as

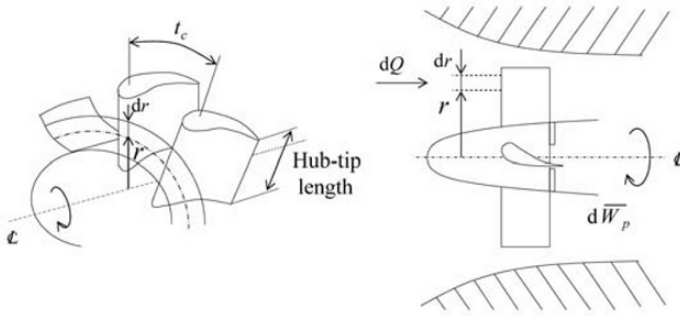


Fig. 4.39 Vane element

$$\begin{aligned} s_c \cdot d\bar{W}_p &= s_c \cdot F_u u dr \\ &= s_c \cdot u F_A (\sin \bar{\beta} \pm \lambda \cos \bar{\beta}) dr \end{aligned} \quad (4.2.27)$$

where s_c is the number of vanes. The flow rate through the element dQ is written as

$$dQ = s_c \cdot t_c dr c_m \quad (4.2.28)$$

where t_c is the pitch of the vanes in the cascade. For $s_c \cdot d\bar{W}_p$ in Eq. (4.2.27), we have the following relationship

$$s_c \cdot d\bar{W}_p = \rho dQ g H_{th} \quad (4.2.29)$$

so that Eq. (4.2.27) is rewritten as

$$s_c \cdot \rho g H_{th} t_c c_m dr = s_c \cdot u F_A (\sin \bar{\beta} \pm \gamma \cos \bar{\beta}) dr \quad (4.2.30)$$

For a two dimensional assumption, Eq. (4.2.30) is integrated with respect to r for a hub-tip length, where we have

$$\begin{aligned} H_{th} &= \frac{F u \sin(\bar{\beta} \pm \gamma)}{\rho g t_c c_m} \\ &= \frac{F_A u (\sin \bar{\beta} \pm \gamma \cos \bar{\beta})}{\rho g t_c c_m} \end{aligned} \quad (4.2.31)$$

Equation (4.2.31) can be further expanded to give a design parameter for the two dimensional cascade, by applying Eq. (4.2.22) with the expression of $F = F_A / \cos \gamma$ as follows

$$H_{th} = C_L \frac{l_c}{t_c} \frac{u}{c_m} \frac{\bar{w}^2}{2g} \frac{\sin(\bar{\beta} \pm \gamma)}{\cos \gamma} \quad (4.2.32)$$

and

$$C_L \frac{l_c}{t_c} = \frac{2gH_{th}c_m \cos \gamma}{\bar{w}^2 u \sin(\bar{\beta} \pm \gamma)} \quad (4.2.33)$$

With reference to the velocity diagram in Fig. 4.38(c), \bar{w} and $\bar{\beta}$ will be given in the following expression

$$\bar{w} = c_m^2 + \left(u - \frac{c_{1u} + c_{2u}}{2} \right)^2 \quad (4.2.34)$$

and

$$\bar{\beta} = \tan^{-1} \left\{ \frac{c_m}{u - (c_{1u} + c_{2u})/2} \right\} \quad (4.2.35)$$

It is noted here that with the lower hub-tip radius ratios, the vanes of a turbomachine will have an appreciable amount of twist along their length so that, in many cases, a three dimensional approach in axial turbomachines, the so-called vortex design, is required. However, with a reasonable degree of accuracy, a two dimensional approach will give a close approximation for axial flow machines with a high hub-tip ratio, such as given in Eqs. (4.2.32) and (4.2.33).

4.2.3 Efficiency and Similarity Rules of Turbomachinery

Definitions of efficiency are always confusing and they, in fact, differ, case by case. Nevertheless, in this section the most commonly used and accepted definitions in the literature of turbomachines are introduced. The total (or overall) efficiency η is defined in such a way that

$$\eta = \frac{\text{mechanical energy available at coupling of output shaft}}{\text{possible maximum energy of fluid}} \quad (4.2.36)$$

The total efficiency η is further decomposed by three independent efficiencies, such as the hydraulic efficiency η_h (or adiabatic efficiency η_t for

gas turbine), the volumetric efficiency η_v and the mechanical efficiency η_m , which are respectively defined as follows

$$\eta_h = \frac{\text{mechanical energy supplied to the rotor}}{\text{possible maximum energy of fluid}} \quad (4.2.37)$$

$$\eta_h = \frac{H - h_l}{H} = \frac{H_{th}}{H} \quad (\text{hydraulic turbine}) \quad (4.2.38)$$

or

$$\eta_h = \frac{H_{th} - h_l}{H_{th}} = \frac{H}{H_{th}} \quad (\text{pump or fan}) \quad (4.2.39)$$

In both cases

$$H_{th} = H \pm h_l \quad (- \text{hydraulic turbine} ; + \text{pump or fan}) \quad (4.2.40)$$

where H is the actual head, h_l the loss head between the inlet and outlet of turbomachines, and H_{th} is the theoretical pressure head.

$$\eta_v = \frac{Q - Q_l}{Q} \quad (\text{hydraulic turbine}) \quad (4.2.41)$$

or

$$\eta_v = \frac{Q}{Q + Q_l} \quad (\text{pump or fan}) \quad (4.2.42)$$

where Q is the volumetric flow rate and Q_l is the volumetric rate of leakage from turbomachines.

$$\eta_m = \frac{\text{shaft power}}{\text{rotor power}} \quad (4.2.43)$$

Altogether, with the definitions of Eqs. (4.2.37–4.2.43), we have the total efficiency η to write

$$\eta = \eta_h \cdot \eta_v \cdot \eta_m \quad (4.2.44)$$

In the design and development of turbomachinery, the widest comprehension of the general behavior is obtained from similitude and dimensional analysis. In engineering practice, for design purposes, we have to depend on test results obtained from experiment with “models”, which are

often smaller in size than the “prototype”. The “prototype” is the full-size device at a preliminary stage of a commercial product. Dimensional analysis based on this similitude can then be applied to predict a prototype’s performance from tests conducted on a scale model, and also to determine the most suitable type of machine for its maximum efficiency, for a specific range of head, speed and flow rate. In a similar manner the dimensional analysis enables data taken from a test machine to reduce into a smaller number of dimensionless groups and given experimental relations between variables to be found with the greatest economy of effect.

We will apply the idea of similitude and dimensional analysis developed in Chapter 6 and in Appendix C to turbomachines in this section. First, we will define our system of a turbomachine, introducing a control volume as shown in Fig. 4.40. The significant parameters for a turbomachine are; discharge Q , power (work transfer) W , rotational (rotational) speed n , representative diameter of rotor D , head gH (g is conventionally inclusive or pressure difference ΔP), efficiency η , density of fluid ρ , viscosity η_0 and some geometric representative scales l_1 and l_2 . The system then can be described, in an arbitrary function, as

$$f\left(Q, n, D, \rho, \eta_0, \frac{l_1}{D}, \frac{l_2}{D}, gH, \eta, W\right) = 0 \quad (4.2.45)$$

With an application of dimensional analysis, say Buckingham π -theorem

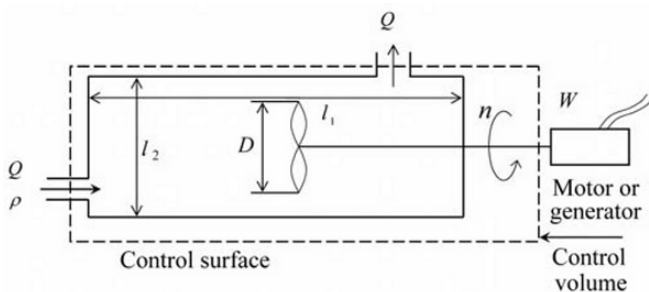


Fig. 4.40 Control volume of turbomachine

with reference to Appendix C-1, we are able to reduce a group of non-dimensional parameters by a functional relationship, using three of the independent variables (ρ, N, D) as common factors (control variables) when considering the three primary (basic) dimensions, i.e. mass, length and time, as follows

$$\varphi = \frac{gH}{(nD)^2} = f_1 \left(\frac{Q}{nD^3}, \frac{\rho nD^2}{\eta_0}, \frac{l_1}{D}, \frac{l_2}{D} \right) \quad (4.2.46)$$

$$\eta = f_2 \left(\frac{Q}{nD^3}, \frac{\rho nD^2}{\eta_0}, \frac{l_1}{D}, \frac{l_2}{D} \right) \quad (4.2.47)$$

$$C_W = \frac{W}{\rho n^3 D^5} = f_3 \left(\frac{Q}{nD^3}, \frac{\rho nD^2}{\eta_0}, \frac{l_1}{D}, \frac{l_2}{D} \right) \quad (4.2.48)$$

In Eqs. (4.2.46–4.2.48), we have the nondimensional parameters

$$\begin{aligned} \varphi &= \frac{gH}{(nD)^2} \text{ (or alternatively, } \varphi = \frac{\Delta P}{\rho \omega^2 D^2} \text{ with angular velocity } \omega) \\ &\equiv \text{Head coefficient (or pressure coefficient)} \end{aligned} \quad (4.2.49)$$

$$\begin{aligned} C_W &= \frac{W}{\rho n^3 D^5} \text{ (or alternatively, } C_W = \frac{W}{\rho \omega^3 D^5} \text{)} \\ &\equiv \text{Power coefficient} \end{aligned} \quad (4.2.50)$$

$$\begin{aligned} C_Q &= \frac{Q}{nD^3} \text{ (or alternatively, } C_Q = \frac{Q}{\omega D^3} \text{)} \\ &\equiv \text{Volumetric flow rate coefficient} \end{aligned} \quad (4.2.51)$$

$$\begin{aligned} Re &= \frac{\rho nD^2}{\eta_0} \text{ (or alternatively, } Re = \frac{\rho \omega D^2}{\eta_0} \text{)} \\ &\equiv \text{Reynolds number} \end{aligned} \quad (4.2.52)$$

The performance parameters in Eqs. (4.2.46–4.2.48) are thus correlated with a group of nondimensional parameters defined in Eqs. (4.2.49–4.2.52). The volumetric flow rate coefficient C_Q in Eq. (4.2.51) is alternatively defined by using the peripheral speed u and the representative fluid speed c_x at a datum point (such as the mean axial speed in a rotor)

$$u \propto nD \quad (4.2.53)$$

$$Q \propto c_x D^2 \quad (4.2.54)$$

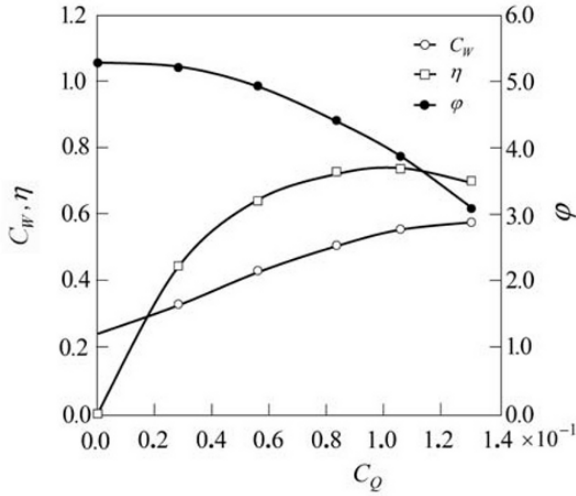


Fig. 4.41 Dimensionless radial flow pump performance curve (Courtesy of Teral Kyokuto Inc.)

so that

$$C_Q = \frac{Q}{nD^3} = \frac{c_x}{u} \quad (4.2.55)$$

For engineering purposes, the kinematic viscosity $\nu = \eta_0 / \rho$ is very small if compared to the inertia $\rho n D^2$ that results in a Reynolds number high. Correspondingly, the flow regime in a turbo machine is usually very turbulent ($Re \gg 10^4$), and experiments confirm that the performance characteristics of a turbomachine is almost independent from the effects of a Reynolds number and can be ignored in a first approximation. It is also a usual practice not to make a correlation between the roughness of the flow channel and the pump losses, assuming that the hydraulic efficiency η_h (or adiabatic efficiency η_t) is constant. With geometric similarity, the model and the prototype are identical in shape, but differ in size. The model ratios l_1 / D and l_2 / D are kept constant and may be eliminated forthwith. Thus, considering the facts above mentioned, the functional relationship for geometrically similar hydraulic turbomachines are then expressed as

$$\phi = f_1(C_Q) \quad (4.2.56)$$

$$\eta = f_2(C_Q) \quad (4.2.57)$$

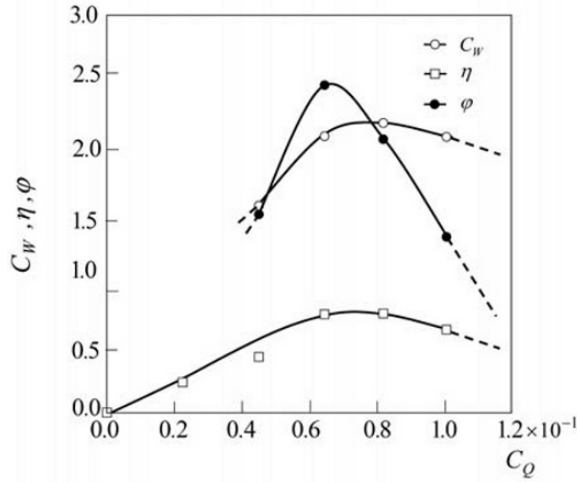


Fig. 4.42 Dimensionless axial flow fan performance curve (Courtesy of Teral Kyokuto Inc.)

$$C_W = f_3(C_Q) \quad (4.2.58)$$

It is noted that the actual form of the functions $f_1 \sim f_3$ in Eqs. (4.2.56–4.2.58) must be determined from results of experimental measurements (or computer simulations). In Figs. 4.41 and 4.42, typical curves of $f_1 \sim f_3$ are displayed for a radial flow pump and an axial flow fan respectively. It should be mentioned that curves for $f_1 \sim f_3$ may vary for types of turbomachines (Refs. Schetz and Fuhs, 1996 and Potter and Wiggent, 1997).

Designers, who wish to obtain a best match with changing flow conditions, can consider off-design operation by considering an additional variable β into Eqs. (4.2.56–4.2.58). For example, in an axial flow pump (or turbine), considering β as the average vane angle $\bar{\beta}$ in Fig. 4.38, which can be set at various values, and we can write as

$$\phi = f_1(C_Q, \beta) \quad (4.2.59)$$

$$\eta = f_2(C_Q, \beta) \quad (4.2.60)$$

Alternatively, we can write

$$\beta = f_4(C_Q, \phi) = f_5(C_Q, \eta) \quad (4.2.61)$$

Therefore, from Eq. (4.2.61), the performance parameter, say η , can be written as

$$\eta = f_6(C_Q, \varphi) \quad (4.2.62)$$

where η is a function of both C_Q and φ , as illustrated in Fig. 4.43 (derived from Fig. 4.42 for varying φ).

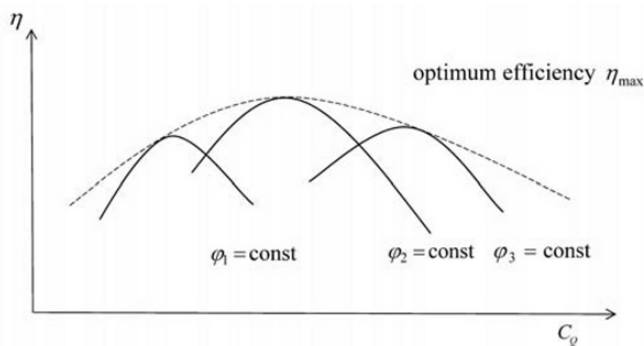


Fig. 4.43 Off-design operation (variable φ)

From the relationship in Eqs. (4.2.53–4.2.55), similar relationships between any two machines from the same geometric family can be straightforwardly derived. Any two machines, identifying M and P as suffix, are

$$\varphi = \text{const.}; \left[\frac{gH}{n^2 D^2} \right]_M = \left[\frac{gH}{n^2 D^2} \right]_P \quad (4.2.63)$$

$$C_Q = \text{const.}; \left[\frac{Q}{n D^3} \right]_M = \left[\frac{Q}{n D^3} \right]_P \quad (4.2.64)$$

$$C_W = \text{const.}; \left[\frac{W}{\rho n^3 D^5} \right]_M = \left[\frac{W}{\rho n^3 D^5} \right]_P \quad (4.2.65a)$$

$$\text{or} \quad \left[\frac{W}{\rho D^2 H^{\frac{3}{2}}} \right]_M = \left[\frac{W}{\rho D^2 H^{\frac{3}{2}}} \right]_P \quad (4.2.65b)$$

Furthermore, for any two identical machines with a different operating condition, for example with a variety of rotational speeds, can set $D_M = D_P$ to Eqs. (4.2.63–4.2.65), identifying the operating conditions by, where we have

$$\frac{H}{H'} = \frac{n^2}{n'^2} \quad , \quad \frac{Q}{Q'} = \frac{n}{n'} \quad , \quad \frac{W}{W'} = \frac{n^3}{n'^3} \quad (4.2.66)$$

Eliminating H and n' from above relationship, we can write

$$\frac{Q^2}{H} = \frac{Q'^2}{H'} \quad , \quad \frac{W}{H^{\frac{3}{2}}} = \frac{W'}{H'^{\frac{3}{2}}} \quad (4.2.67)$$

There is often the case that the turbomachinery designer faces the basic problem of deciding what type of turbomachine will be the best choice. The problem can be solved by correlating a turbomachine of a given family to a nondimensional number that characterizes its operation of optimum conditions. The nondimensional number is termed the specific speed n_s , which is calculated by a preliminary design data and is usually provided to the designer at initial stage of development, with such as H , Q and n for a pump, or W , H and n for a turbine. For any hydraulic turbomachine with fixed geometry, i.e. keeping D as constant, there is a unique relationship between the efficiency and the volumetric flow rate, represented by dimensionless number φ and C_Q , as seen in Fig. 4.41 and in Fig. 4.42. If the optimum efficiency η_{\max} (with reference to Fig. 4.43) is given by a unique value of $C_{Q(0)}$ and $C_{W(0)}$, we can write the similarity relationships in Eqs. (4.2.63–4.2.65) for η_{\max} , $C_{Q(0)}$ and $C_{W(0)}$. Thus, eliminating D from the relationships, combining Eqs. (4.2.63) and (4.2.64) for pump, and Eqs. (4.2.63) and (4.2.65) for turbine, we have

$$n_s = \left[n \frac{Q^{\frac{1}{2}}}{(gH)^{\frac{3}{4}}} \right]_M = \left[n \frac{Q^{\frac{1}{2}}}{(gH)^{\frac{3}{4}}} \right]_P = \frac{C_{Q(0)}^{\frac{1}{2}}}{\eta_{\max}^{\frac{3}{4}}} \quad (4.2.68)$$

$$n_t = \left[n \frac{W^{\frac{1}{2}}}{\rho^{\frac{1}{2}}(gH)^{\frac{5}{4}}} \right]_M = \left[n \frac{W^{\frac{1}{2}}}{\rho^{\frac{1}{2}}(gH)^{\frac{5}{4}}} \right]_P = \frac{C_{w(0)}^{\frac{1}{2}}}{\eta_{\max}^{\frac{5}{4}}} \quad (4.2.69)$$

where n_s is called the specific speed (pump) and n_t is the power specific speed (turbine). It is noted that in Eqs. (4.2.68) and (4.2.69), g and ρ are often eliminated from both $[]_M$ and $[]_P$ in common industrial practices, through which they become dimensional parameter. They are called the homologous specific speed, and in the case of using the homologous specific speed one should be aware of a unit to be used. From industrial experience, in selecting the type of pump based on an impeller (as typically displayed in Fig. 4.34(a)), the specific speed n_s is correlated as follows

$$\begin{aligned} n_s &< 1; \text{ radial flow pump} \\ 1 &< n_s < 4; \text{ mixed flow pump} \\ n_s &> 4; \text{ axial flow pump} \end{aligned} \quad (4.2.70)$$

For further reference, in selecting the type of hydraulic turbine (as typically displayed in Fig. 4.34(b)), the specific speed n_t can be correlated as follows

$$\begin{aligned} 0 &< n_t < 1; \text{ impulse turbine (e.g. Pelton type)} \\ 1 &< n_t < 3.5; \text{ radial turbine (e.g. Francis type)} \\ 3.5 &< n_t < 7.0; \text{ mixed flow turbine} \\ 7.0 &< n_t < 14.0; \text{ axial flow turbine} \end{aligned} \quad (4.2.71)$$

where for Eqs. (4.2.70) and (4.2.71) the units are in n [rad/s = rpm $\times \pi / 30$], Q [m³/s], W [W], ρ [kg/m³] and g [m/s²]. It is noticeable that in general a higher specific speed implies a larger machine, because of a higher volumetric flow rate with a low head (pump) and a higher output power and low head drop (turbine). For economic reasons in developing a turbomachine, it is recommended to select the highest possible specific speed consistent with high efficiency for a given duty. It is also worth noting that larger turbomachines are more efficient than smaller ones of the same geometric family, known as the scale effect. Among many proposed correlations, the following formula is often used in practice, relating efficiencies to size, and according to L. F. Moody (ref. Kittredge, 1968)

$$\eta = 1 - (1 - \eta_M) \left(\frac{D_M}{D} \right)^{\frac{1}{4}} \quad (4.2.72)$$

where η can be used for both pumps and turbines.

4.2.4 Cavitation

Cavitation is the local formation of vapor bubbles in a liquid due to a pressure reduction below the vapor pressure caused by a dynamic action of the liquid, rather than an increase of temperature. The cavitation is largely due to a local boiling in a hydraulic turbomachine (and more generally in an element of a flow channel), through which causes the deterioration of a machine's performance, giving an actual limitation of machine design. Particularly, in selecting a type of turbomachine for a given head H and flow rate Q , it is desirable to choose the highest possible specific speed because of the resulting reduction in size, weight and cost of production. However, this would require the increase in fluid velocities, resulting in a local pressure reduction, and thus causing the cavitation. The lower limit of size in designing a turbomachine is therefore dictated by the cavitation. Figure 4.44 shows a typical performance characteristic, where the $Q-H$ relationship represented in the $c_\phi-\phi$ plot of a radial flow pump, showing the deterioration in performance due to a fully developed cavitation. In the fully developed cavitation state, pockets of vapor are formed, as illustrated in Fig. 4.45 referring to the pressure state diagram Fig. 4.36(b), affecting the whole flow field in vanes.

The cavitation also leads to consequences of structural damage of near solid surfaces, known as cavitation erosion. The cavitation erosion is caused by the following process. When the local pressure in a turbomachine is approached toward a critical pressure, depending upon flow conditions, cavitation occurs. This is called cavitation inception. Bubbles collapse, when they are swept into higher pressure regions, and a pressure wave is produced by a sudden bubble collapse that propagates and hits a solid surface. The repeated action of the bubbles collapsing near the solid surface causes the cavitation erosion over a long time period, and results in a functional failure of turbomachines. In designing turbomachines, the avoidance of cavitation inception is one of the major tasks of design engineers. The cavitation may also cause vibration and noise in turbomachines.

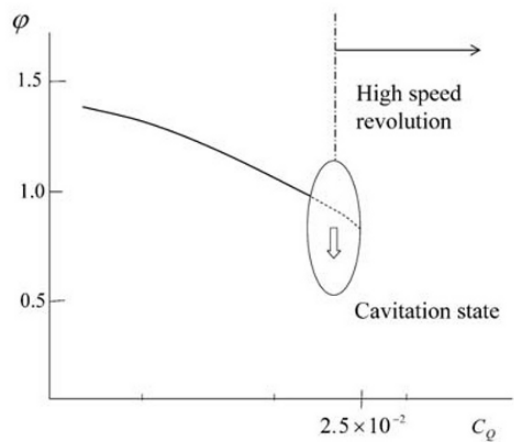


Fig. 4.44 Performance characteristic of a radial flow pump and cavitation

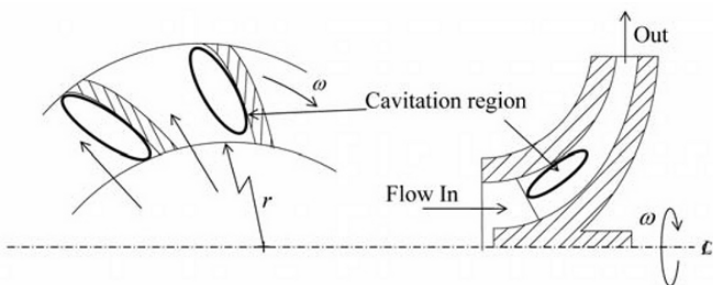


Fig. 4.45 Cavitation region

A criterion for the formation of vapor bubbles is obtained in consideration of the pressure difference between the absolute pressure and the vapor pressure being equal to that of the dynamic pressure of the liquid. In Fig. 4.46, a suction pipe connected to the inlet of a pump (or draft tube connected to discharge of a hydraulic turbine) is illustrated, where H_{sv} is the height (head) of the pump inlet s (the turbine discharge). Also, p_s is the absolute pressure, c_s is the absolute velocity and w_s is the relative velocity

at s . p_e is the absolute pressure at point e in the vane rotor, whereas $\pm h_l$ is the loss head in the pipe and p_a is the atmospheric pressure at the liquid level. The energy balance between 0 and s can be written in terms of head as

$$\frac{p_a}{\rho g} - H_{sv} \pm h_l = \frac{p_s}{\rho g} + \frac{c_s^2}{2g} \quad (4.2.73)$$

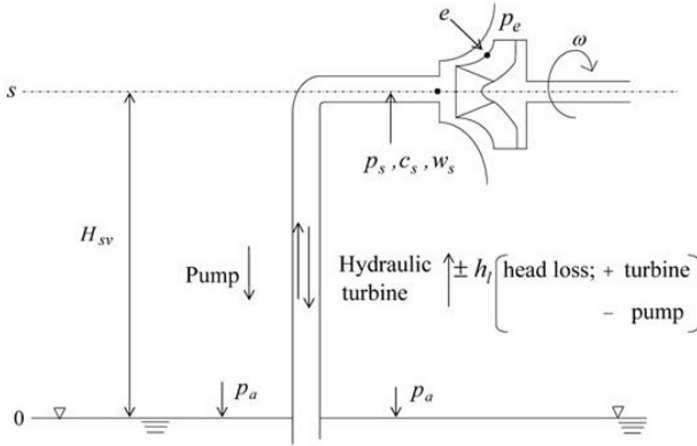


Fig. 4.46 Suction (or draft) configuration

Noting that $\zeta(w_s^2/2g)$ is the dynamic head loss between s and e , and by defining ζ as the loss coefficient, we have

$$\frac{p_s}{\rho g} - \frac{p_e}{\rho g} = \zeta \frac{w_s^2}{2g} \quad (4.2.74)$$

where the constant ζ is determined by a channel configuration. Combining Eq. (4.2.73) with Eq. (4.2.74), we have

$$\begin{aligned} \frac{p_a}{\rho g} - H_{sv} \pm h_l - \frac{p_e}{\rho g} &= \frac{p_s}{\rho g} + \frac{c_s^2}{2g} - \frac{p_e}{\rho g} \\ &= \frac{c_s^2}{2g} + \zeta \frac{w_s^2}{2g} \end{aligned} \quad (4.2.75)$$

Now cases are examined when p_e reaches the saturation vapor pressure p_v where cavitations tend to occur. The condition without cavitations thus can be written as follows

$$\frac{p_a}{\rho g} - H_{sv} \pm h_l - \frac{p_v}{\rho g} = \frac{p_s}{\rho g} + \frac{c_s^2}{2g} - \frac{p_v}{\rho g} \geq \frac{c_s^2}{2g} + \zeta \frac{w_s^2}{2g} \quad (4.2.76)$$

where we set the total dynamic head as

$$H_{sv\max} = \frac{c_s^2}{2g} + \zeta \frac{w_s^2}{2g} \quad (4.2.77)$$

It will prove useful in practical engineering to define the cavitation limit, at which the cavitation occurs, as

$$H_{sv/\text{limit}} = H_{sv} \quad (4.2.78)$$

It is mentioned that H_{sv} depends upon the operating condition of a pump (in the case of pump operation), but $H_{sv/\text{limit}}$ is to be determined uniquely for each individual pump and gives a criterion of cavitation. $H_{sv/\text{limit}}$ is called the net positive suction head (NPSH), through which the critical cavitation number is defined by the following formula

$$\sigma_c = \frac{H_{sv/\text{limit}}}{H} = \left(\frac{p_s}{\rho g} + \frac{c_s^2}{2g} - \frac{p_v}{\rho g} \right)_{\text{limit}} / H \quad (4.2.79)$$

where H is the actual head for a given flow rate Q at a speed of revolution n . In the case of a hydraulic turbine, the critical cavitation number is defined as

$$\sigma_c = \frac{H_{sv/\text{limit}}}{H} = \left(\frac{p_s}{\rho g} - H_s - \frac{p_v}{\rho g} \right)_{\text{limit}} / H \quad (4.2.80)$$

where $H_s = H_{sv} + h_l$. Therefore, the condition to avoid the cavitation is given by the pump

$$\frac{p_s}{\rho g} + \frac{c_s^2}{2g} - \frac{p_v}{\rho g} \geq \sigma_c H \quad (4.2.81)$$

and for the turbine

$$\frac{P_a}{\rho g} - H_s - \frac{P_v}{\rho g} \geq \sigma_c H \quad (4.2.82)$$

In operating turbomachines, the performance laws must include the additional variable H_{sv} , taking into account the effects of cavitation. Considering the similitude at an inlet of the pump (or discharge of hydraulic turbine), we can derive the suction specific speeds, along with Eq. (4.2.68), by replacing H to H_{sv} as follows

$$n_c = n \frac{Q^{\frac{1}{2}}}{(gH_{sv})^{\frac{3}{4}}} \quad (4.2.83)$$

and for the critical cavitation number given in Eq. (4.2.79) as

$$H_{sv/\text{limit}} = \sigma_c H \quad (4.2.84)$$

More conveniently, in practice it is useful to relate n_s and n_c , where we find a relation by substituting $H_{sv/\text{limit}}$ to H_{sv} as in Eq. (4.2.83) with the aid of the definition in Eq. (4.2.68) as follows

$$n_c = n_s / \sigma_c^{\frac{3}{4}} \quad (4.2.85)$$

From past experiences based on experimental results, the cavitation inception occurs almost at the same conditions, satisfying the following relationship.

$$\sigma_c \propto n_s^{\frac{4}{3}} \quad (4.2.86)$$

Equations (4.2.85) and (4.2.86) give the result that values of n_c for all pumps (also for all hydraulic turbines) are kept constant as to designate a resistance to cavitation. They are approximately

$$\text{Pumps ; } n_c = 2.95 \quad (4.2.87)$$

$$\text{Turbines ; } n_c = 3.96 \quad (4.2.88)$$

where n is in $[\text{rpm} \times \pi/30]$, Q is in $[\text{m}^3/\text{s}]$ and gH_{sv} is in $[\text{m}^2/\text{s}^2]$.

Exercise

Exercise 4.2.1 The Pelton Wheel

Turbines (hydraulic steam or gas), with stationary guide vanes and runner (as studied in Section 4.2.2) have a continuous pressure drop when a fluid flows through the passages, where a part of the available head is converted into kinetic energy of flow. These turbines are categorized as the reaction turbine. Reaction turbines usually have sophisticated functions and can run with lower head installations. However, when a very high head is available, it is often more suitable to adopt the impulse type of turbine (particularly in the case of hydraulic power generation). The Pelton wheel is one which is extensively used for high head installations, with its simple construction and thus is economically competitive against reaction turbines.

Considering the theory developed in Exercise 4.1.8, explain the function of a Pelton wheel and discuss the energy conversion characteristics.

Ans.

A Pelton wheel primarily consists of a stationary inlet nozzle, a runner and a casing. The runner has multiple buckets mounted on the periphery of its rotating wheel, as shown in Fig. 4.47(a). The runner is driven by water jets discharged by a nozzle with discharge rate Q . As the jet impacts the rotating buckets with an absolute velocity v_1 , the kinetic energy of the jet is converted into a power to drive the runner. Each bucket has a splitter that divides the jet into two equal streams and each stream leaves the bucket with its relative velocity vector in the horizontal plane. It is noted that in practice, the ideal angle of 180° is limited to a value between 160° and 168° so that the water leaving a bucket may stay free of the trailing buckets.

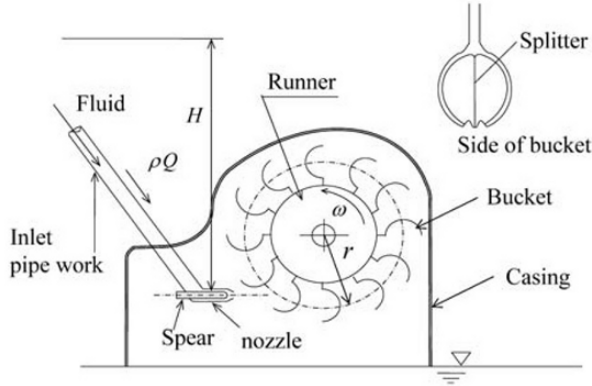
In order to estimate the net power output, we consider a case where the peripheral speed of a bucket, i.e. the circumferential speed, is assumed to be u , and the angle of the leaving jet streams is β_2 , as indicated in Fig. 4.47(b). According to the relationship obtain in Exercise 4.1.8, the torque given to the runner by the water jet is

$$T_r = \rho Q r (v_1 - u)(1 - \cos \beta_2) \quad (1)$$

where r is the runner radius as shown in Fig. 4.47 (a). If the runner rotates with an angular velocity ω , the ideal power output $W_i (= P_w)$ can be written as

$$\begin{aligned}
 W_i &= \rho Q r (v_1 - u)(1 - \cos \beta_2) \omega \\
 &= \rho Q u (v_1 - u)(1 - \cos \beta_2)
 \end{aligned}
 \quad (2)$$

(a) Pelton wheel



(b) Velocity diagram

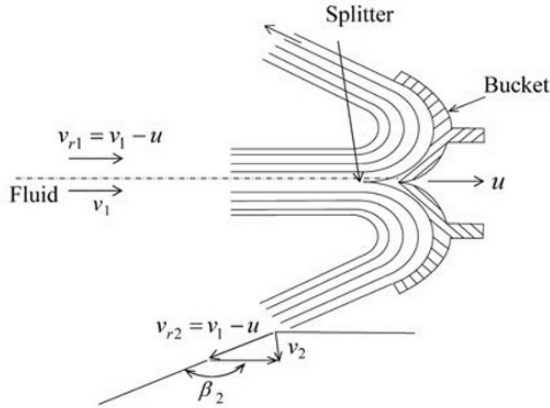


Fig. 4.47 Impulse turbine; the Pelton wheel

Introducing the volumetric efficiency η_v and the mechanical efficiency η_m , with reference to Eqs. (4.2.42) and (4.2.43), the net power output W is obtained from the relation

$$W = W_i \eta_v \eta_m \quad (3)$$

On the other hand, the net power output W is also estimated by the head drop H as follows

$$W = [\rho Q g (H \eta_h)] \eta_v \eta_m \quad (4)$$

and

$$W = \rho Q g H \eta \quad (5)$$

where η_h is the hydraulic efficiency defined in Eq. (4.2.41) and η is the total efficiency defined in Eq. (4.2.44).

From Eqs. (3) and (4), the hydrodynamic coefficient η_h is written where

$$\eta_h = \frac{W_i}{\rho Q g H} = \frac{1}{g H} u (v_1 - u) (1 - \cos \beta_2) \quad (6)$$

The water jet velocity v_1 can be given where the head drop is

$$v_1 = C_v \sqrt{2gH} \quad (7)$$

C_v is the velocity coefficient. Therefore, with Eqs. (6) and (7), we can obtain an expression for η_h where

$$\eta_h = \frac{2C_v^2}{v_1^2} u (v_1 - u) (1 - \cos \beta_2) \quad (8)$$

and

$$\begin{aligned} \eta_h &= \frac{2u}{\sqrt{2gH}} \left(\frac{v_1}{\sqrt{2gH}} - \frac{u}{\sqrt{2gH}} \right) (1 - \cos \beta_2) \\ &= 2\kappa_p (C_v - \kappa_p) (1 - \cos \beta_2) \end{aligned} \quad (9)$$

$\kappa_p = u / \sqrt{2gH}$ is called the speed factor. According to Eq. (8), η_h reaches the maximum when $u = v_1 / 2$, so that it follows that

$$\eta_{h,\max} = \frac{1}{2} C_v^2 (1 - \cos \beta_2) \quad (10)$$

For plotting η_h vs. κ_p in Eq. (9), we have a diagram in Fig. 4.48. If we take representative values (typically) $C_v = 0.94$ and $\beta_2 = 168^\circ$, we have the maximum hydraulic efficiency $\eta_{h,\max} = 0.831$. However, in actual operation, $\eta_{h,\max}$ will be reduced due to the reduction of relative velocity over the bucket via friction and non-uniform velocity splitting, which resultantly alters the Eq. (10) to

$$\eta_{h,\max} = \frac{1}{2} C_v^2 (1 - \varepsilon \cos \beta_2) \quad (11)$$

ε is the friction factor and typically $\varepsilon = 0.9$ in an actual operation.

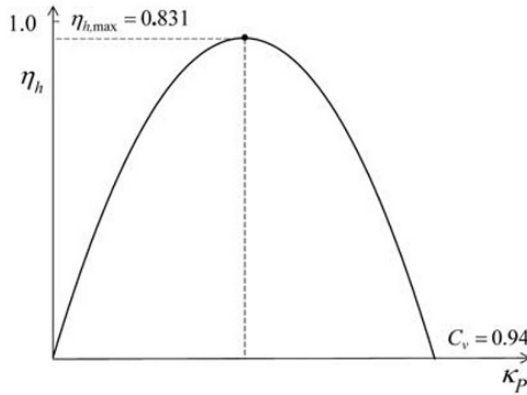


Fig. 4.48 η_h vs. κ_p

Exercise 4.2.2 Radial Flow Impeller for Turbo-Pump

A centrifugal pump with idealized radial flow impeller rotates with $n = 1500$ rpm, as shown in Fig. 4.49. Water enters the impeller axially through the eye, flows radially along the absolute pass line in the blades, and is discharged radially. Denoting the inlet location 1 and the outlet location 2, the idealized velocity diagrams are drawn in Fig. 4.49, using the sign notation of Fig. 4.35(b), where $D_1 = 2r_1$ and $D_2 = 2r_2$ in Fig. 4.49 and their basic dimensions of the impeller are $D_1 = 200$ mm, $D_2 = 400$ mm, $b_1 = 100$ mm, and $b_2 = 50$ mm. If the volumetric flow rate is $Q = 0.25$ m³/s, obtain the theoretical torque T_{th} and Head H_{th} . Also calculate T_{th} and H_{th} when the discharge rate Q is doubled. The meridional component of velocity c_m is assumed to be maintained constant as fluid flows through the

impeller, in which the fluid enters the impeller with a negligible tangential velocity component. It is also assumed that the outlet vane angle β_2 is such that $\beta_2 = 22^\circ$. Show the specific speed n_s for both operation of Q and $2Q$ as well.

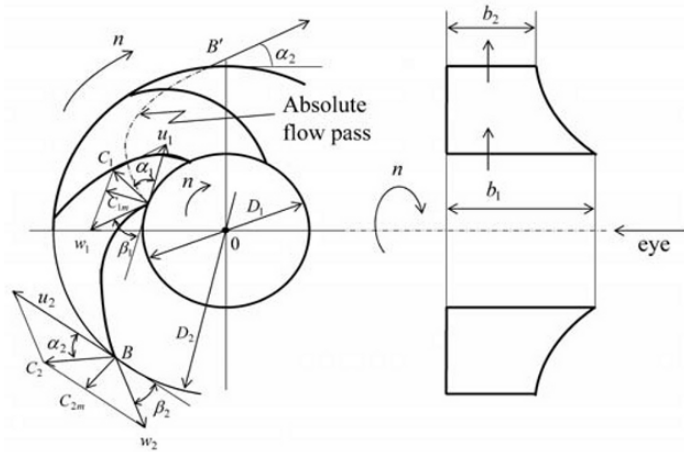


Fig. 4.49 Radial flow impeller of turbo-pump

Ans.

With reference to Fig. 4.49, since the tangential component $c_{1u} = c_1 \cos \alpha_1$ is assumed to be zero, T_{th} can be estimated from Eq. (4.2.1) as

$$T_{th} = \rho Q c_{2u} (D_2 / 2) \quad (1)$$

and from the velocity diagram at the outlet 2, c_{2u} will be derived as

$$c_{2u} = u_2 - c_{2m} \cot \beta_2 \quad (2)$$

where $c_{2m} = Q / \pi D_2 b_2$ and $u_2 = \pi D_2 n / 60$. For the given values of these parameters, we can obtain

$$c_{2m} = 0.25 / (\pi \times 0.4 \times 0.05) = 3.98 \quad [\text{m/s}]$$

$$u_2 = \pi \times 0.4 \times 1500 / 60 = 31.4 \quad [\text{m/s}]$$

$$c_{2u} = 31.4 - 3.98 \cot 22^\circ = 21.5 \quad [\text{m/s}]$$

Therefore, from Eq. (1), we have

$$T_{\text{th}} = \rho Q r_2 c_{2u} = 1000 \times 0.25 \times (0.4/2) \times 21.5 = 1075 \quad [\text{N} \cdot \text{m}]$$

and also from Eq. (4.2.4), H_{th} is

$$H_{\text{th}} = u_2 c_{2u} / g = 31.4 \times 21.5 / 9.81 = 68.8 \quad [\text{m}]$$

When the discharge flow rate Q is doubled

$$Q = 2 \times 0.25 = 0.5 \quad [\text{m}^3/\text{s}]$$

so that

$$c_{2m} = 0.5 / (\pi \times 0.4 \times 0.05) = 7.96 \quad [\text{m/s}]$$

Thus

$$c_{2u} = u_2 - c_{2m} \cot \beta_2 = 31.4 - 7.96 \cot 22^\circ = 11.7 \quad [\text{m/s}]$$

Therefore, in similar manner we have

$$T_{\text{th}} = 1000 \times 0.5 \times (0.4/2) \times 11.7 = 1170 \quad [\text{N} \cdot \text{m}]$$

$$H_{\text{th}} = 31.4 \times 11.7 / 9.81 = 37.4 \quad [\text{m}]$$

The specific speeds for Q and $2Q$ are respectively calculated in Eq. (4.2.68)

$$n_s = n \frac{Q^{1/2}}{(gH)^{3/4}} = \left(1500 \times \frac{\pi}{30} \right) \frac{(0.25)^{1/2}}{(9.81 \times 68.8)^{3/4}} = 0.590$$

$$n'_s = \left(1500 \times \frac{\pi}{30} \right) \frac{(0.5)^{1/2}}{(9.81 \times 37.4)^{3/4}} = 1.32$$

The results show that for $2Q$, $n'_s > 1$, indicating a mixed flow pump may be more appropriate.

Exercise 4.2.3 Power Output from Axial Flow Hydraulic Turbine

For a low head and high specific speed, axial flow hydraulic turbines are often appropriate because of a higher meridional velocity, running faster with higher efficiencies. The propeller turbine with adjustable blades is

known as the Kaplan turbine, which can run with a wide output range by setting the runner blades and guide vanes simultaneously. Referring to Fig. 4.50 (a) representative dimensions, (b) velocity diagrams, (c) draft tube configuration, consider the following problems:

The mean radius R to the runner is $R = 0.5 \text{ m}$, and the width B of it is $B = 0.1 \text{ m}$. The stream of water enters to the runner with an angle of $\alpha_1 = 35^\circ$, and is discharged at atmospheric pressure with an angle of $\beta_2 = 25^\circ$ from the outlet of the runner. The head difference H_1 between the upper level of the water surface and the outlet of runner is $H_1 = 12 \text{ m}$. Before entering the runner, the stream turns to a right angle of the runner, so that the absolute velocity c_2 at the outlet of the runner is perpendicular to the circumferential speed u , i.e. $\alpha_2 = 90^\circ$. It is assumed that there is no radial velocity when water passes through the vanes, and that the axial velocity at the inlet to the runner and the outlet is kept constant.

- (i) Estimate the power transmitted to the runner and the revolutionary speed of the runner, ignoring hydraulic losses.
- (ii) As illustrated in Fig. 4.50(c), if a draft tube of a diffuser type is attached between the outlet of runner to the lower discharged water surface, discuss the change of the power transmitted and revolutionary speed compared to problem (i). Set $H_s = 4 \text{ m}$ for problem (ii).

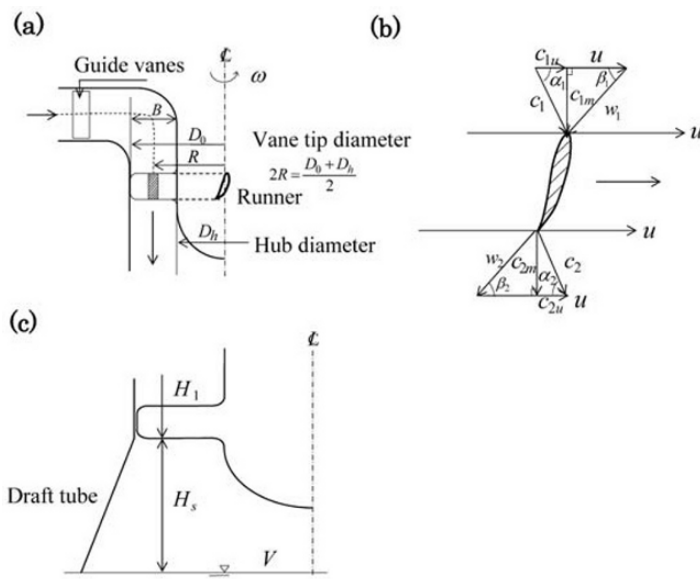


Fig. 4.50 Axial flow propeller turbine; Kaplan turbine

Ans.

(i) Denote the actual head H to the runner is given where

$$H = H_1 - c_2^2 / 2g \quad (1)$$

With the given condition c_{2u} assumed to be zero, so that from Eq. (4.2.4), the theoretical head is to be written as

$$H = uc_{1u} / g \quad (2)$$

By the velocity diagram, c_{1u} can be obtained by knowing that $c_{1m} = c_2$

$$c_{1u} = c_2 \cot \alpha_1 \quad (3)$$

The discharge flow rate Q is also estimated as

$$\begin{aligned} Q &= 2\pi R B c_{1m} \\ &= 2\pi R B c_2 \end{aligned} \quad (4)$$

Knowing the condition at the outlet with reference to Fig. 4.50 (b), the absolute velocity c_2 is written as

$$c_2 = \frac{u}{\cot \beta_2} \quad (5)$$

The key parameters of Q , H , c_2 , c_{1u} , and u in Eqs. (1–5) are thus calculated by the known quantities, R , B , α_1 , β_2 , and H_1 as follows

$$H = \frac{1}{g} c_2 \cot \beta_2 c_2 \cot \alpha_1 = \frac{1}{g} c_2^2 \cot \beta_2 \cot \alpha_1 \quad (6)$$

and with Eqs. (1), (2) and (6), we can obtain the relationship

$$H_1 - \frac{c_2^2}{2g} = \frac{1}{g} c_2^2 \cot \beta_2 \cot \alpha_1 \quad (7)$$

so that c_2 will become

$$c_2 = \sqrt{\frac{2gH_1}{2\cot\beta_2\cot\alpha_1 + 1}} \quad (8)$$

Once c_2 is obtained, therefore, the rest of unknown are readily calculated, using each given value as follows

$$c_2 = \sqrt{\frac{2 \times 9.81 \times 12}{2 \times 2.14 \times 1.43 + 1}} = 5.75 \quad [\text{m/s}]$$

$$H = 12 - \frac{5.75^2}{2 \times 9.81} = 10.31 \quad [\text{m}]$$

$$Q = 2 \times 3.14 \times 0.5 \times 0.1 \times 5.75 = 1.81 \quad [\text{m}^3/\text{s}]$$

As a result, the power (work) W transmitted to the runner is obtained to give

$$W = Q(\rho g H) = 1.81 \times (1000 \times 9.81 \times 10.31) = 183 \quad [\text{kW}]$$

Also with the relation $u = R\omega$, we are able to estimate the revolutionary speed of the runner from the angular velocity ω

$$\omega = \frac{u}{R} = \frac{c_2 \cot \beta_2}{R} = \frac{5.75 \times 2.14}{0.5} = 24.7 \quad [\text{rad/s}]$$

so that we can obtain the revolutionary speed with

$$n = \frac{\omega \times 60}{2\pi} = \frac{24.7 \times 60}{2\pi} = 235 \quad [\text{rpm}]$$

(ii) The installation of the draft tube adds the extra head to H_1 , as illustrated in Fig. 4.50(c), i.e.

$$H = H_1 + H_s \quad (9)$$

With the same manner as verified in problem (i), we should be able to calculate Q and H after obtaining c_2 likewise know that

$$H_1 + H_s = \frac{1}{g} c_2^2 \cot \beta_2 \cot \alpha_1 \quad (10)$$

so that

$$\begin{aligned} c_2 &= \sqrt{\frac{g(H_1 + H_s)}{\cot \beta_2 \cot \alpha_1}} \\ &= \sqrt{\frac{9.81 \times (12 + 4)}{2.14 \times 1.43}} = 7.16 \quad [\text{m/s}] \end{aligned}$$

Thus,

$$Q = 2\pi \times 0.5 \times 0.1 \times 7.16 = 2.25 \text{ [m}^3/\text{s]}$$

$$W = 9.81 \times 2.25 \times (12 + 4) = 353 \text{ [kW]}$$

$$u = 7.16 \times 2.14 = 15.35 \text{ [m/s]}$$

$$n = \frac{15.35/0.5 \times 60}{2\pi} = 293 \text{ [rpm]}$$

There is certainly an improve of the output characteristic of the turbines by adding the draft tube.

Exercise 4.2.4 Maximum Suction Head for Cavitation Limit

A single-suction radial flow pump is to operate for the actual head $H = 50 \text{ m}$, the volumetric flow rate $Q = 0.025 \text{ m}^3/\text{s}$ and the revolutionary speed $n = 2900 \text{ rpm}$. Determine the maximum suction head $H_{sv\max}$, below which the pump can be operated without the cavitation. It is assumed that water temperature in the suction pipe is 60°C and the atmospheric pressure of the water surface at suction is $p_a = 101.3 \text{ kPa}$. It is further assumed that the loss head in the section pipe is $h_l = 1.5 \text{ m}$. The constant for the critical cavitation number σ_c in Eq. (4.2.86) would be obtained from $k_s = 0.236$, where k_s is defined as $\sigma_c = k_s n_s^{4/3}$.

Ans.

The specific speed n_s of the pump is

$$n_s = n \frac{Q^{\frac{1}{2}}}{(gH)^{\frac{3}{4}}} = \left(\frac{2900}{60} \times 2\pi \right) \frac{(0.025)^{\frac{1}{2}}}{(9.81 \times 50)^{\frac{3}{4}}} = 0.459 \quad (1)$$

From Eq. (4.2.86), knowing that the constant is k_s , the critical cavitation number σ_c is thus given where

$$\sigma_c = 0.236 \times (0.459)^{\frac{4}{3}} = 0.084 \quad (2)$$

NPSH is then

$$H_{sv/\text{limit}} = \sigma_c H = 0.084 \times 50 = 4.18 \text{ [m]} \quad (3)$$

The water density is $\rho = 983.2 \text{ kg/m}^3$ and the saturation vapor pressure is $p_v = 19.9 \text{ kPa}$ at the temperature 60°C , which are obtained from a steam table. Therefore, $H_{sv\max}$ will be calculated via Eq. (4.2.82), yielding

$$\begin{aligned} H_{sv\max} &= \frac{p_a}{\rho g} - \frac{p_v}{\rho g} - h_l - H_{sv/\text{limit}} \\ &= \frac{101300}{983.2 \times 9.8} - \frac{19900}{983.2 \times 9.8} - 1.5 - 4.18 \\ &= 2.77 \text{ [m]} \end{aligned}$$

Thus, the suction pipe must be installed as 2.77 m high above the water's surface, so that there would not be cavitation.

Problems

4.2-1 A centrifugal water pump runs at $n = 1450 \text{ rpm}$. The impeller has the following dimensions: $D_2 = 300 \text{ mm}$, $b_2 = 20 \text{ mm}$ and $\beta_2 = 45^\circ$. If the power consumption of the pump is $W = 40 \text{ kW}$, calculate the theoretical discharge Q_{th} and obtain the theoretical head H_{th} . There would be no-slip flow in vanes due to internal circulation flow, so that only a (Euler) theoretical head H_{th} is to be considered. Assume that the hydraulic efficiency is $\eta_h = 0.85$, and the overall efficiency is $\eta = 0.75$. The fluid enters the impeller with a negligible tangential velocity component. Also calculate the actual head.

$$\begin{aligned} \text{Ans. } & \left[\begin{array}{l} W\eta = \rho Q_{th} g (H_{th} \eta_h) \\ gH_{th} = u_2 \left[u_2 - \left(\frac{Q}{\pi D_2 b_2} \right) \cot \beta_2 \right] \\ Q_{th} = 0.0848 \text{ m}^3/\text{s} \\ H_{th} = 42.4 \text{ m} \\ H = 36.04 \text{ m} \end{array} \right] \end{aligned}$$

4.2-2 A model of a centrifugal pump with the impeller diameter of $D_M = 220 \text{ mm}$ is tested at the revolutionary speed of $n_M = 1500 \text{ rpm}$. Results of the test run were such that: the actual head was $H_M = 1.8 \text{ m}$, the actual discharge was $Q_M = 1.75 \text{ m}^3/\text{min}$ and the

mechanical efficiency was $\eta_m = 0.8$. Estimate the head H_P , the discharge Q_P and the shaft input power W_P , when the prototype of a geometrically similar pump is in operation at the rotational speed of $n_P = 800$ rpm. The diameter of the prototype is $D_P = 1000$ mm.

$$\text{Ans. } \begin{bmatrix} H_P = 10.6 \text{ m} \\ Q_P = 87.7 \text{ m}^3/\text{min} \\ W_P = 189 \text{ kW} \end{bmatrix}$$

- 4.2-3 A centrifugal pump is to be operated with an actual head of $H = 15.0$ m. The critical cavitations number is $\sigma_c = 0.08$ at the operating condition. The atmospheric pressure on the suction water surface is $p_a = 101.3$ kPa. The saturation vapor pressure at the operation condition is $p_v = 3.0$ kPa and the head loss along the suction pipe is $h_l = 1.6$ m. Referring Fig. 4.46, obtain the maximum allowable height between the suction water surface to the pump inlet.

$$\text{Ans. } [H_{\text{svmax}} = 7.2 \text{ m}]$$

- 4.2-4 A Pelton wheel with a runner diameter of $D = 200$ mm is generating a power output for a head drop of $H = 100$ m. In order to verify the net power output a braking test was carried out for an ideal nozzle being fully opened. The torque required to hold the wheel was $T_r = 1500$ N·m. Denoting the angle of leaving the jet stream flow from a bucket is $\beta_2 = 12^\circ$ and the overall efficiency of the wheel is $\eta = 0.85$, obtain the rotational speed of the runner and estimate the net power output.

$$\text{Ans. } \begin{bmatrix} n = 713 \text{ rpm} \\ W = 142 \text{ kW} \end{bmatrix}$$

- 4.2-5 An axial flow hydraulic turbine is required to produce the power of $W = 8800$ kW with a given head of $H = 20$ m. The overall efficiency is $\eta = 0.88$, and the hydraulic efficiency is $\eta_h = 0.93$ for the runner of a vane tip diameter of $D_0 = 4$ m and a hob diameter of $D_n = 1.75$ m. Calculate the inlet vane angle β_1 and the outlet vane angle β_2 of the runner. Assume there is no draft tube and the flow is discharged to the atmosphere.

$$Ans. \left[\begin{array}{l} \tan \beta_1 = c_{1m} / (u_1 - u_{1u}) \\ \tan \beta_2 = c_{2m} / u_m \\ \beta_1 = 18.9^\circ \\ \beta_2 = 11.53^\circ \end{array} \right]$$

Nomenclature

A	area
a	sound speed
c	absolute velocity
C_c	contraction coefficient
C_d	discharge coefficient
C_D	drag coefficient
C_L	lift coefficient
C_M	moment coefficient
C_Q	volumetric flow rate coefficient
C_v	velocity coefficient
C_W	power coefficient
$C_0, C_1, C_2, \dots, C_n$	complex constants
D	drag
F, F_i	force, i designated forces
H	total head
H_{th}	theoretical head (Euler head)
k	specific heat ratio
k_s	constant
K_f	flow coefficient
L	lift
l_c	chord length
M	Mach number
\dot{m}	mass flow rate
n_c	critical cavitation number
n_i	toque component ($i=1,2,3$)
n_s	specific speed (pump)
n_t	power specific speed (turbine)
\hat{n}	normal unit vector
P	pressure function
P_c	correlation constant

P_w	power transmitted to (or from) fluid
$p_{\text{atm}} (p_a)$	surrounding pressure
Q	flow rate
q_c	experimental constant
Re	Reynolds number
\mathbf{r}	position vector
r	radius
s_c	number of vanes
T_r	torque
t_c	pitch of vanes
U_∞, u_∞	real constants, average upstream velocity
\mathbf{u}, \mathbf{v}	velocity vector
\mathbf{v}_r	relative velocity vector
W	work transfer, complex potential
$W(z)$	velocity potential
w	complex velocity, relative velocity
z	complex number $z = x + iy$
α, γ	angle
β	angle, diameter ratio
Γ	circulation (potential vortex)
ε_M	(Mach number) correction coefficient
ζ	pressure (head) loss coefficient
η	efficiency, total (overall) efficiency
η_d	diffuser efficiency
η_0	viscosity
η_p	propeller efficiency
κ_p	speed factor
σ_c	critical cavitation number
σ_s	slip factor
τ_{ij}	stress tensor
ν	kinematic viscosity
ξ	correction factor
Φ	scalar potential
ϕ	potential function, velocity potential
φ	head coefficient
ψ	stream function
ω	angular velocity

Bibliography

Some fundamental aspects of turbomachinery with working examples are given in

1. H.S. Bean (edited), *Fluid Meters: their theory and application* (6th Edition), American Society of Mechanical Engineers, New York, 1971.
2. A.H. Shapiro, *The Dynamics and Thermodynamics of Compressible Fluid Flow*, Ronald Press, New York, 1953.
3. M. Massoud, *Engineering Thermofluids*, Springer, 2005.
4. M.C. Potter, D.C. Wiggert, M. Hondzo, *Mechanics of Fluids* (2nd Edition), Prentice-Hall Inc., 1997.
5. S.L. Dixon, *Fluid Mechanics and Thermodynamics of Turbomachinery* (2nd Edition), Pergamon Press, 1975.
6. T. Nishiyama, *Fluid Mechanics*, Vol. I, II (13th Edition), Nikan Kogyo-Shinbunsha, Tokyo, 1989 (in Japanese).
7. J. Katz and A. Plotkin, *Low-Speed Aerodynamics* (2nd Edition), Cambridge University Press, 2001.
8. H. Blasius, *Funktionentheoretische Methoden in der Hydrodynamik*, Math. Zeitschrift, 58, 90–110, 1910.

Great deal of detailed data are available and to be useful for designers of turbomachines. There are useful correlations and definitions for pump design, which are found in

9. C. Pfleiderer, *Die Kreiselpumpen für Flüssigkeiten and Gase*, Springer, 1961.
10. J.A. Schetz and A.E. Fuhs (edited), *Handbook of Fluid Dynamics and Fluid Machinery*, Vol. I, II and III, John Wiley & Sons Inc., 1996.
11. D.N. Roy, *Applied Fluid Mechanics*, Ellis Horwood Ltd, 1988.
12. W. Thomson, (L. Kelvin), *On Vortex Motion*. Trans. Roy. Soc. Edinburgh., 25, 217–260, 1869.

Phenomenological treatment for cavitation is given in greater extend in

13. C.T. Crowe (edited), *Multiphase Flow* (Handbook), Taylor & Francis, CRC Press, 2006.

Rayleigh-Plesset equation for bubble growth is referred from

14. M.S. Plesset, The dynamics of cavitation bubbles, J. Appl. Mech., 1949.
15. M.S. Plesset and A. Prosperetti, Bubble dynamics and cavitation, Ann. Rev. Fluid Mech., 9, 1977.

Estimation of efficiencies in turbomachines are introduced in

16. C.P. Kittredge, Estimating the efficiency of prototype pumps from model tests, Trans, ASME, J. Engg. Power, 90(2), 1968.
17. A.J. Stepanoff, *Centrifugal and Axial Flow Pumps*, John Wiley & Sons Inc., 1957.

5. Compressible Flow

There are many physical processes, when dealing with both gases and liquids, where the density variations are of major importance in determining the character of the flow. In both cases, with regard to high-speed flow, the effects on compressibility cannot be ignored; as a result, a new class of flow effects appears. Such high-speed flows are termed compressible flows. In practice, indeed appreciable density variations are mostly seen in high-speed gas flows. In this chapter we will consider the one dimensional flows of ideal gases, which are important when tackling most physics problems, since they are often involved in compressible flows and are found to be a good approximation of many actual flows.

In applying the one dimensional assumption, we shall restrict the physical situation exclusively to internal flows, where the quantities (such as density, pressure, temperature, velocity and etc.) are uniform over any cross section, and vary only along the channel. Looking at compressible flows, we will consider three conservation laws for mass, momentum, and energy, which are supplemented by thermodynamics state equations together with the definition of sonic speed (related to Mach number). In this chapter, we shall begin to look at the speed of sound which will lead to a better understanding of the role it plays and its effects on more general compressible flows.

5.1 Speed of Sound and Mach Number

If an infinitesimal disturbance occurs in a fluid, the disturbance will propagate through the fluid at a well-defined velocity called the sonic velocity or speed of sound (sometimes called the acoustic velocity). The speed of sound depends upon the properties of the fluid, and may be determined by considering the equation of continuity from Eq. (2.1.5) and the Euler equation from Eq. (4.2). In the case of one dimensional assumption, the equations are written by ignoring the effect of the gravity (body force term)

$$\frac{\partial \rho}{\partial t} + \frac{\partial \rho u}{\partial x} = 0 \quad (5.1.1)$$

$$\rho \left(\frac{\partial u}{\partial t} + u \frac{\partial u}{\partial x} \right) = - \frac{\partial p}{\partial x} \quad (5.1.2)$$

Here, u is the velocity component in the direction of x (one dimensional). Infinitesimal disturbances are thought to occur in a flow at rest (or the undisturbed fluid is moving relative to the propagations of disturbances as $u = u_0 + u'$), assuming $u_0 = 0$ so that

$$u = u' \quad (5.1.3)$$

and

$$p = p_0 + p' \quad (5.1.4)$$

$$\rho = \rho_0 + \rho' \quad (5.1.5)$$

Thus, u_0 , p_0 and ρ_0 are the properties of undisturbed fluid and u' , p' and ρ' are the infinitesimal disturbances of velocity, pressure and density respectively. Equations (5.1.3), (5.1.4) and (5.1.5) are substituted into Eqs. (5.1.1) and (5.1.2). Simplifying and neglecting higher order terms with the conditions of $\partial \rho_0 / \partial t$ and $\partial p_0 / \partial x$ being zero, we have a set of equations for the disturbances

$$\frac{\partial \rho'}{\partial t} + \rho_0 \frac{\partial u'}{\partial x} = 0 \quad (5.1.6)$$

and

$$\frac{\partial u'}{\partial t} = - \frac{1}{\rho_0} \frac{\partial p'}{\partial x} \quad (5.1.7)$$

Eliminating u' from Eqs. (5.1.6) and (5.1.7), we have an equation relating ρ' and p' as follows

$$\frac{\partial^2 \rho'}{\partial t^2} = \frac{\partial^2 p'}{\partial x^2} \quad (5.1.8)$$

In order to make up a closed mathematical model, which deals with the propagation of disturbance, we need to relate ρ' and p' . In engineering fluid mechanics it is reasonable to assume that the thermodynamic process

is in the state of equilibrium and the ideal gas law approximation is valid for low and moderate density gases with a lower temperature gradient process. In view of this consideration, we have the equation of state

$$p\left(\frac{1}{\rho}\right) = RT \quad (5.1.9)$$

or

$$pv = RT \quad (5.1.10)$$

v is the specific volume, R is the ideal (specific) gas constant and T is the absolute temperature. Equation (5.1.9) can be further written in differential form

$$\rho dp - p d\rho = R\rho^2 dT \quad (5.1.11)$$

Next we must introduce the disturbance in addition to Eqs. (5.1.4) and (5.1.5), and that of temperature

$$T = T_0 + T' \quad (5.1.12)$$

These disturbances are then added to Eq. (5.1.11), simplifying and neglecting high order terms with the conditions of

$$dp = dp' \text{ and } d\rho = d\rho' \quad (5.1.13)$$

We can reduce this to the following relation

$$p' = \left(\frac{dp}{d\rho}\right)\rho' \quad (5.1.14)$$

Assuming that $(dp/d\rho)$ is kept constant, we can eliminate p' by substituting Eq. (5.1.14) into Eq. (5.1.8), so that we have

$$\frac{\partial^2 \rho'}{\partial t^2} = \left(\frac{dp}{d\rho}\right) \frac{\partial^2 \rho'}{\partial x^2} \quad (5.1.15)$$

The hyperbolic partial differential equation, Eq. (5.1.15), is a wave equation for ρ' . It is generally known from the wave equation that mathematically ρ' has a solution, which is expressed as

$$\rho' = f(x - at) + g(x + at) \quad (5.1.16)$$

f and g are the wave functions, for example $\rho' = \sin(x \pm at)$. In Eq. (5.1.16), ρ' propagates with the speed of sound a , that is expressed by

$$a^2 = \left(\frac{dp}{d\rho} \right) \quad (5.1.17)$$

It must be emphasized that the disturbance ρ' is infinitesimal, and the process is regarded as reversible, adiabatic and hence isentropic.

Equation (5.1.17), the definition of the speed of sound, can be further rewritten by other fluid properties. When the bulk modulus K of the fluid is considered, from the definition of K , we can write

$$\begin{aligned} dp &= -K \frac{dv}{v} \\ &= K \frac{d\rho}{\rho} \end{aligned} \quad (5.1.18)$$

and

$$\frac{dp}{d\rho} = \frac{K}{\rho} \quad (5.1.19)$$

So, Eq. (5.1.17) may be written as

$$a^2 = \frac{K}{\rho} \quad (5.1.20)$$

Furthermore, since the process is adiabatic, we have the relationship

$$pv^k = \text{const.} \quad (5.1.21)$$

or

$$p \left(\frac{1}{\rho} \right)^k = \text{const.} \quad (5.1.22)$$

Here, k is the specific heat ratio defined as $k = c_p / c_v$. Equation (5.1.22) may be demonstrated as a differential form like so

$$\frac{dp}{d\rho} = \frac{kp}{\rho} \quad (5.1.23)$$

Subsequently, Eq. (5.1.17) can be written

$$a^2 = \frac{kp}{\rho} \quad (5.1.24)$$

Additionally, using the equation of state of ideal gases with reference to Eq. (5.1.9), we can also write Eq. (5.1.24) with the following formula

$$a^2 = kRT \quad (5.1.25)$$

As it is generally directed, the speed of sound is the rate at which a very small disturbance travels through a fluid. In other words, from the under laying physical phenomena, we are to understand that small (infinitesimally small) disturbances in pressure (or density) propagate, as sound waves, with the speed of sound in a fluid. We should next consider how the sound wave (the wave of pressure disturbance) may be propagated when a sound source is at rest in a stationary fluid, or traveling in a straight line with a velocity u in a stationary fluid.

As shown in Fig. 5.1(a), the sound wave propagates radially in all directions with the spherical wave fronts for different transmission times, forming concentric spheres. When the sound source moves with a speed of $u < a$, the waves are no longer concentric, as shown in Fig. 5.1(b), and the spherical wave fronts for different transmission times nest with no intersection. An observer in front of the moving source may experience a Doppler effect after the initial wave front reaches the observer. This situation is called subsonic (in the case of flows, it is called the subsonic flow).

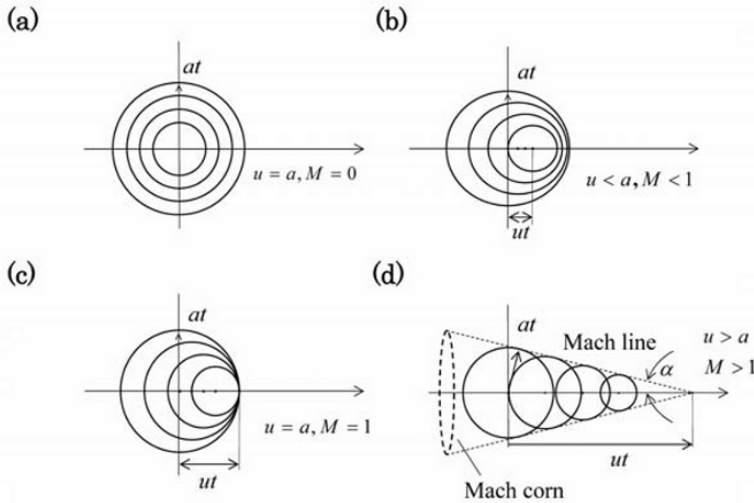


Fig. 5.1 Sound wave propagation

When $u = a$, i.e. the speed of the sound source is equal to the speed of sound, the wave fronts all touch at the position of the sound source as illustrated in Fig. 5.1(c). In this situation, an observer may hear a sudden abrupt sound when the source arrives at the observer, and then after that the observer may experience the Doppler effect. This behavior is called sonic (in the case of flows, it is the sonic flow).

Finally when the speed of sound source exceeds the speed of sound, a conical surface, called the Mach corn, is formed with continuous wave fronts, in which the intersecting spherical waves are contained. The flow is undisturbed outside of the Mach corn and no sound reaches the observer until the Mach corn passes. The half angle of the Mach corn is

$$\alpha = \sin^{-1}\left(\frac{at}{ut}\right) = \sin^{-1}\left(\frac{a}{u}\right) \quad (5.1.26)$$

This is called the Mach angle, and this situation is called supersonic (in the case of flows, it is called the supersonic flow).

The ratio of the local flow speed (or in the case of a moving sound source the traveling speed in a stationary fluid) u to the local speed of sound a is the Mach number as defined by

$$M = \frac{u}{a} \quad (5.1.27)$$

The Mach number is a dimensionless flow property, which characterizes compressible flows.

5.2 Isentropic Flow

Many engineering applications associated with compressible flow can be treated with assumptions of steady and isentropic flow of one dimensional motion. The applications may include gases undergoing appreciable change of density with variations in pressure and temperature through passages of varying cross-section areas. Such problems would be seen with exhaust gases passing through gas turbines, nozzles on rocket engines and gas flow measuring instruments, diffusers of jet engines, etc. These are internal flows where the area change is the predominant case for change of flow conditions.

Consider the steady flow through a channel of changing area A as shown in Fig. 5.2. The flow is isentropic and one dimensional in x direction and has properties of the density ρ , the temperature T and the local

speed of sound a . The continuity equation is, with reference to Eq. (4.1.33), written as

$$\rho Au = \text{const.} \quad (5.2.1)$$

Its differential form is also written as

$$\frac{d\rho}{\rho} + \frac{dA}{A} + \frac{du}{u} = 0 \quad (5.2.2)$$

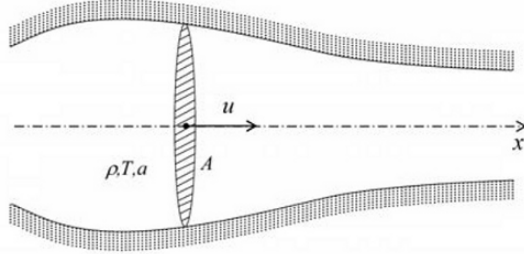


Fig. 5.2 One dimensional isentropic compressible flow

While from the steady one dimensional Euler equation, i.e. Eq. (5.1.2) with $\partial/\partial t = 0$, we have

$$u \frac{\partial u}{\partial x} = -\frac{1}{\rho} \frac{\partial p}{\partial x} \quad (5.2.3)$$

Since the flow is one dimensional, Eq. (5.2.3) can be expressed by the total differential form

$$u du = -\frac{1}{\rho} dp \quad (5.2.4)$$

and from Eqs. (5.1.17), (5.2.4) may be written in terms of the speed of sound as

$$u du = -\frac{a^2}{\rho} d\rho \quad (5.2.5)$$

Finally Eqs. (5.2.5) and (5.2.2) are combined to give, after introducing the Mach number

$$\frac{dA}{A} = \frac{du}{u} (M^2 - 1) \quad (5.2.6)$$

Equation (5.2.6) has a very important relationship for an isentropic uniform flow in a changing area. Equation (5.2.6) is indicating that the

relation between dA/A and du/u changes, depending on the Mach number, i.e. $M < 1$ (subsonic), $M = 1$ (sonic) or $M > 1$ (supersonic). One of the important observations obtained from Eq. (5.2.6) is that for $M = 1$, the area A takes the minimum by denoting A^* . If A is decreased while keeping $M \leq 1$, then there becomes $du \geq 0$, resulting in the appearance of an accelerating flow till $A = A^*$, where $u = u^* = a^*$. Further decreasing in area from A^* may result in no flow existing in the channel. However, if the area is increased from $A = A^*$, du would be positive $du \geq 0$ (accelerating again) for $M \geq 1$. If this flow process is realized, a supersonic flow ($M \geq 1$) would be achieved in the channel. This type of channel is called a Laval tube or supersonic nozzle, which consists of converging and diverging parts with throat in between, as illustrated in Fig. 5.3.

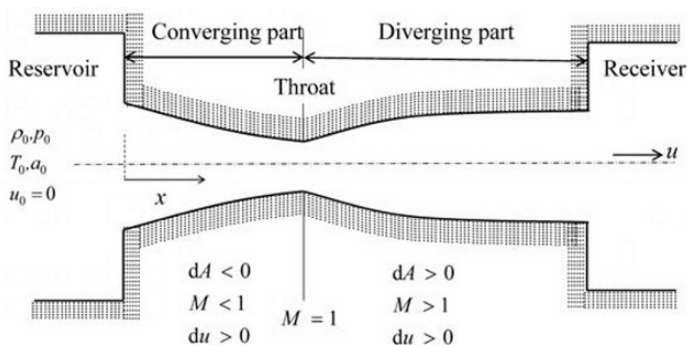


Fig. 5.3 Laval tube; supersonic nozzle

In order to examine the quantitative changes of flow parameters along the flow channel in Fig. 5.3, the isentropic flow is considered in more detail by denoting that the nozzle (Laval tube) is connected with a reservoir, where stagnation quantities, temperature T_0 , pressure p_0 and speed of sound a_0 are defined for $u_0 = 0$, and with a receiver where the (exit) flow conditions are controlled typically by pressure. A direct integration of Eq. (5.2.4) along the channel for x yields an energy equation, with reference to Eq. (4.1.27) without the scalar potential Φ , as follows

$$\frac{1}{2}u^2 + \int \frac{dp}{\rho} = \text{const.} \quad (5.2.7)$$

The flow is isentropic, when the thermodynamic process is kept adiabatic, the pressure function (the second term of Eq. (5.2.7)) can be expressed in terms of the specific heat ratio k in the following manner, using Eq. (5.1.22)

$$\int \frac{dp}{\rho} = \int c_0 k \rho^{k-2} d\rho = \frac{k}{k-1} \frac{p}{\rho} \quad (5.2.8)$$

Therefore, more importantly, we discover that Eq. (5.2.7) is expressed by

$$\frac{1}{2} u^2 + \frac{k}{k-1} \frac{p}{\rho} = \text{const.} \quad (5.2.9)$$

Equation (5.2.7) is also written in various forms, using the speed of sound with Eq. (5.1.24) and the ideal gas relationship with Eq. (5.1.25) respectively as follows

$$\frac{1}{2} u^2 + \frac{a^2}{k-1} = \text{const.} \quad (5.2.10)$$

$$\frac{1}{2} u^2 + \frac{k}{k-1} RT = \text{const.} \quad (5.2.11)$$

and with the Mach number

$$\frac{k-1}{2} M^2 + 1 = \text{const.} \quad (5.2.12)$$

It may prove useful to extend Eq. (5.2.12) further by recognizing that the specific heat $c_p = kR/(k-1)$ and the enthalpy $h = c_p T$ given in Eq. (2.5.17), so as to write the energy equation with an equivalent form as

$$\frac{1}{2} u^2 + h = \text{const.} \quad (5.2.13)$$

When we apply Eqs. (5.2.10–5.2.12) between the reservoir ($u_0 = 0$) and at an appoint x along the channel, subjecting to the adiabatic change for an ideal gas, we have

$$\frac{T_0}{T} = 1 + \frac{k-1}{2} M^2 \quad (5.2.14)$$

$$\frac{p_0}{p} = \left(1 + \frac{k-1}{2} M^2 \right)^{\frac{k}{k-1}} \quad (5.2.15)$$

$$\frac{\rho_0}{\rho} = \left(1 + \frac{k-1}{2} M^2\right)^{\frac{1}{k-1}} \quad (5.2.16)$$

where we have used the following thermodynamic relations

$$\frac{p_0}{p} = \left(\frac{T_0}{T}\right)^{\frac{k}{k-1}} \text{ and } \frac{p_0}{p} = \left(\frac{\rho_0}{\rho}\right)^k \quad (5.2.17)$$

The mass flow rate \dot{m} through the channel is expressed in the continuity equation of Eq. (5.2.1) as

$$\dot{m} = \rho A u \quad (5.2.18)$$

and

$$\rho A u = \rho^* A^* u^* \quad (5.2.19)$$

Note that ρ^* , A^* and u^* are the properties where the flow reaches to the speed of sound, i.e. where the critical values at $M = 1$ (namely $u^* = a^*$). As a result of Eq. (5.2.19), we have

$$\frac{A}{A^*} = \left(\frac{\rho^*}{\rho}\right) \left(\frac{u^*}{u}\right) \quad (5.2.20)$$

Equation (5.2.20) is another form of the continuity equation, which has to be satisfied along the channel. This can be done with following procedure.

For (ρ^*/ρ) in Eq. (5.2.20), we can expand Eq. (5.2.16), by setting $M = 1$ to give

$$\frac{\rho^*}{\rho_0} = \left(\frac{2}{k+1}\right)^{\frac{1}{k-1}} \quad (5.2.21)$$

so that

$$\frac{\rho^*}{\rho} = \left(\frac{\rho^*}{\rho_0}\right) \left(\frac{\rho_0}{\rho}\right) = \left(\frac{2}{k+1}\right)^{\frac{1}{k-1}} \left(1 + \frac{k-1}{2} M^2\right)^{\frac{1}{k-1}} \quad (5.2.22)$$

Similarly for (u^*/u) in Eq. (5.2.20), the critical state can be related by the energy equation of Eq. (5.2.10), by setting $u^* = a^*$ to write

$$\frac{1}{2}u^2 + \frac{a^2}{k-1} = \frac{k+1}{2(k-1)}u^{*2} \quad (5.2.23)$$

By dividing the both sides of this equation by u , we have

$$\frac{1}{2} + \frac{1}{k-1} \frac{a^2}{u^2} = \frac{k+1}{2(k-1)} \left(\frac{u^{*2}}{u^2} \right) \quad (5.2.24)$$

and thus

$$\frac{u^*}{u} = \left[\frac{2(k-1)}{k+1} \left\{ \frac{1}{(k-1)} \frac{1}{M^2} + \frac{1}{2} \right\} \right]^{\frac{1}{2}} \quad (5.2.25)$$

Substitution of Eqs. (5.2.22) and (5.2.25) into Eq. (5.2.20) yields the following relationship

$$\frac{A}{A^*} = \frac{1}{M} \left\{ \frac{2}{k+1} \left(1 + \frac{k-1}{2} M^2 \right) \right\}^{\frac{k+1}{2(k-1)}} \quad (5.2.26)$$

Equation (5.2.26) shows that A/A^* becomes minimum $A/A^* = 1$ for $M = 1$, while $A/A^* > 1$ for $M > 1$ and $M < 1$. This leads the fact that for $A/A^* > 1$ there are two possible states: one is $M < 1$ (subsonic) and the another is $M > 1$ (supersonic). Plots of p/p_0 , A/A^* versus M are displayed for $k = 1.4$ in Fig. 5.4.

The Mach number M is also eliminated by combining Eqs. (5.2.15) and (5.2.26), yielding

$$\frac{A}{A^*} = \left[\left(\frac{k-1}{2} \right)^{\frac{1}{2}} \left(\frac{2}{k+1} \right)^{\frac{k+1}{2(k-1)}} \right] / \left[\left\{ 1 - \left(\frac{p}{p_0} \right)^{\frac{k-1}{k}} \right\}^{\frac{1}{2}} \left(\frac{p}{p_0} \right)^{\frac{1}{k}} \right] \quad (5.2.27)$$

In order to make supersonic flow possible, the Laval tube is considered as previously mentioned, taking into account the pressure variation in Eq. (5.2.27) along the tube, where the stagnation pressure p_0 and all relevant quantities are supposed to be given. With Eq. (5.2.27), the pressure variation p for the tube area A will be obtained as A^* being a variable parameter. The states of pressure variations are displayed in Fig. 5.5(a) and (b), where the area of the throat is denoted as A_t .

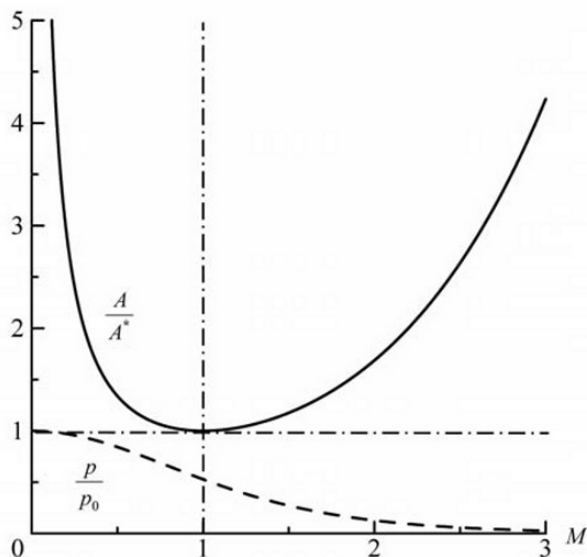
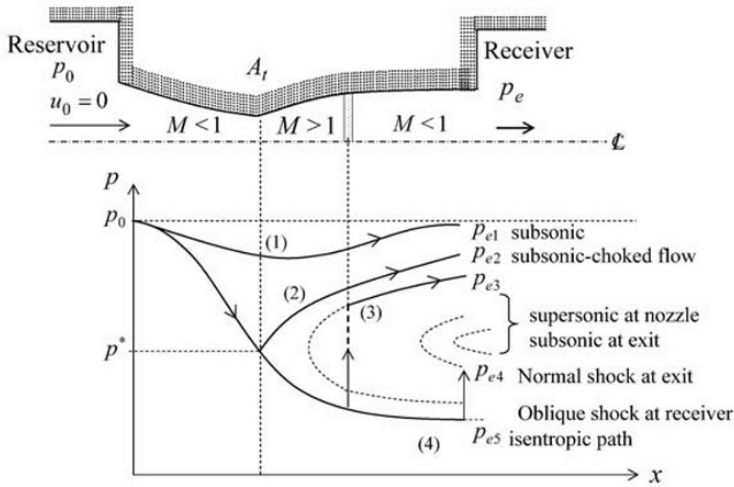


Fig. 5.4 Plots of representative quantities, $k = 1.4$

With reference to Fig. 5.5(a), the flow regimes of those appeared through the tube are dependent upon the pressure p_e and the condition of A , where p_e is the receiver pressure that is kept constant during the development of flow through the tube. p_e can be altered to produce various states of flow as schematically displayed in Fig 5.5(b). Line (1) is one that implies $A^* < A_t$, in which the flow appeared throughout the tube is kept with a subsonic flow. The tube functions as a nozzle and a diffuser. When p_e is further decreased with the condition of $A^* < A_t$, line (2) to line (4) appear, depending on the receiver pressure: p_{e2} to p_{e5} . If the receiver pressure is reduced to p_{e2} , the pressure at the throat reaches a minimum, the critical state in which the flow reaches the speed of sound. However, the flow in the diverging section is still subsonic.

When the receiver pressure is further reduced to p_{e3} , the flow after the throat in some distance becomes supersonic. Then a non-isentropic flow appears followed by a discontinuity in pressure, the normal shock, which renders the isentropic assumption invalid. The flow will be subsonic for the remaining distance to the exit, as indicated by line (3) in Fig. 5.5(a), and schematically in Fig. 5.5(b). The pressure p_{e4} is the condition of the shock that exists at the exit of the Laval tube. There is a receiver pressure p_{e5} with which the flow is isentropic and supersonic in the diverging section. The Mach number associated with p_{e5} is called the design Mach number.

(a)



(b)

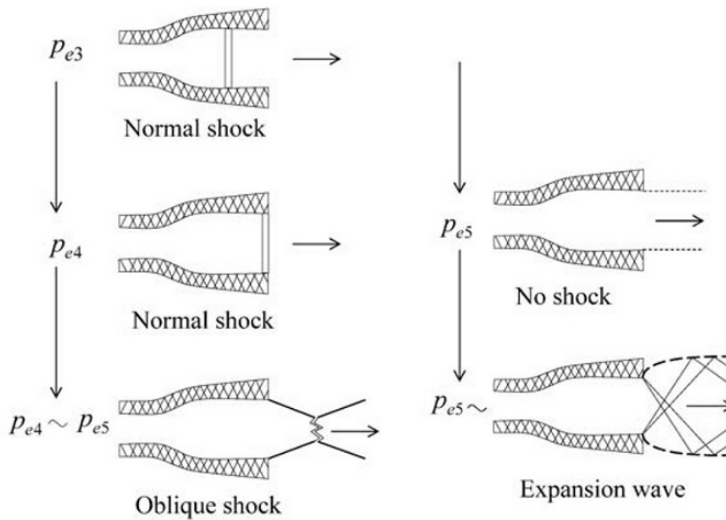


Fig. 5.5 Flow regimes of Laval tube

The pressure variation along the tube follows the isentropic path as indicated in Fig. 5.5(a). Oblique shock patterns occur outside the tube (in the receiver) due to the pressure between $p_{e4} \sim p_{e5}$, where the Laval tube is in

its so-called, over-expanded condition. As pressure p_e approaches to p_{e5} , the oblique shock patters tend to fade away. For the pressure below p_{e5} , Fig. 5.5(b) represents a very complicated flow that exists outside the tube (at the abrupt part of receiver), where expansion waves are formed.

The mass flow rate \dot{m} through the channel in Fig. 5.5(a) increases from line (1) up to line (2). However, at the receiver pressure of p_{e2} and that below line (2), no increase in mass flow is observed to occur, and this situation of flow is said to be choked flow, where the Mach number at the throat is in unity.

In order to verify the choked flow, let us consider a simple converging gas nozzle (as often seen on gas turbines), as shown in Fig. 5.6. The mass flow rate \dot{m} at the exit of the nozzle can be obtained by the mass continuity

$$\dot{m} = \rho_e u_e A_e \quad (5.2.28)$$

The key to establishing a kinematic relationship between the reservoir and receiver is achieved by setting the energy equation between the reservoir and the nozzle exit in Eq. (5.2.9), where we have

$$u_e = \left\{ \frac{2k}{k-1} \left(\frac{p_0}{\rho_0} - \frac{p_e}{\rho_e} \right) \right\}^{\frac{1}{2}} \quad (5.2.29)$$

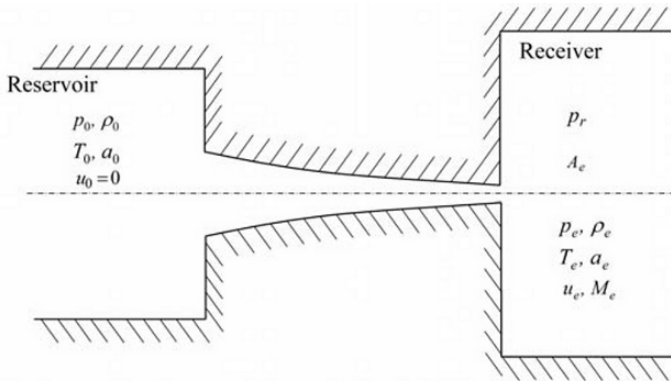


Fig. 5.6 Converging nozzle

so that Eq. (5.2.28) becomes

$$\dot{m} = \rho_e A_e \left\{ \frac{2k}{k-1} \frac{1}{RT_0} \left(\frac{\rho_e^2}{\rho_0^2} - \frac{\rho_e}{\rho_0} \frac{p_e}{p_0} \right) \right\}^{\frac{1}{2}} \quad (5.2.30)$$

Since we assume the isentropic process in the nozzle, denoting that $(\rho_e/\rho_0)^k = p_e/p_0$ in Eq. (5.2.17), we can write Eq. (5.2.30) in the following form

$$\dot{m} = A_e p_0 \left[\frac{2k}{k-1} \frac{1}{RT_0} \left\{ \left(\frac{p_e}{p_0} \right)^{\frac{2}{k}} - \left(\frac{p_e}{p_0} \right)^{\frac{k+1}{k}} \right\} \right]^{\frac{1}{2}} \quad (5.2.31)$$

Equation (5.2.31) indicates that, if we take the receiver conditions as fixed, the mass flow rate \dot{m} only function as p_e for a given A_e . The plotted line in Fig. 5.7 is a curve of Eq. (5.2.31). In actual flow, there is some discrepancy between Eq. (5.2.31) and reality, as indicated in Fig. 5.7 by a solid line. By differentiating Eq. (5.2.31) in terms of (p_e/p_0) and setting the result equal to zero, we found the maximum of \dot{m}_{\max} and its corresponding pressure p_c/p_0 ;

$$\frac{p_c}{p_0} = \left(\frac{k+1}{2} \right)^{\frac{k}{1-k}} \quad (5.2.32)$$

where p_c is called the critical pressure. It is mentioned that experiments show that the nozzle exist (the throat) pressure p_e is never less than the value for the actual maximum pressure. As this is indicated in Fig. 5.7 by the solid line, if the receiver pressure p_r is reduced below p_c , the mass flow rate \dot{m} will not increase, where the condition of choked flow occurs. Upon the condition of choked flow, the mass flow remains at the maximum value and on the exist of the converging nozzle (Fig. 5.6) the fluid undergoes an unrestrained and irreversible expansion to p_e . In practice the flow becomes no longer amendable to simple one dimensional treatment after the onset of the choking condition.

In order to derive an equation of mass flow rate \dot{m} in terms of Mach number, the terms containing (p_e/p_0) in Eq. (5.2.31) are eliminated with the aid of Eq. (5.2.15), thereby giving

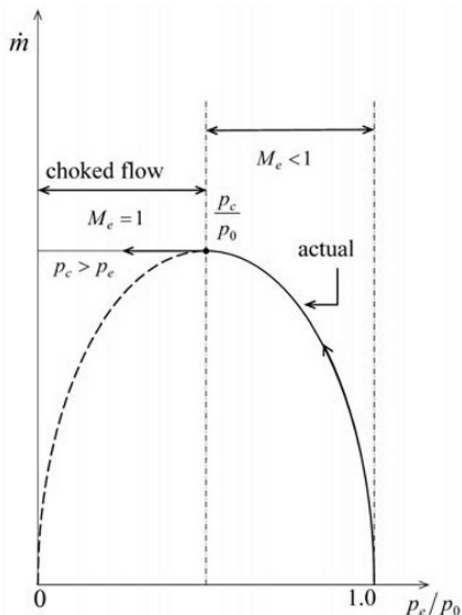


Fig. 5.7 Mass flow rate for variation of p_e

$$\dot{m} = A_e p_0 \sqrt{\frac{k}{RT_0}} M \left(1 + \frac{k-1}{2} M^2 \right)^{\frac{k+1}{2(1-k)}} \quad (5.2.33)$$

If we choose the critical area A^* for $M^* = 1$, we have

$$\dot{m}_{\max} = A^* p_0 \sqrt{\frac{k}{RT_0}} \left(\frac{k+1}{2} \right)^{\frac{k+1}{2(1-k)}} \quad (5.2.34)$$

or

$$\dot{m}_{\max} = A^* \sqrt{k p_0 \rho_0} \left(\frac{k+1}{2} \right)^{\frac{k+1}{2(1-k)}} \quad (5.2.35)$$

Thus, the mass flow rate is only dependent upon the reservoir condition and the throat area A^* . For air, the critical pressure ratio corresponding to

$k = 1.4$ can be calculated from Eq. (5.2.32) to give $(p_c/p_0) = 0.528$, and the maximum flow rate at the choking condition will be given as

$$\dot{m}_{\max} = 0.685 A^* \sqrt{p_0 \rho_0} \quad (5.2.36)$$

Therefore, further reduction of p_r in a receiver below p_c results in no effect on the upstream, since any disturbances caused in the receiver do not travel upstream in the nozzle throat where the Mach number is kept 1. In order to increase the Mach number above its unity through the channel, a diverging section is needed to the converging nozzle section, forming the Laval tube previously discussed.

5.3 Fanno and Rayleigh Lines

There are some flows through a pipe that have friction, whereas the thermodynamic state is kept as isothermal. The situation is often encountered in a gas form, for example natural gas, in a long pipeline. We will treat this problem for an ideal gas in constant cross section channels, where the flow is assumed to be one dimensional and steady. The thermodynamic behavior of such a flow can be obtained by considering a diagram of enthalpy h (or temperature T) versus entropy s . In analyzing a choked flow and shock wave characteristics, the Fanno and Rayleigh lines (curves) plotted on the enthalpy h – entropy s diagram are useful in consideration of a graphical interpretation of the process.

The equations of the Fanno line are derived from the mass continuity, the energy equation and the thermodynamic relations between the stagnation condition and a point in the channel, as long as the channel section is kept adiabatic regardless of the friction.

In Eq. (5.2.18) where $A = \text{const.}$, the continuity equation is written as

$$G = \rho u = \text{const.} \quad (5.3.1)$$

where G is the mass flux. The energy equation of Eq. (5.2.13) is written for an ideal gas, i.e. $h = c_p T$, as

$$\frac{1}{2} u^2 + h = h_0 \quad (5.3.2)$$

The thermodynamic relations, Eq. (2.5.6) and Eqs. (2.5.15–2.5.17), with the adiabatic process, i.e. $p(1/\rho)^k = \text{const.}$, are given in terms of the entropy change as follows

$$s - s_{(1)} = R \ln \left\{ \left(\frac{T}{T_{(1)}} \right)^{\frac{1}{k-1}} \left(\frac{P_{(1)}}{P} \right) \right\} \quad (5.3.3)$$

and

$$s - s_{(1)} = c_v \ln \left[\frac{h}{h_{(1)}} \left(\frac{P_{(1)}}{P} \right)^{k-1} \right] \quad (5.3.4)$$

where suffix $_{(1)}$ is the reference state point with known values of enthalpy $h_{(1)}$, entropy $s_{(1)}$, density $\rho_{(1)}$ and temperature $T_{(1)}$ on the $h-s$ diagram. In Eqs. (5.3.1–5.3.4), the stagnation condition is defined for the enthalpy h_0 , while at an arbitrary point in the channel the quantities are defined without suffix. Combining Eqs. (5.3.1) and (5.3.2), we can write Eq. (5.3.4) as the relation between the enthalpy and the entropy as

$$s - s_{(1)} = c_v \ln \left\{ \left(\frac{\sqrt{2}\rho_{(1)}}{G} \right)^{k-1} \frac{h}{h_{(1)}} (h_0 - h)^{\frac{k-1}{2}} \right\} \quad (5.3.5)$$

Further simplified, we can say

$$s - s_{(1)} = c_v \ln \left\{ \frac{h(h_0 - h)^{\frac{k-1}{2}}}{h_{(1)}(h_0 - h_{(1)})^{\frac{k-1}{2}}} \right\} \quad (5.3.6)$$

Some simplifications are expressed in Eq. (5.3.6), and it maybe written for h as follows

$$h(h_0 - h)^{\frac{k-1}{2}} = C_{(1)} G^{k-1} e^{\left(\frac{k}{c_p} s \right)} \quad (5.3.7)$$

where $C_{(1)}$ is a constant defined as state point (1) in the $h-s$ diagram and is calculated with $G_{(1)}$, $h_{(1)}$ and $s_{(1)}$.

The line of either Eqs. (5.3.6) or (5.3.7) drawn in the $h-s$ diagram is labeled as the Fanno line (or Fanno curve). The Fanno lines given by the function of Eqs. (5.3.6) or (5.3.7) are plotted exaggeratingly in Fig. 5.8(a) and (b) respectively. We can find that s reaches a maximum when s in Eq. (5.3.6) is differentiated with respect to h and setting ds/dh to zero, i.e.

$$\frac{ds}{dh} = c_v \left\{ \frac{1}{h} - \frac{k-1}{2} \left(\frac{1}{h_0 - h} \right) \right\} = 0 \quad (5.3.8)$$

This gives the entropy s maximum for $h = 2h_0/(k+1)$. Furthermore, this $h = 2h_0/(k+1)$ is substituted into Eq. (5.3.2) to give

$$\begin{aligned} u^2 &= h(k-1) \\ &= c_p T(k-1) \\ &= kRT \end{aligned} \quad (5.3.9)$$

Equation (5.3.9) shows that at the maximum entropy, the flow is at the sonic, i.e. $M^2 = u^2/kRT = u^2/a^2 = 1$. Similarly, we can write the gradient of the line from Eq. (5.3.8) in terms of the Mach number

$$\frac{ds}{dh} = \frac{k-1}{a^2} \left[\frac{M^2 - 1}{M^2} \right] \quad (5.3.10)$$

and as a result Eq. (5.3.10) yields the following relations for $k > 1$

$$\frac{ds}{dh} > 0, \quad M > 1 \text{ (supersonic)}$$

$$\frac{ds}{dh} = 0, \quad M = 1 \text{ (sonic)}$$

$$\frac{ds}{dh} < 0, \quad M < 1 \text{ (subsonic)}$$

as indicated in Fig. 5.8(a) and (b). The relations characterize the Fanno line.

The equations of the Rayleigh line are also derived, on the other hand, from the mass continuity and the momentum equation for frictionless flow, lifting the adiabatic condition. The flow under consideration is similarly one dimensional with steady internal flow. Instead of the energy equation, we use the momentum equation per unit area (the momentum flux) from Eq. (4.1.47), i.e.

$$\dot{m}(u_2 - u_1) = (p_1 - p_2)A$$

$$\rho u(u_2 - u_1) = p_1 - p_2$$

and by the mass continuity of Eq. (5.3.1); $\rho u_2 = \rho u_1$, we have the expression

$$\rho u u + p = f = \text{const.} \quad (5.3.11)$$

where f is called the impulse or thrust function as it is kept constant for frictionless flow through the channel. Using the continuity of Eq. (5.3.1) again, we may be able to modify Eq. (5.3.11) to write p explicitly with the formula that follows

$$p = f - \frac{G^2}{\rho} \quad (5.3.12)$$

For an ideal gas, the enthalpy is written by the following formula

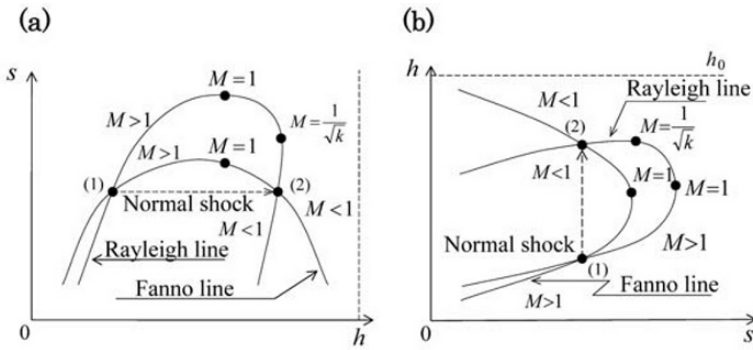


Fig. 5.8 Fanno and Rayleigh lines

$$h = c_p T = c_p \frac{p}{\rho R} = \frac{k p}{\rho(k-1)} \quad (5.3.13)$$

so that

$$\frac{p}{\rho} = \frac{(k-1)h}{k} \quad (5.3.14)$$

Combining Eq. (5.3.12) with Eq. (5.3.14) and eliminating ρ , we can obtain an expression for enthalpy as

$$h = \frac{k(fp - p^2)}{(k-1)G^2} \quad (5.3.15)$$

Nevertheless to convey the essence of the subject, it is required to write p in Eq. (5.3.15) in terms of the entropy in a thermodynamic system. For

an ideal gas, the pressure p is a function of any two thermodynamics parameters, i.e. $p = p(h, s)$. Considering Eqs. (2.5.6) with (2.5.17) by integrating between the state points, we have

$$s - s_{(2)} = c_v \ln \left\{ \left(\frac{p}{p_{(2)}} \right) \left(\frac{\rho_{(2)}}{\rho} \right)^k \right\} \quad (5.3.16)$$

and it follows that

$$\frac{h}{h_{(2)}} = \left(\frac{p}{p_{(2)}} \right)^{\left(\frac{k-1}{k} \right)} e^{\left(\frac{s - s_{(2)}}{c_p} \right)} \quad (5.3.17)$$

where we have used, $h/h_{(2)} = T/T_{(2)}$. Equation (5.3.17) can be further simplified into

$$p = C_{(2)} \left\{ h \cdot e^{\left(\frac{-s}{c_p} \right)} \right\}^{\frac{k}{k-1}} \quad (5.3.18)$$

where $C_{(2)}$ is a constant defined at one state point. The equation of the Rayleigh line is now to be derived by substituting Eq. (5.3.18) into Eq. (5.3.15) to give

$$\left\{ h \cdot e^{\left(\frac{-s}{c_p} \right)} \right\}^{\frac{2k}{k-1}} - \frac{f}{C_{(2)}} \left\{ h \cdot e^{\left(\frac{-s}{c_p} \right)} \right\}^{\frac{k}{k-1}} + \frac{a^2}{C_{(2)}^2} \left(\frac{k-1}{k} \right) h = 0 \quad (5.3.19)$$

In Fig. 5.8(a) and (b), Rayleigh lines are displayed, having common states with the Fanno lines. As in the case of Fanno lines, we are similarly able to obtain the condition at s to be a maximum by differentiating s in Eq. (5.3.19) with respect to h as

$$\frac{ds}{dh} = \frac{M^2 - 1}{kM^2} \left(\frac{1}{T} \right) \quad (5.3.20)$$

where we used the relation in Eq. (5.3.9) similar to the case of the Fanno line. It is denoted that Eq. (5.3.20) is readily obtained by Eqs. (5.3.14) and (10) in Exercises 5.3 together with the thermodynamics relation

$dp = \rho(dh - Tds)$ derived from Eq. (2.5.15). As shown in Fig. 5.8(a) and (b), at $M = 1$ the entropy s reaches the maximum, yielding the flow characteristics for $kM^2 > 1$ as follows

$$\frac{ds}{dh} > 0, \quad M > 1 \text{ (supersonic)}$$

$$\frac{ds}{dh} = 0, \quad M = 1 \text{ (sonic)}$$

$$\frac{ds}{dh} < 0, \quad 1/\sqrt{k} < M < 1 \text{ (subsonic)}$$

It is readily confirmed that at $M = 1/\sqrt{k}$, the enthalpy becomes maximum and for $1/\sqrt{k} < M < 1$, dh/ds is negative, while everything other than this region dh/ds is positive. In Rayleigh flows, as indicated by the Rayleigh line, the increase of entropy is due to heat given from outside the system, since no friction is assumed. Therefore, in comparison with the Fanno flow, which is represented by the Fanno line, self-heating of a compressible flow has an effect to encourage the flow to reach $M = 1$, and this implicitly suggests the friction effect of the Fanno flow.

As we will see later in this chapter, a normal shock is characterized with the mass continuity equation, the momentum equation and the energy equation. Thus, the thermodynamic states represented at points (1) and (2) in Fig. 5.8(a) and (b), where the Fanno and Rayleigh lines across for a given mass flux G , satisfy the three equations for a normal shock. This fact represents that through the occurrence of the normal shock the entropy increases from points (1) to (2) of the thermodynamic states behind and ahead of the normal shock respectively.

5.4 Normal Shock Waves

In a Laval tube, as studied in the previous section, when the exit pressure is well below the reservoir pressure, there is a discontinuity in pressure as observed in Fig. 5.5(a) and (b). The discontinuity of pressure, density and temperature that occurs in the direction of compressible flow is a prominent feature of normal shock. Also for the points where Fanno and Rayleigh lines cross, there is an entropy increase as verified in Fig. 5.8(a) and (b). The points (1) and (2) in Fig. 5.8(a) and (b) meet the following conditions

- (1) one dimensional
- (2) constant cross sectional area through the shock
- (3) ideal gas
- (4) steady state flow
- (5) adiabatic and frictionless

It may be further stated that for the points of cross-lines, the mass continuity, the momentum and the energy equations are simultaneously satisfied. The normal shock, the simplest case of a shock wave, is regarded and is observed in experiments as a surface perpendicular to the direction of flow. Through the shock there is sudden occurrence of discontinuous change of flow properties and the flow is irreversible, so that, although the adiabatic condition is held, the isentropic equations cannot be used. A state of flow for a normal shock is depicted in Fig. 5.9.

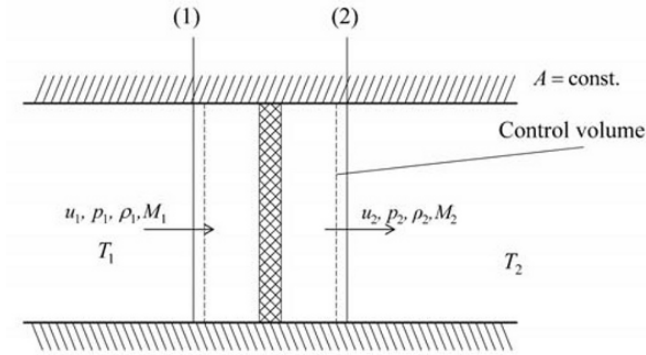


Fig. 5.9 Normal shock

The equations of mass continuity, momentum and energy are repeatedly written for a normal shock as

$$\rho_1 u_1 = \rho_2 u_2 \quad (5.4.1)$$

$$\rho_1 u_1^2 + p_1 = \rho_2 u_2^2 + p_2 \quad (5.4.2)$$

$$\frac{1}{2} u_1^2 + \frac{k}{k-1} \frac{p_1}{\rho_1} = \frac{1}{2} u_2^2 + \frac{k}{k-1} \frac{p_2}{\rho_2} \quad (5.4.3)$$

From Eqs. (5.4.1–5.4.3), we have a relationship among the flow properties between states (1) and (2), respectively in front of and behind the normal shock as follows

$$\frac{u_2}{u_1} = \frac{\rho_1}{\rho_2} = \frac{(k+1) + (k-1)(p_2/p_1)}{(k-1) + (k+1)(p_2/p_1)} \quad (5.4.4)$$

With a definition of the speed of sound as Eq. (5.1.25), we can write Eq. (5.4.4) in terms of a Mach number and its relevant forms such that

$$\frac{u_2}{u_1} = \frac{\rho_1}{\rho_2} = \frac{2 + (k-1)M_1^2}{(k+1)M_1^2} \quad (5.4.5)$$

$$\frac{p_2}{p_1} = \frac{1 + kM_1^2}{1 + kM_2^2} = \frac{2kM_1^2 - k + 1}{k + 1} \quad (5.4.6)$$

$$\frac{T_2}{T_1} = \frac{1 + \frac{1}{2}(k-1)M_1^2}{1 + \frac{1}{2}(k-1)M_2^2} = \frac{(2kM_1^2 - k + 1)(2 + (k-1)M_1^2)}{(k+1)^2 M_1^2} \quad (5.4.7)$$

The formula of Eq. (5.4.4) that relates to pressure and density across a normal shock is known as the Rankine-Hugoniot relationship. This relationship stands for a normal shock wave of any strength without taking in account of any internal structure of the wave.

The equation of a state combined with the thermodynamic expression for entropy change is given as Eq. (5.3.16) and causes the entropy increase as

$$s_2 - s_1 = c_v \left[\ln \left(\frac{p_2}{p_1} \right) - k \ln \left(\frac{\rho_2}{\rho_1} \right) \right] \quad (5.4.8)$$

Substituting Eq. (5.4.4) into Eq. (5.4.8), and denoting $\delta p = p_2 - p_1$ and $\delta s = s_2 - s_1$, we can expand Eq. (5.4.8) to give

$$\delta s = c_v \frac{k^2 - 1}{12k^2} \left(\frac{\delta p}{p_1} \right)^3 + 0(\delta p^4) \quad (5.4.9)$$

Since in the normal shock wave, the entropy increases $\delta s > 0$, it gives a condition that from Eq. (5.4.9), $\delta p > 0$. This for $\delta p > 0$ implies that, from Eqs. (5.4.4) to (5.4.7), the following relations must be met

$$\frac{u_1}{u_2}, \frac{p_2}{p_1}, \frac{T_2}{T_1}, \frac{\rho_2}{\rho_1} > 1 \quad (5.4.10)$$

It is noted that $\delta p/p_1$ in Eq. (5.4.9) is sometimes called the shock strength and for $\delta p > 0$, the thermodynamic process is called the compression. That is to say, the normal shock wave is the compression wave and the following conditions are to be thought:

(i) If the shock strength is small, i.e. $\delta p/p_1 \ll 1$, from Eq. (5.4.8) the flow through the shock is isentropic, i.e. $\delta s \approx 0$.

(ii) Equation (5.4.4) may be written in the following form, by setting $\delta p = p_2 - p_1$ and $\delta \rho = \rho_2 - \rho_1$

$$\frac{\delta p}{\delta \rho} = \frac{k(p_1 + p_2)}{\rho_1 + \rho_2} \quad (5.4.11)$$

and from the momentum equation of Eq. (5.4.2), we have

$$u_1 = \sqrt{\frac{k(p_1 + p_2)}{\rho_1 + \rho_2} \left(\frac{\rho_2}{\rho_1} \right)} = \sqrt{\left(1 + \frac{p_2}{p_1} \right) \frac{k \left(\frac{p_1}{\rho_1} \right)}{1 + \left(\frac{\rho_1}{\rho_2} \right)}} \quad (5.4.12)$$

Consequently according to Eq. (5.4.11), we can identify two conditions for a normal shock wave: for a weak shock, i.e. $\rho_1 \approx \rho_2$ and $p_1 \approx p_2$, Eq. (5.4.12), which becomes

$$u_1 \approx \sqrt{\frac{k p_1}{\rho_1}} = \sqrt{\frac{k p_2}{\rho_2}} = \text{const.} \quad (5.4.13)$$

which is the speed of sound, meaning that the shock propagates with the speed of sound; for a very strong shock, i.e. $p_1 \ll p_2$ and $\rho_1 \ll \rho_2$, Eq. (5.4.12) is certainly greater than the speed of sound, indicating that a very strong shock may propagate faster than a weak shock.

When we consider the critical velocity u^* , i.e. the velocity for the flow reaching the speed of sound a , it will prove useful to write the energy equation Eq. (5.4.3) as

$$\frac{1}{2} u_1^2 + \frac{k}{k-1} \frac{p_1}{\rho_1} = \frac{1}{2} u_2^2 + \frac{k}{k-1} \frac{p_2}{\rho_2} = \frac{k+1}{2(k-1)} a_*^2 \quad (5.4.14)$$

where a_* is invariant between behind and ahead of a normal shock. It is now desired to derive a useful expression for a normal shock. Eliminating p and ρ from Eqs. (5.4.1), (5.4.2) and (5.4.14), we can obtain a simple expression as

$$u_1 u_2 = a_*^2 \quad (5.4.15)$$

This is called as Prandtl relation. As an alternative, Eq. (5.4.15) can also be written by

$$M_{1*} M_{2*} = 1 \quad (5.4.16)$$

Thus, from relationships in Eqs. (5.4.10) and (5.4.16), we have $M_1 > 1$ and $M_2 < 1$, since $M \geq 1$ and $M_* \geq 1$ is respectively true. This indicates that a normal wave can occur only if the upstream flow is supersonic.

It also appears, according to Eq. (5.4.16), that $M_1 \rightarrow \infty$ leads to $\rho_2/\rho_1 = u_1/u_2$ to reach an asymptote of $(k+1)/(k-1)$. If the value of $k=1.4$ represents air, the maximum (the asymptote) is 6, meaning that air cannot be compressed more than 6 times its original density by normal shock, while p_2/p_1 and T_2/T_1 increase infinitely.

Mach number relations across a normal shock wave may be found in the following relation

$$\frac{M_2^2}{M_1^2} = \left(\frac{u_2}{u_1} \right)^2 \frac{T_1}{T_2} \quad (5.4.17)$$

so that with the aid of Eqs. (5.4.5) and (5.4.7) we have

$$M_2^2 = \frac{(k-1)M_1^2 + 2}{2kM_1^2 - (k-1)} \quad (5.4.18)$$

Equation (5.4.18) also indicates that for $M_1 > 1$ and $k > 1$ the flow is subsonic behind a normal shock wave. As for air, for example, with $k=1.4$, Eq. (5.4.18) can be reduced to

$$M_2^2 = \frac{M_1^2 + 5}{7M_1^2 - 1} \quad (5.4.19)$$

5.5 Oblique Shock Wave

When a supersonic incompressible flow passes over a slender wedge, as shown in Fig. 5.10, for example a plane shock wave is formed, when the plane of the shock wave is inclined by an angle of β with respect to the incoming flow direction. This plane shock wave, termed an oblique shock wave, is attached to the nose of the wedge, and acts to turn the flow through a semi-vertex angle (wedge angle) of θ so that the flow becomes parallel to the wedge downstream from the shock. An oblique shock wave is often observed at the nose of a supersonic aircraft.

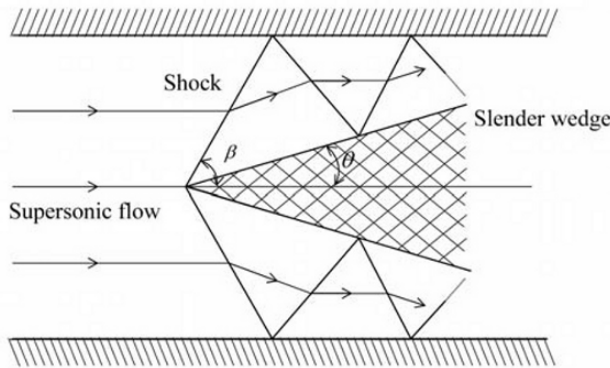


Fig. 5.10 Supersonic flow past a wedge

Figure 5.11 shows a schematic diagram of an oblique shock wave that has been assigned kinematic properties. In dealing with an oblique shock wave, mass continuity, momentum, and energy equations are to be solved in the same manner as a normal shock wave. However, it should be kept in mind that by conservation of momentum, since there is no pressure change along the shock wave and there is no force acting on the fluid along the shock wave plane, the tangential component of velocity u_t is continuous across the shock wave

$$\rho_1 u_{n1} u_{t1} = \rho_2 u_{n2} u_{t2} \quad (5.5.1)$$

Thus, with the aid of the relation $\rho_1 u_{n1} = \rho_2 u_{n2}$ (Eq. 5.4.1), we have

$$u_{t1} = u_{t2} = u_t \quad (5.5.2)$$

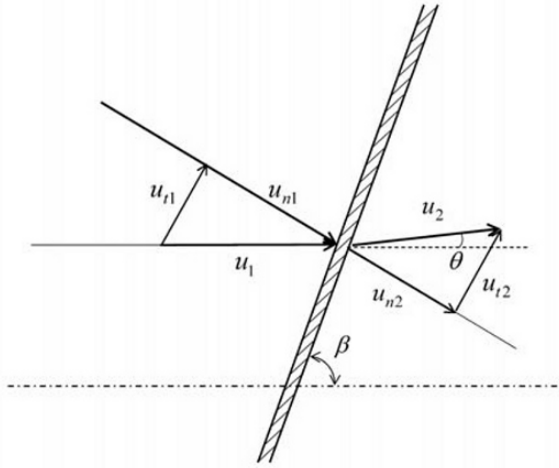


Fig. 5.11 The oblique shock

The normal components of velocity u_{n1} and u_{n2} are related to the normal shock relations of the previous section. Therefore, the mass continuity, momentum and energy equations in the normal direction to the shock are written identically for an oblique shock when the flow properties, such as pressure, density, temperature and etc, are related in the same way as with the normal shock. Thus, it would be useful to write the energy equation as

$$\frac{1}{2}(u_{n1}^2 + u_{t1}^2) + \frac{k}{k-1} \frac{p_1}{\rho_1} = \frac{1}{2}(u_{n2}^2 + u_{t2}^2) + \frac{k}{k-1} \frac{p_2}{\rho_2} = \frac{k+1}{k(k-1)} a_*^2 \quad (5.5.3)$$

Furthermore, with the condition of Eq. (5.5.2) we have

$$\frac{1}{2} u_{n1}^2 + \frac{k}{k-1} \frac{p_1}{\rho_1} = \frac{1}{2} u_{n2}^2 + \frac{k}{k-1} \frac{p_2}{\rho_2} = \frac{k+1}{2(k-1)} \left(a_*^2 - \frac{k-1}{k+1} u_t^2 \right) \quad (5.5.4)$$

Equation (5.5.4) is exactly the same as Eq. (5.4.14) by replacing a_*^2 from Eq. (5.4.14) with $a_*^2 - (k-1)u_t^2/(k+1)$, so that the Rankine-Hugoniot relationship of a normal shock wave can still be valid for the oblique shock. The Prandtl relation for the oblique shock is also written as follows

$$u_{n1}u_{n2} = a_*^2 - \frac{k-1}{k+1} u_t^2 \quad (5.5.5)$$

With the aid of the velocity diagram in Fig. 5.11, the velocity ratios for u_n and u_t are expressed in terms of the shock inclination angle β and the velocity deflection angle θ as

$$\frac{u_{n1}}{u_t} = \tan \beta \quad \text{and} \quad \frac{u_{n2}}{u_t} = \tan(\beta - \theta) \quad (5.5.6)$$

By defining $M_1 = u_1 / a_1$, we can write $u_{n1} / a_1 = M_1 \sin \beta$ since typically $u_{n1} = u_1 \sin \beta$. Thus, the normal shock relationship from Eq. (5.5.5) can be written for the oblique shock relationship by replacing M_1 in Eq. (5.4.5) with $M_1 \sin \beta$, which gives

$$\frac{u_{n1}}{u_{n2}} = \frac{\rho_2}{\rho_1} = \frac{(k+1)(M_1^2 \sin^2 \beta)}{(k-1)M_1^2 \sin^2 \beta + 2} \quad (5.5.7)$$

Perhaps it is worth taking a moment to consider the relationship between the shock inclination angle β and the wedge angle θ . Substituting the relations from Eq. (5.5.6) into Eq. (5.5.7), we can derive the following relationship between β and θ

$$\frac{\tan(\beta - \theta)}{\tan \beta} = \frac{(k-1)M_1^2 \sin^2 \beta + 2}{(k+1)(M_1^2 \sin^2 \beta)} \quad (5.5.8)$$

By solving Eq. (5.5.8) for θ , we can write the angle θ as

$$\tan \theta = \frac{2(M_1^2 \sin^2 \beta - 1)}{M_1^2(k + \cos 2\beta) + 2} \cot \beta \quad (5.5.9)$$

Depending on M_1 , Eq. (5.5.9) shows that θ will be zero for β , equal to either $\pi/2$ or $\sin^{-1}(1/M_1)$, or somewhere within this range, noting that there is a maximum of θ . Figure 5.12 is a plot of θ versus β for a given M_1 , where the dashed line is a curve for θ_{\max} . Figure 5.12 indicates that there are two possible solutions of β for θ ($\theta < \pi/4$). In practice it is observed that the solution (to a weak shock) occurs and has a weaker discontinuity, with a remainder of $M_2 > 1$ (except for in a region between the lines $M_2 = 1$ and θ_{\max}). That is, two solutions are derived from the jump conditions, which are in effect characterized by different shock inclinations angles and shock intensities. The solutions are known as the weak and strong solutions. Phenomenologically the strong solution indicates a flow which is subsonic downstream from the shock with $\theta_{\max} < \beta < \pi/2$,

whereas the weak solution describes a flow which is supersonic downstream from the shock in β less than the line of $M_2 = 1$. With a symmetrical slender wedge, u_1 is parallel to the surface of the wedge with an angle of θ , so that when M_1 is specified, the shock inclination angle β will be calculated from Eq. (5.5.9).

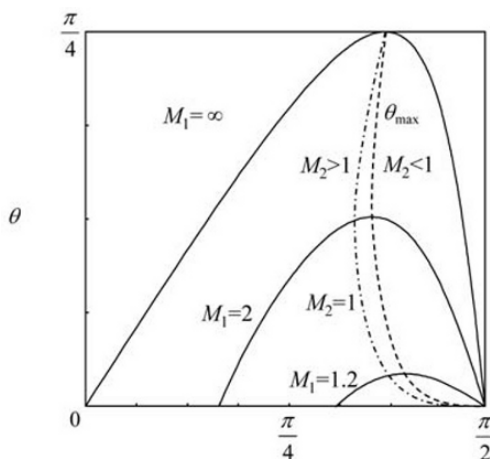


Fig. 5.12 $\theta - \beta$ plot for an oblique shock

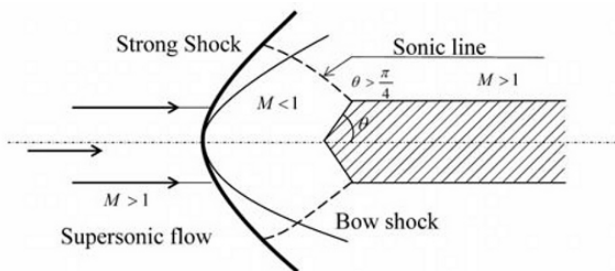


Fig. 5.13 Detached shock wave

It is interesting to see the flow phenomena if θ is greater than $\pi/4$. It appears that neither an oblique shock nor a normal shock is possible and it is observed from experiment that the shock becomes detached. That is to say, the shock curves around the wedge are not touching the wedge, as schematically displayed in Fig. 5.13. The phenomenon also occurs with a blunt body. There are some regions after the curved shock wave, called the bow shock, as shown in Fig. 5.13. The dotted line, which corresponds to

$M=1$, is called the sonic line and divides the two regions of supersonic and subsonic flow. It is found that the drag on a blunt body (or higher deflection angled wedge) is higher than that of a slender body when the body is traveling with supersonic speed. This is due to the shock wave being detached, and to reduce the drag it is advantageous to adopt a small nose angle (wedge angle) for supersonic crafts so that the oblique shock may be formed on the body.

Exercise

Exercise 5.1 The Compressibility Factor

In an isentropic flow through a channel from a reservoir, the pressure in the reservoir is such that the velocity of flow is identically zero. In contrast to the reservoir, when an isotropic flow is brought to rest at any point of a flow field, the pressure with zero velocity can be obtained with the same treatment as the case of a reservoir. The stagnation pressure is such that a flow is brought to rest. We will now consider the stagnation pressure p_0 for an isentropic flow in terms of the Mach number.

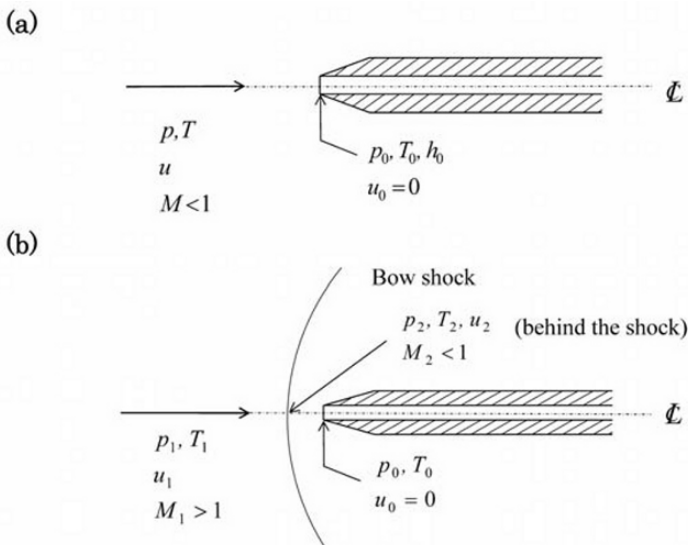


Fig. 5.14 The stagnation pressure; Pitot tube configuration

The typical application of such a flow is found by measuring its velocity via the Pitot tube, as depicted in Fig. 5.14(a) and (b). Show the effect of Mach number in measuring the stagnation pressure, and thus the velocity of flow for an ideal gas.

Ans.

Let consider the energy equation of Eq. (5.2.13) between the upstream and the stagnation, as indicated in Fig. 5.14(a)

$$\frac{1}{2}(u^2 - u_0^2) = h_0 - h \quad (1)$$

For an ideal gas we may write the enthalpy with the aid of the relations $h = c_p T$ and $h_0 = c_p T_0$. Also using $M = u/a$ and $c_p = kR/(k-1)$, we can reduce Eq. (1) to the following form, by setting $u_0 \rightarrow 0$

$$\frac{T_0}{T} = 1 + \frac{k-1}{2} M^2 \quad (2)$$

For the isentropic flow, we have a thermodynamic relation

$$\frac{p_0}{p} = \left(\frac{T_0}{T} \right)^{\frac{k}{k-1}} \quad (3)$$

In combination with Eqs. (2) and (3), the stagnation pressure p_0 is thus expressed by

$$\frac{p_0}{p} = \left(1 + \frac{k-1}{2} M^2 \right)^{\frac{k}{k-1}} \quad (4)$$

If this equation is expressed with a binomial expansion for the Mach number, we have

$$\frac{p_0}{p} = 1 + \frac{k}{2} M^2 + \frac{k}{8} M^4 + \frac{k(2-k)}{48} M^6 + \dots \quad (5)$$

and

$$p_0 - p = \frac{pkM^2}{2} \left\{ 1 + \frac{M^2}{4} + \frac{2-k}{24} M^4 + \dots \right\} \quad (6)$$

It will prove useful to write the leading term of the right hand of Eq. (6) as

$$\frac{pkM^2}{2} = \frac{p}{2} k \frac{u^2}{kRT} = \frac{1}{2} \frac{p}{RT} u^2 = \frac{1}{2} \rho u^2$$

Thus, Eq. (6) becomes

$$\frac{p_0 - p}{\frac{1}{2} \rho u^2} = 1 + \frac{M^2}{4} + \frac{2-k}{24} M^4 + \dots = \alpha_c \quad (7)$$

The right hand side of Eq. (7) can be represented by α_c , which is called the compressibility factor. For example, in the case of air $k=1.4$, it is calculated that $\alpha_c=1.276$ at $M=1$ and in a lower Mach number case, we can say that $\alpha_c=1.022$ at $M=0.3$. Thus, for measuring the velocity by a Pitot tube, we can write the Eq. (7) as

$$u = \sqrt{\frac{2(p_0 - p)}{\rho}} (\alpha_c)^{-\frac{1}{2}} \quad (8)$$

The actual velocity measured by a Pitot tube for a flow of $M=0.3$ is approximately 1.1% less than that of incompressible flow measurement.

In supersonic flow, however, a detached shock wave may be formed ahead of a Pitot tube as shown in Fig. 5.14(b). Along the center line, the relationship across a normal shock can be applied that are found in Eqs. (5.4.18) and (5.4.6), written as

$$M_2^2 = \frac{(k-1)M_1^2 + 2}{2kM_1^2 - (k-1)} \quad \text{and} \quad \frac{p_2}{p_1} = \frac{2kM_1^2 - (k-1)}{k+1} \quad (9)$$

The isentropic relation of Eq. (4) can be used between the point of after shock to the stagnation point as indicated in Fig. 5.14(b), which is given as

$$\frac{p_0}{p_2} = \left(1 + \frac{k-1}{2} M_2^2 \right)^{\frac{k}{k-1}} \quad (10)$$

With Eqs. (9) and (10), eliminating M_2 and p_2 , we can derive the following relationship between the upstream and the stagnation point

$$\frac{p_0}{p} = \left[\frac{\left(\frac{M_1^2}{2} \right)^k (k+1)^{k+1}}{2kM_1^2 - (k-1)} \right]^{\frac{1}{k-1}} \quad (11)$$

Equation (11) relates the stagnation pressure for a supersonic flow and the formula is called the Rayleigh's Pitot-tube relation.

Exercise 5.2 Fanno-line Flow Relations and Chocking

Consider a flow of ideal gas in a horizontal tube of constant cross-section. The flow in the tube is assumed adiabatic, but with friction, i.e. the existence of wall shear stress. Derive Fanno-line flow relations and discuss the possibility of choking condition.

Ans.

Let denote A as the cross-section area and dx as a small increment of x as indicated in Fig. 5.15, where the control volume is defined by dotted line together with flow and thermodynamic parameters. For the control volume, we will apply (i) the mass continuity, (ii) the momentum and (iii) the energy equations as described below.

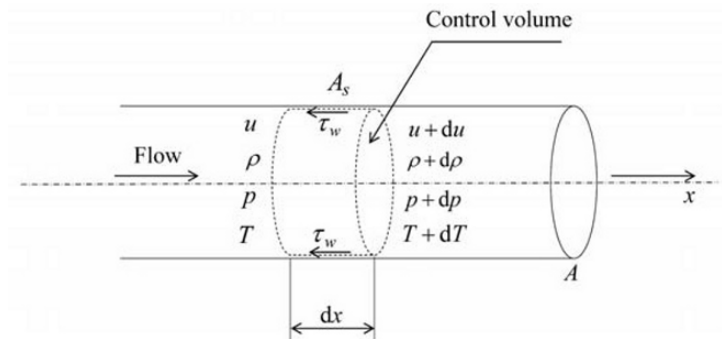


Fig. 5.15 Fanno-line flow, τ_w the wall shear stress

(i) Mass continuity equation

$$\rho u A = \text{const.} \quad (1)$$

For A constant, we can write Eq. (1) in a differential form as

$$\frac{d\rho}{\rho} + \frac{du}{u} = 0 \quad (2)$$

(ii) Momentum equation

The momentum balance of the control volume is

$$\rho u A [(u + du) - u] = pA - (p + dp)A - \tau_w A_s \quad (3)$$

where τ_w is the wall shear stress and A_s is the wall surface area of the control volume. τ_w can be defined, using the friction factor c_f , as

$$\tau_w = c_f \left(\frac{1}{2} \rho u^2 \right) \quad (4)$$

We can assume that c_f is kept constant along the channel. It is reassuring to know that the constant of c_f is justified since it is kept around $c_f = 0.004 \sim 0.003$ for the Reynolds number $10^9 \sim 10^6$, although c_f is a function of the Reynolds number, the Mach number and surface roughness ε (RMS) of tube wall, $c_f = c_f(Re, M, \varepsilon/D)$. In a case of circular tube of diameter D , i.e. $A_s = \pi D dx$, Eq. (1) can be rearranged as follows

$$\frac{du}{u} + \frac{1}{kM^2} \frac{dp}{p} + \frac{c_f}{2} \left(\frac{4}{D} \right) dx = 0 \quad (5)$$

where for $\rho u^2 = (p/RT)M^2 a^2 = k p M^2$ is used and, a is the speed of sound.

(iii) Energy equation

The energy equation of an ideal gas with the enthalpy defined as $h = c_p T$ is written from Eq. (5.2.13) as

$$u du + c_p dT = 0 \quad (6)$$

By dividing the both sides by $c_p T$ and recognizing $c_p = kR/(k-1)$, we can obtain

$$\frac{dT}{T} + (k-1)M^2 \frac{du}{u} = 0 \quad (7)$$

It should be kept in mind that, as in Eqs. (1) to (7), there is no particular thermodynamic process mentioned for the control volume, but with the adiabatic condition to the control volume being assumed, we can assume there is no heat transfer to or from the control volume.

(iv) Entropy change and Mach number

The equation of state for an ideal gas is written as $p/\rho = RT$, and its differential form is

$$\frac{dp}{p} = \frac{d\rho}{\rho} + \frac{dT}{T} \quad (8)$$

The entropy change of the control volume is, from the second law of thermodynamics

$$\begin{aligned} ds &= c_v \frac{dT}{T} - R \frac{d\rho}{\rho} \\ &= \frac{R}{k-1} \frac{dT}{T} - R \frac{d\rho}{\rho} \end{aligned} \quad (9)$$

It is noted again that the adiabatic condition to the control volume does not directly mean it is isentropic, since we are considering the friction of flow. From the definition of the Mach number $M = u/\sqrt{kRT}$, a differential form is

$$\frac{dM}{M} = \frac{du}{u} - \frac{1}{2} \frac{dT}{T} \quad (10)$$

Now we are able to reduce the Fanno-line of flow relations in terms of the Mach number, using Eqs. (1) to (10). To begin with, eliminating dT/T as in Eqs. (7) and (10) and by combining them with Eq. (2), we can obtain

$$\frac{du}{u} = \frac{1}{2} \left\{ \frac{1}{M^2} - \frac{(k-1)}{(k-1)M^2 + 2} \right\} dM^2 = -\frac{d\rho}{\rho} \quad (11)$$

Equation (11) is substituted into Eq. (7) and we have the relationship that follows

$$\frac{dT}{T} = -\frac{1}{M} \left\{ \frac{2(k-1)M^2}{(k-1)M^2 + 2} \right\} dM \quad (12)$$

In the same manner, Eqs. (11) and (12) are substituted into Eq. (8) to give

$$\frac{dp}{p} = -\left\{ \frac{1}{M} + \frac{(k-1)M}{(k-1)M^2 + 2} \right\} dM \quad (13)$$

Thus, from the relationships derived from above, the entropy change is given by substituting Eqs. (11) and (12) into Eq. (9)

$$\frac{ds}{R} = \left\{ \frac{1}{M} - \frac{(k+1)M}{(k-1)M^2 + 2} \right\} dM \quad (14)$$

Similarly, the actual change of the Mach number itself will be given by substituting Eqs. (11) and (13) to Eq. (5) to give

$$4c_f \frac{dx}{D} = \left\{ \frac{2}{k} \frac{1}{M^3} - \frac{(k+1)}{k} \frac{1}{M} + \left(\frac{k+1}{k} \right) \frac{(k-1)M}{(k-1)M^2 + 2} \right\} dM \quad (15)$$

Table 5.1 Change of properties in the Fanno-line flow

Property	Subsonic flow $M < 1$	Supersonic flow $M > 1$
s	\rightarrow	\rightarrow
M	\rightarrow	\rightarrow
u	\rightarrow	\rightarrow
ρ	\rightarrow	\rightarrow
T	\rightarrow	\rightarrow
p	\rightarrow	\rightarrow

Equations (11) to (15) give the change of properties, u , ρ , T , p , s and M . It will be convenient to verify the changes of a state by the Mach number whether the flow is subsonic or supersonic. Table 5.1 shows the summarized results. As seen in Table 5.1, for subsonic flow ($M < 1$), when the Mach number increases, the change of the Mach number along the tube will be $dM/dx > 0$ from Eq. (15), implying the fact that the effective cross section area decreases. This effect concerns the effective increase of the thickness of the boundary layer, since the flow includes the effect of viscosity.

From Table 5.1, we also see that the frictional effects cause the fluid to tend toward $M = 1$ for both initially subsonic and supersonic conditions.

This fact indicates, if a tube length is sufficiently long enough, that the flow is choked off due to the friction. We may be able to integrate Eqs. (11)~(15) between a reference point of flow to a point where the flow reaches the Mach number, as schematically depicted in Fig. 5.16. For example, if we integrate Eq. (15), we obtain

$$\frac{4c_f}{D} \int_x^{x^*} dx = \int_M^1 \frac{2}{k} \frac{1}{M^3} \left\{ \frac{2(1-M^2)}{(k-1)M^2 + 2} \right\} dM \quad (16)$$

and

$$\frac{4c_f}{D} L_{\max} = \frac{k+1}{2k} \ln \left\{ \frac{(k+1)M^2}{(k-1)M^2 + 2} \right\} - \frac{M-1^2}{kM^2} \quad (17)$$

where we set $L_{\max} = x^* - x$.

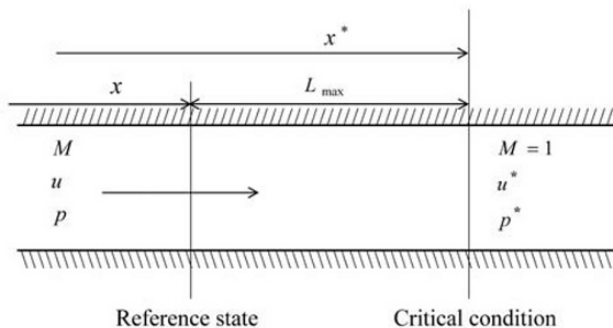


Fig. 5.16 Approach to critical condition

It appears that the flow reaches the choking condition at $x = x^*$ from an arbitrary point x in a tube. L_{\max} is the maximum length, which is called the limiting length.

Now cases are examined in order to gain the trend in the properties change along the distance, particularly in the Mach number. From Eq. (17), Fig. 5.17 is a plot of a Mach number M_2 at a distance x_2 from a reference point x , where a reference Mach number is denoted by M_2 . For example, a flow with a Mach number $M = 0.7$ at a point of x reaches $M_2 = 1$ at approximately $L_{2\max} = 0.2$ where the flow is choked. In the case where the length of tube is longer than $L_{2\max}$, the flow cannot reach $M = 1$ along the tube, but only at the exit, where the flow is choked. The mass flow rate decreases in the case of a tube longer than $L_{2\max}$. When a flow is

supersonic upstream, for example $M = 2.0$, the choking occurs at approximately $L_{2\max} = 0.3$. Further extending the tube length causes a formation of a normal shock wave upstream and at the exit of the tube, where the flow reaches $M_2 = 1$. The mass flow rate does not change for a tube greater than $L_{2\max}$. The position of the shock is that subsonic flow behind the shock accelerates to sonic condition $M_2 = 1$ at the exit.

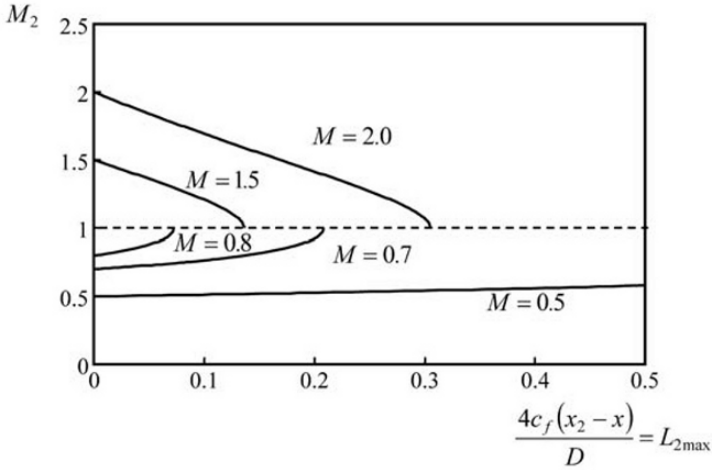


Fig. 5.17 Variation of Mach number

Similarly the integration of Eqs. (11) to (15) yields the following relationships

$$\frac{u}{u^*} = M \left\{ \frac{k+1}{(k-1)M^2 + 2} \right\}^{\frac{1}{2}} = \frac{\rho^*}{\rho} \quad (18)$$

$$\frac{T}{T^*} = \frac{k+1}{(k-1)M^2 + 2} = \left(\frac{a}{a^*} \right)^2 \quad (19)$$

$$\frac{p}{p^*} = \frac{1}{M} \left\{ \frac{k+1}{(k-1)M^2 + 2} \right\}^{\frac{1}{2}} \quad (20)$$

$$\frac{s^* - s}{R} = \ln \frac{1}{M} \left\{ \frac{(k-1)M^2 + 2}{k+1} \right\}^{\frac{k+1}{2(k-1)}} \quad (21)$$

and writing Eq. (21) by T/T^* using Eq. (19), we have

$$\frac{s - s^*}{R} = \ln \left[\left(\frac{T}{T^*} \right)^{\frac{1}{k-1}} \left\{ \frac{(k+1) - 2(T/T^*)}{k-1} \right\}^{\frac{1}{2}} \right] \quad (22)$$

As an alternative of Eq. (22), T/T^* can be replaced by the enthalpy, using the relationship $h/h^* = c_p T/c_p T^* = T/T^*$. This resultant expression gives the equivalent form of Eq. (5.3.6)

Exercise 5.3 Rayleigh-line Flow Relations and Chocking

Consider a flow of an ideal gas in a horizontal tube in a constant cross section. The flow in the tube is assumed to be frictionless, but there is heat transfer between the tube wall and the fluid. Such a flow is called the Rayleigh-line flow. Derive the Rayleigh-line flow relationships and discuss the possibility of chocking condition.

Ans.

As schematically indicated in Fig. 5.18, we will apply the mass continuity, the momentum and the energy equations, denoting that δq is the heat transfer to the control volume.

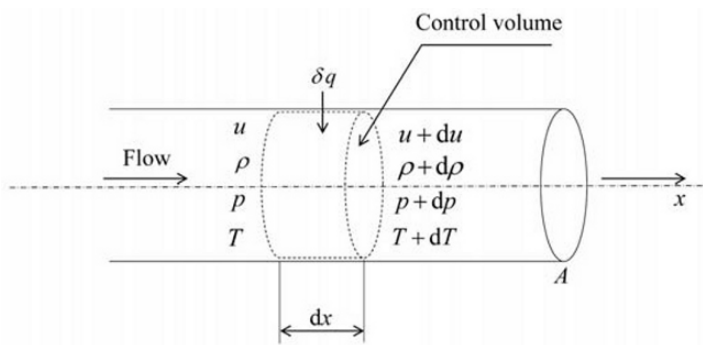


Fig. 5.18 Rayleigh-line flow, δq the heat transfer

(i) Mass continuity equation

$$\frac{d\rho}{\rho} + \frac{du}{u} = 0 \quad (1)$$

where the cross-section area A is constant.

(ii) Momentum equation

$$\frac{du}{u} + \frac{1}{kM^2} \frac{dp}{p} = 0 \quad (2)$$

Denote that τ_w in Eq. (3) in Exercise 5.2 is set at zero, and letting $a^2 = kp/\rho$.

(iii) Energy equation

For an open system at a steady state, the energy balance equation of the control volume can be written as

$$\delta q = de + d(pv) + u \times du + dL_t \quad (3)$$

where de is the increase of internal energy, $d(pv) = d(p/\rho)$ is the increase of flow work, udu is the increment of kinetic energy, and dL_t is the work transfer (including work done due to a frictional effect). Defining enthalpy $h = e + pv$ and recognizing $h = c_p T$ for an ideal gas, we can reduce Eq. (3) for a frictionless flow under a condition of no work transfer, i.e. $dL_t = 0$, as follows

$$\begin{aligned} \delta q &= dh + udu \\ &= c_p dT + udu \end{aligned} \quad (4)$$

Both side of Eq. (4) is divided by $c_p T$, and by defining the stagnation enthalpy $h_0 = c_p T_0$, we have (similar to Eq. (7) in Exercise 5.2)

$$\frac{\delta q}{h} = \frac{dT}{T} + (k-1)M^2 \frac{du}{u} = \frac{dT_0}{T} = \frac{dh_0}{h} \quad (5)$$

(iv) The entropy change and Mach number.

From the definition of entropy for a reversible process, it follows that

$$\frac{ds}{R} = \frac{\delta q}{RT} \quad (6)$$

The increase of a Mach number is written, according to Eq. (10) in Exercise 5.2, as

$$\frac{dM}{M} = \frac{du}{u} - \frac{1}{2} \frac{dT}{T} \quad (7)$$

Along the similar manner to derive the Fanno-line flow relationships, we can now derive the Rayleigh-line flow relationships in terms of the Mach number as written below

$$\frac{du}{u} = \frac{2}{M} \left(\frac{1}{1 + kM^2} \right) dM = - \frac{d\rho}{\rho} \quad (8)$$

$$\frac{dT}{T} = \frac{1}{M} \left\{ \frac{2(1 - kM^2)}{1 + kM^2} \right\} dM \quad (9)$$

$$\frac{dp}{p} = 2M \left(\frac{-k}{1 + kM^2} \right) dM = \frac{kM^2}{M^2 - 1} \frac{\delta q}{h} \quad (10)$$

The entropy change is also derived from Eq. (6), to give

$$\frac{ds}{R} = \frac{1}{M} \left[\left(\frac{k}{k-1} \right) \left\{ \frac{2(1 - M^2)}{1 + kM^2} \right\} \right] dM \quad (11)$$

and, the change of the total temperature dT_0 in Eq. (5) is derived from

$$\frac{dT_0}{T} = \frac{2}{M} \left(\frac{1 - kM^2}{1 + kM^2} \right) dM \quad (12)$$

Equations (8) to (12) give the change of properties, u , ρ , T , s , M and T_0 for a state of a Mach number, to which in Table 5.2 the summarized results are listed in a case of heating, $\delta q > 0$. It should be kept in mind that in the case of cooling, $\delta q < 0$, the trends in Table 5.2 are opposite. From Table 5.2, we see that the heating of an ideal gas flow causes the fluid to tend toward $M = 1$ for both initially subsonic and supersonic conditions. Therefore, if a tube is heated to transfer heat to an ideal gas, the flow is choked; likewise in the Fanno-line flow (in the case of frictional effect). This phenomenon is sometimes called thermal choking.

Table 5.2 Change of property in Rayleigh-line flow ($\delta q > 0$)

Property	Subsonic flow $M < 1$	Supersonic flow $M > 1$
s	\rightarrow	\rightarrow
M	\rightarrow	\rightarrow
u	\rightarrow	\rightarrow
ρ	\rightarrow	\rightarrow
T	$M < 1/\sqrt{k} \rightarrow$	\rightarrow
	$M > 1/\sqrt{k} \rightarrow$	
p	\rightarrow	\rightarrow
T_0	\rightarrow	\rightarrow

In order to verify thermal choking, we will consider the total temperature ratio T_0/T_0^* . It is readily confirmed that T_0/T_0^* can be directly obtained by integrating Eq. (12) from an arbitrary point to $M = 1$, yielding

$$\frac{T}{T^*} = \left\{ \frac{(1+k)M}{1+kM^2} \right\}^2 = \left(\frac{a}{a^*} \right)^2 \quad (13)$$

and using Eq. (5.4.7) together with following two relations for $M = 1$

$$\frac{T_0}{T} = 1 + \frac{k-1}{2} M^2 \quad (14)$$

$$\frac{T^*}{T_0^*} = \frac{2}{k+1} \quad (15)$$

By eliminating T and T^* from Eqs. (13), (14) and (15), we have

$$\frac{T_0}{T_0^*} = \frac{M^2(1+k)\{2 + (k-1)M^2\}}{(1+kM^2)^2} \quad (16)$$

Now consider a case with reference to Fig. 5.19, where a section of a tube is heated by q (heat transfer to the flow), as is written below

$$q = c_p(T_{02} - T_{01}) \quad (17)$$

where T_{01} and T_{02} are the temperatures at the points where 1 and 2 are along the tube respectively. It will be convenient to write Eq. (17) as

$$\frac{T_{02}}{T_{01}} = 1 + \frac{q}{c_p T_{01}} \quad (18)$$

Thus, as a result, the temperature rises due to heating, as written as Eq. (18) and now it is desired as an expression in terms of the Mach numbers at point (1) and point (2), which is given as

$$\frac{T_{02}}{T_{01}} = \left(\frac{T_{02}}{T_0^*} \right) \left(\frac{T_0^*}{T_{01}} \right) = \left(\frac{M_2}{M_1} \right)^2 \left(\frac{1 + kM_1^2}{1 + kM_2^2} \right) \left\{ \frac{2 + (k-1)M_2^2}{2 + (k-1)M_1^2} \right\} \quad (19)$$

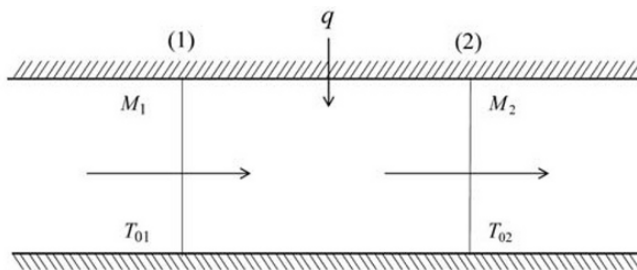


Fig. 5.19 Chocking by heating in Rayleigh-line flow

In order to characterize the system, Fig. 5.20 is a plot for T_{02}/T_{01} of Eq. (19) versus M_2 , while keeping M_1 constant. As seen in the diagram, when a flow at point (1) is subsonic $M < 1$ and the total temperature of T_{01} , the total temperature T_{02} at point (2) rises due to heating (according to Eq. (18)), for example (1)→(2) in $M_1 = 0.5$ as indicated in Fig. 5.20, following the simultaneous rise of the Mach number of M_2 . Then, at $M_2 = 1$, T_{02}/T_{01} reaches its maximum for a given M_1 and T_{01} , where the Rayleigh-line flow becomes sonic, and the flow is said to be thermally choked.

If the cooling is started from the point (2) to down stream, the total temperature drops and the supersonic flow becomes possible. Further cooling the tube to absolute zero, the Mach number of the flow asymptotically approaches infinity. In contrast, if the section of the tube is further heated, T_{02} rises, for example with reference to Fig. 5.20 (2)→(2)', where we keep the state choked at $M_2 = 1$, since the only maximum Mach number possible at M_2 is $M_2 = 1$. With reference to the state at (2)', the Mach

number at point (1) should be lower, for example, with reference to Fig. 5.20 (1) \rightarrow (1)', when followed by the Rayleigh-line flow, while T_{01} is kept constant. In this situation, the mass flow rate drops, compared to that of the original state.

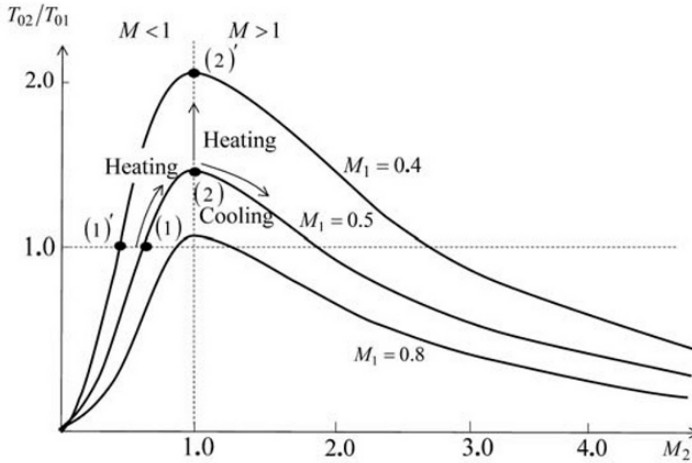


Fig. 5.20 T_{01}/T_{02} , Mach number relation (for $k = 1.4$) in subsonic flow case

In this case, if the Mach number at point (1) is supersonic $M_1 > 1$ and a section of the tube is heated, the Mach number at the exist of a tube, where $T_{02} = T_0^*$, becomes the sonic $M_2 = 1$, leading the flow thermally choked.

Figure 5.21 is a plot of Eq. (16) for air $k = 1.4$. As the section is heated from a total temperature of T_{01} with supersonic flow M_1 at the point (1), the Mach number M along the tube decreases to point (2). If there is a normal shock wave that exists in a section of the tube, the Mach number jumps to a state of (2)', where the Mach number behind the shock wave is subsonic. From (2)', the Mach number again increases toward the exit, where the Mach number is in unity. When the heating is high enough, the shock wave is formed further upstream, i.e. shifting (2) to further high Mach numbers and resulting in (2)' to a further lower Mach number toward the point (1), where the heating is originally started in the section of the tube.

In engineering practice of observing shock wave formation, a higher heating of the section of the tube may shift the shock wave to the throat of a Laval nozzle, in which the shock disappears. As it has been verified, it is

interesting to note that the heating (and cooling) can control the shock wave positions in a tube.

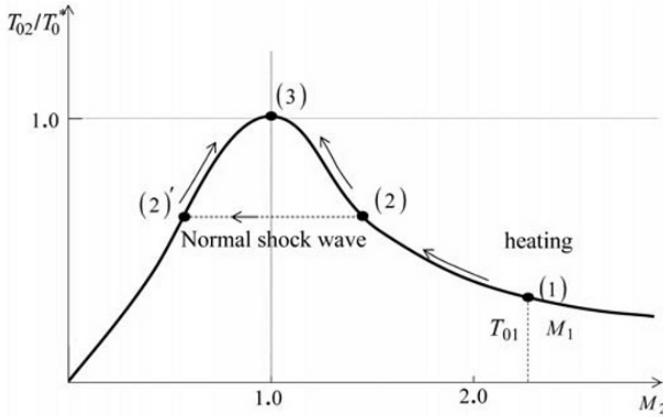


Fig. 5.21 T_{02}/T_0^* , Mach number relation (for air $k = 1.4$) in supersonic flow case

Similar to the Fanno-line flow, the integration of Eqs. (8) to (11) yields the following relations

$$\frac{u}{u^*} = \frac{(1+k)M^2}{1+kM^2} = \frac{\rho^*}{\rho} \quad (20)$$

$$\frac{p}{p^*} = \frac{1+k}{1+kM^2} \quad (21)$$

$$\frac{s-s^*}{R} = \frac{k}{k-1} \ln \left[M^2 \left\{ \frac{1+k}{1+kM^2} \right\}^{\frac{k+1}{k}} \right] \quad (22)$$

$$= \frac{k}{k-1} \ln \left[\left(\frac{T}{T^*} \right)^{\frac{1}{k}} \left\{ \frac{(k+1) \pm \sqrt{(k+1)^2 - 4k(T/T^*)}}{2k} \right\}^{\frac{k-1}{k}} \right] \quad (23)$$

It is noted that as an alternative of Eq. (23), T/T^* can be also replaced by the enthalpy, using the relation $h/h^* = c_p T / c_p T^* = T/T^*$, and the resultant expression gives the equivalent form of Eq. (5.3.19).

Problems

- 5-1. A model wing is placed in a uniform air flow of pressure $p_1 = 0.45 \times 10^5 \text{ N/m}^2$ and the temperature is $T_1 = 253\text{K}$. When a measurement of pressure and the Mach number on a wing was carried out, they were, respectively, $p_2 = 0.35 \times 10^5 \text{ N/m}^2$ and $M_2 = 0.75$. Obtain the speed and the Mach number of the uniform air flow, assuming that the flow is isentropic.

Ans. [$u_1 = 134 \text{ m/s}$ and $M_1 = 0.42$]

- 5-2. A supersonic plane traveling at a speed with a Mach number of 2.25 passes 12000 m above an observer. Determine how far does the plane travel from the point beyond the observer, when the acoustic disturbance of the plane was first heard. Assume the speed of sound to be 330 m/s, and that it is independent of the altitude.

Ans. [24174 m after $\Delta t = 32.5 \text{ s}$]

- 5-3. A compressed gas of a specific heat ratio k is discharged in the atmospheric pressure $p_2 = p_a$ through the Borda's mouth piece of a cross-section area A_1 from a large reservoir tank, where the pressure is kept p_0 , as schematically displayed in Fig. 5.22. If the area of the vena contracta is A_2 and the Mach number is M_2 at the vena contracta, prove that the contraction coefficient $C_c = A_2/A_1$, is given by the following formula

$$C_c = \left(\frac{p_0}{p_2} - 1 \right) / k M_2^2 \quad (1)$$

and for isentropic flow also prove this is written as

$$C_c = \frac{1}{k M_2^2} \left\{ \left(1 + \frac{k-1}{2} M_2^2 \right)^{\frac{1}{k-1}} - 1 \right\} \quad (2)$$

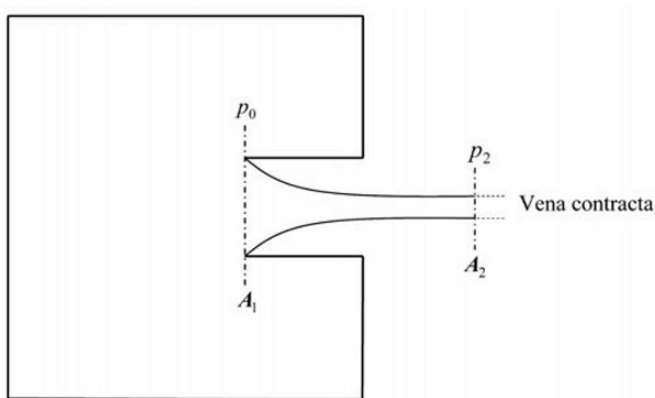


Fig. 5.22 Flow through Borda's mouth piece

5-4. An incompressible gas of the specific heat ratio k is passing through a sudden expansion as shown in Fig. 5.23. The flow is subsonic and the conditions at (1) and (2) are respectively

(1) $A_1, p_1, \rho_1, u_1, M_1$

(2) $A_2, p_2, \rho_2, u_2, M_2$

show that

$$p_2 - p_1 = \rho_2 u_2 (u_1 - u_2)$$

$$\frac{p_2}{p_1} = \frac{1 + k M_1^2 (A_1 / A_2)}{1 + k M^2}$$

where the flow is assumed to be adiabatic.

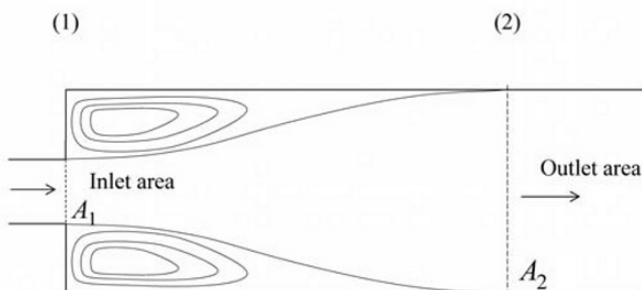


Fig. 5.23 Gas flow through sudden expansion

- 5-5. Air at a pressure of $p_1 = 2.15 \times 10^5 \text{ N/m}^2$, a temperature of $T_1 = 303 \text{ K}$ and a Mach number of $M_1 = 0.25$ is discharged to the atmosphere $p_a = 1.013 \times 10^5 \text{ N/m}^2$ through a convergent nozzle whose throat area is $A_e = 5.0 \times 10^{-3} \text{ m}^2$. Calculate the exit pressure p_e and the mass flow rate \dot{m} , describing the exit condition.

$$\text{Ans. } \left[\begin{array}{l} \text{choking at exist and} \\ p_e = 1.19 \times 10^5 \text{ N/m}^2, \dot{m}^* = \dot{m} = 2.59 \text{ kg/s} \end{array} \right]$$

- 5-6. A normal traveling shock wave passes through stagnant air with a speed of 680 m/s . In the stagnant air, the static temperature is 15°C and static pressure is $0.75 \times 10^5 \text{ N/m}^2$. Obtain pressure p_2 and temperature T_2 down stream of the shock wave.

$$\text{Ans. } [M_1 = 2.0, p_2 = 3.37 \times 10^5 \text{ N/m}^2, T_2 = 213^\circ\text{C}]$$

- 5-7. A stream of air $k = 1.4$ is flowing through a converging-diverging nozzle as shown in Fig. 5.24. At a position (1), the cross-section area is $A_1 = 1.0 \times 10^{-2} \text{ m}^2$, the static pressure is $p_1 = 0.75 \times 10^5 \text{ N/m}^2$ and the Mach number is $M_1 = 0.45$. The cross-section area at position (2) is $A_2 = 1.5 \times 10^{-2} \text{ m}^2$. The flow is assumed to be isentropic between position (1) to (2). Answer the following questions:

(i) Calculate the Mach number M_2 and the static pressure p_2 at the position (2).

(ii) At a position x , where the cross-section area A_x is given to be $A_x = 1.15 \times 10^{-2} \text{ m}^2$, a normal shock wave was found. Determine M_2, p_2 , at position (2).

$$\text{Ans. } \left[\begin{array}{l} \text{(i) } M_2 = 0.28, p_2 = 0.816 \times 10^5 \text{ N/m}^2 \\ \text{or } M_2 = 2.29, p_2 = 0.070 \times 10^5 \text{ N/m}^2 \\ \text{(ii) } M_2 = 0.40, p_2 = 0.56 \times 10^5 \text{ N/m}^2 \end{array} \right]$$

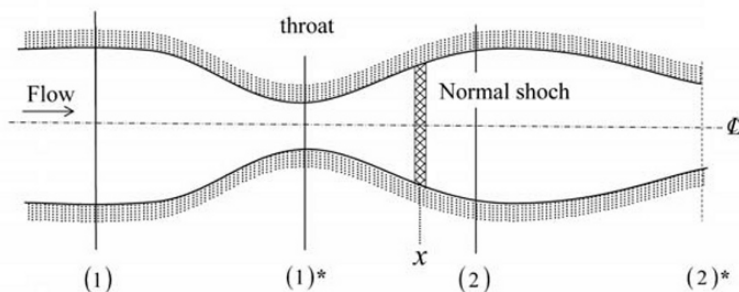


Fig. 5.24 A flow through a converging diverging nozzle

- 5-8. An oblique shock wave was observed at a slender wedge, referring to Fig. 5.10 of semi-vertex angle $\theta = 10^\circ$. The shock was reflected at an angle of $\beta = 30^\circ$ in the original flow direction. Estimate the Mach number of the air flow.

Ans. $[M_1 = 2.68]$

- 5-9. Air flows in a 0.02 m diameter pipe with a pressure of $p_1 = 2.5 \times 10^5 \text{ N/m}^2$, a temperature of $T_1 = 310 \text{ K}$ and a Mach number of $M_1 = 0.24$ at position (1) of $x = x_1$, and leaves from exit position (2) of $x = x_2$. As shown in Fig. 5.25, the length l between position (1) and position (2) is $l = 10.3 \text{ m}$. The flow is assumed to be adiabatic and the friction coefficient c_f is 0.0036 along the pipe.

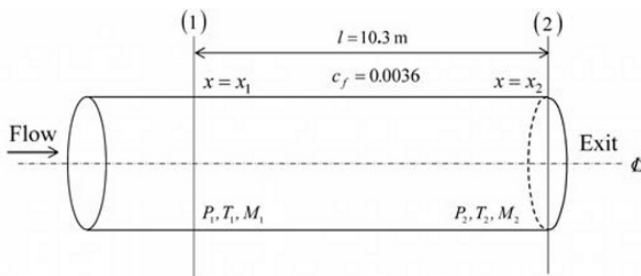


Fig. 5.25 Flow with friction in a pipe, Fanno-line flow

- (i) Determine the mass flow rate \dot{m} , the pressure p_2 , the temperature T_2 , the velocity u_2 at the exit of position (2). Also obtain the total temperature T_0 and the total pressure loss $p_{01} - p_{02}$ between position (1) and position (2).
- (ii) Calculate the mass flow rate \dot{m} at the choking condition, when the mass flow is increased, keeping the total temperature T_0 and the exit pressure p_2 constant.

$$\text{Ans. } \left[\begin{array}{l} \text{(i) } \dot{m} = 0.0748 \text{ kg/s}, p_2 = 1.41 \times 10^5 \text{ N/m}^2, \\ T_2 = 303 \text{ K and } u_2 = 147 \text{ m/s} \\ p_{01} - p_{02} = 1.15 \times 10^5 \text{ N/m}^2, T_{01} = 314 \text{ K} \\ \text{(ii) For choking condition,} \\ \dot{m} = 0.192 \text{ kg/s} \end{array} \right]$$

- 5-10. Consider the airflow without friction ($k = 1.4$ and $R = 267.1 \text{ J/kg} \cdot \text{K}$) in a pipe ($A = 7.5 \times 10^{-3} \text{ m}^2$) heated through the pipe wall between position (1) and position (2) as shown in Fig. 5.26. The heat transfer q to the unit mass of flow in the section of the pipe is $q = 2037 \text{ kJ/kg}$. The total temperature of air is $T_0 = 500 \text{ K}$ and the velocity $u_1 = 89.7 \text{ m/s}$ at position (1) is discharged into the atmospheric pressure $p_2 = p_a = 1 \times 10^5 \text{ N/m}^2$ at the exit position (2). Calculate the pressure p_1 and the total pressure p_0 at position (1) and the velocity u_2 and the temperature T_2 at the exit of position (2). Also determine the mass flow rate \dot{m} discharged to the atmosphere and the total pressure loss $p_{01} - p_{02}$.

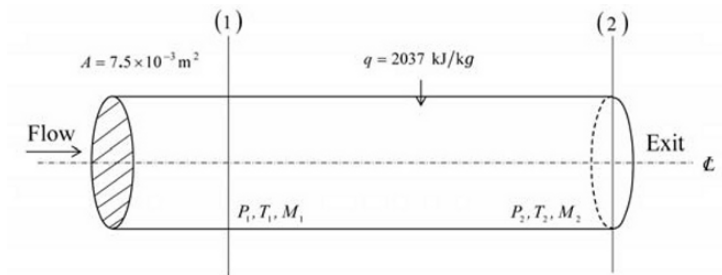


Fig. 5.26 Flow with heat transfer in a pipe, Rayleigh-line flow

$$\text{Ans. } \left[\begin{array}{l} p_1 = 1.53 \times 10^5 \text{ N/m}^2, p_{01} = 1.57 \times 10^5 \text{ N/m}^2, \\ u_2 = 641 \text{ m/s}, T_2 = 2324 \text{ K}, \dot{m} = 0.72 \text{ kg/s} \\ \text{and } p_{01} - p_{02} = 0.228 \times 10^5 \text{ N/m}^2 \end{array} \right]$$

Nomenclature

A	cross-section area of channel
A_t	area of throat
a	speed of sound
C_c	contraction coefficient
c_f	friction factor (coefficient)
c_p	specific heat at constant pressure
c_v	specific heat at constant volume
d_c	compressibility tensor
e	internal energy
f	impulse (or thrust) function
G	mass flux
h	enthalpy
K	bulk modulus
k	specific heat ratio c_p/c_v
L, ℓ	length of channel (section)
L_t	work transfer
M	Mach number
\dot{m}	mass flow rate
P	pressure
p_a	atmospheric pressure
q	heat transfer rate
R	ideal (specific) gas constant
s	entropy
T	absolute temperature
t	time
u	velocity
x, y, z	Cartesian coordinates system
α	Mach angle
α_c	compressibility factor
β	shock inclination angle
ε	surface roughness (RMS)

θ	semi-vertex angle (wedge angle)
τ_w	wall shear stress
ν	kinematic viscosity $1/\rho$
ρ	density
Superscripts	
*	critical properties
Subscripts	
0	stagnation properties
i	$i \equiv$ designated number or symbols, points along flow channel

Bibliography

The most fundamental treatment of gas dynamics is given in the classical texts:

1. H.W. Liepmann and A. Roshko, *Elements of Gasdynamics*, John Wiley, 2 Sons, Inc., Hoboken, NJ, 1957.
2. L.D. Landau and E.M. Lifshitz, *Fluid Mechanics* (2nd Edition), (Translation) Butterworth and Heinemann, Woburn, MA, 1987.

Some fundamental aspects of steady compressible flows with working examples are given in

3. D.N. Roy, *Applied Fluid Mechanics*, Ellis Horwood Limited, 1988.
4. W.F. Hughes and J.A. Brighton, *Theory and Problems of Fluid Dynamics*, McGraw-Hill Book Company, New York, 1967.
5. E. Krause, *Fluid Mechanics*, Springer, New York, 2005.

Inviscid compressible flow problems are treated in view of Computational Fluid Mechanics (CFD) by

6. T. Cebeci, J.P. Shao, F. Kafyeke and E. Laurendeau, *Computational Fluid Dynamics for Engineers*, Springer, New York, 2005.

Advanced treatments in compressible fluids are found in

7. D.D. Joseph, *Fluid Dynamics of Viscoelastic Liquids*, Springer-Verlag, New York, 1990.
8. E. Feireisl, *Dynamics of Viscous Compressible Fluids*, Oxford University Press, Oxford, 2004.

6. Newtonian Flow

The system of conservation equations in continuum mechanics, as discussed in Chapter 2, is valid for any fluid motion. In dealing with flow problems in engineering the type of fluid used, as encountered in various problems, determines flows characteristics and their associated phenomena. The first step to tackle these problems is to know the type of fluid in the system and then to set up governing equations of flows to be solved or to applied. Fluids of the most commonly encountered in fluid engineering are water and air, and also, include structurally simple fluids with low molecular weight, are found to obey “Newton’s law of viscosity”. Such fluids are referred to as Newtonian fluids. The Newton’s law of viscosity states that the shearing force (per unit area) τ_{yx} is proportional to the shear rates (the rate of shear strain) $\partial u/\partial y$, and that they may be expressed as follows

$$\tau_{yx} = \eta_0 \frac{\partial u}{\partial y} \quad (6.1)$$

or alternatively in our tensor index notation in Cartesian coordinates

$$\tau_{21} = \eta_0 \frac{\partial u_1}{\partial x_2} \quad (6.2)$$

The proportionality in Eq. (6.1) or Eq. (6.2) is regarded as a property of the fluid, and is defined as the viscosity. It is often convenient to use the kinematic viscosity ν , which is given as

$$\nu = \frac{\eta_0}{\rho} \quad (6.3)$$

instead of η_0 . Fortunately, the Newtonian model can be applied to many actual fluids in engineering problems. The surface forces due to pressure and stresses are derived from the microscopic momentum flux across a surface from the molecular point of view. The shear stress τ_{yx} is a part of the momentum flux tensor, or simply the stress tensor, which is the molecular rate of transport of momentum. An equation that assigns a value to

the stress tensor is called a “constitutive equation”. Equation (6.1) or Eq. (6.2) are the constitutive equations of a Newtonian fluid in its most simple presentation. The constitutive equation of the Newtonian fluid is associated with the viscosity of the fluid and the rate of shear strain. More specifically, the Newtonian fluid that is at the shear stress is lineally proportional to the rate of shear strain with a proportionally called the viscosity.

The most appropriate generalization of the constitutive equation of the Newtonian fluid is derived from a linear Stokesian fluid, and that is presented by

$$\mathbf{T} = -(p - \lambda_0 \nabla \cdot \mathbf{u})\mathbf{I} + 2\eta_0 \mathbf{e} \quad (6.4)$$

where λ_0 is the constant, called the second viscosity coefficient, and \mathbf{e} is the rate of strain tensor with reference to Eq. (1.1.16). Note that for a linear Stokesian fluid λ_0 is associated only with a volume expansion and it is customarily called the bulk viscosity coefficient. The stress tensor of a Newtonian fluid is symmetric and obtained under an assumption of the general isotropic tensor for the stress components being dependent upon the rates of a strain tensor, as given in Eq. (6.4). The constants λ_0 and η_0 can be related, considering an incompressible limit, where the pressure is the mean of the principal stress with reference to Eq. (1.6.15), where

$$\frac{1}{3} T_{ii} = -p + \left(\lambda_0 + \frac{2}{3} \eta_0 \right) \frac{\partial u_i}{\partial x_i} \quad (6.5)$$

It is reassuring that in the incompressible limit, i.e. $\nabla \cdot \mathbf{u} = 0$, p is the thermodynamic pressure at the equilibrium. If we take $-\bar{p}$ as the mean of the principal stress (the physical or mechanical pressure), we can write

$$\bar{p} - p = - \left(\lambda_0 + \frac{2}{3} \eta_0 \right) \nabla \cdot \mathbf{u} \quad (6.6)$$

and

$$\bar{p} - p = \left(\lambda_0 + \frac{2}{3} \eta_0 \right) \frac{1}{\rho} \frac{D\rho}{Dt} \quad (6.7)$$

Furthermore, we may be able to choose a constant of the proportionality of Eq. (6.7) as

$$\kappa_d = \lambda_0 + \frac{2}{3} \eta_0 \quad (6.8)$$

so that $\lambda_0 = \kappa_d - (2/3)\eta_0$, where κ_d is referred to as the dilatational viscosity, through which there is an additional transport property in generalizing Newton's law of viscosity. κ_d is identically zero for ideal, monatomic gases, while it is not true for polyatomic gases or liquids. The dilatational viscosity is the fluid property, which relates to the degree of departure of the physical pressure from its thermodynamic pressure. However, unless there are extreme cases of the rate of expansion, we may be able to disregard the inclusion of dilatational viscosity κ_d in the constitutive relation of Eq. (6.4). For incompressible liquids, i.e. $\nabla \cdot \mathbf{u} = 0$, the term containing κ_d in Eq. (6.4) vanishes and consequently for motions of fluid it becomes unimportant.

As an alternative, the constitutive equation for the Newtonian fluid can be written, using the dilatational viscosity κ_d , as

$$\mathbf{T} = -\left\{ p - \left(\kappa_d - \frac{2}{3}\eta_0 \right) \nabla \cdot \mathbf{u} \right\} \mathbf{I} + 2\eta_0 \mathbf{e} \quad (6.9)$$

and equivalently with the tensor index notation in Cartesian coordinates, we can write

$$T_{ij} = -\left\{ p - \left(\kappa_d - \frac{2}{3}\eta_0 \right) \frac{\partial u_k}{\partial x_k} \right\} \delta_{ij} + 2\eta_0 e_{ij} \quad (6.10)$$

As another part of correspondence, it is important to know that an argument on κ_d is a controversial subject. Namely, if we follow Stokes' hypothesis, we may simply set $\lambda_0 + (2/3)\eta_0$ equal to zero, assuming that the pressure p can be identified with a mean stress $-(1/3)T_{ii}$, i.e. the procedure is the equivalent of $\kappa_d = 0$, so that we can write Eq. (6.10) to give

$$T_{ij} = -\left\{ p + \frac{2}{3}\eta_0 \frac{\partial u_k}{\partial x_k} \right\} \delta_{ij} + 2\eta_0 e_{ij} \quad (6.11)$$

Determination of λ_0 is, however, still controversial. The second type of treatment for λ_0 is simply to ignore the $\lambda_0 \nabla \cdot \mathbf{u}$ term identically, since the $\lambda_0 \nabla \cdot \mathbf{u}$ term is found in many, very small situations. However, in dealing with a shock wave or sound absorption, the argument for λ_0 must be included. Nevertheless, in the limit of an incompressible fluid, the constitutive equation is given, knowing that

$$\nabla \cdot \mathbf{u} = 0, \text{ by } T_{ij} = -p\delta_{ij} + 2\eta_0 e_{ij} \quad (6.12)$$

The viscosity of Newtonian fluids is a function of temperature, and is generally of a concentration and a pressure. However, with moderate operating conditions, i.e. room temperature range, the viscosity of Newtonian fluids is only a function of temperature. The typical physical properties, including the viscosity, are tabulated in Appendix A. Unless otherwise mentioned, the viscosity in the text will be treated as constant, i.e. conventionally notating $\eta = \eta_0$ in Newtonian fluids.

It will be useful to know that the viscosity of low density nonpolar gases may be given by Maxwell's molecular dynamics treatment as

$$\eta_0 = \frac{2}{3d^2} \sqrt{\frac{mk_B T}{\pi^3}} \quad (6.13)$$

where m is a mass of the molecular, d the diameter of the molecular, T the temperature and k_B the Boltzmann constant.

6.1 Navier-Stokes Equation

Cauchy's equation of motion given in Eq. (2.2.6) holds for any continuum, whatever the stress \mathbf{T} , and has constitutive relationships. When we consider Newtonian fluids and adapt the Stokes hypothesis, the constitutive equation Eq. (6.4) that can be substituted into Eq. (2.2.4), i.e. where the conservation form of the linear momentum, so that we have

$$\frac{\partial \rho u_i}{\partial t} + \frac{\partial (\rho u_j u_i)}{\partial x_j} = -\frac{\partial}{\partial x_j} \left(p\delta_{ij} - \lambda_0 \frac{\partial u_k}{\partial x_k} \delta_{ij} \right) + \frac{\partial}{\partial x_j} (2\eta_0 e_{ij}) + \rho g_i \quad (6.1.1)$$

where e_{ij} is a tensor index notation of the rate of a strain tensor, which is repeatedly written as

$$e_{ij} = \frac{1}{2} \left(\frac{\partial u_i}{\partial x_j} + \frac{\partial u_j}{\partial x_i} \right) \quad (6.1.2)$$

The equation (6.1.1) with Eq. (6.1.2) yields

$$\frac{\partial \rho u_i}{\partial t} + \frac{\partial (\rho u_j u_i)}{\partial x_j} = -\frac{\partial p}{\partial x_i} + (\lambda_0 + \eta_0) \frac{\partial}{\partial x_i} \left(\frac{\partial u_k}{\partial x_k} \right) + \eta_0 \frac{\partial^2 u_i}{\partial x_j^2} + \rho g_i \quad (6.1.3)$$

and as an alternative with a vector notation, we have

$$\frac{\partial \rho \mathbf{u}}{\partial t} + \frac{\partial \rho \mathbf{u} \mathbf{u}}{\partial \mathbf{x}} = -\frac{\partial p}{\partial \mathbf{x}} + (\lambda_0 + \eta_0) \frac{\partial}{\partial \mathbf{x}} \left(\frac{\partial \mathbf{u}}{\partial \mathbf{x}} \right) + \eta_0 \frac{\partial^2 \mathbf{u}}{\partial \mathbf{x}^2} + \rho \mathbf{g} \quad (6.1.4)$$

Equivalently using $\text{grad}(\text{div } \mathbf{u}) = \nabla(\nabla \cdot \mathbf{u})$ and the Laplace of \mathbf{u} as $\nabla^2 \mathbf{u}$, we can write Eq. (6.1.4) as follows

$$\frac{\partial \rho \mathbf{u}}{\partial t} + \nabla(\rho \mathbf{u} \mathbf{u}) = -\nabla p + (\lambda_0 + \eta_0) \nabla(\nabla \cdot \mathbf{u}) + \eta_0 \nabla^2 \mathbf{u} + \rho \mathbf{g} \quad (6.1.5)$$

It is mentioned here that the gravity acceleration \mathbf{g} is introduced here for the body force \mathbf{g} . Equations (6.1.3) or (6.1.4) and (6.1.5) are called the Navier-Stokes equation in honor of C.L.M.H. Navier, and G.G. Stokes, who separately formulated them in 1822 and 1845, respectively. The non-conservation form of this equation can be written, according to Eq. (2.2.7) as

$$\rho \left(\frac{\partial \mathbf{u}}{\partial t} + \mathbf{u} \nabla \mathbf{u} \right) = -\nabla p + (\lambda_0 + \eta_0) \nabla(\nabla \cdot \mathbf{u}) + \eta_0 \nabla^2 \mathbf{u} + \rho \mathbf{g} \quad (6.1.6)$$

For incompressible flow, i.e., $\nabla \cdot \mathbf{u} = 0$, the Eq. (6.1.6) can reduce the form as

$$\rho \left(\frac{\partial \mathbf{u}}{\partial t} + \mathbf{u} \cdot \nabla \mathbf{u} \right) = -\nabla p + \eta_0 \nabla^2 \mathbf{u} + \rho \mathbf{g} \quad (6.1.7)$$

It is reassuring that, if a perfect fluid is considered, Eq. (4.1) is substituted into Eq. (2.2.7) with the same manner, or alternatively by setting $\eta_0 \rightarrow 0$ in Eq. (6.1.7), we can obtain the following equation

$$\rho \left(\frac{\partial \mathbf{u}}{\partial t} + \mathbf{u} \cdot \nabla \mathbf{u} \right) = -\nabla p + \rho \mathbf{g} \quad (6.1.8)$$

This equation (6.1.8) is previously derived and referred to as the Euler equation, which was historically derived prior to Navier-Stokes equation. The Euler equation is valid for inviscid flow in general.

In many flow problems, the Navier-Stokes equation is solved with the equation of continuity Eq. (2.1.5) and the equation of energy conservation Eq. (2.5.23), both of which give appropriate conditions to reduce the governing equations into the most suitable forms. In the following sections, we will find some typical problems in fluid engineering, and in the problems the most appropriate forms of the governing equations are introduced.

The components of the Navier-Stokes equation are found in the Appendix B, together with the equation of continuity and the equation of energy conservation.

As another point of correspondence, it will be shown that alternative forms of the Navier-Stokes equation of incompressible flow can be considered, taking into account the secondary flow field variables, such as the vorticity vector, for certain problems when pressure and the gravity conditions are not defined explicitly in the boundary conditions. In such a flow system, conservation equation of the vorticity can be obtained by taking the rotation of the linear momentum equation and substituting the deviatoric stress of Newtonian fluids into the vorticity transport equation (2.2.9) with the following procedure

$$\boldsymbol{\tau} = 2\eta_0 \mathbf{e} \quad (6.1.9)$$

$$\rho \frac{\partial \boldsymbol{\omega}}{\partial t} + \rho \mathbf{u} \cdot \nabla \boldsymbol{\omega} - \rho \boldsymbol{\omega} \cdot \nabla \mathbf{u} = \nabla \times (\nabla \cdot \boldsymbol{\tau}) \quad (6.1.10)$$

and resultantly we have

$$\rho \frac{\partial \boldsymbol{\omega}}{\partial t} + \rho \mathbf{u} \cdot \nabla \boldsymbol{\omega} = \rho \boldsymbol{\omega} \cdot \nabla \mathbf{u} + \eta_0 \nabla^2 \boldsymbol{\omega} \quad (6.1.11)$$

The first term appeared in the right hand side of Eq. (6.1.11) can be further reduced to

$$\begin{aligned} \boldsymbol{\omega} \cdot \nabla \mathbf{u} &= \frac{1}{2} \boldsymbol{\omega} \cdot \left\{ (\nabla \mathbf{u} + \nabla \mathbf{u}^T) + (\nabla \mathbf{u} - \nabla \mathbf{u}^T) \right\} \\ &= \boldsymbol{\omega} \cdot (\mathbf{e} + \boldsymbol{\omega}) \\ &= \boldsymbol{\omega} \cdot \mathbf{e} - \boldsymbol{\omega} \times \boldsymbol{\omega} \\ &= \boldsymbol{\omega} \cdot \mathbf{e} \end{aligned} \quad (6.1.12)$$

Therefore, using the relation of Eq. (6.1.12) into Eq. (6.1.11), we obtain the vorticity transport equation of Newtonian fluid for an incompressible flow as

$$\rho \frac{\partial \boldsymbol{\omega}}{\partial t} + \rho \mathbf{u} \cdot \nabla \boldsymbol{\omega} = \rho \boldsymbol{\omega} \cdot \mathbf{e} + \eta_0 \nabla^2 \boldsymbol{\omega} \quad (6.1.13)$$

The left hand side terms imply the time change and convection of vorticity respectively. The right hand side terms represent vorticity amplification

due to the local rate of strain \mathbf{e} and diffusion of vorticity with the viscosity as a diffusivity coefficient respectively. It is interesting to see that the first term in the right hand side of Eq. (6.1.13) leads to the concept of strain in a vortex line. The vortex line, as mentioned in Section 4.1, is a line that is instantaneously formed, joining every point aligned with $\boldsymbol{\omega}$; the stream line is similarly aligned with \mathbf{u} . The vortex lines are either extended or contracted, depending on $\boldsymbol{\omega} \cdot \mathbf{e}$. With mass conservation, it is seen that extended vortex lines move closer together, while contracted lines move further apart. A detailed presentation of vorticity dynamics is given in Wu et al. (2006).

Problems

6.1-1 Write the mass continuity, Navier-Stokes, and energy equations of incompressible flow in $x-y$ plane in Cartesian coordinates system.

$$\text{Ans.} \left[\text{Appendix B-6, B-8, and B-9 with } u_z = 0 \text{ and } \frac{\partial}{\partial z} = 0 \right]$$

6.1-2 Write the mass continuity, Navier-Stokes, and energy equations of incompressible flow in $r-z$ plane in cylindrical coordinates systems, assuming that the flow is uni-directional and axisymmetric.

$$\text{Ans.} \left[\text{Appendix B-6, B-8, and B-9 with } u_\theta = 0 \text{ and } \frac{\partial}{\partial \theta} = 0 \right]$$

6.1-3 Write the mass continuity, Navier-Stokes, and energy equation of incompressible flow in $r-\theta$ plane in a spherical coordinates system, assuming the flow is axisymmetric to an axis of rotation through the center.

$$\text{Ans.} \left[\text{Appendix B-6, B-8, and B-9 with } \frac{\partial}{\partial \varphi} = 0 \right]$$

6.1-4 Write the vorticity transport equation of Eq. (6.1.13) in $x-y$ plane in Cartesian coordinates system, assuming that the velocity field is expressed by the stream function and that the only non-zero vorticity component is ω_z

$$\text{Ans.} \left[\begin{array}{l} \frac{\partial \omega_z}{\partial t} + u_x \frac{\partial \omega_z}{\partial x} + u_y \frac{\partial \omega_z}{\partial y} = \nu \left(\frac{\partial^2 \omega_z}{\partial x^2} + \frac{\partial^2 \omega_z}{\partial y^2} \right) \\ u_x = \frac{\partial \psi}{\partial y}, \quad u_y = -\frac{\partial \psi}{\partial x} \end{array} \right]$$

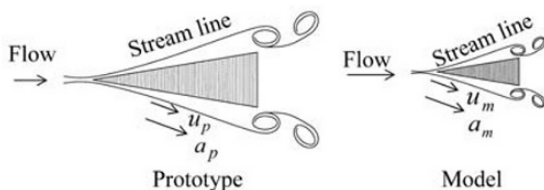
6.2 Similitude and Nondimensionalization

In the design of fluid machineries and systems, before constructing the full-size device or system, called a prototype, we exploit experimental modeling as a fundamental method. With the same idea in the solution of many fundamental fluid mechanics problems, theoretical analysis with a fluid flow approach is valid only for a limited number of simple problems, so that in these circumstances we have to depend on test results obtained from experimental modeling as well. Models, which are usually smaller in size than the prototype, are tested. If necessary, with a different kind of fluid, model experiments are utilized for the prototype from the law of similarity. Similitude is the study of predicting prototype conditions from model experiments.

(a) geometric similarity



(b) kinematic similarity



(c) dynamic similarity (subject to inertial force F_i , pressure force F_p and viscous force F_v)

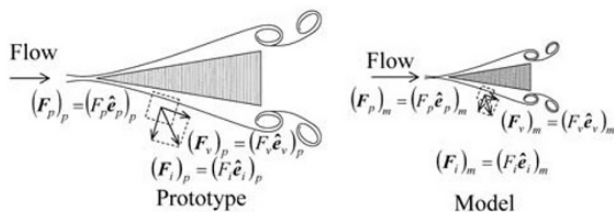


Fig. 6.1 Similitude

Experimental modeling in the design of fluid machineries and systems may be found in developing aircrafts in wind tunnels, fluid machineries and ships in towing tanks, tidal waves in rivers, and so forth. In the similitude there are the similarity conditions to be met in applying test results obtained from models to the prototype. They are (i) the geometric similarity, (ii) the kinematics similarity, (iii) the dynamic similarity and (iv) the thermal similarity in some case. The law of similarity for (i) to (iii) are schematically displayed in Fig. 6.1.

(i) Geometric similarity

The length ratio must be constant between all corresponding points in the flow fields, when the model and the prototype are identical in shape but differ in size. Thus, geometrical similarity requires that a scale model has to have the precise shape of the prototype with the model ratios;

Model ratio

$$l_r = \frac{l_m}{l_p} \quad (6.2.1)$$

Area ratio

$$A_r = \frac{A_m}{A_p} = \frac{l_m^2}{l_p^2} = l_r^2 \quad (6.2.2)$$

Volume ratio

$$V_r = \frac{V_m}{V_p} = \frac{l_m^3}{l_p^3} = l_r^3 \quad (6.2.3)$$

where subscript m and p denote the model and prototype respectively as shown in Fig. 6.1(a). The geometric similarity also requires roughness of objective surface between the model and the prototype. Difference in roughness may differ with the onset of turbulence, resulting in failure of similitude. In some problems, however, roughing the surface of the model may result in holding the geometric similarity. For example, scaling model of large buildings in a city may face the similar problem, depending on the magnitude of scaling, i.e. the model ratio scale effect.

(ii) Kinematic similarity

The velocity ratio must be a constant between all corresponding points in the flow fields for the model and the prototype, where their streamlines are geometrically similar. In satisfying kinematic similarity, velocities and

accelerations are in the same ratio for corresponding control volumes in the flow fields as shown in Fig. 6.1(b);

Velocity ratio

$$u_r = \frac{u_m}{u_p} = \frac{l_m/t_m}{l_p/t_p} = \frac{l_r}{t_r} \quad (6.2.4)$$

Acceleration ratio

$$a_r = \frac{a_m}{a_p} = \frac{u_m^2/l_m}{u_p^2/l_p} = \frac{u_r^2}{l_r} \quad (6.2.5)$$

or

$$a_r = \frac{l_m/t_m^2}{l_p/t_p^2} = \frac{l_r}{t_r^2} \quad (6.2.6)$$

where t_r is the time scale ratio. As seen from Eqs. (6.2.4) to (6.2.6), when the model ratio and the time scale ratio are fixed, the flow will be kinematically similar. The time scale ratio becomes particularly important for unsteady flow, indicating that geometrical similarity is not necessarily kinematically similar to flows. With satisfying both geometric similarity and kinematic similarity, we can write the inertial force ratio as

$$\frac{(F_i)_m}{(F_i)_p} = \frac{a_m m_m}{a_p m_p} = a_r m_r \quad (6.2.7)$$

where m_r is the mass ratio. Equation (6.2.7) shows that the inertial force ratio becomes constant when the acceleration ratio between corresponding points on the model and prototype is assured to be constant, if the mass ratio of corresponding control volume is kept constant.

(iii) Dynamic similarity

The forces acting on corresponding control volume in the model flow and the prototype flow are in the same ratio in the flow fields. Characteristics of the flow fields are governed by the force acting on fluid elements, so that as seen from Eq. (6.2.7), the kinematic similarity is satisfied when geometric and dynamic similarities exist between model and prototype flows.

Suppose that inertial forces F_i , pressure forces F_p , viscous forces F_v , gravity force F_g , surface tension forces F_s and compression forces F_c are present in the flow fields of the model and prototype. From Newton's

second law of dynamics, we can equate the inertial force with its summation if the other forces are

$$\mathbf{F}_i = \mathbf{F}_p + \mathbf{F}_v + \mathbf{F}_g + \mathbf{F}_s + \mathbf{F}_c \quad (6.2.8)$$

When all forces are present, dynamic similarity requires that, at corresponding points in the flow fields, the following quotient relation of the model and prototype should hold

$$\frac{(F_i)_m}{(F_i)_p} = \frac{(F_p)_m}{(F_p)_p} = \frac{(F_v)_m}{(F_v)_p} = \frac{(F_g)_m}{(F_g)_p} = \frac{(F_s)_m}{(F_s)_p} = \frac{(F_c)_m}{(F_c)_p} \quad (6.2.9)$$

These can be rearranged with respect to the inertial force F_i to read

$$\left(\frac{F_i}{F_p} \right)_m = \left(\frac{F_i}{F_p} \right)_p, \quad \frac{F_i}{F_p} \equiv \text{Euler number} \equiv Eu \quad (6.2.10)$$

$$\left(\frac{F_i}{F_v} \right)_m = \left(\frac{F_i}{F_v} \right)_p, \quad \frac{F_i}{F_v} \equiv \text{Reynolds number} \equiv Re \quad (6.2.11)$$

$$\left(\frac{F_i}{F_g} \right)_m = \left(\frac{F_i}{F_g} \right)_p, \quad \frac{F_i}{F_g} \equiv \text{Froude number} \equiv Fr \quad (6.2.12)$$

$$\left(\frac{F_i}{F_s} \right)_m = \left(\frac{F_i}{F_s} \right)_p, \quad \frac{F_i}{F_s} \equiv \text{Weber number} \equiv We \quad (6.2.13)$$

$$\left(\frac{F_i}{F_c} \right)_m = \left(\frac{F_i}{F_c} \right)_p, \quad \frac{F_i}{F_c} \equiv \text{Mach Number} \equiv M \quad (6.2.14)$$

where Eu , Re , Fr , We and M are the nondimensional numbers which appear in characterizing flow fields. According to dynamic similarity expressed in Eqs. (6.2.10) to (6.2.14), Newton's second law given in Eq. (6.2.8) is expressed in terms of these nondimensional numbers as

$$\left(\frac{F_i}{F_i} \right) \hat{\mathbf{e}}_i = \left(\frac{F_p}{F_i} \right) \hat{\mathbf{e}}_p + \left(\frac{F_v}{F_i} \right) \hat{\mathbf{e}}_v + \left(\frac{F_g}{F_i} \right) \hat{\mathbf{e}}_g + \left(\frac{F_s}{F_i} \right) \hat{\mathbf{e}}_s + \left(\frac{F_c}{F_i} \right) \hat{\mathbf{e}}_c \quad (6.2.15)$$

$$\hat{\mathbf{e}}_i = \left(\frac{c_1}{Eu} \right) \hat{\mathbf{e}}_p + \left(\frac{c_2}{Re} \right) \hat{\mathbf{e}}_v + \left(\frac{c_3}{Fr^2} \right) \hat{\mathbf{e}}_g + \left(\frac{c_4}{We} \right) \hat{\mathbf{e}}_s + \left(\frac{c_5}{M^2} \right) \hat{\mathbf{e}}_c \quad (6.2.16)$$

where $\hat{\mathbf{e}}_i \sim \hat{\mathbf{e}}_e$ are unit vectors associated with the forces, as some of them are representatively shown in Fig. 6.1(c), and $c_1 \sim c_5$ are dimensionless constants.

Consequently, to ensure complete dynamic similarity, Eq. (6.2.16) has simultaneously to be applied to both the model and the prototype system, where the nondimensional numbers and their associated constants are kept identical for both systems. For those nondimensional numbers appeared in Eq. (6.2.16), each nondimensional number is defined by taking l as the characteristic length of the system as follows

$$\frac{F_i}{F_p} \propto \frac{\rho l^2 U^2}{p l^2} \propto \frac{U^2}{p/\rho} = Eu \quad (\text{or} = Eu^{-1}) \quad (6.2.17)$$

$$\frac{F_i}{F_v} \propto \frac{\rho l^2 U^2}{\eta_0 U l^2} \propto \frac{U l}{(\eta_0/\rho)} = Re \quad (6.2.18)$$

$$\frac{F_i}{F_g} \propto \frac{\rho l^2 U^2}{\rho l^3 g} \propto \frac{U^2}{l g} = Fr^2 \quad (\text{or} = Fr) \quad (6.2.19)$$

$$\frac{F_i}{F_c} \propto \frac{\rho l^2 U^2}{K_0 l^2} \propto \frac{U^2}{K_0/\rho} = M^2 \quad (6.2.20)$$

$$\frac{F_i}{F_s} \propto \frac{\rho l^2 U^2}{\sigma l} \propto \frac{U^2}{\sigma/\rho l} = We \quad (6.2.21)$$

The idea of deriving Eq. (6.2.16) (the dynamic similarity) comes from the similitude between the model and prototype systems that are completely ensured if the nondimensional numbers and their associated constants in the governing equations are identical with the same boundary conditions (satisfying the geometric and the kinematic similarity). We will see that the nondimensional numbers naturally appear in the governing equations of flow when the equations are nondimensionalized.

It is mentioned here that nondimensionalization of the flow equations should also, besides giving the reason of the similitude of dynamic systems, give two other reasons. The first is that the number of physical parameters desired to solve the flow problem can be reduced drastically. Thus, there will be less work involved in solving the equations for given parameter ranges. This is particularly advantageous in CFD. The second reason is to give a clue to make rational simplification to the flow equations. This is particularly advantageous to gain approximation solutions based on order-of-magnitude arguments in some flow problems.

With the same process the dynamic similarity applied to the momentum equation of Eq. (6.2.8), we are able to obtain the nondimensional

governing equations for Newtonian fluids. For the sake of simplicity, as discussed in the previous section in dealing the second coefficient of viscosity λ_0 , we will ignore the $\lambda_0 \nabla \cdot \mathbf{u}$ term identically, thereafter. The mass continuity equation and the Navier-Stokes equations are written respectively as

$$\frac{\partial \rho}{\partial t} + \nabla \cdot \rho \mathbf{u} = 0 \quad (6.2.22)$$

$$\rho \left(\frac{\partial \mathbf{u}}{\partial t} + \mathbf{u} \cdot \nabla \mathbf{u} \right) = -\nabla p + \eta_0 \nabla^2 \mathbf{u} + \rho \mathbf{g} \quad (6.2.23a)$$

or

$$\rho \frac{D\mathbf{u}}{Dt} = -\nabla p + \eta_0 \nabla^2 \mathbf{u} + \rho \mathbf{g} \quad (6.2.23b)$$

Nondimensionalization of Eqs. (6.2.22) and (6.2.23) is accomplished by dividing both side of the equations by an appropriate combination of characteristic dimensions. Particularly, for the momentum equation, i.e. the Navier-Stokes equation (force per volume) of Eq. (6.2.23), the division is done by the inertial force dimension, thereby making each term dimensionless. By common variables of characteristic dimension, we choose l as a characteristic length, U as characteristic velocity, ρ_0 as characteristic density, p_0 as characteristic pressure and t_0 as characteristic time. We firstly write nondimensional parameters (denoted by asterisk) by scaling quantities with the characteristic dimensions as

$$\begin{aligned} \mathbf{x}^* &= \frac{\mathbf{x}}{l}, \quad t^* = \frac{t}{t_0} \quad (\text{and } t^* = \frac{tU}{l}) \\ \mathbf{u}^* &= \frac{\mathbf{u}}{U}, \quad p^* = \frac{p}{p_0}, \quad \rho^* = \frac{\rho}{\rho_0} \\ \nabla^* &= l \frac{\partial}{\partial x_i} \hat{\mathbf{e}}_i, \quad \nabla^{*2} = l^2 \frac{\partial^2}{\partial x_i^2} \hat{\mathbf{e}}_i \end{aligned} \quad (6.2.24)$$

Thus, by using those nondimensional parameters, Eqs. (6.2.22) and (6.2.23) can be reduced to

$$\left(\frac{U}{l} \rho_0 \right) \left(\frac{\partial \rho^*}{\partial t^*} + \nabla^* \cdot \rho^* \mathbf{u}^* \right) = 0 \quad (6.2.25)$$

$$\begin{aligned} & \rho^* \left\{ \left(\frac{l}{Ut_0} \right) \frac{\partial \mathbf{u}^*}{\partial t^*} + \mathbf{u}^* \cdot \nabla^* \mathbf{u}^* \right\} \\ &= - \left(\frac{p_0}{\rho_0 U^2} \right) \nabla^* p + \left(\frac{\eta_0}{\rho_0 U l} \right) \nabla^{*2} \mathbf{u}^* + \left(\frac{g l}{U^2} \right) \rho^* \hat{\mathbf{e}}_g \end{aligned} \quad (6.2.26)$$

Using notation by Eqs. (6.2.17) to (6.2.21), we can write Eqs. (6.2.25) and (6.2.26), by dropping an asterisk * for brevity's sake, as

$$\frac{\partial \rho}{\partial t} + \nabla \cdot \rho \mathbf{u} = 0 \quad (6.2.27)$$

$$\rho \left(St \frac{\partial \mathbf{u}}{\partial t} + \mathbf{u} \cdot \nabla \mathbf{u} \right) = - \frac{1}{Eu} \nabla p + \frac{1}{Re} \nabla^2 \mathbf{u} + \frac{\rho}{Fr^2} \hat{\mathbf{e}}_g \quad (6.2.28)$$

where $St = l/Ut = \omega l/U$ is identified as the Strouhal number (=centrifugal force/inertial force). Note that for a periodic flow motion (ω as angular velocity), such as vortex shedding (for example, flow past cylinder, flow through turbomachinery, etc.), it is necessary to model the effect of periodicity, which is in effect included with the Strouhal number. With a similar process, the Navier-Stokes equation in non-conservation form may be simply written as, instead of Eq. (6.2.28)

$$\rho \frac{D\mathbf{u}}{Dt} = - \frac{1}{Eu} \nabla p + \frac{1}{Re} \nabla^2 \mathbf{u} + \frac{\rho}{Fr^2} \hat{\mathbf{e}}_g \quad (6.2.29)$$

Equation (6.2.29) is the same formulation defined in Eq. (6.2.16).

There are some variations on the nondimensionalizing Navier-Stokes equation, however, depending upon the systems and how those characteristic parameters are to be chosen.

For example, in natural convection, there is no characteristic velocity defined in fluid flow systems, where flow is driven by a buoyant force due to a small change in density. In such a system, the density can be linearly approximated with respect to the temperature change as

$$\rho \approx \rho_0 \{1 - \beta_T (T - T_0)\} \quad (6.2.30)$$

where β_T is the coefficient of thermal expansion defined by Eq. (2.5.25). The characteristic velocity U can be replaced by $\eta/(\rho_0 l)$. A new non-dimensional number may appear for a natural convection, when the Navier-Stokes equation is appropriately simplified, where the non-dimensional number is given in

$$Gr = \frac{g\beta_T \rho_0^2 l^3 (T - T_0)}{\eta_0^2} = \frac{gl^3 \Delta\rho}{\rho_0 \nu^2} = \text{Grashof number} \quad (6.2.31)$$

The derivation of nondimensionalized Navier-Stokes equation, with a Boussinesq approximation, is given in Exercise 6.2.1.

Up to this point we have dealt with flow problems in which the temperature was assumed constant. However, when the heat and work transfer to the fluid system are to be considered, the energy equation has to be coupled with the momentum and the mass continuity equation. Thermal similarity between the model and the prototype system, or more specifically for a scaled experiment, is treated with the same manner. This is done straightforwardly, by nondimensionalizing the energy equation of Eq. (2.5.24) to give

$$\rho c_p \frac{DT}{Dt} = \nabla \cdot (k_c \nabla T) + \Phi + \beta_T T \frac{Dp}{Dt} \quad (6.2.32)$$

where $\Phi = \boldsymbol{\tau} : \nabla \mathbf{u}$ is the dissipation function and the heat transfer $\mathbf{q} = -k_c \nabla T$ (Fourier's law) is assumed by a conduction, knowing that the internal heat generation term ρb in Eq. (2.5.24) is ignored. Note that k_c is the reference thermal conductivity. Nondimensional parameters (denoted by an asterisk) are defined by scaling quantities with characteristic dimensions as

$$T^* = \frac{T - T_0}{T_w - T_0}, \quad \Phi^* = \frac{l^2}{\eta U^2} \quad (6.2.33)$$

where T_w is the boundary temperature and T_0 the reference temperature. Using quantities in Eqs. (6.2.33) and (6.2.24) that are substituted into Eq. (6.2.32), the final result of the energy equation takes the following form, after dropping the asterisk

$$\frac{DT}{Dt} = \frac{1}{Re \cdot Pr} \nabla^2 T + Ec \frac{Dp}{Dt} + \frac{Ec}{Re} \Phi \quad (6.2.34)$$

Nondimensional numbers appeared in Eq. (6.2.34) other than in Eq. (6.2.29), such as

$$Ec = \frac{U^2}{c_p T_0} = \text{Eckert number} \quad (6.2.35)$$

or alternatively, for an ideal gas (denoting k as the specific heat ratio. i.e.

$$k = c_p / c_v)$$

$$Ec = \frac{U^2}{c_p T_0} = \frac{U^2}{\{kR/(k-1)\}T_0} = (k-1) \frac{U^2}{kRT_0} = (k-1) \frac{U^2}{a_0^2} = (k-1)M^2$$

$$Pr = \frac{\eta_0 c_p}{k_c} = \frac{\nu}{k_\alpha} = \text{Prandtl number} \quad (6.2.36)$$

$$Pe = Re \cdot Pr = \text{Peclet number} \quad (6.2.37)$$

$$Br = Ec \cdot Pr = \text{Brinkman number} \quad (6.2.38)$$

Thus, taking into account new nondimensional numbers in Eq. (6.2.34), the similitude of the two systems, i.e. the model and prototype, can be held when the temperature field is considered.

Solving Eqs. (6.2.27); $\nabla \cdot \mathbf{u} = 0$ for incompressible flow, Eqs. (6.2.28 or 6.2.29) and (6.2.34) with given boundary conditions, would give similarity solutions that represent flow fields of any similar systems simultaneously. It is seen from the nondimensionalized governing equations that choosing the nondimensional numbers controls the flow fields of the systems. Thus, the similarity solutions are the function of the nondimensional numbers, represented as

$$f(Re, Eu, Fr, Ec, Pr) = 0 \quad (6.2.39)$$

where Re , Eu , Fr , Ec and Pr are the nondimensional numbers that appeared in the governing equations discussed above.

In the study of engineering fluid mechanics, there are very few problems that are actually solved using the differential equations discussed above and have the similarity solutions as represented by a form of Eq. (6.2.39). Instead of actually solving the system of differential equations, we may be able to adopt dimensional analysis to predict prototype conditions from model observations that are based on the notion of dimensional homogeneity. With dimensional analysis we can find essential nondimensional numbers, which contributes to similitude with the two systems. The Buckingham π -theorem is a very powerful tool to derive the essential nondimensional numbers. Particularly in experimental studies in fluid mechanics involving the use of scaled models, the π -theorem is effective for correlating experimental results. In Appendix C, the Buckingham π -theorem is demonstrated. The reader may refer to the point that the nondimensional numbers obtained in Eq. (6.2.16) are also straightforwardly derived by the π -theorem.

Exercise

Exercise 6.2.1 The Boussinesq Approximation

There are situations of practical occurrence, where the validity of physical properties in a fluid is due to small variations in temperature. In natural convection applications of fluid under gravity and buoyancy for variations in temperature of only moderate levels, the Navier-Stokes equation may be simplified so as to put buoyancy into evidence. In such a case, we may treat the density as a constant ρ_0 in all terms in the Navier-Stokes equation of incompressible media, except for the one in the buoyancy term due to gravity. This is called the Boussinesq approximation. In the energy equation, the viscous dissipation term Φ can be ignored owing to the fact that the prevailing velocity field is weak. The basic equations in the Boussinesq approximation are written as

$$\nabla \cdot \mathbf{u} = 0 \quad (1)$$

$$\rho_0 \frac{D\mathbf{u}}{Dt} = -\nabla p' + \eta_0 \nabla^2 \mathbf{u} + (\rho - \rho_0)\mathbf{g} \quad (2)$$

$$\rho_0 c_p \frac{DT}{Dt} = k_c \nabla^2 T \quad (3)$$

$$\rho = \rho_0 \{1 - \beta_T (T - T_0)\} \quad (4)$$

and

$$p' = p + \phi_0 \quad (5)$$

where ϕ_0 is the gravitational potential, such as defined by $\phi_0 = -\rho_0 g z$ in Cartesian coordinates system.

Nondimensionalize the equations (1) to (3), using the following non-dimensional parameters

$$\mathbf{u}^* = \frac{\mathbf{u}}{U} = \frac{\mathbf{u}}{\eta_0 / (\rho_0 l)}, \quad t^* = \frac{t}{t_0} = \frac{t}{(\rho_0 l^2) / \eta_0}, \quad p^* = \frac{p'}{\rho_0 U^2} = \frac{p'}{\eta_0^2 / (\rho_0 l^2)}$$

$$T^* = \frac{T - T_0}{T_w - T_0}$$

where U and t_0 are replaced by $U = \eta_0 / (\rho_0 l)$ and $t_0 = (\rho_0 l^2) / \eta_0$ respectively. Also, consider a heat transfer through a boundary with an appropriate nondimensional number.

Ans.

The basic equations are nondimensionalized as

$$\left(\frac{\eta_0}{\rho_0 l^2} \right) \nabla^* \mathbf{u}^* = 0 \quad (6)^*$$

$$\left(\frac{\eta_0^2}{\rho_0 l^3} \right) \left(\frac{D^* \mathbf{u}^*}{D^* t^*} \right) = - \left(\frac{\eta_0^2}{\rho_0 l^3} \right) \nabla^* p^* + \left(\frac{\eta_0^2}{\rho_0 l^3} \right) \nabla^{*2} \mathbf{u}^* - \rho_0 \beta_T (T_w - T_0) T^* g \hat{\mathbf{e}}_g \quad (7)^*$$

$$(T_w - T_0) \left(\frac{c_p \eta_0}{l^2} \right) \frac{D^* T^*}{D^* t^*} = (T_w - T_0) \frac{k_c}{l^2} \nabla^{*2} T^* \quad (8)^*$$

so that, for nondimensional equations after dropping the asterisk

$$\nabla \cdot \mathbf{u} = 0 \quad (9)$$

$$\frac{D\mathbf{u}}{Dt} = -\nabla p + \nabla^2 \mathbf{u} - Gr T^* \hat{\mathbf{e}}_g \quad (10)$$

$$\frac{DT}{Dt} = \frac{1}{Pr} \nabla^2 T \quad (11)$$

At a boundary in natural convection, the heat transferred q_w (heat flux) to the fluid is customarily defined such that q_w is proportional to $\Delta T = T - T_w$ as

$$q_w = h_w \Delta T \quad (12)$$

where h_w is called the heat transfer coefficient. h_w may be non-dimensionalized either by

$$Sn = \frac{q_w}{\rho_0 c_p U (T_w - T_0)} = \frac{h_w}{\rho_0 c_p U} \quad (13)$$

where Sn is called Stanton number, or

$$Nu = \frac{h_w l}{k_c} \quad (14)$$

where Nu is called a Nusselt number. Sn and Nu are related by

$$Nu = SnRePr \quad (15)$$

where Re is defined by the characteristic length l . Thus, from the argument given above for the natural convection, if Nu is chosen as a thermal characteristic parameter, a characteristic in a thermally similar system may be determined where

$$Nu = f(Gr, Pr) \quad (16)$$

For a very simple basic system in natural convection, for example, called the Benard's convection, Nu around the onset of a natural convection from the heat conduction mode is almost a function of $Gr \times Pr$, as show in Fig. 6.2. The data referred in Fig. 6.2 is a case for the Benard's convection, where the lower plate is heated while the upper plate is cooled for fluids contained in an infinite slab. As the experimental results indicate that Nu becomes a function of $Gr \times Pr$, which is defined as a Rayleigh number, i.e. $Ra = Gr \times Pr$, after the onset of a natural convection that is observed after Nu deviates from value of 1 around $Ra \approx 1708$, as seen in Fig. 6.2. The natural convection occurs from a state of equilibrium in heat conduction mode at the critical Rayleigh number Ra_c , where the value of Ra_c in Fig. 6.2 is approximately $Ra_c \approx 1708$, which is also verified by an instability analysis. For a limited range of Ra , it is possible to express the Nusselt number Nu by the relationship

$$Nu = f(Ra) \quad (17)$$

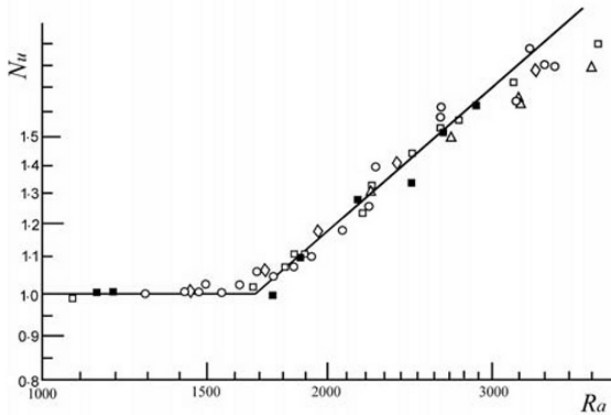


Fig. 6.2 Benard's convection at onset of natural convection
(Replotted after Silveston, 1958)

Problems

6.2-1 Give the definition for each nondimensional number in Eqs. (6.2.10) to (6.2.14); Eu, Re, Fr, We and M in view of the dynamic similarity.

6.2-2 For steady state flows in a horizontal pipe of diameter d and length l with the roughness ε (RMS), the dominant forces will be the driving force (pressure), resisting force (wall shear), and the inertial force. Find the governing nondimensional numbers.

$$Ans. \left[c_p = f \left(Re, \frac{l}{d}, \varepsilon \right) \right]$$

6.2-3 A prototype propeller of a wind power generator of diameter 50 m is to be tested in a wind tunnel using a 1/50 scaled model. If the prototype propeller is to run at 60 rpm, what should be the speed (revolution per minutes) of the model? What is the ratio of prototype torque and model torque? The fluid properties for the prototype and model are the same.

$$Ans. \left[Fr = \frac{n^2 d}{g} = \frac{n_m^2 d_m}{g}, n_m = n \sqrt{\left(\frac{d}{d_m} \right)} = 60\sqrt{50} = 424 \text{ rpm} \right]$$

6.2-4 Assume that the critical Rayleigh number of the natural convection is $Ra_c = 1708$ for an infinite slab. For water as a working fluid, estimate the temperature difference ΔT between the lower hot surface and upper cold surface, when the thickness of the slab is 20 mm. Take a reference temperature at 20°C .

$$Ans. \left[\begin{aligned} Ra_c = Gr \cdot Pr &= \frac{g \beta_f \rho_0^2 l^3 (T - T_0)}{\eta_0^2} \cdot \frac{\nu}{k_\alpha} = \frac{g \beta_f \rho_0 l^3 \Delta T}{\eta_0 k_\alpha} \\ \Delta T &= \frac{Ra_c \eta_0 k_\alpha}{g \beta_f \rho_0 l^3} = 16.1 \text{ K} \end{aligned} \right]$$

6.3 Basic Flows Derived from Navier-Stokes Equation

There are certain cases for viscous flows where the Navier-Stokes equation is rationally simplified so that analytical solutions can be obtained. In the most of the cases that the analytical solutions are available, the nonlinear term (the convective term) in the Navier-Stokes equation is either omitted or linearized in consideration of the types of flow with appropriate assumptions to avoid further intricate problems.

We will see a number of basic flows in which such results are valid within a certain range of Reynolds numbers. In order to gain further engineering significance, some cases are extended to include higher Reynolds numbers, illuminating pure viscous flow phenomena.

6.3.1 Unidirectional Flow in a Gap Space

M. Couette (1880) conducted experiments on the flow between stationary and moving concentric cylinders. Flows in a narrow gap, including parallel plates and concentric cylinders, are treated here.

(i) Flow in parallel plates is considered firstly as one of the simplest geometrical configuration of flow, referred to Fig. 6.3(a). As schematically displayed in the diagram, the flow configuration is such that the length of the gap is h and the upper plate moves with velocities $u = \pm U$, while the lower plate is kept stationary. Assume that flow is unidirectional to x direction, incompressible and steady, neglecting the body force or may be included in p as the gravitational potential as previously described. For example, the conditions are

$$\mathbf{u} \equiv (u_x, u_y, u_z) = (u, 0, 0) \quad (6.3.1)$$

$$\nabla p \equiv \left(\frac{\partial p}{\partial x}, \frac{\partial p}{\partial y}, \frac{\partial p}{\partial z} \right) = \left(\frac{\partial p}{\partial x}, 0, 0 \right) \quad (6.3.2)$$

and

$$u = u(y) \quad (6.3.3)$$

$$\frac{\partial p}{\partial x} = \text{const.} \quad (6.3.4)$$

$$\nabla \cdot \mathbf{u} = 0, \quad \frac{\partial}{\partial t} = 0, \quad \rho \mathbf{g} = 0 \quad (6.3.5)$$

The governing equations of flow in Cartesian coordinates systems are written as

$$\text{Continuity: } \frac{\partial u}{\partial x} = 0 \quad (6.3.6)$$

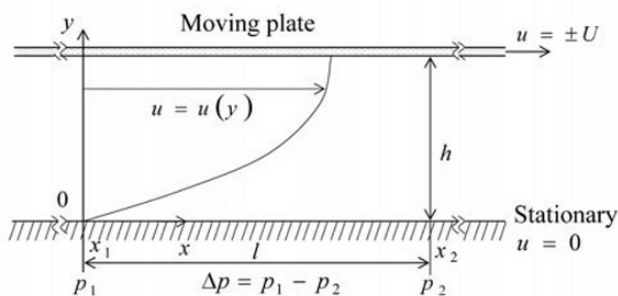
$$\text{N-S equation: } 0 = -\frac{\partial p}{\partial x} + \eta_0 \frac{\partial^2 u}{\partial y^2} \quad (6.3.7)$$

The boundary conditions are such that with reference to Fig. 6.3(a)

$$u = 0 \quad \text{for } y = 0 \quad (6.3.8)$$

$$u = \pm U \quad \text{for } y = h \quad (6.3.9)$$

(a) Flow between parallel plates



(b) Flow between concentric rotating cylinders

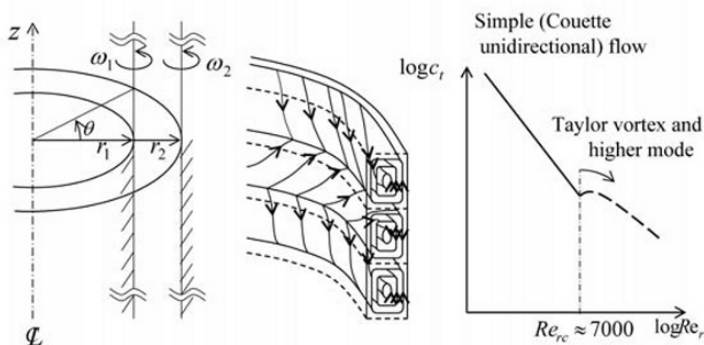


Fig. 6.3 Flows in narrow gap

The solution in Eq. (6.3.6) is $u = \text{Constant}$ for x direction, indicating that the flow is fully developed toward its motion.

Equation (6.3.7) is solved for $u(y)$ with the boundary conditions in Eqs. (6.3.8) and (6.3.9), giving solutions as

$$u = \frac{\Delta p}{2\eta_0 l} (h - y)y \pm \frac{Uy}{h} \quad (6.3.10)$$

where the pressure difference Δp between the points in x -direction x_1 and x_2 are defined by, as in Eq. (6.3.4)

$$\frac{dp}{dx} = c \text{ (constant)} \quad (6.3.11)$$

so that

$$p_2 - p_1 = c(x_2 - x_1) \\ -\Delta p = cl, \Delta p = p_1 - p_2 \geq 0$$

and

$$c = -\frac{\Delta p}{l} \quad (6.3.12)$$

The solutions (6.3.10) indicate that the velocity profiles appearing in the flow field is parabolic in nature, and this flow is called the plane Poiseuille flow, particularly in the case when $U = 0$. On the contrary, when $h \ll 1$, the second term in Eq. (6.3.10) dominates the flow field, yielding

$$u = \pm \frac{U}{h} y \quad (6.3.13)$$

The flow of Eq. (6.3.13) has a linear velocity profile, and is called the plane Couette flow, which is independent from the viscous effect.

The volume flow rate Q through the gap is then calculated from Eq. (6.3.10) such that

$$Q = \int_0^h u \, dy = \frac{\Delta p h^3}{12\eta_0 l} \pm \frac{Uh}{2} \quad (6.3.14)$$

and the average velocity \bar{u} is also defined by

$$\bar{u} = \frac{Q}{h} = \frac{\Delta p h^2}{12\eta_0 l} \pm \frac{U}{2} \quad (6.3.15)$$

Using the average velocity \bar{u} for the plane Poiseuille flow ($U = 0$), the flow through the channel (the gap) length l may be characterized by the

friction coefficient λ , or referred as Darcy friction factor, defined along with the Darcy-Weisbach equation

$$\Delta p = \lambda \left(\frac{h}{l} \right) \left(\frac{1}{2} \rho \bar{u}^2 \right) \quad (6.3.16)$$

in which

$$\lambda = \frac{24}{Re} \quad (6.3.17)$$

where the Reynolds number Re is defined as

$$Re = \frac{\bar{u}h}{(\eta_0/\rho)} \quad (6.3.18)$$

It is also desired to derive an expression for the wall shear stress τ_w to give

$$\tau_w = \tau_{xy} \Big|_{y=0} = \frac{6\eta_0 \bar{u}}{h} \quad (6.3.19)$$

which, furthermore, is nondimensionalized as

$$c_f = \frac{\tau_w}{\frac{1}{2} \rho \bar{u}^2} = \frac{12}{Re} \quad (6.3.20)$$

In a similar way, the plane Couette flow is also characterized as follows

$$\lambda = \frac{4}{Re} \text{ and } c_f = \frac{2}{Re} \quad (6.3.21)$$

The flow expressed with Eq. (6.3.10) is laminar and is maintained up to the incipience of the turbulent flow mode, in the order of $Re \cong 1000$ for the plane Poiseuille flow and $Re \cong 1900$ for plane Couette flow.

(ii) The flow between two concentric rotating cylinders as shown in Fig. 6.3(b) is another flow field that is obtained by solving Navier-Stokes equation with rational simplification. The geometric configuration of flow is particularly important for lubrication of a rotating shaft, a cylindrical viscometer and other similar designs. The analytical solution of laminar flow will be found for fairly slow relative rotational speeds between the inner cylinder with an angular velocity of ω_1 and an outer cylinder with that of ω_2 . Assume that the flow is unidirectional for θ direction, incompressible

and steady, neglecting the body force or inclusive in p , i.e. the conditions are

$$\mathbf{u} = (u_r, u_\theta, u_z) = (0, u, 0) \quad (6.3.22)$$

$$\nabla p = \left(\frac{\partial p}{\partial r}, \frac{1}{r} \frac{\partial p}{\partial \theta}, \frac{\partial p}{\partial z} \right) = \left(\frac{\partial p}{\partial r}, 0, 0 \right) \quad (6.3.23)$$

and

$$u = u(r) \quad (6.3.24)$$

$$\frac{\partial u}{\partial \theta} = 0, \quad \frac{\partial u}{\partial z} = 0 \quad (6.3.25)$$

$$\nabla \cdot \mathbf{u} = 0, \quad \frac{\partial}{\partial t} = 0, \quad \rho \mathbf{g} = 0 \quad (6.3.26)$$

The governing equations of flow in cylindrical coordinates systems are written as

$$\text{Continuity : } \frac{1}{r} \frac{\partial u}{\partial \theta} = 0 \quad (6.3.27)$$

$$\text{N-S equation : } 0 = \eta_0 \left(\frac{\partial^2 u}{\partial r^2} + \frac{1}{r} \frac{\partial u}{\partial r} - \frac{u}{r^2} \right) \quad (6.3.28)$$

The boundary conditions are such that, with reference to Fig. 6.3(b)

$$u = r_1 \omega_1 \text{ for } r = r_1 \quad (6.3.29)$$

$$u = r_2 \omega_2 \text{ for } r = r_2 \quad (6.3.30)$$

where it is noted that ω_1 and ω_2 include the direction \pm for the laboratory (fixed) frame of reference.

The solution of Eq. (6.3.27) is $u = \text{Constant}$ for θ direction, indicating that the flow is fully developed toward its motion.

In order to solve Eq. (6.3.28), it will prove useful to write the equation with

$$\frac{d^2 u}{dr^2} + \frac{d}{dr} \left(\frac{u}{r} \right) = 0 \quad (6.3.31)$$

and then it is solved with the boundary conditions in Eqs. (6.3.29) and (6.3.30), giving the solution:

$$u = \left(\frac{r_2^2 \omega_2 - r_1^2 \omega_1}{r_2^2 - r_1^2} \right) r + \left[\frac{r_1^2 r_2^2 (\omega_1 - \omega_2)}{r_2^2 - r_1^2} \right] \frac{1}{r} \quad (6.3.32)$$

Among a number of situations in combination of ω_1 and ω_2 , we shall examine a case where $\omega_2 = 0$, i.e. the outer cylinder being kept stationary, as is often the case in engineering applications. We have a solution from Eq. (6.3.32) that says

$$u = \frac{r_1^2 \omega_1}{r_2^2 - r_1^2} \left(\frac{r_2^2}{r} - r \right) \quad (6.3.33)$$

The shear stress τ_{wl} acting on the wall of the inner cylinder is $-\tau_{r\theta}$ and it is calculated by

$$\begin{aligned} \tau_{wl} = -\tau_{r\theta} &= -\eta_0 \left[r \frac{\partial}{\partial r} \left(\frac{u}{r} \right) \right]_{r=r_1} \\ &= \left(\frac{2\eta_0 r_2^2}{r_2^2 - r_1^2} \right) \omega_1 \end{aligned} \quad (6.3.34)$$

The net torque T_r exerted on the inner cylinder, whose length is l , is obtained as

$$\begin{aligned} T_r &= \tau_{wl} (2\pi r_1 l) r_1 \\ &= \left(\frac{4\pi \eta_0 r_1^2 r_2^2}{r_2^2 - r_1^2} \right) l \omega_1 \end{aligned} \quad (6.3.35)$$

It is useful to mention that Eq. (6.3.35) gives a principle of Couette rheometer and, with that, the viscosity η_0 is obtained by measuring the torque T_r for the various shear rate $\dot{\gamma}$ with the known geometry r_1 , r_2 and l as follows

$$\begin{aligned} \eta_0 &= \frac{T_r [1 - (r_1/r_2)^2]}{4\pi r_2^2 (r_1/r_2)^2 \omega_1} \\ &= \frac{T_r}{4\pi r_2^2 l} \left(\frac{1}{\dot{\gamma}} \right) \end{aligned} \quad (6.3.36)$$

where k_r is the radius ratio (r_1/r_2) and $\dot{\gamma}$ is the shear rate defined as

$$\dot{\gamma} = \frac{k_r^2 \omega_1}{1 - k_r^2} \approx \frac{\omega_1}{1 - k_r} \quad (\text{for small gap as } k_r \rightarrow 1) \quad (6.3.37)$$

In the case of the lubrication of a rotating shaft, the power P to overcome the resistance of viscosity of a lubricant is obtained by multiplying the torque T_r by the rotational speed ω_1 , where

$$\begin{aligned} P &= T_r \cdot \omega_1 \\ &= \left(\frac{4\pi\eta_0 r_1^2 r_2^2}{r_2^2 - r_1^2} \right) l \omega_1^2 \end{aligned} \quad (6.3.38)$$

The power P is normally dissipated into heat and thus results in a temperature increase. The removal of heat from the lubricant often requires heat exchangers. For a rheometer, the temperature of a test liquid must also be controlled since η_0 is a function of temperature.

The laminar flow solution in Eq. (6.3.33) for the inner cylinder rotation with a fixed outer cylinder is valid up to a rotational Reynolds number Re_r , approximately 7000 (or Taylor number Ta , $Ta_c \approx 1700$). Above the critical value of approximately $Re_{rc} \approx 7000$, the flow mode changes from a simple unidirectional flow to a flow with a secondary flow in the meridional plane, where the velocity distribution in the gap changes with the appearance of strong u_r and u_z components. The flow phenomena was first studied by G.I. Taylor (1923), and found that there appears a cellular pattern in the meridional plane, called the Taylor vortex, which is schematically depicted in Fig. 6.3(b). The occurrence of the flow phenomena is due to the flow instability. Numerous flow modes appear after the incipience of the Taylor vortex, when the rotational speed is increased further from Re_{rc} , and eventually the flow becomes turbulent. These flow transitions are also observed by plotting the torque coefficient c_t for the rotational Reynolds number Re_r (or Ta), as indicated in the graph in Fig. 6.3(b).

$$c_t = \frac{T_r}{\rho r_1^5 \omega_1^2} \quad (6.3.39)$$

$$Re_r = \frac{r_1 \omega_1 (r_2 - r_1)}{(\eta_0 / \rho)} \quad (6.3.40a)$$

or

$$Ta = \frac{\omega_1^3 r_1 (r_2 - r_1)^3}{(\eta_0 / \rho)^2} \quad (6.3.40b)$$

It must be noted that for measuring the viscosity η_0 in Eq. (6.3.36) one should be aware of the limitation of the validity ($Re_r < 7000$). It is also mentioned that the case is different, in view of the flow instability, when the outer cylinder is rotated while the inner cylinder is kept stationary. The unidirectionality of u_θ is kept for further higher Reynolds numbers, since the flow in the gap is stable in the laminar flow regime.

6.3.2 Lubrication Theory

Flow in a varying gap of space is generally regarded as a superposition of the plane of Couette flow and the plane of Poiseuille flow. Lubrication flows are generally accomplished by a thin film of viscous fluid in such a moving wall channel. The theory of lubrication is generally applicable to the processing of materials in liquid form, film coatings, mechanical lubrication on the slipper-pad bearings and others. The theory was first developed by Reynolds (1886). The general Reynolds equation in a general lubrication problem can be derived for a flow between the upper and lower walls under the assumption that $h \ll 1$, which may be moving tangentially or normally as schematically displayed in Fig. 6.4, by means of the control volume principle on the mass continuity equation.

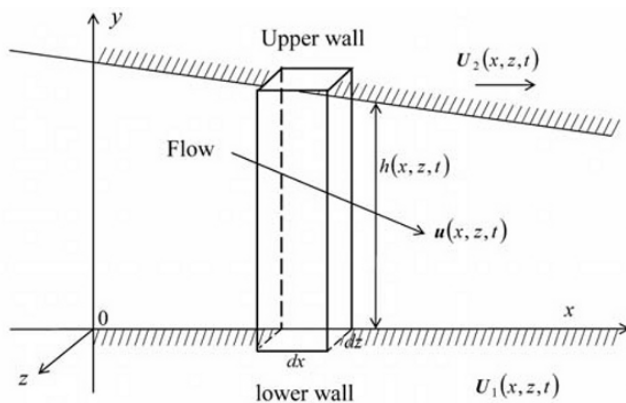


Fig. 6.4 Lubrication flow in a gap

Based on Eqs. (2.1.3) and (2.1.5), the integration form of the mass continuity is written as

$$\frac{\partial}{\partial t} \int_V \rho dV + \int_V \nabla \cdot \rho \mathbf{u} dV = 0 \quad (6.3.41)$$

The integration can be performed for the control volume, i.e. $\int_0^h (dx dz) dy$, and we can reduce Eq. (6.3.41) to the following form

$$\left[\frac{\partial}{\partial t} \int_0^h \rho dy \right] dx dz + \left[\nabla \cdot \rho \int_0^h \mathbf{u} dy \right] dx dz = 0$$

where we have

$$\frac{\partial \rho h}{\partial t} + \nabla \cdot \rho \mathbf{q}_V = 0 \quad (6.3.42)$$

where we assumed that the change of ρ in h height is small due to a thin film of fluid and \mathbf{q}_V is the volume flux through the gap, which is defined as

$$\mathbf{q}_V = \int_0^h \mathbf{u} dy \quad (6.3.43)$$

The flow velocity $\mathbf{u}(x, z, t)$ may be written with reference to the solution given by Eq. (6.3.10)

$$\mathbf{u} = \left(\frac{1}{2\eta_0} \nabla p \right) y(h-y) + \left(\frac{\mathbf{U}_2 - \mathbf{U}_1}{h} \right) y + \mathbf{U}_1 \quad (6.3.44)$$

Substitution of Eq. (6.3.44) into Eq. (6.3.43), and rearranging Eq. (6.3.42), we get the resultant equation where

$$\nabla \cdot \left(\frac{\rho h^3}{12\eta_0} \nabla p \right) = \nabla \cdot \left[\frac{1}{2} \rho (\mathbf{U}_2 + \mathbf{U}_1) h \right] + \frac{\partial(\rho h)}{\partial t} \quad (6.3.45)$$

Equation (6.3.45) is called the Reynolds equation for lubrication. It is mentioned here that ρ may be dropped from the equation for incompressible fluid although in the case when the variation of density is accounted for, in such as gas bearings, ρ has to be included.

In an application of the Reynolds equation, i.e. Eq. (6.3.45), consider a slipper-pad bearing as sketched in Fig. 6.5(a). Let us assume the lower

wall is flat and moves with a constant velocity of U_1 . The upper wall, called the slipper block, is inclined where $h(x)$ is given by the function

$$h(x) = h_0 + (h_l - h_0) \frac{x}{l} \quad (6.3.46)$$

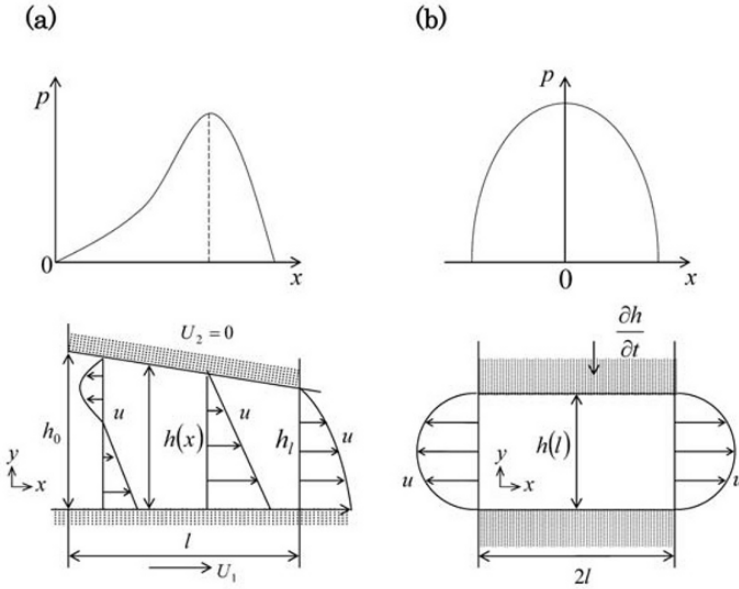


Fig. 6.5 (a)Slipper-pad bearing (b)Squeezed film

As a bearing, the lubricant fluid provides a high lift force to the slipper block that supports a large load without the block touching the lower wall and thus prevents wear. To prove the function, we obtain the pressure force acting on the block. If we consider the unidirectional (x direction), incompressible and steady state flow, Eq. (6.3.45), it can be written as

$$\frac{\partial}{\partial x} \left(h^3 \frac{\partial p}{\partial x} \right) = 6\eta_0 U_1 \frac{\partial h}{\partial x} \quad (6.3.47a)$$

and the boundary condition is such that

$$p = 0 \text{ at } x = 0 \text{ and } p = 0 \text{ at } x = l \quad (6.3.47b)$$

Equation (6.3.47) is then solved with Eq. (6.3.46) and the boundary condition which yields the solution to give

$$p = \frac{6\eta_0 U_1 (h - h_l)x}{h^2 (h_0 + h_l)} \quad (6.3.48)$$

The distribution of p as the function of x is shown in a graph found in Fig. 6.5(a), where the velocity profiles $u = u(y)$, which are obtained in Eq. (6.3.44), are known by given conditions. The total load-bearing capacity F (per unit depth) is

$$F = \int_0^l p dx = \frac{6\eta_0 U_1 l^2}{(h_0 - h_l)^2} \left[\ln\left(\frac{h_0}{h_l}\right) - 2\left(\frac{h_0 - h_l}{h_0 + h_l}\right) \right] \quad (6.3.49)$$

The maximum value of F is found by differentiating Eq. (6.3.49) with respect to (h_0/h_l) and equating it to zero, and which gives

$$F_{\max} = 0.16 \frac{\eta_0 U_1 l^2}{h_l^2} \quad (6.3.50)$$

where $h_0/h_l = 2.2$. The total drag force F_D (per unit depth) for the width l can be calculated as

$$F_D = \int_0^l \tau_w dx \quad (6.3.51)$$

where $\tau_w = -\eta_0 (\partial u / \partial y)_{y=0}$, the wall of shear stress. F_D is obtained by the known velocity profile, and it is

$$F_D = \frac{\eta_0 U_1 l}{(h_0 - h_l)} \left[4 \ln\left(\frac{h_0}{h_l}\right) - 6\left(\frac{h_0 - h_l}{h_0 + h_l}\right) \right] \quad (6.3.52)$$

The drag-lift ratio F_D/F_{\max} for the maximum load-bearing capacity will be calculated to give

$$F_D/F_{\max} = 2.14 \left(\frac{h_0}{l} \right) \quad (6.3.53)$$

for $h_0/h_l = 2.2$ as a representative value (for maximum load-bearing capacity).

The slipper-pad bearing is often used as a thrust bearing for heavy turbomachineries, such as for a hydraulic turbine. It is mentioned that reversing the wall direction $U_1 < 0$ may cause cavitation and form a vapor region in the gap and may not necessarily exert the required load-bearing capacity.

The flow configuration of the slipper-pad bearing can be applied to a journal bearing, where the eccentric annular gap between two rotating cylinder shafts is filled with lubricant. In the case of a rotating journal bearing, where the gap contracts and then expands in a rotating direction so that a partial cavitation often occurs.

The next illustrative example of the Reynolds equation is the squeezed film problem, which is seen in a squeezed film damper or a modeling of a knee joint, etc. The basic configuration is displayed in Fig. 6.5(b), where the upper wall moves toward the lower wall, keeping h being parallel to the both walls. Let us consider the following condition for the problem

$$v = -\frac{\partial h}{\partial t}, \quad U_1 = U_2 = 0 \quad \text{and} \quad \nabla h = 0 \quad (6.3.54)$$

where the gap width h is a function of time, i.e. $h = h(t)$ and the fluid is assumed incompressible. Thus, Eq. (6.3.45) is reduced to

$$h^3 \nabla^2 p = -12\eta_0 v \quad (6.3.55)$$

and for the unidirectional flow of the pressure p , we have

$$\frac{\partial^2 p}{\partial x^2} = -\frac{12\eta_0}{h^3} v \quad (6.3.56)$$

Equation (6.3.56) is directly solved for p with the boundary condition of

$$\begin{aligned} x = 0, \quad \frac{\partial p}{\partial x} &= 0; \text{ symmetry} \\ x = \pm l, \quad p &= 0; \text{ boundary} \end{aligned}$$

so that the solution p is given as

$$p(x, t) = \frac{6\eta_0 v}{h^3} (l^2 - x^2) \quad (6.3.57)$$

The pressure distribution $p(x, t)$ is sketched in the graph in Fig. 6.5(b), which shows the parabolic distribution. The velocity profile in the gap is essentially the plane Poiseuille flow as also indicated in the figure, which is easily verified from Eq. (6.3.44). The total load capacity F (per unit depth) exerted on the upper wall (or the lower wall) is

$$F = 2 \int_0^l p dx = \frac{8\eta_0 v}{h^3} l^3 \quad (6.3.58)$$

Since $h \ll 1$ and if h is the decreasing function of t , the total load capacity increases drastically as $F \rightarrow +\infty$, indicating a large suspending force that can be produced by the squeezing of the film flow on the gap walls.

To convey the essence of the subject, although it is hard to survey all the interesting possibilities, we are able to introduce an interesting application of the Reynolds equation, the so-called Hele-Shaw flow. The flow has a nature of a viscid potential flow, which observes streamline patterns of a potential flow in laboratory demonstrations. The flow is provided in a Hele-Shaw cell, that is made of two stationary parallel transparent plates with a precise small gap distance h , as shown in Fig. 6.6. When an object, whose characteristic length l is much larger than h to ensure a no-slip condition on the object surface, is placed in the cell, a two dimensional potential flow around the object appears for an incompressible fluid, entering the cell from one end at a uniform rate. This phenomena is found in the fact that the pressure p in the cell is considered to be followed from Eq. (6.3.45) where

$$\nabla^2 p = 0 \quad (6.3.59)$$

where ρ and h are assumed constant with $U_1 = U_2 = 0$. Thus, the corresponding velocity field is, from Eq. (6.3.44), obtained to write

$$\mathbf{u} = \frac{1}{2\eta_0} y(h-y)\nabla p \quad (6.3.60)$$

Equation (6.3.60) indicates that in plan view, i.e. the x - z plane, the streamlines are in parallel with the pressure gradient, through which the rotation of Eq. (6.3.60) yields

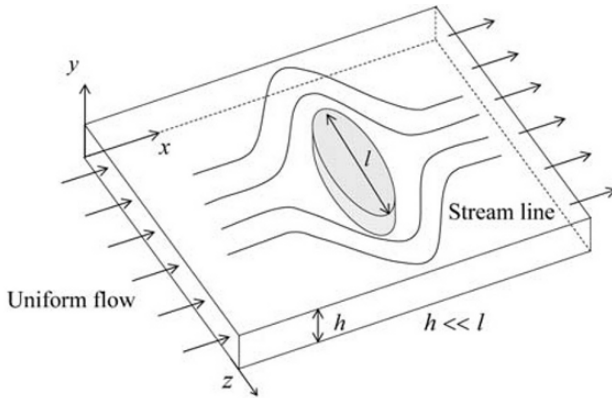


Fig. 6.6 Hele-Shaw flow cell

$$\nabla \times \mathbf{u} = \frac{1}{2\eta_0} y(h-y) \nabla \times \nabla p = 0 \quad (6.3.61)$$

Therefore, the two dimensional flow field is irrotational and \mathbf{u} can be described by a scalar potential (velocity potential) ϕ in x - z plane, such that $\mathbf{u} = \nabla \phi$, where p itself acts as the velocity potential, satisfying the Laplace's equation in Eq. (6.3.59).

6.3.3 Flow Around a Sphere

Consider a small sphere descending in a viscous fluid. The falling sphere attains a so-called terminal velocity, when the acceleration becomes zero after sometime from the incipient motion. In the situation where the buoyant force plus the drag force on the sphere consequently become equal to its gravity force.

Defining the Reynolds number $Re = Ud/(\eta_0/\rho)$, where d is the diameter of the sphere, U the terminal velocity, η_0 the viscosity of fluid and ρ the density of fluid, we will obtain the drag force and show it to measure the viscosity of fluid, noting ρ_s being the density of the material of the sphere. The discussion is supposed to be valid for approximately $Re < 0.1$.

Let us begin to consider an axisymmetric flow around a sphere, as depicted in Fig. 6.7. Due to the axisymmetric flow field where $u_\phi = 0$ in the spherical coordinates system, the flow field can be described by the stream function $\psi = (r, \theta)$ (the Stokes stream function), which identically satisfied the continuity equation of incompressible fluid. The velocity components of u_r and u_θ are thus written by ψ as

$$u_r = -\frac{1}{r^2 \sin \theta} \frac{\partial \psi}{\partial \theta}, \quad u_\theta = \frac{1}{r \sin \theta} \frac{\partial \psi}{\partial r} \quad (6.3.62)$$

The Navier-Stokes equation in r and θ coordinates, without inertia terms, i.e. the creep flow limit and neglecting the gravity acceleration, are written as

$$0 = -\frac{\partial p}{\partial r} + \eta_0 \left[\frac{1}{r^2} \frac{\partial^2}{\partial r^2} (r^2 u_r) + \frac{1}{r^2 \sin \theta} \frac{\partial}{\partial \theta} \left(\sin \theta \frac{\partial u_r}{\partial \theta} \right) \right] \quad (6.3.63)$$

and

$$0 = -\frac{1}{r} \frac{\partial p}{\partial \theta} + \eta_0 \left[\frac{1}{r^2} \frac{\partial}{\partial r} \left(r^2 \frac{\partial u_\theta}{\partial r} \right) + \frac{1}{r^2} \frac{\partial}{\partial \theta} \left(\frac{1}{r \sin \theta} \frac{\partial}{\partial \theta} (u_\theta \sin \theta) \right) + \frac{2}{r^2} \frac{\partial u_r}{\partial \theta} \right] \quad (6.3.64)$$

Substituting u_r and u_θ in Eq. (6.3.62) into Eqs. (6.3.63) and (6.3.64) and eliminating the pressure terms, we can obtain

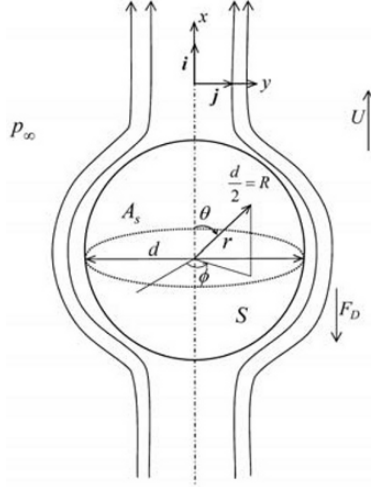


Fig. 6.7 Creeping flow past a sphere

$$\left\{ \frac{\partial^2}{\partial r^2} + \frac{\sin \theta}{r^2} \frac{\partial}{\partial \theta} \left(\frac{1}{\sin \theta} \frac{\partial}{\partial \theta} \right) \right\} \left[\left\{ \frac{\partial^2}{\partial^2 r} + \frac{\sin \theta}{r^2} \frac{\partial}{\partial \theta} \left(\frac{1}{\sin \theta} \frac{\partial}{\partial \theta} \right) \right\} \psi \right] = 0 \quad (6.3.65)$$

and using the differential operator E^2 , we can alternatively write

$$E^2(E^2\psi) = 0 \quad (6.3.66)$$

or

$$E^4\psi = 0 \quad (6.3.67)$$

The solutions in Eq. (6.3.66) or Eq. (6.3.67) are harmonic functions in polar coordinates systems, $\psi = \psi(r, \theta)$, with the following boundary conditions on the sphere

$$u_r = u_\theta = 0 \quad \text{for } r = \frac{d}{2} (= R) \quad (6.3.68)$$

which implies

$$\frac{\partial \psi}{\partial r} = 0 \quad \text{and} \quad \frac{\partial \psi}{\partial \theta} = 0 \quad (6.3.69)$$

At infinity, $r \rightarrow \infty$

$$u = U_r \hat{e}_r + U_\theta \hat{e}_\theta = U(\cos \theta \hat{e}_r - \sin \theta \hat{e}_\theta) \quad (6.3.70)$$

which implies that

$$\frac{\partial \psi}{\partial r} = -U r \sin^2 \theta \quad \text{and} \quad \frac{\partial \psi}{\partial \theta} = U r^2 \sin \theta \cos \theta \quad (6.3.71)$$

Equation (6.3.71) gives ψ at $r \rightarrow \infty$ by the integration of

$$\psi = \int d\psi = \int \frac{\partial \psi}{\partial r} dr + \int \frac{\partial \psi}{\partial \theta} d\theta = -\frac{1}{2} U r^2 \sin^2 \theta \quad (6.3.72)$$

Equation (6.3.72) might assume the form of the solution in Eq. (6.3.67) as

$$\psi = f(r)g(\theta) \quad (6.3.73)$$

In order to seek a solution in Eq. (6.3.67), it may be appropriate to set $g(\theta) = \sin^2 \theta$ and substitute Eq. (6.3.73) for Eq. (6.3.64), where

$$\left(\frac{d^2}{dr^2} - \frac{2}{r^2} \right)^2 f(r) \cdot \sin^2 \theta = 0 \quad (6.3.74)$$

In order to satisfy Eq. (6.3.74) for r and θ simultaneously, we must satisfy

$$\left(\frac{d^2}{dr^2} - \frac{2}{r^2} \right)^2 f(r) = 0 \quad (6.3.75)$$

The solutions of f in Eq. (6.3.75) must satisfy the following differential equation (equidimensional equation)

$$r^4 f''' - 4r^2 f'' + 8rf' - 8f = 0 \quad (6.3.76)$$

Equation (6.3.76) is the so-called Euler's differential equation, to which the general solution to this equation is given as

$$f(r) = \frac{c_1}{r} + c_2 r + c_3 r^2 + c_4 r^4 \quad (6.3.77)$$

where constants c_1 , c_2 , c_3 and c_4 are determined from the boundary conditions in Eqs. (6.3.68) and (6.3.69). The final solution in Eq. (6.3.73) is given with the aid of the functional form of Eq. (6.3.73) where

$$\psi = U \frac{1}{2} r^2 \left(1 - \frac{3}{2} \frac{R}{r} + \frac{1}{2} \frac{R^3}{r^3} \right) \sin^2 \theta \quad (6.3.78)$$

Equation (6.3.78) also gives the velocity components as

$$u_r = -U \left(1 - \frac{3}{2} \frac{R}{r} + \frac{1}{2} \frac{R^3}{r^3} \right) \cos \theta \quad (6.3.79)$$

$$u_\theta = U \left(1 - \frac{3}{4} \frac{R}{r} - \frac{1}{4} \frac{R^3}{r^3} \right) \sin \theta \quad (6.3.80)$$

Knowing the velocity field given in Eqs. (6.3.79) and (6.3.80), we can obtain the pressure field by substituting Eqs. (6.3.79) and (6.3.80) into Eqs. (6.3.63) and (6.3.64), and carrying out the integration to yield $p(r, \theta)$ as

$$p(r, \theta) = \int dp = \int \frac{\partial p}{\partial r} dr + \int \frac{\partial p}{\partial \theta} d\theta = p_\infty - \frac{3}{2} \eta_0 R U \frac{\cos \theta}{r^2} \quad (6.3.81)$$

where p_∞ is the pressure at infinity, i.e. $r \rightarrow \infty$.

As another point of correspondence, it will now be shown that the drag force F_D , which is the net force acting on the sphere in the flow direction \mathbf{i} in Fig. 6.7, may be calculated by obtaining the stress component t_x on the sphere in direction \mathbf{i} . This will be done by knowing the stress vector \mathbf{t} on the sphere as follows

$$\begin{aligned} \mathbf{t} &= \hat{\mathbf{e}}_r \cdot \mathbf{T} = \hat{\mathbf{e}}_r \cdot (-p \mathbf{I} + \boldsymbol{\tau}) = (-p + \tau_{rr}) \hat{\mathbf{e}}_r + \tau_{r\theta} \hat{\mathbf{e}}_\theta \\ &= (-p + \tau_{rr}) (\cos \theta \mathbf{i} + \sin \theta \mathbf{j}) + \tau_{r\theta} (-\sin \theta \mathbf{i} + \cos \theta \mathbf{j}) \end{aligned} \quad (6.3.82)$$

The stress component t_x is thus

$$t_x = \mathbf{i} \cdot \mathbf{t} = (-p + \tau_{rr}) \cos \theta - \tau_{r\theta} \sin \theta \quad (6.3.83)$$

where τ_{rr} and $\tau_{r\theta}$ are components of the viscous stress tensor of a Newtonian fluid, and which are given by the following constitutive equations

$$\tau_{rr} = 2\eta_0 \frac{\partial u_r}{\partial r}, \quad \tau_{r\theta} = \eta_0 \left[r \frac{\partial}{\partial r} \left(\frac{u_\theta}{r} \right) + \frac{1}{r} \frac{\partial u_r}{\partial \theta} \right] \quad (6.3.84)$$

The velocity components u_r and u_θ of Eqs. (6.3.79) and (6.3.80) are then substituted into the relationship in Eq. (6.3.84), and consequently t_x will be obtained as

$$t_x = -p_\infty \cos \theta + \frac{3}{2} \frac{\eta_0}{R} U \quad (6.3.85)$$

Thus, as a result, the drag force F_D is calculated to integrate t_x over the spherical surface S

$$\begin{aligned} F_D &= \int_S t_x dS = \int_0^{2\pi} \int_0^\pi t_x R^2 \sin \theta d\theta d\phi \\ &= 6\pi \eta_0 R U \\ &= 3\pi \eta_0 d U \end{aligned} \quad (6.3.86)$$

Equation (6.3.86) states that at the creep flow limit the drag force is linearly proportional to the speed of flow passing a small sphere (or a descending sphere with a constant speed). This is called Stokes' law.

It is noted that $-p_\infty \cos \theta$ does not contribute the drag F_D due to its symmetry, as previously described, indicating that the potential flow, which has only a contribution of $-p_\infty \cos \theta$, does not influence the drag, but only that the viscous contribution found in Eq. (6.3.85) does in the case of viscous flow. If the drag coefficient c_D is defined such that

$$c_D = \frac{F_D}{1/2 \rho U^2 A_s} \quad (6.3.87)$$

where A_s is the frontal area of the sphere. Then we can reduce Eq. (6.3.86) to give the drag coefficient in terms of the Reynolds number

$$c_D = \frac{F_D}{1/2 \rho U^2 (\pi d^2/4)} = \frac{24}{Re} \quad (6.3.88)$$

If $Re < 0.1$, which implies a small sphere in a high viscous fluid, the Stokes' law is valid and for a sphere at the terminal velocity U , the buoyant force F_b plus the drag force F_D become equal to the gravity force F_g , that is

$$\frac{\pi}{6} d^3 \rho g + 3\pi\eta_0 U d = \frac{\pi}{6} d^3 \rho_s g \quad (6.3.89)$$

An important application of Eq. (6.3.89) is to measure the viscosity η_0 by measuring the terminal velocity U for a falling sphere in a transparent cylinder, containing the viscous fluid to be tested. According to Eq. (6.3.89) η_0 can be obtained where

$$\eta_0 = \frac{(\rho_s - \rho)gd^2}{18U} \quad (6.3.90)$$

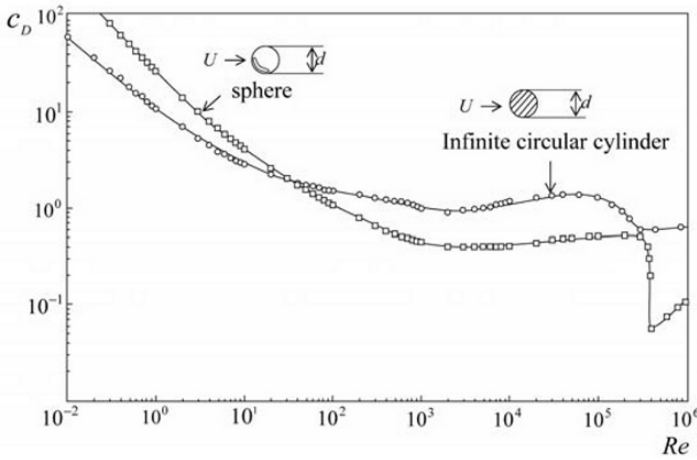


Fig. 6.8 Drag coefficient of a sphere and an infinite cylinder (From various sources, and data for $Re \geq 10^4$ is replotted after Achenback, 1971 and 1972)

The drag coefficient c_D given by Stoke's law, i.e. Eq. (6.3.88), is further extended to validate in higher Reynolds numbers by Oseen (1910)

$$c_D = \frac{24}{Re} \left(1 + \frac{3}{16} Re \right)^n \quad (6.3.91)$$

where $Re < 1$ for $u = 1$ m/s. If n is chosen at 0.5, Eq. (6.3.91) is extended to $Re \approx 100$. Typical changes of c_D versus Re are displayed in Fig. 6.8 for a sphere and an infinite cylinder for the sake of comparison. It is seen in both cases at approximately $Re \approx 3 \times 10^5 \sim 5 \times 10^5$, there is a sudden drop

in the value of c_D . This is due to phenomena caused by a transition of laminar flow to turbulence. The boundary layer, which is described in more detail in later sections, is the cause of this phenomenon.

Problems

6.3-1 Describe how the resultant flow between the concentric rotating cylinders can be used as a means of measuring the viscosities of fluids. Give comments on the feasibility of the method of measuring viscosity.

6.3-2 A slipper-pad bearing is running with a speed of $U_1 = 2$ m/s. The representative dimensions are such that, $h_0 = 0.8 \times 10^{-4}$ m, $h_l = 0.4 \times 10^{-4}$ m and $l = 0.3$ m. The viscosity of the lubricant oil is $\eta_0 = 2 \times 10^{-5}$ Pa · s at a constant operating temperature. Find the total load-bearing capacity to maintain the gap. Also calculate the drag-lift ratio.

$$Ans. \left[\begin{array}{l} F = 354 \text{ N} \\ F_D / F_{\max} = 0.655 \times 10^{-5} \end{array} \right]$$

6.3-3 Design an appropriate experimental apparatus for examining a potential flow around an infinite cylinder.

6.3-4 A small sphere of diameter d and density ρ_s is dropped from a rest position in a viscous fluid with density ρ . Write the equation of motion of this sphere and find the terminal velocity. The viscosity of the fluid is η_0 . Assume that the Stokes' law is in effect to the motion of the sphere.

$$Ans. \left[\begin{array}{l} \left(\frac{\pi}{6} d^3 \rho_s \right) \frac{dU}{dt} = -\frac{\pi}{6} d^3 \rho g - 3\pi\eta_0 U d + \frac{\pi}{6} d^3 \rho_s g \\ U = \frac{(\rho_s - \rho) g d^2}{18\eta_0} \text{ for } \frac{dU}{dt} = 0 \end{array} \right]$$

6.3-5 Find the time elapsed to the fall distance $l = 0.01$ m for a sphere of $d = 1 \times 10^{-5}$ m and $\rho_s = 5 \times 10^3$ kg/m³ released from a position of rest in a viscous fluid of viscosity $\eta_0 = 1 \times 10^{-1}$ Pa · s and the density $\rho = 2 \times 10^3$ kg/m³.

$$Ans. [\text{Approx. } 9001 \text{ s.}]$$

6.4 Flow Through Pipe

The circular pipe flow is probably the most celebrated viscous flow in the development of fluid dynamics, in view of the fundamental importance of, as well as, basic fluid engineering applications. We shall start to consider a straight circulation pipe connected to a reservoir tank, as illustrated in Fig. 6.9. In many practical engineering applications, a pipe is usually connected to a reservoir tank or a source, and the flow in the pipe starts to move forward, downstream. Note that the entrance is supposed to be a bell mouth shape to avoid boundary layer separation. There will be an “entrance effect”, where a shear layer (boundary layer; details of which will be studied in later section) on the pipe wall and an inviscid core (uniform constant velocity region along axis of the pipe) that develops toward the downstream of flow near the entering region of the pipe.

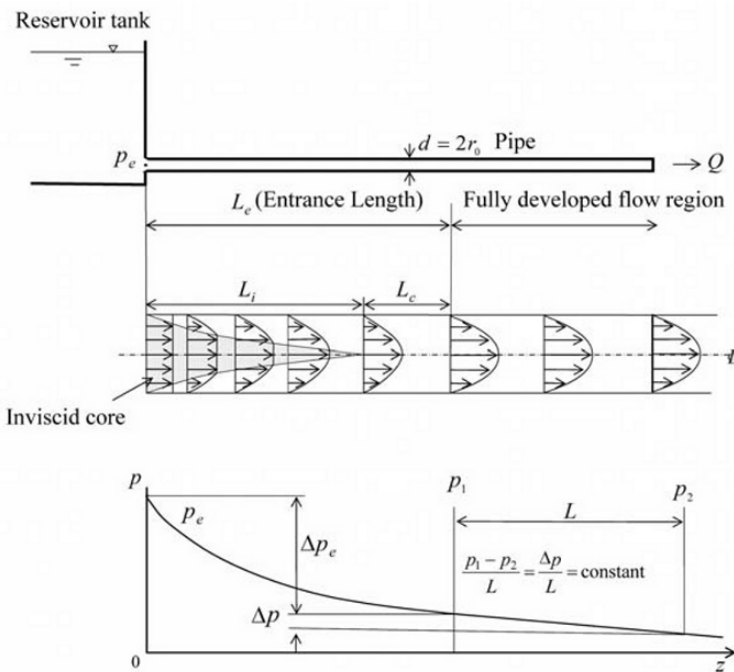


Fig. 6.9 Circular pipe flow through entrance

As indicated in Fig. 6.9, the shear layer grows and meets at the axis as the inviscid core disappears within the length L_i termed as the inviscid core length, at which the viscous stress dominates the entire cross section. The profile then continues to change due to the viscous effect until a developed flow is achieved, where the length is often termed as the profile development region L_c . The total length $L_i + L_c$ is called the entrance length L_e , and after which the flow is fully developed, where the velocity profile across the cross section does not change toward the downstream.

6.4.1 Entrance Flow

The entrance length for a laminar flow can be correlated in the forms

$$\frac{L_e}{d} = 0.065 Re \quad (\text{Boussinesq, 1891 and Nikuradse, 1933}) \quad (6.4.1)$$

$$\frac{L_e}{d_h} = 0.5 + 0.05 Re_h \quad (\text{Shah and London, 1978}) \quad (6.4.2)$$

where Reynolds number Re is based on the average velocity \bar{U} through a cross section area and the diameter d , i.e. $Re = \bar{U}d/\nu$. Note that the Shah-London correlation is valid for an arbitrary pipe shape in a cross section, where d_h is the hydraulic diameter (four times hydraulic radius r_h), which is defined by

$$d_h = 4 \left(\frac{A}{l_p} \right) = 4r_h \quad (6.4.3)$$

where A is the cross-section area and l_p is the wetted perimeter, that perimeter where the fluid is in contact with the solid boundary. The limit of the Reynolds number is approximately 2300 for engineering applications, whereas with carefully controlled conditions the Reynolds number may go up to higher values in excess of 40,000.

For a turbulent flow, the situation is somewhat different from the laminar case. In order to observe the entrance length L_e of the fully developed turbulent flow, an extra length may be needed for the detailed structure of the turbulent flow to develop in addition to the profile development region. For the high turbulent strength flow at the inlet of the pipe, the entrance length L_e is given by the following correlation at the Reynolds numbers normally encountered

$$\frac{L_e}{d} = 4.4 Re^{\frac{1}{6}} = (25 \sim 40) \quad (\text{Nikuradse, 1933}) \quad (6.4.4)$$

The pressure variation along the pipe length from the inlet is sketched in Fig. 6.9, where the inlet pressure is p_e . The pressure loss at the entrance length occurs due to an acceleration of flow, i.e. the kinetic energy loss, and the viscous friction loss. The pressure loss Δp_e solely due to the kinetic energy loss can be estimated in consideration of the energy flux at a representative cross sectional area as follows

$$\Delta p_e = \frac{(E_f - E_e)}{\pi r_0^2 \bar{U}} \quad (6.4.5)$$

where E_f and E_e are the kinetic energy through a cross section of pipe at the entrance length L_e and the inlet respectively. They are, therefore, given by the following formula

$$E_{f \text{ and } e} = \int_0^{r_0} u \left(\frac{1}{2} \rho u^2 \right) 2\pi r dr \quad (6.4.6)$$

For the laminar flow, the velocity profile in the fully developed flow is given by well known Hagen-Poiseuille flow, which will be explained in the subsequent section (with reference to Eq. (6.4.33)), as follows

$$u(r) = 2\bar{U} \left(1 - \frac{r}{r_0} \right)^2 \quad (6.4.7)$$

where, at the inlet of the pipe, the velocity profile can be assumed to be constant where

$$u(r) = \bar{U} \quad (6.4.8)$$

Substituting Eqs. (6.4.7) and (6.4.8) into Eq. (6.4.6) and calculating Δp_e from Eq. (6.4.5), we can obtain

$$\Delta p_e = \frac{\rho}{2} \bar{U}^2 \quad (6.4.9)$$

If the pressure loss coefficient ζ based on a loss of head is defined by

$$\frac{\Delta p_e}{\rho g} = \zeta \left(\frac{\bar{U}^2}{2g} \right) \quad (6.4.10)$$

ζ is obtained for the laminar flow as

$$\zeta = 1 \quad (6.4.11)$$

In the case of the turbulent flow, ζ is given by 1/7 power law (Eq. 6.4.53)

$$\zeta = 0.09 \quad (6.4.12)$$

The actual pressure loss (defining $\zeta = \zeta_0$ as the total pressure loss coefficient) at the entrance length is usually higher than that of the kinetic energy loss due to the viscous friction loss, and they are found by using the Hagen's experiments

$$\zeta_0 = 1.7 \text{ for laminar flow} \quad (6.4.13)$$

$$\zeta_0 = 0.4 \text{ without bell mouth entrance for turbulent flow} \quad (6.4.14)$$

In the flow beyond the entrance length the pressure variation tends to decrease linearly along the axial distance z and the pressure gradient

$$-\frac{\partial p}{\partial z} = \frac{p_1 - p_2}{L} = \frac{\Delta p}{L} \quad (6.4.15)$$

is kept constant for both the laminar and turbulent flows.

6.4.2 Fully Developed Flow in Pipe

For $z > L_e$, the velocity becomes a solely axial and only with the lateral coordinates in the fully developed flow in a circular pipe, as sketched in Fig. 6.9, where the flow is non-accelerating and is driven by the pressure gradient (when the gravitational body force is ignored for a horizontal straight pipe or, if at all, it can be incorporated in the pressure term as the potential energy function). In general terms, such a (nearly) non-accelerating flow of an incompressible Newtonian fluid in a steady state of motion is treated as the so-called Stokes' equation, which is written with the continuity equation as follows

$$\nabla \cdot \mathbf{u} = 0 \quad (6.4.16)$$

and

$$-\nabla p + \eta_0 \nabla^2 \mathbf{u} = 0 \quad (6.4.17)$$

It should be noted that the Stokes' equation (6.4.17) is reduced from the Navier-Stokes equation Eq. (6.1.7), by setting the inertia term zero, and is valid for not so large Reynolds number where the flow tends to become turbulent. The flow field derived from Eq. (6.4.17) is independent of the density, and the flows followed in Eq. (6.4.17) are so-called creeping flows, even though the Reynolds number need not be small (and in fact the Reynolds number is not even a required parameter).

It is now desired to consider the fully developed, pressure-driven laminar flow in a circular pipe where the flow is assumed to be steady, axisymmetric and rectilinear. This flow is termed as the Hagen-Poiseuille flow, which implies that in the flow field there is only an axial velocity component u_z , while the radial u_r and circumferential u_θ velocity components are, respectively, $u_r = 0$ and $u_\theta = 0$. In the cylindrical coordinates system u_z may be the function of r, θ, z , i.e. $u_z = u_z(r, \theta, z)$. However with the condition of axisymmetry, i.e.

$$\frac{\partial u_z}{\partial \theta} = 0 \quad (6.4.18)$$

and from the mass continuity

$$\frac{\partial u_z}{\partial z} = 0 \quad (6.4.19)$$

u_z is only the function of r , i.e. $u_z = u_z(r)$. In the fully developed rectilinear flows, the pressure gradient in the axial direction is kept constant as is referred to in Eq. (6.4.15), i.e.

$$-\frac{\partial p}{\partial z} = \text{const.}(=c) \quad (6.4.20)$$

It will prove useful to consider the nondimensionalization of the Stokes' equation in Eq. (6.4.17), which can be carried out by taking the pipe radius r_0 as follows

$$r^* = \frac{r}{r_0}, \quad u^* = \frac{\eta_0 u_z}{r_0^2 (-\partial p / \partial z)} \quad (6.4.21)$$

Resultantly we have

$$\nabla^{*2}(u^*) = -1 \quad (6.4.22)$$

It should be kept in mind that the negative pressure gradient is adopted to make u^* a positive quantity. Eq. (6.4.22) can now be solved for

$$\frac{1}{r^*} \frac{d}{dr^*} \left(r^* \frac{du^*}{dr^*} \right) = -1 \quad (6.4.23)$$

with the boundary conditions,

$$u^* = 0 \text{ (no-slip at wall) for } r^* = 1 \quad (6.4.24)$$

and

$$u^* = \text{finite (along the axis of symmetry) for } r = 0 \quad (6.4.25)$$

The solution of Eq. (6.4.23) is expressed by

$$u^* = -\frac{1}{4} r^{*2} + C_1 \ln r^* + C_2 \quad (6.4.26)$$

and with the boundary conditions $C_1 = 0$ and $C_2 = 1/4$, we can write a rigorous solution for u_z as follows

$$u_z = \frac{1}{4\eta_0} \left(-\frac{\partial p}{\partial z} \right) (r_0^2 - r^2) \quad (6.4.27)$$

The velocity profile in Eq. (6.4.27) is a paraboloid, termed as the Poiseuille paraboloid of a revolution about the axis of pipe, as shown in Fig. 6.10. Note that Eq. (6.4.27) carries a dimension. The flow expressed in Eq. (6.4.27) is called the Hagen-Poiseuille flow.

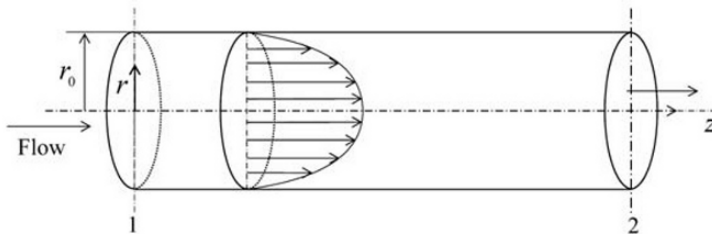


Fig. 6.10 Poiseuille paraboloid

Now, the flow properties associated with the Hagen-Poiseuille flow are examined, knowing that the flow is fully developed that at any cross sec-

tion of the pipe, the flow profile is kept identical.

$$\tau_{rz} = \frac{\partial u_z}{\partial r} = \frac{1}{2\eta_0} \left(\frac{dp}{dz} \right) r \quad (6.4.28)$$

and the wall shear stress τ_w is calculated by setting $r = r_0$

$$\tau_w = -\tau_{rz} \Big|_{r=r_0} = -\frac{1}{2\eta_0} \left(\frac{\partial p}{\partial z} \right) r_0 \quad (6.4.29)$$

The volume flow rate Q through the cross sectional area is given where

$$Q = \int_0^{r_0} u_z 2\pi r dr = -\frac{\pi}{8\eta_0} \left(\frac{\partial p}{\partial z} \right) r_0^4 \quad (6.4.30)$$

This is called the Hagen-Poiseuille equation, and the average velocity \bar{U} is thus given as

$$\bar{U} = \frac{Q}{\pi r_0^2} = -\frac{1}{8\eta_0} \left(\frac{\partial p}{\partial z} \right) r_0^2 \quad (6.4.31)$$

The maximum velocity $u_{z,\max}$ occurs at $r = 0$, i.e. at the axis of the pipe, to write

$$u_{z,\max} = -\frac{1}{4\eta_0} \left(\frac{\partial p}{\partial z} \right) r_0^2 \quad (6.4.32)$$

The velocity profile given in Eq. (6.4.27) can be alternatively written by \bar{U} or $u_{z,\max}$ as follows

$$u_z = 2\bar{U} \left(1 - \frac{r}{r_0} \right)^2 \quad (6.4.33)$$

or

$$u_z = u_{z,\max} \left(1 - \frac{r}{r_0} \right)^2 \quad (6.4.34)$$

The pressure drop in an arbitrary section L with reference to Fig. 6.9 is given in Eq. (6.4.20), and the integration gives

$$\begin{aligned}
 p_2 - p_1 &= c \int_{z_1}^{z_2} dz \\
 &= cL
 \end{aligned}$$

so that

$$c = -\frac{\partial p}{\partial z} = \frac{p_1 - p_2}{L} = \frac{\Delta p}{L} \quad (6.4.35)$$

Note that Eq. (6.4.35) is equivalent to Eq. (6.4.15). With the aid of Eq. (6.4.31), the pressure drop Δp can be expressed in the following form

$$\begin{aligned}
 \Delta p &= 64 \left(\frac{\eta_0}{\rho} \right) \left(\frac{L}{2r_0} \right) \left(\frac{1}{2} \rho \bar{U}^2 \right) \\
 &= \frac{64}{Re} \left(\frac{L}{d} \right) \left(\frac{1}{2} \rho \bar{U}^2 \right)
 \end{aligned} \quad (6.4.36)$$

From the Darcy-Weisbach equation below

$$\Delta p = \lambda \left(\frac{L}{d} \right) \left(\frac{1}{2} \rho \bar{U}^2 \right) \quad (6.4.37)$$

the (Darcy) friction factor λ is thus given in Eq. (6.4.36) as

$$\lambda = \frac{64}{Re} \quad (6.4.38)$$

When the wall of shear stress τ_w given in Eq. (6.4.29) is non-dimensionalized as is commonly used in the literature, the skin-friction coefficient c_f (or Fanning friction factor) is defined in such a way that

$$c_f = \frac{\tau_w}{\frac{1}{2} \rho \bar{U}^2} = \frac{1}{4} \lambda \quad (6.4.39)$$

The friction factor λ derived from the Poiseuille parabolic, namely the solution of the fully developed laminar pipe flow, is in a generally good agreement with the experiment as compared with the data (Nikuradse 1933) in Fig. 6.11 with the relationship between λ and Re . When the Reynolds number exceeds approximately 2300, in most of engineering applications, the flow undergoes a transition to turbulence, and above approximately 3000 the pipe flow becomes fully turbulent. There is no rigor-

ous solution for turbulent flow in a pipe, where λ in Eq. (6.4.37) is customarily extended in the turbulent flow regime, as shown in Fig. 6.11. It should be mentioned that Fig. 6.11 is based on experimental data obtained from various degrees of roughness of a pipe wall (after Nikuradse experiments with pipes of sand roughness), where ε is the roughness (R.M.S) and d is the diameter of pipe. As effects of the roughness are exemplified in the diagram, when ε/d increases, λ raises, indicating a higher pressure drop (higher wall shear) in the turbulent regime, whereas in the laminar regime, as λ is expressed by $64/Re$, there would not be the effect of the roughness on the pressure drop.

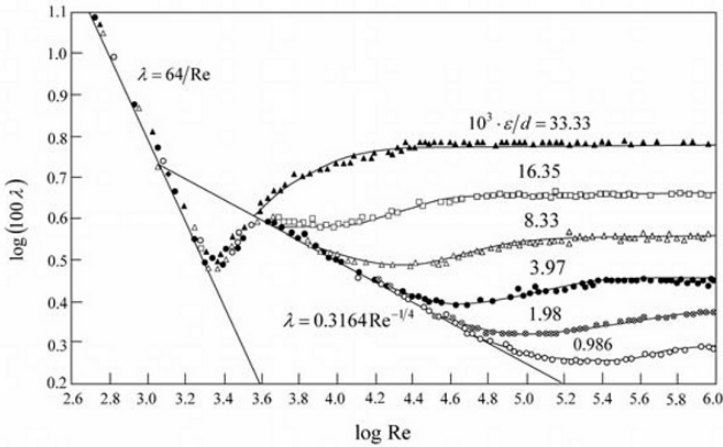


Fig. 6.11 λ vs Re in straight pipe (replotted after Nikuradse, 1933)

With hydrodynamically smooth pipes that are independent of the surface roughness, a curve fitted correlation to a turbulent flow data is given as

$$\lambda = 0.3164 Re^{-1/4} \quad \text{for } Re = 3 \times 10^3 \sim 10^5 \quad (6.4.40)$$

The empirical equation (6.4.40) is called the Blasius formula (1913) that only depends on the Reynolds number, and is often used for practical purposes in engineering. There are several empirical relations for λ in hydrodynamically smooth pipes. Among those, Prandtl's universal law of friction for smooth pipes is valid for a wide range of Reynolds numbers in turbulent flows, which is given as

$$\frac{1}{\sqrt{\lambda}} = 2 \log(Re\sqrt{\lambda}) - 0.8 \quad (6.4.41)$$

C.F. Colebrook (1939) extended the relationship to include the roughness effect for commercial pipes, which is written as

$$\frac{1}{\sqrt{\lambda}} = 1.14 - 2 \log\left(\frac{\varepsilon}{d} + \frac{9.35}{Re\sqrt{\lambda}}\right) \quad (6.4.42)$$

It is of interest to know the velocity profile for fully developed turbulent flows in a circular pipe from experimental verifications. This can be reduced from the Blasius formula (6.4.40) with the definition of the skin-friction coefficient in Eq. (6.4.39) as follows

$$\tau_w = \frac{\lambda}{8} \rho \bar{U}^2 \quad (6.4.43)$$

$$\lambda = \frac{0.3164}{(\bar{U}d/\nu)^{1/4}} \quad (6.4.44)$$

Substituting Eq. (6.4.44) into Eq. (6.4.43) yields τ_w as

$$\tau_w = 0.03326 \eta_0^{1/4} r_0^{-1/4} \bar{U}^{7/4} \rho^{3/4} \quad (6.4.45)$$

If we, as Blasius suggested, assume the power law velocity profile for axisymmetric fully developed a turbulent flow, as schematically shown in Fig. 6.12, we can write

$$\frac{u}{u_{\max}} = \left(\frac{y}{r_0}\right)^n \quad (6.4.46)$$

where u_{\max} is the maximum velocity at the axis of the pipe, $y = r_0 - r$ is the wall distance and n is the power index to be determined. It is noted that u is the time average velocity here in Eq. (6.4.46). The volume flow rate Q is then calculated as

$$\begin{aligned} Q &= \pi r_0^2 \bar{U} = \int_0^{r_0} u(2\pi r dr) \\ &= \int_0^{r_0} u_{\max} \left(\frac{y}{r_0}\right)^n 2\pi(r_0 - y) dy \end{aligned} \quad (6.4.47)$$

Thus

$$\frac{\bar{U}}{u_{\max}} = \frac{2}{(n+1)(n+2)} \quad (6.4.48)$$

and in Eq. (6.4.46), \bar{U} can be written as

$$\bar{U} = \frac{2}{(n+1)(n+2)} u \left(\frac{r_0}{y} \right)^n \quad (6.4.49)$$

Substituting Eq. (6.4.49) into Eq. (6.4.45), we have

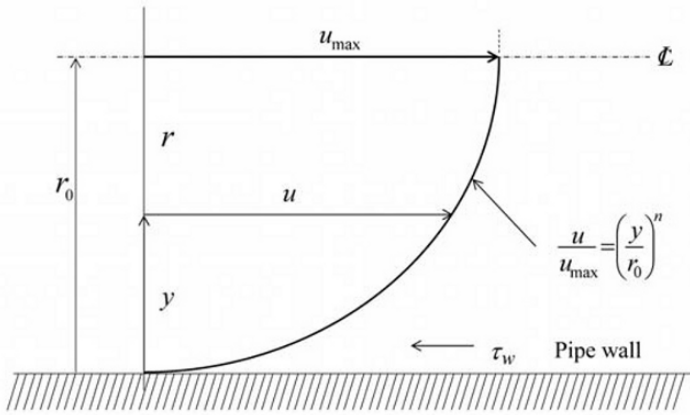


Fig. 6.12 Power law for turbulent velocity profile

$$\tau_w = 0.03326 \left\{ \frac{2}{(n+1)(n+2)} \right\}^{\frac{7}{4}} \eta_0^{\frac{1}{4}} r_0^{-\left(\frac{1}{4}\right) + \left(\frac{7n}{4}\right)} u^{\frac{7}{4}} \rho^{\frac{3}{4}} y^{-\frac{7n}{4}} \quad (6.4.50)$$

It should be reasonable to think that τ_w depends only on fluid properties and the velocity profile u so that τ_w would not include the effect on the radius r_0 in its formulation. This thought would lead to the fact that the power of r_0 in Eq. (6.4.50) is null, i.e.

$$-\frac{1}{4} + \frac{7n}{4} = 0 \quad (6.4.51)$$

And thus, we can obtain n for

$$n = \frac{1}{7} \quad (6.4.52)$$

Consequently, the velocity profile u is written as

$$\begin{aligned} \frac{u}{u_{\max}} &= \left(\frac{y}{r_0} \right)^{\frac{1}{7}} \\ &= \left(1 - \frac{r}{r_0} \right)^{\frac{1}{7}} \end{aligned} \quad (6.4.53)$$

The formula given in Eq. (6.4.53) is termed as the $1/7$ power law of a turbulent velocity profile. By using Eq. (6.4.48), it can be shown that the average velocity u_{\max} are related as

$$\bar{U} = \frac{49}{60} u_{\max} \quad (6.4.54)$$

The turbulent velocity profile near the solid wall will be further extended in consideration with the boundary layer theory, which is studied in later sections.

6.4.3 Transient Hagen-Poiseuille Flow in Pipe

The time development of flow at the rest to the Poiseuille flow can be obtained as an exact solution of a reduced Navier-Stokes equation. Consider a Newtonian flow likewise, as in the previous sections, which are initially at rest in an infinitely long horizontal pipe with a radius r_0 . We will examine the transient behavior where a constant pressure gradient dp/dz is applied at $t = 0$.

The governing equation of this system is such that, i.e. in the cylindrical axisymmetric rectilinear system, without the body force

$$\rho \frac{\partial u_z}{\partial t} = -\frac{\partial p}{\partial z} + \eta_0 \left(\frac{\partial^2 u_z}{\partial r^2} + \frac{1}{r} \frac{\partial u_z}{\partial r} \right) \quad (6.4.55)$$

where u_z is a function of both r and t , i.e. $u_z = u_z(r, t)$. Similar to Eqs. (6.4.23), (6.4.55) can be nondimensionalized through the following relations

$$r^* = \frac{r}{r_0}, \quad t^* = \frac{(\eta_0/\rho)}{r_0^2} t = \frac{\nu}{r_0^2} t \quad \text{and} \quad u^* = \frac{4\eta_0 u_z}{r_0^2 (-\partial p/\partial z)} \quad (6.4.56)$$

The resultant nondimensional equation can be written in the following form

$$\frac{\partial u^*}{\partial t^*} = 4 + \frac{\partial^2 u^*}{\partial r^{*2}} + \frac{1}{r^*} \frac{\partial u^*}{\partial r^*} \quad (6.4.57)$$

For the transient Poiseuille flow from at rest, the initial and boundary conditions to be imposed in Eq. (6.4.57) are

$$\begin{aligned} u^*(r^*, t^*) &= 0 & \text{for } t^* = 0, \quad 0 \leq r^* \leq 1 \\ u^*(r^*, t^*) &= u_{\max}^* & \text{for } t^* > 0, \quad r^* = 0 \\ u^*(r^*, t^*) &= 0 & \text{for } t^* > 0, \quad r^* = 1 \end{aligned} \quad (6.4.58)$$

In order to obtain the analytical solution of Eq. (6.4.57), we decompose u_z with the steady state Poiseuille flow (for $t = \infty$) and the transient term u'_z as follows

$$u_z(r, t) = \frac{1}{4\eta_0} \left(-\frac{\partial p}{\partial z} \right) (r_0^2 - r^2) - u'_z(r, t) \quad (6.4.59)$$

which is rewritten in a nondimensional form

$$u^* = (1 - r^{*2}) - u_p^* \quad (6.4.60)$$

Equation (6.4.57) is then written in terms of u_p^* after the substitution of Eq. (6.4.60) as follows

$$\frac{\partial u_p}{\partial t} = \frac{\partial^2 u_p}{\partial r^2} + \frac{1}{r} \frac{\partial u_p}{\partial r} \quad (6.4.61)$$

It is noted that for a sake of simplicity * will be dropped from the equation in (6.4.61). The new boundary conditions of Eq. (6.4.61) are

$$\begin{aligned} u_p(r, t) &= 1 - r^2 & \text{for } t = 0, \quad 0 \leq r \leq 1 \\ u_p(r, t) &= 1 - u_{\max} & \text{for } t > 0, \quad r = 0 \\ u_p(r, t) &= 0 & \text{for } t > 0, \quad r = 1 \end{aligned} \quad (6.4.62)$$

Equation (6.4.61) can be solved by using a separation of the variable in the following manner

$$u_p(r, t) = R(r) \cdot T(t) \quad (6.4.63)$$

so that we have two ordinary differential equations:

$$\frac{dT}{dt} + T = 0 \quad (6.4.64)$$

$$\frac{d^2 R}{dr^2} + \frac{1}{r} \frac{dR}{dr} + R = 0 \quad (6.4.65)$$

The solution in Eq. (6.4.64) is rather straightforward to give

$$T = T_0 e^{-t} \quad (6.4.66)$$

whereas Eq. (6.4.65) is a Bessel's differential equation of a general form

$$\ddot{R} + \frac{1}{r} \dot{R} + \left(1 - \frac{n^2}{r^2}\right) R = 0 \quad (6.4.67)$$

where $n \geq 0$. It is known that the general solution of the Bessel's equation is given in the following form

$$R = c_1 J_n(r) + c_2 Y_n(r) \quad (6.4.68)$$

The solution $J_n(r)$, which has a finite limit as $r \rightarrow 0$, is called a Bessel function of the first kind. The solution $Y_n(r)$, which has no finite limit as $r \rightarrow 0$, is called a Bessel function of the second kind. The solutions for $R(r)$ and $T(t)$ are thus obtained with the boundary conditions (6.4.62), where we have

$$u(r, t) = (1 - r^2) - u_p(r, t) \\ = (1 - r^2) - \left\{ 8 \sum_{n=1}^{\infty} \lambda_n^{-3} J_1^{-1}(\lambda_n) J_0(\lambda_n r) e^{-\lambda_n^2 t} \right\} \quad (6.4.69)$$

as J_0 and J_1 are the zero-th and first order of Bessel's function, which are generated by the following recurrence formula

$$\frac{2n}{r} J_n(r) = J_{n+1}(r) + J_{n-1}(r) \quad (6.4.70)$$

and for the n positive integer we have

$$J_0(r) = 1 - \frac{r^2}{2^2} + \frac{r^4}{2^2 4^2} - \frac{r^6}{2^2 4^2 6^2} + \dots \quad (6.4.71)$$

In Fig. 6.13, some $J_n(r)$ are displayed for a reference. λ_n that appeared in (6.4.69) is the n th root of $J_0(\lambda) = 0$, which are given as

$$\lambda_n = \frac{\pi}{4} m \left\{ 1 + \frac{2}{(\pi m)^2} - \frac{62}{3(\pi m)^4} + \frac{15116}{15(\pi m)^6} - \dots \right\} \quad (6.4.72)$$

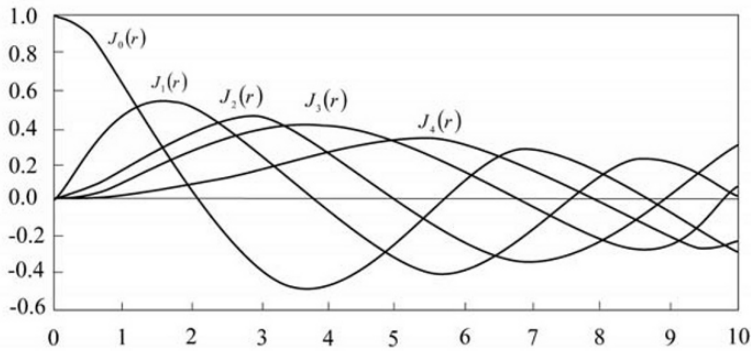


Fig. 6.13 Bessel's function of first kind

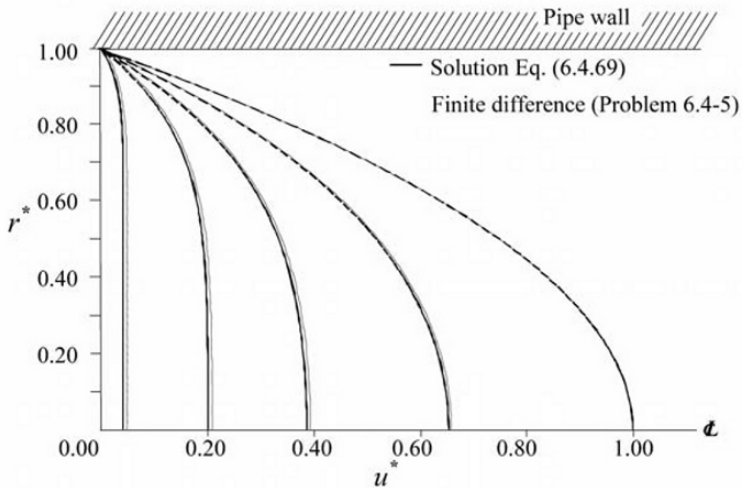


Fig. 6.14 Transient Poiseuille flow

where $m = 4n - 1$. The detailed derivation of the solution (6.4.69) is found in Szymaniski (1932) and Papanastasiou et al. (2000).

As a result of the solution expressed in Eq. (6.4.69), the transient behavior of the flow is shown in Fig. 6.14, where it is seen that two (both analytical and numerical) flow velocities evolve from a rest position as time elapses to reach the maximum center speed $u(0, \infty) = 1$.

It is mentioned that Eq. (6.4.57) is a partial differential equation of a parabolic type that is solved numerically fairly easily, such as the finite difference method. In Fig. 6.14, as an example, a numerical solution by the finite difference method is displayed in comparison with the analytic solution of Eq. (6.4.69).

Exercise

Exercise 6.4.1 Inclined Plane Poiseuille Flow

Let's us consider the incompressible steady laminar flow between two inclined plates as shown in Fig. 6.15. Obtain the velocity profile of u as a function of y for the one dimensional rectilinear flow in $x-y$ plane, assuming the pressure gradient $\partial p / \partial x$ is constant.

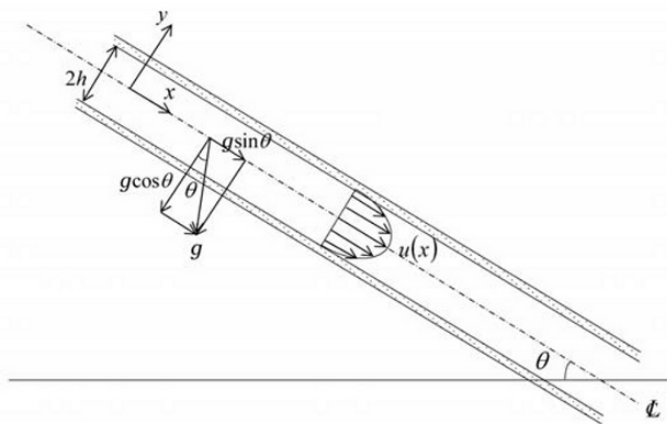


Fig. 6.15 Inclined plane Poiseuille flow

Ans.

The Navier-Stokes equation can be reduced to the following form in the $x-y$ plane

$$0 = -\frac{\partial p}{\partial x} + \eta_0 \frac{\partial^2 u}{\partial y^2} + \rho g \sin \theta \quad (1)$$

With the boundary conditions such that

$$\frac{du}{dy} = 0 \quad \text{for } y = 0 \quad (2)$$

and

$$u = 0 \quad \text{for } y = h \quad (3)$$

Equation (1) can be solved for u , which yields the solution as

$$u(y) = \frac{1}{2\eta_0} \left(-\frac{\partial p}{\partial x} + \rho g \sin \theta \right) (h^2 - y^2) \quad (4)$$

The body force (the gravity) is added to the pressure gradient to increase, depending on the sign of $\sin \theta$.

Exercise 6.4.2 Laminar Flow in a Square Duct

Suppose that an incompressible Newtonian fluid is flowing through an infinitely long square duct. The flow is assumed laminar with the constant pressure gradient along the flow direction z . Determine the velocity profile in the square cross section of the $x-y$ plane, as depicted in Fig. 6.16.

Ans.

The situation is that the non-accelerating and unidirectional flow of the velocity component u_z is persisting in the duct with a constant pressure gradient. We apply the Stokes' equation given in Eq. (6.4.17) in z -direction, so that we can write the governing equation of flow as

$$\frac{\partial^2 u_z}{\partial x^2} + \frac{\partial^2 u_z}{\partial y^2} = -\frac{1}{\eta_0} \frac{\partial p}{\partial z} \quad (1)$$

Equation (1) can be nondimensionalized by the relationships

$$x^* = \frac{x}{a}, \quad y^* = \frac{y}{a} \quad \text{and} \quad u^* = \frac{2\eta_0 u_z}{a^2(-\partial p/\partial z)} \quad (2)$$

through which the resultant nondimensionalized equation for Eq. (1) will be written as

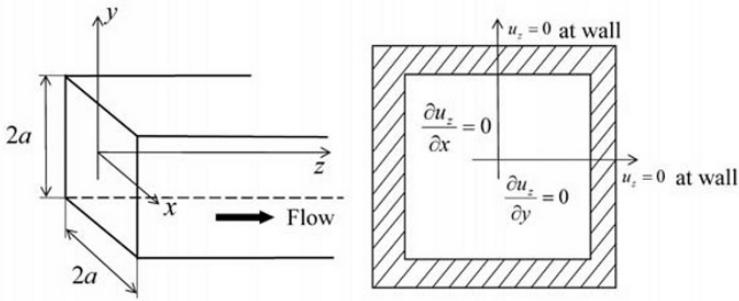


Fig. 6.16 Flow in a square duct

$$\frac{\partial^2 u}{\partial x^2} + \frac{\partial^2 u}{\partial y^2} = -2 \quad (3)$$

It is noted that * is dropped in Eq. (3) for a sake of clarity. The boundary conditions in the first quadrant plane (due to symmetry) are written below. Note that at the center of the duct the symmetric conditions in both x and y axis are given respectively together with the no-slip conditions at the wall.

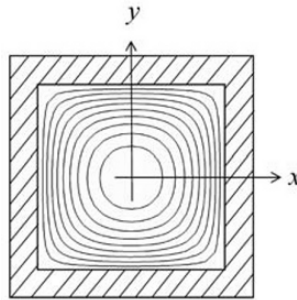


Fig. 6.17 Velocity contour in a duct flow

$$\begin{aligned}
\frac{\partial u}{\partial y} &= 0 & \text{for } x &= 0 \\
\frac{\partial u}{\partial x} &= 0 & \text{for } y &= 0 \\
u &= 0 & \text{for } x &= 1 \\
u &= 0 & \text{for } y &= 1
\end{aligned} \tag{4}$$

Similar to Eq. (6.4.59), by decomposing u_z with the plane Poiseuille flow, we have

$$u_z(x, y) = \frac{1}{2\eta_0} \left(-\frac{\partial p}{\partial z} \right) (a^2 - y^2) + u'_z(x, y) \tag{5}$$

and with a nondimensional form, we can write

$$u = (1 - y^2) + u_p \tag{6}$$

Equation (3) of the Poisson equation can now be reduced into the Laplace's equation by substituting Eq. (6) into Eq. (3) to write

$$\frac{\partial^2 u_p}{\partial x^2} + \frac{\partial^2 u_p}{\partial y^2} = 0 \tag{7}$$

The boundary conditions for u_p are newly written as

$$\begin{aligned}
\frac{\partial u_p}{\partial y} &= 0 & \text{for } x &= 0 \\
\frac{\partial u_p}{\partial x} &= 0 & \text{for } y &= 0 \\
u_p &= -(1 - y^2) & \text{for } x &= 1 \\
u_p &= 0 & \text{for } y &= 1
\end{aligned} \tag{8}$$

In Eq. (7) the boundary conditions (8) are the same as the heat conduction problem in a square plate, to which the analytical solution is possible by solving the equation through the method of the separation of variables. The solution for u_p consists of particular product solutions in the form

$$u_p(x, y) = X(x)Y(y) \tag{9}$$

Substituting Eq. (9) into Eq. (7) yields

$$\frac{d^2 X}{dx^2} Y + X \frac{d^2 Y}{dy^2} = 0 \quad (10)$$

and after separating the variables, we may be able to set the equation to the flow

$$-\frac{1}{X} \frac{d^2 X}{dx^2} = \frac{1}{Y} \frac{d^2 Y}{dy^2} = c^2 \quad (11)$$

where c^2 is the arbitrary constant. As a result, there follows a set of ordinary differential equations

$$\frac{d^2 X}{dx^2} + c^2 X = 0 \quad (12)$$

$$\frac{d^2 Y}{dy^2} - c^2 Y = 0 \quad (13)$$

Equations (12) and (13) constitute a Sturm-Liouville problem through which the characteristic values are given where

$$c = c_n = (2n-1)\frac{\pi}{2} \quad \text{for } n=1,2,3,\dots \quad (14)$$

It follows that the solution is written for a series of the form where

$$u_p = \sum_{n=1}^{\infty} a_n \cos(c_n y) \cosh(c_n x) \quad (15)$$

and a_n satisfies Eq. (7) with the boundary conditions in (8). The final form of u_p is given as

$$u_p = \sum_{n=1}^{\infty} 4 \frac{(-1)^n}{c_n^3 \cosh(c_n)} \cos(c_n y) \cosh(c_n x) \quad (16)$$

It should be kept in mind that the actual solution of u is expressed with Eq. (6) by substituting u_p in Eq. (16). In Fig. 6.17, the velocity profile is schematically drawn by velocity contour, which is the same as the temperature contour in the case of a heat conduction problem.

Note that Eq. (7) is a partial differential equation of the elliptic type. The equation can be fairly easily solved by a numerical method, such as

the finite difference method. The reader may be worth trying to write a program code to solve the problem. This is left to reader's own discretion, similar to the Problem in 6.4-5 (which is a type of parabolic partial differential equation).

Problems

- 6.4-1. Can the Poiseuille flow be used as a means of measuring the viscosities of liquids? Describe how and give a limitation for the method.

Ans. [Yes, within the laminar flow]

- 6.4-2. In a horizontal circular pipe with a diameter of $10 \times 10^{-3} \text{ m}$, a fluid with a viscosity of $1 \times 10^{-2} \text{ Pa} \cdot \text{s}$ and density $1.2 \times 10^3 \text{ kg/m}^3$ is flowing. The discharge is $4.0 \times 10^{-7} \text{ m}^3/\text{s}$. Find the pressure drop in a 10m section, and a maximum velocity in the pipe cross section.

$$\text{Ans. } \left[\begin{array}{l} \Delta p = 1.63 \times 10^6 \text{ N/m}^2 \\ u_{\max} = 1.02 \text{ m/s} \end{array} \right]$$

- 6.4-3. Find the laminar flow velocity profile in a circular annulus for $a \leq r \leq b$. Assume that the pressure drop in a length l is Δp . The fluid properties are such that the density is ρ and the viscosity is η_0 , which are kept constant. Also show that the maximum velocity occurs at $r = \{0.5(b^2 - a^2)/\ln(b/a)\}^{\frac{1}{2}}$.

$$\text{Ans. } \left[u = \frac{\Delta p}{4\eta_0 l} \left\{ (b^2 - a^2) \frac{\ln(b/r)}{\ln(a/b)} + (b^2 - r^2) \right\} \right]$$

- 6.4-4. Prove Eq. (6.4.50).

- 6.4-5. Write a finite difference code for solving Eq (6.4.57).

Ans. [Refer Section 7.3.3.2]

- 6.4-6. Show that the velocity profile of the laminar flow in a square duct is equivalent to the temperature distribution of the heat conduction of an identical square plate (without internal heat generation).

- 6.4-7. Verify that the volumetric flow rate Q through a square duct is given where

$$Q = -\frac{4}{3\eta_0} \left(\frac{\partial p}{\partial z} \right) a^4 \left[1 - 6 \sum_{n=1}^{\infty} \left\{ \frac{\tanh(c_n)}{c_n^5} \right\} \right]$$

for a steady laminar flow of Newtonian fluid.

6.5 Laminar Boundary Layer Theory

The conceptual thought on the boundary layer is already given in the previous sections, for example, in the Problems 4.1-6, 4.1-8, and Section 6.3.3. From a phenomenological point of view, the boundary layer is important to flow, as in confined narrow regions near solid walls, where the effect of viscosity comes into play. In addition, all the previous examples of the viscous flow, in one way or another, have hinted strongly at boundary layer behavior.

The idea about a boundary layer was first put forth by Prandtl (1904), in his celebrated boundary layer equations, and a great deal of quantitative information was also obtained in the exact solutions given by his student, Blasius (1908). Von Kármán (1921), suggested an integral method over the thickness of the boundary layer, using a guessed velocity profile rather than obtaining the exact solution of the equations. The excellent idea of Kármán's leads to estimate the drag and wall shear of a viscous flow past a flat plate at a high Reynolds number, and that is valid, in effect, for either laminar or turbulent flow. The theory of the boundary layer carries particular importance in designing aircrafts, turbo blades in various turbo machineries, and those are categorized as external flows. In this section, the thin boundary layer approximations will be discussed. The boundary layer is laminar at first and, as the Reynolds number increases, it undergoes a transition to turbulence. In order to convey the essence of the theory, the flows that we discuss in this chapter are laminar, for which the Reynolds numbers are not too high. We will begin to study a two dimensional laminar boundary layer flow in order to gain a fundamental insight within the framework of the traditional approach.

6.5.1 Flow over a Flat Plate

Consider the laminar flow over a flat plate when the Reynolds number, which we have yet to define, is high enough, before it undergoes a transition to turbulence. Here, we expect that the flow of an incompressible

Newtonian fluid with density ρ and viscosity η_0 is planar, with no cross-stream velocity component, as indicated in Fig. 6.18. The flow in the confined narrow region of high shear stress beginning from the leading edge close to the plate, whose thickness is $\delta(x)$, is two dimensional with velocity components, $\mathbf{u} = (u_x, u_y, 0) = (u, v, 0)$. The boundary layer thickness $\delta(x)$ is defined in such way that the height about the plate is $u = 0.99U$, meaning that the streamwise velocity component u is within 1% of the free stream velocity U , although u to U is asymptotic in direction. The velocity boundary conditions of the boundary layer require no-slip and no penetration at the wall of the flat plate, i.e. $u(x, 0) = 0$ and $v(x, 0) = 0$ for $x \geq 0$. Also, above the plate, outside the boundary layer the flow is treated as the inviscid, i.e. $u(x, y) = U$ and $v(x, y) = 0$ for $x > 0$ and $y \gg \delta(x)$.

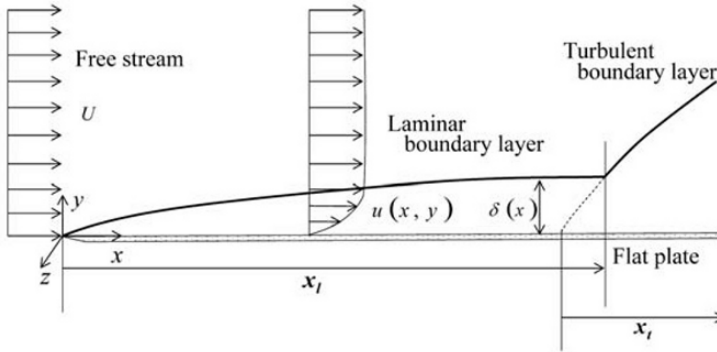


Fig. 6.18 Boundary layer over a flat plate

In the boundary layer, more importantly inertial effects and viscous effects are both significant, so that it appears that we need to solve the Navier-Stokes equation, whereas outside the boundary layer the Euler equation may be used. By focusing our attention within the boundary layer, we may write the continuity equation and the Navier-Stokes equation, as the starting point for a discussion on flat plate boundary layer flow. The non-dimensionalized governing equations are given by taking the representative length scale as x , velocity as U , time scale as x/U and pressure scale as ρU^2 , as follows

$$\frac{\partial u^*}{\partial x^*} + \frac{\partial v^*}{\partial y^*} = 0 \quad (6.5.1)$$

$\mathcal{O}(1) \quad \mathcal{O}(1)$

$$\frac{\partial u^*}{\partial t^*} + u^* \frac{\partial u^*}{\partial x^*} + v^* \frac{\partial u^*}{\partial y^*} = -\frac{\partial p^*}{\partial x^*} + \frac{1}{Re_x} \left(\frac{\partial^2 u^*}{\partial x^{*2}} + \frac{\partial^2 u^*}{\partial y^{*2}} \right) \quad (6.5.2)$$

$\mathcal{O}(1) \quad \mathcal{O}(1) \quad \mathcal{O}(1) \quad \mathcal{O}(\delta^{*2}) \left\{ \mathcal{O}(1) \mathcal{O}\left(\frac{1}{\delta^{*2}}\right) \right\}$

$$\frac{\partial v^*}{\partial t^*} + u^* \frac{\partial v^*}{\partial x^*} + v^* \frac{\partial v^*}{\partial y^*} = -\frac{\partial p^*}{\partial y^*} + \frac{1}{Re_x} \left(\frac{\partial^2 v^*}{\partial x^{*2}} + \frac{\partial^2 v^*}{\partial y^{*2}} \right) \quad (6.5.3)$$

$\mathcal{O}(\delta^*) \quad \mathcal{O}(\delta^*) \quad \mathcal{O}(\delta^*) \quad \mathcal{O}(\delta^{*2}) \left\{ \mathcal{O}(\delta^*) \mathcal{O}\left(\frac{1}{\delta^{*2}}\right) \right\}$

In applying Eqs. (6.5.1), (6.5.2) and (6.5.3) to the boundary layer, substantial simplification of these equations can be made by recalling that;

(i) the flow is predominantly parallel to the plate, i.e. $u \gg v$

(ii) the boundary layer thickness $\delta(x)$ is very thin, i.e. $\delta(x) \ll x$

implying that axial derivatives of velocity components are much smaller than the transverse derivatives of those same components, and that the transverse pressure gradient is much smaller than the axial pressure gradient.

Using the conditions from (i) and (ii), we can perform an order-of-magnitude analyses. In order to make the point clear in Eqs. (6.5.1), (6.5.2) and (6.5.3), the order of each term is shown in the equations below, where $\mathcal{O}(1)$ is determined such a way that, for example, $u^* = u/U \approx 1$ and $x^* \approx 1$ so that $\partial u^*/\partial x^* \approx \mathcal{O}(1)$, whereas $v^* = v/U \approx \delta^*$ and $y^* = \delta/x \approx \delta^*$ so that $\partial v^*/\partial y^* \approx \mathcal{O}(1)$, and so on. Let Re_x denote the Reynolds number, defined by

$$Re_x = \frac{Ux}{(\eta_0/\rho)} = \frac{Ux}{\nu} \quad (6.5.4)$$

The important issue that arises for the viscous terms of $\partial^2 u^*/\partial y^{*2}$ and $\partial^2 v^*/\partial y^{*2}$, for which as $Re_x \rightarrow \infty$ and $\delta^* \rightarrow 0$, the condition of Eqs. (6.5.2) and (6.5.3) not being reached to the inviscid limit is that

$$\frac{1}{Re_x} \times \frac{\partial^2 u^*}{\partial y^{*2}} \approx o(1) \quad (6.5.5)$$

and Eq. (6.5.5) indicates that Re_x has to have the order

$$Re_x \approx \frac{1}{\delta^{*2}} \quad (6.5.6)$$

as already displayed below, each term in Eqs. (6.5.2) and (6.5.3). Eq. (6.5.6) consequently shows the important fact that the boundary layer thickness $\delta(x)$ becomes thicker toward downstream, along the axial direction followed by the relation

$$\delta \approx \frac{x}{\sqrt{Re_x}} \quad (6.5.7)$$

The pressure is such that $p^* \approx o(1)$, and since in y direction the variation of p^* is very small, i.e. $\partial p^* / \partial y^* \approx o(\delta^*)$, p^* is in effect given by the inviscid flow outside the boundary layer.

It is now desired to derive an expression for the boundary layer flow by using the order-of-magnitude analysis, and as a result we obtain the set of simplified equations in a dimensional form as follows

$$\frac{\partial u}{\partial x} + \frac{\partial v}{\partial y} = 0 \quad (6.5.8)$$

$$\rho \left(\frac{\partial u}{\partial t} + u \frac{\partial u}{\partial x} + v \frac{\partial u}{\partial y} \right) = -\frac{\partial p}{\partial x} + \eta_0 \left(\frac{\partial^2 u}{\partial y^2} \right) \quad (6.5.9)$$

$$0 = -\frac{\partial p}{\partial y} \quad (6.5.10)$$

and for the inviscid core flow

$$\frac{\partial U}{\partial t} + U \frac{\partial U}{\partial x} = -\frac{1}{\rho} \frac{\partial p}{\partial x} \quad (6.5.11)$$

These are the so-called Prandtl's boundary layer equation. The boundary layer equations however, are still kept in nonlinear terms (as seen in Eq. (6.5.9) in convective terms. Nevertheless, one of the important aspects of the equations is that the pressure gradient in Eq. (6.5.9) may be determined

by knowing the pressure distribution in the inviscid core flow given in Eq. (6.5.11) over the same surface shape.

It should be mentioned that the boundary layer equations are valid for moderately curved surfaces, and for that

$$\frac{\partial p}{\partial y} = \varepsilon_x \rho u^2 \quad (6.5.12)$$

where ε_x is a representative curvature of the curved surface.

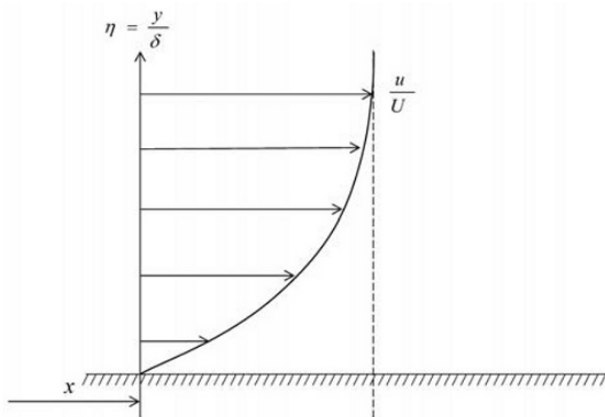


Fig. 6.19 Nondimensional velocity profile by η

Blasius gave analytical solutions to the boundary layer equations, assuming that the flow is steady and the pressure distribution in an inviscid flow over a flat plate is uniform, i.e. $\partial p / \partial x = 0$, so that we have

$$\frac{\partial u}{\partial x} + \frac{\partial v}{\partial y} = 0 \quad (6.5.13)$$

$$\rho \left(u \frac{\partial u}{\partial x} + v \frac{\partial u}{\partial y} \right) = \eta_0 \left(\frac{\partial^2 u}{\partial y^2} \right) \quad (6.5.14)$$

Blasius showed that a similarity solution (the velocity profile) of these equations can be obtained by introducing a new parameter

$$\eta = \frac{y}{\delta} = \frac{y}{\sqrt{\nu x / U}} = \frac{y}{x} Re_x^{\frac{1}{2}} \quad (6.5.15)$$

where δ is adopted from Eq. (6.5.7). Note that η is a conventionally defined parameter (it should not be confused with the viscosity), which scales the directional distance from the wall at position x , as shown in Fig. 6.19. It is reasonable to state that the nondimensional velocity distribution function f_n would be expressed in terms of η to write

$$\frac{u}{U} = f_n(\eta) \quad (6.5.16)$$

Since the velocity profile would be written in terms of η , we may be able to introduce a stream function ψ by letting $\int f_n(\eta) d\eta = f(\eta)$, as follows

$$\psi(x, y) = \sqrt{\nu U x} f(\eta) \quad (6.5.17)$$

Using Eq. (6.5.17), we are able to write the velocity component u and v where

$$u = \frac{\partial \psi}{\partial y} = U f'(\eta) \quad (6.5.18)$$

$$v = -\frac{\partial \psi}{\partial x} = \frac{1}{2} \sqrt{\frac{\nu U}{x}} \{ \eta f'(\eta) - f(\eta) \} \quad (6.5.19)$$

and a substitution of Eqs. (6.5.18) and (6.5.19) to Eq. (6.5.14) yields

$$2f''' + ff'' = 0 \quad (6.5.20)$$

Equation (6.5.20) is the Blasius equation, which is a nonlinear, third-order, ordinary differential equation that is solved for the boundary conditions

$$f = \frac{df}{d\eta} = 0 \text{ for } \eta = 0 \quad (6.5.21)$$

and

$$\frac{df}{d\eta} \rightarrow 1 \text{ as } \eta \rightarrow \infty \quad (6.5.22)$$

It is mentioned that the function $f(\eta)$ that satisfies Eq. (6.5.20) and the boundary condition is the Blasius solution.

The exact analytic solution has not yet been obtained. Otherwise, matching inner and outer series solutions is found to be one of techniques for solving the equation such as shown by Meksyn (1961) and Rosenhead

(1963) that gives:

(i) Near wall;

$$f(\eta) = \sum_{n=0}^{\infty} \left(-\frac{1}{2}\right)^n \frac{\alpha^{n+1} C_n}{(3n+2)!} \eta^{3n+2} \quad (6.5.23)$$

where $C_0 = 1$, $C_1 = 1$, $C_2 = 11$, $C_3 = 375$, $C_4 = 27897$ and $C_5 = 3817137$.

(ii) Infinite distance from wall;

$$f(\eta) = \eta - \beta + \gamma \int_{\eta}^{\infty} d\eta \int_{\eta}^{\infty} e^{-\left(\frac{1}{4}\right)(\eta-\beta)^2} d\eta \quad (6.5.24)$$

(iii) Matching α , β and γ ;

Matching Eqs. (6.5.23) and (6.5.24) is given by taking the constants

$$\alpha = 0.332, \beta = 1.73 \text{ and } \gamma = 0.231$$

where f , f' and f'' are joined in the region of the solution.

The numerical solution for the Blasius equation is readily available. Note that at the edge of the boundary layer, which is defined as the location where $u^* = u/U = 0.99$, occurs for $\eta = 4.91 \approx 5.0$, the result of a numerical solution for the Blasius equation. Therefore, we have a value of 99% boundary layer thickness given as

$$\delta \approx 5.0xRe_x^{-\frac{1}{2}} \quad (6.5.25)$$

It is confirmed that the Blasius solution does agree with experiments, such as Liepmann's (1943), showing that the similarity of the velocity profile in the flat plate is held.

Note that from experimental verification, the turbulent boundary layer starts to persist for a flat plate with a zero attack angle for $Re_x \geq 5 \times 10^5$.

6.5.2 Integral Analysis of Boundary Layer Equation

The direct analytical approach to solve the boundary layer equation involves much difficulties, as seen from the solution of the Blasius equation. However, if the velocity profile within the boundary layer can be assumed to be known, we may be able to gain a great deal of quantitative informa-

tion by simply integrating Prandtl's boundary layer equation. Particularly, in most of engineering problems, estimation of a frictional drag force over an objective solid wall is of primary importance.

In this section, we will derive the momentum integral equation, following an idea first put forth by von Kármán (1921), and calculate the frictional drag on a flat plate at high Reynolds numbers. The control volume chosen for the analysis is sketched in Fig. 6.20, where the velocity is defined at a downstream position x from the leading edge of a flat plate.

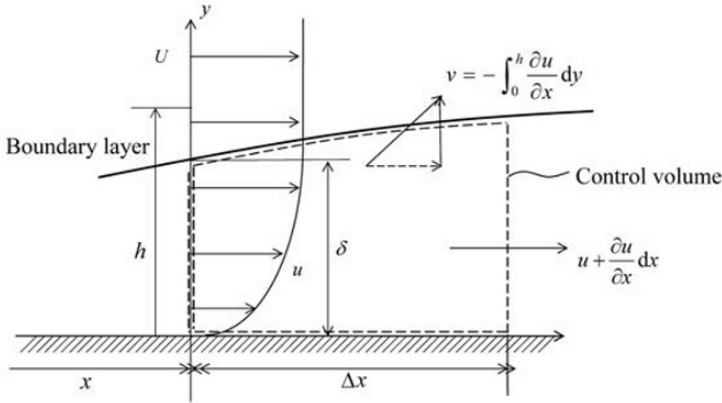


Fig. 6.20 Control volume for a boundary layer

Consider the boundary layer equation, the momentum equation in x direction given in Eq. (6.5.9), and integrate the equation from the wall to the height beyond the thickness of the boundary layer, i.e. $0 \leq y \leq h$, as follows

$$\int_0^h \frac{\partial u}{\partial t} dy + \int_0^h u \frac{\partial u}{\partial x} dy + \int_0^h v \frac{\partial u}{\partial y} dy = - \int_0^h \frac{1}{\rho} \frac{\partial p}{\partial x} dy + v \frac{\partial u}{\partial y} \Big|_0^h \quad (6.5.26)$$

The last term on the right hand side of Eq. (6.5.26) can be written as

$$\begin{aligned} v \frac{\partial u}{\partial y} \Big|_0^h &= v \left(\frac{\partial u}{\partial y} \right)_h - \frac{1}{\rho} \left(\eta_0 \frac{\partial u}{\partial y} \right)_0 = 0 - \frac{1}{\rho} \tau_w \\ &= - \frac{1}{\rho} \tau_w \end{aligned} \quad (6.5.27)$$

when τ_w is the wall of shear stress. The last term of Eq. (6.5.26) can be written as

$$\nu \frac{\partial u}{\partial y} \Big|_0^h = \frac{1}{\rho} \int_0^h \frac{\partial \tau}{\partial y} dy = -\frac{\tau_w}{\rho} \quad (6.5.28)$$

It should be kept in mind that Eq. (6.5.27) or (6.5.28) can be valid for any flow mode (laminar or turbulence). Similarly, the continuity equation in Eq. (6.5.8) is integrated to give

$$v = - \int_0^h \left(\frac{\partial u}{\partial x} \right) dy \quad (6.5.29)$$

Using Eq. (6.5.29), the last term on the left hand side of Eq. (6.5.26) can be reduced to the following form, after eliminating v and carrying out the integration by parts

$$\begin{aligned} \int_0^h v \frac{\partial u}{\partial y} dy &= - \int_0^h \left(\frac{\partial u}{\partial y} \int_0^h \frac{\partial u}{\partial x} dy \right) dy \\ &= -U \int_0^h \frac{\partial u}{\partial x} dy + \int_0^h u \frac{\partial u}{\partial x} dy \end{aligned} \quad (6.5.30)$$

The momentum equation is thus written altogether as

$$\int_0^h \frac{\partial u}{\partial t} dy + \int_0^h 2u \frac{\partial u}{\partial x} dy - U \int_0^h \frac{\partial u}{\partial x} dy = - \int_0^h \frac{1}{\rho} \frac{\partial p}{\partial x} dy - \frac{\tau_w}{\rho} \quad (6.5.31)$$

The pressure term in Eq. (6.5.31) is eliminated by the inviscid flow equation in Eq. (6.5.11), and after some arrangements, we can write the equation to give

$$\begin{aligned} \int_0^h \frac{\partial U}{\partial t} dy - \int_0^h \frac{\partial u}{\partial t} dy + \int_0^h U \frac{\partial u}{\partial x} dy + \int_0^h u \frac{\partial U}{\partial x} dy \\ - \int_0^h 2u \frac{\partial u}{\partial x} dy + \int_0^h U \frac{\partial U}{\partial x} dy - \int_0^h u \frac{\partial U}{\partial x} dy = \frac{\tau_w}{\rho} \end{aligned} \quad (6.5.32)$$

The resultant integral equation of momentum change seems formidable at first glance, but leads to no novel algebraic difficulties by reducing the common terms together as follows

$$\int_0^h \frac{\partial}{\partial t} (U - u) dy + \int_0^h \frac{\partial}{\partial x} [u(U - u)] dy + \frac{\partial U}{\partial x} \int_0^h (U - u) dy = \frac{\tau_w}{\rho} \quad (6.5.33)$$

Some simplifications are expressed in Eq. (6.5.33) by virtue of defining the properties of δ' and θ by taking $h \rightarrow \infty$, where for the fixed control volume the integral equation of Eq. (6.5.33) is rewritten with the following compact form

$$\frac{\partial(U\delta')}{\partial t} + \frac{\partial}{\partial x}(U^2\theta) + U\delta' \frac{\partial U}{\partial x} = \frac{\tau_w}{\rho} \quad (6.5.34)$$

where we define δ' and θ respectively

$$\delta' = \int_0^\infty \left(1 - \frac{u}{U}\right) dy \quad (6.5.35)$$

$$\theta = \int_0^\infty \left(1 - \frac{u}{U}\right) \left(\frac{u}{U}\right) dy \quad (6.5.36)$$

Equation (6.5.34) was first derived by von Kàrmàn (1921) and is often referred to as the Kàrmàn integral equation. The equation is valid for both laminar and turbulence flows, as long as the velocity profile $u(x, y, t)$ is known *a priori*. The boundary conditions for the integration in Eq. (6.5.34) are

$$u = 0 \quad \text{for } y = 0$$

$$u = U \quad \text{and} \quad \frac{\partial u}{\partial y} = 0 \quad \text{for } y = \infty \quad (6.5.37)$$

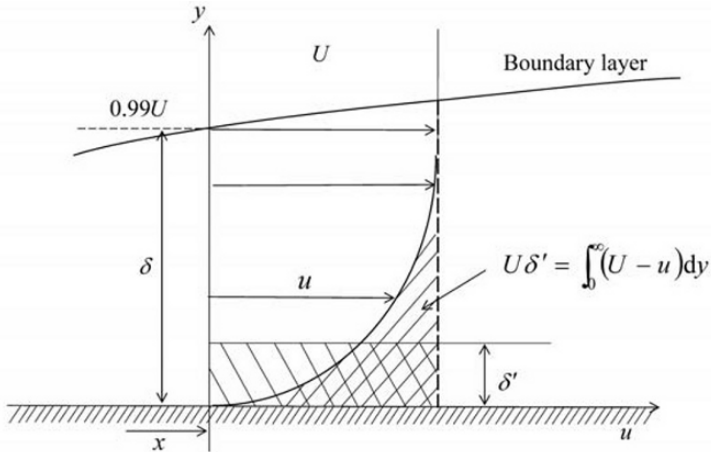


Fig. 6.21 Displacement thickness

As seen in Eq. (6.5.34), there are two new additional lengths in boundary layer theory, as defined in Eqs. (6.5.35) and (6.5.36). There are the displacement thickness δ' and the momentum thickness θ . The displacement thickness is the equivalent thickness of the deficit of volume flow rate in the boundary layer compared to the inviscid flow limit by the continuity consideration, as schematically shown in Fig. 6.21. The momentum thickness is the equivalent thickness of the momentum loss due to the deficit of mass (volume flow rate) in the boundary layer.

For a steady flow over a flat plate with a zero pressure gradient, that is $\partial p / \partial x = 0$ and $U(x) = U = \text{const.}$, i.e. $\partial U / \partial x = 0$, the momentum loss is solely due to wall friction, and this is simply expressed in Eq. (6.5.34) as

$$\tau_w = \rho U^2 \frac{\partial \theta}{\partial x} \quad (6.5.38)$$

The momentum thickness θ is often used to represent a characteristic length in turbulent boundary layer studies.

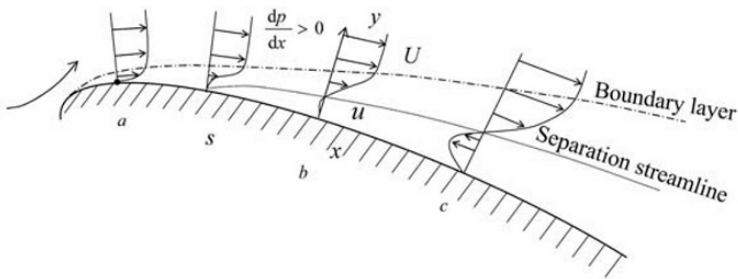
6.5.3 Boundary Layer Separation

The boundary layer theory based on thin layer approximations discussed in this chapter does not apply in so-called separated regions, such as observed along curved surfaces. Nevertheless, the boundary layer theory can give an estimate to the point of occurrence of the separation, and is able to give an explanation of the phenomena. Here we will consider the phenomenon of boundary layer separation and vortex formation behind bluff bodies.

The velocity profile in the boundary layer depends upon the potential flow outside the boundary layer. The core flow, which may be accelerated or decelerated, is determined by the flow situation and geometry of the wall. The phenomenon of boundary layer separation occurs for flow, which has an adverse pressure gradient, $dp/dx > 0$, as illustrated in Fig. 6.22(a). Particularly with a flow over a curved surface, such as flow over an airfoil, as representatively displayed in Fig. 6.22(a), the inviscid flow is decelerated, the separation of boundary layer from the wall starts at s and in the downstream b and c , the reverse flow persists with $\partial u / \partial y < 0$, whereas in the upstream a the flow is forward at x direction with $\partial u / \partial y > 0$. The separation streamline, which is of a zero velocity contour coincides with the wall, leaves the surface at the separation point s and extends toward the downstream. When the Reynolds number of flow is sufficiently high, at the downstream of the separation point below the separation streamline, the wake takes place which is typically characterized by irregular eddies.

In the wake, large energy loss due to high mixing may occur, resulting in a large pressure loss, and causes a higher pressure difference between the leading edge and the trailing edge, increasing in the pressure drag. The boundary layer separation may be seen in a diffuser or in a highly divergent channel in which there exists a strong adverse pressure gradient. However, there would not be boundary layer separation for a flow over a flat plate at a zero attack angle since the pressure gradient is always kept negative, and the laminar boundary layer formed close to the leading edge grows and changes to a turbulent passing through a transition region, when the plate is sufficiently long.

(a)



(b)

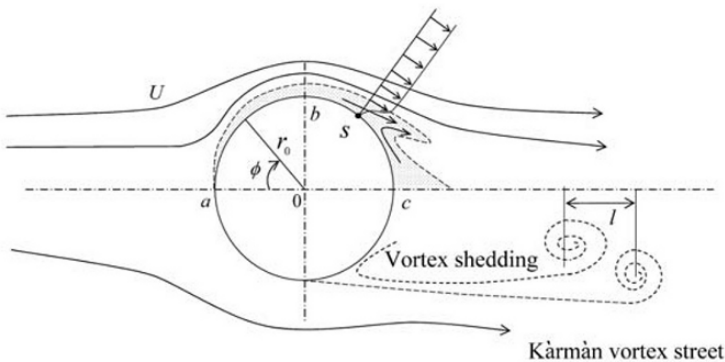


Fig. 6.22 Boundary layer separation and vortex formation

The very important phenomenon of boundary layer separation can be more clearly explained by considering the flow around a circular cylinder, as illustrated in Fig. 6.22(b). In consideration of an inviscid fluid, the flow is accelerated on the upstream cylindrical surface, a to b, and decelerated on the downstream surface, b to c. The adverse pressure gradient occurs in the region of b to c and the boundary layer below the inviscid flow would separate at point s on the cylindrical surface. As illustrated in Fig. 6.22(b), after the point s, backward flow in vicinity of the wall, due to higher pressure in flow direction and toward flow in the upper layer of separation a streamline causes the vortex formation. The separation point is predicted at the angle of $\phi \geq 90^\circ$ with the boundary layer theory based on inviscid outer flow. However, for viscous flow, the situation is somewhat different from the inviscid flow case. For example, at a Reynolds number of $Re = 9500$ (based on radius r_0), the angle of separation point s is approximately $\phi \approx 80.5^\circ$ (Hiemez, experiment 1911), which is quite different from the inviscid flow. The boundary layer approximation gives a first order estimate, but is inadequate in the separated flow since a large scale separation may alter the flow field greatly.

The vortex generated in the vicinity of the separation point s is increased in size and becomes separated shortly afterwards and sheds from the wall, regularly and alternately from opposite sides. The resulting flow downstream, in the wake, is often referred to as a Kármán vortex street. It occurs in the Reynolds number (based on diameter, $Re = dU/\nu$), $40 \leq Re \leq 10000$, and is accompanied by turbulence. In order to quantify the vortex shedding, dimensional analysis may be applied by defining the Strouhal number where

$$St = \frac{fd}{U} \quad (6.5.39)$$

where f is the frequency of shedding the vortices. The dimensional analysis yields, so that St is a function of the Reynolds number and can be expressed by an empirical relation

$$St = 0.198(1 - 19.7Re^{-1}) \quad (6.5.40)$$

for the range of $250 \leq Re \leq 2 \times 10^5$. As found in Eq. (6.5.40), St approaches to the value of 0.198 as the Reynolds number becomes high. Therefore, the frequency f is directly proportional to the velocity U and inverse of the diameter d for a large Reynolds number, i.e. $f \approx 0.198(U/d)$.

Vortex shedding from an object (such as a cylindrical object) in a flow may cause periodic lateral forces, when the frequency of a vortex shedding is equal to the natural frequency of the object. The phenomenon of resonance may occur in the object, appearing as the aerodynamic vibration. The engineer must be very careful to be aware that such an aerodynamic vibration can cause a failure of structures, such as towers, chimneys, suspension wire-bridge, and so forth. Furthermore, a long continuous aerodynamic vibration may cause metal fatigue, leading structures to malfunction.

6.5.4. Integral Relation for Thermal Energy

In the case of heating on a flat plate, the energy equation is used to estimate local values of heat transfer and the associated thickness of a thermal boundary layer. The basic concept of the development of a thermal boundary layer is sketched in Fig. 6.23, where the flow is heated at a constant temperature with T_w beginning at the point of x_{r0} .

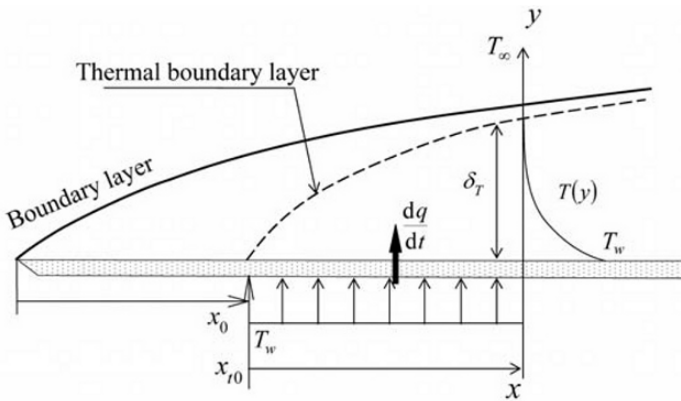


Fig. 6.23 Thermal boundary layer

In order to derive an expression for the thermal boundary layer, we must first look into the energy equation where there is a heat transfer from the plate to the flow in the vicinity of the wall. The nondimensionalized energy equation in Eq. (6.2.34), will be written in two dimensional $x-y$ coordinates system, assuming the flow is incompressible and the thermal conductivity k_c of fluid is kept constant, as follows

$$\begin{aligned}
& \left(\frac{\partial T^*}{\partial t^*} + u^* \frac{\partial T^*}{\partial x^*} + v^* \frac{\partial T^*}{\partial y^*} \right) \\
&= \frac{1}{Re_x} \left(\frac{1}{Pr} \right) \left(\frac{\partial^2 T^*}{\partial x^{*2}} + \frac{\partial^2 T^*}{\partial y^{*2}} \right) \\
& \quad + \frac{1}{Re_x} (Ec) \left\{ 2 \left(\frac{\partial u^*}{\partial x^*} \right)^2 + 2 \left(\frac{\partial v^*}{\partial y^*} \right)^2 + \left(\frac{\partial u^*}{\partial y^*} + \frac{\partial v^*}{\partial x^*} \right)^2 \right\} \quad (6.5.41)
\end{aligned}$$

Then we carry out the order-of-magnitude analysis, similar to the Prandtl boundary layer equations, discarding the terms $(\partial u^*/\partial x^*)^2$ and $\partial^2 T^*/\partial x^{*2}$, where we have the energy equation for the thermal boundary in resultant dimensional form

$$\rho c_p \left(\frac{\partial T}{\partial t} + u \frac{\partial T}{\partial x} + v \frac{\partial T}{\partial y} \right) = k_c \frac{\partial^2 T}{\partial y^2} + \eta_0 \left(\frac{\partial u}{\partial y} \right)^2 \quad (6.5.42)$$

The boundary conditions are, with the aid of Fig. 6.23, given as

$$\begin{aligned}
T(x, 0, t) &= T_w(x, t) \\
T(x, \infty, t) &= T_\infty(x, t)
\end{aligned} \quad (6.5.43)$$

For the initial and inlet conditions, respectively

$$\begin{aligned}
T(x, y, 0) &\equiv \text{given} \\
T(x_0, y, t) &\equiv \text{given}
\end{aligned} \quad (6.5.44)$$

Equation (6.5.42) is also written in terms of thermodynamic properties and the shear stress in the conservation form as

$$\frac{\partial(\rho h_0)}{\partial t} + \frac{\partial(\rho u h_0)}{\partial x} + \frac{\partial(\rho v h_0)}{\partial y} = \frac{\partial}{\partial y} (-q + u \tau_{xy}) \quad (6.5.45)$$

where $h_0 = c_p T + u^2/2$ is the total enthalpy of the flow. Neglecting the kinetic energy of $u^2/2$, since $c_p T \gg u^2/2$, the integral form of Eq. (6.5.45) is thus, for the wall heat transfer q_w , written as

$$q_w = \frac{\partial}{\partial t} \left(\int_0^\infty \rho c_p T dy \right) + \frac{\partial}{\partial x} \left\{ \int_0^\infty \rho u (h_0 - h_{0\infty}) dy \right\} + \rho c_p v T \Big|_0^\infty - u \tau_{xy} \Big|_0^\infty$$

$$\approx \frac{\partial}{\partial t} \left(\int_0^\infty \rho c_p T dy \right) + \frac{\partial}{\partial x} \left\{ \int_0^\infty \rho u (h_0 - h_{0\infty}) dy \right\} \quad (6.5.46)$$

Furthermore, for the steady flow, i.e. $\partial/\partial t = 0$, we can write the heat transfer quantity q_w as

$$q_w = \frac{d}{dx} \left[\int_0^\infty \rho u \left\{ \left(h + \frac{1}{2} u^2 \right) - \left(h_\infty + \frac{1}{2} U^2 \right) \right\} dy \right] \quad (6.5.47)$$

where at the flat plate wall, $q_w = -k_c \partial T / \partial y \big|_{y=0}$. It should be kept in mind that Eq. (6.5.47) is usually valid for a low speed laminar flow or a turbulent boundary layer, customarily neglecting kinetic energy of $u^2/2$ and $U^2/2$ (as $Ec \ll 1$). Thus the energy integral relation in the thermal boundary layer, we can write

$$q_w = \frac{d}{dx} \left\{ \int_0^\infty \rho c_p u (T - T_\infty) dy \right\} \quad (6.5.48)$$

From Eq. (6.5.48) it is useful to derive an expression for the wall heat transfer by defining the enthalpy thickness δ_h defined as

$$\delta_h = \int_0^\infty \left(\frac{T - T_\infty}{T_w - T_\infty} \right) \frac{u}{U} dy \quad (6.5.49)$$

so that we have

$$q_w = \rho U c_p (T_w - T_\infty) \frac{d\delta_h}{dx} = -k_c \frac{\partial T}{\partial y} \bigg|_{y=0} \quad (6.5.50)$$

where the thermophysical properties, ρ , c_p , η_0 and k_c are assumed to be kept constant throughout the flow and thermal boundary layer.

Exercise

Exercise 6.5.1 Estimation of Drag Coefficient on Flat Plate

Consider a flat plate with a zero attack angle and obtain the drag force on one side of the surface with a width of b and a length of l , assuming that

the flow is isothermal, incompressible and in a steady laminar flow. The fundamental geometrical configuration is shown in Fig. 6.24.

Ans.

For a flat plate with a zero attack angle, the condition for an inviscid core flow parallel to the plate is given as $dU/dx = 0$, so that from the Kàrmàn integral equation, the local wall shear stress τ_w is expressed in Eq. (6.5.38) to be written as

$$\tau_w(x) = \rho U^2 \frac{d\theta}{dx} \quad (1)$$

where θ is the momentum thickness and is a function of x . θ can be determined if the velocity profile in the boundary layer is known. We will exploit a similarity solution of the velocity profile

$$\frac{u}{U} = f_n(\eta) = f(\eta) \quad (2)$$

where η is the y -directional distance from the wall defined by $\eta = y/\delta(x)$, and $\delta(x)$ is the boundary layer thickness. θ and τ_w , thus, will be expressed in terms of η as follows

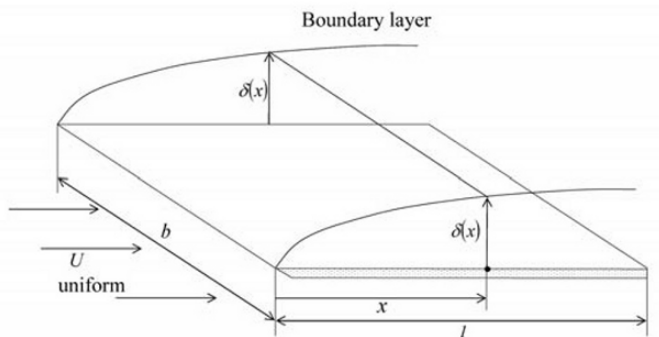


Fig. 6.24 Flow over a flat plate

$$\begin{aligned} \theta &= U^{-2} \int_0^\infty u(U-u)dy = \delta \int_0^1 f(1-f)d\eta \\ &= c_1 \delta \end{aligned} \quad (3)$$

$$\begin{aligned}
 \tau_w &= \eta_0 \left(\frac{\partial u}{\partial y} \right)_{y=0} = \eta_0 \frac{U}{\delta} \left[\frac{\partial(u/U)}{\partial \eta} \right]_{\eta=0} \\
 &= c_2 \frac{\eta_0 U}{\delta}
 \end{aligned} \tag{4}$$

where $c_1 = \int_0^1 f(1-f) d\eta$ and $c_2 = f'(0)$. Substituting Eqs. (3) and (4) into Eq. (1), we have a new equation

$$\delta \frac{d\delta}{dx} = \left(\frac{c_2}{c_1} \right) \frac{\nu}{U} \tag{5}$$

and is solved for δ where

$$\delta = \sqrt{2 \left(\frac{c_2}{c_1} \right)} \sqrt{\frac{\nu x}{U}} \tag{6}$$

Therefore, if the displacement thickness δ' is defined, such that

$$\delta' = c_3 \delta \tag{7}$$

where $c_3 = \int_0^1 (1-f) d\eta$, we have

$$\delta' = c_3 \sqrt{2 \left(\frac{c_2}{c_1} \right)} \sqrt{\frac{\nu x}{U}} \tag{8}$$

and for θ , similarly

$$\theta = c_1 \sqrt{2 \left(\frac{c_2}{c_1} \right)} \sqrt{\frac{\nu x}{U}} \tag{9}$$

The required drag force F_D on one side of the flat plate is thus calculated as

$$\begin{aligned}
 F_D &= \int_0^l b \tau_w dx \\
 &= \int_0^l \rho b U^2 d\theta \\
 &= b \sqrt{2 c_1 c_2} \sqrt{\nu \rho^2 l U^3}
 \end{aligned}$$

$$= \sqrt{2c_1c_2} \sqrt{\nu \rho^2 b^2 l U^3} \quad (10)$$

and the drag coefficient c_f is expressed by definition to be written as

$$c_f = \frac{F_D}{bl \left(\frac{1}{2} \rho U^2 \right)} = \frac{2\sqrt{2c_1c_2}}{\sqrt{\frac{Ul}{\nu}}} = 2\sqrt{2c_1c_2} Re_l^{-\frac{1}{2}} \quad (11)$$

It is therefore mentioned that F_D and c_f are obtained by simply calculating c_1 and c_2 by giving the velocity distribution function $f(\eta)$.

In order to calculate Eqs. (10) and (11), we will take an approach of guessing $f(\eta)$ in the first place. Let us assume that $f(\eta)$ is the polynomial function of the 4th order, where

$$f(\eta) = \alpha_0 + \alpha_1\eta + \alpha_2\eta^2 + \alpha_3\eta^3 + \alpha_4\eta^4 \quad (12)$$

where constants $\alpha_0 \sim \alpha_4$ are determined from the following physical conditions of the boundary layer.

$$(i) \ u = 0 \text{ so that } f(0) = 0 \quad \text{for } y = 0$$

$$(ii) \ \nu \frac{\partial^2 u}{\partial y^2} = \frac{1}{\rho} \frac{dp}{dx} = -U \frac{dU}{dx} \quad \text{so that } f''(0) = 0 \text{ for } y = 0$$

$$(iii) \ u = U \text{ so that } f(1) = 1 \quad \text{for } y = \delta$$

$$(iv) \ \frac{\partial u}{\partial y} = 0 \text{ so that } f'(1) = 0 \quad \text{for } y = \delta$$

$$(v) \ \frac{\partial^2 u}{\partial y^2} = 0 \text{ so that } f''(1) = 0 \text{ for } y = \delta$$

It is noted that for $y = 0$, there is no-slip condition on the wall, i.e. $\nu = 0$ and $u = 0$, so that ν does not appear in the conditions (i) ~ (v). By applying the conditions (i) ~ (v) to Eq. (12), we can obtain the constants

$$\alpha_0 = 0, \alpha_1 = 2, \alpha_2 = 0, \alpha_3 = -2 \text{ and } \alpha_4 = 1$$

that give the velocity distribution function f as

$$f(\eta) = 2\eta - 2\eta^3 + \eta^4 \quad (13)$$

Thus, the drag force F_D and the drag coefficient c_f are given, according

to Eqs. (10) and (11) and calculating c_1 and c_2 from Eqs. (3) and (4), by

$$F_D = 0.6854\sqrt{\nu\rho^2b^2IU^3} \quad (14)$$

and

$$c_f = 1.371Re_l^{-\frac{1}{2}} \quad (15)$$

Note that from the Blasius' analytical solution, c_f is given where

$$c_f = 1.328Re_l^{-\frac{1}{2}} \quad (16)$$

The difference between Eqs. (15) and (16) is small, showing that the approach taken for the von Kàrmàn integral equation by adopting a guess-velocity profile is correct. c_f in Eq. (15) or (16) is valid for $10^3 \leq Re_l \leq 5 \times 10^5$, as long as the boundary layer is thin enough ($\delta \ll x$). The method of the guess-velocity for the Kàrmàn integral equation is also used for turbulent flows, by giving an appropriate turbulent velocity profile in the boundary layer.

Exercise 6.5.2 Heat Transfer from a Flat Plate

Assume the profile of thermal boundary layer with reference to Fig. 6.23 is given by a following second order polynomial function, similar to a second order polynomial function guessed by velocity profile (see Problem 6.5-1), such that

$$T - T_\infty = (T_w - T_\infty) \left\{ 1 - 2\left(\frac{y}{\delta_T}\right) + \left(\frac{y}{\delta_T}\right)^2 \right\} \quad (1)$$

Estimate the heat transfer from the flat plate to the fluid. Note that the heating region begins at the leading edge, $x_0 = 0$, with reference to Fig. 6.23, and that u is given where

$$u = U \left\{ 2\left(\frac{y}{\delta}\right) - \left(\frac{y}{\delta}\right)^2 \right\} \quad (2)$$

Ans.

The heat transfer rate q_w from the plate wall to the fluid is given in Eq.

(6.5.48), and with the given temperature profile in Eq. (1) and the velocity profile in Eq. (2), we have

$$q_w = \rho U c_p (T_w - T_\infty) \frac{d}{dx} \int_{\delta_0}^{\delta_\infty} \left\{ 1 - 2 \left(\frac{y}{\delta_T} \right) + \left(\frac{y}{\delta_T} \right)^2 \right\} \left\{ 2 \left(\frac{y}{\delta} \right) - \left(\frac{y}{\delta} \right)^2 \right\} dy$$

$$= -k_c \left. \frac{\partial T}{\partial y} \right|_{y=\infty} \quad (3)$$

Taking into account that for the integration over the thermal boundary layer thickness δ_T

$$\delta|_0^\infty = \delta|_{y=\infty} - \delta|_{y=0} \approx \delta_T = \zeta \delta \quad (4)$$

so that Eq. (3) can be written as

$$\rho U c_p (T_w - T_\infty) \frac{d}{dx} \left[\delta \left(\frac{\zeta^2}{6} - \frac{\zeta^3}{30} \right) \right] = \frac{2k_c (T_w - T_\infty)}{\zeta \delta} \quad (5)$$

where $\zeta = \delta_T / \delta$ is the boundary thickness ratio. Eq. (5) is further reduced to the form after differentiation to write

$$\frac{d\delta}{dx} \frac{1}{6} \left(\zeta^3 - \frac{\zeta^4}{5} \right) = \frac{2}{\delta U} \left(\frac{k_c}{\rho c_p} \right) \quad (6)$$

For the velocity profile in Eq. (2), we have (see Problem 6.5.1)

$$\delta^2 = \frac{30\eta_0 x}{\rho U} \quad \text{or} \quad \frac{\delta}{x} = 5.5 Re_x^{-\frac{1}{2}} \quad (7)$$

and

$$\delta \frac{d\delta}{dx} = \frac{15\eta_0}{\rho U} \quad (8)$$

Substituting Eq. (8) for Eq. (6), and after rearranging, we have a non-dimensional equation

$$\zeta^3 - \frac{\zeta^4}{5} \approx \frac{4}{5} \frac{k_\alpha}{\nu} = 0.8 Pr^{-1} \quad (9)$$

where k_α is the thermal diffusivity $k_\alpha = k_c / \rho c_p$ and Pr is the Prandtl number. The solution in Eq. (9) for ζ with Pr being not too far from

unity is obtained to be

$$\zeta \approx Pr^{\frac{1}{3}} \quad (10)$$

Thus the local heat transfer q_w is written with the aid of Eqs. (7) and (10) as

$$q_w \approx 2k_c (T_w - T_\infty) \frac{Re_x^{\frac{1}{2}} Pr^{\frac{1}{3}}}{5.5x} \quad (11)$$

Furthermore, the local Nusselt number can be obtained as

$$Nu_x = \frac{q_w x}{k_c (T_w - T_\infty)} = 0.364 Re_x^{\frac{1}{2}} Pr^{\frac{1}{3}} \quad (12)$$

For comparison reasons it is quoted that the analytical solution is available in Schlichting (1955), for Nu_x to give

$$Nu_x = 0.339 Re_x^{\frac{1}{2}} Pr^{\frac{1}{3}} \quad (13)$$

The difference is not as large as obtained in Eq. (12) from the guessed profile method.

In two dimensional boundary layer flow, if Pr is not far from unity, there exists a relationship between the heat flux q_w and the wall shear stress τ_w as follows

$$\frac{q_w}{\tau_w} = \frac{k_c \left(\frac{\partial T}{\partial y} \right)_w}{\eta_0 \left(\frac{\partial u}{\partial y} \right)_w} = \frac{k_c}{\eta_0} \left| \frac{dT}{du} \right|_w \quad (14)$$

where it is assumed that the behavior of u and T in the boundary layer is similar. The relation (14) is known as the Reynolds' analogy. Considering Eq. (11) in Exercise 6.5.1 and Eq. (12) in Exercise 6.5.2 to Eq. (14), we can relate Nu_x (representing q_w) and c_f (representing τ_w) as follows

$$Nu_x = \frac{1}{2} c_f Re_x Pr^{\frac{1}{3}} \quad (15)$$

For $Pr = 1$, we have the relationship

$$Nu_x = \frac{1}{2} c_f Re_x \quad (16)$$

Equation (16) is the simplest form of the Reynolds' analogy. It is of interest to consider that the expression Eq. (15) is expanded in more general form of the Reynolds' analogy, which is valid for all laminar boundary layer flow, and is written as

$$Nu_x = \frac{1}{2} c_f Re_x f\left(\frac{x}{l}, Pr\right) \quad (17)$$

where $f(x/l, Pr)$ is a function determined by experiments or analysis. It is noted that frequently in practice, the Stanton number Sn (the local Stanton number Sn_x) is used instead of the Nusselt number, which is defined as

$$Sn_x = \frac{Nu_x}{Re_x Pr} \quad (18)$$

Using Sn_x , Eq. (15) it is written as

$$Sn_x = \frac{1}{2} c_f Pr^{-\frac{2}{3}} \quad (19)$$

Problems

6.5-1. The guessed laminar and turbulent velocity profiles in the boundary layer on a flat plate with a zero attack angle is given by the parabolic and the 1/7-power law respectively as follows

$$\frac{u}{U} = 2\left(\frac{y}{\delta}\right) - \left(\frac{y}{\delta}\right)^2; \text{ laminar} \quad (1)$$

and

$$\frac{u}{U} = \left(\frac{y}{\delta}\right)^{\frac{1}{7}}; \text{ turbulence} \quad (2)$$

Show that

(i) for a laminar flow; $Re_x \leq 5 \times 10^5$

$$\delta \approx 5.5xRe_x^{-\frac{1}{2}} \quad (3)$$

$$c_f \approx 0.73Re_x^{-\frac{1}{2}} \quad (4)$$

(ii) for a turbulent flow; $5 \times 10^5 \leq Re_x \leq 1 \times 10^7$

$$\delta \approx 0.38xRe_x^{-\frac{1}{5}} \quad (5)$$

$$c_f \approx 0.059Re_x^{-\frac{1}{5}} \quad (6)$$

6.5-2. Define the boundary layer thickness δ , the displacement thickness δ' and the momentum thickness θ , and give the physical interpretation by discussing the importance of the three thicknesses.

6.5-3. Give the limitation of applying the boundary layer theory to an actual viscous flow over a bluff body.

6.5-4. For a flat plate with a zero attack angle, calculate the boundary layer thickness at a point of $x = 0.5\text{m}$ from the leading edge, if the free stream velocity of air is $U = 0.05\text{m/s}$, where the density is $\rho = 1.16\text{ kg/m}^3$ and the kinematic viscosity is $\nu = 1.60 \times 10^{-5}\text{ m}^2/\text{s}$. Also, predict the net drag force for one side of the plate if the surface is 2 m wide and 4 m long. Is the flow laminar or turbulence? If the free stream velocity of the inviscid core flow is increased to $U = 5\text{ m/s}$, predict the net drag force, taking into account of the laminar portion, where $Re_x \leq 5 \times 10^5$. Use relations in Problem 6.5-1 (to be more precise relations Exercise 6.6.1 may be used and also see Problem 6.6-4).

$$Ans. \left[\begin{array}{l} \text{For } U = 0.05\text{ m/s, } Re_x = 1560 \text{ laminar, } \delta = 0.07\text{ m} \\ F_D = 2.14\text{ N} \\ \text{For } U = 5.0\text{ m/s, } F_D \approx 0.553\text{ N} \end{array} \right]$$

6.5-5. Prove Eq. (5) in Exercise 6.5.2.

$$\begin{aligned}
 & \left[\begin{aligned}
 q_w &\approx \frac{d}{dx} \left\{ \int_{\delta_0}^{\delta_w} \rho_p U (T_w - T_\infty) \left(\frac{2y}{\delta} - \frac{y^2}{\delta^2} \right) \left(1 - \frac{2y}{\delta_r} + \frac{y^2}{\delta_r^2} \right) dy \right\} \\
 &\approx \frac{d}{dx} \left\{ \rho_p U (T_w - T_\infty) \int_{\delta_0}^{\delta_w} \left(\frac{2y}{\delta} - \frac{y^2}{\delta^2} \right) \left(1 - \frac{2y}{\delta_r} + \frac{y^2}{\delta_r^2} \right) dy \right\} \\
 \delta|_\infty - \delta|_0 &= [\delta]_0^\infty = \delta_r = \zeta \delta \\
 \int_{\delta_0}^{\delta_w} \left(\frac{2y}{\delta} - \frac{4y^2}{\zeta^2 \delta^2} + \frac{2y^3}{\zeta^2 \delta^3} - \frac{y^2}{\delta^2} + \frac{2y^3}{\zeta^2 \delta^3} - \frac{y^4}{\zeta^2 \delta^5} \right) dy &= \delta \left(\frac{\zeta^2}{6} - \frac{\zeta^3}{30} \right) \\
 \therefore q_w &\approx \frac{d}{dx} \left[\rho_p U (T_w - T_\infty) \delta \left(\frac{\zeta^2}{6} - \frac{\zeta^3}{30} \right) \right]
 \end{aligned} \right]
 \end{aligned}$$

6.6 Turbulent Flow

Osborne Reynolds (1895) tried to give theoretical explanation for the empirical criterion $Ud/\nu \leq 2300$ that rules out turbulent flow, observed in his celebrated experimental apparatus, the Reynolds tank. He manipulated the continuity and Navier-Stokes equations into a form that can predict the time-averaged behavior of turbulence. When entering into the subject of turbulent flow, it is essential to understand that, in most engineering applications, the kind of flows is shear flow. They can be bound by a solid wall or they may be free, such as with boundary layers and pipe flows, or free jets and wakes. In this section, greater emphasis is placed on the flow characteristics of a mean flow from the act of turbulence, rather than on turbulent motions and their associated structure. Moreover, we will combine the subject into incompressible Newtonian flows for the sake of clear understanding.

The nature of turbulent flow is three dimensional, at which velocity and pressure at a certain point do not remain constant with time but perform highly irregular fluctuations, and mixing of fluid in a turbulent flow, is much higher than in laminar flow, resulting in a more uniform mean of velocity distribution in comparison to a laminar flow, owing to a mixed dispersion of momentum. Also the intermittency is of notable phenomenon, as observed in measuring a turbulent flow field, such as the velocity record in relation to time variations. This phenomenon can occur when noticing the Reynolds number is close to the transition between the laminar and the turbulent flow in pipes and boundary layers.

Turbulent motions of fluid particles are so complex that they cannot be treated individually, although they are deterministic and predictable in

principle from the mass and momentum equations, once an appropriate boundary and initial conditions are given. In practice, because of the apparent randomness of turbulent flows, we will take an averaging approach to obtain the means of motion to enable us to discover a statistical flow description that includes turbulent properties. The average value of a flow quantity f (such as u or p) of a Eulerian flow description in turbulent flows is obtained via an ensemble average that is defined by

$$\overline{f}(\mathbf{x}, t) = \lim_{N \rightarrow \infty} \frac{1}{N} \left[\sum_{i=1}^N f(\mathbf{x}, t)_i \right] \quad (6.6.1)$$

where all samples are drawn at the same time with the same position relative to the flow field boundaries. The ensemble average expressed in Eq. (6.6.1) allows for the possibility of an unsteady mean flow. However, from a practical point of view, data drawn from an ensemble average of nominally identical experiments is never available. Indeed, in turbulent flows, most available quantitative information will be gained for flows that are statistically stationary flows, the average of f given by the time average that is defined as

$$\overline{f}(\mathbf{x}_0, t) = \frac{1}{T} \int_{t_0}^{t_0+T} f(\mathbf{x}_0, t) dt \quad (6.6.2)$$

where \mathbf{x}_0 is a point $\mathbf{x} = \mathbf{x}_0$, T the averaging time and t_0 the starting time. Note that t_0 is not important. Nevertheless, T must be large enough so that any further time elapsed has no significant effect on the measured value of \overline{f} . For f in the statistically stationary flows, the ergodic hypothesis is held such that the ensemble average of each flow variable is the same as its time average in certain fairly general conditions.

According to Reynolds, we decompose each flow variable f as a sum of the mean value \overline{f} and the fluctuation f' from the mean. Thus,

$$f(\mathbf{x}, t) = \overline{f}(\mathbf{x}, t) + f'(\mathbf{x}, t) \quad (6.6.3)$$

and simply, as illustrated in Fig. 6.25, we can write

$$f = \overline{f} + f' \quad (6.6.4)$$

It is clearly shown that

$$\overline{f'} = 0 \text{ and } \overline{\overline{f}} = \overline{f} \quad (6.6.5)$$

and that for the differential operation we have

$$\overline{\nabla f} = \nabla \bar{f} \quad \text{and} \quad \frac{\partial \bar{f}}{\partial t} = \frac{\partial \bar{f}}{\partial t} \quad (6.6.6)$$

It will prove useful to mention that the root mean square of f' , i.e. $\left(\overline{|f'|^2}\right)^{\frac{1}{2}}$ is not zero, and in consideration of f as the instantaneous velocity \mathbf{u} in the turbulent flow field (i.e. $f \equiv \mathbf{u}$), we can define the relative turbulent intensity I as

$$I = \frac{\left(\overline{|u'|^2}\right)^{\frac{1}{2}}}{|\bar{\mathbf{u}}|} \quad (6.6.7)$$

The turbulent intensity is often used for determining the level of turbulent intensity. In a typical turbulent flow in an engineering application, the turbulent intensity is approximately $I \approx 0.1$. Note that the critical Reynolds number at the transition depends upon I in the upstream.

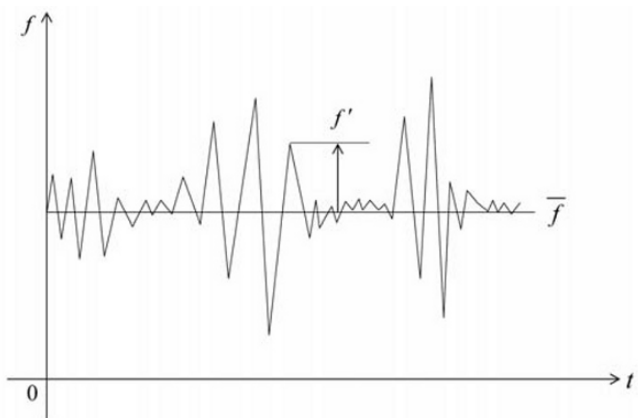


Fig. 6.25 Superimposition of turbulent fluctuation f' and the mean value \bar{f}

Now we shall consider the mass and momentum conservation equations for an incompressible, isothermal, Newtonian fluid of density ρ and viscosity η_0 , respectively:

$$\nabla \cdot \mathbf{u} = 0 \quad (6.6.8)$$

and

$$\rho \left(\frac{\partial \mathbf{u}}{\partial t} + \nabla \cdot \rho \mathbf{u} \mathbf{u} \right) = -\nabla p + \eta_0 \nabla^2 \mathbf{u} \quad (6.6.9)$$

where the gravitational (body force) term is ignored. Decomposing \mathbf{u} and p respectively where

$$\mathbf{u} = \bar{\mathbf{u}} + \mathbf{u}' \quad (6.6.10)$$

$$p = \bar{p} + p' \quad (6.6.11)$$

and substituting into Eqs. (6.6.8) and (6.6.9) yields

$$\nabla \cdot (\bar{\mathbf{u}} + \mathbf{u}') = 0 \quad (6.6.12)$$

and

$$\begin{aligned} & \rho \left[\frac{\partial (\bar{\mathbf{u}} + \mathbf{u}')}{\partial t} + \nabla \cdot (\bar{\mathbf{u}} \bar{\mathbf{u}} + \bar{\mathbf{u}} \mathbf{u}' + \mathbf{u}' \bar{\mathbf{u}} + \mathbf{u}' \mathbf{u}') \right] \\ & = -\nabla (\bar{p} + p') + \eta_0 \nabla^2 (\bar{\mathbf{u}} + \mathbf{u}') \end{aligned} \quad (6.6.13)$$

Taking the average of each term in Eqs. (6.6.12) and (6.6.13) as a result, we can obtain

$$\nabla \cdot \bar{\mathbf{u}} = 0 \quad (6.6.14)$$

and

$$\rho \frac{\partial \bar{\mathbf{u}}}{\partial t} + \nabla \cdot \rho \bar{\mathbf{u}} \bar{\mathbf{u}} = -\nabla \bar{p} + \eta_0 \nabla^2 \bar{\mathbf{u}} + \nabla \cdot (-\rho \overline{\mathbf{u}' \mathbf{u}'}) \quad (6.6.15)$$

Equation (6.6.15) differs from the Navier-Stokes equation for the average flow because of the extra term on the last term in the right hand side of the equation. This quantity

$$\boldsymbol{\tau}_R = -\rho \overline{\mathbf{u}' \mathbf{u}'} \quad (6.6.16)$$

is called the Reynolds stress, and Eq. (6.6.15) is called the Reynolds equation. The Reynolds stress $\boldsymbol{\tau}_R$ acts on a control surface that moves with the local averaging velocity $\bar{\mathbf{u}}$, just as though a stress equals to $-\hat{\mathbf{n}} \cdot (\rho \overline{\mathbf{u}' \mathbf{u}'})$.

There is a closure problem in the Reynolds equation for the Reynolds stress in Eq. (6.6.16), which has to be attained with an appropriate equation. In order to eliminate the closure problem and to obtain an appropriate equation, we may be able to set a transport equation for $\overline{\mathbf{u}'\mathbf{u}'}$, by setting

$$\text{Eq. (6.6.13)} \overline{\mathbf{u}' \cdots \mathbf{u}'} \text{ dyadic product of } \mathbf{u}' \text{ to Eq. (6.6.13) then averaging} \quad (6.6.17)$$

Equation (6.6.17), after some manipulation, however, generates a higher order of terms, such as $\nabla \cdot \overline{\mathbf{u}'\mathbf{u}'\mathbf{u}'}$, and consequently it requires another effort to give an equation for $\overline{\mathbf{u}'\mathbf{u}'\mathbf{u}'}$, and so forth. This would require endless labor without knowing substantial information. In order to make the problem easier, we need an independent equation for the Reynolds stress. The independent equation for the nature of a constitutive equation or a so-called turbulent model may be necessary.

It is appropriate to give a turbulent model analogous to a Newtonian constitutive equation, by referring to Eq. (6.11), to the Reynolds stress where

$$-\rho \overline{\mathbf{u}'\mathbf{u}'} = \eta_t \left(\nabla \overline{\mathbf{u}} + \nabla \overline{\mathbf{u}}^T \right) - \frac{2}{3} \rho k \mathbf{I} \quad (6.6.18)$$

or in tensor notation

$$-\rho \overline{u'_i u'_j} = \eta_t \left(\frac{\partial \overline{u}_i}{\partial x_j} + \frac{\partial \overline{u}_j}{\partial x_i} \right) - \frac{2}{3} \rho k \delta_{ij} \quad (6.6.19)$$

where η_t is defined as the eddy viscosity and k is the average kinetic energy of the turbulence per unit mass, which is defined as

$$\begin{aligned} k &= \frac{1}{2} \overline{\mathbf{u}' \cdot \mathbf{u}'} \\ &= \frac{1}{2} \overline{u'^2_{ii}} = \frac{1}{2} \overline{u'^2_{jj}} \end{aligned} \quad (6.6.20)$$

It should be mentioned that the addition of the second term in Eq. (6.6.18) or Eq. (6.6.19) is due to the result of defining k as expressed in Eq. (6.6.20). From the definition of k in Eq. (6.6.20), \sqrt{k} is used as a characteristic scale of velocity if no other velocity characterizes the turbulent flow. Thus, it is appropriate to define the Reynolds number for the turbulence as

$$Re_t = \frac{\sqrt{k}l_c}{(\eta_0/\rho)} = \frac{\sqrt{k}l_c}{\nu} \quad (6.6.21)$$

where l_c is the characteristic length, which can also be chosen as the length scale of the largest fluctuations, such as a diameter in a pipe flow.

It is necessary to estimate the scales of time and the length in a turbulent flow for a consideration of the turbulence structure and a statistical description of the fluctuations. The important scales of length and time are the Kolmogorov scales. The argument used to estimate those scales is based on the idea that the kinetic energy is transferred down the energy cascade to smaller and smaller length scales with an increased rate of deformation induced by the smallest eddies. There would be an end of energy cascade where the length is sufficiently small enough for the energy to be dissipated by a viscous action. The mean rate of dissipation energy per unit of mass ε is brought in the equilibrium region by larger eddies, where the turbulence is assured to be locally isotropic. At the equilibrium region the kinematic viscosity $\nu = \eta_0/\rho$ is also an important parameter to control the dynamics. Thus, at the equilibrium region, the length scale λ_k and time scale τ_k for the smallest eddies, or the smallest fluctuations can be obtained by combination of the dimensions L^2/T^3 and L^2/T for ε and ν respectively, as

$$\lambda_k = \left(\frac{\nu^3}{\varepsilon}\right)^{\frac{1}{4}} \text{ and } \tau_k = \left(\frac{\nu}{\varepsilon}\right)^{\frac{1}{2}} \quad (6.6.22)$$

where λ_k and τ_k are called the Kolmogorov (or dissipation) scales of length and time respectively. It may be speculated from energy accounting that ε is proportional to $(\sqrt{k})^3/l_c$, so that in Eq. (6.6.22) we can write for λ_k as

$$\lambda_k \approx \frac{l_c}{Re_t^{\frac{3}{4}}} \quad (6.6.23)$$

It should be further considered that multiplication of τ_k and \sqrt{k} can give an estimate of the average length scale of the fluctuations λ_T , which is called the Taylor microscale, which is given by

$$\lambda_T \approx \frac{l_c}{Re_t^{\frac{1}{2}}} \quad (6.6.24)$$

Thus, from Eqs. (6.6.23) and (6.6.24) we have reached an important relationship where

$$\frac{\lambda_T}{\lambda_k} \approx Re_t^{\frac{1}{4}} \quad (6.6.25)$$

Namely, Eq. (6.6.25) shows that the average length scale of the fluctuation of order is $Re_t^{\frac{1}{4}}$ times the Kolmogorov scale (the smallest scale).

6.6.1 Turbulence Models

There are numerous turbulence models, ranging from the simplest algebraic correlations to second-closure models by Wilcox (1998), which are further extended to be based on CFD with large eddy simulations (LES) and direct numerical simulations (DNS). In the proceeding sections, in view of engineering applications, we shall look into the most basic models of zero-equation models: one-equation models and two-equation models, all of which deal with the eddy viscosity η_t and the average kinetic energy of turbulence k .

(i) Zero-equation model

In a two dimensional turbulent boundary layer flow of an incompressible fluid, denoting $\bar{\mathbf{u}} = (\bar{u}, \bar{v}, 0)$ and $\mathbf{u}' = (u', v', 0)$, we have the following set of equations from Eqs. (6.6.14) and (6.6.15), such as

$$\frac{\partial \bar{u}}{\partial x} + \frac{\partial \bar{v}}{\partial y} = 0 \quad (6.6.26)$$

$$\rho \left[\frac{\partial \bar{u}}{\partial t} + \frac{\partial}{\partial x} (\bar{u}^2) + \frac{\partial}{\partial y} (\bar{u} \bar{v}) \right] = - \frac{\partial \bar{p}}{\partial x} + \eta_0 \frac{\partial^2 \bar{u}}{\partial y^2} + \frac{\partial}{\partial y} (-\rho \overline{u'v'}) \quad (6.6.27)$$

$$- \frac{\partial \bar{p}}{\partial y} - \frac{\partial}{\partial y} (\rho \overline{v'^2}) = 0 \quad (6.6.28)$$

For the inviscid flow from Euler equation, Eq. (6.5.11), we have

$$\frac{\partial \bar{U}}{\partial t} + \bar{U} \frac{\partial \bar{U}}{\partial x} = -\frac{1}{\rho} \frac{\partial \bar{p}}{\partial x} \quad (6.6.29)$$

In the momentum equation in Eq. (6.6.27), the third term in the right hand side of the equation includes the turbulent shear stress τ_t ,

$$\tau_t = -\rho \overline{u'v'} \quad (6.6.30)$$

The simplest way to give a constitutive relation to τ_t is to introduce the eddy viscosity η_t as analogous to the molecular shear viscosity with reference to either Eq. (6.6.18) or (6.6.19)

$$\tau_t = \eta_t \left(\frac{\partial \bar{u}}{\partial y} \right) \quad (6.6.31)$$

It is noted that η_t is not a fluid property, but depending upon flow conditions and thus varying with position, η_t is a positive value, and the gradient $(\partial \bar{u} / \partial y)$ is positive under typical boundary layer flows. For a positive η_t in Eq. (6.6.31), the shear correlation $\overline{u'v'}$ must thus be negative, which is supported by experimental observation.

One successful approach to estimate η_t is the mixing length concept of Prandtl (1925). The basic idea is to assume that u' and v' are each proportional to $(\partial \bar{u} / \partial y)$, i.e.

$$-\rho \overline{u'v'} \approx \rho \left(l_1 \frac{\partial \bar{u}}{\partial y} \right) \cdot \left(l_2 \frac{\partial \bar{u}}{\partial y} \right) \quad (6.6.32)$$

where l_1 and l_2 are mixing lengths. l_1 and l_2 represent a degree of average eddy size, and may be conveniently replaced by a representative length l . Thus using l , Eq. (6.6.32) may be written as

$$-\rho \overline{u'v'} = \rho l^2 \left| \frac{\partial \bar{u}}{\partial y} \right| \left(\frac{\partial \bar{u}}{\partial y} \right) \quad (6.6.33)$$

Comparing Eq. (6.6.33) with Eq. (6.6.31), we can write η_t where

$$\eta_t \approx \rho l^2 \left| \frac{\partial \bar{u}}{\partial y} \right| \quad (6.6.34)$$

Thus the difficulty arises again to determine l , which is just replaced in ignorance of $\overline{u'v'}$. However, if we can relate the mixing length l to the flow condition, the model will be completely determined as a closed system that deals with l . We will look into the turbulent boundary layer in more detail by decomposing the turbulent flow over a flat plate for the sake of clearness, as schematically shown in Fig. 6.26. As indicated in Fig. 6.26, the turbulent boundary layer is composed chiefly by two layers: one is a thin inner layer close to the wall, where the viscous effects are significant; another is a thicker outer layer where the viscous effect is insignificant. There is a region called an overlap layer in-between the inner and outer layers, where the inertial and viscous effects are both insignificant. In the free stream, viscous and Reynolds stresses do not play important roles. As it is shown further in Fig. 6.26, from inside of the inner layer, there are two distinct layers, and they are identified as buffer layers and linear sublayers. Those two layers are altogether called viscous sublayers, where viscous effects are significant. In the linear sublayer, the Reynolds stress effects are insignificant, while in the buffer layer viscous and Reynolds stress effects are comparable.

As to the mixing length l , the primary effect is the distance from the wall. The following correlations were suggested by Prandtl and Kàrmàn

$$\text{In the viscous sublayer: } l \approx y^2 \quad (6.6.35)$$

$$\text{In the overlap layer: } l \approx ay \quad (6.6.36)$$

$$\text{In the outer layer: } l \approx \text{constant} \quad (6.6.37)$$

It will prove useful to nondimensionalize the quantity $\overline{u'v'}$ by knowing the parameters ρ , ν , y and τ_w in the boundary layer as follows

$$\frac{\overline{u'v'}}{u_\tau^2} = g\left(\frac{yu_\tau}{\nu}\right) \text{ and } \frac{\bar{u}}{u_\tau} = f\left(\frac{yu_\tau}{\nu}\right) \quad (6.6.38)$$

where we define the velocity u_τ , the so-called friction velocity which is given as

$$u_\tau = \sqrt{\frac{\tau_w}{\rho}} \quad (6.6.39)$$

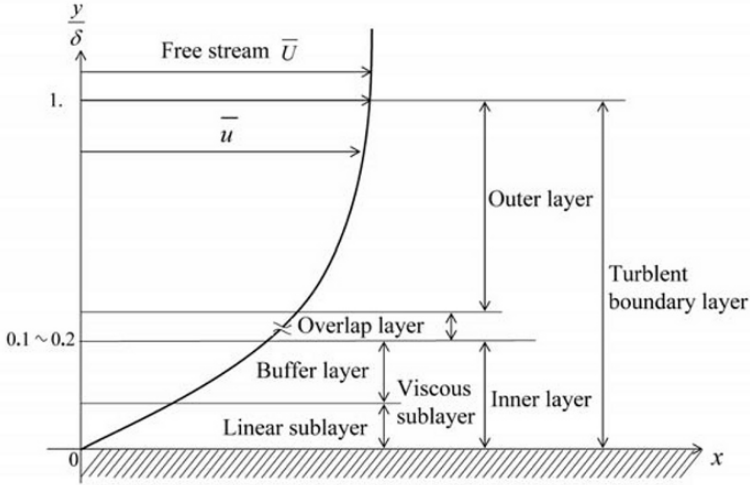


Fig. 6.26 Structure of turbulent boundary layer over a flat plate

Using conventional notations for these nondimensional parameters

$$u^+ = \frac{\bar{u}}{u_\tau} \quad \text{and} \quad y^+ = \frac{y u_\tau}{\nu} \quad (6.6.40)$$

we can write Eq. (6.6.38) simply by

$$\frac{\overline{u'v'}}{u_\tau^2} = g(y^+) \quad \text{and} \quad u^+ = f(y^+) \quad (6.6.41)$$

The correlational expression of Eq. (6.6.41) is called the law of the wall. From the argument of the law of the wall, we can readily calculate the velocity profile in the overlapping layer for hydrodynamically smooth flat plates with a zero attack angle and a zero pressure gradient (the total shear stress is constant near the wall), assuming that the turbulent (shear) stress τ_t is written as the eddy viscosity η_t (with reference to Eq. (6.6.34)) and the mixing length l (with reference to Eq. (6.6.36)) as follows

$$\tau_t = (\eta_0 + \eta_t) \left(\frac{\partial \bar{u}}{\partial y} \right) = \rho l^2 \left| \frac{\partial \bar{u}}{\partial y} \right| \left(\frac{\partial \bar{u}}{\partial y} \right) = \rho \alpha^2 y^2 \left| \frac{\partial \bar{u}}{\partial y} \right| \left(\frac{\partial \bar{u}}{\partial y} \right) \quad (6.6.42)$$

Via the assumption of $\eta_t \gg \eta_0$ in the overlap layer, we can relate the velocity profile u_τ with a shear stress, using Eq. (6.6.39), in the following manner

$$\rho a^2 y^2 \left(\frac{\partial \bar{u}}{\partial y} \right)^2 = \rho u_\tau^2 \quad (6.6.43)$$

Solving Eq. (6.6.43) for \bar{u} and using the notation from Eq. (6.6.41), we can obtain a correlation of $f(y^+)$ as

$$u^+ = \frac{1}{a} \ln(y^+) + b \quad (6.6.44)$$

The expression is called the logarithmic velocity distribution, where a and b are suggested, for example, by Coles and Hirst (1968) as

$$a \approx 0.41 \text{ and } b \approx 5.0$$

With these constants, Eq. (6.6.44) gives good estimate for $35 \leq y^+ \leq 350$ with ordinary flow conditions. Analogous to Eq. (6.6.44), the correlation may be extended to the outer layer via the relationship where

$$\bar{U}^+ - u^+ = -\frac{1}{a} \ln\left(\frac{y}{\delta}\right) + c \quad (6.6.45)$$

where $\bar{U}^+ = \bar{U}/u_\tau$ and c are constant depending upon the pressure gradient, and often upon flow parameters. In order to cover the correlation between the viscous sublayers, the following expression by van Driest (1956), is helpful

$$l \approx ay \left[1 - e^{-\left(\frac{y^+}{A}\right)} \right] = ay \alpha_D \quad (6.6.46)$$

where α_D is the damping factor and A is the configuration parameter. Adopting Eq. (6.6.46), the velocity profile may be given in the following form, similar to Eq. (6.6.44), as follows

$$u^+ = \int_0^{y^+} \frac{2dy^+}{1 + \left(1 + 4a^2 y^{+2} \alpha_D^2\right)^{\frac{1}{2}}} \quad (6.6.47)$$

It is noted that $A = 26$ is given to a case of flow over a flat plate.

In the most adjacent layer to the wall, where the viscous effect dominates the flow, i.e. $\eta_0 \gg \eta_t$, we may write the turbulent shear stress as

$$\tau_t = (\eta_0 + \eta_t) \left(\frac{\partial \bar{u}}{\partial y} \right) \approx \eta_0 \left(\frac{\partial \bar{u}}{\partial y} \right) = \rho u_\tau^2 \quad (6.6.48)$$

which gives a simple differential equation for u^+

$$\frac{\partial u^+}{\partial y^+} = e \quad (6.6.49)$$

and thus with a boundary condition, i.e. $u^+ = 0$ for $y^+ = 0$, we have

$$u^+ = c_0 y^+ \quad (6.6.50)$$

where c_0 is a constant. Equation (6.6.50) gives a linear velocity profile in the linear sublayer. The range of Eq. (6.6.50) is valid within approximately $y^+ \leq 30 \sim 50$ (the buffer layer)

(ii) One-equation model

This is a model to unite an equation for k given in Eq. (6.6.20), and the momentum equation in Eq. (6.6.15) which is solved in coupled with the continuity equation of Eq. (6.6.14).

We shall now write a transport equation for k , by starting to obtain a mechanical energy equation, multiplying (dyadic product of) \mathbf{u} (or u_i) to the Navier-Stokes equation where

$$\rho u_i \left(\frac{\partial u_i}{\partial t} + u_j \frac{\partial u_i}{\partial x_j} \right) = u_i \left[-\frac{\partial p}{\partial x_i} + \eta_0 \frac{\partial^2 u_i}{\partial x_j^2} \right] \quad (6.6.51)$$

which directly gives

$$\begin{aligned} \frac{\partial}{\partial t} \left(\frac{u_i u_i}{2} \right) &= -\frac{\partial}{\partial x_i} \left\{ u_i \left(\frac{p}{\rho} + \frac{u_j u_j}{2} \right) \right\} \\ &+ \nu \frac{\partial}{\partial x_j} \left\{ u_i \left(\frac{\partial u_i}{\partial x_j} + \frac{\partial u_j}{\partial x_i} \right) \right\} - \nu \left(\frac{\partial u_i}{\partial x_j} + \frac{\partial u_j}{\partial x_i} \right) \frac{\partial u_i}{\partial x_j} \end{aligned} \quad (6.6.52)$$

Now we will write Eq. (6.6.52) in terms of average and fluctuating quantities, substituting the following relationship in Eq. (6.6.52)

$$u_i = \bar{u}_i + u_i' \quad (6.6.53)$$

$$p = \bar{p} + p' \quad (6.6.54)$$

$$u_i u_i = \bar{u}_i \bar{u}_i + 2\bar{u}_i u'_i + u'_i u'_i \quad (6.6.55)$$

and taking the time average of both sides. Then we subtract with the Reynolds equation in Eq. (6.6.15) after multiplying \bar{u}_i to it, and resultantly we obtain

$$\begin{aligned} & \frac{\partial}{\partial t} \left(\frac{\overline{u'_i u'_i}}{2} \right) + \frac{\partial}{\partial x_i} \left(\frac{\overline{-u'_j u'_j}}{2} \right) \\ &= -\frac{\partial}{\partial x_i} \left\{ \overline{u'_i \left(\frac{p'}{\rho} + \frac{u'_j u'_j}{2} \right)} \right\} - \overline{u'_i u'_j} \frac{\partial \bar{u}_j}{\partial x_i} \\ &+ \nu \frac{\partial}{\partial x_i} \left\{ \overline{u'_j \left(\frac{\partial u'_i}{\partial x_j} + \frac{\partial u'_j}{\partial x_i} \right)} \right\} - \nu \left(\frac{\partial \bar{u}'_i}{\partial x_j} + \frac{\partial \bar{u}'_j}{\partial x_i} \right) \frac{\partial \bar{u}'_j}{\partial x_i} \end{aligned} \quad (6.6.56)$$

where $k = \overline{u'_j u'_j} / 2$. Each term of Eq. (6.6.56) contains identifiable energy as counting from the 1st term on the left hand side of the equation to right and over to the right hand side of the equation:

1. time rate of change of k
2. convection of k by means of the mean flow
3. convection of total energy by means of turbulence
4. production of turbulence taken from the mean flow
5. work done by viscous effect due to turbulence motion
6. dissipation of turbulence by turbulence motion

Equation (6.6.56) seems formidable, but the introduction of the parameter leads to a lose of novel algebraic difficulties and as a result it will be written in the boundary layer form, with a non-conservation form, as follows

$$\frac{\partial k}{\partial t} + \bar{u}_i \frac{\partial k}{\partial x_i} = -\frac{\partial}{\partial x_i} \left\{ \overline{u'_i \left(\frac{p'}{\rho} + k \right)} \right\} - \overline{u'_i u'_j} \frac{\partial \bar{u}_j}{\partial x_i} - \nu \frac{\partial \bar{u}'_j}{\partial x_i} \frac{\partial \bar{u}'_j}{\partial x_i} \quad (6.6.57)$$

In one equation model, the three terms appearing on the right hand side of Eq. (6.6.57) are replaced by each appropriate term. Typically, in the first term, the convection of total energy can be replaced by a gradient diffusion, such that

$$\frac{\partial}{\partial x_i} \left\{ -u'_i \left(\frac{p'}{\rho} + k \right) \right\} \approx \frac{\partial}{\partial x_i} \left(\alpha_1 \frac{\partial k}{\partial x_i} \right) \quad (6.6.58)$$

where, by analogy with turbulent shear stress, α_1 is a constant. The second term, the production of turbulence, has already been modeled by the eddy viscosity η_t in Eq. (6.6.30), so that

$$-\overline{u'_i u'_j} \left(\frac{\partial \overline{u_j}}{\partial x_i} \right) = \frac{\eta_t}{\rho} \left(\frac{\partial \overline{u_j}}{\partial x_i} \right)^2 = \nu_t \left(\frac{\partial \overline{u_j}}{\partial x_i} \right)^2 \quad (6.6.59)$$

The third term, the dissipation of turbulence, is a difficult term to tackle as it stands. The term, setting ε , carries units of power per mass or (velocity)³ per length, so that dimensionally it is convenient to relate ε by

$$\nu \frac{\partial \overline{u'_j}}{\partial x_i} \frac{\partial \overline{u'_j}}{\partial x_i} = \varepsilon \propto k^m l^n \quad (6.6.60)$$

where k is the average kinetic energy of turbulence and l is a length scale of an eddy moving with the velocity scale $(k)^{1/2}$. Therefore, using Eq. (6.6.60), ε may be written as

$$\varepsilon = \alpha_2 \frac{k^{\frac{3}{2}}}{l} \quad (6.6.61)$$

where α_2 is a constant. Using Eqs. (6.6.58), (6.6.59) and (6.6.61) we can write the energy equation, the so-called k -equation, as follows

$$\frac{\partial k}{\partial t} + u_i \frac{\partial k}{\partial x_i} = \frac{\partial}{\partial x_i} \left(\alpha_1 \frac{\partial k}{\partial x_i} \right) + \nu_t \left(\frac{\partial \overline{u_j}}{\partial x_i} \right)^2 - \alpha_2 \frac{k^{\frac{3}{2}}}{l} \quad (6.6.62)$$

However, it should be kept in mind that Eq. (6.6.62) is not yet in closed form since l has not been correlated for with flow properties. For given α_1 and α_2 , “ l ” may be correlated by experimental verification by Kline et al. (1968). One needs so much effort to solve Eq. (6.6.62), together with finding a correlation for l , and so far, one-equation model represented by Eq. (6.6.62) is not popular, except for one particular problem.

(iii) Two-equation model

As we see in one equation model, the difficulty is to determine the characteristic length l , or alternatively, to determine ε in the k -equation given in Eq. (6.6.62). The two-equation model is generally based on an idea that the characteristic length can be obtained by writing an additional equation for the k -equation. Among the most popular of the two-equation model is the $k-\varepsilon$ model. With the $k-\varepsilon$ model, the eddy viscosity η_t is further written with k and ε as

$$\eta_t = \frac{c_\ell \rho k^2}{\varepsilon} \quad (\text{or } \nu_t = \frac{c_\ell k^2}{\varepsilon}) \quad (6.6.63)$$

where c_ℓ is a constant to be determined by experimental observation.

Similar to the one-equation model in Eq. (6.6.62), a set of $k-\varepsilon$ equations is written by Tennekes and Lumley (1972) as follows:

k -equation:

$$\frac{\partial k}{\partial t} + \overline{u_i} \frac{\partial k}{\partial x_i} \approx \frac{\partial}{\partial x_i} \left(\frac{\nu_t}{\sigma_k} \frac{\partial k}{\partial x_i} \right) + \nu_t \frac{\partial \overline{u_j}}{\partial x_i} \left(\frac{\partial \overline{u_j}}{\partial x_i} + \frac{\partial \overline{u_i}}{\partial x_j} \right) - \varepsilon \quad (6.6.64)$$

ε -equation:

$$\frac{\partial \varepsilon}{\partial t} + \overline{u_i} \frac{\partial \varepsilon}{\partial x_i} \approx \frac{\partial}{\partial x_i} \left(\frac{\nu_t}{\sigma_\varepsilon} \frac{\partial \varepsilon}{\partial x_i} \right) + c_1 \frac{\varepsilon}{k} \nu_t \frac{\partial \overline{u_j}}{\partial x_i} \left(\frac{\partial \overline{u_j}}{\partial x_i} + \frac{\partial \overline{u_i}}{\partial x_j} \right) - c_2 \frac{\varepsilon^2}{k} \quad (6.6.65)$$

There are five empirical constants appearing in $k-\varepsilon$ equations. The $k-\varepsilon$ model is widely used for analysis of two dimensional turbulent shear flows at high Reynolds numbers. The five empirical constants were obtained via experiments and are recommended for calculations:

$$c_1 = 1.44, \quad c_2 = 1.92, \quad c_\ell = 0.09, \quad \sigma_k = 1.0 \quad \text{and} \quad \sigma_\varepsilon = 1.3 \quad (6.6.66)$$

Note that they are not universal constants, but can be modified for specific problems. The constants given in (6.6.66) give good estimate for turbulent flow characteristic for a flat plate with high Reynolds numbers. It is further mentioned that $\sigma_k = \nu_t / \nu_k$ and $\sigma_\varepsilon = \nu_t / \nu_\varepsilon$ are effective Prandtl numbers defined by the eddy diffusivity.

In practical engineering applications the $k-\varepsilon$ equations, Eqs. (6.6.64) and (6.6.65), are solved with the continuity and momentum equations where, respectively, Eqs. (6.6.14) and (6.6.15) are attained by numerical methods. However, the models (the $k-\varepsilon$ model) are designated to the fully turbulent region away from solid walls. In the near region of solid walls, due to strong viscous effects, the velocity gradient is very high, so

that in practical computations, there are needs for a large number of mesh points to give sufficient resolutions. Even with modern super computers, the number of mesh to gain sufficient resolution for turbulence motion is not enough. There could be some methods to overcome the problem. One of the most fundamental methods is to use a wall-function to give an estimate of turbulent properties at the first node point in a computational mesh in the overlapping layers; with that, the calculation in the lower layer close to the wall will not be necessary. In the region of the overlapping layer, $35 \leq y^+ \leq 350$, the turbulence energy production and dissipation is balanced so that other terms beside the production and dissipation are unimportant. In this region, some significant use is expressed by virtue of the logarithmic velocity distribution in Eq. (6.6.44), which gives a first estimate for the $k - \varepsilon$ parameters for the closest node y_p^+ to the wall, as schematically displayed in Fig. 6.27. Then the $k - \varepsilon$ equations are solved to give converged solutions by a numerical procedure. According to the idea close to the wall, $u^+ = u_p^+$ will be then given via y_p^+ using the wall-function as

$$\frac{\bar{u}}{u_\tau} = \frac{1}{a} \ln(y_p^+ B), \text{ and } y_p^+ = \frac{y u_\tau}{\nu} \quad (6.6.67)$$

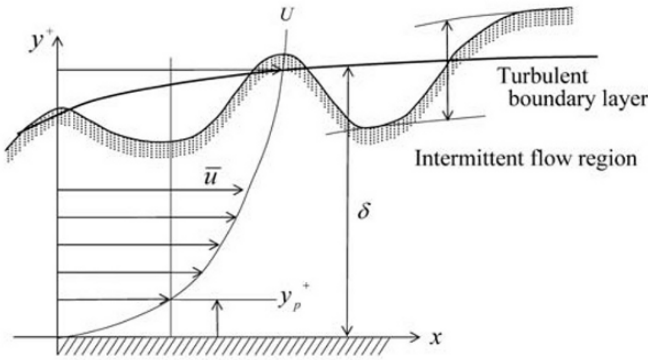


Fig. 6.27 Node point y_p^+ with wall-function

where $a = 0.41$ and $B = 7.77$. In order to examine k close to the wall, the k -equation in the two dimensional turbulent boundary layer in the overlapping layer is considered to be

$$\eta_t \left(\frac{\partial \bar{u}}{\partial y} \right) \left(\frac{\partial \bar{u}}{\partial y} \right) - \rho \varepsilon = 0 \quad (6.6.68)$$

It is further known that the shear stress $\eta_t \left(\frac{\partial \bar{u}}{\partial y} \right)$ is nearly equal to the wall of shear stress $\tau_w = \rho u_\tau^2$, so that we can write

$$\eta_t \left(\frac{\partial \bar{u}}{\partial y} \right) \approx \tau_w = \rho u_\tau^2 \quad (6.6.69)$$

Using the expression in Eq. (6.6.63) for η_t , we can calculate k where

$$k = \frac{u_\tau^2}{\frac{1}{c_l^2}} \quad (6.6.70)$$

Thus, k is determined by u_τ with Eq. (6.6.70). Similarly, for ε in Eq. (6.6.68), we can obtain

$$\varepsilon = \frac{\eta_t}{\rho} \left(\frac{\partial \bar{u}}{\partial y} \right)^2 \quad (6.6.71)$$

Using Eqs. (6.6.67) and (6.6.69), ε is further written where

$$\varepsilon = \frac{u_\tau^3}{ky} \quad (6.6.72)$$

Therefore, when u_τ is given *a priori* as a guessed value, k and ε at y_p^+ will be estimated. It is mentioned that u_τ is a quantity entirely determined by a whole turbulent flow field calculation, provided that only u_τ is finally determined at the end of recurrence procedure in a numerical calculation. It is also useful to give \bar{u} and u_τ a relationship, which is given in Eq. (6.6.67) as

$$\frac{\bar{u}}{u_\tau^2} c_l^{\frac{1}{4}} k^{\frac{1}{2}} = \frac{1}{a} \ln \left(B y_p \frac{c_l^{\frac{1}{4}} k^{\frac{1}{2}}}{\nu} \right) \quad (6.6.73)$$

for y_p at y_p^+ , we set $y_p^+ = y_p c_l^{1/4} k^{1/2} / \nu$.

6.6.2 Turbulent Heat Transfer

In a non-isotropic temperature field, it becomes necessary to take into account the energy equation in addition to the continuity and momentum equations in turbulent flows. Particularly, in a compressible flow there appears a strong interaction between the velocity and temperature field. The general treatment for a turbulent heat transfer is far from complete, and rather it is at the developing stage in the research of turbulent flows. In this section of the chapter, we shall look into the characterization of turbulent heat transfer in two dimensional consideration of the averaged energy equation in turbulent boundary layers, using the Reynolds' analogy as examined earlier (in Exercise 6.5.2).

The energy equation given with Eq. (2.5.29) can be written for an incompressible Newtonian fluid in the conservation form, ignoring the body force term, as follows

$$\frac{\partial \rho c_p T}{\partial t} + \nabla \cdot \rho c_p T \mathbf{u} = \nabla \cdot (k_c \nabla T) + 2\eta_0 \mathbf{e} \cdot \mathbf{e} \quad (6.6.74)$$

where \mathbf{e} is the rate of strain tensor given in either Eq. (1.1.19) or (6.1.2). For a turbulent flow, likewise, what we had done to the velocity, temperature T is also decomposed into its average part \bar{T} and its fluctuating part T' , where

$$T = \bar{T} + T' \quad (6.6.75)$$

Substituting Eq. (6.6.75), together with the velocity of Eq. (6.6.10) to Eq. (6.6.74), and taking the average from the equation, we have

$$\frac{\partial \rho c_p \bar{T}}{\partial t} + \nabla \cdot (\rho c_p \bar{\mathbf{u}} \bar{T}) + \nabla \cdot (\rho c_p \overline{\mathbf{u}' T'}) = \nabla \cdot (k_c \nabla \bar{T}) + 2\eta_0 \overline{(\mathbf{e} + \mathbf{e}')^2} \quad (6.6.76)$$

With a non-conservation form with tensor notation, we can write

$$\begin{aligned} \rho c_p \frac{D\bar{T}}{Dt} = \frac{\partial}{\partial x_i} \left(k_c \frac{\partial \bar{T}}{\partial x_i} \right) - \frac{\partial}{\partial x_i} (\rho c_p \overline{u'_i T'}) \\ + 2\eta_0 \left\{ \overline{\left(\frac{\partial \bar{u}_i}{\partial x_j} + \frac{\partial \bar{u}_j}{\partial x_i} \right)} + \overline{\left(\frac{\partial u'_i}{\partial x_j} + \frac{\partial u'_j}{\partial x_i} \right)} \right\}^2 \end{aligned} \quad (6.6.77)$$

In order not to lose the generality and to convey the essence of the subject, it appears that Eq. (6.6.76) can be written in a two dimensional boundary layer over a flat plate:

$$\rho c_p \left(\frac{\partial \bar{T}}{\partial t} + \bar{u} \frac{\partial \bar{T}}{\partial x} + \bar{v} \frac{\partial \bar{T}}{\partial y} \right) = \frac{\partial}{\partial y} \left(k_c \frac{\partial \bar{T}}{\partial y} \right) - \frac{\partial \bar{q}_y}{\partial y} + \left(\eta_0 \frac{\partial \bar{u}}{\partial y} + \eta_t \frac{\partial \bar{u}}{\partial y} \right) \left(\frac{\partial \bar{u}}{\partial y} \right) \quad (6.6.78)$$

where \bar{q}_y is defined as the turbulent heat flux against the molecular heat flux (laminar heat flux) given by the term $\partial/\partial y (k_c \partial \bar{T}/\partial y)$ where

$$\bar{q}_y = -\rho c_p \bar{v}' T' \quad (6.6.79)$$

It has been mentioned that $\eta_t (\partial \bar{u}/\partial y)$ in Eq. (6.6.78) is introduced analogous to the turbulent shear stress expressed in Eq. (6.6.31). It is further postulated that in order to render Eq. (6.6.78) to make an amenable practical calculation that \bar{q}_y may be set, in analogous to the Fourier's law in laminar flow case, where

$$\bar{q}_y = -c_p A_t \left(\frac{\partial \bar{T}}{\partial y} \right) \quad (6.6.80)$$

where A_t is the turbulent heat flux coefficient. Consequently, Eq. (6.6.78) can be written as

$$\rho c_p \left(\frac{\partial \bar{T}}{\partial t} + \bar{u} \frac{\partial \bar{T}}{\partial x} + \bar{v} \frac{\partial \bar{T}}{\partial y} \right) = \frac{\partial}{\partial y} \left[(k_c + c_p A_t) \frac{\partial \bar{T}}{\partial y} \right] + (\eta_0 + \eta_t) \left(\frac{\partial \bar{u}}{\partial y} \right)^2 \quad (6.6.81)$$

The complete derivation of the energy equation of a turbulent heat transfer is given first by Schlichting (1955).

The turbulent energy equation expressed in Eq. (6.6.81) is solved by combining the continuity equation in Eq. (6.6.26) with the appropriate momentum equations, for example, $k - \varepsilon$ equations for Eqs. (6.6.64) and (6.6.65).

However, the problem arose where there exists another unknown quantity A_t in Eq. (6.6.81) that must be determined by the flow and thermal variables. Considering the temperature field in heat transfer situation, there exists an intimate connection between heat and momentum transfer in general. Owing to this fact, we can extend the Reynolds' analogy to the turbulent heat transfer. In order to formulate the idea we can relate the eddy viscosity η_t (the momentum exchange coefficient) and the turbulent heat flux coefficient A_t (the heat exchange coefficient), with the reason that both of which have the common dimension of the molecular viscosity. A new non-dimensional number, so-called the turbulent Prandtl number Pr_t is analo-

gous to the molecular Prandtl number ($Pr = \eta_0 c_p / k_c$), is a convenient parameter to relate the quantities

$$Pr_t = \frac{\eta_t}{A_t} \quad (6.6.82)$$

While we have the relationship of

$$\frac{\bar{q}_y}{\tau_t} = \frac{-c_p A_t \left(\frac{\partial \bar{T}}{\partial y} \right)}{\eta_t \left(\frac{\partial \bar{u}}{\partial y} \right)} = - \frac{c_p \left(\frac{\partial \bar{T}}{\partial y} \right)}{Pr_t \left(\frac{\partial \bar{u}}{\partial y} \right)} \quad (6.6.83)$$

We are able to collect the molecular heat conduction q_c and the turbulent heat transfer q_t terms in a kind of total rate of heat transfer q where

$$q = q_c + q_t = -c_p \left(\frac{\eta_0}{Pr} + \frac{\eta_t}{Pr_t} \right) \left(\frac{\partial \bar{T}}{\partial y} \right) \quad (6.6.84)$$

$\partial \bar{T} / \partial y$ is taken as the positive gradient.

The analogy between the heat and momentum transfer in a flow over a flat plate with a zero attack angle is discussed here in succession for the laminar boundary layer case. With reference to Fig. 6.28, consider the linear sublayer in the turbulent boundary layer with Reynolds' analogy, in particular, where the momentum and heat transfer exchange (with coefficients respectively with η_t and A_t) are thought to be insignificant. Therefore, it may not be far from reality to write the relationship between (Exercise 6.5.2, Eq. (14)), assuming that $Pr_t \approx 1$, where

$$\frac{q_w}{\tau_w} = - \frac{k_c}{\eta_0} \left(\frac{dT}{du} \right)_w \quad (6.6.85)$$

On the other hand, with the turbulent outer layer as indicated in Fig. 6.28, the molecular coefficients of η_0 and k_c can be neglected, where it is assumed that $Pr_t \approx 1$, so that Eq. (6.6.83) will become

$$\frac{\bar{q}_y}{\tau_t} = -c_p \left(\frac{d\bar{T}}{d\bar{u}} \right) \quad (6.6.86)$$

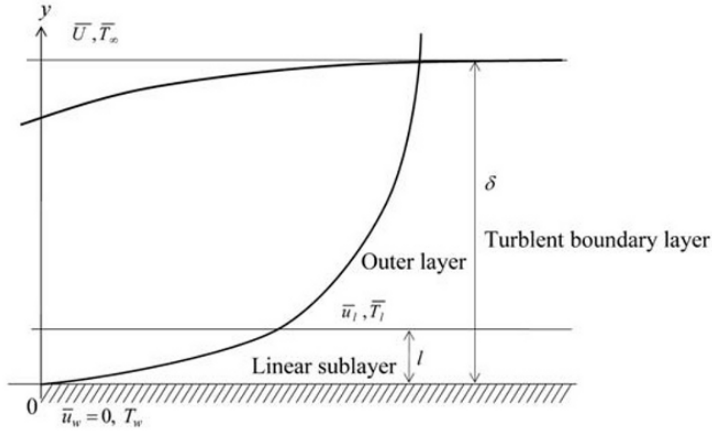


Fig. 6.28 Boundary values in turbulent boundary layer

Equations (6.6.85) and (6.6.86) now can be integrated over each layer separately, referring each boundary value as indicated in Fig. 6.28, to give

$$\frac{q_w}{\tau_w} = -\frac{k_c}{\eta_0} \frac{\bar{T}_l - T_w}{\bar{u}_l} = -\frac{k_c}{\eta_0 \bar{U}} \frac{\bar{T}_l - T_w}{(\bar{u}_l / \bar{U})} \quad (6.6.87)$$

and

$$\frac{q}{\tau} = -c_p \frac{\bar{T}_l - \bar{T}_\infty}{\bar{u}_l - \bar{U}} \quad (6.6.88)$$

It is reasonable, therefore, to assume that the ratio q_w / τ_w and q / τ (similarly q_w / τ_w and \bar{q}_y / τ_t for each layer in the integration) remains constant across the whole width δ of the boundary layer. Furthermore, since $Pr \approx 1$, we can set the similarity of the velocity and temperature profile as

$$\frac{\bar{u}}{\bar{U}} = \frac{\bar{T} - T_\infty}{\bar{T}_\infty - T_w} \quad (6.6.89)$$

Equating Eqs. (6.6.87) and (6.6.89), we can now obtain a relationship between the velocity and temperature where

$$\left(\frac{T_w - \bar{T}_\infty}{\bar{T}_l - T_w} \right) Pr = -\frac{\bar{U}}{\bar{u}_l} \left[1 + \frac{\bar{u}_l}{\bar{U}} (Pr - 1) \right] \quad (6.6.90)$$

In many situations in engineering, it proves useful to consider the local heat transfer coefficient h_x that can be defined as

$$h_x = \frac{q_w}{T_w - \bar{T}_\infty} \quad (6.6.91)$$

This can be further reduced to a more convenient form with Eqs. (6.6.91) and (6.6.87) where

$$\begin{aligned} h_x &= - \left[\frac{Pr}{1 + (\bar{u}_l / \bar{U})(Pr - 1)} \right] \left[\frac{(\bar{u}_l / \bar{U})}{(\bar{T}_l - T_w)} \right] q_w \\ &= \frac{1}{1 + (\bar{u}_l / \bar{U})(Pr - 1)} \frac{c_p}{\bar{U}} \tau_w \end{aligned} \quad (6.6.92)$$

As an alternative expression to the local heat coefficient h_x , the non-dimensional parameter, the local Nusselt number Nu_x (as defined in Exercise 6.5.2) can be written by other flow field parameters

$$Nu_x = \frac{\frac{1}{2} c_f Re_x Pr}{1 + (\bar{u}_l / \bar{U})(Pr - 1)} \quad (6.6.93)$$

Further, the Stanton number is similarly given where

$$Sn_x = \frac{\frac{1}{2} c_f}{1 + (\bar{u}_l / \bar{U})(Pr - 1)} \quad (6.6.94)$$

The expression in Eq. (6.6.93) is derived from Prandtl and G.I. Taylor independently as the extension of the Reynolds' analogy to the turbulent heat transfer. The case, when $Pr_t \neq 1$, was studied more by Ambrok (1957). Numerical treatment of the turbulent flow problem in the $k - \varepsilon$ equation is found in Jones and Lunder (1972).

Exercise

Exercise 6.6.1 Estimation of Drag Coefficient on Flat Plate for Turbulent Flow

Based on the momentum integral analysis, estimate the drag coefficient for turbulent flow over a flat plate with a zero attack angle. Let us assume here, for simplicity, that the turbulent boundary layer grows from the leading edge of the flat plate. The flow is a steady flow over a flat plate with a

zero pressure gradient so that the stream velocity \bar{U} is kept constant. Consider a case of the mean velocity distribution for the turbulent boundary layer to be the power law

$$\frac{\bar{u}}{\bar{U}} = \left(\frac{y}{\delta}\right)^{\frac{1}{n}} = \left(\frac{y}{\delta}\right)^{\frac{1}{7}} \quad (1)$$

Ans.

By the Kàrmàn integral equation, the local friction coefficient c_{f_x} can be written by

$$c_{f_x} = \frac{\tau_w}{\frac{1}{2}\rho\bar{U}^2} = 2\frac{d\theta}{dx} \quad (2)$$

θ is the momentum thickness, which is given where

$$\theta = \int_0^\infty \left(1 - \frac{\bar{u}}{\bar{U}}\right) \left(\frac{\bar{u}}{\bar{U}}\right) dy \quad (3)$$

Setting $\eta = y/\delta$, the velocity distribution is expressed by the power law, as assumed where

$$\frac{\bar{u}}{\bar{U}} = \eta^{\frac{1}{7}} \quad (4)$$

The wall of shear stress τ_w of pipe given by Blasius' formula in Eq. (6.4.40) is transformed to the flat plate coordinates by setting $\delta = r_0 = d/2$, and $U_{\max} = 60\bar{U}/49$ with reference to Eq. (6.4.54), so that for the boundary layer over a flat plate, we have

$$\tau_w = 0.0233\rho\bar{U}^2(\delta\bar{U}/\nu)^{-\frac{1}{4}} \quad (5)$$

The integral equation for Eq. (2) can be rewritten by using Eqs. (3) and (4), which is further equated with Eq. (5) as follows

$$\bar{U}^2 \frac{d\delta}{dx} \left\{ \frac{d}{dx} \int_0^1 \eta^{\frac{1}{7}} \left(1 - \eta^{\frac{1}{7}}\right) d\eta \right\} = 0.0223\bar{U}^2 (\bar{U}\delta/\nu)^{-\frac{1}{4}} \quad (6)$$

Equation (6) is an ordinary differential equation with respect to $\delta(x)$, and is solved by assuming $\delta = 0$ for $x = 0$ to give

$$\delta^{\frac{1}{4}} d\delta = 0.24(\nu/\bar{U})^{\frac{1}{4}} dx \quad (7)$$

Resultantly, it follows

$$\delta = \frac{0.382x}{(\bar{U}x/\nu)^{\frac{1}{5}}} = 0.382x Re_x^{-\frac{1}{5}} \quad (8)$$

It is noted here that the boundary layer thickness $\delta(x)$ of the turbulent flow $\delta(x) \approx x^{4/5}$ is far thicker than that of a laminar boundary layer $\delta(x) \approx x^{1/2}$, as is evident by comparison between Eq. (8) and Eq. (6.5.25). Now the local value of the shear stress τ_w of Eq. (5) can be evaluated by using $\delta(x)$ in Eq. (8), so that

$$\begin{aligned} \tau_w &= 0.0296 \rho \bar{U}^2 (\bar{U}x/\nu)^{-\frac{1}{5}} \\ &= 0.0296 \rho \bar{U}^2 Re_x^{-\frac{1}{5}} \end{aligned} \quad (9)$$

which gives

$$c_{f_x} = 0.0592 Re_x^{-\frac{1}{5}} \quad \text{for } Re_x = 10^7 \quad (10)$$

Thus, the required drag force F_D on one side of the flat plate is calculated, according to Eq. (10) in Exercise 6.5.1, as

$$\begin{aligned} F_D &= \int_0^l b \tau_w dx \\ &= 0.037 \rho \bar{U}^{\frac{9}{5}} \nu^{\frac{1}{5}} l^{\frac{4}{5}} b \end{aligned} \quad (11)$$

The drag coefficient is

$$\begin{aligned} c_f &= \frac{F_D}{bl \left(\frac{1}{2} \rho \bar{u}^2 \right)} \\ &= 0.074 Re_l^{-\frac{1}{5}} \quad \text{for } 5 \times 10^5 \leq Re_l \leq 10^7 \end{aligned} \quad (12)$$

c_{f_x} and c_f given in Eqs. (10) and (12) respectively give good estimate values for the Reynolds number range indicated in the equations.

For reference, Schlichting (1955) proposed c_{f_x} and c_f , using the logarithmic law of the wall, and those are in good agreement with experimental data in the Reynolds number range, $10^7 \leq Re_l \leq 10^9$, which is

$$c_{f_x} = (2 \log Re_x - 0.65)^{-2.3} \quad (13)$$

and

$$c_f = \frac{0.455}{(\log Re_l)^{2.58}} \quad (14)$$

Note that c_f shown in Eqs. (12) and (14) is subjected to the turbulent boundary layer developed from the leading edge. However, in practice, the laminar boundary is usually developed immediately after the leading edge toward the position of the transition region that usually lies in the range, $3 \times 10^5 \leq Re_x \leq 3 \times 10^6$, so that, when the transition is assumed to occur at $Re_x \approx 5 \times 10^5$, it is convenient to write c_f for a fully developed turbulent boundary flow as $c_{fp} = c_f - 1700/Re_x$.

$$5 \times 10^5 \leq Re_x \leq 10^7 \text{ or } 10^9 \quad (15)$$

where c_f is given either by Eq. (12) or (14), depending upon the upper range of Re_x .

Exercise 6.6.2 The Temperature Law of the Wall

The total rate of heat transfer q_w from a flat plate is written by using the turbulent Prandtl number with reference to Eq. (6.6.84) where

$$q_w = c_p \left(\frac{\eta_0}{Pr} + \frac{\eta_t}{Pr_t} \right) \frac{d\bar{T}}{dy} \quad (1)$$

$d\bar{T}/dy$ is taken for the negative gradient from the wall. If η_t/η_0 is given via a linear function of y^+ where

$$\frac{\eta_t}{\eta_0} = ky^+ \quad (2)$$

Show that \bar{T} is a logarithmic function of y^+ . Note that y^+ is defined by the friction velocity u_τ , such that

$$y^+ = \frac{yu_\tau}{\nu} = y \sqrt{\frac{\tau_w}{\rho}} \frac{\rho}{\eta_0} \quad (3)$$

Ans.

Equation (1) can be integrated to give

$$T^+ = \frac{T_w - \bar{T}}{T_t} = \int_0^{y^+} \frac{dy^+}{\left\{ \frac{1}{Pr} + \left(\frac{\eta_t}{\eta_0} \right) \frac{1}{Pr_t} \right\}} \quad (4)$$

where T_t is defined analogous to the friction velocity, such that

$$T_t = \frac{q_w}{\rho c_p u_\tau} \quad (5)$$

T^+ given in Eq. (4) is the so-called temperature law of the wall, analogous to the law of the wall variable y^+ as defined in Equation (3). Equation (4) together with the relation of (η_t/η_0) , as given in Eq. (2), yields the following expression:

$$T^+ = \frac{Pr_t}{a} \ln y^+ + B(Pr) \quad (6)$$

where a is an experimental constant (such as in Eq. (6.6.67)) and B is an integration constant given at a boundary of y^+ . The expression is the logarithmic expression for the distribution of temperature in the turbulent boundary layer. The similarity of velocity distribution in the temperature is evident. Note that very near to the wall, where $\eta_t \ll \eta_0$, the thermal sublayer has the following linear temperature distribution, that is represented by

$$T^+ = Pr y^+ \quad (7)$$

There are some expressions for $B(Pr)$ that are obtained from experimental verification. For example, by referring Kader (1981) where

$$B(Pr) \approx \left(3.85 Pr^{\frac{1}{3}} - 1.3 \right)^2 + 2.12 \ln Pr \quad (8)$$

Equation (8) is valid for air, water and etc. for $0.7 \leq Pr \leq 170$.

Problems

- 6.6-1. Derive the relationship to describe a turbulent velocity profile in a pipe with radius r_0 from the definition of the eddy viscosity η_t and of the eddy diffusivity $\nu_t = \eta_t / \rho$ in the turbulent boundary layer of a flat plate.

$$\text{Ans.} \quad \left[\left(1 - \frac{y^+}{r_0^+} \right) = \left(1 + \frac{\nu_t}{\nu} \right) \frac{du^+}{dy^+} \right]$$

- 6.6-2. The velocity profile in the turbulence core for a smooth pipe can be expressed in the logarithmic form

$$u^+ = 2.5 \ln y^+ + 5.5$$

Find ν_t / ν with the functional form, using the result from previous question.

$$\text{Ans.} \quad \left[\frac{y^+}{2.5} \left(1 - \frac{y^+}{r_0^+} \right) - 1 \right]$$

- 6.6-3. Air is flowing on a flat plate with a zero attack angle. Sketch how the boundary layer is developed on the plate, assuming that, at the same distance, x from the leading edge, where the flow is reached to be a turbulent flow from a laminar flow at $Re_{\text{critical}} = \bar{U}x/\nu$, the turbulent boundary layer has started to be developed onward.

Ans. [Ref. Fig. 6.18 for example]

- 6.6-4. In problem 6.5-4, denote that the free stream velocity is 5 m/s and the kinematic viscosity of air is $1.6 \times 10^{-5} \text{ m}^2/\text{s}$. The length and width of the plate is 4 m and 2 m respectively. Estimate the boundary layer thickness at the end of the plate surface, and calculate the total drag force acting on one side of the plate. Assume that the critical Reynolds number from laminar to turbulent is approximately $Re_{\text{critical}} = 5 \times 10^5$.

$$\text{Ans.} \quad [\delta_{\text{end}} = 0.11 \text{ m}, F_D = 0.098 \text{ N}]$$

- 6.6-5 Compare the velocity profile and temperature profile over the turbulent boundary layer with a heat transfer from a flat plate with a zero attack angle. Assume $Pr \approx 1.0$ and $Pr_t = 1.0$, and use Kader's expression with reference to Exercise 6.6.2, Eq. (8).

Nomenclature

A	configuration parameter
a, b, c	constant in a turbulent flow
a_0	speed of sound
b	internal heat generation
Br	Brinkman number
c_D, c_f	drag coefficients and friction coefficient
c_p, c_v	specific heat
$c_0, c_1, c_2 \dots c_n$	constants
d	diameter $d = 2r_0$
d_h	hydraulic diameter
\mathbf{e}	rate of strain tensor
$\hat{\mathbf{e}}_i$	unit vectors
Ec	Eckert number
Eu	Euler number
\mathbf{F}, \mathbf{F}	force, vector
F_D	drag force
Fr	Froude number
f	frequency
\mathbf{g}	body force
\mathbf{g}	gravitational acceleration
h	height or thickness or enthalpy per unit mass or heat transfer coefficient
h_w	wall heat transfer coefficient
$\mathbf{i}, \mathbf{j}, \mathbf{k}$	unit vectors in Cartesian coordinates system
\mathbf{I}	unit tensor
K	constant in a turbulent
K_0	bulk modulus
k	average kinetic energy of turbulence or specific heat ratio
k_c	thermal conductivity
k_B	Boltzmann constant
k_r	radius ratio
k_α	thermal diffusivity
L, l	length or l ; length scale of an eddy or ; mixing length
L_c	characteristic length

l_p	wetted perimeter
l_m	mean free path
m	mass
\hat{n}	unit normal
P	power
p	pressure
Pe	Peclet number
Pr	Prandtl number
Pr_t	turbulent Prandtl number
q, \mathbf{q}	heat flux, vector
q_w	wall heat flux, wall heat transfer rate
Q	volumetric flow rate
R	(specific) gas constant
Ra	Rayleigh number
Re	Reynolds number
r_0	radius
r_h	hydraulic radius
S	area
Sn	Stanton number
St	Strouhal number
s	specific entropy
t, t_0	time, reference time or starting time
\mathbf{t}	stress vector
\mathbf{T}	total stress tensor
T	temperature or averaging time
T_r	torque
\mathbf{u}	velocity vector
u_τ	friction velocity
U	speed or potential core speed
\bar{U}	average velocity
u, v, w	velocity components in Cartesian coordinates system
V	volume
We	Weber number
x, y, z	Cartesian coordinates system
r, θ, z	cylindrical coordinates system
r, θ, ϕ	spherical coordinates system
α, β, γ	matching constants
α_D	damping factor

$\alpha_0, \alpha_1, \dots, \alpha_4$	constants
β_T	coefficient of thermal expansion
$\dot{\gamma}$	shear rate
δ	boundary layer thickness or shear layer thickness
δ'	displacement thickness
δ_h	enthalpy thickness
δ_T	thermal boundary layer thickness
ε	roughness or dissipation energy of turbulence
ζ	pressure loss coefficient
ς	boundary thickness ratio
η	similarity variable
η_0	Newtonian viscosity
η_t	eddy viscosity
θ	momentum thickness
κ_d	dilatational viscosity
λ	friction factor
λ_k	Kolmogorov scale of length
λ_T	Taylor microscale
λ_0	second viscosity coefficient
ρ	density
σ	surface tension
$\boldsymbol{\tau}$	stress tensor
τ_w	wall stress
τ_t	turbulent (shear) stress
τ_k	Kolmogorov scale of time
$\boldsymbol{\tau}_R$	Reynolds stress tensor
ν	kinematic viscosity
ν_1	kinematic eddy viscosity
ϕ_0	gravitational potential
Φ	dissipation function
ψ	stream function
ω	angular frequency
$\boldsymbol{\omega}$	spin tensor
$\boldsymbol{\omega}$	vorticity (vector)
Superscripts	
*	dimensionless variable
+	values based on law of wall

, fluctuating component
– time average

Subscripts

e entrance value
 m model
 p prototype
 x value based on axial position
 w wall value
 0 initial value or base value
 ∞ value at infinity
 $1,2$ inner and outer respectively

Bibliography

Recent development of Newtonian viscous fluid flow is well documented together with fundamental concepts in fluid mechanics, including the flow instability, in

1. F.M. White, *Viscous Fluid Flow* (3rd Edition), McGraw Hill International, New York, 2006.
2. F.S. Sherman, *Viscous Flow*, McGraw Hill Publishing Company, New York, 1990.

The most classic text book in boundary layer theory is

3. H. Schlichting, *Boundary-Layer Theory* (7th Edition 1979), McGraw-Hill book company Inc., New York, 1955.
4. L. Rosenhead, *Laminar Boundary Layer*, Oxford University, Oxford, Press, 1963.
5. D. Meksyn, *New Methods in Laminar Boundary Theory*, Pergamon, London, 1961.

Basic treatment on incompressible viscous flows with details on dimensional analysis is found in

6. R.L. Panton, *Incompressible Flow* (2nd Edition), John Willey & Sons, Inc., Hoboken, NJ, 1996.

Extensive literature review for developing flows are found in

7. A.J. Word-Smith, *Internal Fluid Flow*, Clarendon Press, England, 1980.

Experimental techniques on Newtonian fluid flow and visualization methods are documented in

8. W.J. Yang, *Handbook of Flow Visualization*, Hemisphere Publishing Corp., New York, 1989.

Flow phenomena, specific data, correlations and approximations referred in the text are presented in

9. J. Boussinesq, *Thiorie Analytique de la chaleur*, 2, 172, Gauthier-Villars, Paris, 1903.
10. P.L. Silveston, Warmedurchgang in waagerechten flüssigkeitsschichten, Part I Forsch. Ing. Wes. 24,29–32 and 59–69, 1958.
11. H.S. Hele-Shaw, Investigation of the nature of surface resistance of water and of stream motion under certain experimental conditions, Frans. Inst. Naval Arch., 11, 1898.
12. G.G. Stokes, Mathematical and physical papers I, 75, Trans. Camb. Soc., 8, 1845.
13. C.W. Oseen, On the Stokes' problem and on the fundamental problems of hydrodynamics (German), Ark. F. Mat. Astr. og Fys., 6 (29), 1910.
14. J. Boussinesq, *Comptes Reudus*, 9, 1891.
15. Prandtl-Tietjens, *Hydro und Aeromechanics*, Bd.II, 1931.
16. R.K. Shah and A.L. London, *Laminar Flow Forced Convection in Ducts*, Academic Press, New York, 1978.
17. J. Nikuradse, Strömungsgesetze in rauhen Rohen, Forsch. Arb. Ing.-Wes., (361), 1933.
18. L. Prandtl, Über flussigkeitsbewegung bei sehr kleiner reibung. Verhndlungen des III. Internationalen Mathematiker-Kongrees, Heidelberg, 1904.
19. L. Prandtl, Über flussigkeitsbewegung bei sehr kleiner reibung, Proc.Third Int. Math. Congr. Heidelberg (NACA Technical Memo.452 in English), 1908.
20. L. Prandtl, Über die ausgebildete turbblenz, Z. Angew. Math. Mech., 5, 1925.
21. H. Blasius, Grenzsichten in flüssikeiten mit kleiner reibung, Z. Angew. Math. Phys., 56 [NACA Technical Memo.1256 in English], 1908.
22. T. von Kàrmàn, Über den mechanismus des widerstandes, den ein bewegter Körper in einer flüssigkeit erzeugt, Nachr. Ges. Wiss. Göttingen Math. –Phys. Kl.II, 1921.

23. H.W. Liepmann, Investigation on curved boundary layer stability and transition on curved boundaries, NACA Wartime Report W107 (ACR 3H30) or [NACA Technical Memo.1196], 1943.
24. D.C. Wilcox, *Turbulence Modeling for CFD* (2nd Edition), DCW Industries, La Cañada, CA, 1998.
25. D.E. Coles and E.A. Hirst (editors), *Proceedings on Computational Turbulent Boundary Layers*, 2, Stanford University Press, Stanford, CA, 1968.
26. E.R. van Driest, On turbulent flow near a wall, *J. Aeronaut. Sci.*, 23, 1956.
27. S.J. Kline, M.V. Morkovin, G. Sovran and D.J. Cockrell, *Computation of Turbulent Boundary Layers*, AFOSR-IFP Stanford conference, Proceedings of the 1968 Conference, 1, Stanford University Press, Stanford, CA, 1968.
28. H. Tennekes and J.L. Lumley, *A First Course in Turbulence*, M.I.T.Press, Cambridge, MA, 1972.
29. G.S. Ambrok, Approximate solutions of equations for the thermal boundary layer with variations in the boundary layer structure, *Soviet Phys. -Tech. Phys.*, 2 (9), 1957.
30. W.P. Jones and B.E. Lunder, The prediction of laminarization with a two-equation model of turbulence, *Int. J. Heat Mass Transfer*, 15, 1972.
31. B.A. Kader, Temperature and concentration profile in fully turbulent boundary layers, *Int. J. Heat Mass transfer*, 24(9), 1981.
32. R.B. Bird, W.E. Stewart and E.N. Lightfoot, *Transport Phenomena* (2nd Edition) John Wiley & Sons, Inc., Hoboken, NJ, 2002.
33. F. Szymanski, Quelques solutions exactes des equations de l'hydrodynamique de fluide visqueux dans le cas d'un tube cylindrique, *J., Math., pure Appl.*, Ser. 9, 11, 1932.
34. T.C. Papanastasiou, G.C. Georgiou and A.N. Alexandrou, *Viscous Fluid Flow*, CRC Press LLC, Boca Raton, FL, 2000.
35. K. Hiemez, Die Grenzschicht an einem in den gleich förmigen Flüssigkeitsstrom eingetauchten geraden Kreiszylinder, *Dingler's Polytech. J.*, 326, 1911.
36. E. Achenback, Influence of surface roughness on the cross-flow around a circular cylinder, *J. Fluid Mech.*, 46, 1971, and Experiments on the flow past spheres at very high Reynolds number, *J. Fluid Mech.*, 54, 1972.
37. M. Couette, Etudes sur le frottement des liquides, *Ann. Chim. Phys.*, ser. 6, 21, 433–510.
38. G.I. Taylor, Stability of a Viscous Liquid Contained between Two Rotating Cylinders, *Philosophical Transactions of the Royal Society of London. Series A, Containing Papers of a Mathematical or Physical Character*, 223, 289–343, 1923.

39. O. Reynolds, On the Theory of Lubrication and Its Application to Mr. Beauchamp Tower's Experiments, Including an Experimental Determination of the Viscosity of Olive Oil, Philosophical Transactions of the Royal Society of London, 177, 157–234, 1886.
40. O. Reynolds, On the dynamical theory of incompressible viscous fluids and the determination criterion. Philosophical Transactions of the Royal Society of London, 14, 123–164, 1895.
41. C.F. Colebrook, Turbulent flow in pipes with particular reference to the transition region between the smooth and rough pipe laws. J. Institution Civil Engineers, 1939.
42. W.P. Jones and B.E. Launder, The Prediction of Laminarization with a Two-equation Model of Turbulence, Int. J. Heat Mass Transfer, 15, 301–314, 1972.

The vorticity vortex dynamics is well documented with details in

43. J.Z. Wu, H.Y. Ma and M.D. Zhou, *Vorticity and Vortex Dynamics*, Springer, New York, 2006.

7. Non-Newtonian Fluid and Flow

In a general sense, fluids that exhibit characters not predicted by the Newtonian constitutive equation given in Eq. (6.4) are non-Newtonian. The exceptions to the Newtonian fluids are not of rare occurrence, and in fact many common fluids are non-Newtonian. Some examples are: paints, solutions of various polymers and molten plastics; food products such as apple sauce, ketchup and other mammalian whole foods; synovial fluid found in joints, blood and other organic fluids; many solid-liquid and liquid-liquid suspensions such as fibers in a liquid paper pulp, coal slurries, emulsions of water in oil or oil in water, and so on. The so-called non-Newtonian fluids, as mentioned above, are often found in many fields of engineering fluid mechanics as well as in bio-medical fields, and exhibit interesting, useful and even exciting characteristics differed from those found in Newtonian fluids.

Many difficulties are encountered to predict non-Newtonian flow due to the reason that the theoretical predictions are usually based upon the use of idealizing rheological fluid properties with associated constitutive equations that are often difficult to verify under conditions of complex flows. However, in recent years extensive efforts have been carried out to construct more general constitutive equations and to calculate the flows of practical configurations by using high-speed computers. Knowledge gained from CFD efforts presents the greatest amount of insight into many unexpected flow phenomena and explain the causes. The discovery, for example, so-called Toms effect (1948), that high molecular weight additives could lower the friction factor for flow of a polymer solution below that of the Newtonian solvent, is recognized nowadays that the drag reduction is a much wider spread phenomenon than originally thought. These problems are studied extensively, although not being quoted in the text, in conjunction with turbulence structure and flow instability with an aid of CFD.

In this chapter we will begin to describe characteristics and a rheological classification of non-Newtonian fluids. Then we will proceed to describe the standard flows, which are commonly used to characterize the rheology of non-Newtonian fluids. Subjecting a fluid to a standard flow we will then be able to define material functions, which are to be derived from a constitutive equation. After this initial background, we will study some

of the non-Newtonian constitutive equations with applications to basic engineering flows.

7.1 Non-Newtonian Fluids and Generalized Newtonian Fluid Flow

There exists a variety of substances for which the mechanical properties differ from Newton's viscous laws to a greater or lesser extent. In the present section, we shall discuss the rheological characteristics of non-Newtonian fluids that are chiefly based on a shear stress and their associated viscosity. Viscoelasticity is also introduced later in this section for further interpretations into non-Newtonian fluids.

Some typical flows are studied in view of engineering applications in connection with a discussion of rheological characteristics, considering an interpretation of generalized Newtonian viscous laws.

7.1.1 Rheological Classifications

We shall deal with incompressible medium of non-Newtonian fluids as commonly found in practice of engineering. The rheological characterization is done by experimental measurements. To convey the measurements of the subject, one approach specifies a deformation imposed on by a fluid and then measures the stresses generated by the flowing fluid through a specified channel geometry.

(i) Pure viscous non-Newtonian fluids

The most of the non-Newtonian fluids that we encounter practically usually fall into this category. These fluids are also termed as time-independent fluids (fully reversible without time-lag), and are subdivided into several groups, as graphically shown by Fig. 7.1. A Newtonian fluid is defined by Newton's law of viscosity, with reference to Eq. (6.1) as follows

$$\tau_{yx} = \eta \frac{\partial u}{\partial y} = \eta \dot{\gamma} \quad (7.1.1)$$

where η is the viscosity and $\dot{\gamma}$ the shear rate. It is noted that Fig. 7.1(a) is called the flow curve, which is the plot of τ_{yx} and $\dot{\gamma}$, the shear stress versus the shear rate. Similarly, Fig. 7.1(b) is a plot of η and $\dot{\gamma}$, the shear

viscosity versus the shear rate. η is a function of $\dot{\gamma}$ and is sometimes called the apparent viscosity η_a , which is defined, from Eq. (7.1.1), as

$$\eta_a = \tau_{yx} / \dot{\gamma} \tag{7.1.2}$$

In case of a Newtonian fluid, $\eta = \eta_a = \eta_0 = \text{constant}$, as is indicated in Fig. 7.1(b).

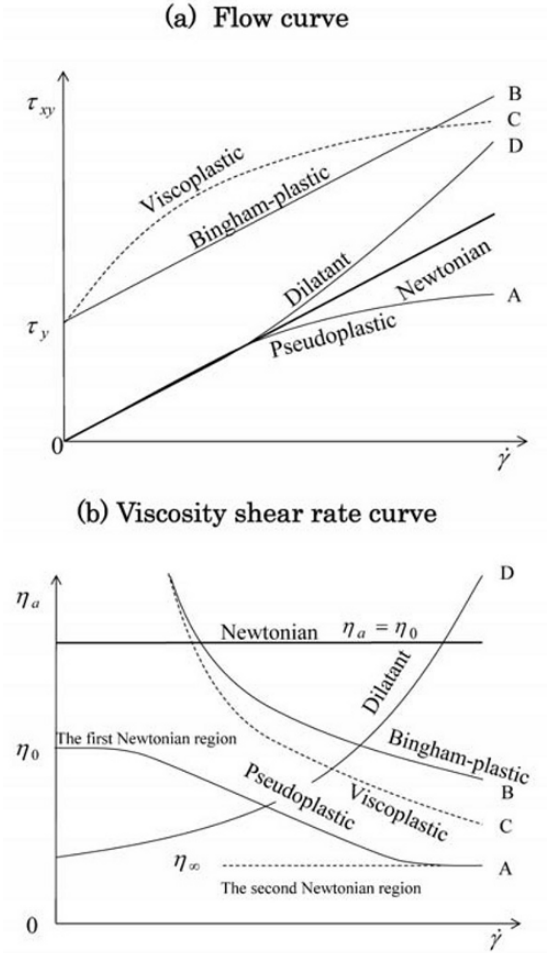


Fig. 7.1 Pure viscous Non-Newtonian fluids

A. Pseudoplastic fluids (shear thinning fluids)

Pseudoplastic fluids, as the ones indicated on curve A in Fig. 7.1(a) and (b), are characterized by a decreasing slope of a flow curve; equivalently,

the apparent viscosity decreases with increasing shear rate. The pseudoplastic fluid often has a rheological behavior that at very low and very high shear rates the apparent viscosity becomes constant; respectively, we have η_0 (called zero-shear rate viscosity) and η_∞ , regions which are respectively called the first Newtonian region and the second Newtonian region, where the flow curves are linear. Pseudoplastic fluids are found in many real fluids, such as polymer melts and solutions, starch paste, and glass melt.

There are a number of empirical relationships, among which the simplest is the power law suggested by Ostwald (1925). It may be written as

$$\tau_{xy} = m|\dot{\gamma}|^{n-1}\dot{\gamma} \quad (7.1.3)$$

where m and n are constant for a particular fluid. The fluids described in Eq. (7.1.3) are generally called power law fluids. In particular, when $n < 1$, the fluid shows the shear thinning behavior and is characterized as a pseudoplastic fluid. It appears that for a Newtonian fluid $n=1$ and $m = \eta_0$. Equation (7.1.3) is the most widely used in a less rigorous manner in many practical applications. There are some difficulties that should be kept in mind in applications of Eq. (7.1.3); one such instance occurs where the dimensions of m depend upon n ; therefore, m is not a material property. Another difficulty is that for real fluids, as mentioned above, n may not be constant over the entire range of $\dot{\gamma}$, with which the apparent viscosity η_a is written as

$$\eta_a = m|\dot{\gamma}|^{n-1} \quad (7.1.4)$$

However, n is effective in a limited range of $\dot{\gamma}$ for m to be constant.

Many other empirical formulae have been proposed to overcome some of the objections of the power law. One example is given where

$$\text{Ree-Eyring; } \tau_{xy} = \sum_{i=1}^m C_i \sinh^{-1}(\beta_i \dot{\gamma}) \quad (7.1.5)$$

C_i and β_i are constants to be determined as specific molecular parameters. Some rheological formulae for the apparent viscosity are

$$\text{Carreau-Yasuda; } \frac{\eta - \eta_\infty}{\eta_0 - \eta_\infty} = \left[1 + (\lambda \dot{\gamma})^a \right]^{\frac{n-1}{a}} \quad (7.1.6)$$

where η_0 is the zero-shear rate viscosity, $\eta_0 = \eta_a$ as $\dot{\gamma} \rightarrow 0$, a is a constant and λ is the time constant.

$$\text{Oldroyd; } \frac{\eta}{\eta_0} = \left(\frac{1 + C_1 \dot{\gamma}^2}{1 + C_2 \dot{\gamma}^2} \right) \quad (7.1.7)$$

Here, C_1 and C_2 are constants.

B. and C. Bingham-plastic and viscoplastic fluids

Viscoplastic fluids, as indicated on curve C in Fig. 7.1(a) and (b), are often characterized by the generalized Bingham model, which is written as

$$\tau_{xy} = \tau_y + m|\dot{\gamma}|^{n-1} \dot{\gamma} \quad (7.1.8)$$

where τ_y is termed as the yield stress. It should be kept in mind that the yield stress is a finite stress required to initiate flow and represents the value of τ_{xy} as $\dot{\gamma} \rightarrow 0$. The Bingham plastics (fluids) behave like a straight line in a flow curve after the yield stress, as indicated in curve B in Fig. 7.1, with the setting $n=1$ and $m=\eta_p$ in Eq. (7.1.8). The formula of a Bingham plastic (fluid) is thus expressed where

$$\tau_{xy} = \tau_y + \eta_p \dot{\gamma} \quad (7.1.9)$$

η_p is called the plastic viscosity. Some real fluids behave like the Bingham plastics, such as slurries, plastics, emulsions such as paint, and suspensions of finely divided solids in a liquid. Some electro-rheological fluids (ER fluid) have been found to be closely approximated to the behavior of a Bingham fluid, in which the yield stress is a function of the strength of electric field.

D. Dilatant fluids (shear thickening fluids)

Dilatant fluids, as indicated in curve D in Fig. 7.1(a) and (b), are similar to pseudoplastic fluids, but differ in that the slope of the flow curve decreases with an increasing of the shear rate, and equivalently, the apparent viscosity increases with increasing of the shear rate. These fluids are less common than with pseudoplastic fluids. As with pseudoplastic fluids, they are represented by the power law found in Eq. (7.1.3), where $n > 1$. The dilatant fluids have been found to closely approximate the behavior of some real fluids, such as starch in water and an appropriate mixture of sand and water. The term dilatant is also used to describe volumetric dilatancy, which is the tendency of suspensions to expand in a volume during flowing situations. It must be noted that dilatant fluids in this text are rheological dilatancy.

(ii) Thixotropic and rheopectic fluids

There are some fluids, which are more complex in structure than those found in time independent (pure viscous) fluids, and to which the apparent viscosity depends not only on the shear rate, but also on the time when the shear has been applied or ceased. For example, in a certain colloidal system, more particularly in a suspension, the apparent viscosity decreases during the mixing process, but on cessation of the shearing the viscosity recovers to its original value.

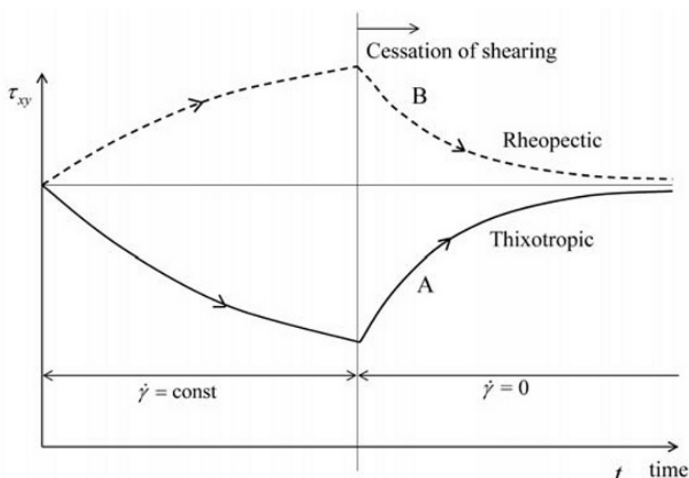


Fig. 7.2 Time dependent fluids

There are two general classes of such fluids: A. thixotropic fluids, in which the shear stress decreases with time as the fluids are sheared; and B. rheopectic fluids, in which the shear stress increases with time as the fluids are sheared. Figure 7.2 shows a schematic of the thixotropic and rheopectic fluid behavior in a symmetrical manner. Figure 7.2 is the simplest case of a symmetrical thixotropy or rheopecty in which the structure of the fluid is broken down (thixotropic fluid) or built up (rheopectic fluid) under increasing duration of applying a constant shear rate. In case of the symmetrical thixotropy, on cessation of shearing the structure can build up at the same rate as the break-down process. Therefore, it is symmetrical in this sense; the opposite type is the symmetrical rheopecty. There are many cases in which the structure does not recover completely upon the cessation of shearing, often indicating hysteresis, and as a result, some factors other than time, such as total strain, may be influential. Certain type of ink shows thixotropy. Other examples include the beating and thickening of egg whites, which shows rheopecty. It appears that many substances,

however, loses their time-independent rheological characteristics at extremely high shearing and can behave in a totally different manner as expected.

(iii) Viscoelastic fluids

Consider a dynamic system, where one may take the stress τ as a dynamic property and the strain γ as a geometric property. For the sake of simplicity, the system can be regarded as temperature independent and that the response time is so short that the inertia effect would be negligible. When a material exhibits such a way that there is a unique relationship between τ and γ , the material is called an elastic body (or elastic material). If there is a linear relationship between τ and γ , we have

$$\tau = G\gamma \quad (7.1.10)$$

The material is said to be a linear elastic body (or linear elastic material), where Eq. (7.1.10) is called Hooke's law, where G is the Young's modulus. In similar manner, as described in Eq. (7.1.1), when there is a unique relationship between τ and $\dot{\gamma}$, the material is called a viscous fluid. If τ is taken for the shear stress τ_{xy} and $\dot{\gamma} = d\gamma/dt$ for the shear rate, we can write the linear relationship of τ and $\dot{\gamma}$ for a Newtonian fluid where

$$\tau = \eta\dot{\gamma} \quad (7.1.11)$$

η is the viscosity (or coefficient of viscosity).

A viscoelastic material exhibits both elastic and viscous properties. The constitutive equation is written for a viscoelastic material where

$$\tau = f(\gamma, \dot{\gamma}) \quad (7.1.12)$$

However, for many realistic viscoelastic materials, including high molecular weight polymer materials, there is a complicated constitutive relationship, which is generally written in the following functional form

$$\phi\left(\tau, \frac{d\tau}{dt}, \frac{d^2\tau}{dt^2}, \dots, \gamma, \frac{d\gamma}{dt}, \frac{d^2\gamma}{dt^2}, \dots\right) = 0 \quad (7.1.13)$$

It must be kept in mind that τ and γ are to be treated *vis a vis* a tensor quantity in general. Some details of viscoelastic fluids and flows are treated in Section 7.3. Viscoelastic fluids under applied stress deform, but when stress is removed, the stress inside the viscoelastic fluid does not instantly vanish due to sustained stress by the internal molecular structure. This unique behavior is termed as the memory effect, which often characterizes flows of the viscoelastic fluid. In order to gain a qualitative

understanding of the fluid memory, more in-depth treatment will be provided in Section 7.3.

7.1.2 Generalized Newtonian Fluid Flows

In many engineering flows of non-Newtonian fluids, the most important rheological parameter is the non-Newtonian viscosity, which often has a substantial dependence on the shear rate, resulting in enormous change in pressure loss, volumetric flow rates and their associated flow characteristics. In this section we shall extend the Newton's viscous law to allow for a change of viscosity via the shear rate.

The deviatoric stress tensor of an incompressible Newtonian fluid is written with reference to Eq. (6.4) as follows

$$\begin{aligned}\boldsymbol{\tau} &= 2\eta \mathbf{e} \\ &= \eta \dot{\boldsymbol{\gamma}} \quad (\text{or } \eta \dot{\gamma}_{ij})\end{aligned}\tag{7.1.14}$$

$\dot{\boldsymbol{\gamma}}$ is the rate of strain tensor, i.e. $\nabla \mathbf{u} + \nabla \mathbf{u}^T$. In order to extend the idea of a varying viscosity with the shear rate $\dot{\boldsymbol{\gamma}}$ to an arbitrary flow, we are able to write the viscosity with the function of the scalar invariants of $\dot{\boldsymbol{\gamma}}$. Here for the sake of clarity, the invariants of $\dot{\boldsymbol{\gamma}}$ are denoted as I_e (The first invariant of the rate of strain tensor), II_e (The second invariant of the rate of strain tensor) and III_e (The third invariant of the rate of strain tensor), which are defined by

$$I_e = \text{tr } \dot{\boldsymbol{\gamma}} = \dot{\gamma}_{ii}\tag{7.1.15}$$

$$II_e = \text{tr } \dot{\boldsymbol{\gamma}}^2 = \dot{\gamma}_{ij}\dot{\gamma}_{ji}\tag{7.1.16}$$

$$III_e = \det \dot{\boldsymbol{\gamma}} = \varepsilon_{ijk}\dot{\gamma}_{1i}\dot{\gamma}_{2j}\dot{\gamma}_{3k}\tag{7.1.17}$$

so that η would be written as

$$\eta = \eta(I_e, II_e, III_e)\tag{7.1.18}$$

Considering incompressible flow, i.e. $\nabla \cdot \mathbf{u} = 0$, I_e becomes zero. In addition, if the flow field is assumed to be shear dominant, III_e would be regarded as zero, noting that for the simple shear flow III_e becomes identically zero. By virtue of the conditions above, it would be appropriate to regard that η would be the only function of II_e . Furthermore, it is more

useful to use the shear rate $\dot{\gamma}$ than Π_e if one thinks of empiricism, as discussed in the previous section, and with the fact $\dot{\gamma}$ is calculated as the magnitude of the rate of the strain tensor $\dot{\gamma}$ as follows

$$\dot{\gamma} = \sqrt{\frac{1}{2} \dot{\gamma}_{ij} \dot{\gamma}_{ji}} = \sqrt{\frac{1}{2} \Pi_e} \quad (7.1.19)$$

Therefore, the constitutive equation of the generalized Newtonian fluid is written as

$$\boldsymbol{\tau} = \eta(\dot{\gamma}) \dot{\gamma} \quad (7.1.20)$$

$\dot{\gamma}$ is given in Eq. (7.1.19). For example, in a simple shear, it is readily calculated that Π_e is $2\dot{\gamma}^2$.

If we assume that the fluid is inelastic and obeys the power law expression in Eq. (7.1.3), we can write general form of the power law fluid as

$$\boldsymbol{\tau} = m \left\{ \left(\frac{1}{2} \Pi_e \right)^{\frac{1}{2}} \right\}^{n-1} \dot{\gamma} \quad (7.1.21)$$

where the apparent viscosity is defined by

$$\eta_a = m \left(\frac{1}{2} \Pi_e \right)^{\frac{n-1}{2}} \quad (7.1.22)$$

It is mentioned that the expression of the shear dependent viscosity $\eta(\dot{\gamma})$ in Eq. (7.1.20) can be applied for other empirical formulae, as mentioned in the previous section by calculating the flow characteristics of a steady state shear flow of non-Newtonian fluids, using $\dot{\gamma}$ given in Eq. (7.1.19).

It may be useful to use nondimensionalized governing equations in flow calculations. Let us demonstrate how to nondimensionalize governing equations by using the generalized power law. It is assumed that the flow is incompressible and isothermal without body force. Denote that scaling parameters with the characteristic dimensions are such that

$$\mathbf{x}^* = \frac{\mathbf{x}}{l}, t^* = \frac{t}{t_0}, \mathbf{u}^* = \frac{\mathbf{u}}{U}, p^* = \frac{p}{\rho U^2} \text{ and } \boldsymbol{\tau}^* = \frac{\boldsymbol{\tau}}{\rho U^2} \quad (7.1.23)$$

Using the notations in Eq. (7.1.23), the continuity and Cauchy's equation of motion (the linear momentum equation) can now be respectively

written as

$$\nabla \cdot \mathbf{u}^* = 0 \quad (7.1.24)$$

and

$$St \frac{\partial \mathbf{u}^*}{\partial t^*} + \mathbf{u}^* \cdot \nabla \mathbf{u}^* = -\nabla p^* + \nabla \cdot \boldsymbol{\tau}^* \quad (7.1.25)$$

where the constitutive equation for the generalized power law model is

$$\boldsymbol{\tau}^* = \frac{1}{Re^*} \left(\frac{1}{2} \Pi_e^* \right)^{\frac{n-1}{2}} \dot{\gamma}^* \quad (7.1.26)$$

The nondimensional parameters that appear in the equations are the Strouhal number St and the generalized Reynolds number Re^* , which are respectively written where

$$St = \frac{l}{U t_0} \quad \text{and} \quad Re^* = \frac{\rho U^{2-n} l^n}{m} \quad (7.1.27)$$

Therefore, in order to keep the similarity of the flow of power law fluids for a constant St , the generalized Reynolds number Re^* , which includes power law constants m and n , must be kept constant.

Exercise

Exercise 7.1.1 The Second Invariant of the Rate of Strain Tensor

Write the second invariant of the rate of strain tensor Π_e and obtain the shear rate $\dot{\gamma}$ for a given (unidirectional) velocity component in the case of a simple shear flow in a Cartesian coordinates system, the cylindrical coordinates system and the spherical coordinates system.

Ans.

Set the velocity components such that

$$\mathbf{u} = u_i \quad (1)$$

and the rate of the strain tensor equates to

$$\dot{\gamma} = \dot{\gamma}_{ij} \quad (2)$$

i and j is x, y, z in a Cartesian coordinates system and r, θ, z in a cylindrical coordinates system and r, θ, ϕ in the spherical coordinates system. The second invariant of the rate of strain tensor Π_e is thus, written in Eq. (7.1.16), where

$$\Pi_e = \gamma_{11}^2 + \gamma_{22}^2 + \gamma_{33}^2 + 2(\gamma_{23}^2 + \gamma_{31}^2 + \gamma_{12}^2) \quad (3)$$

the rate of the strain tensor is assumed to be symmetric, i.e. $\gamma_{23} = \gamma_{32}$, $\gamma_{31} = \gamma_{13}$ and $\gamma_{12} = \gamma_{21}$. For a simple shear flow, the shear rate $\dot{\gamma}$ will be given in Eq. (7.1.19) for the given coordinates systems as follows

$$\dot{\gamma} = \sqrt{\frac{1}{2}(2\dot{\gamma}_{12}^2)} = \dot{\gamma}_{12} \quad (4)$$

so that

(i) Cartesian coordinates system, $\mathbf{u} = (u_x, 0, 0)$

$$\dot{\gamma} = \dot{\gamma}_{xy} = \frac{\partial u_x}{\partial x} \quad (5)$$

(ii) Cylindrical coordinates system, $\mathbf{u} = (0, u_\theta, 0)$, $\partial/\partial\theta = 0$

$$\dot{\gamma} = \dot{\gamma}_{r\theta} = r \frac{\partial}{\partial r} \left(\frac{u_\theta}{r} \right) \quad (6)$$

(iii) Spherical coordinates system, $\mathbf{u} = (0, 0, u_\phi)$, $\partial/\partial\phi = 0$

$$\dot{\gamma} = \dot{\gamma}_{r\phi} = r \frac{\partial}{\partial r} \left(\frac{u_\phi}{r} \right) \quad (7)$$

Exercise 7.1.2 Power Law Fluid in a Pipe

Consider the steady state laminar and isothermal flow in a horizontal pipe. The fluid in the pipe is incompressible and can be treated by the power law fluid. Find the fully developed flow velocity profile at an arbitrary cross section of the pipe, and calculate the relevant flow properties, such as the flow rate, the average velocity and the pressure drop along the pipe.

Ans.

Assume that the flow is axisymmetric so that the velocity components in the cylindrical coordinates (r, θ, z) are

$$\mathbf{u} = (0, 0, u_z) \quad (1)$$

where u_z is the axial velocity component and is an only function of r as depicted in Fig. 7.3. Ignoring the inertial and body force term, the Cauchy's equation of motion in the unidirectional flow (z directional) is written to show

$$0 = -\frac{\partial p}{\partial z} + \frac{1}{r} \frac{\partial}{\partial r} (r \tau_{rz}) \quad (2)$$

The component of the shear stress $\boldsymbol{\tau}$ is given by the power law

$$\tau_{rz} = m |\dot{\gamma}|^{n-1} \dot{\gamma} \quad (3)$$

where $\dot{\gamma}$ is the shear rate $\dot{\gamma} = \dot{\gamma}_{rz}$, and which is given as

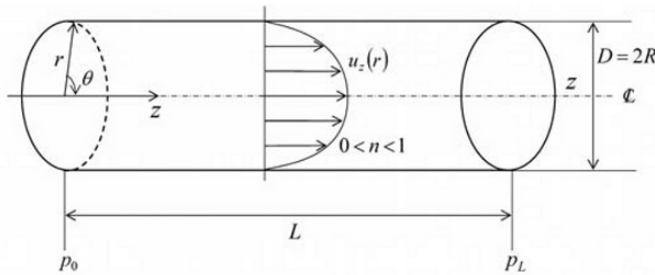


Fig. 7.3 Pipe flow of power law fluid

$$\dot{\gamma} = \frac{\partial u_z}{\partial r} \quad (4)$$

Equation (2) can be integrated to obtain τ_{rz} by the separation of variables so that we have

$$\tau_{rz} = \frac{1}{2} \left(\frac{\partial p}{\partial z} \right) r + \frac{C_1}{r} \quad (5)$$

where C_1 is a constant. Since τ_{rz} has a finite value at the center line, i.e. $r = 0$, C_1 must be zero.

From Eqs. (3), (4) and (5), we can write an equation for u_z where

$$m \left| \frac{\partial u_z}{\partial r} \right|^{n-1} \left(-\frac{\partial u_z}{\partial r} \right) = \frac{1}{2} \left(-\frac{\partial p}{\partial z} \right) r \quad (6)$$

Note that in the pipe flow we take the sign convention for a negative, since the velocity gradient $\partial u_z / \partial r$ and the pressure gradient $\partial p / \partial z$ are both negative. Equation (6) is now integrated for u_z by a separation of variables as follows

$$\frac{\partial u_z}{\partial r} = - \left\{ \frac{1}{2m} \left(-\frac{\partial p}{\partial z} \right) r \right\}^{\frac{1}{n}} \quad (7)$$

and

$$u_z = -\frac{n}{n+1} \left\{ \frac{1}{2m} \left(-\frac{\partial p}{\partial z} \right) \right\}^{\frac{1}{n}} r^{\frac{n+1}{n}} + C_2 \quad (8)$$

where C_2 is a constant that is obtained by the boundary condition, i.e. $u_z(R) = 0$. Resultantly, the velocity profile u_z will be given where

$$u_z = \frac{n}{n+1} \left\{ \frac{1}{2m} \left(-\frac{\partial p}{\partial z} \right) \right\}^{\frac{1}{n}} R^{\frac{n+1}{n}} \left[1 - \left(\frac{r}{R} \right)^{\frac{n+1}{n}} \right] \quad (9)$$

The speed at the axis is to be the maximum speed U_{\max} and is given by the setting $r = 0$ to yield

$$U_{\max} = \frac{n}{n+1} \left[\frac{1}{2m} \left(-\frac{\partial p}{\partial z} \right) \right]^{\frac{1}{n}} R^{\frac{n+1}{n}} \quad (10)$$

As a result, the velocity profile u_z will now be alternatively expressed with U_{\max} as follows

$$u_z = U_{\max} \left[1 - \left(\frac{r}{R} \right)^{\frac{n+1}{n}} \right] \quad (11)$$

The flow rate Q is thus calculated by integrating u_z across the radius to give

$$Q = 2\pi \int_0^R u_z r dr = \frac{n+1}{3n+1} \pi R^2 U_{\max} \quad (12)$$

The average velocity \bar{u} is also obtained from Eq. (12) where

$$\bar{u} = \frac{Q}{\pi R^2} = \frac{n+1}{3n+1} U_{\max} \quad (13)$$

The pressure gradient $-\partial p/\partial z$ is constant along the z axis, which is given by

$$-\frac{\partial p}{\partial z} = \frac{p_0 - p_L}{L} = \frac{\Delta p}{L} \quad (14)$$

where Δp is the pressure drop, leaving $\Delta p > 0$. Using Eq. (14), the (Darcy) friction factor λ , Δp is obtained by

$$\begin{aligned} \Delta p &= \lambda \left(\frac{L}{d} \right) \left(\frac{1}{2} \rho \bar{u}^2 \right) \\ &= \frac{8[2(3n+1)/n]^n}{Re^*} \left(\frac{L}{d} \right) \left(\frac{1}{2} \rho \bar{u}^2 \right) \end{aligned} \quad (15)$$

Re^* is the generalized Reynolds number defined in Eq. (7.1.27)

Note that the velocity distribution given in Eq. (11) shows flatter near the axis due to shear thinning, i.e. $0 < n < 1$. As $n \rightarrow 1$, when the Poiseuille paraboloid tends to persist, and when $n = 1$ the friction factor becomes $\lambda = 64/Re$.

Exercise 7.1.3 Spherical Gap Flow with Power Law Fluid

Examine the flow of power law fluid contained in a gap between two concentric spheres, where the inner sphere rotates at a given constant angular velocity ω , while the outer sphere is kept stationary. Assume that the gap is sufficiently narrow so that the simple shear flow persists, referring to section 6.3.1. Find the unidirectional velocity profile $u_\phi(r)$ and the torque to rotate the inner sphere against the frictional force. The geometric configuration is shown in Fig. 7.4.

Let u_ϕ be the circumferential velocity (velocity component of ϕ direction) and be the only function for r , i.e. $\mathbf{u} = (0, 0, u_\phi)$ and $u_\phi = u_\phi(r)$, as indicated in Fig. 7.4. By ignoring the inertial term and the body force term, the pressure gradient in the circumferential direction (ϕ direction) is null

due to the symmetry, provided that only the Cauchy's equation of motion in the circumferential direction is written where

$$0 = \frac{1}{r^3} \frac{\partial}{\partial r} (r^3 \tau_{r\phi}) \quad (1)$$

The shear stress $\tau_{r\phi}$ is given where the power law gives

$$\tau_{r\phi} = m |\dot{\gamma}|^{n-1} \dot{\gamma} \quad (2)$$

$\dot{\gamma}$ is the shear rate $\dot{\gamma} = \dot{\gamma}_{r\phi}$, which is written as

$$\dot{\gamma} = r \frac{\partial}{\partial r} \left(\frac{u_\phi}{r} \right) \quad (3)$$

Equation (1), together with Eqs. (2) and (3), is then solved with the boundary conditions:

$$u_\phi = r_1 \omega \quad \text{for } r = r_1 \quad (4)$$

and

$$u_\phi = 0 \quad \text{for } r = r_2 \quad (5)$$

These give the solution for u_ϕ , as follows

$$u_\phi = \left[\frac{r\omega}{(1+\beta)^{3/n} - 1} \right] \left[\left(\frac{1+\beta}{r/r_1} \right)^{3/n} - 1 \right] \quad (6)$$

Note that in Eq. (6), β is the gap ratio defined as

$$\beta = \frac{r_2 - r_1}{r_1} \quad (7)$$

The net torque T_r needed to rotate the inner sphere is governed by the shear stress $\tau_{r\phi}$ acting on the inner sphere; this is calculated by integrating $\tau_{r\phi}$ over the inner sphere with

$$T_r = 2\pi r_1^3 \int_0^\pi \tau_{r\phi} \sin^2 \theta d\theta \quad (8)$$

Note that Eq. (8) is valid for an axisymmetric flow, i.e. $\partial/\partial\phi = 0$, in general without $\tau_{\phi\phi}$ contribution.

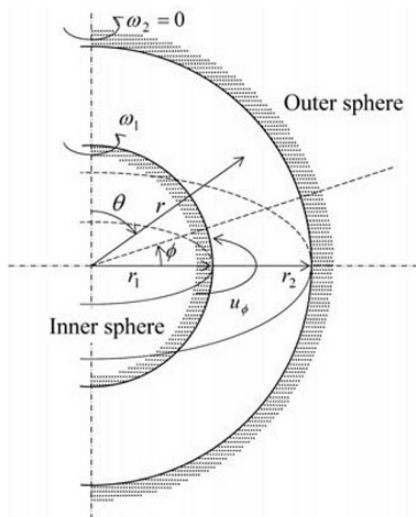


Fig. 7.4 Flow of a power law fluid between concentric rotating spheres

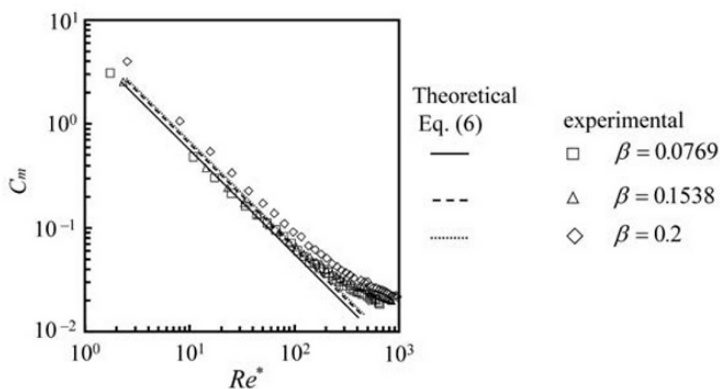


Fig. 7.5 Torque characteristic in a spherical gap flow

It is often convenient to nondimensionalize the torque T_r in such a way that

$$C_m = \frac{T_r}{\rho r_1^5 \omega_1^2} \quad (9)$$

where ρ is the liquid density and C_m is called the torque coefficient. Substituting Eq. (6) for Eq. (3), as well as for Eq. (2), we can obtain the torque coefficient C_m through Eqs. (8) and (9), as follows

$$C_m = 2\pi \frac{1}{Re^*} (1 + \beta)^3 \left[\frac{(3/n)\beta}{(1 + \beta)^{\frac{3}{n}} - 1} \right]^n \int_0^\pi \sin^{2+n}\theta d\theta \quad (10)$$

Re^* is the generalized (rotational) Reynolds number given where

$$Re^* = \frac{\rho(r_1\omega_1)^{2-n}(r_2 - r_1)^n}{m} \quad (11)$$

For reference, the results of Eq. (10) are representatively presented in Fig. 7.5 for a relatively low concentration of a polyacrylamide-water solution of 2000 ppm with various β . As observed in Fig. 7.5, the departure of experimental data plots from Eq. (10) are speculated to be caused by the appearance of flow instability, Yamaguchi, et al. (1997).

Problems

7.1-1 For a flow between two concentric rotating cylinders, with reference to Fig. 6.3(b) in Section 6.3.1, when the outer cylinder is kept stationary, find the expression for the shear rate $\dot{\gamma} = \dot{\gamma}_{r\theta}$. A power law fluid is assumed in the simple shear flow. Denote m and n are power law constants and k_r is the radius ratio defined by $k_r = r_1/r_2$.

$$\text{Ans. } \left[\dot{\gamma} = \left(\frac{r_2}{r} \right)^{\frac{2}{n}} \left[\frac{2\omega_1}{n \left[(1/k_r)^{\frac{2}{n}} - 1 \right]} \right] \right]$$

and for smaller gap $k_r \rightarrow 1 \quad \dot{\gamma} \approx \frac{\omega_1}{1 - k_r}$

7.1-2 For a helical flow in a cylindrical annular, where the inner cylinder rotates with the stationary outer cylinder, find the second invariant of the rate of the deformation tensor, and the shear viscosity $\eta(\dot{\gamma})$ from the power law. Note that the helical flow is such as that there is a flow along the rotational axis with the velocity component of u_z with the circumferential velocity component u_θ , whereas the radial velocity component u_r is kept zero in the cylindrical annular, as indicated in Fig. 7.6.

$$\begin{aligned}
 \text{Ans. } & \left[\begin{aligned} \dot{\gamma}_{rz} = \dot{\gamma}_{rz} = \frac{\partial u_z}{\partial r} \text{ and } \dot{\gamma}_{\theta r} = \dot{\gamma}_{r\theta} = r \frac{\partial}{\partial r} \left(\frac{u_\theta}{r} \right) \\ \Pi_e = 2(\dot{\gamma}_{rz}^2 + \dot{\gamma}_{\theta r}^2) = 2 \left[\left(\frac{\partial u_z}{\partial r} \right)^2 + \left\{ r \frac{\partial}{\partial r} \left(\frac{u_\theta}{r} \right) \right\}^2 \right] \\ \eta = m \left[\left(\frac{1}{2} \Pi_e \right)^{\frac{1}{2}} \right]^{n-1} = m \left[\left(\frac{\partial u_z}{\partial r} \right)^2 + \left\{ r \frac{\partial}{\partial r} \left(\frac{u_\theta}{r} \right) \right\}^2 \right]^{\frac{n-1}{2}} \end{aligned} \right]
 \end{aligned}$$

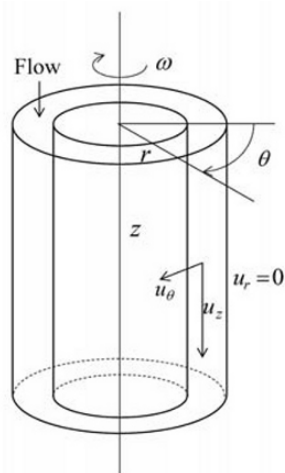


Fig. 7.6 Helical flow in a cylindrical annular

7.1-3 If the temperature distribution T of a steady state laminar flow in a horizontal pipe is given in the following energy equation

$$-\frac{k_c}{r} \frac{\partial}{\partial r} \left(r \frac{\partial T}{\partial r} \right) = \eta (\dot{\gamma}) \left(\frac{\partial u_z}{\partial r} \right)^2$$

Show that T in a power law fluid is calculated by

$$\frac{T - T_w}{T_0 - T_w} = 1 - \left(\frac{r}{R} \right)^{\frac{3n+1}{n}}$$

where T_0 and T_w are the temperatures at the axis ($r=0$) and at the

wall ($r = R$) respectively while k_c is the thermal conductivity of the fluid. Compare the temperature profile with the velocity profile [Eq. (11) in Exercise 7.1.2] and provide comments.

- 7.1-4 Show the difference between the power law model in Eq. (7.1.4) and the Carreau-Yasuda model in Eq. (7.1.6) when a set of viscosity-shear rate data is given as displaced in Fig. 7.7. Determine the constants in both models, when the data in Fig. 7.7 is fitted by both models.

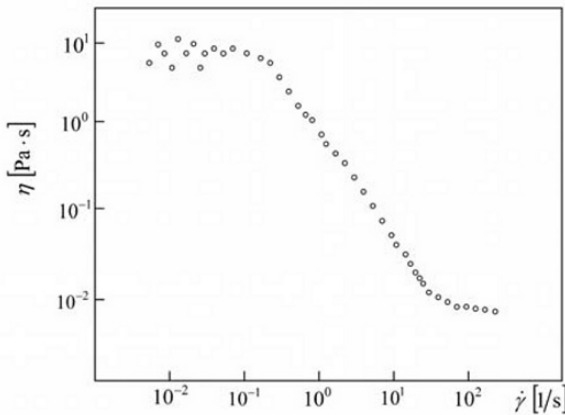


Fig. 7.7 Sample data of a shear thinning fluid

7.2 Standard Flow and Material Functions

In the previous section, we discovered that the dynamic property of a Newtonian fluid in an isothermal condition is characterized by a single material constant, namely the viscosity. However, in non-Newtonian fluids it is suggested that the material constant depends upon any deformation, time and/or other conditions yet to be examined. The dynamic properties of the materials (the interest in this text lies only in substances classifiable as fluids) that are used to determine the material constants in specific non-Newtonian constitutive equations or simply used to present mechanical property in engineering problem, are called material functions. The method of determining the material functions of fluids via experimental means is called rheometry, in which in classic approach basic rheometric or viscometric flows are introduced to give stress behavior under any given uniform deformation. The most common types of flow, used as standard flow

patterns in rheometric work, are the simple shear flow and simple shear-free flow.

In this section, we shall also look into the most commonly used rheometries based on the standard flow patterns and find approaches to obtain their material functions.

7.2.1 Simple Shear Flow

A simple shear flow is most typically understood as the plane Couette flow given in Eq. (6.3.13) as follows

$$u_x = \dot{\gamma}_{yx} y = \frac{U}{h} y = \dot{\gamma} y, \quad u_y = 0 \quad \text{and} \quad u_z = 0 \quad (7.2.1)$$

The absolute value of $\dot{\gamma}_{yx}$, i.e. the shear component of the rate of deformation tensor, is written as the shear rate $\dot{\gamma}$ in a rheometric flow. In the rheometry in a steady state measurement, as sketched in Fig. 7.8(a), it is assumed that $\dot{\gamma}$ is kept constant for such a long time that all associated stresses generated in a test fluid are time independent in isothermal condition.

The stress tensor associated with a simple shear flow is given in the following equation, referring to Eq. (1.6.13)

$$\mathbf{T} = -p\mathbf{I} + \boldsymbol{\tau} = \begin{bmatrix} -p + \tau_{xx} & \tau_{yx} & 0 \\ \tau_{xy} & -p + \tau_{yy} & 0 \\ 0 & 0 & -p + \tau_{zz} \end{bmatrix} \hat{\mathbf{e}}_i \hat{\mathbf{e}}_j \quad (7.2.2)$$

(a) Simple shear flow

(b) Shearfree (or elongational) flow

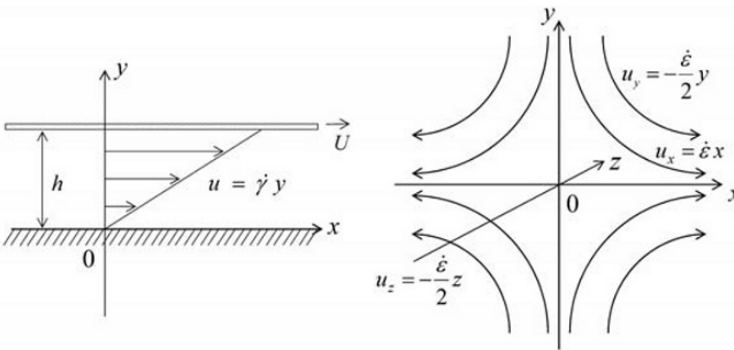


Fig. 7.8 Rheometric (viscometric) flows

For rheometric flows, the fluid is assumed to be isotropic so that it has no preferred direction other than the unidirectional flow field. In Eq. (7.2.2), $\boldsymbol{\tau}$ is sometimes called the deviatoric stress tensor in order to distinguish it from the total stress tensor \mathbf{T} .

Due to the symmetric nature of \mathbf{T} , recognizing the fluid as a non-polar fluid, the shear stresses τ_{xy} and τ_{yx} are the same in their value and τ_{yx} will be written by using the non-Newtonian viscosity $\eta(\dot{\gamma})$ as previously defined in Eq. (7.1.1)

$$\tau_{yx} = \eta(\dot{\gamma})\dot{\gamma} \quad (7.2.3)$$

In incompressible fluids, which are subject to study in most non-Newtonian fluids practice, the pressure p in Eq. (7.2.2) cannot be separated from normal stress measurements on a solid interface, so that in order to isolate p from the measurements two normal stress differences are only meaningful when determining the material functions, such that

$$N_1 = \tau_{xx} - \tau_{yy} = \psi_1(\dot{\gamma})\dot{\gamma}^2 \quad (7.2.4)$$

and

$$N_2 = \tau_{yy} - \tau_{zz} = \psi_2(\dot{\gamma})\dot{\gamma}^2 \quad (7.2.5)$$

where the functions ψ_1 and ψ_2 are called the first and the second normal stress coefficients respectively. It is noted that $\dot{\gamma}^2$ is used instead of $\dot{\gamma}$ for the reason that the sign of the two normal stress differences are not to be changed for the choice of the sign for $\dot{\gamma}$.

η , ψ_1 and ψ_2 are the material functions, which are often referred to as the viscometric functions. They are directly connected with a design of unit operations for processing viscoelastic materials and the mechanical performance of lubricants. The first normal difference N_1 has significant effects on unique viscoelastic flow phenomena, such as die swell, Weissenberg effect and etc. Both τ_{xy} and N_1 can be routinely measured by commercially available instruments. The second normal stress difference N_2 , however, receives less attention due to difficulties in its measurements, and for the smallness of its value. For many materials, N_2 would be usually an order of magnitude smaller than, and have the opposite sign to, that of N_1 . In Fig. 7.9, the representative data trends of viscometric functions are displayed. The graphs are typical of many

polymeric liquids (Huilgol and Phan-Thien, 1997). Viscometric functions are important parameters in order to describe flow characteristics of non-Newtonian fluids, the determining suitability of the constitutive equation. It is reassuring that in Newtonian fluids, the total stress tensor for the simple shear flow is expressed by a tensor form

$$\mathbf{T} = -p\mathbf{I} + \boldsymbol{\tau} = \begin{bmatrix} -p & \tau_{yx} & 0 \\ \tau_{xy} & -p & 0 \\ 0 & 0 & -p \end{bmatrix} \hat{\mathbf{e}}_i \hat{\mathbf{e}}_j \quad (7.2.6)$$

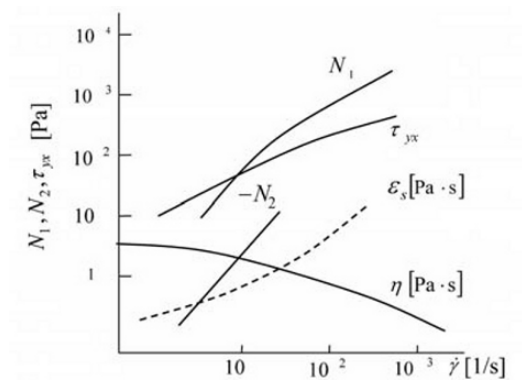


Fig. 7.9 Typically observed viscometric functions (replotted after Huilgol and Phan-thien, 1997); Polyiso-butylenes in cetane

As it is readily verified in Eq. (7.2.6), the normal stress components in a deviatoric stress tensor are all zero, i.e. $\tau_{xx} = \tau_{yy} = \tau_{zz} = 0$. Therefore, with Newtonian fluids, η is constant for $\dot{\gamma}$ and both N_1 and N_2 are null. There are many complex and unique flow phenomena that appear in non-Newtonian fluids due to the fact that there exist normal stresses beside the non-linearity of the non-Newtonian viscosity.

The appearance of a normal stress in cases of viscoelastic fluids, such as often seen in polymeric fluids, is particularly important to understand flow behavior. In such a case, the generations of normal stresses are closely connected with the elasticity of viscoelastic fluids. A measure of the elasticity is often quoted by the so-called stress ratio defined as

$$\varepsilon_s = \frac{\tau_{xx} - \tau_{yy}}{\tau_{yx}} \quad (7.2.7)$$

In many polymeric fluids, ε_s is a monotonic increasing function for an increasing $\dot{\gamma}$, as representatively shown in Fig. 7.9, while in Newtonian fluids ε_s is always kept at zero.

7.2.2 Shearfree Flow

Shearfree flows are flows in which there is no shear velocity gradient $\dot{\gamma}_{ij} = 0 (i \neq j)$ in the rate of the deformation tensor, but only a shearfree (normal) velocity gradient $\dot{\gamma}_{ii}$. There are some variations to achieve an ideal shearfree flow; they are defined by introducing the elongation rate $\dot{\varepsilon}$ along one arbitrary axis, such as

$$\frac{\partial u_x}{\partial x} = \dot{\gamma}_{xx} = \dot{\varepsilon} \quad (7.2.8)$$

In dealing with incompressible non-Newtonian fluids, the continuity equation can be written as

$$\frac{\partial u_x}{\partial x} + \frac{\partial u_y}{\partial y} + \frac{\partial u_z}{\partial z} = 0 \quad (7.2.9)$$

To satisfy Eq. (7.2.9), the other normal velocity gradients have to be written in the following forms, taking into account Eq. (7.2.8) so that

$$\frac{\partial u_y}{\partial y} = -\frac{\dot{\varepsilon}}{2}(1+k) \quad (7.2.10)$$

and

$$\frac{\partial u_z}{\partial z} = -\frac{\dot{\varepsilon}}{2}(1-k) \quad (7.2.11)$$

The choice of the axis is arbitrary due to the assumption of isotropic and frame invariance. The flow fields of shearfree flows defined in Eqs. (7.2.8), (7.2.10) and (7.2.11) are given by

$$u_x = \dot{\varepsilon} x \quad (7.2.12)$$

$$u_y = -\frac{1}{2}\dot{\varepsilon}(1+k)y \quad (7.2.13)$$

and

$$u_z = -\frac{1}{2}\dot{\epsilon}(1-k)z \quad (7.2.14)$$

k is constant and has the range in $0 \leq k \leq 1$. In particular, for rheometric flows, there are some shearfree flows by choice of $\dot{\epsilon}$ and k as follows

(i) $k=0$, $\dot{\epsilon} > 0$

$$u_x = \dot{\epsilon}x, \quad u_y = -\frac{1}{2}\dot{\epsilon}y, \quad u_z = -\frac{1}{2}\dot{\epsilon}z \quad (7.2.15)$$

The flow is called an elongational (or extensional) flow, as representatively shown in Fig. 7.8(b). The flow uniaxially stretches in x -direction, while contracting toward the center from the y and z axis points.

(ii) $k=0$, $\dot{\epsilon} < 0$

$$u_x = \dot{\epsilon}x, \quad u_y = -\frac{1}{2}\dot{\epsilon}y, \quad u_z = -\frac{1}{2}\dot{\epsilon}z \quad (7.2.16)$$

The flow is called a biaxial stretching flow. This is opposite to (i), where in y and z , a directional stretching flow persists, while along the x direction the flow is contracting.

(iii) $k=1$

$$u_x = \dot{\epsilon}x, \quad u_y = -\dot{\epsilon}y, \quad u_z = 0 \quad (7.2.17)$$

The flow is called a planar elongational flow. The flow appears along both the x and y plane, where in x direction flow stretches and in y direction flow contracts, and vice versa, depending upon the choice of the sign of $\dot{\epsilon}$.

Similar to a steady shear flow, $\dot{\epsilon}$ is kept constant for such a long time that all associated stresses generated in test fluids are time independent at isothermal conditions. The stress tensor associated with shearfree flows are given via the following equation

$$\mathbf{T} = -p\mathbf{I} + \boldsymbol{\tau} = \begin{pmatrix} -p + \tau_{xx} & 0 & 0 \\ 0 & -p + \tau_{yy} & 0 \\ 0 & 0 & -p + \tau_{zz} \end{pmatrix} \hat{\mathbf{e}}_i \hat{\mathbf{e}}_j \quad (7.2.18)$$

Along with the thought of a simple shear flow, two normal stress differences are only meaningful when determining the material functions for a shearfree flow, i.e.

$$\tau_{xx} - \tau_{yy} = \eta_1(\dot{\epsilon}, k) \dot{\epsilon} \quad (7.2.19)$$

and

$$\tau_{yy} - \tau_{zz} = \eta_2(\dot{\epsilon}, k) \dot{\epsilon} \quad (7.2.20)$$

where η_1 and η_2 are the viscometric functions for shearfree flows of isotropic fluids. Particularly in view of rheometry, the case of $k = 0$ is important, so that Eqs. (7.2.19) and (7.2.20) become

$$\eta_1(\dot{\epsilon}, 0) = \eta_e = \frac{\tau_{xx} - \tau_{yy}}{\dot{\epsilon}} \quad (7.2.21)$$

and

$$\eta_2(\dot{\epsilon}, 0) = 0 \quad (7.2.22)$$

η_e is called the elongational viscosity (or extensional viscosity) and also called the Trouton viscosity. It is readily obtain through the elongational viscosity η_e of the fluid, i.e. $\eta_e = 3\eta_0$, a result found via Trouton (1906). The rheometric measurement of an elongational viscosity is not easy, as is the shear viscosity in general, due to the difficulties of the isolation of shear influences. A typical measurement for data is displayed in Fig. 7.10, for a polystyrene melt (replotted after Munstedt 1993). In many polymeric fluids, the elongational viscosity is typically much larger (at least three times larger than a zero-shear viscosity) than its viscometric counterpart. It is noted that in Fig. 7.10, $\eta(\dot{\gamma}) \rightarrow \eta_0$ as $\dot{\gamma} \rightarrow 0$, η_0 is the zero-shear viscosity.

As observed in Fig. 7.10, the elongational viscosity η_e approaches to the value of $3\eta_0$ as $\dot{\gamma} \rightarrow 0$, where (at very low shear rate region) the shear stress is almost proportional to $\dot{\gamma}$, showing Newtonian fluid characteristics and the region called the first Newtonian region (also see Fig. 7.1(b)). Some rheometric measurements on elongational viscosity are found in reference to Tirtaatmadja et al. (1993).

There are some elongational flow fields typically encountered in engineering practice. They are, for example, converging and diverging channels, squeezing film, spinning synthetic fibers from molten liquid and so forth. The tubeless-siphon, in which a siphon continues to ascend even though the upstream end has been withdrawn from the fluid surface, is also prominently dominated by the elongational flow field. And, moreover flow behavior in viscoelastic fluids is widely discussed from the view point of elongational viscosity in recent years.

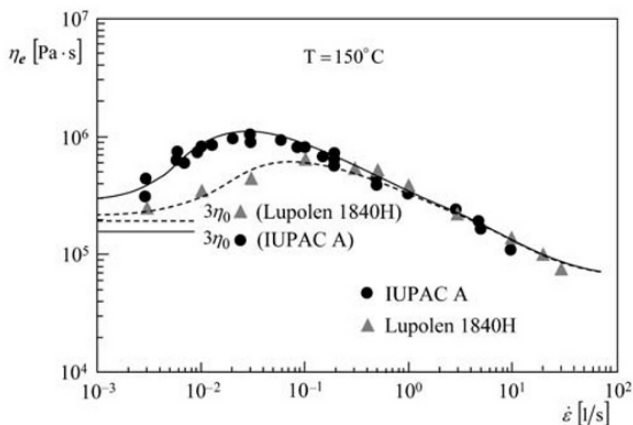


Fig. 7.10 Elongational viscosity (replotted after Munstedt 1993)

7.2.3 Oscillatory Rheometric Flow

Viscometric functions η , ψ_1 , ψ_2 and η_e , derived from standard flow patterns, which, in view of rheometric work, are commonly the simple shear and shearfree flows, are defined as time independent variable functions. However, in dealing with viscoelastic fluids, the dynamic properties and time dependent material functions, are of considerable practical importance, as flow behavior can often be directly related to the viscous, as well as elastic parameters, where the fluids undergo the transient process. In view of processing such material, the dynamic properties can also yield strong insight into the microstructure of the material. Among other time dependent material functions, the most widely used rheometric flow to determine the linear viscoelastic properties of polymeric fluids is a small amplitude oscillatory shear flow. The idealistic flow configuration is that the upper plate of Fig. 7.8(a), i.e. the simple shear flow, is oscillated with a small amplitude to give the shear strain γ as a function of time in such a way that

$$\gamma(t) = \gamma_0 \sin(\omega t) \quad (7.2.23)$$

where γ_0 is the shear strain amplitude and ω is the frequency. The shear strain rate $\dot{\gamma}$ is then obtained by differentiating Eq. (7.2.23) to give

$$\dot{\gamma} = \gamma_0 \omega \cos(\omega t) = \dot{\gamma}_0 \cos(\omega t) \quad (7.2.24)$$

where $\dot{\gamma}_0$ is the shear rate amplitude.

By subjecting to the limit of linear viscoelasticity (such that the viscoelastic material under this study may follow both Hooke's law and Newton's law simultaneously) stress is linearly dependent upon the shear strain and the shear strain rate at any time. This is the basic idea of the Boltzmann's superposition principle, and that is directly applied to developing the mathematical modeling of linear viscoelastic materials. From the rheometric point of view, the basic theory of linear viscoelasticity constitutes a convenient and a rather accurate analytical tool to analyze rheometric experimental data. In following the principle of superposition, we can write the shear stress τ_{yx} as linear in the strain or strain rate with corresponding forms of Eqs. (7.2.23) and (7.2.24), assuming that the relevant strain or strain rates are small enough

$$\tau_{yx} = |G^*| \gamma_0 \sin(\omega t + \delta) \quad (7.2.25)$$

$$\tau_{yx} = |\eta^*| \dot{\gamma}_0 \cos(\omega t - \phi) \quad (7.2.26)$$

where δ and ϕ are phase-shifts that are sometimes called mechanical loss angles. Note that $|G^*| \gamma_0$ and $|\eta^*| \dot{\gamma}_0$ give the stress amplitudes. Instead of relating $\delta(\omega)$ and $\phi(\omega)$ with material functions, it is customary to write these relationships in the following forms, using trigonometric identity

$$\tau_{yx} = \gamma_0 [G'(\omega) \sin(\omega t) + G''(\omega) \cos(\omega t)] \quad (7.2.27)$$

$$\tau_{yx} = \dot{\gamma}_0 [\eta'(\omega) \cos(\omega t) + \eta''(\omega) \sin(\omega t)] \quad (7.2.28)$$

There are two sets of linear viscoelastic material functions, namely G' , G'' and η' , η'' , appearing in Eqs. (7.2.27) and (7.2.28), where G' is called the storage modulus, and G'' is called the loss modulus and η' is called the dynamic viscosity.

It is sometimes convenient to consider $G'(\omega)$ and $G''(\omega)$ as real and imaginary components of a complex number respectively, defined as follows

$$G^*(\omega) = G'(\omega) + iG''(\omega) \quad (7.2.29)$$

where G^* is called the complex modulus. Thus, from Eq. (7.2.29), the magnitude of G^* is given:

$$|G^*| = \sqrt{(G')^2 + (G'')^2} \quad (7.2.30)$$

Furthermore, in Eq. (7.2.27), G' and G'' are expressed in terms of a phase-shift where

$$G' = |G^*| \cos(\delta) \text{ and } G'' = |G^*| \sin(\delta) \quad (7.2.31)$$

Alternatively, we may be able to define the complex viscosity $\eta^*(\omega)$ by writing

$$\eta^*(\omega) = \eta'(\omega) - i\eta''(\omega) \quad (7.2.32)$$

where

$$|\eta^*| = \sqrt{(\eta')^2 + (\eta'')^2}$$

As a result, we have the following relationship

$$\eta' = |\eta^*| \sin \delta = G''/\omega \text{ and } \eta'' = |\eta^*| \cos \delta = G'/\omega \quad (7.2.33)$$

The typical trends of experimental observation on G' , G'' and η' , η'' are sketched for linear polymeric fluids in Fig. 7.11.

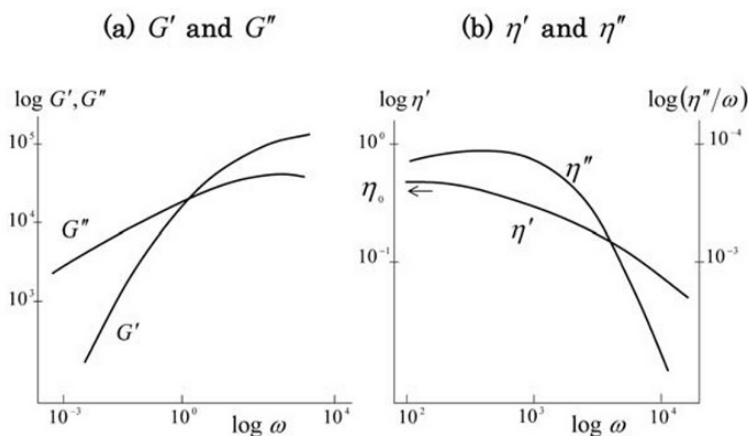


Fig. 7.11 Time dependent material functions; (a) G' and G'' for typically polyethylene melt; (b) η' and η'' for a typically narrow distribution linear polymer

It will now prove useful to speculate on the limiting behavior of the storage and the loss moduli at low frequencies as $\omega \rightarrow 0$; and at high frequencies as $\omega \rightarrow \infty$ for linear viscoelastic fluids. At low frequencies, as

expected from a linear viscoelastic fluid, we may find that viscous effects dominate the behavior so that

$$\lim_{\omega \rightarrow 0} (G''/\omega) = \lim_{\omega \rightarrow 0} \eta' = \eta_0 \quad (7.2.34)$$

$$\lim_{\omega \rightarrow 0} G' = \lim_{\omega \rightarrow 0} \eta'' = 0 \quad (7.2.35)$$

$$\lim_{\omega \rightarrow 0} G'' = 0 \quad (7.2.36)$$

where η_0 is the zero-shear viscosity. Furthermore, it is known that G'/ω^2 approaches a non-zero limiting value, for low frequencies

$$\lim_{\omega \rightarrow 0} (G'/\omega^2) = \lim_{\omega \rightarrow 0} (\eta''/\omega) = A_G \quad (7.2.37)$$

where A_G is a limiting value for $\omega \rightarrow 0$.

At high frequencies, the elasticity effects come to dominate the behavior in such a way that

$$\lim_{\omega \rightarrow \infty} G' = G_g \quad (7.2.38)$$

$$\lim_{\omega \rightarrow \infty} G'' = \lim_{\omega \rightarrow \infty} \eta'' = \lim_{\omega \rightarrow \infty} \eta' = 0 \quad (7.2.39)$$

where G_g is referred to as the glassy modulus; moreover, η''/ω becomes proportional to ω^{-2} . At very high frequencies, the fluid becomes like an elastic solid, where no viscous effects tend to appear.

There are some useful relationships involving viscometric functions to relate time-independent and time-dependent material functions. One of the most quoted relationships among many others is the Cox-Merz (Cox and Mertz, 1958) rule, which is expressed as

$$\eta(\dot{\gamma}) = |\eta^*(\omega)| \quad \text{by setting } \omega \approx \dot{\gamma} \quad (7.2.40)$$

This rule has been found to be relatively reliable for fluids with flexible molecules, and other relationships as the ones proposed by Laun (1986) for the first normal stress coefficient ψ_1 where

$$\psi_1(\dot{\gamma}) = 2 \frac{G'}{\omega^2} \left[1 + (G'/G'')^2 \right]^{0.7} \quad (7.2.41)$$

This relationship is tested for melts of some low- and high-density polymers, Laun (1986).

7.2.4 Viscometric Flow in Rheometry

Through the determination of material functions, we have discussed viscometric (or rheometric) flows that are equivalent to steady (or unsteady) simple shear flows, such as Couette flows, and shearfree flows, such as elongational flows. In this section, we shall pay more attention to practical measurements that determine those material functions, specifically the viscosity, the two normal stress differences, and the elongational viscosity.

The time-dependent material functions of kinematically variable viscometric flows and shearfree flows may be readily established from the time independent rheometric flows although, in practice, in precision measurements they are not at all easy a matter to achieve. As we have restricted material functions in non-Newtonian fluids, the fluids are assumed to be incompressible and isothermal. There are only two cases of typically studied flow configurations (in a sense that they are most widely utilized as practical rheometric measurements) that are considered in this section.

(i) The cone and plate rheometer

That is probably the most popular geometry for rheological measurements of viscoelastic fluids. It is usually used for measuring the shear viscosity and the first normal stress difference simultaneously. Additionally, the second normal stress difference can be determined from the relationship $N_1 + 2N_2$, a value of which is measurable by means of measuring the pressure distribution across a plate. An ideal cone and plate arrangement is illustrated in Fig. 7.12(a). A more practical arrangement in an actual rheometer is also displayed for a reference. In order to recognize the usefulness of a practical arrangement in Fig. 7.12(b), it is worth noting that the reason for utilizing a truncated cone is to avoid frictional torque at the contact with the plate, and with which it becomes easier to set the correct gap as required by the geometry of Fig. 7.12(a). The sample fluid is then placed in the space between the truncated cone and cup.

In order to verify the measuring principle, we shall look the basic arrangement of the cone and plate. As shown in Fig. 7.12(a), a spherical coordinates system (r, θ, ϕ) is used to analyze the flow field, assuming that the cone is rotated at the angular velocity Ω (either the cone or the plate can be rotated) at a symmetric axis. Due to the rotational symmetry, $\partial/\partial\phi$ components become identically zero and as the cone angle θ_0 is taken to be very small, i.e. approximately in a range where $0 < \theta_0 \leq 3^\circ$, the flow can be regarded as a narrow gap flow, namely with the condition of the velocity \mathbf{u} of the fluid that can be treated as $\mathbf{u} = (0, 0, u_\phi)$. The velocity

profile u_ϕ is also regarded as linear to the position (r, θ) in the gap and is approximated as

(a) Cone and plate geometry (b) Truncated cone and cup geometry

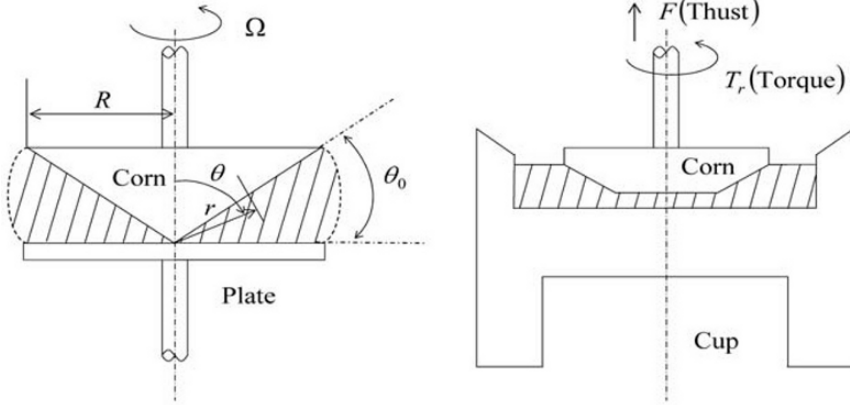


Fig. 7.12 Viscometric (or rheometric) flow

$$u_\phi \approx r\Omega \left(\frac{\pi}{2} - \theta \right) / \theta_0 \quad (7.2.42)$$

The shear rate $\dot{\gamma}$ in a spherical coordinates system is the $\theta\phi$ -component $\dot{\gamma}_{\theta\phi}$ with the rate of strain tensor $\dot{\gamma}$, which is written as

$$\dot{\gamma} = \dot{\gamma}_{\theta\phi} = \frac{\sin\theta}{r} \left[\frac{\partial}{\partial\theta} \left(\frac{u_\phi}{\sin\theta} \right) \right] \quad (7.2.43)$$

The substitution of Eq. (7.2.42) for Eq. (7.2.43) yields

$$\dot{\gamma} = -\frac{\Omega}{\theta_0} \quad (7.2.44)$$

since here we assume $\sin\theta \approx 1$ and $\cos\theta \approx 0$. The importance of Eq. (7.2.44) is that $\dot{\gamma}$ is independent from the position (r, θ) (free from coordinates) and that $\dot{\gamma}$ is only determined by the fixed angle θ_0 and the rotational speed (angular speed) Ω . It is repeatedly stated that Eq. (7.2.44) is only true for θ_0 if it is very small.

The viscosity η can be obtained from the actual measurement of torque T_r , which is exerted on the shaft of a cone to rotate at a given rotational speed Ω . The net torque on the surface of cone is given where

$$\begin{aligned}
 T_r &= \int_S \Delta T_r dS \\
 &= \int_S -\tau_{\theta\phi} r \sin\theta dS \\
 &= -\int_0^R \int_0^{2\pi} \tau_{\theta\phi} r^2 \sin^2\theta d\phi dr \\
 &= -2\pi \int_0^R \tau_{\theta\phi} r^2 dr \\
 &= -\frac{2}{3} \pi R^3 \tau_{\theta\phi}
 \end{aligned} \tag{7.2.45}$$

since $\sin\theta \approx 1$ and $\tau_{\theta\phi}$ is independent from coordinates system (r, θ, ϕ) for $\theta_0 \ll 1$. Note that $-\text{sign}$ to $\tau_{\theta\phi}$ reflects the shear stress on the solid surface of a cone. The viscometric function η , the viscosity, will be obtained by substituting Eqs. (7.2.44) and (7.2.45) to Eq. (7.1.1), yielding

$$\eta(\dot{\gamma}) = \frac{\tau_{\theta\phi}}{\dot{\gamma}} = \frac{\theta_0}{\Omega} \frac{3T_r}{2\pi R^3} \tag{7.2.46}$$

Therefore, from Eq. (7.2.46), the viscosity is readily determined by measuring T_r for a given Ω with fixed geometric constants θ_0 and R . The simplicity of the result given in Eq. (7.2.46) explains why the cone and plate rheometer is so widely used. In the most of commercially available rheometers, the range of $\dot{\gamma}$ [1/s] is approximately $10^{-1} \leq \dot{\gamma} \leq 10^4$ for precise measurements, although it is dependent upon a sample fluid.

More importantly, normal stress differences N_1 and N_2 can be determined by a cone and a plate rheometer. Particularly, it is ideal for a cone and plate geometry to measure the first normal stress difference N_1 . The two normal stress differences for N_1 and N_2 in a spherical coordinates system are defined as

$$N_1(\dot{\gamma}) = \tau_{\phi\phi} - \tau_{\theta\theta} \tag{7.2.47}$$

and

$$N_2(\dot{\gamma}) = \tau_{\theta\theta} - \tau_{rr} \tag{7.2.48}$$

Cauchy's equation of motion given in Eq. (2.2.6), ignoring the inertial term $\rho D\mathbf{u}/Dt$ and the body force term $\rho\mathbf{g}$, can be written as

$$0 = \nabla \cdot \mathbf{T} \quad (7.2.49)$$

where \mathbf{T} is the total stress tensor defined in Eq. (1.6.13). The $r\theta$ - and the $r\phi$ - components of the stress are to be zero. There is no shear force acting in r - direction, and the flow is assumed to be symmetrical with respect to ϕ . We can simply write the total stress tensor as follows

$$T_{rr} = -p + \tau_{rr}, \quad T_{\theta\theta} = -p + \tau_{\theta\theta} \quad \text{and} \quad T_{\phi\phi} = -p + \tau_{\phi\phi} \quad (7.2.50)$$

The Cauchy's equation, thus, in a spherical coordinates system will be written in the component form where

$$0 = \frac{\partial T_{rr}}{\partial r} - \frac{1}{r}(T_{\theta\theta} + T_{\phi\phi}) + \frac{2}{r}T_{rr} \quad (7.2.51)$$

Equation (7.2.51) is further rearranged to give

$$\begin{aligned} \frac{\partial T_{rr}}{\partial r} &= \frac{1}{r}(T_{\phi\phi} - T_{\theta\theta}) + \frac{2}{r}T_{\theta\theta} - \frac{2}{r}T_{rr} \\ &= \frac{1}{r}(T_{\phi\phi} - T_{\theta\theta}) + \frac{2}{r}(T_{\theta\theta} - T_{rr}) \end{aligned}$$

and therefore

$$\frac{\partial T_{rr}}{\partial \ln r} = (T_{\phi\phi} - T_{\theta\theta}) + 2(T_{\theta\theta} - T_{rr}) \quad (7.2.52)$$

Using the relationship of Eq. (7.2.50) with Eqs. (7.2.47) and (7.2.48), we can rewrite Eq. (7.2.52) as follows

$$\frac{\partial (-p + \tau_{rr})}{\partial \ln r} = N_1 + 2N_2. \quad (7.2.53)$$

Equation (7.2.53) will become a more convenient form for actual measurement when $T_{rr} = -p + \tau_{rr}$ is eliminated. Rewriting of Eq. (7.2.53) can be done for $N_2(\dot{\gamma})$, being as a unique function of $\dot{\gamma}$ and independent from r so that

$$\frac{\partial T_{rr}}{\partial \ln r} = \frac{\partial T_{\theta\theta}}{\partial \ln r} = \frac{\partial (-p + \tau_{\theta\theta})}{\partial \ln r} \quad (7.2.54)$$

The value of Eq. (7.2.54) is kept constant since $N_1 + 2N_2$ is also a unique function of $\dot{\gamma}$, showing that plotting $T_{\theta\theta}$ against $\ln(r/R)$, on a

semi-logarithmic scale should yield a straight line, the slope of which is $N_1 + 2N_2$, i.e.

$$T_{\theta\theta}(r) - T_{\theta\theta}(R) = (N_1 + 2N_2) \ln \left(\frac{r}{R} \right) \quad (7.2.55)$$

where Eq. (7.2.55) is obtained by integrating Eq. (7.2.53) from $r = r$ to $r = R$. However, the measurement for the (total) pressure $T_{\theta\theta} = -p + \tau_{\theta\theta}$ is a very difficult task, even when using very small and sensitive flush-mounted pressure transducers along the plate wall.

On the other hand, the primary normal stress difference N_1 can be readily determined by measuring the axial net force (net thrust force) F exerted on a cone (or plate). This is a widely used technique for rheometry. F is generally related to the normal stress $\tau_{\theta\theta}$ and the atmospheric pressure p_a on a cone through the following algebraic manipulation

$$\begin{aligned} F &= \int_S \Delta F - \pi R^2 p_a \\ &= \int_0^R \int_0^{2\pi} (T_{\theta r} \cos \theta - T_{\theta\theta} \sin \theta) dS - \pi R^2 p_a \\ &= \int_0^R \int_0^{2\pi} (T_{\theta r} \cos \theta - T_{\theta\theta} \sin \theta) r \sin \theta d\phi dr - \pi R^2 p_a \\ &= - \int_0^R \int_0^{2\pi} T_{\theta\theta} r d\phi dr - \pi R^2 p_a \end{aligned} \quad (7.2.56)$$

since $\theta \approx \pi/2$, $\cos \theta \approx 0$ and $\sin \theta \approx 1$. Substituting Eq. (7.2.55) for Eq. (7.2.56) and integrating the equation, we have

$$\begin{aligned} F &= -2\pi(N_1 + 2N_2) \int_0^R \ln \left(\frac{r}{R} \right) r dr - 2\pi \int_0^R T_{\theta\theta}(R) r dr - \pi R^2 p_a \\ &= \frac{1}{2} \pi R^2 (N_1 + 2N_2) - \pi R^2 T_{\theta\theta}(R) - \pi R^2 p_a \end{aligned} \quad (7.2.57)$$

We assure that the free surface at $r = R$ is at the atmospheric pressure p_a , i.e. $T_{rr}(R) = -p_a$, so that we can write N_2 as

$$\begin{aligned} N_2 &= T_{\theta\theta}(R) - T_{rr}(R) = T_{\theta\theta}(R) - (-p_a) \\ &= T_{\theta\theta}(R) + p_a \end{aligned} \quad (7.2.58)$$

Combining Eq. (7.2.57) with Eq. (7.2.58) yields the final form

$$N_1 = \frac{2F}{\pi R^2} \quad (7.2.59)$$

Equation (7.2.59) indicates that N_1 will be readily determined by measuring the net axial force (net thrust force) F for a given geometry R , subject to the assumption that a small cone angle, a negligible fluid inertial and edge effect (including surface tension) are involved. For precise measurements, corrections for these possible errors are recommended in Carreau, et al. (1997).

Other commonly used rotational rheometers are the parallel plate (or tensional) rheometer, and the concentric cylinder rheometer (referring to Section 6.3.1). The common features of these rheometers are based on the narrow gap flow where the shear rate is to be regarded as being independent from the spatial coordinates.

(ii) The elongational rheometer

There is an increasing amount of effort for polymer solutions for applications such as lubrication, turbulent drag reduction, coatings and atomization, in which the elongational (or extensional) flow field pre-dominates the mode of deformation. Continuing interest in polymer melts stems from the fact that polymer processing operations such as flat film extrusion, film blowing, fiber spinning and flow molding involve such elongational deformation that have been in fact subject of research for many decades. To characterize the flow of non-Newtonian fluids in the elongational deformation and to verify their constitutive relations, particularly for those derived from molecular dynamics, it is necessary to measure the material functions for shearfree flows. In view of investigating the elongational properties of polymer solutions, and a higher elongational rate for polymer melts, the two elongational flow fields, which have been used to try to generate a uniaxial stretching, are introduced in this section. In order to realize the flow field, some basic configurations for the types are exemplified via fiber spinning (or extrudate drawing), and pressure driven flows in a converging channel, as illustrated in Fig. 7.13(a) and (b) respectively. There are numerous modifications from the basic configurations, and therefore there is room for further precision measurements, for example, Collyer, et al. (1988) and Dealy, et al. (1999).

An apparent elongational viscosity $\bar{\eta}_e$ defined in Eq. (7.2.21) for uniaxial stretching is measured by using the relationship

$$\bar{\eta}_e = \eta_1 \approx \frac{\tau_E}{\dot{\epsilon}_E} \quad (7.2.60)$$

where τ_E is the net tensile stress, which can be approximated for $\tau_E = \tau_{yy} - \tau_{xx}$, and $\dot{\epsilon}_E$ is the tensile strain rate. The basic configuration for measuring $\bar{\eta}_e$ comes from a fiber-spinning apparatus, as illustrated in Fig. 7.13(a), where the test fluid, usually in the state of melt, is forced through a spinneret by means of a pressurized reservoir. Using a technique with an extrudate drawing, the filament (fiber) is cooled by exposure to ambient air, and is drawn down by means of a take-up drum.

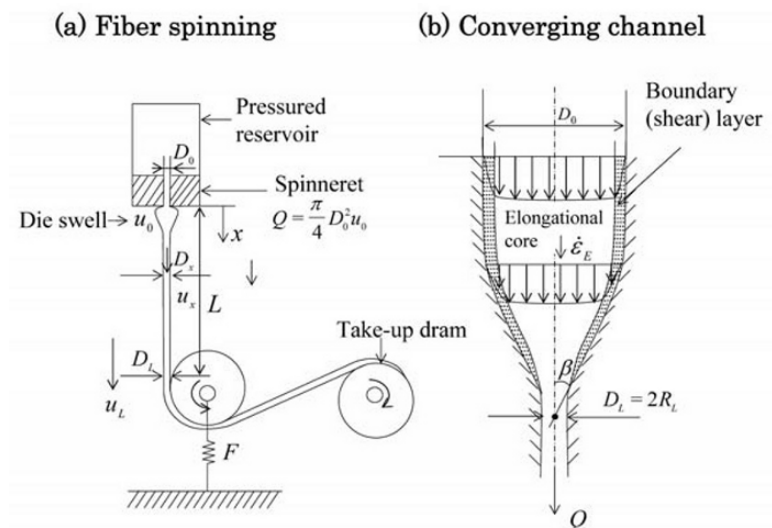


Fig. 7.13 Elongational rheometer

The vertical tensile force F in the filament is then measured on the rotating drum as indicated in Fig. 7.13(a). There are obviously sources for error associated with the measurement. They are, for example, the stress history through the spinneret and the exit point of the capillary channel (where the die swell occurs), surface tensile, inertia and air friction.

Neglecting these uncertainties and assuming that the force in the filament is kept constant along its length, the tensile stress would be given where

$$\tau_E = \frac{F}{\frac{\pi}{4} D_L^2} \quad (7.2.61)$$

With the continuity of the volume flow rate Q i.e. $Q = \pi D_L^2 u_L / 4 = \pi D_0^2 u_0 / 4$, where u_0 and u_L are the speed of flow at the position $x = 0$ and $x = L$. Equation (7.2.61) is written as

$$\tau_E = \frac{u_L}{u_0} \frac{F}{\pi D_0^2} \text{ (or } \frac{u_L}{Q} F \text{)} \quad (7.2.62)$$

If the cross section area of the filament varies with the axial distance x , for example, according to

$$A(x) = A_0 e^{-x} \quad (7.2.63)$$

A_0 and $A(x)$ are the cross section area at $x=0$ and x respectively. It proves useful to justify the derivation of Eq. (7.2.63). That is originated from the thought that a measure for the amount of elongation ε_E is often described by the so-called Hencky strain, defined as

$$\varepsilon_E = \ln \left(\frac{A_0}{A_x} \right) = \ln \left(\frac{x}{x_0} \right) \quad (7.2.64)$$

The strain rate $\dot{\varepsilon}_E$ is thus expressed as

$$\dot{\varepsilon}_E = \frac{d\varepsilon_E}{dt} = \frac{1}{x} \frac{dx}{dt} \quad (7.2.65)$$

So that, for a constant $\dot{\varepsilon}_E$, the length x increases with time t exponentially with the expression

$$x = x_0 e^{\dot{\varepsilon}_E t} \quad (7.2.66)$$

and for the cross section area where

$$A = A_0 e^{-\dot{\varepsilon}_E t} \quad (7.2.67)$$

Equation (7.2.63) is thus recovered by assuming that $\dot{\varepsilon}_E$ is kept constant along its length to give x with, likewise, only a function of time where

$$x = \dot{\varepsilon}_E t \quad (7.2.68)$$

For $x=L$, knowing u_L , Eq. (7.2.63) may be approximated through the following form

$$\frac{\pi}{4} D_L^2 \approx \frac{\pi}{4} D_0^2 e^{-\dot{\varepsilon}_E \frac{L}{u_L}} \quad (7.2.69)$$

Equation (7.2.66) can then be written for $\dot{\varepsilon}_E$ as

$$\begin{aligned}
 \dot{\epsilon}_E &= \frac{u_L}{L} \ln \left[c \left(\frac{D_0}{D_L} \right)^2 \right] \\
 &= \frac{u_L}{L} \ln \left(c \frac{u_L}{u_0} \right)
 \end{aligned}
 \tag{7.2.70}$$

c is an experimental constant. Thus, from Eq. (7.2.62) and Eq. (7.2.70), the apparent viscosity defined in Eq. (7.2.60) is readily calculated where

$$\bar{\eta}_e = \frac{4L}{u_0\pi} \frac{F}{D_0^2 \ln \left(c \frac{u_L}{u_0} \right)}
 \tag{7.2.71}$$

In order to minimize the error and to achieve a more idealistic state to validate Eq. (7.2.71), the filament can be extruded in isothermal canbers, for example, Sampers and Leblans (1988).

Test fluids with higher fluidity and at higher elongational rate may be tested for measuring the apparent elongational viscosity by using a pressure-driven converging channel as illustrated in Fig. 7.13(b). The average velocity increases monotonically as fluid particles move toward the apex. There appears an elongational flow field, though we must aware of the fact that there exists a boundary (shear) layer along the channel wall. To have a well-defined elongational flow field in the channel, the upstream section of the channel needs to be a tube with a large diameter D_0 relative to the throat diameter D_L . The entering flow also has to be moderate. The relative amount of a shear layer and an elongational core will depend on the geometry of the channel, the volumetric flow rate and the fluid's properties. To minimize the presence of the shear layer, it has been proposed that the channel walls may have to be lubricated with a relatively low viscosity fluid (Hsu et al. 1980), although it is difficult to form a uniform layer of lubricant along the channel wall.

Considering the elongational rheometer, an injection molding machine is often used as a rheometer head. Cogswell (1978) derived an expression for calculating an apparent elongational viscosity by using a die entry flow field. See reference to Fig. 7.13(b) for a nomenclature in cylindrical coordinates. The entry pressure drop Δp_{ent} is assumed to have two contributing parts where

$$\Delta p_{\text{ent}} = \Delta p_s + \Delta p_e
 \tag{7.2.72}$$

Δp_s is the shear flow contribution and Δp_e is the elongational flow contribution. The velocity through the channel is calculated by the power law model with a power law index n , and for the power law fluid, the average shear viscosity (shear thinning viscosity $n < 1$) η_a is obtained via the apparent shear rate $\dot{\gamma}_a$ in the capillary viscometer whose radius is R_L , such that

$$\dot{\gamma}_a = \frac{4Q}{\pi R_L^3} \quad (7.2.73)$$

This is also the so-called Newtonian wall shear rate (see Exercise 7.2.4). The derived expression for the apparent elongational viscosity $\bar{\eta}_e$ is given in Gogswell (1978) as

$$\tau_E = \frac{3}{8}(n+1)\Delta p_{\text{ent}} \quad (7.2.74)$$

$$\dot{\epsilon}_E = \frac{4\dot{\gamma}_a\eta_a}{3(n+1)\Delta p_{\text{ent}}} \quad (7.2.75)$$

so that

$$\bar{\eta}_e = \frac{9(n+1)^2 \Delta p_{\text{ent}}^2}{32\eta_a \dot{\gamma}_a^2} \quad (7.2.76)$$

The measuring technique with a pressure-driven converging channel has an advantage in the case of a rheometric measurement. However, an unknown flow field in the channel would lead to future questions of equivalency to simple uniaxial stretching that is based on a shearfree flow, no matter how drastic assumptions have to be made. This is, in fact, the difficulty of measuring the elongational viscosity in general.

Exercise

Exercise 7.2.1 N_1 *Measurement by a Cylindrical Couette Flow*

By utilizing a simple shear flow in concentric rotating cylinders (referring to in Fig. 6.3(b)) the normal stress difference, especially the 1st normal stress difference $N_1 = \tau_{rr} - \tau_{\theta\theta}$ in cylindrical coordinates system, can be measured. Discuss the principle of the measurement, assuming that in the gap there are non-zero stress components of $\tau_{r\theta}$, τ_{rr} , $\tau_{\theta\theta}$ and τ_{zz} .

Consider a case when the inner cylinder is rotated with an angular velocity ω for a small gap ratio $k_r = r_1/r_2 \approx 1$.

Ans.

With a simple shear flow, $\mathbf{u} = (0, u_\theta, 0)$, and Cauchy's equation of motion in r direction, ignoring the body force term, we have

$$-\rho \frac{u_\theta^2}{r} = -\frac{\partial p}{\partial r} + \frac{1}{r} \frac{\partial}{\partial r} (r \tau_{rr}) - \frac{\tau_{\theta\theta}}{r} \quad (1)$$

Equation (1) can be rearranged, using rr -component of the total stress tensor T_{rr} as follows

$$-\frac{\partial T_{rr}}{\partial r} = -\frac{\partial(-p + \tau_{rr})}{\partial r} = \rho \frac{u_\theta^2}{r} + \frac{\tau_{rr} - \tau_{\theta\theta}}{r} \quad (2)$$

Since T_{rr} is an only function of r , i.e. infinite length cylinder approximation, Eq. (2) can be integrated with respect to r to obtain T_{rr}

$$T_{rr}(r_1) - T_{rr}(r_2) = \int_{r_1}^{r_2} \left(\rho \frac{u_\theta^2}{r} + \frac{\tau_{rr} - \tau_{\theta\theta}}{r} \right) dr \quad (3)$$

resulting in

$$T_{rr}(k_r r_2) - T_{rr}(r_2) = \int_{r_2}^{r_1} \left(\rho \frac{u_\theta^2}{r} + \frac{N_1}{r} \right) dr \quad (4)$$

In the case of a small gap, the cylindrical Couette flow, the shear rate $\dot{\gamma} = \dot{\gamma}_{r\theta}$ can be reduced to (Eq. 6.3.37)

$$\dot{\gamma} = \dot{\gamma}_{r\theta} \approx \frac{\omega}{1 - k_r} \quad (5)$$

which is assumed to be kept constant in the gap, so that u_θ becomes the linear velocity profile as follows

$$u_\theta \approx \frac{\omega}{1 - k_r} k_r r_2 \left(1 - \frac{r}{r_2} \right) \quad (6)$$

Substituting Eq. (6) for Eq. (4), and noting $N_1 = N_1(r)$, Eq. (4) can now be integrated to obtain

$$T_{rr}(k_r r_2) - T_{rr}(r_2) = \rho \left(\frac{\omega}{1 - k_r} \right)^2 (k_r r_2^2) \left\{ \frac{1}{2} (1 - k_r^2) - 2(1 - k_r) + \ln \left(\frac{1}{k_r} \right) \right\} + N_1 \ln \left(\frac{1}{k_r} \right) \quad (7)$$

and to set

$$\Delta \bar{p} = \phi(\omega) + N_1 \ln \left(\frac{1}{k_r} \right) \quad (8)$$

$\Delta \bar{p}$ is the measured pressure difference between the outer and inner cylindrical walls. $\Delta \bar{p}$ is the actual value of the pressure difference, which includes the normal stress components and is measurable by such flash mount pressure transducers. $\phi(\omega)$ is a known function, which is written as

$$\phi(\omega) = \rho \left(\frac{\omega}{1 - k_r} \right)^2 (k_r r_2^2)^2 \left\{ \frac{1}{2} (1 - k_r^2) - 2(1 - k_r) + \ln \left(\frac{1}{k_r} \right) \right\} \quad (9)$$

Therefore, N_1 can be obtained in principle from Eqs. (7) and (9) where

$$N_1 = \frac{\Delta \bar{p} - \phi(\omega)}{\ln \left(\frac{1}{k_r} \right)} \quad (10)$$

Exercise 7.2.2 Energy Dissipation

Give an expression for the energy dissipation W_c per cycle per unit of volume in an oscillatory shear.

Ans.

The energy dissipation W_c is equal to the work done per unit volume of a fluid undergoing one cycle in an oscillatory shear τ_{yx} , so that W_c can be written as

$$W_c = \int_0^T \tau_{yx} \dot{\gamma}(t) dt \quad (1)$$

The shear rate $\dot{\gamma}(t)$ and τ_{yx} in Eq. (1) are given in Eqs. (7.2.24) and in (7.2.25) as follows

$$\dot{\gamma}(t) = \dot{\gamma}_0 \cos(\omega t) \quad (2)$$

$$\tau_{yx} = \tau_{yx0} \sin(\omega t + \delta) \quad (3)$$

$\dot{\gamma}_0$ is the shear rate amplitude, τ_{yx0} is the stress amplitude and δ is the mechanical loss angle for the angular velocity $\omega = \omega_\phi$. It is noted that τ_{yx0} given in Eq. (7.2.25) is as follows

$$\tau_{yx0} = |G^*| \gamma_0 \quad (4)$$

where $|G^*|$ is the magnitude of the complex modulus and γ_0 is the shear strain amplitude.

Substituting Eqs. (2) and (3) for (1) and integrating gives

$$\begin{aligned} W_c &= \int_0^{2\pi} \tau_{yx0} \dot{\gamma}_0 \cos(\omega t) \sin(\omega t + \delta) dt \\ &= \tau_{yx0} \dot{\gamma}_0 \pi \sin \delta \\ &= \tau_{yx0} \dot{\gamma}_0 \pi \sin \delta \\ &= |G^*| \pi \sin \delta \dot{\gamma}_0 \gamma_0 \end{aligned} \quad (5)$$

From the relationship in Eq. (7.2.31), we find that

$$W_c = G'' \pi \dot{\gamma}_0 \gamma_0 \quad (6)$$

Therefore, the energy dissipation is directly proportional to the loss modulus.

Exercise 7.2.3 Dynamic Properties of G' and G''

Examine the storage of G' and loss of G'' moduli for a Newtonian fluid and a Hookean solid where subjected to an oscillatory shear.

Ans.

For a Newtonian fluid, we have a linear pure viscous constitutive relationship where

$$\tau_{yx} = \eta \dot{\gamma} \quad (1)$$

For the oscillatory shear, we have this from Eq. (7.2.24):

$$\tau_{yx} = \eta \dot{\gamma}_0 \cos(\omega t) \quad (2)$$

In comparison with Eq. (7.2.28), we can derive the relationship

$$\eta = \eta'(\omega) = G''/\omega \quad \text{and} \quad G' = 0 \quad \text{due to} \quad \eta''(\omega) = 0 \quad (3)$$

This shows that the mechanical loss angle (phase-shift) is $\pi/2$ since $\sin(\omega t + 2/\pi) = \cos(\omega t)$.

For a Hookean solid, we have a linear pure elastic constitutive relation where

$$\tau_{yx} = G\gamma \quad (4)$$

G is a shear modulus while the oscillatory shear from Eq. (7.2.23) leads to

$$\tau_{yx} = G\gamma_0 \sin(\omega t) \quad (5)$$

Similarly, in comparison with Eq. (7.2.27), we can obtain results that give us

$$G = G' \quad \text{and} \quad G'' = 0$$

These show that the mechanical loss angle (phase-shift) is zero.

Exercise 7.2.4 Rabinowitsch Procedure

Knowing a constitutive relationship for a non-Newtonian fluid (typically for power law fluids) or a Newtonian fluid, an apparent viscosity given in Eq. (7.1.2) is measured by a capillary rheometer. Show the principle of the measurement and apply it to a power law fluid, for example.

Ans.

Consider a flow in a capillary tube with reference to Exercise 7.1.2. The shear stress τ_{rz} is given in Eq. (5) in Exercise 7.1.2 as follows:

$$\tau_{rz} = \frac{r}{2} \left(\frac{\partial p}{\partial z} \right) \quad (1)$$

At the tube wall, i.e. $r = R$, the wall shear stress τ_w is written as

$$\tau_w = \frac{R}{2} \left(\frac{\partial p}{\partial z} \right) \quad (2)$$

From Eqs. (1) and (2), we can write τ_{rz} as

$$\tau_{rz} = \frac{\tau_w}{R} r \quad (3)$$

Note that Eq. (3) is valid for any fluid in a fully developed pipe flow.

For a steady state of fully developed unidirectional flow, the velocity profile u_z at a given cross section is only a function of r , so that the shear rate $\dot{\gamma}_{rz} = \Delta u_z / \Delta z < 0$ may be written by a function g as follows

$$\frac{\partial u_z}{\partial r} = -g(\tau_{rz}) \quad (4)$$

Here, g is a positive function of τ_{rz} and τ_{rz} is a function of r . Integrating Eq. (4) for given boundary conditions, i.e. $u_z = 0$ for $r = R$, we have

$$u_z = \int_r^R g(\tau_{rz}) dr \quad (5)$$

Equation (5) can be transformed into an integration with respect to τ as

$$u_z = \frac{R}{\tau_w} \int_{\tau}^{\tau_w} g(\tau) d\tau \quad (6)$$

where we can write $\tau = \tau_{rz}$ for brevity's sake.

It is now desired to derive an expression for the flow rate Q , which is calculated by

$$\begin{aligned} Q &= \int_0^R 2\pi r u_z dr \\ &= - \int_0^R \pi r^2 \left(\frac{\partial u}{\partial r} \right) dr \end{aligned} \quad (7)$$

$$= \int_0^R \pi r^2 g(\tau) dr \quad (8)$$

The integration parameter r in Eq. (8) can be transformed into τ with the aid of Eq. (3) to give

$$Q = \frac{\pi R^3}{\tau_w^3} \int_0^{\tau_w} g(\tau) \tau^2 d\tau \quad (9)$$

Setting the shear rate $\dot{\gamma} = \dot{\gamma}_{rz}$ in Eqs. (4), (5) is now rewritten as

$$\frac{\tau_w^3 Q}{\pi R^3} = \int_0^{\tau_w} \dot{\gamma} \tau^2 d\tau \quad (10)$$

Equation (10) is also written as a differential equation of Q by differentiating τ_w to give

$$\frac{1}{\pi R^3} \left(\tau_w^3 \frac{dQ}{d\tau_w} + 3\tau_w^2 Q \right) = \dot{\gamma}_w \tau_w^2 \quad (11)$$

and

$$\dot{\gamma}_w = \frac{1}{\pi R^3} \frac{1}{\tau_w^2} \frac{d(\tau_w^3 Q)}{d\tau_w} \quad (12)$$

where $\dot{\gamma}_w$ is the wall shear rate at $r = R$. Equation (11) is often called the Rabinowitsch equation, noting that Eq. (11) can be written in term of the pressures difference $\Delta p = p_0 - p_L$ for a given section L , as exemplified in Fig. 7.3, with the following formula

$$\dot{\gamma}_w = \frac{1}{\pi R^3} \left(3Q + \Delta p \frac{dQ}{d\Delta p} \right) \quad (13)$$

where a relationship $\tau_w = R\Delta p/(2L)$ is used for Eq. (12).

Equation (12) can be further reduced to a preferable expression to fit a monotonous, simple polynomial form as follows:

$$\begin{aligned} \dot{\gamma}_w &= \frac{1}{4\tau_w^2} \frac{d}{d\tau_w} \left(\tau_w^3 \frac{4Q}{\pi R^3} \right) \\ &= \frac{3}{4} \left(\frac{4Q}{\pi R^3} \right) + \frac{1}{4} \left(\frac{4Q}{\pi R^3} \right) \frac{d \ln \left(\frac{4Q}{\pi R^3} \right)}{d \ln \tau_w} \end{aligned} \quad (14)$$

In order to simplify Eq. (14), we may introduce parameter n' by defining

$$\frac{1}{n'} = \frac{d \ln \left(\frac{4Q}{\pi R^3} \right)}{d \ln \tau_w} \quad (15)$$

so that Eq. (14) can be newly expressed as

$$\begin{aligned} \dot{\gamma}_w &= \frac{3n' + 1}{4n'} \left(\frac{4Q}{\pi R^3} \right) \\ &= \frac{3n' + 1}{4n'} \dot{\gamma}_a \end{aligned} \quad (16)$$

where $\dot{\gamma}_a$ is the apparent Newtonian wall shear rate. Here, the term $(3n'+1)/4n'$ is usually called the Rabinowitsch correction. The non-Newtonian viscosity η is thus determined with a shear rate $\dot{\gamma}_w$ where

$$\eta(\dot{\gamma}_w) = \frac{\tau_w}{\dot{\gamma}_w} \quad (17)$$

Let us examine a case of a power law fluid along with the abovementioned procedure

$$\tau_w = m |\dot{\gamma}_w|^n \quad (18)$$

The logarithm form of Eq. (18) is

$$\ln \tau_w = \ln m + n \ln |\dot{\gamma}_w| \quad (19)$$

By combining Eq. (19) with Eq. (16) and setting $\dot{\gamma}_w = \dot{\gamma}_a$, we have

$$\ln \tau_w = \ln m + n \ln \left(\frac{3n' + 1}{4n'} \right) + n \ln \left(\frac{4Q}{\pi R^3} \right) \quad (20)$$

The differentiation of Eq. (20) with respect to $\ln(4Q/\pi R^3)$ gives

$$\frac{d \ln \tau_w}{d \ln \left(\frac{4Q}{\pi R^3} \right)} = n' = n \quad (21)$$

Therefore, a flow curve of τ_w vs $\dot{\gamma}_w$ is plotted in log-log scale as shown schematically in Fig. 7.14, where the slop is equal to the power law index n . The intercept p of $\ln \tau_w$ and $\ln(4Q/\pi R^3)$ at a given $\dot{\gamma}_w = \dot{\gamma}_{wp}$ and $\dot{\tau}_w = \dot{\tau}_{wp}$ will give m as

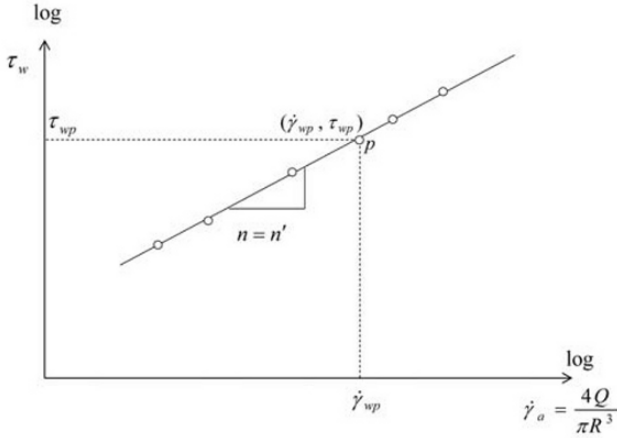


Fig. 7.14 Flow curve of power law fluid

$$\ln \tau_{wp} = \ln m + n \ln \left\{ \left(\frac{3n+1}{4n} \right) \cdot \dot{\gamma}_{wp} \right\} \quad (22)$$

so that

$$m = \tau_{wp} \left\{ \frac{4n}{(3n+1)\dot{\gamma}_{wp}} \right\}^n \quad (23)$$

Thus, knowing m and n in Eq. (18), the non-Newtonian viscosity η will be obtained readily by the relationship given in Eq. (17).

Problems

7.2-1 In Exercise 7.2.1, show that N_1 can be further simplified to the form

$$N_1 \approx \frac{\Delta \bar{p}}{(k_r - 1)}$$

when the inertial term is ignored. Note that $\ln(1/k_r) \approx 1 - k_r$ and

$$1 - k_r^2 = (1 + k_r)(1 - k_r) \approx 2(1 - k_r) \text{ for } k_r \approx 1.$$

7.2-2 A power law fluid is flowing in a pipe with a 0.05 m diameter at a volume flow rate of $0.1 \times 10^{-4} \text{ m}^3/\text{s}$. If the power law index n is 0.7,

estimate the apparent shear rate and show the difference if the flow is assumed to be Newtonian.

Ans.

	Power law fluid
	$\dot{\gamma}_w = \frac{3 \times 0.7 + 1}{4 \times 0.7} \left\{ \frac{4 \times 0.1 \times 10^{-4}}{\pi \left(\frac{0.05}{2} \right)^3} \right\} = 0.902 \left[1/s \right]$
	Newtonian fluid
	$\dot{\gamma}_w = \frac{3 \times 1 + 1}{4 \times 1} \left\{ \frac{4 \times 0.1 \times 10^{-4}}{\pi \left(\frac{0.05}{2} \right)^3} \right\} = 0.815 \left[1/s \right]$

7.2-3 When a rod is rotated at an interface of a viscoelastic fluid, the fluid climbs the rod (see Fig. 7.15). The phenomenon is called the Weissenberg effect. Explain this phenomenon, considering the pressure difference $\Delta \bar{p}$ given in Eq. (8) in Exercise 7.2.1 (cylindrical Couette flow). Thoughts on viscoelastic phenomena would be great help, where details will be studied in Section 7.3.

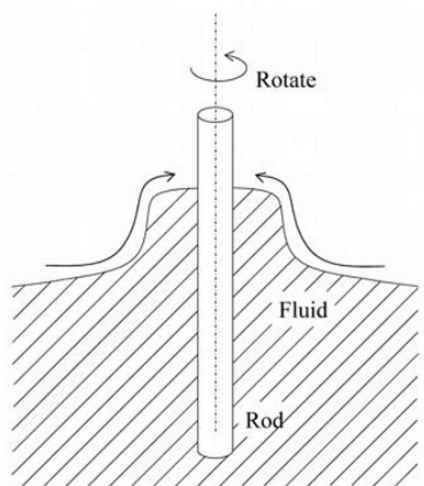


Fig. 7.15 Weissenberg effect

7.2-4 Discuss and specify difficulties for measuring the elongational viscosity by utilizing the converging channel (refer Fig. 7.13 (b)).

7.3 Viscoelastic Fluid and Flow

There are flow phenomena that cannot be explained by the Newtonian viscous law. Of which, the best known is the Weissenberg effect, in Problem 7.2.3, where some non-Newtonian fluids climb up a rod when it is inserted perpendicular to the fluid interface and rotated along its axis. The phenomena can be seen easily by stirring paint or cream in daily life. Another phenomenon associated with behavior of non-Newtonian fluids is the extrudate (die) swell in which the fluid emerges from a capillary tube and the diameter increases in vicinity of the exit (for example see Fig. 7.13(a)). This phenomenon is often experienced in the extrusion of meltplastic. These phenomena of non-Newtonian fluids are responsible for normal stress effects, contrary to what the Newtonian viscous effect (shear stress) does. The normal stress effects are an expression of a fluid elasticity, which is added to the viscous effects when the fluid is in motion. The viscoelastic fluids possess both viscous and elastic characters, with a nature unto themselves.

There are so many attempts to include the elastic effect in a macroscopic constitutive equation, with which unique phenomena of viscoelastic fluids would be explained. Although it is almost impossible to categorize the viscoelastic constitutive equation, historically, there might be three approaches to construct the equations: the first approach is one that is developed from a simple one dimensional rheological equation using a spring and a dashpot together with the concept of continuum mechanics, based on experimental facts and, moreover, experiences; the second approach is one that is derived from the general concept of genuine continuum mechanics; and the third approach is one that is developed from molecular dynamics in combination with the continuum concept, considering the molecular structures of the fluids, chiefly for polymeric fluids. In this text we shall follow the first approach in great detail.

The application of a constitutive equation for viscoelastic fluids to flow phenomena is another problem. Particularly, flows in actual engineering are very complicated where, in analysis, the nonlinear constitutive equation is highly coupled with its continuity, the linear momentum and energy equations. In such situations, the only possible way to tackle these problems is to rely on numerical analysis. Nevertheless, there are some analytical solutions possible for a simple geometry of flow. In this text we will

see some of these simple flows of viscoelastic fluids, which are described with linear viscoelastic models.

7.3.1 Linear Viscoelastic Rheological Equations

For a linear viscoelastic rheological equation, the constitutive equation is generally expressed by Eq. (7.1.13) with a linear relationship between τ , γ and their time derivatives.

The most fundamental theory in the case of an elastic liquid is derived from the so-called Maxwell element, as schematically shown in Fig. 7.16. The model consists of a series arrangement of a purely viscous element assigned as dashpot, where η is the viscosity and a perfectly elastic body is assigned as a spring where G is the modulus. The Maxwell model of viscoelasticity is obtained by thought of the Maxwell element, which is subjected to a sudden elongation and the force is then calculated as a function of time. As seen from the mechanical assembly in Fig. 7.16, the Maxwell element has no unique reference length and it will deform indefinitely when a force (per unit area) τ is applied. This behavior is analogous to the liquid-like behavior of a melt of an uncross-linked polymeric material over its glass transition.

Assume that the stress τ_1 , (the force per unit area) in the spring is $G\gamma_1$ and the stress τ_2 in the dashpot is $\eta(\partial\gamma_2/\partial t) = \eta\dot{\gamma}_2$. Here, we have a relationship between τ_1 and τ_2 where

$$\tau = \tau_1 = \tau_2 \quad (7.3.1)$$

since these are connected in series. In the system where the total strain of the system is written as

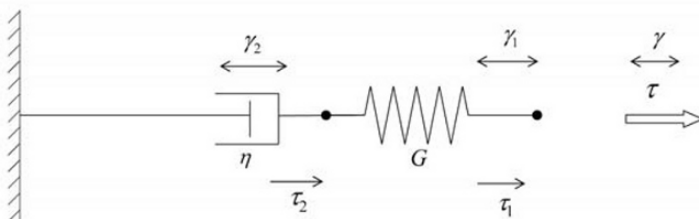


Fig. 7.16 Maxwell element

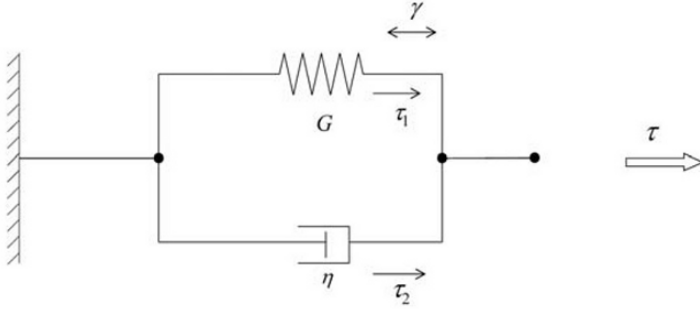


Fig. 7.17 Voigt element (or Kelvin element)

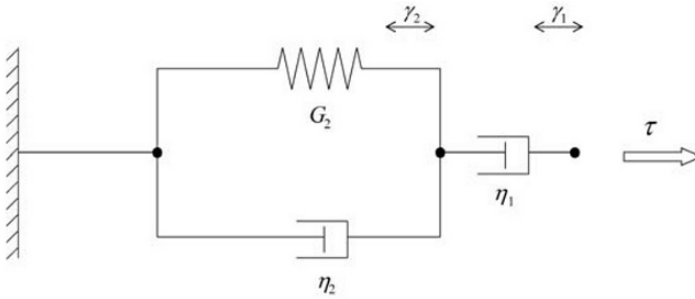


Fig. 7.18 Jeffreys element

$$\gamma = \gamma_1 + \gamma_2 \quad (7.3.2)$$

By differentiating Eq. (7.3.2) with respect to time t , we have

$$\frac{\partial \gamma}{\partial t} = \frac{\partial \gamma_1}{\partial t} + \frac{\partial \gamma_2}{\partial t} \quad (7.3.3)$$

so that with Eq. (7.3.1), we are able to write an equation relating the stress and strain rate

$$\begin{aligned} \frac{\partial \gamma}{\partial t} &= \frac{\left(\frac{\partial \tau_1}{\partial t} \right)}{G} + \frac{\tau_2}{\eta} \\ &= \frac{\left(\frac{\partial \tau}{\partial t} \right)}{G} + \frac{\tau}{\eta} \end{aligned} \quad (7.3.4)$$

Equation (7.3.4) can be further reduced as an expression for τ where

$$\tau + \lambda \frac{\partial \tau}{\partial t} = \eta \frac{\partial \gamma}{\partial t} \quad (7.3.5)$$

$\lambda = \eta/G$ is called the relaxation time. Equation (7.3.5) is the Maxwell model of a viscoelastic fluid. Equation (7.3.5) is a first order ordinary differential equation of τ . Since τ is only a function of time, Eq. (7.3.5) can be solved for τ to give

$$\tau = e^{-\frac{t}{\lambda}} \left[\int \frac{\eta}{\lambda} \left(\frac{\partial \gamma}{\partial t'} \right) e^{\frac{t'}{\lambda}} dt' + c \right]$$

and using $\dot{\gamma}$

$$\tau = \int_{-\infty}^t \left[\frac{\eta}{\lambda} e^{-\frac{(t-t')}{\lambda}} \right] \dot{\gamma}(t') dt' \quad (7.3.6)$$

where the stress τ at $t = -\infty$ is determined to have a finite value $\tau(-\infty)$ for the finite value of the strain rate $\dot{\gamma}(-\infty) = (\partial \gamma / \partial t)_{t=-\infty}$ at $t = -\infty$, i.e. to satisfy the following condition

$$\lim_{t \rightarrow -\infty} \tau(t) = \lim_{t \rightarrow -\infty} \frac{\frac{\eta}{\lambda} \dot{\gamma}(t) e^{\frac{t}{\lambda}}}{\frac{1}{\lambda} e^{\frac{t}{\lambda}}} = \eta \dot{\gamma}(-\infty) \quad (7.3.7)$$

It should be mentioned that Eq. (7.3.5) is the differential equation for the Maxwell model and Eq. (7.3.6) is the integral equation for the Maxwell model, both of which are equivalent. Equation (7.3.6) can be further reduced to the following expression with the integration by parts where

$$\tau(t) = - \int_{-\infty}^t \left\{ \frac{\eta}{\lambda^2} e^{-\frac{(t-t')}{\lambda}} \right\} \gamma(t, t') dt' \quad (7.3.8)$$

In Eq. (7.3.8), we used the strain at a past time t' relative to the reference state at the present time t . This is due to the reason that there would not be a unique configuration for the fluid at time past, but with only a reference state at the present time. Thus, the relationship between the strain and strain rate will be given where

$$\gamma(t, t') = \int_t^{t'} \dot{\gamma}(u) du$$

Equivalently,

$$\dot{\gamma}(t') = \frac{\partial}{\partial t'} \gamma(t, t') = \frac{\partial}{\partial t'} \int_t^{t'} \dot{\gamma}(u) du \quad (7.3.9)$$

The mechanical assembly that consists of a spring in parallel with a dashpot is called a Voigt (or Kelvin) element, or body, as schematically displayed in Fig. 7.17. The schematic of the assembly is where the body returns to a unique length, to the rest of the length of the spring, when the force (per unit area) is absent. The Voigt element is not intended to be a model for an elastic rubber; however, qualitative characteristics are quite similar to those exhibited by rubbers for its response to changes in applied force, showing that the Voigt element is analogous to the behavior of a viscoelastic solid.

With Voigt element, the strain γ is the same at both of the spring and dashpot, besides for the overall force (per unit area) τ of the parameter assembly, we can write

$$\tau = \tau_1 + \tau_2 \quad (7.3.10)$$

so that the following relationship exists

$$\tau = G\gamma + \eta \frac{\partial \gamma}{\partial t} \quad (7.3.11)$$

Equation (7.3.11) is the Voigt model of a viscoelastic solid and can be solved for $\gamma(t)$ with an initial condition of $\tau = \tau_0$ and $\varepsilon = 0$ at time $t = 0$, to yield

$$\gamma = \frac{\tau_0}{G} \left(1 - e^{-\frac{G}{\eta} t} \right) \quad (7.3.12)$$

The important point of the model is that the viscous resistance to elongation brings a time dependency into the response of the body. Equation (7.3.12) may be alternatively written in the following form, by setting $\lambda = \eta/G$ and $\gamma_\infty = \tau_0/G$

$$\gamma = \gamma_\infty \left(1 - e^{-\frac{t}{\lambda}} \right) \quad (7.3.13)$$

This indicates that for a sudden change in force (per unit area) τ_0 , the strain γ approaches its plateau γ_∞ asymptotically as time elapses. This indicates that a viscoelastic solid has a time constant λ and cannot respond instantaneously to changes in stress. This is called the retarded elasticity, and the time to reach $1/e$ of γ_∞ is called the retardation time. The strain change $\gamma(t)$ in time t for a given stress τ_0 is called the creep.

While dealing with more realistic viscoelastic materials, the basic models (i.e. the Maxwell element and Voigt element) are not necessarily adequate to apply with their own form. There are typically some combinations of these mechanical assemblies, and along which are the three elemental models of viscoelastic liquids called the Jeffreys elements, as indicated in Fig. 7.18. For the three elements models, we have the following stress-strain relations

$$\tau = \eta_1 \frac{\partial \gamma_1}{\partial t} \quad (7.3.14)$$

$$\tau = G_2 \gamma_2 + \eta_2 \frac{\partial \gamma_2}{\partial t} \quad (7.3.15)$$

From Eqs. (7.3.14) and (7.3.15), we can write an expression after differentiating both sides

$$G_2 \tau + (\eta_1 + \eta_2) \frac{\partial \tau}{\partial t} = \eta_1 G_2 \frac{\partial \gamma}{\partial t} + \eta_1 \eta_2 \frac{\partial^2 \gamma}{\partial t^2} \quad (7.3.16)$$

By knowing that τ and γ are functions of time only, we can write Eq. (7.3.16) with the simple form

$$\tau + a_1 \frac{\partial \tau}{\partial t} = b_1 \frac{\partial \gamma}{\partial t} + b_2 \frac{\partial}{\partial t} \left(\frac{\partial \gamma}{\partial t} \right) \quad (7.3.17)$$

where a_1 , b_1 and b_2 are the new constants defined where

$$a_1 = \frac{\eta_1 + \eta_2}{G_2}, \quad b_1 = \eta_1 \quad \text{and} \quad b_2 = \frac{\eta_1 \eta_2}{G_2} \quad (7.3.18)$$

The three new constants have relationships:

$$a_1 - \frac{b_2}{b_1} = \frac{\eta_1}{G_2} \quad (7.3.19)$$

and

$$a_1 > \frac{b_2}{b_1} \quad (7.3.20)$$

Herewith, both a_1 and b_2/b_1 have a unit of time where we can replace them with new notations

$$a_1 = \lambda_1 \text{ and } \frac{b_2}{b_1} = \lambda_2 \quad (7.3.21)$$

Using λ_1 and λ_2 , Eq. (7.3.17) can be rewritten where

$$\tau + \lambda_1 \frac{\partial \tau}{\partial t} = \eta_0 \left(\dot{\gamma} + \lambda_2 \frac{\partial \dot{\gamma}}{\partial t} \right) \quad (7.3.22)$$

with $\eta_0 = b_1$ and $\lambda_1 > \lambda_2$. Equation (7.3.22) is a constitutive equation of the Jeffreys model that contains two time constants λ_1 and λ_2 ; these are relaxation time constant and retardation time constant, respectively.

Since τ is a function of only time, Eq. (7.3.22) is a first order ordinary differential equation and there is a solution via an integral form as follows

$$\tau(t) = \int_{-\infty}^t \left\{ \frac{\eta_0}{\lambda_1} \left(1 - \frac{\lambda_2}{\lambda_1} \right) e^{-\left(\frac{t-t'}{\lambda_1} \right)} + \frac{2\eta_0\lambda_2}{\lambda_1} \delta(t-t') \right\} \dot{\gamma}(t') dt' \quad (7.3.23)$$

where $\delta(t)$ is the Dirac delta function. Equation (7.3.23) can be further reduced to the following form with an integration by parts

$$\tau(t) = - \int_{-\infty}^t \left\{ \frac{\eta_0}{\lambda_1^2} \left(1 - \frac{\lambda_2}{\lambda_1} \right) e^{-\left(\frac{t-t'}{\lambda_1} \right)} + \frac{2\eta_0\lambda_2}{\lambda_1} \delta'(t-t') \right\} \gamma(t-t') dt' \quad (7.3.24)$$

where we used following relationship of the delta function

$$\int_{-a}^a f(x) \delta(x) dx = 2 \int_0^a f(x) \delta(x) dx = f(0) \quad (7.3.25)$$

and

$$\int_{-a}^a f(x) \delta'(x) dx = -f'(0) \quad (7.3.26)$$

Experiments thought of vis a vis the Maxwell element, Voigt body and Jeffreys model are subjected to a sudden unidirectional elongation in

which the forces (per unit area) are calculated as a function of time. The analogous rheological experiment is one in which a sample of viscoelastic material is suddenly deformed: γ_0 at time $t=0$, and then the resulting stress $\tau(t)$ is measured as a function of time, that is

$$\tau(t) = G(t, \gamma_0) \gamma_0 \quad (7.3.27)$$

$G(t, \gamma_0)$ is called the relaxation modulus. This is called a stress relaxation experiment. As the most fundamental point of correspondence, we will now show that for a very small strain $\gamma_0 \ll 1$, G is independent of γ_0 in general, so that a linear relationship may stand, such that

$$\tau(t) = G(t) \gamma_0 \quad (7.3.28)$$

This very small-strain behavior is called a linear viscoelasticity.

A general equation that describes all types of linear viscoelastic behavior may be derived from the idea of a superposition principle, called the Boltzmann's superposition principle as shown in Fig. 7.19. Consider a sequence of a very small strain occurring at time t_1, t_2, t_3 , so that we have the relationship, according to the principle

$$\begin{aligned} \tau(t) &= G(t-t_1) \delta\gamma(t_1) + G(t-t_2) \delta\gamma(t_2) + \dots \\ &= \sum_{i=1}^N G(t-t_i) \delta\gamma(t_i) \quad (t > t_N) \\ &\approx \int_{-t}^t G(t-t') \delta\gamma(t') \quad (7.3.29) \end{aligned}$$

For an interval of a step strain $\delta\gamma(t')$, we may write $\delta\gamma(t') = \dot{\gamma} dt'$, so that Eq. (7.3.29) can be rewritten where

$$\tau(t) = \int_{-\infty}^t G(t-t') \dot{\gamma} dt' \quad (7.3.30)$$

It is noted that $\tau(-\infty)$ is defined by a mathematical convenience, with reference to Eq. (7.3.7), so that the stress τ has a finite value at $t = -\infty$. Equation (7.3.30) can be further reduced to another expression in terms of the strain γ (instead of the strain rate $\dot{\gamma}$) *vis a vis* the integration by parts, using the relationship of Eq. (7.3.9), as follows

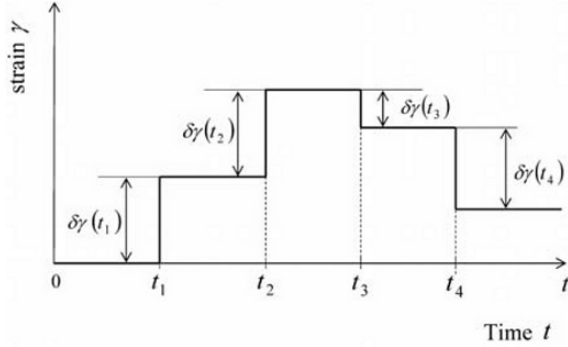


Fig. 7.19 Step strain in superposition principle

$$\begin{aligned}\tau(t) &= - \int_{-\infty}^t \frac{\partial G(t-t')}{\partial t'} \gamma(t, t') dt' \\ &= - \int_{-\infty}^t M(t-t') \gamma(t, t') dt'\end{aligned}\quad (7.3.31)$$

$M(t-t')$ is called the memory function. Both integral expressions in Eqs. (7.3.30) and (7.3.31) show that the stress at the present time t depends on the history of the state of the strain for all times past $-\infty < t' \leq t$.

In summarizing this section, let us look at the linear viscoelastic fluids relaxation modulus where the Maxwell model and the Jeffreys model are respectively given as

$$G(t-t') = \frac{\eta}{\lambda} e^{-\left(\frac{t-t'}{\lambda}\right)} \quad (7.3.32)$$

and

$$G(t-t') = \frac{\eta_0}{\lambda_1} \left(1 - \frac{\lambda_2}{\lambda_1}\right) e^{-\left(\frac{t-t'}{\lambda_1}\right)} + 2 \frac{\eta_0 \lambda_2}{\lambda_1} \delta(t-t') \quad (7.3.33)$$

Similarly, the memory functions are respectively given where

$$M(t-t') = \frac{\eta}{\lambda^2} e^{-\left(\frac{t-t'}{\lambda}\right)} \quad (7.3.34)$$

and

$$M(t-t') = \frac{\eta_0}{\lambda_1^2} \left(1 - \frac{\lambda_2}{\lambda_1}\right) e^{-\left(\frac{t-t'}{\lambda_1}\right)} + \frac{2\eta_0\lambda_2}{\lambda_1} \delta'(t-t') \quad (7.3.35)$$

It is mentioned that the exponential factors in G and M describe the fading memory, which is the decay of a weighting factor (both the relaxation modulus and the memory function) as time elapses from its original state.

7.3.2 Linear and Nonlinear Viscoelastic Models

Linear viscoelastic rheological equations can now be generalized to arbitrary small displacement flows, recognizing, first of all, that the relaxation process is independent, not only of the magnitude of the strain γ , but also of kinematics of the deformation. This can be done by replacing the strain γ by the strain tensor $\boldsymbol{\gamma}$ and the strain rate $\dot{\gamma}$ by the rate of the strain tensor $\dot{\boldsymbol{\gamma}}$ for infinitesimal deformations. In addition, the stress τ to achieve via the stress tensor $\boldsymbol{\tau}$ is used to obtain the following alternative forms of the Boltzmann's superposition principle:

$$\boldsymbol{\tau}(t) = \int_{-\infty}^t G(t-t') \dot{\boldsymbol{\gamma}}(t, t') dt' \quad (7.3.36)$$

and

$$\boldsymbol{\tau}(t) = - \int_{-\infty}^t M(t-t') \boldsymbol{\gamma}(t, t') dt' \quad (7.3.37)$$

Then the Maxwell model is written via integral equation

$$\boldsymbol{\tau}(t) = - \int_{-\infty}^t \left[\frac{\eta_0}{\lambda^2} e^{-\left(\frac{t-t'}{\lambda}\right)} \right] \boldsymbol{\gamma}(t, t') dt' \quad (7.3.38)$$

Equivalently, with use of a differential equation, we have

$$\boldsymbol{\tau} + \lambda \frac{\partial \boldsymbol{\tau}}{\partial t} = \eta_0 \dot{\boldsymbol{\gamma}} \quad (7.3.39)$$

Similarly, the Jeffreys model is also written as an integral equation, giving us

$$\boldsymbol{\tau}(t) = - \int_{-\infty}^t \left[\frac{\eta_0}{\lambda_1^2} \left(1 - \frac{\lambda_2}{\lambda_1} \right) e^{-\left(\frac{t-t'}{\lambda_1} \right)} + \frac{2\eta_0\lambda_2}{\lambda_1} \delta'(t-t') \right] \boldsymbol{\gamma}(t, t') dt' \quad (7.3.40)$$

Again, an equivalent form via a differential equation:

$$\boldsymbol{\tau} + \lambda_1 \frac{\partial \boldsymbol{\tau}}{\partial t} = \eta_0 \left(\dot{\boldsymbol{\gamma}} + \lambda_2 \frac{\partial \dot{\boldsymbol{\gamma}}}{\partial t} \right) \quad (7.3.41)$$

In Eqs. (7.3.38) to (7.3.41), we used η_0 as the zero shear rate viscosity.

These linear viscoelastic constitutive equations derived from generalized Maxwell and Jeffreys models are based on the idea that flows undergo infinitesimal displacement gradients. However, flows with large displacement gradients are found to be more realistic in practice, and constitutive equations are obtained on the basis of large displacement gradients that are found to be more appropriate in comparison with experiments. Also, some molecular theories, such as Bird et al., (1987 vol. 2), suggest very strongly that it is more appropriate to adopt the concept of large displacement gradients. Owing to these reasons, it is thought to take a fairly large displacement gradient into consideration in order to construct a viscoelastic constitutive equation.

An admissible viscoelastic constitutive equation would be obtained from a thought of relative strain tensor $\boldsymbol{\gamma}_R(t, t') = \mathbf{C}^{-1} - \mathbf{I}$ given in Eq. (1.4.6), where \mathbf{C}^{-1} is the Finger tensor. $\boldsymbol{\gamma}_R$, a symmetric tensor, contains information about the orientations of the three principle axes of stretch ratios and the magnitudes of the three principle stretch ratios. It should be kept in mind, as verified in Section 1.4, that \mathbf{C}^{-1} itself does not contain information about the rotation of material lines that occurs during the deformation.

With the argument introducing the relative strain tensor $\boldsymbol{\gamma}_R$ in a viscoelastic constitutive equation, we shall replace $\boldsymbol{\gamma}(t, t')$ in Eq. (7.3.37) with $\boldsymbol{\gamma}_R(t, t')$, to give

$$\begin{aligned} \boldsymbol{\tau}(t) &= - \int_{-\infty}^t M(t-t') (\mathbf{C}^{-1} - \mathbf{I}) dt' \\ &= - \int_{-\infty}^t M(t-t') \boldsymbol{\gamma}_R(t, t') dt' \end{aligned} \quad (7.3.42)$$

The model of Eq. (7.3.42) is referred to as a Lodge network (rubberlike) liquid and has a linear dependence on the history of a relative strain tensor, although a relative strain tensor is itself nonlinear in the displacement gradients. In this sense, the model may be regarded as quasi-linear. By adopting

the memory function $M(t-t')$ from the Maxwell model given in Eq. (7.3.34), we have a constitutive equation when writing

$$\boldsymbol{\tau}(t) = - \int_{-\infty}^t \left[\frac{\eta}{\lambda^2} e^{-\left(\frac{t-t'}{\lambda}\right)} \right] \boldsymbol{\gamma}_R(t, t') dt' \quad (7.3.43)$$

Equation (7.3.43) is known as the Lodge equation, which is really a nonlinear equation similar to the Maxwell model in terms of the displacement gradients. In similar fashion, the specific choices for memory function, for example, the Jeffreys model given by Eq. (7.3.35), will lead to another type of nonlinear version of the model.

A simple integral constitutive equation of a nonlinear version, such as Equation (7.3.43), can be converted to an equivalent differential form by differentiating the equation via the present time t . The time dependent term appears in the integral in three places; they are: in the memory function, in the Finger tensor, and in the upper limit of integration. Now we can see the conversion of the integral constitutive equation of Eq. (7.3.43) into the differential form

$$\begin{aligned} \dot{\boldsymbol{\tau}} = & \left[\frac{\eta_0}{\lambda^2} \boldsymbol{\gamma}_R(t') e^{-\left(\frac{t-t'}{\lambda}\right)} \right]_{t'=t} \Big|_{(1)} \\ & - \left[\frac{\eta_0}{\lambda^3} \int_{-\infty}^t e^{-\left(\frac{t-t'}{\lambda}\right)} \boldsymbol{\gamma}_R(t') dt' \right]_{(2)} \\ & + \left[\frac{\eta_0}{\lambda} \int_{-\infty}^t e^{-\left(\frac{t-t'}{\lambda}\right)} \dot{\mathbf{C}}^{-1}(t') dt' \right]_{(3)} \end{aligned} \quad (7.3.44)$$

In using the following identity for the time derivative of a Finger tensor

$$\begin{aligned} \dot{\mathbf{C}}^{-1}(t) &= \frac{\partial \mathbf{C}^{-1}}{\partial t} = \frac{\partial}{\partial t} (\mathbf{E}^{-1} \cdot \mathbf{E}^{-1T}) \\ &= \nabla \mathbf{u} \cdot \mathbf{C}^{-1} + \mathbf{C}^{-1} \cdot \nabla \mathbf{u}^T \end{aligned} \quad (7.3.45)$$

we have a differential form of the constitutive equation where

$$\begin{aligned} \dot{\boldsymbol{\tau}} = & \left[\frac{\eta_0}{\lambda^2} \mathbf{0} \right]_{(1)} - \left[\frac{1}{\lambda} \boldsymbol{\tau} \right]_{(2)} + [\nabla \mathbf{u} \cdot \boldsymbol{\tau} + \boldsymbol{\tau} \cdot \nabla \mathbf{u}^T]_{(3)} \\ & + \left[\frac{\eta_0}{\lambda} (\nabla \mathbf{u} + \nabla \mathbf{u}^T) \right]_{(3)} \end{aligned} \quad (7.3.46)$$

Each bracket...(1), (2) and (3)...implies that of Eq. (7.3.44). Rearrangement of the terms in Eq. (7.3.46) yields

$$\boldsymbol{\tau} + \lambda \overset{\nabla}{\boldsymbol{\tau}} = 2\eta_0 \mathbf{e} \quad (7.3.47)$$

where $\overset{\nabla}{\boldsymbol{\tau}}$ denotes the upper convective time derivative defined in Eq. (1.3.13), i.e.

$$\overset{\nabla}{\boldsymbol{\tau}} = \dot{\boldsymbol{\tau}} - \nabla \mathbf{u} \cdot \boldsymbol{\tau} - \boldsymbol{\tau} \cdot \nabla \mathbf{u}^T \quad (7.3.48)$$

\mathbf{e} is the rate of the strain tensor defined in Eq. (1.1.16), i.e.

$$2\mathbf{e} = \dot{\boldsymbol{\gamma}} = \nabla \mathbf{u} + \nabla \mathbf{u}^T \quad (7.3.49)$$

Equation (7.3.47) is called the upper convective Maxwell (UCM) equation. As discussed in Section 1.3, the UCM equation does obey the material objectivity, equivalent for the principle of the frame invariance. Furthermore, in view of satisfying the material objectivity, the UCM equation is extended to be written as

$$\boldsymbol{\tau} + \lambda \overset{\Delta}{\boldsymbol{\tau}} = 2\eta_0 \mathbf{e} \quad (7.3.50)$$

as well as

$$\boldsymbol{\tau} + \lambda \overset{\circ}{\boldsymbol{\tau}} = 2\eta_0 \mathbf{e} \quad (7.3.51)$$

where $\overset{\Delta}{\boldsymbol{\tau}}$ and $\overset{\circ}{\boldsymbol{\tau}}$ denote the lower convective time derivative and the corotational or Jaumann time derivative respectively, referring to Eqs. (1.3.14) and (1.3.15). These equations are called, respectively, the lower convective Maxwell (LCM) equation and the corotational Maxwell (CRM) equation. It appears that UCM equation is more commonly used in practice than the other two Maxwell models. This is chiefly because of the reason that the other Maxwell model (LCM in particular) does not give a qualitative agreement in comparison with rheological experimental data, and have no molecular basis, while the UCM equation does gain its background from the molecular based dynamic theories from Bird et al. (1977). The integral

form of the CRM equation is often called the Goddard–Miller equation (1966), which contains a spectrum of relaxation times.

In carrying out a numerical simulation to a flow of viscoelastic fluid, the differential type of constitutive equation is often more preferable than the integral type in discretizing procedure.

In similar fashion, the integral constitutive equation of the Jeffreys model given in Eq. (7.3.40), can be converted into differential equations. Resultantly, they are, as proposed by Oldroyd

$$\boldsymbol{\tau} + \lambda_1 \overset{\nabla}{\boldsymbol{\tau}} = 2\eta_0 \left(\mathbf{e} + \lambda_2 \overset{\nabla}{\mathbf{e}} \right) \quad (7.3.52)$$

and

$$\boldsymbol{\tau} + \lambda_1 \overset{\Delta}{\boldsymbol{\tau}} = 2\eta_0 \left(\mathbf{e} + \lambda_2 \overset{\Delta}{\mathbf{e}} \right) \quad (7.3.53)$$

These two equations are also frame invariants, meeting the requirements from the material objectivity. Equation (7.3.52) is called the Oldroyd-B equation, and Eq. (7.3.53) the Oldroyd-A equation. As mentioned earlier, Oldroyd-A equation is not used due to the reasons inherited from the problems of LCM. In addition to the Oldroyd-A and B equations, there is an equation, called the corotational Jeffreys equation, which has the expression

$$\boldsymbol{\tau} + \lambda_1 \overset{\circ}{\boldsymbol{\tau}} = 2\eta_0 \left(\mathbf{e} + \lambda_2 \overset{\circ}{\mathbf{e}} \right) \quad (7.3.54)$$

Oldroyd's equations have an additional term, $\lambda_2 \overset{\nabla}{\mathbf{e}}$, $\lambda_2 \overset{\Delta}{\mathbf{e}}$ (or $\lambda_2 \overset{\circ}{\mathbf{e}}$) to Maxwell's equations, which are inherited from the retardation term of the Jeffreys model given in Eq. (7.3.22). This term can be regarded as arising from stresses in a solvent of polymeric solutions (denote the solvent stress $\boldsymbol{\tau}_s$ and the polymer stress $\boldsymbol{\tau}_p$). In the case of Oldroyd-B equation, the (total) stress $\boldsymbol{\tau}$ can be regarded as a simple summation of $\boldsymbol{\tau}_p$ and $\boldsymbol{\tau}_s$ as

$$\boldsymbol{\tau} = \boldsymbol{\tau}_p + \boldsymbol{\tau}_s \quad (7.3.55)$$

where for, with $\boldsymbol{\tau}_p$ and $\boldsymbol{\tau}_s$, the following constitutive equations can be applied:

$$\boldsymbol{\tau}_p + \lambda_1 \overset{\nabla}{\boldsymbol{\tau}_p} = 2\eta_p \mathbf{e} \quad (7.3.56)$$

and

$$\boldsymbol{\tau}_s = 2\eta_s \mathbf{e} \quad (7.3.57)$$

Equations (7.3.56) and (7.3.57) are respectively the UCM equation and the Newtonian viscous equation. Any constant appearing in Eqs. (7.3.56) and (7.3.57) can be related by

$$\eta_0 = \eta_p + \eta_s \text{ and } \lambda_2 = \frac{\eta_s \lambda_1}{\eta_p + \eta_s} \quad (7.3.58)$$

where η_p and η_s are respectively the viscosity of a polymer contribution and a solvent viscosity. It is further noted that the Oldroyd-B model has a molecular basis from the elastic dumbbell in a solvent. Oldroyd (1958) proposed an extension of the B-equation, introducing 8 constants in the equation, which are also subject to the constraints of frame invariance. The Oldroyd 8-constant equation yields a reasonable account for estimating non-Newtonian viscosity and normal stress differences for incompressible viscoelastic fluids. In opposition to what has just been stated, there is a disadvantage for a model that, at a higher shear rate, the model tends to lose its quantitative agreement with actual experimental data.

We now look into a strongly nonlinear case, while as we have seen thus far, the Maxwell equations and Oldroyd's equations are, in a sense, quasi-linear, where the stress and strain relationship is indeed linear. Giesekus (1982) proposed a model like the UCM equation, in which a nonlinear term, derived from the viewpoint of a molecular basis, is appended. Namely, the constitutive equation is given where

$$\boldsymbol{\tau}_p + \lambda_1 \overset{\nabla}{\boldsymbol{\tau}_p} + \alpha \frac{\lambda_1}{\eta_p} \boldsymbol{\tau}_p \cdot \boldsymbol{\tau}_p = 2\eta_p \mathbf{e} \quad (7.3.59)$$

with auxiliary equations written as

$$\boldsymbol{\tau} = \boldsymbol{\tau}_s + \boldsymbol{\tau}_p \quad (7.3.60)$$

and

$$\boldsymbol{\tau}_s = 2\eta_s \mathbf{e} \quad (7.3.61)$$

Note that $\boldsymbol{\tau}_s$ and $\boldsymbol{\tau}_p$ are, respectively, solvent and polymer contributions to the stress tensor $\boldsymbol{\tau}$. The Giesekus model contains four constants, in which λ_1 is a relaxation time, η_s and η_p are respectively the solvent and polymer contributions to the zero-shear rate viscosity η_0 and α is a non-dimensional parameter called the mobility factor. The term involving α is originally derived from a molecular theory associated with anisotropic

hydrodynamic drag on the constituent polymer molecules, Giesekus (1966). The model is originally designated as an application for polymer solutions. The range of the mobility factor α lies between 0 and 1, where $\alpha = 0$ corresponds to the minimum anisotropies (isotropic drag) where the UCM equation is recovered, while $\alpha = 1$ corresponds to the strongest anisotropic drag. It is worthily mentioned that, when $\alpha = 1$, a steady state shear and an elongational stress are identical to those obtained from CRM equations. It appears that Eq. (7.3.59), the polymer contribution constitutive equation, is found to give a good rheological characterization to polymer melts.

Equations (7.3.59), (7.3.60) and (7.3.61) can be converted to a single constitutive equation with the following relationship

$$\boldsymbol{\tau}_p = \boldsymbol{\tau} - 2\eta_s \mathbf{e} \quad (7.3.62)$$

which is substituted in Eq. (7.3.59) to give

$$\begin{aligned} & \boldsymbol{\tau} + \lambda_1 \overset{\nabla}{\boldsymbol{\tau}} + \beta \frac{\lambda_1}{\eta_0} \boldsymbol{\tau} \cdot \boldsymbol{\tau} - 2\beta\lambda_2 (\mathbf{e} \cdot \boldsymbol{\tau} + \boldsymbol{\tau} \cdot \mathbf{e}) \\ & = 2\eta_0 \left(\mathbf{e} + \lambda_2 \overset{\nabla}{\mathbf{e}} - 2\beta \frac{\lambda_2^2}{\lambda_1} \mathbf{e} \cdot \mathbf{e} \right) \end{aligned} \quad (7.3.63)$$

where constants have a mutual relationship to satisfy

$$\eta_0 = \eta_s + \eta_p, \quad \lambda_2 = \lambda_1 \frac{\eta_s}{\eta_0} \quad \text{and} \quad \beta = \frac{\alpha}{1 - \lambda_2 / \lambda_1} \quad (7.3.64)$$

It will prove useful to note that with the constitutive equation of Eq. (7.3.63), the shear viscosity has a finite value as the shear rate $\dot{\gamma}$ approaches infinity, satisfying the rheological characters of polymeric solutions. The Giesekus model can be reduced to a number of constitutive equations referred to in the literature. For example, by setting $\lambda_2 = 0$ and $\alpha = 1/2$, the Leonov-like model (1976) of a steady shear and a shearfree flows are reduced.

There are some useful nonlinear constitutive equations, which are listed below.

Differential form:

(i) The White–Metzner model (1963)

$$\boldsymbol{\tau}_p + \frac{\eta(\dot{\gamma})}{G} \boldsymbol{\tau} = 2\eta(\dot{\gamma}) \mathbf{e} \quad (7.3.65)$$

where G is a constant modulus and $\dot{\gamma}$ is defined as

$$\dot{\gamma} = \left(\frac{1}{2} \dot{\gamma} : \dot{\gamma} \right)^{1/2} = \left(\frac{1}{2} \Pi_e \right)^{1/2} \quad (7.3.66)$$

(ii) The Phan-Thien and Tanner model (1977)

$$\lambda \overset{*}{\boldsymbol{\tau}} + Y(t_r, \boldsymbol{\tau}) \boldsymbol{\tau} = 2\eta_0 \mathbf{e} \quad (7.3.67)$$

$\overset{*}{\boldsymbol{\tau}}$ is an interpolated derivative defined by the following formula using Eq. (7.3.63)

$$\overset{*}{\boldsymbol{\tau}} = \frac{d\boldsymbol{\tau}}{dt} - \boldsymbol{\omega}^T \cdot \boldsymbol{\tau} - \boldsymbol{\tau} \cdot \boldsymbol{\omega} + c \left\{ \frac{1}{2} \left(\overset{\Delta}{\boldsymbol{\tau}} - \overset{\nabla}{\boldsymbol{\tau}} \right) \right\} \quad (7.3.68)$$

and

$$Y(t_r, \boldsymbol{\tau}) = e^{\frac{\varepsilon \lambda}{\eta_0}(t_r, \boldsymbol{\tau})} = 1 + at_r \boldsymbol{\tau} \quad (7.3.69)$$

where a , c and ε are constants. Y , as a function of $t_r, \boldsymbol{\tau}$ given in Eq. (7.3.69), is used for curve fitting for certain rheological data with a being a constant of small argument approximations and for $\eta_0 = G\lambda_0$.

Integral form:

(i) The convected generalized Maxwell model (Lodge network model, 1964 and 1983)

$$\boldsymbol{\tau} = - \int_{-\infty}^t \left[\sum_{i=1}^n \frac{\eta_i}{\lambda_i^2} e^{-\left(\frac{t-t'}{\lambda_i}\right)} \right] \boldsymbol{\gamma}_R(t, t') dt' \quad (7.3.70)$$

where the bracket is the memory function. The model is derived from a molecular theory of polymer melts, and also gives a constitutive equation for dilute polymer solutions, by giving explicit expressions for η_i and λ_i .

(ii) The Factorized K-BKZ equation:

$$\boldsymbol{\tau} = - \int_{-\infty}^t M(t-t') \left[\frac{\partial W(\mathbf{I}, \mathbf{II})}{\partial \mathbf{I}} \boldsymbol{\gamma}_R(t, t') + \frac{\partial W(\mathbf{I}, \mathbf{II})}{\partial \mathbf{II}} \boldsymbol{\gamma}^R(t, t') \right] dt' \quad (7.3.71)$$

In Eq. (7.3.71), W is a scalar (potential) function that gives strain energy and $U(\mathbf{I}, \mathbf{II}, t-t')$ is the free energy of elastic deformation as follows

$$U(\mathbf{I}, \mathbf{II}, t-t') = M(t-t') W(\mathbf{I}, \mathbf{II}) \quad (7.3.72)$$

where \mathbf{I} and \mathbf{II} are scalars defined from the Finger tensor \mathbf{C}^{-1} as follows

$$\mathbf{I} = t_r \mathbf{C}^{-1} \quad (7.3.73)$$

and

$$\mathbf{II} = \frac{1}{2} \left[\left(t_r \mathbf{C}^{-1} \right)^2 - t_r \mathbf{C}^{-2} \right] \quad (7.3.74)$$

Some simplifications are expressed with an incompressible flow limit, i.e.

$$\mathbf{III} = \det \mathbf{C}^{-1} = 1 \quad (7.3.75)$$

and with the Cayley-Hamilton theorem

$$\mathbf{C}^{-2} - \mathbf{I} \mathbf{C}^{-1} + \mathbf{II} \mathbf{I} = \mathbf{C} \quad (7.3.76)$$

Taking the determinant to both sides, we have

$$\mathbf{II} = t_r \mathbf{C} \quad (7.3.77)$$

where \mathbf{C} is known as the Cauchy strain tensor, defined where

$$\mathbf{C} \cdot \mathbf{C}^{-1} = \mathbf{I} \quad (7.3.78)$$

Also, the term $\boldsymbol{\gamma}^R$ that appears in the second term of Eq. (7.3.71) is the (another form of) relative strain tensor, namely

$$\boldsymbol{\gamma}^R = \mathbf{I} - \mathbf{C} \quad (7.3.79)$$

As an alternative, Eq. (7.3.71) is also written in its original form as follows:

$$\boldsymbol{\tau} = - \int_{-\infty}^t \left[\frac{\partial U(\mathbf{I}, \mathbf{II}, t-t')}{\partial \mathbf{I}} \boldsymbol{\gamma}_R + \frac{\partial U(\mathbf{I}, \mathbf{II}, t-t')}{\partial \mathbf{II}} \boldsymbol{\gamma}^R \right] dt' \quad (7.3.80)$$

Equation (7.3.80) is proposed independently by Kaye (1962) and Bernstein, et al. (1963), and is widely known as the K-BKZ equation, which is developed around ideas of rubber elastic theories.

Equation (7.3.71) can be reduced to a number of constitutive equations, as is often referred in the literature. For example, by setting

$$M(t-t') = \frac{96\eta_0}{\lambda^2} \sum_{\alpha(\text{odd})} e^{-\pi^2 \alpha^2 (t-t')/\lambda} \quad (7.3.81)$$

and

$$W(I, II) = \frac{5}{4\pi} \int \ln(C^{-1} : \hat{n}\hat{n}) d\hat{n} \quad (7.3.82)$$

we can obtain the Curtiss–Bird (1981) constitutive equation.

7.3.3 Viscoelastic Models to Standard Flow and Application to Some Engineering Flow Problems

In the preceding section we shall see the rheological predictions of some simple viscoelastic constitutive equations. However, it should be kept in mind that these viscoelastic constitutive equations would be used to portray the rheological properties that are observed in typical polymeric fluids. There are, in fact, a wide variety of material functions, as overviewed in Section 7.2. The cases examined here are chiefly based on the properties, in view of applying the equations to engineering problems, that are dependent upon the shear viscosity $\eta(\dot{\gamma})$ and the first normal stress coefficient $\psi_1(\dot{\gamma})$ in steady, simple shear flows, and also the elongational viscosity $\eta_e(\dot{\epsilon})$ at finite level of the elongational rate $\dot{\epsilon}$ in particular.

Some of typical flow problems are exemplified in the later section to illustrate the methods of applying the equations.

7.3.3.1 UCM, CRM and Giesekus Equations

In order to examine rheological characteristics of the constitutive equations at a steady state, an assumption is made to state that a time period after imposing a steady shear or elongation is much longer than the relaxation time constant, which is a property of fluid at rest.

We shall begin to examine the UCM equation given in Eq. (7.3.47), for simple shear and shearfree flows. Firstly, in the simple shear flow, UCM equation is written (with reference to Exercise 7.3.1) where

$$\begin{pmatrix} \tau_{xx} & \tau_{xy} & 0 \\ \tau_{xy} & \tau_{yy} & 0 \\ 0 & 0 & \tau_{zz} \end{pmatrix} - \lambda \dot{\gamma} \begin{pmatrix} 2\tau_{xy} & \tau_{yy} & 0 \\ \tau_{yy} & 0 & 0 \\ 0 & 0 & 0 \end{pmatrix} = \eta_0 \dot{\gamma} \begin{pmatrix} 0 & 1 & 0 \\ 1 & 0 & 0 \\ 0 & 0 & 0 \end{pmatrix} \quad (7.3.83)$$

Thus, from Eq. (7.3.83) we are able to obtain the material functions as

$$\tau_{xy} = \eta_0 \dot{\gamma}, \quad N_1 = \tau_{xx} - \tau_{yy} = 2\lambda \eta_0 \dot{\gamma}^2 \quad \text{and} \quad N_2 = \tau_{yy} - \tau_{zz} = 0 \quad (7.3.84)$$

which gives us

$$\eta = \frac{\tau_{xy}}{\dot{\gamma}} = \eta_0, \quad \psi_1 = \frac{N_1}{\dot{\gamma}^2} = 2\lambda \eta_0 \quad \text{and} \quad \psi_2 = \frac{N_2}{\dot{\gamma}^2} = 0 \quad (7.3.85)$$

Secondly, in shearfree flows, the UCM equation is similarly written as its component form

$$\begin{pmatrix} \tau_{xx} & 0 & 0 \\ 0 & \tau_{yy} & 0 \\ 0 & 0 & \tau_{zz} \end{pmatrix} - 2\lambda \dot{\epsilon} \begin{pmatrix} \tau_{xx} & 0 & 0 \\ 0 & -\frac{1}{2}(1+k)\tau_{yy} & 0 \\ 0 & 0 & -\frac{1}{2}(1-k)\tau_{zz} \end{pmatrix} \\ = \eta_0 \dot{\epsilon} \begin{pmatrix} 2 & 0 & 0 \\ 0 & -(1+k) & 0 \\ 0 & 0 & -(1-k) \end{pmatrix} \quad (7.3.86)$$

Thus, from Eq. (7.3.86) in the case of uniaxial stretching, i.e. $k=0$, in an elongational flow, the elongational viscosity η_e is obtained where

$$\eta_e = \frac{\tau_{xx} - \tau_{yy}}{\dot{\epsilon}} = \frac{3\eta_0}{(1 - 2\lambda \dot{\epsilon})(1 + \lambda \dot{\epsilon})} \quad (7.3.87)$$

In a similar manner, the CRM equation given in Eq. (7.3.51), in a simple shear flow, can be written as its component form

$$\begin{pmatrix} \tau_{xx} & \tau_{xy} & 0 \\ \tau_{xy} & \tau_{yy} & 0 \\ 0 & 0 & \tau_{zz} \end{pmatrix} + \lambda \dot{\gamma} \begin{pmatrix} -\tau_{xy} & \frac{\tau_{xx} - \tau_{yy}}{2} & 0 \\ \frac{\tau_{xx} - \tau_{yy}}{2} & \tau_{xy} & 0 \\ 0 & 0 & 0 \end{pmatrix}$$

$$= \eta_0 \dot{\gamma} \begin{pmatrix} 0 & 1 & 0 \\ 1 & 0 & 0 \\ 0 & 0 & 0 \end{pmatrix} \quad (7.3.88)$$

Thus, from Eq. (7.3.88), the material functions are

$$\tau_{xy} = \frac{\eta_0}{1 + (\lambda \dot{\gamma})^2} \dot{\gamma}, \quad N_1 = \frac{2\lambda \eta_0 \dot{\gamma}^2}{1 + (\lambda \dot{\gamma})^2} \quad \text{and} \quad N_2 = -\frac{\eta_0 \lambda \dot{\gamma}^2}{1 + (\lambda \dot{\gamma})^2} \quad (7.3.89)$$

which gives us

$$\eta = \frac{\eta_0}{1 + (\lambda \dot{\gamma})^2}, \quad \psi_1 = \frac{2\lambda \eta_0}{1 + (\lambda \dot{\gamma})^2} \quad \text{and} \quad \psi_2 = -\frac{\eta_0 \lambda}{1 + (\lambda \dot{\gamma})^2} \quad (7.3.90)$$

If we proceed along the same line of reasoning, for the shearfree flow, the CRM equation is written as

$$\begin{pmatrix} \tau_{xx} & 0 & 0 \\ 0 & \tau_{yy} & 0 \\ 0 & 0 & \tau_{zz} \end{pmatrix} + \lambda \mathbf{0} = \eta_0 \dot{\epsilon} \begin{pmatrix} 2 & 0 & 0 \\ 0 & -(1+k) & 0 \\ 0 & 0 & -(1-k) \end{pmatrix} \quad (7.3.91)$$

which readily gives the elongational viscosity in its simplest form for $k=0$ as follows

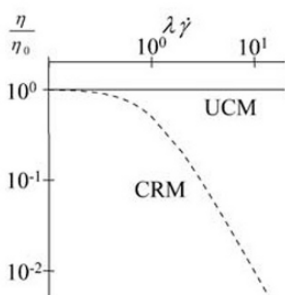
$$\eta_e = 3\eta_0 \quad (7.3.92)$$

Figure 7.20 shows a qualitative comparison of rheological predictions of UCM and CRM equations for: (a) normalized viscosities η/η_0 , (b) normalized first normal stress coefficients $\psi_1/2\eta_0\lambda$, (c) normalized second normal stress coefficients $-\psi_2/\eta_0\lambda$, and (d) normalized elongational viscosities $\eta/3\eta_0$. The CRM equation gives fairly good qualitative predictions on shear thinning characters. However, with the CRM equation, the elongational viscosity becomes constant for all $\dot{\epsilon}$, giving a Trouton value of $\eta = 3\eta_0$, which is not realistic with general polymeric fluids, which often show the strain hardening.

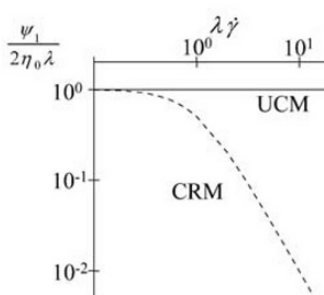
It is useful to mention that the shear viscosity given in Eq. (7.3.90) can be modified to write:

$$\frac{\eta}{\eta_0} = \left[1 + (\lambda \dot{\gamma})^2 \right]^{\frac{n-1}{2}} \quad (7.3.93)$$

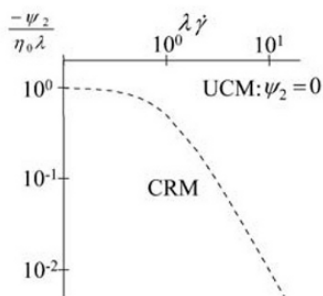
(a) Normalized shear viscosity



(b) Normalized first normal stress coefficient



(c) Normalized second normal stress coefficient



(d) Normalized elongational viscosity

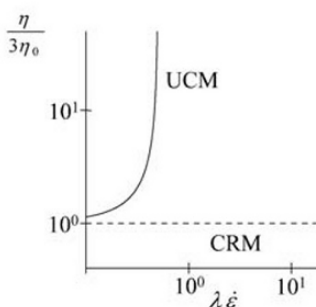


Fig. 7.20 Rheological predictions via UCM and CRM equations

Namely, Eq. (7.3.93) is the equivalent form with the Carreau-Yasuda formula presented in Eq. (7.1.6) where $a=2$ and $\eta_\infty=0$. Usually, the shear dependent material functions given in Eq. (7.3.93) give too large prediction to agree with most data on polymeric fluids, for which the range of n is $0.5 \leq n \leq 1.0$.

The Giesekus equation given in Eq. (7.3.59) is a nonlinear constitutive equation, which contains the quadratic term of $\boldsymbol{\tau}$ with a given constant of the mobility factor α . Choosing α gives more realistic predictions in both melts and solutions of polymeric fluids. Now, cases are examined for the

equation in steady simple shear flow:

$$\begin{pmatrix} \tau_{xx} & \tau_{xy} & 0 \\ \tau_{xy} & \tau_{yy} & 0 \\ 0 & 0 & \tau_{zz} \end{pmatrix} - \lambda_1 \dot{\gamma} \begin{pmatrix} 2\tau_{xy} & \tau_{yy} & 0 \\ \tau_{yy} & 0 & 0 \\ 0 & 0 & 0 \end{pmatrix} + \frac{\alpha}{G} \begin{pmatrix} \tau_{xx}^2 + \tau_{xy}^2 & \tau_{xx}\tau_{xy} + \tau_{xy}\tau_{yy} & 0 \\ \tau_{xx}\tau_{xy} + \tau_{xy}\tau_{yy} & \tau_{xy}^2 + \tau_{yy}^2 & 0 \\ 0 & 0 & \tau_{zz}^2 \end{pmatrix} = \eta_P \dot{\gamma} \begin{pmatrix} 0 & 1 & 0 \\ 1 & 0 & 0 \\ 0 & 0 & 0 \end{pmatrix} \quad (7.3.94)$$

where G is defined by $G = \eta_P / \lambda_1$. Equation (7.3.94) has, thus, algebraic relationships for four stress components as follows

$$\tau_{xx} - 2\lambda_1 \dot{\gamma} \tau_{xy} + \frac{\alpha}{G} (\tau_{xx}^2 + \tau_{xy}^2) = 0 \quad (7.3.95)$$

$$\tau_{yy} + \frac{\alpha}{G} (\tau_{xy}^2 + \tau_{yy}^2) = 0 \quad (7.3.96)$$

$$\tau_{xy} - \lambda_1 \dot{\gamma} \tau_{yy} + \frac{\alpha}{G} (\tau_{xx}\tau_{xy} + \tau_{xy}\tau_{yy}) - \eta_P \dot{\gamma} = 0 \quad (7.3.97)$$

$$\tau_{zz} + \frac{\alpha}{G} \tau_{zz}^2 = 0 \quad (7.3.98)$$

Solving Eqs. (7.3.95) to (7.3.98) for each stress component τ_{xx} , τ_{yy} , τ_{xy} and τ_{zz} , we can obtain a steady state of normalized material functions for the simple shear flow, where $\eta = \tau_{xy} / \dot{\gamma}$ and

$$\frac{\eta}{\eta_P} = \frac{(1-\zeta)^2}{1+(1-2\alpha)\zeta} \quad (7.3.99)$$

$$\frac{\psi_1}{2\eta_P \lambda_1} = \frac{\zeta(1-\alpha\zeta)}{\alpha(1-\zeta)(\lambda_1 \dot{\gamma})^2} \quad (7.3.100)$$

$$-\frac{\psi_2}{\eta_P \lambda_1} = \frac{\zeta}{(\lambda_1 \dot{\gamma})^2} \quad (7.3.101)$$

ζ is a parameter defined by

$$\zeta = \frac{1 - \xi}{1 + (1 - 2\alpha)\xi} \quad (7.3.102)$$

and for ξ

$$\xi^2 = \frac{\left\{1 + 16\alpha(1 - \alpha)(\lambda_1 \dot{\gamma})^2\right\}^{\frac{1}{2}} - 1}{8\alpha(1 - \alpha)(\lambda_1 \dot{\gamma})^2} \quad (7.3.103)$$

The elongational viscosity predicted from the Giesekus equation may be obtained for the steady shearfree flow of uniaxial stretching, i.e. $k = 0$, as follows

$$\begin{aligned} & \begin{pmatrix} \tau_{xx} & 0 & 0 \\ 0 & \tau_{yy} & 0 \\ 0 & 0 & \tau_{zz} \end{pmatrix} + \lambda_1 \dot{\epsilon} \begin{pmatrix} -2\tau_{xx} & 0 & 0 \\ 0 & \tau_{yy} & 0 \\ 0 & 0 & \tau_{zz} \end{pmatrix} + \frac{\alpha}{G} \begin{pmatrix} \tau_{xx}^2 & 0 & 0 \\ 0 & \tau_{yy}^2 & 0 \\ 0 & 0 & \tau_{zz}^2 \end{pmatrix} \\ &= \eta_P \dot{\epsilon} \begin{pmatrix} 2 & 0 & 0 \\ 0 & -1 & 0 \\ 0 & 0 & -1 \end{pmatrix} \end{aligned} \quad (7.3.104)$$

Equation (7.3.104) contains three stress components, for which the algebraic equations can be written where

$$\tau_{xx} - 2\lambda_1 \dot{\epsilon} \tau_{xx} + \frac{\alpha}{G} \tau_{xx}^2 - 2\eta_P \dot{\epsilon} = 0 \quad (7.3.105)$$

$$\tau_{yy} + \lambda_1 \dot{\epsilon} \tau_{yy} + \frac{\alpha}{G} \tau_{yy}^2 + \eta_P \dot{\epsilon} = 0 \quad (7.3.106)$$

$$\tau_{zz} + \lambda_1 \dot{\epsilon} \tau_{zz} + \frac{\alpha}{G} \tau_{zz}^2 + \eta_P \dot{\epsilon} = 0 \quad (7.3.107)$$

Solving Eqs. (7.3.105) to (7.3.107) yields the normalized elongational viscosity to write

$$\frac{\eta_e}{3\eta_p} = \frac{1}{2\alpha} + \frac{\left\{1 - 4(1 - 2\alpha)(\lambda_1 \dot{\epsilon}) + 4(\lambda_1 \dot{\epsilon})^2\right\}^{\frac{1}{2}}}{6\alpha(\lambda_1 \dot{\epsilon})} - \frac{\left\{1 + 2(1 - 2\alpha)(\lambda_1 \dot{\epsilon}) + (\lambda_1 \dot{\epsilon})^2\right\}^{\frac{1}{2}}}{6\alpha(\lambda_1 \dot{\epsilon})} \quad (7.3.108)$$

In the application of polymeric solutions, the Giesekus equation can be written in the form given in Eq. (7.3.63), where the parametric relationship is given in Eq. (7.3.64). Using the notation found in Eq. (7.3.64), the steady state normalized material functions are calculated to give, for the simple shear flow by letting $\eta_0 = \eta_s + \eta_p = \tau_{xy}/\dot{\gamma}$

$$\frac{\eta}{\eta_0} = \frac{\lambda_2}{\lambda_1} + \left(1 - \frac{\lambda_2}{\lambda_1}\right) \frac{(1 - \zeta)^2}{1 + (1 - 2\alpha)\zeta} \quad (7.3.109)$$

$$\frac{\psi_1}{2\eta_0(\lambda_1 - \lambda_2)} = \frac{\zeta(1 - \alpha\zeta)}{\alpha(1 - \zeta)(\lambda_1 \dot{\gamma})^2} \quad (7.3.110)$$

$$-\frac{\psi_2}{\eta_0(\lambda_1 - \lambda_2)} = \frac{\zeta}{(\lambda_1 \dot{\gamma})^2} \quad (7.3.111)$$

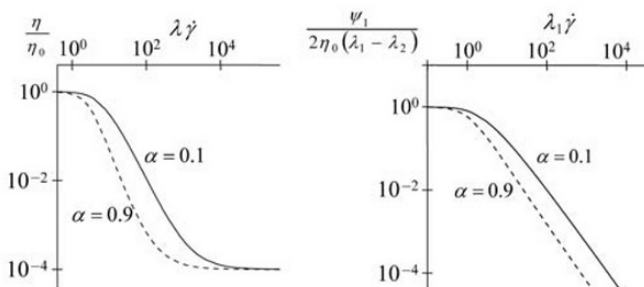
and for the shearfree flow of uniaxial stretching:

$$\begin{aligned} \frac{\eta_e}{3\eta_0} &= \frac{\lambda_2}{\lambda_1} + \frac{1}{2\alpha} \left(1 - \frac{\lambda_2}{\lambda_1}\right) \\ &+ \frac{1}{6\alpha(\lambda_1 \dot{\epsilon})} \left(1 - \frac{\lambda_2}{\lambda_1}\right) \left\{1 - 4(1 - 2\alpha)(\lambda_1 \dot{\epsilon}) + 4(\lambda_1 \dot{\epsilon})^2\right\}^{\frac{1}{2}} \\ &- \frac{1}{6\alpha(\lambda_1 \dot{\epsilon})} \left(1 - \frac{\lambda_2}{\lambda_1}\right) \left\{1 + 2(1 - 2\alpha)(\lambda_1 \dot{\epsilon}) + (\lambda_1 \dot{\epsilon})^2\right\}^{\frac{1}{2}} \end{aligned} \quad (7.3.112)$$

In Fig. 7.21, similar to the cases of the UCM and CRM equations in Fig. 7.20, the rheological predictions via the Giesekus equation for solutions are also plotted qualitatively from Eqs. (7.3.109) to (7.3.112) for $\lambda_2/\lambda_1 = 0.001$ (i.e. for a relatively small retardation time). The choice of the mobility factor α would soften the material functions with an idea that $\alpha = 0$ gives the limit of the UCM equation. The Giesekus model often

gives a good rheological estimate for melts and solutions in practical use, which also reflects the popular quotation found in the CFD.

(a) Normalized shear viscosity (b) Normalized first normal stress coefficient



(c) Normalized second normal stress coefficient (d) Normalized elongational viscosity coefficient

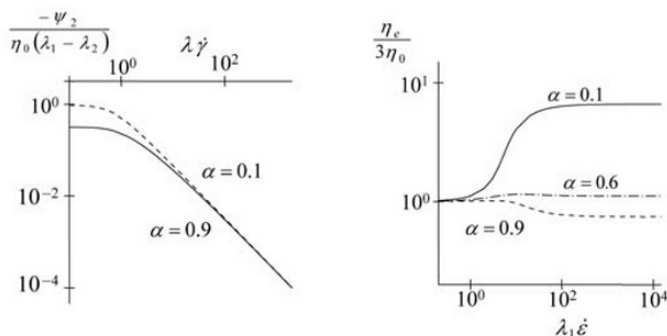


Fig. 7.21 Rheological predictions via the Giesekus equation for example; $\lambda_2/\lambda_1 = 0.001$

7.3.3.2 Unidirectional Basic Flow Problems

There are many interesting and rather unexplained flow phenomena that occur in a flow of viscoelastic fluids. In engineering flow situations they are extremely complicated due to viscous and elastic effects interacting in the flow field where, in most cases, the only way to examine the flows is to obtain the numerical solutions. One particular problem arises, however, when a realistic constitutive equation is used to simulate viscoelastic flows, while the convergence of numerical solutions is often difficult due to the nonlinearity of the constitutive equation and the boundary conditions, whether if they are no-slip or slip conditions at a given wall.

In this section of the chapter, we will try to interpret some of viscoelastic flows using simple linearized theories. This certainly limits the type of results we can obtain, bearing in mind.

As a representative case, the transient Poiseuille flow of a viscoelastic fluid may be treated numerically using a simple finite difference technique. Note that the configuration has already been treated in Section 6.4.3 in the Newtonian case.

Denote the unidirectional flow field in a cylindrical coordinates system when $u_z = u(r, t)$, and the shear stress $\tau = \tau_{rz}(r, t)$. The equation of motion, the Cauchy's equation of motion, for the cylindrical flow problem, is written as

$$\rho \frac{\partial u}{\partial t} = P(t) + \frac{1}{r} \frac{\partial(r\tau)}{\partial r} \quad (7.3.113)$$

where $P(t) = -\partial p / \partial z$. We assume a linear viscoelastic fluid represented by the Maxwell model from Eq. (7.3.39), setting $\tau = \tau_{xy}$ as follows

$$\tau + \lambda \frac{\partial \tau}{\partial t} = \eta_0 \frac{\partial u}{\partial r} \quad (7.3.114)$$

Following the nondimensional parameters defined in Eq. (6.4.56) repeatedly, they are

$$r^* = \frac{r}{r_0}, \quad t^* = \frac{(\eta_0 / \rho) t}{r_0^2} = \frac{\nu}{r_0^2} t \quad \text{and} \quad u^* = \frac{4\eta_0 u}{r_0^2 P} \quad (7.3.115)$$

also, defining a nondimensional stress and relaxation time as

$$\tau^* = \frac{4}{r_0 P} \tau \quad \text{and} \quad \zeta = \frac{\nu \lambda}{r_0^2} \quad (7.3.116)$$

Therefore, for a set of flow field and constitutive equations, Eqs. (7.3.113) and (7.3.114) are written respectively by

$$\frac{\partial u^*}{\partial t^*} = 4 + \frac{\partial \tau^*}{\partial r^*} + \frac{\tau^*}{r^*} \quad (7.3.117)$$

and

$$\tau^* + \zeta \frac{\partial \tau^*}{\partial t^*} = \frac{\partial u^*}{\partial r^*} \quad (7.3.118)$$

These equations are to be solved with the boundary and initial conditions of the problem. They are respectively

$$\frac{\partial u^*(0, t^*)}{\partial r^*} = 0 \text{ and } u^*(1, t^*) = 0 \quad (7.3.119)$$

and

$$u^*(r^*, 0) = 0 \text{ and } \tau^*(r^*, 0) = 0 \quad (7.3.120)$$

Equation (7.3.120) represents the start-up flow from a rest with no-slip at wall and Eq. (7.3.119) represents the symmetric condition at the center of pipe. We will impose one more condition on the pressure that follows step change in pressure gradient imposed upon the fluid at rest, i.e.

$$P(t^*) = 0 \quad \text{for } -\infty \leq t^* \leq 0 \quad (7.3.121)$$

and

$$P(t^*) = \text{Constant} \quad \text{for } 0 \leq t^* \leq \infty \quad (7.3.122)$$

From a view of CFD, we shall here take an approach to obtain numerical solutions, by using a finite difference technique. The most direct means of discretisation is provided by replacing the derivatives of Eqs. (7.3.117) and (7.3.118) by equivalent finite difference expressions. The algebraic equations produced by the discretisation with 2nd order central difference in space and 1st order forward difference in time (the so-called Euler method) would be

$$\frac{u_{i,k+1} - u_{i,k}}{\Delta t} = 4 + \frac{\tau_{i+1,k} - \tau_{i-1,k}}{2\Delta r} + \frac{\tau_{i,k}}{r_i} \quad (7.3.123)$$

and

$$\tau_{i,k+1} + \zeta \frac{\tau_{i,k+1} - \tau_{i,k-1}}{\Delta t} = \frac{u_{i,k+1} - u_{i,k-1}}{2\Delta r} \quad (7.3.124)$$

which gives explicit finite difference formulation

$$u_{i,k+1} = u_{i,k} + \Delta t \left(4 + \frac{\tau_{i+1,k} - \tau_{i-1,k}}{2\Delta r} + \frac{\tau_{i,k}}{r_i} \right) \quad (7.3.125)$$

and

$$\tau_{i,k+1} = \frac{\zeta}{\Delta t + \zeta} \tau_{i,k-1} + \frac{\Delta t}{2\Delta r(\Delta t + \zeta)} (u_{i+1,k} - u_{i-1,k}) \quad (7.3.126)$$

where $r_i = i\Delta r$ for $i=0, 1, 2, \dots, m$ and $t_k = k\Delta t$ for $k=0, 1, 2, 3, \dots, \infty$.

Note that for simplicity asterisk * in Eqs. (7.3.117) and (7.3.118) is dropped in the resultant finite difference equations of Eqs. (7.3.125) and (7.3.126).

For given initial and boundary conditions, i.e. Eqs. (7.3.119) to (7.3.122), repeated use of Eqs. (7.3.125) and (7.3.126) generates the numerical solution at all interior grid points r_i at time level $k+1$. That is, incrementing k for time and substituting the known values of $u_{i,k+1}$ and $\tau_{i,k+1}$ into the right hand side of Eqs. (7.3.125) and (7.3.126) allows the discrete solution to be marched toward in time. A typical numerical solution of $u_{1,k}$, the time development of the axial velocity at the center of pipe, is displayed in Fig. 7.22. As seen in the figure, an overshooting and damping oscillation of the velocity are displayed for a step change of the pressure gradient. It should be mentioned here that there might be some difficulties for obtaining convergence of numerical solutions, depending upon ζ and other geometric parameters.

The overshooting of flow parameters is typically observed phenomena in viscoelastic fluid flow at sudden start-up condition. Etter and Schowalter (1965) calculated the transient behavior of viscoelastic flow of the same problem, using Oldroyd-B model and showed similar overshooting character of the flow parameter.

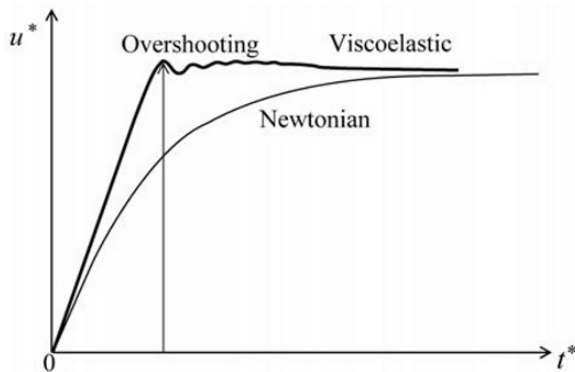


Fig. 7.22 Overshooting of flow parameter at start-up flow

The next important problem in viscoelastic fluid flow is the boundary layer problem. In many engineering flow problems with viscoelastic fluids, the pressure loss along the channel is a major concern, which is also directly connected with the formation of a boundary layer on the solid wall of the channel. Let us examine the two dimensional boundary layer on a flat plate (see Section 6.5.1 and refer Fig. 6.18). The effect of fluid elasticity

represented in the UCM equation of Eq. (7.3.47) can be included in the integral analysis of a boundary layer equation given in Eq. (6.5.33) by denoting that the extra stress in an axial flow direction will introduce additional terms inherited from the UCM equation. Denoting b as the width of the flat plate, the integral momentum equation at a steady state is written as

$$b \int_0^x \tau_w(x') dx' = \rho b \int_0^h u(U - u) dy \quad (7.3.127)$$

τ_w is the wall shear stress, u is the axial velocity in the boundary layer, U is the velocity in the potential core and h is the boundary thickness $h \geq \delta$. In the region $0 \leq y \leq h$, a Maxwellian fluid is assumed to add the axial extra stress to the Newtonian wall shear stress τ_w , so that Eq. (7.3.127) will be newly written as

$$b \int_0^x \tau_w(x') dx' + b \int_0^h \tau_{xx}(y) dy = \rho b \int_0^h u(U - u) dy \quad (7.3.128)$$

With regard to the axial extra stress contribution in Eq. (7.3.128), τ_{xx} of the UCM equation in simple shear flow is readily obtained from Eq. (7.3.84) and it is

$$\tau_{xx} = 2\lambda\eta_0 \left(\frac{\partial u}{\partial y} \right)^2 \quad (7.3.129)$$

Substituting Eq. (7.3.129) for Eq. (7.3.128) and differentiating the equation with respect to x yields

$$\nu \left(\frac{\partial u}{\partial y} \right)_w = \frac{d}{dx} \int_0^h \left[u(U - u) - 2\lambda\nu \left(\frac{\partial u}{\partial y} \right)^2 \right] dy \quad (7.3.130)$$

where $\nu = \eta_0/\rho$ is the kinematic viscosity. Therefore, as seen in Eq. (7.3.130), the wall shear stress $\tau_w = \eta_0 (\partial u / \partial y)_w$ is increased by the presence of elasticity. As in the Newtonian case, it is assumed that the similarity of the velocity profiles is held at various sections along the boundary layer development direction x . We can transform Eq. (7.3.130) into the differential form for the boundary layer thickness δ as follows

$$\delta \left(1 - \frac{2\lambda\nu c_4}{c_1 \delta^2} \right) \frac{d\delta}{dx} - \frac{c_2 \nu}{c_1 U} = 0 \quad (7.3.131)$$

where

$$c_1 = \int_0^1 f(1-f)d\eta, \quad c_2 = \left(\frac{df}{d\eta} \right)_{\eta=0} = f'(0) \quad \text{and} \quad c_4 = \int_0^1 (f')^2 d\eta \quad (7.3.132)$$

It is noted that f and η are defined in Section 6.5, see Exercise 6.5.1, and that $f_n(\eta) = f(\eta)$. With the boundary condition $\delta = \delta_0$ at $x=0$, Eq. (7.3.132) is integrated to give

$$\left(\frac{\nu c_2}{U} \right) x - \frac{c_1 \delta_0^2}{2} \left[\left(\frac{\delta}{\delta_0} \right)^2 - 1 \right] + 2\lambda \nu c_4 \ln \left(\frac{\delta}{\delta_0} \right) = 0 \quad (7.3.133)$$

The root (δ/δ_0) in Eq. (7.3.133) would give us an insight on the phenomenological explanation of the boundary layer development along a flat plate, knowing that δ/δ_0 is a function of x , when implicitly calculated for the variation of x . Figure 7.23 schematically shows the profiles of the viscoelastic and the Newtonian boundary layer. The boundary layer profile for the viscoelastic flow tends, asymptotically, to Newtonian case at downstream, which is given as

$$\delta(x) = \sqrt{2 \left(\frac{c_2}{c_1} \right)} \sqrt{\frac{\nu x}{U}} \quad (7.3.134)$$

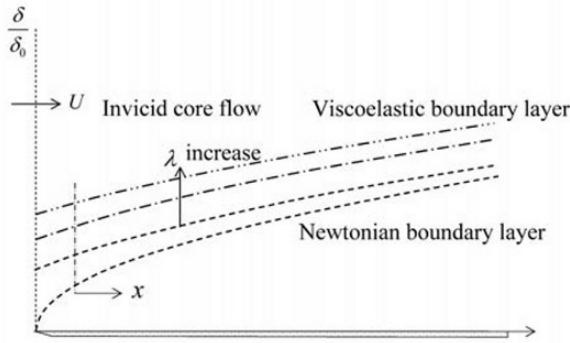


Fig. 7.23 Viscoelastic boundary layer

This is the same value as given in Eq. (6) in Exercise 6.5.1. As observed in Fig. 7.23, the viscoelastic effect presented by adding the normal stress to the Newtonian shear stress leads to the thickening of the boundary layer, though giving a finite boundary layer thickness at the leading edge, i.e. δ_0 at $x=0$.

The physical interpretation of the thickening of the boundary layer may be regarded as due to tensile stresses in the layer causing a thickening layer while stretching the layer in an axial direction. At the leading edge, due to a sudden thickening of the boundary layer formation, a finite value of δ_0 appears, which is, in effect, a purely hypothetical boundary condition in terms of treating the problem via the constitutive equation.

Exercise

Exercise 7.3.1 Strains in Standard Flow

Display convective derivatives of the rate of a strain tensor for the simple shear and shearfree flows at a steady state. Also show the relative strain tensor for the simple shear and shearfree flows at a steady state. In like manner obtain the convective derivatives of the stress tensors as well. Consider the problems in Cartesian coordinates system.

Ans.

For the simple shear flow, we have relationships such that $u_x = \dot{\gamma}_{yx}y = \dot{\gamma}(t)y$, $u_y = 0$ and $u_z = 0$, considering that the steady state shear rate $\dot{\gamma}$ be constant. Similarly, for the shearfree flow, we can write relationships such that

$$u_x = \dot{\epsilon}_{xx}x = \dot{\epsilon}(t)x, \quad u_y = -\dot{\epsilon}(t)(1+k)y/2$$

$$\text{and} \quad u_z = -\dot{\epsilon}(t)(1-k)z/2$$

where k is a constant $-1 \leq k \leq 1$, considering that the steady state elongational rate $\dot{\epsilon}$ be constant.

The rate of strain tensor for the simple shear flow is given via its components

$$\begin{aligned} \dot{\gamma} &= \nabla \mathbf{u} + \nabla \mathbf{u}^T \\ &= \begin{pmatrix} 0 & 1 & 0 \\ 0 & 0 & 0 \\ 0 & 0 & 0 \end{pmatrix} \dot{\gamma} + \begin{pmatrix} 0 & 0 & 0 \\ 1 & 0 & 0 \\ 0 & 0 & 0 \end{pmatrix} \dot{\gamma} = \begin{pmatrix} 0 & 1 & 0 \\ 1 & 0 & 0 \\ 0 & 0 & 0 \end{pmatrix} \dot{\gamma} \end{aligned} \quad (1)$$

The upper convective derivative of the rate of strain tensor is written by

$$\begin{aligned}
\overset{\nabla}{\dot{\gamma}} &= \frac{D\dot{\gamma}}{Dt} - (\nabla \mathbf{u} \cdot \dot{\gamma} + \dot{\gamma} \cdot \nabla \mathbf{u}^T) \\
&= \frac{\partial}{\partial t} \begin{pmatrix} 0 & 1 & 0 \\ 1 & 0 & 0 \\ 0 & 0 & 0 \end{pmatrix} \dot{\gamma} - \begin{pmatrix} 0 & 1 & 0 \\ 0 & 0 & 0 \\ 0 & 0 & 0 \end{pmatrix} \begin{pmatrix} 0 & 1 & 0 \\ 1 & 0 & 0 \\ 0 & 0 & 0 \end{pmatrix} \dot{\gamma}^2 - \begin{pmatrix} 0 & 1 & 0 \\ 1 & 0 & 0 \\ 0 & 0 & 0 \end{pmatrix} \begin{pmatrix} 0 & 0 & 0 \\ 1 & 0 & 0 \\ 0 & 0 & 0 \end{pmatrix} \dot{\gamma}^2 \\
&= \begin{pmatrix} 0 & 1 & 0 \\ 1 & 0 & 0 \\ 0 & 0 & 0 \end{pmatrix} \frac{\partial \dot{\gamma}}{\partial t} - 2 \begin{pmatrix} 1 & 0 & 0 \\ 0 & 0 & 0 \\ 0 & 0 & 0 \end{pmatrix} \dot{\gamma}^2 = \mathbf{0} - 2 \begin{pmatrix} 1 & 0 & 0 \\ 0 & 0 & 0 \\ 0 & 0 & 0 \end{pmatrix} \dot{\gamma}^2 = -2 \begin{pmatrix} 1 & 0 & 0 \\ 0 & 0 & 0 \\ 0 & 0 & 0 \end{pmatrix} \dot{\gamma}^2 \quad (2)
\end{aligned}$$

Note that higher order upper convective derivative $n \geq 2$ is expressed by $\overset{\nabla(n)}{\dot{\gamma}}$ and $\mathbf{0}$ is designated zero tensor (null tensor). Similarly, the corotational convective derivative of the rate of strain tensor is expressed by

$$\begin{aligned}
\overset{\circ}{\dot{\gamma}} &= \frac{D\dot{\gamma}}{Dt} - \boldsymbol{\omega} \cdot \dot{\gamma} + \dot{\gamma} \cdot \boldsymbol{\omega} \\
&= \mathbf{0} - \begin{pmatrix} 0 & 1 & 0 \\ -1 & 0 & 0 \\ 0 & 0 & 0 \end{pmatrix} \begin{pmatrix} 0 & 1 & 0 \\ 1 & 0 & 0 \\ 0 & 0 & 0 \end{pmatrix} \frac{\dot{\gamma}^2}{2} + \begin{pmatrix} 0 & 1 & 0 \\ 1 & 0 & 0 \\ 0 & 0 & 0 \end{pmatrix} \begin{pmatrix} 0 & 1 & 0 \\ -1 & 0 & 0 \\ 0 & 0 & 0 \end{pmatrix} \frac{\dot{\gamma}^2}{2} \\
&= \begin{pmatrix} -1 & 0 & 0 \\ 0 & 1 & 0 \\ 0 & 0 & 0 \end{pmatrix} \dot{\gamma}^2 \quad (3)
\end{aligned}$$

The rate of strain tensor for the shearfree flow is similarly obtained where

$$\begin{aligned}
\dot{\gamma} &= \mathbf{0} + \begin{pmatrix} 1 & 0 & 0 \\ 0 & -\frac{1}{2}(1+k) & 0 \\ 0 & 0 & -\frac{1}{2}(1-k) \end{pmatrix} \dot{\varepsilon} + \begin{pmatrix} 1 & 0 & 0 \\ 0 & -\frac{1}{2}(1+k) & 0 \\ 0 & 0 & -\frac{1}{2}(1-k) \end{pmatrix} \dot{\varepsilon} \\
&= \begin{pmatrix} 2 & 0 & 0 \\ 0 & -(1+k) & 0 \\ 0 & 0 & -(1-k) \end{pmatrix} \dot{\varepsilon} \quad (4)
\end{aligned}$$

and

$$\begin{aligned}
 \overset{\nabla}{\dot{\boldsymbol{\gamma}}} &= \mathbf{0} - \begin{pmatrix} 1 & 0 & 0 \\ 0 & -\frac{1}{2}(1+k) & 0 \\ 0 & 0 & -\frac{1}{2}(1-k) \end{pmatrix} \begin{pmatrix} 2 & 0 & 0 \\ 0 & -(1+k) & 0 \\ 0 & 0 & -(1-k) \end{pmatrix} \dot{\boldsymbol{\varepsilon}}^2 \\
 &- \begin{pmatrix} 2 & 0 & 0 \\ 0 & -(1+k) & 0 \\ 0 & 0 & -(1-k) \end{pmatrix} \begin{pmatrix} 1 & 0 & 0 \\ 0 & -\frac{1}{2}(1+k) & 0 \\ 0 & 0 & -\frac{1}{2}(1-k) \end{pmatrix} \dot{\boldsymbol{\varepsilon}}^2 \\
 &= - \begin{pmatrix} 4 & 0 & 0 \\ 0 & +(1+k)^2 & 0 \\ 0 & 0 & +(1-k)^2 \end{pmatrix} \dot{\boldsymbol{\varepsilon}}^2
 \end{aligned} \tag{5}$$

$$\begin{aligned}
 \overset{\circ}{\dot{\boldsymbol{\gamma}}} &= \mathbf{0} - \mathbf{0} \\
 &= \mathbf{0}
 \end{aligned} \tag{6}$$

The relative strain tensor will be calculated by defining the displacement functions $\mathbf{r}(t) = [x(t), y(t), z(t)]$ and $\mathbf{r}'(t') = [x'(t'), y'(t'), z'(t')]$, when we assume the simple shear flow equates to

$$u_x = \frac{\partial x}{\partial t} = \dot{\gamma}_{yx}(t)y, \quad u_y = \frac{\partial y}{\partial t} = 0 \quad \text{and} \quad u_z = \frac{\partial z}{\partial t} = 0 \tag{7}$$

The displacement function $\mathbf{r}'(t, t')$ is written via the component form

$$\begin{aligned}
 x' &= x + \int_{t'}^t \dot{\gamma}_{yx}(t'')y dt'' = x + \gamma_{yx}(t, t')y = x + \gamma y \\
 y' &= y
 \end{aligned} \tag{8}$$

and

$$z' = z \tag{9}$$

The relative strain tensor $\boldsymbol{\gamma}_R$ is written by definition, and which can be reduced to its component form likewise

$$\boldsymbol{\gamma}_R = \mathbf{C}^{-1} - \mathbf{I} = \mathbf{E}^{-1} \cdot \mathbf{E}^{-1T} - \mathbf{I} = \frac{\partial \mathbf{r}'(t, t')}{\partial \mathbf{r}} \cdot \frac{\partial \mathbf{r}'(t, t')^T}{\partial \mathbf{r}} - \mathbf{I}$$

$$= \begin{pmatrix} 1 & \gamma & 0 \\ 0 & 1 & 0 \\ 0 & 0 & 1 \end{pmatrix} \begin{pmatrix} 1 & 0 & 0 \\ \gamma & 1 & 0 \\ 0 & 0 & 1 \end{pmatrix} - \begin{pmatrix} 1 & 0 & 0 \\ 0 & 1 & 0 \\ 0 & 0 & 1 \end{pmatrix} = \begin{pmatrix} \gamma^2 & \gamma & 0 \\ \gamma & 0 & 0 \\ 0 & 0 & 0 \end{pmatrix} \quad (10)$$

In a similar fashion its inverse is given, where

$$\begin{aligned} \gamma^R &= \mathbf{I} - \mathbf{C} = \mathbf{I} - (\mathbf{C}^{-1})^{-1} \\ &= \begin{pmatrix} 1 & 0 & 0 \\ 0 & 1 & 0 \\ 0 & 0 & 1 \end{pmatrix} - \begin{pmatrix} 1 & -\gamma & 0 \\ -\gamma & 1 + \gamma^2 & 0 \\ 0 & 0 & 1 \end{pmatrix} = \begin{pmatrix} 0 & \gamma & 0 \\ \gamma & -\gamma^2 & 0 \\ 0 & 0 & 0 \end{pmatrix} \end{aligned} \quad (11)$$

Next, let us follow the same procedure where the relative strain tensors are obtained for the shearfree flow by writing the velocity components as

$$u_x = \dot{\varepsilon}x, \quad u_y = -\frac{\dot{\varepsilon}}{2}(1+k)y \quad \text{and} \quad u_z = -\frac{\dot{\varepsilon}}{2}(1-k)z \quad (12)$$

The displacement function $\mathbf{r}'(t, t')$ is written via its component form

$$x' = xe^{\varepsilon(t-t')} = x\lambda_x$$

$$y' = ye^{-\frac{1}{2}\varepsilon(t-t')(1+k)} = y\lambda_y$$

and

$$z' = ze^{-\frac{1}{2}\varepsilon(t-t')(1-k)} = z\lambda_z \quad (13)$$

where ε is the elongational strain defined as

$$\varepsilon(t, t') = \int_{t'}^t \dot{\varepsilon}(t'') dt'' \quad (14)$$

This is called the Hencky strain. Thus, the relative strain tensors are expressed via the following forms

$$\gamma_R = \mathbf{C}^{-1} - \mathbf{I} = \begin{bmatrix} \lambda_x^2 - 1 & 0 & 0 \\ 0 & \lambda_y^2 - 1 & 0 \\ 0 & 0 & \lambda_z^2 - 1 \end{bmatrix} \quad (15)$$

and

$$\boldsymbol{\gamma}^R = \mathbf{I} - \mathbf{C} = \begin{bmatrix} 1 - \frac{1}{\lambda_x^2} & 0 & 0 \\ 0 & 1 - \frac{1}{\lambda_y^2} & 0 \\ 0 & 0 & 1 - \frac{1}{\lambda_z^2} \end{bmatrix} \quad (16)$$

Similarly the deviatoric stress tensors $\boldsymbol{\tau}$ for the simple shear and uni-axial stretching (shearfree) flows are written respectively

$$\boldsymbol{\tau} = \begin{bmatrix} \tau_{xx} & \tau_{xy} & 0 \\ \tau_{yx} & \tau_{yy} & 0 \\ 0 & 0 & \tau_{zz} \end{bmatrix} \quad (17)$$

and

$$\boldsymbol{\tau} = \begin{bmatrix} \tau_{xx} & 0 & 0 \\ 0 & \tau_{yy} & 0 \\ 0 & 0 & \tau_{zz} \end{bmatrix} \quad (18)$$

The upper convective and corotational derivatives are thus obtained for $\dot{\gamma} = \gamma_{xy} = du_x/dy$ as follows

$$\begin{aligned} \overset{\nabla}{\boldsymbol{\tau}} &= \frac{D\boldsymbol{\tau}}{Dt} - [\nabla \mathbf{u} \cdot \boldsymbol{\tau} + \boldsymbol{\tau} \cdot \nabla \mathbf{u}^T] \\ &= \mathbf{0} - \dot{\gamma} \begin{pmatrix} 0 & 1 & 0 \\ 0 & 0 & 0 \\ 0 & 0 & 0 \end{pmatrix} \begin{pmatrix} \tau_{xx} & \tau_{xy} & 0 \\ \tau_{yx} & \tau_{yy} & 0 \\ 0 & 0 & \tau_{zz} \end{pmatrix} - \dot{\gamma} \begin{pmatrix} \tau_{xx} & \tau_{xy} & 0 \\ \tau_{yx} & \tau_{yy} & 0 \\ 0 & 0 & \tau_{zz} \end{pmatrix} \begin{pmatrix} 0 & 0 & 0 \\ 1 & 0 & 0 \\ 0 & 0 & 0 \end{pmatrix} \\ &= -\dot{\gamma} \begin{pmatrix} \tau_{yx} & \tau_{yy} & 0 \\ 0 & 0 & 0 \\ 0 & 0 & 0 \end{pmatrix} - \dot{\gamma} \begin{pmatrix} \tau_{xy} & 0 & 0 \\ \tau_{yy} & 0 & 0 \\ 0 & 0 & 0 \end{pmatrix} = -\dot{\gamma} \begin{pmatrix} 2\tau_{xy} & \tau_{yy} & 0 \\ \tau_{yy} & 0 & 0 \\ 0 & 0 & 0 \end{pmatrix} \quad (19) \end{aligned}$$

and

$$\begin{aligned}
\overset{\circ}{\boldsymbol{\tau}} &= \frac{D\boldsymbol{\tau}}{Dt} - \boldsymbol{\omega} \cdot \boldsymbol{\tau} + \boldsymbol{\tau} \cdot \boldsymbol{\omega} \\
&= \mathbf{0} - \frac{\dot{\gamma}}{2} \begin{pmatrix} 0 & 1 & 0 \\ -1 & 0 & 0 \\ 0 & 0 & 0 \end{pmatrix} \begin{pmatrix} \tau_{xx} & \tau_{xy} & 0 \\ \tau_{yx} & \tau_{yy} & 0 \\ 0 & 0 & \tau_{zz} \end{pmatrix} + \frac{\dot{\gamma}}{2} \begin{pmatrix} \tau_{xx} & \tau_{xy} & 0 \\ \tau_{yx} & \tau_{yy} & 0 \\ 0 & 0 & \tau_{zz} \end{pmatrix} \begin{pmatrix} 0 & 1 & 0 \\ -1 & 0 & 0 \\ 0 & 0 & 0 \end{pmatrix} \\
&= \dot{\gamma} \begin{pmatrix} -\tau_{xy} & \frac{\tau_{xx} - \tau_{yy}}{2} & 0 \\ \frac{\tau_{xx} - \tau_{yy}}{2} & \tau_{xy} & 0 \\ 0 & 0 & 0 \end{pmatrix} \quad (20)
\end{aligned}$$

Similarly setting the elongational rate at $\dot{\epsilon} = \dot{\epsilon}_{xx} = \partial u_x / \partial x$ for a shear-free flow, where $\dot{\epsilon}$ is kept constant, the upper convective derivative and the corotational derivative of $\boldsymbol{\tau}$ are obtained respectively where

$$\begin{aligned}
\overset{\nabla}{\boldsymbol{\tau}} &= \mathbf{0} - \dot{\epsilon} \begin{pmatrix} 1 & 0 & 0 \\ 0 & -\frac{1}{2}(1+k) & 0 \\ 0 & 0 & -\frac{1}{2}(1-k) \end{pmatrix} \begin{pmatrix} \tau_{xx} & 0 & 0 \\ 0 & \tau_{yy} & 0 \\ 0 & 0 & \tau_{zz} \end{pmatrix} \\
&\quad - \dot{\epsilon} \begin{pmatrix} \tau_{xx} & 0 & 0 \\ 0 & \tau_{yy} & 0 \\ 0 & 0 & \tau_{zz} \end{pmatrix} \begin{pmatrix} 1 & 0 & 0 \\ 0 & -\frac{1}{2}(1+k) & 0 \\ 0 & 0 & -\frac{1}{2}(1-k) \end{pmatrix} \\
&= -2\dot{\epsilon} \begin{pmatrix} \tau_{xx} & 0 & 0 \\ 0 & -\frac{1}{2}(1+k)\tau_{yy} & 0 \\ 0 & 0 & -\frac{1}{2}(1-k)\tau_{zz} \end{pmatrix} \quad (21)
\end{aligned}$$

and

$$\overset{\circ}{\boldsymbol{\tau}} = \mathbf{0} - \mathbf{0} = \mathbf{0} \quad (22)$$

Exercise 7.3.2 Integral UCM Equation in Standard Flow

Consider the integral UCM equation of Eq. (7.3.43), for the simple shear flow and the shearfree flow at steady state. Give the rheological predictions on the shear viscosity, the first normal stress difference, the second normal stress difference and the elongational viscosity.

Ans.

The integral UCM equation is given via the following form, using the relative strain tensor

$$\begin{aligned}\boldsymbol{\tau} &= - \int_{-\infty}^t \left[\frac{\eta_0}{\lambda^2} e^{-\frac{t-t'}{\lambda}} \right] \boldsymbol{\gamma}_R(t, t') dt' \\ &= - \int_{-\infty}^t \left[\frac{\eta_0}{\lambda^2} e^{-\frac{t-t'}{\lambda}} \right] [\mathbf{C}^{-1}(t, t') - \mathbf{I}] dt'\end{aligned}\quad (1)$$

where \mathbf{C}^{-1} is the Finger tensor. To obtain the shear viscosity $\eta = \eta(j) = \tau_{xy} / \dot{\gamma}$, $C_{12}^{-1} = C_{xy}^{-1}$ component of the Finger tensor must be obtained for the simple shear flow, namely, as it is exemplified in Exercise 7.3.1

$$\begin{aligned}\gamma_{Rxy} &= C_{xy}^{-1} - 0 \\ &= \dot{\gamma}(t - t')\end{aligned}\quad (2)$$

Therefore, η is computed where

$$\begin{aligned}\eta &= \frac{\tau_{xy}}{\dot{\gamma}} = \frac{1}{\dot{\gamma}} \int_{-\infty}^t \frac{\eta_0}{\lambda^2} e^{-\left(\frac{t-t'}{\lambda}\right)} \dot{\gamma}(t - t') dt' \\ &= \eta_0\end{aligned}\quad (3)$$

Thus, according to Eq. (3), η is kept constant for the variation of $\dot{\gamma}$. The first normal stress difference $N_1 = \tau_{xx} - \tau_{yy}$ is obtained similarly when, inserting $C_{xx}^{-1} - C_{yy}^{-1} = \dot{\gamma}^2(t - t')^2 dt'$, we have

$$\begin{aligned}N_1 &= \tau_{xx} - \tau_{yy} = \int_{-\infty}^t \frac{\eta_0}{\lambda^2} e^{-\left(\frac{t-t'}{\lambda}\right)} (C_{xx}^{-1} - C_{yy}^{-1}) dt' \\ &= 2\lambda\eta_0 \dot{\gamma}^2\end{aligned}\quad (4)$$

The first normal stress coefficient ψ_1 is as well computed when

$$\psi_1 = \frac{N_1}{\dot{\gamma}^2} = 2\lambda\eta_0 \quad (5)$$

Thus, ψ_1 is also kept constant for the variation of $\dot{\gamma}$. The second normal stress difference N_2 is, however, zero since $C_{yy}^{-1} - C_{zz}^{-1} = 0$ for the simple shear flow. Thus, for all $\dot{\gamma}$, we have

$$N_2 = 0 \quad (6)$$

and

$$\varphi_2 = 0 \quad (7)$$

For the uniaxial stretching, i.e. $k=0$ in Eq. (7.2.15), with the constant elongational rate $\dot{\epsilon}$, the elongational viscosity η_e is obtained with reference to Exercise 7.3.1, with the following formulation

$$\begin{aligned} \eta_e &= \frac{\tau_{11} - \tau_{22}}{\dot{\epsilon}} = \frac{1}{\dot{\epsilon}} \int_{-\infty}^t \frac{\eta_0}{\lambda^2} e^{-\left(\frac{t-t'}{\lambda}\right)} (C_{xx}^{-1} - C_{yy}^{-1}) dt' \\ &= \frac{1}{\dot{\epsilon}} \int_{-\infty}^t \frac{\eta_0}{\lambda^2} e^{-\left(\frac{t-t'}{\lambda}\right)} [e^{2\dot{\epsilon}(t-t')} - e^{-\dot{\epsilon}(t-t')}] dt' \\ &= \frac{\eta_0}{\lambda^2 \dot{\epsilon}} \int_{-\infty}^t \left[e^{-(t'-t)(2\dot{\epsilon}-1/\lambda)} - e^{-(t'-t)(\dot{\epsilon}-1/\lambda)} \right] dt' \\ &= \frac{3\eta_0}{(1-2\lambda\dot{\epsilon})(1+\lambda\dot{\epsilon})} \end{aligned} \quad (8)$$

It is mentioned that in Eq. (8) $\eta_e \rightarrow \infty$ as $\dot{\epsilon} \rightarrow 1/2\lambda$. Consequently, the results from (3) to (7) agree with those obtained from the differential UCM equation, as examined in Eqs. (7.3.85) and (7.3.87).

Exercise 7.3.3 Oldroyd-B Equation

Examine the Oldroyd-B equation for the simple shear flow and shearfree flow at a steady state.

Ans.

The Oldroyd-B equation given in Eq. (7.3.52) contains two time constants, namely λ_1 and λ_2 , which are, respectively, the relaxation

time constant and the retardation time constant, with η_0 being the zero shear rate viscosity. The rheological predictions of this quasi-linear equation are useful to expand more admissible constitutive equations. Now let us start again to consider the steady simple shear flow by writing the equation

$$\begin{pmatrix} \tau_{xx} & \tau_{xy} & 0 \\ \tau_{xy} & \tau_{yy} & 0 \\ 0 & 0 & \tau_{zz} \end{pmatrix} - \lambda_1 \dot{\gamma} \begin{pmatrix} 2\tau_{xy} & \tau_{yy} & 0 \\ \tau_{xx} & 0 & 0 \\ 0 & 0 & 0 \end{pmatrix} = \eta_0 \left[\begin{pmatrix} 0 & 1 & 0 \\ 1 & 0 & 0 \\ 0 & 0 & 0 \end{pmatrix} \dot{\gamma} - 2\lambda_2 \begin{pmatrix} 1 & 0 & 0 \\ 0 & 0 & 0 \\ 0 & 0 & 0 \end{pmatrix} \dot{\gamma}^2 \right] \quad (1)$$

which gives the following relationships:

$$\tau_{xy} = \eta_0 \dot{\gamma}, \quad N_1 = \tau_{xx} - \tau_{yy} = 2\eta_0(\lambda_1 - \lambda_2)\dot{\gamma}^2 \quad (2)$$

and

$$N_2 = \tau_{yy} - \tau_{zz} = 0 \quad (3)$$

Resultantly, we can obtain the material functions where

$$\eta = \eta_0, \quad \psi_1 = 2\eta_0(\lambda_1 - \lambda_2) \text{ and } \psi_2 = 0 \quad (4)$$

As it is obviously seen in comparison with Eq. (3) to (7) in the previous Exercise of 7.3.2, we have the same material functions as those of the UCM equation with respect to the steady shear flow.

In the case of a shearfree flow, however, the Oldroyd-B equation can be written in components form:

$$\begin{pmatrix} \tau_{xx} & 0 & 0 \\ 0 & \tau_{yy} & 0 \\ 0 & 0 & \tau_{zz} \end{pmatrix} - 2\lambda_1 \dot{\epsilon} \begin{pmatrix} \tau_{xx} & 0 & 0 \\ 0 & -\frac{1}{2}(1+k)\tau_{yy} & 0 \\ 0 & 0 & -\frac{1}{2}(1-k)\tau_{zz} \end{pmatrix} = \eta_0 \left[\dot{\epsilon} \begin{pmatrix} 2 & 0 & 0 \\ 0 & -(1+k) & 0 \\ 0 & 0 & -(1-k) \end{pmatrix} - \lambda_2 \dot{\epsilon}^2 \begin{pmatrix} 4 & 0 & 0 \\ 0 & +(1+k)^2 & 0 \\ 0 & 0 & +(1-k)^2 \end{pmatrix} \right] \quad (5)$$

From such a deduction, each stress component is given where

$$\begin{aligned}
(1 - 2\lambda_1 \dot{\epsilon})\tau_{xx} &= 2\eta_0 \dot{\epsilon} - 4\lambda_2 \eta_0 \dot{\epsilon}^2 \\
&= 2\eta_0 \dot{\epsilon} (1 - 2\lambda_2 \dot{\epsilon}) \\
\tau_{xx} &= \frac{2\eta_0 \dot{\epsilon} (1 - 2\lambda_2 \dot{\epsilon})}{1 - 2\lambda_1 \dot{\epsilon}} \\
[1 + (1 + k)\lambda_1 \dot{\epsilon}]\tau_{yy} &= -\eta_0 \dot{\epsilon} (1 + k) - \lambda_2 \eta_0 \dot{\epsilon}^2 (1 + k)^2 \\
\tau_{yy} &= \frac{-(1 + k)\eta_0 \dot{\epsilon} [1 + \lambda_2 (1 + k)\dot{\epsilon}]}{1 + (1 + k)\lambda_1 \dot{\epsilon}}
\end{aligned}$$

and

$$\begin{aligned}
[1 + (1 - k)\lambda_1 \dot{\epsilon}]\tau_{zz} &= -\eta_0 \dot{\epsilon} (1 - k) - \lambda_2 \eta_0 \dot{\epsilon}^2 (1 - k)^2 \\
\tau_{zz} &= \frac{-(1 - k)\eta_0 \dot{\epsilon} [1 + \lambda_2 (1 - k)\dot{\epsilon}]}{1 + (1 - k)\lambda_1 \dot{\epsilon}}
\end{aligned}$$

Thus, in the case of uniaxial stretching, i.e. $k = 0$, we can obtain the elongational viscosity from the Oldroyd-B equation, which is

$$\begin{aligned}
\eta_e &= \frac{\tau_{xx} - \tau_{yy}}{\dot{\epsilon}} = \frac{2\eta_0(1 - 2\lambda_2 \dot{\epsilon})}{1 - 2\lambda_1 \dot{\epsilon}} + \frac{\eta_0(1 + \lambda_2 \dot{\epsilon})}{1 + \lambda_1 \dot{\epsilon}} \\
&= \frac{2\eta_0(1 - 2\lambda_2 \dot{\epsilon})(1 + \lambda_1 \dot{\epsilon}) + \eta_0(1 + \lambda_2 \dot{\epsilon})(1 - 2\lambda_1 \dot{\epsilon})}{(1 - 2\lambda_1 \dot{\epsilon})(1 + \lambda_1 \dot{\epsilon})} \\
&= \frac{3\eta_0 - 3\eta_0 \lambda_2 \dot{\epsilon} (1 + 2\lambda_1 \dot{\epsilon})}{(1 - 2\lambda_1 \dot{\epsilon})(1 + \lambda_1 \dot{\epsilon})} \tag{6}
\end{aligned}$$

It is noted that the steady material function in a shearfree flow becomes infinite at the critical strain rates, i.e. $\lambda_1 = 1/(2\dot{\epsilon})$.

Exercise 7.3.4 Nondimensional Parameters in a Viscoelastic Model Equation

Consider the White-Metzner constitutive equation given in Eq. (7.3.65). Assuming isothermal flow, nondimensionalize the equation with the following nondimensional parameters

$$\mathbf{x}^* = \frac{\mathbf{x}}{l}, \quad \mathbf{u}^* = \frac{\mathbf{u}}{U}, \quad t^* = \frac{t}{t_0} \quad \text{and} \quad \boldsymbol{\tau}^* = \frac{\boldsymbol{\tau}}{\eta_0 (U/l)^n} \tag{1}$$

where l is the characteristic length, U is the characteristic velocity, t_0 is the reference time, and η_0 is the zero shear rate viscosity. Set n and s to be power index (constants) for the power law given below

$$\eta(\dot{\gamma}) = \eta_0 \left(\frac{1}{2} \|\mathbf{e}\| \right)^{\frac{n-1}{2}} \quad (2)$$

and

$$\lambda = \frac{\eta(\dot{\gamma})}{G} = \lambda_0 \left(\frac{1}{2} \|\mathbf{e}\| \right)^{\frac{s-n-1}{2}} \quad (3)$$

Ans.

The constitutive equation is, according to Eq. (7.3.65), written as

$$\begin{aligned} \dot{\boldsymbol{\tau}} + \lambda_0 \left(\frac{1}{2} \|\mathbf{e}\| \right)^{\frac{s-n-1}{2}} \left(\frac{D\boldsymbol{\tau}}{Dt} - \nabla \mathbf{u} \cdot \boldsymbol{\tau} - \boldsymbol{\tau} \cdot \nabla \mathbf{u}^T \right) \\ = 2\eta_0 \left(\frac{1}{2} \|\mathbf{e}\| \right)^{\frac{n-1}{2}} \mathbf{e} \end{aligned} \quad (4)$$

Using the relationship in Eq. (1), the constitutive equation is non-dimensionalized as follows

$$\begin{aligned} \boldsymbol{\tau}^* + \frac{\lambda_0}{t_0} \left(\frac{U}{l} \right)^{s-n-1} \left(\frac{1}{2} \|\mathbf{e}^*\| \right)^{\frac{s-n-1}{2}} \frac{D\boldsymbol{\tau}^*}{Dt^*} \\ + \lambda_0 \left(\frac{U}{l} \right)^{s-n} \left(\frac{1}{2} \|\mathbf{e}^*\| \right)^{\frac{s-n-1}{2}} \left(-\nabla \mathbf{u}^* \cdot \boldsymbol{\tau}^* - \boldsymbol{\tau}^* \cdot \nabla \mathbf{u}^{*T} \right) \\ = 2 \left(\frac{1}{2} \|\mathbf{e}^*\| \right)^{\frac{n-1}{2}} \mathbf{e}^* \end{aligned} \quad (5)$$

We have two nondimensionalized parameters that appear at the second and the third term of the left hand side of the equation. They are

$$De = \frac{\lambda_0}{t_0} \left(\frac{U}{l} \right)^{s-n-1} = \frac{\lambda}{t_{\text{flow}}} = \frac{\text{time scale of fluid (relaxation time)}}{\text{time scale of flow system}} \quad (6)$$

and

$$We = \lambda_0 \left(\frac{U}{l} \right)^{s-n} = \lambda \gamma = \frac{\text{relaxation time}}{\text{second characteristic time}} \quad (7)$$

where γ is the characteristic strain rate. De and We are respectively called the Deborah number and the Weissenberg number. De is interpreted as dynamic of a polymeric fluid, as the ratio of the magnitude of the elastic forces to that of the viscous forces, and, in-between De and We , there is the relationship

$$De = We \cdot St \quad (8)$$

where St is the Strouhal number defined in Eq. (6.2.28) as $St = l/Ut_0$. In application of the similarity law to dynamic problems of viscoelastic fluid flow, either De or We can be used to characterize the flow phenomena. In general, We is often used for steady state flow dynamics together with the Reynolds number Re . It should be mentioned that the symbol of We is conventionally used for the Weber number defined in Eq. (6.2.13); thus, care must be taken to avoid misuse of the symbolism for the Weissenberg number.

Problems

7.3-1 Sketch the behavior of G' , G'' , η' and η'' for the Oldroyd-B equation, when $\lambda_2 = 0.1\lambda_1$ is assumed. What are the physical implications for the assumption of $\lambda_2 > \lambda_1$?

Ans. For simple shear flow, consider the transient behavior of the shear stress.

7.3-2 Explain the physical implications of the Carreau-Yasuda formula, given in Eq. (7.1.6) from the viewpoint of the CRM equation.

Ans. Shear thinning with power index of n

7.3-3 In treating the same problem found in Eqs. (7.3.113) and (7.3.114), a method of Laplace transform may be adopted to obtain an analytical solution. Here the constitutive equation is given by an integral

equation. Derive an ordinary differential equation given by the following form after Laplace transform.

$$-\frac{1}{1+s\zeta} \frac{d}{dr^*} \left(r^* \frac{d\phi}{dr^*} \right) + \frac{4}{\zeta} = s\phi - u^*(r^*, 0)$$

where s is taken as complex number with mathematical convention, defining $s = r + iy$, and $r = x$ for insuring the convergence of inverse transformation, otherwise r being arbitrary, and ϕ is such that

$$\phi(r^*, s) = \int_{-\infty}^{\infty} e^{-\zeta \xi} u^*(r^*, \xi) d\xi$$

Ans.
$$\left[\begin{aligned} & \frac{1}{r^*} \frac{\partial}{\partial r^*} \left[r^* \int_0^{t^*} \left\{ \frac{\eta_0}{\lambda} e^{-\left(\frac{t^* - t'}{\zeta} \right)} \right\} \frac{\partial u^*}{\partial r^*} dt' \right] \\ & + 4 = \frac{\partial u^*}{\partial t^*}, \text{transform} \\ & \text{this equation with B.C.} \\ & \text{by Laplace transform} \end{aligned} \right]$$

7.3-4 Plot velocity profile of the transient Poiseuille flow of a viscoelastic fluid (as studied in Section 7.3.3.2 and Problem 7.3-3) and compare the Newtonian case as indicated in Fig. 7.24. Finite difference cord developed in Section 7.3, Eqs. (7.3.125) and (7.3.126) are helpful.

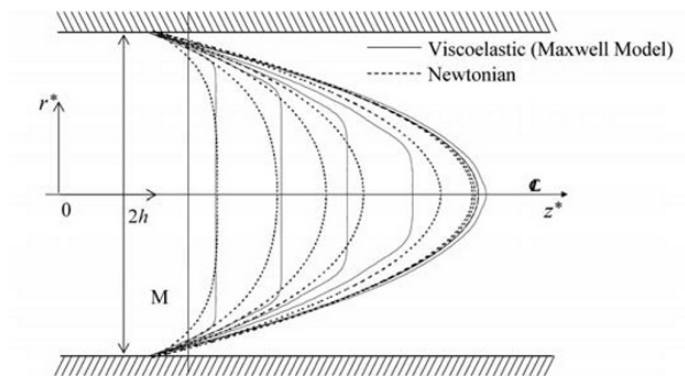


Fig. 7.24 Viscoelastic fluid in start-up transient Poiseuille flow

Nomenclature

a, a_1, a_2	: constants
b, b_1, b_2	: constants
c, C	: constants
c_1, c_2, c_3, \dots	: parameters
C_m	: torque coefficient
\mathbf{C}	: Cauchy tensor
\mathbf{C}^{-1}	: Finger tensor
D, d	: diameter of take = $2R, 2r$
De	: Deborah number
\mathbf{e}	: rate of strain tensor
\mathbf{F}, F	: force vector, thrust force
G	: modulus, relaxation modulus
G'	: storage modulus
G''	: loss modulus
G^*	: complex modulus
G_g	: Glassy modulus
k	: constant, $0 \leq k \leq 1$
k_c	: thermal conductivity
L, l	: length scale
h	: gap distance
n	: power law index
$\hat{\mathbf{n}}$: normal unit vector
m	: material constant for power law
N_1, N_2	: respectively the first and second normal stress differences
p	: pressure
R, r	: radius
Q	: flow rate
Re	: Reynolds number
Re^*	: generalized Reynolds number
St	: Strouhal number
s	: power law index, parameter in Laplace transform
t	: time
T	: temperature
T_r	: torque
\mathbf{T}	: total stress tensor
U	: bulk (characteristic) velocity, free energy

u	: local velocity
\bar{u}	: mean (average) flow velocity
W	: scalar (potential) function
W_c	: energy dissipation
We	: Weissenberg number
x, y, z	: Cartesian coordinates system
r, θ, z	: cylindrical coordinates system
r, θ, φ	: spherical coordinates system
α	: mobility factor
β	: gap ratio
γ	: strain
$\dot{\gamma}$: shear rate (rate of strain)
$\dot{\gamma}_a$: apparent Newtonian wall shear rate
$\dot{\gamma}_w$: wall shear rate
$\boldsymbol{\gamma}$: strain tensor
$\boldsymbol{\gamma}_R, \boldsymbol{\gamma}^R$: relative strain tensor
ε	: elongational strain
ε_s	: stress ratio
$\dot{\varepsilon}$: elongational (strain) rate
$\dot{\varepsilon}_E$: tensile (elongational) strain rate
ζ, ξ	: parameters
η	: viscosity
η'	: dynamic viscosity
η^*	: complex viscosity
η_a	: apparent viscosity
η_e	: elongational viscosity
η_0	: Newtonian viscosity, zero shear (rate) viscosity
η_s	: solvent contribution viscosity
η_p	: polymer contribution viscosity, plastic viscosity
θ, θ_0	: angle
λ, λ_1	: relaxation time constant,
λ_i	: multiple relaxation time conditions
λ_2	: retardation time constant
δ	: mechanical loss angle (phase-shift)
$\boldsymbol{\tau}$: (deviatoric) stress tensor
τ_{ij}	: components of (deviatoric) stress tensor

τ_E	: net tensile stress
τ_p	: polymer stress tensor
τ_s	: solvent stress tensor
τ_w	: wall shear stress
ϕ	: mechanical loss angle (phase-shift), scalar function
ψ_1, ψ_2	: respectively the first and second normal stress difference coefficients
ω	: frequency
Ω	: rotational speed

Bibliography

The most fundamental treatment of non-Newtonian fluids, in particular to polymeric liquids, is found in rather authoritative texts, with which every student of non-Newtonian fluid mechanics should be acquainted:

1. R.B. Bird, R.C. Armstrong and O. Hassager, *Dynamics of polymeric liquids*, 1. Wiley, New York, 1977.
2. R.B. Bird, C.F. Curtiss, R.C. Armstrong and O. Hassager, *Dynamics of Polymeric Liquids*, Vol.1 *Fluid Mechanics* and Vol. 2 *Kinetic Theory* (2nd Edition), A Wiley-Interscience Publication, New York, NY, 1987.
3. R.B. Bird, W.E. Stewart and E.N. Lightfoot, *Transport Phenomena* (2nd Edition), John Wiley & Sons, Inc., Hoboken, NJ, 2002.

A lucid mathematical treatment on flows of non-Newtonian fluids, in which conceptual and logical thinking is developed, is given with

4. J. Harris, *Rheology and Non-Newtonian Flow*, Longman Inc., New York, 1977.
5. R.R. Huilgol and N. Phan-Thien, *Fluid Mechanics of Viscoelasticity*, Elsevier Science Publishers B.V., Amsterdam, 1997.
6. N.W. Tschoegl, *The Phenomenological Theory of Linear Viscoelastic Behavior*, Springer-Verlag, New York, 1989.

Some of flow problems, the boundary layer behavior, are derived from the reference 3. Some selective topics of flow problems in viscoelastic liquids with a good deal of literature citation is found in

7. D.D. Joseph, *Fluid Dynamics of Viscoelastic Liquids*, Springer-Verlag New York Inc., New York, 1990.

The current approach in flow problems of non-Newtonian fluids is largely dependent upon numerical analysis with ultrahigh performance computer. A basic computational viscoelastic fluid dynamic is found in the reference 4, and

8. R.G. Owens and T.N. Phillips, *Computational Rheology*, Imperial College Press, London, 2002.
9. M.J. Crochet, A.R. Davies and K. Walters, *Numerical Simulation of Non-Newtonian Flow* (3rd Edition), Elsevier Science Publishers B.V., Amsterdam, 1991.

Rheological treatment of non-Newtonian fluids and the derivation of the expression for the constitutive equations are well presented in

10. F.A. Morrison, *Understanding Rheology*, Oxford University Press, Inc., Oxford, 2001.
11. R.I. Tanner, *Engineering Rheology*, Oxford University, Inc., Oxford, (Reprinted) 1992.
12. P.J. Carreau, D.C.R. De Kee, and R.P. Chhabra, *Rheology of Polymeric Systems*, Hanser/Gardner Publications, Inc., Cincinnati, OH, 1997.
13. R.G. Larson, *Constitutive Equations for Polymer Melts and Solutions*, Butterworths Series in Chemical Engineering, AT&T Bell Laboratories, Inc., Murray Hill, NJ, 1988

The transport phenomena in simple flows, including the boundary layer flows in power law fluids, are well presented in the reference 11. A few texts of standard measurement methods and the contribution of the melt rheology contain some useful materials on industrial applications. Three examples are those by

14. A.A. Collyer and D.W. Clegg, *Rheological Measurement*, Elsevier Applied Science Publishers LTD, Amsterdam, 1988.
15. J.M. Dealy and K.F. Wissbrun, *Melt Rheology and Its Role in Plastics Processing*, Kluwer Academic Publishers, Boston, MA (Reprinted) 1999.
16. J.R.A. Pearson, *Mechanics of Polymer Processing*, Elsevier Applied Science Publishers, LTD, Amsterdam, (Reprinted) 1986.

In particular, although not being quoted in the present text, but as one of current topics in engineering fluid mechanics, the drag reduction of turbulent flows in view of dilute polymeric substance adding is found in

17. A. Gyr and H.W. Bewersdorff, *Drag Reduction of Turbulent Flows by Additives*, Kluwer Academic Publishers, Boston, MA, 1995.

Flow Phenomena, specific data, correlations and approximations that are referred to in this text are presented in

18. W. Ostwald, Quantitative Filtrationsanalyse als dispersoidanalytische Methode, *Kolloid Z.*, 36, 1925.
19. K. Yasuda, Ph.D thesis, Massachusetts Institute of Technology, Cambridge, MA, 1979. also K. Yasuda, R.C. Armstrong and R.E. Cohen, Shear flow properties of concentrated solutions of linear and star branched polyst, *Rheol. Acta*, 20. pp. 163–178, 1981
20. T. Ree and H. Eyring, Theory of Non-Newtonian Flow. I. Solid Plastic System, *Appl. Phys.*, 26(7), 1955.
21. J.G. Oldroyd, The interpretation of observed pressure gradients in laminar flow of non-Newtonian liquids through tubes, *J. Coll. Sci.*, 4, 1949.
22. J.G. Oldroyd, On the formulation of rheological equations of state, *Proc. Roy. Soc.*, A200, 1950.
23. J.G. Oldroyd, Finite strains in an anisotropic elastic continuum, *Proc. Roy. Soc.*, A202, 1950.
24. J.G. Oldroyd, Non-Newtonian effects in steady motion of some idealized elastico-viscous liquids, *Proc. Roy. Soc.*, A245, 1958.
25. E.C. Bingham, *Fluidity and Plasticity*, McGraw-Hill, New York, NY, 1922.
26. H. Yamaguchi, Behavior of laminar boundary layer with shear thickening-thinning characteristics of non-Newtonian flows, *Soc. Rheol. Japan*, 22(2), 1994.
27. H. Yamaguchi, J. Fujiyoshi and H. Matsui, Spherical Couette flow of a viscoelastic fluid, *J. Non-Newtonian Fluid Mech.*, Part I and Part II, 69, 1997.
28. F.T. Trouton, The pressure in equilibrium with substances holding varying amounts of moisture, *Proc. Roy. Soc.*, A77, 1906.
29. M. Sentmanat, B.N. Wang and G.H. McKinley, Measuring the transient extensional rheology of polyethylene melts using the SER universal testing platform, *J. Rheol.*, 49, 2005.
30. V. Tiratmadja and T. Snidhar, A filament stretching device for measurement of extensional viscosity, *J. Rheol.*, 37(6), 1993.
31. W.P. Cox and E.H. Mertz, Correlation of dynamic and steady flow viscosities, *J. Polym. Sci.*, 28, 1958.
32. H.M. Laun, Prediction of elastic strains of polymer melts in shear and elongation, *J. Rheol.*, 30, 1986.
33. J. Sampers and P.J.R. Leblans, An experimental and theoretical study of the effect of the elongational history on the dynamics of isothermal melt spinning, *J. Non-Newtonian Fluid Mech.*, 30, 1988.

34. T. Hsu, P. Shirodkar, R.L. Laurence and H.H. Winter, The wall effect in orthogonal stagnation flow, *Proc. 8th Int. Congr. Rheol.*, 2, 1980.
35. F.N. Cogswell, Converging flow and stretching flow : a compilation, *J. Non-Newtonian Fluid Mech.*, 4, 1978.
36. B.Z. Rabinowitsch, *Physik chemie*, A145, 1929.
37. H. Giesekus, A simple constitutive equation for polymer fluids based on the concept of deformation-dependent tensorial mobility, *J. Non-Newtonian Fluid Mech.*, 11, 1982.
38. A.I. Leonov, Nonequilibrium thermodynamics and rheology of viscoelastic polymer media, *Rheol. Acta*, 15(2), 1976.
39. N. Phan-Thien and R.I. Tanner, A new constitutive equation derived from network theory , *J. Non-Newtonian Fluid Mech.*, 2, 1977.
40. A.S. Lodge, *Elastic Liquids*, Academic Press, New York, NY, 1964.
41. A. Kaye, A study of stress relaxation with finite strain, College of Aeronautics Cranfield, UK Note 134, 1962.
42. B. Bernstein, E.A. Kearsley and L.J. Zapas, *Irans. Soc. Rheol.*, 7, 1963.
43. C.F. Curtiss and R.B. Bird, A kinetic theory for polymer melts, *J. Chem. Phys.*, 74(3), 1981.
44. I. Etter and W.R. Schowalter, Unsteady flow of an Oldroyd fluid in a circular tube, *Trans. Soc. Rheol.*, 9(2), 1965.
45. J.D. Goddard and C. Miller, An inverse for the Jaumann derivative and some applications to the rheology of viscoelastic fluids, *Rheol. Acta*, 5, 1966
46. B.A. Toms, Some observations on the flow of linear polymer solutions through straight tubes at large Reynolds numbers, North Holland, Amsterdam, *Proc. 1st Intern. Congr. on Rheol.* 2, 135–141.
47. J.L. White and A.B. Metzner, Development of constitutive equations for polymeric melts and solutions, *J. Appl. Polym. Sci.*, 1867–1889. 1963.
48. K. Nakamura, *Non-Newtonian Fluid Mechanics*, Corona Pub. Co., LTD., Tokyo, 1997 (in Japanese).
49. H. Giesekus, Die Elastizitat von Flussigkeiten, *Rheol Acta* 5, 29–35, 1966.

8. Magnetic Fluid and Flow

Magnetic fluid, or alternatively called ferrofluid, is a colloidal suspension system of nano-sized ferro- or ferri-magnetic particles stably dispersed in a carrier (or base) liquid. Magnetic fluid is an artificial material rather than formed naturally. It has prominent character of the fluidity and also possesses magnetic properties. Magnetic fluid can be manipulated to position or forced to flow by means of a magnetic force.

Magnetic fluid and its concept of usage appeared in a 1965 research product for space technology in NASA. Since the time of the first appearance of magnetic fluid, much progress has been made in producing various types of high quality magnetic fluids associated with applications in many fields of technology, medicine and science. Many efforts have been also made to establish thermo-mechanical equations of magnetic fluids in order to deal with colloidal magnetic particles in a carrier liquid in an applied magnetic field, where the local moment of momentum exchange between particles and a fluid must be taken into account. The intrinsic angular momentum of particles under the influence of magnetic field introduces a volumetric force that couples into the governing equations of fluid motion. A quasi-stationary approximation is, however, possible in many practical situations, where the magnetization can be treated as an equilibrium in many processes, so that magnetic fluids can be only assumed as single-phase, homogeneous isotropic continuous media with magnetic forces, which is in many respects similar to the effects of the gravitational body force.

There are many striking phenomena in the physical behavior of magnetic fluids that are activated by imposing magnetic fields. Those responses include the normal field instability represented by the appearance of spikes on a fluid surface; the labyrinthine instability formed in a thin layer; the self-levitation of an immersed magnet; magnetocaloric effects, and so on. These phenomena are now well understood by the fluid dynamics and the thermodynamics of magnetic fluids based on the continuum mechanical approach via microscopic description. The complexity of the system with its chemical composition requires distinct knowledge in a physico-chemistry in order to synthesize the fluids. In addition, the utilization of the system requires a firm knowledge of continuum mechanics and

thermodynamics with an understanding of magnetic field theory. The field of study in magnetic fluids is recognized as “Ferrohydrodynamics,” as attributed to R. Rosensweig, (1985). The overall field of study in magnetic fluid has a highly interdisciplinary character, including physics, chemistry, engineering, mathematics and even medicine in practical applications.

In this chapter, in view of engineering fluid mechanics, fundamental aspects of continuum mechanics and some basic properties of magnetic fluids are introduced. Also, some typical technological applications are described in consideration with magnetoviscous effects.

8.1 Thermophysical Properties

The magnetic fluids available today are liquids containing small magnetic particles, in a so-called suspension (a colloidal system). In manufacturing magnetic fluids, mainly three components are required: namely such as a base liquid (or a carrier liquid), magnetic particles of a colloidal size and stabilizer (or repelling electric charge) to disperse the magnetic particles from aggregation. The size of magnetic particles must be sufficiently small enough since the stability of a magnetic fluid, such as a colloidal system, is ensured by thermal motion of the particles, preventing agglomeration and precipitation. The particle material must have a high level of magnetizability. Most common magnetic fluids are usually composed of 3 to 15 nm sized particles of solid, magnetic, single-domain particles coated with a molecular layer of dispersant (surfactant, such as oleic acid), where the particles are suspended in a liquid carrier. The basic mechanism of the suspension is such that thermal agitation of Brownian motion keeps the particles suspended and the coatings of the particles from sticking to each other. It should be kept in mind that the particles must not to be too small, since at sizes less than 1 to 2 nm their magnetic properties tend to disappear. Figure 8.1 shows a schematic diagram of magnetic fluids: (a) with a surfactant coating (separating of particles by the effect of steric repulsion); (b) with ionic surface charge (separating of particles by the effect of electric repulsion); and (c) also shows an electron micrograph of a magnetic fluid. A typical thermophysical property of magnetic fluid, a commercially available magnetic fluid, is tabulated in Table 8.1.

In typical thermomagnetic properties of magnetic fluids, Fig. 8.2 shows: (a) equilibrium magnetization (M) vs. magnetic field strength (H), and (b) equilibrium saturation magnetization (M_s) vs. temperature (T). The particles in a magnetic fluid (each with the magnetic moment m) are analogous to the molecules of a paramagnetic gas. The magnetization law

for the paramagnetic gas is described by the Langevin function $L(\zeta)$ with the following formula

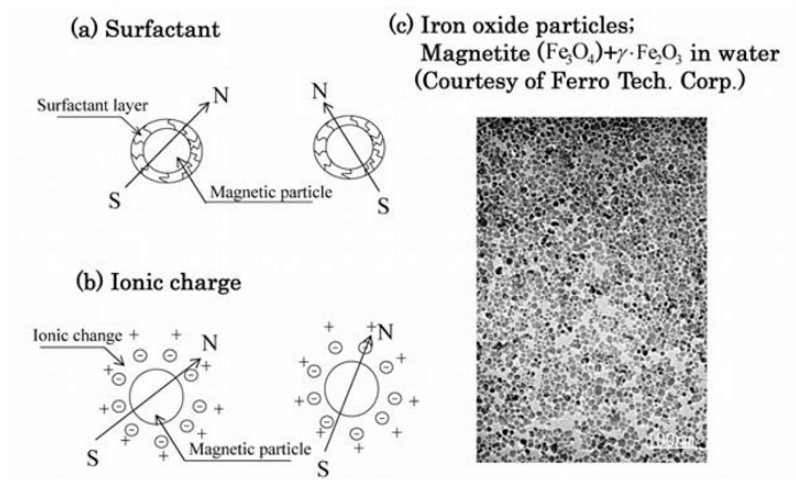
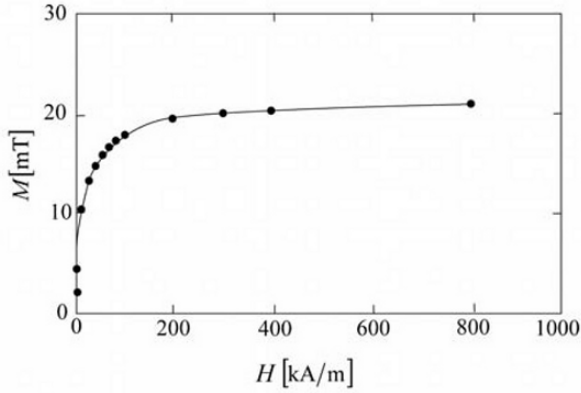


Fig. 8.1 Magnetic Fluid

Table 8.1 Magnetic fluids (MK-340; Courtesy of Ferro Tech. Corp.)

Appearance	Black-brown or red-brown viscous fluid
Carrier liquid	Synthetic hydrocarbon
Saturation magnetization(M_s)	11.0 mT
Viscosity (at 27 °C)	100 mPa · s
Density	0.94 kg/m ³
Pour point	- 56 °C
Flash point	>200 °C
Thermal conductivity (at 38 °C)	150 mW/(m · K)
Surface tension (at 25 °C)	32 mN/m
Coefficient of thermal expansion	7.5×10^{-4} /K

- (a) Magnetic curve of Iron oxide particles in synthetic hydrocarbon oil based magnetic fluid (Courtesy of Taihokohzai Co. Ltd)



- (b) Temperature-sensitive magnetic fluid of Mn-Zn ferrite in Kerosene base (Courtesy of Taihokohzai Co. Ltd)

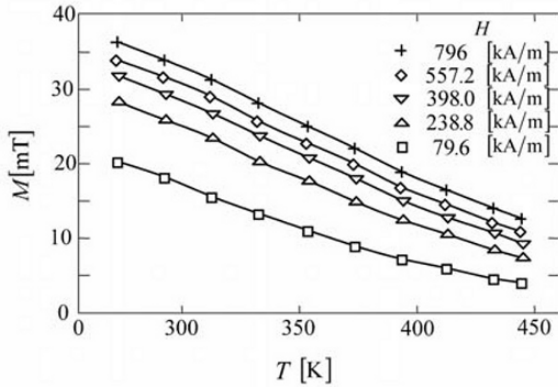


Fig. 8.2 Magnetization characteristic

$$M = Nm \left(\coth \zeta - \frac{1}{\zeta} \right) = M_s L(\zeta) \quad (8.1.1)$$

where N is the number of particles per unit volume, $\zeta = mH/k_B T$ (Langevin argument), k_B is the Boltzmann constant and m is the

magnetic moment. It should be mentioned that the saturation magnetization M_S can be written in terms of the colloid density ρ , which is $\rho = N\varpi$, where ϖ is the mass of a particle with attached carrier liquid molecules, in such a manner as to propose

$$M_S = \left(\frac{m}{\varpi} \right) \rho \quad (8.1.2)$$

The character of this magnetization by Eq. (8.1.1) is called superparamagnetism as displayed in Fig. 8.2(a).

In narrow ranges of magnetic fluid strength and temperature, the equation for the magnetic state of an incompressible magnetic fluid with the equilibrium magnetization of a magnetic fluid $\mathbf{M}(\mathbf{H}, T)$ is approximated with an accuracy to the first order term as follows

$$\mathbf{M}(\mathbf{H}, T) = \bar{\mathbf{M}} + \left(\frac{\partial \mathbf{M}}{\partial T} \right)_H (T - \bar{T}) + \left(\frac{\partial \mathbf{M}}{\partial H} \right)_T (\mathbf{H} - \bar{\mathbf{H}}) \quad (8.1.3)$$

$\bar{\mathbf{H}}$ and \bar{T} are some mean values which satisfy $\bar{\mathbf{M}} = \mathbf{M}(\bar{\mathbf{H}}, \bar{T})$. The quantity $(\partial \mathbf{M} / \partial H)_T = \chi$ is called the differential magnetic susceptibility of a magnetic fluid (for a ferromagnetic solid $\chi = M/H$ is the magnetic susceptibility). The other quantity appears in Eq. (8.1.3) is $K = \left| \left(\partial \mathbf{M} / \partial T \right)_H \right|$, which is called the pyromagnetic coefficient. Using the linear relationship in Eq. (8.1.3), the curve ($\zeta \ll 1$) of magnetization of a magnetic fluid is well approximated as representatively displayed in Fig. 8.2(b).

The field dependence of the equilibrium magnetization is the key parameter in discussing the dynamics of the magnetic fluid, and which also provides valuable information about the constituent elements of the fluid. The physical prerequisite for the existence of equilibrium magnetization is the assumption that the equilibrium is achieved by the relocation of the orientation of elementary magnetic moments along the applied magnetic field. There are two different relaxation processes after the applied field has been changed.

In the first mechanism we can assume that the magnetic moment of the particle is fixed with respect to its crystal structure and the relocation takes place by a rotation of the whole particle. This process is characterized by a respective time, called a Brown rotational diffusion time τ_B , Brown (1963), which is given where

$$\tau_B = \frac{3\tilde{V}\eta_0}{k_B T} \quad (8.1.4)$$

\tilde{V} is the hydrodynamic volume of the particle, including the surfactant layer, η_0 is the viscosity of the carrier liquid.

In the second mechanism, the magnetic moment may rotate inside the particle relative to the crystal structure. This process, called Néel relaxation, Néel (1949), is characterized by a respective relaxation time τ_N , which is given where

$$\tau_N = \frac{1}{f_0} e^{\frac{KV}{k_B T}} \quad (8.1.5)$$

K is the anisotropy constant of the particles, f_0 is the Larmor frequency of the magnetization having the approximate value of 10^9 Hz and V is the volume of the magnetic core of the particle. The Néel relaxation takes place if the thermal energy $k_B T$ is high enough to overcome the energy barrier KV , which is given by the crystallographic anisotropy of the magnetic particle. The relaxation of magnetization in a nano-dispersed suspension will follow the process with a shorter relaxation time, $\tau_B \ll \tau_N$ or $\tau_B \gg \tau_N$. When $\tau_B \ll \tau_N$, the magnetic material is said to have the extrinsic superparamagnetism; oppositely where $\tau_B \gg \tau_N$, it is said to have the intrinsic superparamagnetism. In either case, the magnetic fluid has an apparent superparamagnetism described in Eq. (8.1.1) and shown in Fig. 8.2(a). In comparison with Eqs. (8.1.4) and (8.1.5), for bigger particle sizes, τ_B becomes smaller than τ_N and the Brownian relaxation will take place due to a rotation of the whole particle. Note that in a real magnetic fluid the relaxation process may be very complicated due to the particle distribution, where a part of the particles relaxes by the Néel process, while another part of the particles relaxes by the Brownian process, depending on the size of each constituent particle. For example, the critical diameter d_{crit} , where the condition $\tau_N = \tau_B$ is met, is 18nm for Fe_3O_4 particle (with $K = 14 \text{ J/m}^3$ and $\eta_0 = 10^{-2} \text{ kg/m} \cdot \text{s}$), Odenbach (2002). The important aspect in the equilibrium magnetization is that the mean value of magnetization is achieved almost instantaneously within a time much shorter than the characteristic time scale of a macroscopic process, such as the fluid dynamical motion, where the magnetization vector \mathbf{M} becomes paralleled to the vector of a magnetic field of intensity \mathbf{H} at a given instant, i.e. $\mathbf{M} // \mathbf{H}$.

Another important property of magnetic fluids, particularly with regard to the magnetoviscous effect, is the apparent viscosity η_a in the absence of the magnetic field. η_a may vary from that of the carrier liquid due to the presence of the suspended particles. In the first approach, we may be able to use a well-known theoretical prediction by Einstein (1906) for diluted suspensions

$$\eta_a = \eta_0 \left(1 + \frac{5}{2} \phi_v \right) \quad (8.1.6)$$

where ϕ_v is the volume fraction of all suspended particles, including the surfactant layer, given as

$$\phi_v = \phi_m \left(\frac{d + 2s}{d} \right)^3 \quad (8.1.7)$$

In Eq. (8.1.7), ϕ_m is the volume fraction of the magnetic material, d is the average diameter of particle and s is the thickness of the surfactant layer. For example, for typical values of $d \approx 10\text{nm}$ and $s \approx 2\text{nm}$ of a magnetic fluid $\phi_m = 0.1$, ϕ_v would be calculated as $\phi_v = 0.27$. It should be aware that Einstein's formula, i.e. Eq. (8.1.6) is, however, no longer valid for higher concentration suspensions, such as $\phi_m > 0.1$ and this fact must be kept in mind in dealing with actual magnetic fluids.

A realistic correlation is proposed by Rosensweig, (1985) written where

$$\eta_a = \eta_0 \left(1 - \frac{5}{2} \phi_v + b \phi_v^2 \right)^{-1} \quad (8.1.8)$$

b is given by a function such that

$$b = \frac{\left(\frac{5}{2} \phi_c - 1 \right)}{\phi_c^2} \quad (8.1.9)$$

ϕ_c in Eq. (8.1.9) is a critical volume fraction of suspended material, which is obtained under the assumption that the suspension's apparent viscosity diverges at a given value of ϕ_c . For example, $\phi_c = 0.74$ would give a good estimate for η_a/η_0 for a kerosene-based magnetic fluid, Odenbach (2002).

Exercise

Exercise 8.1.1 Langevin Argument

The equilibrium magnetization of magnetic fluids is described by the Langevin formula in Eq. (8.1.1), when the saturation dipole moment m_d of the bulk of a magnetic solid is related to the saturation magnetization M_S through the volume fraction ϕ_m of a magnetic material

$$M_S = \phi_m m_d \quad (1)$$

Write the Langevin argument ζ in terms of the particle diameter d .

Ans.

The saturation magnetization M_S of the magnetic fluid is given in terms of the particle dipole moment m as defined in Eq. (8.1.2) by

$$M_S = Nm \quad (2)$$

while the Langevin argument ζ is given where

$$\zeta = \frac{mH}{k_B T} \quad (3)$$

Using Eqs. (1) and (2), Eq. (3) becomes

$$\zeta = \frac{H}{k_B T} \frac{m_d}{N} \phi_m \quad (4)$$

Since $\phi_m/N = V$, where V is the volume of the magnetic core of a particle, Eq. (4) can be reduced to the following expression:

$$\zeta = \frac{H}{k_B T} m_d V = \frac{\pi}{6} d^3 \frac{H m_d}{k_B T} \quad (5)$$

Note that V is given by $V = \pi d^3/6$ in Eq. (5)

Exercise 8.1.2 Relaxation of Magnetization

Consider two relaxation mechanisms by which the magnetization of magnetic fluid suspensions relax after the applied magnetic field has been

altered. Draw curves of τ_N and τ_B for the diameter of a colloidal particle of a magnetic fluid. Also compare the results if the effective relaxation time τ_f is given via the following expression, Martsenyuk et al. (1974)

$$\tau_f = \frac{\tau_B \tau_N}{\tau_B + \tau_N} \quad (1)$$

Use the following representative values of the properties of a magnetic fluid, if necessary

$K; (\text{for Fe})$	$K = 0.47 \times 10^5$	$\left[\frac{\text{J}}{\text{m}^3} \right]$
$f_0;$	$f_0 = 1 \times 10^9$	$\left[\frac{1}{\text{s}} \right]$
$k_B;$	$k_B = 1.38 \times 10^{-23}$	$\left[\frac{\text{J}}{\text{K}} \right]$
$\eta_0; (\text{for Kerosene})$	$\eta_0 = 0.2 \times 10^{-3}$	$\left[\frac{\text{kg}}{\text{m} \cdot \text{s}} \right]$

Ans.

Let the temperature be 25°C , i.e. $T = 25 + 273 = 298\text{K}$. \tilde{V} appearing in Eq. (8.1.3) includes the thickness of the surfactant layer, which gives \tilde{V} to write

$$\tilde{V} = \frac{\pi}{6} (d + 2s)^3 \quad (2)$$

where $s = 2 \times 10^{-9}\text{m}$ is assumed. Thus, the relaxation time due to the Néel relaxation τ_N given in Eq. (8.1.5) and the relaxation time due to the Brownian relaxation τ_B given in Eq. (8.1.4) are respectively written as

$$\tau_N = 10^{-9} \exp \left[0.47 \times 10^5 \times \frac{\pi}{6} d^3 \left/ (1.38 \times 10^{-23} \times 298) \right. \right] \quad (3)$$

$$\tau_B = 3 \times \frac{\pi}{6} (d + 2 \times 2 \times 10^{-9})^3 \times 0.2 \times 10^{-3} \left/ (1.38 \times 10^{-23} \times 298) \right. \quad (4)$$

The effective relaxation time τ_f can be calculated in Eq. (1), knowing τ_N and τ_B from Eqs. (3) and (4). The curves of Eqs. (1), (3) and (4) are

displayed in Fig. 8.3. In a real magnetic fluid, due to a broad size distribution, the exact evaluation of the relaxation time is difficult. A precise determination of the relaxation times requires direct experimental observation.

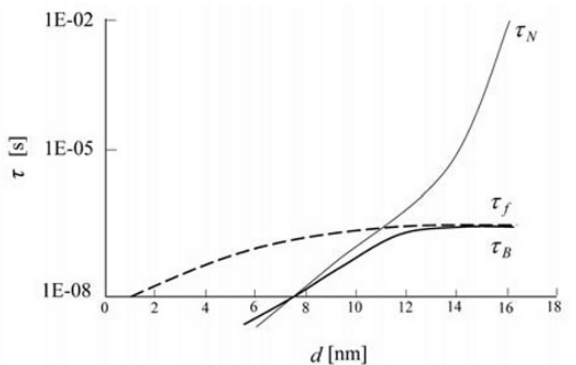


Fig. 8.3 Relaxation of magnetization

Problems

- 8.1-1 Plot the equilibrium magnetization curve using the Langevin function given in Eq. (8.1.1). Use values of the parameters, if necessary, for the particle size $d = 10\text{nm}$ at the temperature $T = 298\text{K}$ with $\phi_m = 0.041$ and $M_s = 0.04\text{Tesla}$.
- 8.1-2 In taking into account the parallelism of \mathbf{M} and \mathbf{H} , i.e. $\mathbf{M} \parallel \mathbf{H}$, the induction of \mathbf{B} can be expressed by the magnetic permeability μ_s of a magnetic fluid. Show that μ_s contains the magnetic susceptibility χ and the permeability of free space μ_0 .

$$\text{Ans. } \begin{bmatrix} \mathbf{B} = \mu_0 \mathbf{H} + \mathbf{M} \\ \mathbf{B} = \mu_0 \mathbf{H} + \mathbf{M} \\ = \mu_0 \mathbf{H} + \chi \mathbf{H} \\ = (\mu_0 + \chi) \mathbf{H} \\ = \mu_s \mathbf{H} \end{bmatrix}$$

- 8.1-3 Draw a curve for the viscosity ratio η_a/η_0 of a magnetic fluid as a function ϕ_v under no magnetic field, referring to Eq. (8.1.8). Use a value of $\phi_c \approx 0.74$ for the result.

8.2 Ferrohydrodynamic Equations

In the theory of magnetic fluid, ferrohydrodynamic equations are derived from a continuum mechanics on a microscopic treatment used to predict its dynamic behavior, establishing the state of equilibrium, motion and heat transfer. The concept to establish a dynamic theory of magnetic fluid is based on the idea that in a magnetic field, nano-scaled magnetic particles suspended in a non-magnetic fluid media, produces effects that are led by forces that draw from a dynamic system into a translational and rotational motion. When a magnetic fluid is in motion, under the applied magnetic field, the ferromagnetic phase interacts with a carrier liquid through a viscous friction. The establishment of basic equations for magnetic fluid came from an approach of a quasi-stationary one-phase fluid whose magnetization is in equilibrium in any dynamical process, Neuringer and Rosensweig (1964).

The outline for the governing equations of flow is described below from the basic concepts of continuum mechanics of polar material. Ferrohydrodynamic equations are thereafter derived by the determination of constitutive equations.

The continuity equation, which is derived from the mass conservation discussed in Section 2.1, is of the same form for an ordinary fluid

$$\frac{\partial \rho}{\partial t} + \nabla \cdot \rho \mathbf{u} = 0 \quad (8.2.1)$$

The equation of motion derived from the principle of the conservation of linear momentum is written by an unconstituted form of Cauchy's equation of motion, as it appears in Section 2.2, as follows

$$\rho \frac{D\mathbf{u}}{Dt} = \nabla \cdot \mathbf{T} + \rho \mathbf{g} \quad (8.2.2)$$

where \mathbf{g} is the body force and \mathbf{T} is the total stress tensor.

The equation of the internal angular momentum for a polar fluid that is derived from the conservation law of angular momentum of a polar material in Section 2.3 is written below:

$$\rho \frac{Ds}{Dt} = \rho \mathbf{f} + \nabla \cdot \mathbf{c} + \mathbf{A} \quad (8.2.3)$$

s is the intrinsic (internal) angular momentum per unit mass, \mathbf{c} is the couple stress tensor, \mathbf{A} is the vector of the tensor \mathbf{T} given in Eq. (2.3.9) and \mathbf{f} is the body couple per unit mass.

The energy equation for internal energy u_m is derived by the first law of the thermodynamics for non-(electrically) conductive mediums followed by Rosensweig (2002):

$$\rho \frac{Du_m}{Dt} = -\nabla \cdot \mathbf{q} + \mathbf{T}^T : \nabla \mathbf{u} + \mathbf{c}^T : \nabla \boldsymbol{\omega}_p - \mathbf{T} : (\boldsymbol{\varepsilon} \cdot \boldsymbol{\omega}_p) - [\mathbf{H}\mathbf{B} - (\mathbf{B} \cdot \mathbf{H})\mathbf{I}] : \nabla \mathbf{u} + \mathbf{H} \cdot \frac{D\mathbf{M}}{Dt} - \frac{\mu_0 H^2}{2} \nabla \cdot \mathbf{u} + \rho b \quad (8.2.4)$$

$\boldsymbol{\omega}_p$ is the average spin angular velocity of particles about their own center given by the expression:

$$\mathbf{s} = \frac{I\boldsymbol{\omega}_p}{\rho} \quad (8.2.5)$$

Here, I is the moment of inertia per unit of mass for a monodispersion of spherical particles. Note that \mathbf{B} in Eq. (8.2.4) is the magnetic induction and b is the amount of heat generated per unit mass. It should be kept in mind that u_m in Eq. (8.2.4) is the internal energy exclusive of field energy associated with the space the medium occupies, and of which it is given, where

$$u_m = u - \frac{\mu_0 H^2}{2\rho} \quad (8.2.6)$$

u is the internal energy of the system defined in Eq. (2.4.1) and μ_0 is the permeability of free space, i.e. $\mu_0 = 4\pi \times 10^{-7} \text{ H} \cdot \text{m}^{-1}$. In a magnetic medium, \mathbf{B} , \mathbf{H} and \mathbf{M} are related by the magnetic polarization relation given where

$$\mathbf{B} = \mu_0 \mathbf{H} + \mathbf{M} \quad (8.2.7)$$

It is noted that in SI units, the magnetic field \mathbf{H} has units of $\text{A} \cdot \text{m}^{-1}$, and the magnetization \mathbf{M} and the magnetic induction \mathbf{B} both have units of $\text{kg} \cdot \text{s}^{-2} \cdot \text{A}^{-1} = \text{Tesla}$.

Equations (8.2.2), (8.2.3), and (8.2.4) are unconstituted equations to which constitutive equations of \mathbf{T} , \mathbf{c} , \mathbf{f} , \mathbf{A} , \mathbf{M} and \mathbf{q} are to be determined in order to derive ferrohydrodynamic equations. Each constitutive equation can be determined such that thermophysical characteristics of magnetic fluids are satisfied.

In general, magnetic fluids are treated as incompressible and non-(electrically) conductive mediums. These conditions immediately give the continuity equation of Eq. (8.2.1) to express

$$\nabla \cdot \mathbf{u} = 0 \quad (8.2.8)$$

The total stress tensor \mathbf{T} in Eq. (8.2.2) may be decomposed by following stress tensors:

$$\mathbf{T} = -p_0 \mathbf{I} + \mathbf{T}^{(v)} + \mathbf{T}_{em} \quad (8.2.9)$$

p_0 is the hydrostatic pressure, $\mathbf{T}^{(v)}$ is the viscous stress tensor and is further expanded to show, referring to Eq. (2.3.8)

$$\mathbf{T}^{(v)} = \mathbf{T}_s + \mathbf{T}_a \quad (8.2.10)$$

where \mathbf{T}_s is the symmetric part and \mathbf{T}_a is the skew-symmetric part of the tensor $\mathbf{T}^{(v)}$. \mathbf{T}_s and \mathbf{T}_a have their own constitutive equations, which are, respectively, written with the following formulae:

$$\mathbf{T}_s = 2\eta_a \mathbf{e} \quad (8.2.11)$$

and

$$\mathbf{T}_a = \frac{1}{2} \boldsymbol{\varepsilon} \cdot \mathbf{A} = 2\zeta \boldsymbol{\varepsilon} \cdot (\boldsymbol{\Omega} - \boldsymbol{\omega}_p) \quad (8.2.12)$$

Note that \mathbf{T}_s is the Newtonian contribution to the symmetric part of the viscous stress tensor. In Eq. (8.2.11), \mathbf{e} is the rate of strain tensor, defined in Eq. (1.1.16), and η_a is the apparent viscosity of a suspension in the absence of a magnetic field, as, for example, it is given in Eq. (8.1.6) or Eq. (8.1.8).

Also it should be noted that $\mathbf{A} = -4\zeta(\boldsymbol{\omega}_p - \boldsymbol{\Omega})$ in Eq. (8.2.12) is the pseudovector, which is a vector of a tensor, defined in Eqs. (2.3.9) and (2.3.10) in Section 2, where \mathbf{A} is given from a consideration of the angular momentum equation and ζ is known as the vortex viscosity. It is further noted that in Eq. (8.2.12), $\boldsymbol{\Omega}$ is the angular velocity of a fluid particle with a rigid rotation defined by $\boldsymbol{\Omega} = 1/2\nabla \times \mathbf{u}$ and $\boldsymbol{\omega}_p$ is the average angular velocity of a constituent particle. Giving the definition of \mathbf{A} , \mathbf{A} will be further discussed in the angular momentum equation.

The Maxwell stress tensor in the electromagnetic field, assuming that the magnetic fluid is nonconductive, is proposed by Landau and Lifshitz (1960)

$$\mathbf{T}_{em} = -P_{em} \mathbf{I} + \mathbf{H}\mathbf{B} \quad (8.2.13)$$

where P_{em} is the electromagnetic energy per unit volume in a vacuum space, which is understood as

$$P_{em} = \mu_0 \int_0^H \left\{ M - \rho \left(\frac{\partial M}{\partial \rho} \right)_{T,H} \right\} dH + \mu_0 \frac{H^2}{2} \quad (8.2.14)$$

For magnetic fluids with a Langevin magnetization as in Eq. (8.1.1), M is proportional to ρ and resultantly M would be equal to $\rho(\partial M/\partial \rho)_{T,H}$ so that the first term of Eq. (8.2.14), may vanish.

The substitution of Eq. (8.2.8) together with constitutive equations to the Cauchy's equation of motion given in Eq. (8.2.2), regarding magnetic fluids as nonconductive, i.e. $\nabla \times \mathbf{H} = 0$, and with the continuation of magnetic induction \mathbf{B} , i.e. $\nabla \cdot \mathbf{B} = 0$, we can derive the linear momentum equation as follows

$$\rho \frac{D\mathbf{u}}{Dt} = -\nabla p^* + \eta_a \nabla^2 \mathbf{u} + \mathbf{M} \cdot \nabla \mathbf{H} + \frac{I}{2\tau_s} \nabla \times (\boldsymbol{\omega}_p - \boldsymbol{\Omega}) + \rho \mathbf{g} \quad (8.2.15)$$

where p^* is the total pressure, $p^* = p_0 + \mu_0 H^2/2$ and τ_s is the rotational relaxation time of particles due to the vortex viscosity. It will prove useful to consider here, as another point of correspondence that will be discussed to a larger extent in the angular momentum treatment, to write Eq. (8.2.15) with the field parameters of \mathbf{M} and \mathbf{H} , eliminating the parameter $\boldsymbol{\omega}_p$ of a microscopic concept.

From the angular momentum equation of magnetic fluids, if one assumes that τ_s is sufficiently small and the spin diffusion is ignored, it is reasonable to minute its relationship from Eq. (8.2.25), where

$$\frac{I}{\tau_s} (\boldsymbol{\omega}_p - \boldsymbol{\Omega}) = \mathbf{M} \times \mathbf{H} \quad (8.2.16)$$

It is noted that \mathbf{A} given where $\mathbf{A} = -4\zeta(\boldsymbol{\omega}_p - \boldsymbol{\Omega})$ is replaced by the relationship $2\zeta = I/2\tau_s$. Thus, the substitution of Eq. (8.2.16)–(8.2.15) yields the linear momentum equation of magnetic fluids, that is written as

$$\rho \frac{D\mathbf{u}}{Dt} = -\nabla p^* + \eta_a \nabla^2 \mathbf{u} + \mathbf{M} \cdot \nabla \mathbf{H} + \frac{1}{2} \nabla \times (\mathbf{M} \times \mathbf{H}) + \rho \mathbf{g} \quad (8.2.17)$$

Equation (8.2.17) includes the term $\mathbf{M} \cdot \nabla \mathbf{H}$, which is the so-called the Kelvin force density, derived from the stress of an electromagnetic field, and the term $1/2 \nabla \times (\mathbf{M} \times \mathbf{H})$, which is derived from the consideration of

an internal angular momentum to give the skew-symmetric part of the viscous stress tensor.

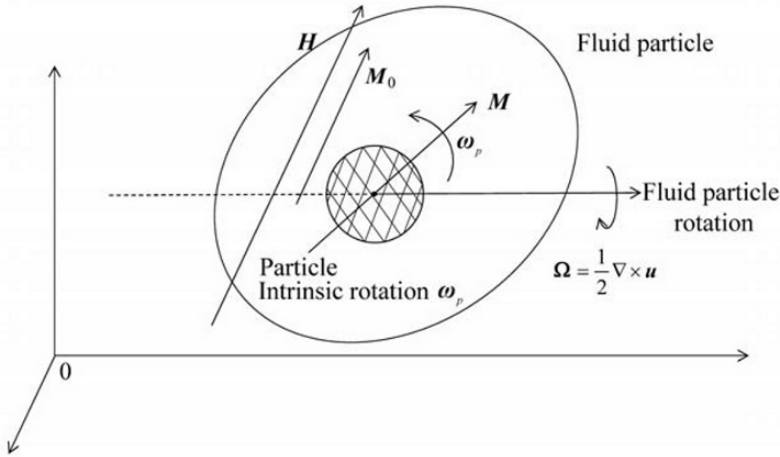


Fig. 8.4 Intrinsic rotation of magnetic particle against rotation of fluid particle

In order to derive the angular momentum equation of a magnetic fluid, it is useful to give a visual image of the intrinsic rotation of a magnetic particle as schematically represented in Fig. 8.4. We will consider that the magnetic moment of the particle is fixed within the particle, assuming that the magnetization relaxation occurs by means of the Brownian relaxation, as discussed earlier. The situation sketched in Fig. 8.4 is that a magnetic field H is applied to the suspension under a shear flow, where the rotation of fluid particles is given in Ω . The applied magnetic field will then try to align the magnetic moment m (where $m = \mu_0 M \delta V$; δV for the volume element of a magnetic body) with the same direction of H , while the viscous torque exerted by the flow tries to rotate the fluid particle with Ω . Thus the direction of m (or M) will be misaligned with the direction of H , since the moment is fixed in the particle. This misalignment with M and H gives rise to a magnetic torque that tries to realign the magnetic moment, which counteracts the viscous torque. The particle will then rotate to a frame of reference with the angular velocity of ω_p , which is different from the rotation Ω of the fluid particle, as indicated in Fig. 8.4. Thus, the particle rotates internally in the fluid particle with the torque counteracting

the free rotation of the particle, and resultantly this torque gives rise to an increase of the fluid's viscosity.

In this case, however, when the magnetic field \mathbf{H} is applied as colinear with the rotation $\mathbf{\Omega}$ of the fluid particle, the magnetic moment \mathbf{m} (or \mathbf{M}) will be aligned with the same direction of \mathbf{H} ($\mathbf{M} // \mathbf{H}$), and with that there is not any field influence, rotating the particle with the same angular velocity $\mathbf{\Omega}$ ($\boldsymbol{\omega}_p = \mathbf{\Omega}$). Obviously, when there is no magnetic field $\mathbf{H} = 0$, the particle has no preferable direction to be oriented, and rotates freely with the same angular velocity of the fluid particle. The theoretical explanation of magnetoviscous effect in diluted magnetic fluids was given by Shliomis (1972); this also gives the basis for the development of ferrohydrodynamic equations.

By considering the establishment of the angular momentum equation of magnetic fluid, we can write Eq. (8.2.3), using the stress tensor given in Eq. (8.2.9), as follows

$$I \frac{D\boldsymbol{\omega}_p}{Dt} = \nabla \cdot \mathbf{c} + \boldsymbol{\varepsilon} : (\mathbf{T}^{(v)} + \mathbf{T}_{em}) \quad (8.2.18)$$

Here, it is mentioned that $\rho \mathbf{s}$ is replaced by the intrinsic angular momentum of the particles with the particles rotation $\boldsymbol{\omega}_p$, as $\rho \mathbf{s} = I\boldsymbol{\omega}_p$. Denote that the explicit expression of $\rho \mathbf{f}$ in Eq. (8.2.3) is disregarded here at this point.

The constitutive equation for the couple stress tensor or the surface couple stress tensor \mathbf{c} is difficult to obtain, but it is simply assumed that \mathbf{c} is symmetric and diffusive by the intrinsic rotation $\boldsymbol{\omega}_p$ (the angular spin rate) analogous to the Newtonian viscous fluid, which is dependent upon the rate of strain, Rosensweig (1985), as follows

$$\mathbf{c} = \lambda' (\nabla \cdot \boldsymbol{\omega}_p) \mathbf{I} + \eta' (\nabla \boldsymbol{\omega}_p + \nabla \boldsymbol{\omega}_p^T) \quad (8.2.19)$$

where, by analogy, η' and λ' are respectively called the shear and bulk coefficients of the spin viscosity.

The terms, $\boldsymbol{\varepsilon} : \mathbf{T}^{(v)}$ and $\boldsymbol{\varepsilon} : \mathbf{T}_{em}$, that appear in Eq. (8.2.18) are treated with the following considerations. Firstly, we can consider the origin of $\boldsymbol{\varepsilon} : \mathbf{T}^{(v)}$ that is derived from an extraneous magnetic torque to maintain $\boldsymbol{\omega}_p$ against $\mathbf{\Omega}$ under magnetic field, Rosensweig (1988)

$$\boldsymbol{\varepsilon} : \mathbf{T}^{(v)} = -\frac{I}{\tau_s} (\boldsymbol{\omega}_p - \mathbf{\Omega}) \quad (8.2.20)$$

$$= -4\zeta (\boldsymbol{\omega}_p - \mathbf{\Omega}) \quad (8.2.21)$$

I/τ_s is replaced by the vortex viscosity ζ with the relationship $I/\tau_s = 4\zeta$. It is noted that Eq. (8.2.21) gives the definition to the pseudovector \mathbf{A} as it appears in Eq. (8.2.12), so that, as a result

$$\mathbf{A} = -4\zeta(\boldsymbol{\omega}_p - \boldsymbol{\Omega}) \quad (8.2.22)$$

As for the second variant $\boldsymbol{\varepsilon}:\mathbf{T}_{em}$, we can calculate the tensor product by substituting the Maxwell stress tensor given in Eq. (8.2.13) together with the polarization relationship given in Eq. (8.2.7) to yield

$$\boldsymbol{\varepsilon}:\mathbf{T}_{em} = \mathbf{M} \times \mathbf{H} \quad (8.2.23)$$

Therefore, after giving the constitutive relationships discussed above, substituting the expressions from Eqs. (8.2.19), (8.2.21) and (8.2.23), into Eq. (8.2.18), we can obtain the angular momentum equation of a magnetic fluid by writing:

$$I \frac{D\boldsymbol{\omega}_p}{Dt} = (\lambda' + \eta') \nabla(\nabla \cdot \boldsymbol{\omega}_p) + \eta' \nabla^2 \boldsymbol{\omega}_p - \frac{I}{\tau_s} (\boldsymbol{\omega}_p - \boldsymbol{\Omega}) + \mathbf{M} \times \mathbf{H} \quad (8.2.24)$$

It has been mentioned that $\mathbf{M} \times \mathbf{H}$ that appears in Eq. (8.2.24) is equivalent to the body couple $\rho \mathbf{f}$ in Eq. (8.2.3), which is the torque density (torque per unit volume).

In a case when τ_s is sufficiently small and the diffusion and convection of the particle rotation $\boldsymbol{\omega}_p$ are regarded as minimal, we can write Eq. (8.2.24) in a further simplified form where

$$\frac{I}{\tau_s} (\boldsymbol{\omega}_p - \boldsymbol{\Omega}) = \mathbf{M} \times \mathbf{H} \quad (8.2.25)$$

Note that $\tau_s = I/6\eta_0\phi_v = \rho_s d^2/60\eta_0 \approx 1 \times 10^{-11}$ for $d \approx 10$ nm, $\eta_0 \approx 10^{-3}$ kg/m·s and $\rho_s = 6 \times 10^3$ kg/m³, where ρ_s is a particle material density.

The energy equation given in Eq. (8.2.4) is constituted by giving \mathbf{q} and \mathbf{c} , where \mathbf{q} may be straightforwardly constituted by the Fourier's law of Eq. (2.5.28) and \mathbf{c} is given in Eq. (8.2.19). However, at this stage it is appropriate to reduce the equation to the most widely used (or rather practical) expression under assumptions that: the magnetic fluid is (electrically) nonconductive disregarding intrinsic rotation; the magnetization is linear in terms of H and T ; it is incompressible with constant coefficients; and neglects all heat sources due to magnetoviscous and viscous effects and internal heat generation. The resultant equation is written in the following expression where

$$\left[\rho c_p - H \left(\frac{\partial M}{\partial T} \right)_H \right] \frac{DT}{Dt} + T \left(\frac{\partial M}{\partial T} \right)_H \frac{DH}{Dt} = k_c \nabla^2 T \quad (8.2.26)$$

In Eq. (8.2.26) the second term at the left hand side represents the magnetocaloric effect, where the magnetocaloric effect is associated with the change of magnetic field intensity with time at $\partial H / \partial t$ and the fluid traveling through the magnetic field $\mathbf{u} \cdot \nabla \mathbf{H}$. However, for a small dependence of magnetization M on temperature change, i.e. $(\partial M / \partial T)_H \approx 0$ (except for a temperature sensitive magnetic fluid, which has a large temperature dependence on magnetization), Eq. (8.2.26) can be reduced to the conventional temperature field equation as follows

$$\rho c_p \frac{DT}{Dt} = k_c \nabla^2 T \quad (8.2.27)$$

Probably the most characteristic treatment in deriving ferrohydrodynamic equations is that the instantaneous magnetization \mathbf{M} of the suspension is different from the equilibrium magnetization \mathbf{M}_0 , which is given for a diluted suspension from the Langevin magnetization formula of Eq. (8.1.1). In addition, as described in association with Fig. 8.4, the relaxation of \mathbf{M} is coupled with a dynamic change of the flow field. Shliomis (1972, also reviewed article 2002), obtains a phenomenological expression of the magnetization of magnetic fluids, transferring the Debye relaxation equation (1929) of a rotating (local) frame of reference, which rotates with a magnetic particle ω_p , to the fixed (laboratory) system in the following manner.

The Debye-like magnetization equation in the rotating frame of reference is given as

$$\frac{d'\mathbf{M}}{dt} = -\frac{1}{\tau_B} (\mathbf{M} - \mathbf{M}_0) \quad (8.2.28)$$

The rates of change of any vector, say in our case \mathbf{M} , in the rotating frame of reference to the fixed system can be expressed by the relationship

$$\frac{d\mathbf{M}}{dt} = \omega_p \times \mathbf{M} + \frac{d'\mathbf{M}}{dt} \quad (8.2.29)$$

Combing Eq. (8.2.28) and (8.2.29), we have

$$\frac{d\mathbf{M}}{dt} = \omega_p \times \mathbf{M} - \frac{1}{\tau_B} (\mathbf{M} - \mathbf{M}_0) \quad (8.2.30)$$

where τ_B is the Brownian relaxation of time at a constant. With the aid of the torque balance equation obtained in Eq. (8.2.25), Eq. (8.2.30) can be rearranged to yield

$$\frac{d\mathbf{M}}{dt} = \mathbf{\Omega} \times \mathbf{M} - \frac{1}{\tau_B} (\mathbf{M} - \mathbf{M}_0) - \frac{1}{6\eta_0\phi_v} \mathbf{M} \times (\mathbf{M} \times \mathbf{H}) \quad (8.2.31)$$

The equation derived in Eq. (8.2.31) is the Shliomis magnetic relaxation equation.

It proves useful to derive an expression of a linear form of Eq. (8.2.31) and this is done by letting the last quadratic term of the equation to become

$$\begin{aligned} -\frac{1}{6\eta_0\phi_v} \mathbf{M} \times (\mathbf{M} \times \mathbf{H}) &= -\frac{NmL(\zeta)}{6\eta_0\phi_v} \frac{\mathbf{H} \times (\mathbf{M} \times \mathbf{H})}{H} \\ &= -\frac{NmL(\zeta)H}{6\eta_0\phi_v} \frac{\mathbf{H} \times (\mathbf{M} \times \mathbf{H})}{H^2} \end{aligned} \quad (8.2.32)$$

by letting $(\mathbf{M} - \mathbf{M}_0)$ be respectively split into parallel and perpendicular parts to the applied field \mathbf{H} , as

$$\mathbf{M} - \mathbf{M}_0 = \frac{\mathbf{H} \{(\mathbf{M} - \mathbf{M}_0) \cdot \mathbf{H}\}}{H^2} + \frac{\mathbf{H} \times \{(\mathbf{M} - \mathbf{M}_0) \times \mathbf{H}\}}{H^2} \quad (8.2.33)$$

Combining Eqs. (8.3.32) and (8.3.33) with Eq. (8.3.30), we have a linearized magnetization equation to obtain

$$\begin{aligned} \frac{d\mathbf{M}}{dt} &= \mathbf{\Omega} \times \mathbf{M} - \frac{1}{\tau_B} \frac{\mathbf{H} \{(\mathbf{M} - \mathbf{M}_0) \cdot \mathbf{H}\}}{H^2} - \frac{1}{\tau_B} \frac{\mathbf{H} \times (\mathbf{M} \times \mathbf{H})}{H^2} \\ &\quad - \left(\frac{NmL(\zeta)H}{6\eta_0\phi_v} \right) \frac{\mathbf{H} \times (\mathbf{M} \times \mathbf{H})}{H^2} \\ &= \mathbf{\Omega} \times \mathbf{M} - \frac{1}{\tau_{\parallel}} \frac{\mathbf{H} [(\mathbf{M} - \mathbf{M}_0) \cdot \mathbf{H}]}{H^2} - \frac{1}{\tau_{\perp}} \frac{\mathbf{H} \times (\mathbf{M} \times \mathbf{H})}{H^2} \end{aligned} \quad (8.2.34)$$

where two characteristic relaxation times τ_{\parallel} and τ_{\perp} for respectively paralleled and perpendicular contributions are defined where

$$\tau_{\parallel} = \tau_B \quad (8.2.35)$$

and

$$\begin{aligned}\frac{1}{\tau_{\perp}} &= \frac{1}{\tau_B} + \frac{NmHL(\zeta)}{6\eta_0\phi_v} \\ &= \frac{1}{\tau_B} \left\{ 1 + \frac{1}{2}\zeta L(\zeta) \right\}\end{aligned}$$

so that τ_{\perp} is written as

$$\tau_{\perp} = \frac{2\tau_B}{2 + \zeta L(\zeta)} \quad (8.2.36)$$

Consequently, for a stationary limit, Eq. (8.3.34) gives a solution in the linear order

$$\mathbf{M} - \mathbf{M}_0 \approx \tau_{\perp} (\boldsymbol{\Omega} \times \mathbf{M}_0) \quad (8.2.37)$$

Finally, in electromagnetic fields, magnetic fluids are treated as non-conductive mediums in continuum, and to which Maxwell equations are written as

$$\nabla \times \mathbf{H} = 0 \quad (8.2.38)$$

and for the magnetic induction

$$\nabla \cdot \mathbf{B} = 0 \quad (8.2.39)$$

Equations (8.2.38) and (8.2.39) were already used to reduce ferrohydrodynamic equations. Note that the induction \mathbf{B} in a continuum has a difference from the magnetic field (intensity) \mathbf{H} by the magnetization \mathbf{M} . This relation is given in Eq. (8.2.7).

Based on the thought of the intrinsic rotation of magnetic particles, a phenomenological explanation for the increase of apparent viscosity under applying magnetic field is possible, which is found in Exercise 8.2.2. Applications for controlling the viscosity of a continuum by external means are enormous, such as in damping and activating systems in engineering.

Exercise

Exercise 8.2.1 Rosensweig Equation

By considering the linear momentum equation given in Eq. (8.2.17) of magnetic fluids, show a new set of ferrohydrodynamic equations, assuming that the fluids are incompressible and at a quasi-stationary when the relaxation rate is so fast that \mathbf{M} and \mathbf{H} are sensibly collinear, i.e. $\mathbf{M} \parallel \mathbf{H}$.

Also assume that all heat sources and the magnetocaloric effect are identically neglected in the energy equation.

Ans.

The continuity equation of an incompressible medium is written as

$$\nabla \cdot \mathbf{u} = 0 \quad (1)$$

under the assumption of $\mathbf{M} \parallel \mathbf{H}$, that is

$$\rho \frac{D\mathbf{u}}{Dt} = -\nabla p^* + \eta_a \nabla^2 \mathbf{u} + M \nabla H + \rho \mathbf{g} \quad (2)$$

The equation (2) is a so-called Rosensweig equation, first proposed by Ronald Rosensweig (1964). The research of magnetic fluids has continued from the original work of Rosensweig (1964).

The energy equation is reduced to the temperature field equation, and is written repeatedly as

$$\left[\rho c_p - H \left(\frac{\partial M}{\partial T} \right)_H \right] \frac{DT}{Dt} + T \left(\frac{\partial M}{\partial T} \right)_H \frac{DH}{Dt} = k_c \nabla^2 T \quad (3)$$

The magnetization is expressed by the magnetic state equation $M = M(H, T)$, so that it is written by the Langevin formula as

$$M = NmL(\zeta) \text{ for } \zeta = mH/k_B T \quad (4)$$

where $L(\zeta) = \coth \zeta - \zeta^{-1}$.

Treating the magnetic fluids to be nonconductive, the electromagnetic field equations are then written where

$$\nabla \times \mathbf{H} = 0 \text{ and } \nabla \cdot \mathbf{B} = 0 \quad (5)$$

For magnetic polarization of magnetic fluids, we have

$$\mathbf{B} = \mu_0 \mathbf{H} + \mathbf{M} \quad (6)$$

This set of equations, which are yielded in a closed system, can be solved with appropriate boundary conditions.

Exercise 8.2.2 Rotational Viscosity

Probably one of the most noticeable features of magnetic fluids is an increase of apparent viscosity under a magnetic field. Based on the idea that

the intrinsic rotation ω_p of a particle deviates from the angular velocity Ω of the fluid particle, it will be reasonable to think that the difference leads to an additional dissipation, which may be understood to contribute an increase of apparent viscosity. An example of the simple flow field is displayed in Fig. 8.5.

Verify the increase of the apparent viscosity under the condition where the applied magnetic field \mathbf{H} is perpendicular to Ω .

Ans.

In considering Eq. (8.2.33), the perpendicular part of $(\mathbf{M} - \mathbf{M}_0)$ to the applied field \mathbf{H} is written as

$$\mathbf{M} - \mathbf{M}_0 = \frac{1}{H} \left[\left(\frac{\mathbf{H}}{H} \right) \times \{ (\mathbf{M} - \mathbf{M}_0) \times \mathbf{H} \} \right]_{\perp} \quad (1)$$

The steady state solution of Eq. (8.2.34) is given where, i.e. from the resultant Eq. (8.2.37),

$$\mathbf{M} - \mathbf{M}_0 = \tau_{\perp} (\Omega \times \mathbf{M}_0) \quad (2)$$

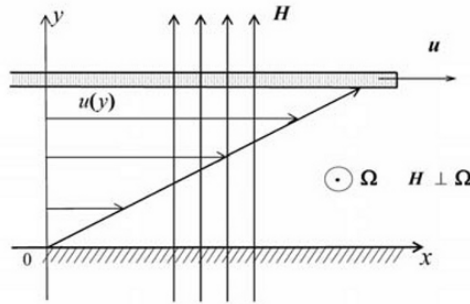


Fig. 8.5 One example of $\mathbf{H} \perp \Omega$ in a Couette flow

Using these conditions, i.e. $\mathbf{H} \parallel \mathbf{M}_0$ and $\mathbf{H} \perp \Omega$, a combination of Eqs. (1) and (2) yields

$$\tau_{\perp} M_0 H \Omega = -(\mathbf{M} \times \mathbf{H}) \quad (3)$$

By noting that $\Omega = (\nabla \times \mathbf{u})/2$ and substituting Eq. (3) to the linear momentum equation given in Eq. (8.2.17), we have

$$\begin{aligned}
\rho \frac{D\mathbf{u}}{Dt} &= -\nabla p^* + \eta_a \nabla^2 \mathbf{u} + \frac{1}{2} \nabla \times (\mathbf{M} \times \mathbf{H}) + \mathbf{M} \cdot \nabla \mathbf{H} + \rho \mathbf{g} \\
&= -\nabla p^* + \left(\eta_a + \frac{1}{4} \tau_{\perp} M_0 H \right) \nabla^2 \mathbf{u} + \mathbf{M} \cdot \nabla \mathbf{H} + \rho \mathbf{g}
\end{aligned} \tag{4}$$

As the results obtained from the form of Eq. (4), the second term of the right hand side of the equation indicates that there appears an additional viscous term η_r where

$$\eta_r = \frac{1}{4} \tau_{\perp} M_0 H \tag{5}$$

The increase of the apparent viscosity in η_r is regarded as the rotational viscosity, Shliomis (1972). Eq. (5) can be expressed in combination with the Langevin formula given in Eq. (8.1.1) and the definition τ_{\perp} given in Eq. (8.2.36) as follows

$$\eta_r(\zeta) = \frac{3}{2} \eta_0 \phi_v \frac{\zeta \mathcal{L}(\zeta)}{2 + \zeta \mathcal{L}(\zeta)} = \frac{3}{2} \eta_0 \phi_v \frac{\zeta - \tanh \zeta}{\zeta + \tanh \zeta} \tag{6}$$

In the absence of a magnetic field, i.e. $\zeta = 0$, Eq. (6) leads $\eta_r(0) = 0$, in which an individual particle rotates with the same angular velocity as a fluid particle, followed by $\boldsymbol{\omega}_p = \boldsymbol{\Omega}$. On the other hand, in the limiting case for $\zeta \rightarrow \infty$, we have

$$\eta_r(\infty) = \frac{3}{2} \eta_0 \phi_v \tag{7}$$

Problems

8.2-1 Prove that τ_{\perp} is expressed in the formula given in Eq. (8.2.36).

Ans. [Exercise 8.1.1 are useful.]

8.2-2 Sketch the curve given in Eq. (6) in Exercise 8.2.2, and discuss the increase of the apparent viscosity where $\eta_r(\zeta)$. Keep other parameters constants.

8.2-3 Assuming $\omega_p = 0$, Eq. (8.2.25) gives $\mathbf{M} \times \mathbf{H} = -6\eta_0\phi_v\mathbf{\Omega}$. Substitution of this $\mathbf{M} \times \mathbf{H}$ to Eq. (8.2.17), gathering the viscous terms, yields $(\eta_a + 3/2 \cdot \eta_0\phi_v)\nabla^2\mathbf{u}$. Derive this expression and discuss the consequence of Exercise 8.2.2, i.e. $\eta_r(\infty) = 3/2 \cdot \eta_0\phi_v$.

$$\text{Ans.} \left[\begin{array}{l} \zeta = 0 \text{ implies the} \\ \text{rolling of particles,} \\ \text{while } \zeta = \infty \text{ implies} \\ \text{the slipping of particles} \end{array} \right]$$

8.3 Basic Flows and Applications

Among many interesting phenomena that often characterize magnetic fluids, some typical cases are explained in this text. In order to avoid confusion and complexity, phenomenological explanations are chiefly given here, trying not to go into too much detailed mathematical treatments. One very characteristic response is the normal field instability. The spontaneous generation of an ordered pattern of peaks (spikes) on the interface (the surface exposed to atmosphere for example) occurs when a uniform magnetic field (exceeding a critical intensity) is applied perpendicular to the interface of a magnetic fluid. Figure 8.6 displays the surface spikes generated due to a normal instability. Among other interesting phenomena connected with the instability problem in a magnetic fluid is that an instability produces a labyrinthine or maze pattern that occurs in a thin layer of a magnetic fluid, when the layer is contained between a closely spaced flat surfaces, where furthermore possible patterns can appear in different configurations of imposing magnetic fields. These phenomena are known mathematically as a bifurcation and are treated as a critical phenomenon, resulting in many patterns appearing at supercritical stages of new equilibrium flow fields. The thermomagnetic convection followed by the appearance of cell patterns is also generated due to the flow instability under various conditions of magnetic fields. This is known as thermoconvective instability.

In this section we shall start our discussion to derive the ferrohydrodynamic Bernoulli equation. Many flow problems in magnetic fluid's technology can be explained similar to, yet in a more augmented way, the Bernoulli equation. Some problems of the thermoconvective instability are treated, taking account of the temperature dependence of magnetization.



Fig. 8.6 Surface spikes due to the normal instability

8.3.1 Generalized Bernoulli Equation

Denoting that magnetic fluids are incompressible and at quasi-stationary where $\mathbf{M} \parallel \mathbf{H}$ is satisfied, the ferrohydrodynamic equation represented by a Rosensweig equation is written as

$$\rho \frac{D\mathbf{u}}{Dt} = -\nabla p^* + \eta_a \nabla^2 \mathbf{u} + M \nabla H + \rho \mathbf{g} \quad (8.3.1)$$

A peculiar feature of the equation describing magnetic fluids is associated with an additional volume force $M \nabla H$, the Kelvin force density and the composite pressure p^* appearing in place of a hydrostatic pressure p . In this sense, Eq. (8.3.1) is an extended Navier-Stokes equation. Denote that $\rho \mathbf{g}$ is the gravitational body force in Eq. (8.3.1).

Along with assumptions adapted for derivation of a Bernoulli equation in Chapter 4, we assume that the fluid is inviscid $\eta_a = 0$, irrotational $\omega = \nabla \times \mathbf{u} = 0$ and isothermal $T = \text{Constant}$. With the condition of a steady state $\partial \mathbf{u} / \partial t = 0$, Eq. (8.3.1) can be reduced to the following form

$$\nabla \left(p^* + \frac{1}{2} \rho u^2 + \Phi - \int_0^H M(H') dH' \right) = 0 \quad (8.3.2)$$

where $\Phi = \rho g z$ is the gravitational potential. The last term can be alternatively written by using the field-averaged magnetization, which is defined as

$$\overline{M} = \frac{1}{H} \int_0^H M(H') dH' \quad (8.3.3)$$

so that

$$\int_0^H M(H') dH' = \overline{M}H \quad (8.3.4)$$

The integration (along the stream line or vortex line) of Eq. (8.3.2) yields a more convenient form where

$$\frac{1}{2} \rho u^2 + p^* + \rho g z - \overline{M}H = \text{const.} \quad (8.3.5)$$

In comparing Eq. (8.3.5) with Eq. (4.1.38), Eq. (8.3.5) is called a ferrohydrodynamic Bernoulli equation, where a new term $-\overline{M}H$ appears in the Bernoulli equation. The importance of Eq. (8.3.5) in view of engineering flow problems will be illustrated in proceeding sections.

8.3.2 Hydrostatics

With a limit of flow speed $u \rightarrow 0$, the state of fluids is at a hydrodynamically static state, where the pressure distribution in a stationary magnetic fluid is described as a static equilibrium equation, derived from Eq. (8.3.5), as follows

$$p^* = p_0^* - \rho g(z - z_0) + \int_{H_0}^H M(H') dH' \quad (8.3.6)$$

where p_0^* is the composite pressure at the point where $\mathbf{x}_0 = (x_0, y_0, z_0)$ in which $H = H_0$ and the axis z is directed vertically upward.

Now let us consider a situation when a nonmagnetic body immersed in a magnetic fluid, similar to that what considered in Fig.3.3. The force acting on a body is determined by a stress T_{nn} on the surface element $d\mathbf{S}$, as similarly treated in Eq. (3.1.9)

$$\begin{aligned} \mathbf{F} &= \int_S T_{nn} d\mathbf{S} \\ &= \int_S \left[-p_0 \mathbf{I} - \frac{\mu_0}{2} H^2 \mathbf{I} + \mathbf{H}\mathbf{B} \right]_{nn} \hat{\mathbf{n}} dS \end{aligned} \quad (8.3.7)$$

T_{nn} is derived from Eq. (8.2.9), together with the Maxwell stress tensor in Eq. (8.2.13) for the condition of hydrodynamically static state. At the boundary (at the surface) of the body, the induction \mathbf{B} has to satisfy the condition

$$\int_S \mathbf{B} \cdot d\mathbf{S} = 0 \quad (8.3.8)$$

Leading to Eq. (8.3.7) to write

$$\mathbf{F} = \int_S \left(-p_0 - \frac{1}{2} (\mathbf{M}_n)^2 \right) \hat{\mathbf{n}} dS \quad (8.3.9)$$

Equation (8.3.9) indicates that at the surface of body, the pressure boundary condition becomes

$$p_0 + \frac{1}{2} M_n^2 = \text{Const.} \quad (8.3.10)$$

The second term of Eq. (8.3.10) is called the magnetic normal traction, indicating that there would be a magnetic pressure jump at the interface of a body and a magnetic fluid. Extensive discussion on the magnetic normal traction is found in Berkovsky et al. (1993).

In general, the calculation of the surface integral for Eq. (8.3.9) yields the net force \mathbf{F} . However, in reality obtaining $M_n = M_n(H)$ is difficult since a non-magnetic body immersed in a magnetic fluid disturbs an external field and resultantly alters $H = H(\mathbf{x})$ at the surface of the body. Within the tolerance it is reasonable to assume that $\mathbf{M}_n \ll \mathbf{H}$, which enables us to neglect the magnetic normal traction. The force \mathbf{F} is thus, by using Eq. (8.3.6), written as

$$\mathbf{F} = - \int_S p^* \hat{\mathbf{n}} dS = \int_S \left\{ \rho g z - \int_{H_0}^H M(H') dH' \right\} \hat{\mathbf{n}} dS \quad (8.3.11)$$

where the magnetic field $H = H(x)$ is assumed the same as those prior to immersing the body.

Equation (8.3.11) can also be rewritten by the Gauss' divergence theorem as follows

$$\begin{aligned} \mathbf{F} &= - \int_S p^* \hat{\mathbf{n}} ds = - \int_V \nabla p^* dV \\ &= \int_V (\rho \mathbf{g} + M \nabla H) dV \end{aligned} \quad (8.3.12)$$

If we further assume that within the volume of a non-magnetic body, $M\nabla H$ is kept constant as \mathbf{g} does, we can write Eq. (8.3.12) to give

$$\mathbf{F} = -\rho\mathbf{g}V - (M\nabla H)V \quad (8.3.13)$$

The first term in Eq. (8.3.13) is the buoyant force known as the principle of Archimedes with reference to Eq. (3.1.30); the second term of the equation is the magnetic buoyant force, whose direction is determined by ∇H of a magnetic field (where we assume $\mathbf{M} \parallel \mathbf{H}$).

When the choice of the direction of ∇H is controlled to be the same as the gravity acceleration \mathbf{g} , which effectively increases the flotation effect for a non-magnetic body. This effect leads to wide applications in practical engineering. One of which is ore separation with respect to specific gravities, as schematically displayed in Fig. 8.7(a). The buoyant force of the preset magnitude is applied to floating valuable substances, separated from other grains of ore. On the contrary, in a case where the flotation conditions of non-magnetic bodies change in the presence of an external non-uniform field, magnetic bodies are self-levitating. For example, if a permanent magnet is placed in a non-magnetic vessel filled with a magnetic fluid, the magnet floats stably alone at the bottom of the vessel, being repelled from the side walls and resultantly occupying a position in the vessel, as sketched in Fig. 8.7(b). The self-levitating effect is the basis for the development of accelerometers, level meter or inertia dampers in engineering applications.

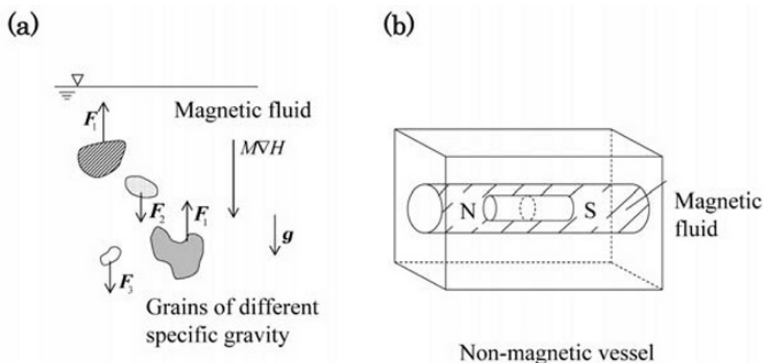


Fig. 8.7 Magnetostatic buoyancy effects

The magnetic hydrostatic equation given in Eq. (8.3.6), suggests that the body force due to the field gradient yields a pressure gradient, as is straightforwardly stated from the Rosensweig equation given in Eq. (8.3.1) for the static condition of $\mathbf{u} = 0$. The presence of a pressure gradient under

a magnetic body force seems to be one of the most attractive effects in magnetic fluid statistics. Since the appearance of magnetic fluids, the principal application of magnetic fluids is largely found in rotary shaft seals, as displayed schematically in Fig. 8.8. As seen in Fig. 8.8(a), a small volume of a magnetic fluid is sustained in the annular region between a rotating shaft and a surrounding cylindrical magnetic pole, where the magnetic fluid maintains direct contact with both shaft and pole piece, providing a virtually leak-proof liquid seal. The pressure difference between the inner and outer housing, say p_3 (high pressure side) and p_4 (low pressure side) with reference to Fig. 8.8(b), can be maintained under a rotating shaft condition. The pressure difference $\Delta p = p_3 - p_4$, i.e. the seal pressure, can be estimated by the static equilibrium equation in Eq. (8.3.6), assuming that the gravitational force is ignored and the magnetic fluid in the gap is in a static state with a condition of the magnetic field to be tangential at the interface, i.e. $M_n = 0$. With the magnetic condition at the interface, there would not be a magnetic pressure jump, so that $p_1^* = p_3$ and $p_2^* = p_4$. Thus, at first approximation, the pressure difference Δp can be estimated by

$$\Delta p = p_3 - p_4 = p_1^* - p_2^* = \int_{H_1}^{H_2} M(H') dH' \quad (8.3.14)$$

The integral in Eq. (8.3.14) depends on the magnetization law. In a weak magnetic field, i.e. $M = \chi H$, so that the integral is given where

$$\int_{H_1}^{H_2} M(H') dH' = \chi \int_{H_1}^{H_2} H' dH' = \frac{1}{2} \chi (H_2^2 - H_1^2) \quad (8.3.15)$$

In a case of strong magnetic fields, $M(H) = M_S$, and the integral is of the form

$$\int_{H_1}^{H_2} M(H') dH' = M_S (H_2 - H_1) \quad (8.3.16)$$

where M_S is the equilibrium saturation magnetization given in Eq. (8.1.2).

In a general case, the Langevin formula given in Eq. (8.1.1) can be used to calculate the integral, which is found to give

$$\int_{H_1}^{H_2} M(H') dH' = N k_B T \ln \left\{ \zeta^{-1} \sinh(\zeta) \right\} \Big|_{H_1}^{H_2} \quad (8.3.17)$$

The magnetic fluid seals are in commercial use as pressure-, vacuum- and dust-seals employed in both rotary and reciprocating shafts. As verified in the text above, the main characteristic ensuring the seal performance is the magnetic field strength in a gap space. In more technical views,

care must be taken to choose the most appropriate type of magnetic fluid to prevent deterioration or evaporation of carrier liquids, depending upon the combination of the contact fluids.

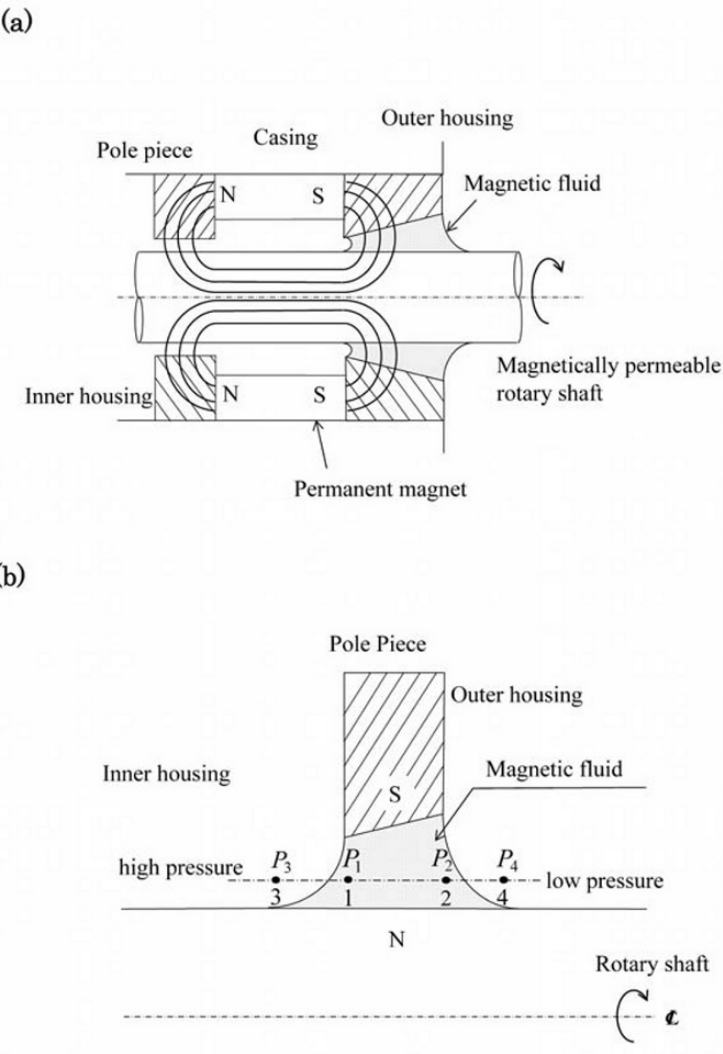


Fig. 8.8 Rotating shaft magnetic fluid seal

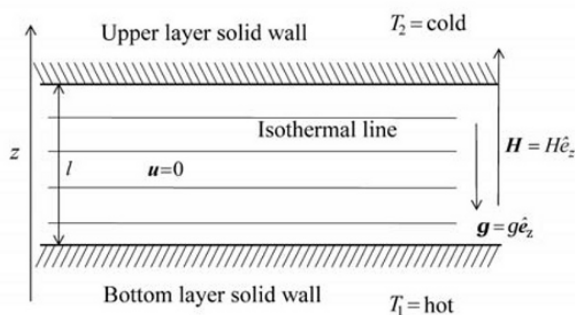
8.3.3 Thermoconvective Phenomena

The Kelvin force density $M\nabla H$ that appeared in the Rosensweig equation is an additional body force term for the gravitational body force (if the fluid motion under the gravity field is considered). The term $M\nabla H$, as seen in the previous section, plays an important part in determining the flow behavior of magnetic fluids. Let us now consider, if a temperature field $T(x)$ is introduced into the flow field of internal flows, a situation of a thermomagnetic natural convection that is analogous to a thermal gravitational natural convection.

The problems found in determining the thermomagnetic natural convection are similar to what was considered in the thermal gravitational natural convection in the way that the onset of a natural convection is caused by a hydrodynamic instability that breaks the mechanical equilibrium of fluid at a hydrodynamically static state, Landau and Lifshitz (1959) and Gershuni and Zhukhvitkii (1976). In this section, for the sake of clarity the simplest case of the natural convection, the so-called Benard convection, is considered as schematically represented in Fig. 8.9. As shown in Fig. 8.9(a) and (b), the thermal configuration is such that two dimensional infinite solid horizontal layers are arranged in parallel, in which the temperature of the interface of the bottom layer is set higher than that of the upper layer. Between the two layers a magnetic fluid is charged, where the density ρ and magnetization M of the magnetic fluid posses a spatial non-uniformity due to a temperature distribution. It is assumed that the two solid layers have an infinite magnetic permeability and a thermal conductivity.

At the beginning, the state of the fluid is at a quiescent state of mechanical equilibrium $\mathbf{u} = 0$, where an externally applied magnetic field \mathbf{H} and temperature difference $\Delta T = |T_2 - T_1|$ are very small, and the heat is transferred from the bottom wall to the upper wall by the thermal conduction through the magnetic fluid layer, as indicated in Fig. 8.9(a). This is the conduction state, where isothermal temperature distribution persists. As thermal and/or magnetic conditions are changed, as we will discuss here, there should be a threshold condition, upon which a natural convection mode appears, followed with the appearance of cellular structure of flow, known as the Benard cell as schematically shown in Fig. 8.9(b). With this mode of flow, i.e. at the state of a natural convection, the heat transfer rate increases drastically compared to the thermal conduction state due to a convective motion of flow.

(a)



(b)

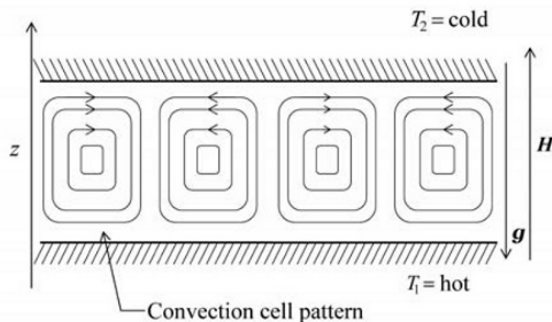


Fig. 8.9 Problem of Benard convection in thermomagnetic natural convection

In order to develop knowledge in critical phenomena at the occurrence of a thermomagnetic natural convection, we will examine the mechanism by firstly writing conditions for a mechanical equilibrium. The requisite mechanical equilibrium is given by taking the rotation of the Rosensweig equation at the hydrodynamically static state $\mathbf{u} = 0$, as follows

$$\nabla \rho \times \mathbf{g} + \nabla M \times \nabla H = 0 \quad (8.3.18)$$

In examining appropriateness of Eq. (8.3.18), we shall assume here that the temperature dependence for the properties of $\rho = \rho(T)$ and

$M = M(T, H)$, where T varies in position z likewise $T = T(z)$, so that we have

$$\nabla \rho = \left(\frac{\partial \rho}{\partial T} \right) \nabla T \text{ and } \nabla M = \left(\frac{\partial M}{\partial T} \right)_H \nabla T + \left(\frac{\partial M}{\partial H} \right)_T \nabla H \quad (8.3.19)$$

It is further mentioned that the magnetic fluid is assumed to be homogeneous in terms of the concentration of a magnetic phase in a fluid. The substitution of Eq. (8.3.18) to Eq. (8.3.19) yields the necessary condition of a mechanical equilibrium, that is

$$\left\{ \left(\frac{\partial \rho}{\partial T} \right) \mathbf{g} + \left(\frac{\partial M}{\partial T} \right) \nabla H \right\} \times \nabla T = 0 \quad (8.3.20)$$

The existence of the critical phenomena, namely the transition to a flow of natural convection from the state of thermal conduction requires the parallelity of ∇T to \mathbf{g} and ∇H . At a condition when this parallelity is broken, the equilibrium (the static) state would not be possible, at which moment the onset of a convection motion, $\mathbf{u} \neq 0$, appears.

Thermal characteristics found in problems of the Benard convection are solely determined by the Rayleigh number Ra as discussed in Exercise 6.2.1, which is defined as

$$Ra = Gr \times Pr = \frac{\rho_0 g \beta_T |\nabla T| c_p l^4}{k_c \nu} \quad (8.3.21)$$

The temperature gradient ∇T is defined by $|\Delta T/l|$, c_p is the specific heat, k_c is the thermal conductivity, ν is the kinematic viscosity. Note that β_T is the coefficient of thermal expansion that is defined as

$$\rho = \rho_0 \{1 - \beta_T (T - T_0)\} \quad (8.3.22)$$

It is further mentioned that ρ_0 and T_0 are a reference density and temperature respectively. All thermophysical values are bulk values of a magnetic fluid.

Some simplifications are expressed by assuming a linear magnetization relationship, a so-called soft magnet approximation to the magnetic fluid. By the use of that from Eq. (8.1.3), the magnetization can be written analogously to Eq. (8.3.22),

$$M = M_0 \{1 - \beta_m (T - T_0)\} \quad (8.3.23)$$

where β_m is defined as the relative pyromagnetic coefficient.

Satisfying the condition of parallelity given in Eq. (8.3.20), i.e. $\mathbf{g} // \nabla H$, with the critical phenomena of the natural convection of a magnetic fluid, the Rayleigh number defined in Eq. (8.3.21) can be modified to write

$$Ra^* = (\rho_0 g \beta_T - \beta_m M_0 \frac{dH}{dz}) (-\frac{dT}{dz}) c_p l^4 / k_c \nu \quad (8.3.24)$$

The important consequence of deriving the expression found in Eq. (8.3.24) is that the flow instability at the onset of a natural convection is adequately described by the known solutions of ordinary thermoconvective stability problems, by adding an extra term of thermomagnetic force action to the buoyant force effect.

Taking into account of the magnetic polarization relation expressed in Eq. (8.2.7), the magnetic field gradient dH/dz can be rewritten by the following sequence

$$\nabla \cdot \mathbf{H} = -\frac{1}{\mu_0} \nabla \cdot \mathbf{M} \quad (8.3.25)$$

Equation (8.3.19) has a scalar component for H where

$$\begin{aligned} \nabla H &= -\frac{1}{\mu_0} \nabla M \\ &= -\frac{1}{\mu_0} \left\{ \left(\frac{\partial M}{\partial T} \right)_H \nabla T + \left(\frac{\partial M}{\partial H} \right)_T \nabla H \right\} \end{aligned} \quad (8.3.25)$$

so that

$$\frac{dH}{dz} = -\frac{1}{\mu_0} \left\{ (-M_0 \beta_m) \frac{dT}{dz} + \chi \frac{dH}{dz} \right\} \quad (8.3.26)$$

where the field gradient is given as

$$\frac{dH}{dz} = \frac{M_0 \beta_m}{\left(1 + \frac{\chi}{\mu_0} \right)} \left(\frac{dT}{dz} \right) \quad (8.3.27)$$

Therefore, Ra^* in Eq. (8.3.24) can be decomposed into two basic terms as we substitute Eq. (8.3.27) for Eq. (8.3.24), yielding

$$\begin{aligned}
 R_a^* &= -\rho_0 g \beta_T \left(\frac{dT}{dz} \right) \frac{c_p l^4}{k_c \nu} + \frac{\mu_0 M_0^2 \beta_m^2}{(\mu_0 + \chi)} \left(\frac{dT}{dz} \right)^2 \frac{c_p l^4}{k_c \nu} \\
 &= R_a + R_m
 \end{aligned} \tag{8.3.28}$$

The first term R_a is an ordinary (thermogravitational Rayleigh number) and the second term R_m is defined as the magnetic Rayleigh number. An important result obtained from Eq. (8.3.28) is that the R_m in all directions of $\nabla T = dT/dz$ is positive, indicating that in the irrespective of the direction of the magnetic field gradient $\nabla H = dH/dz$ the temperature perturbation of the magnetizing field always leads to the thermoconvective fluid destabilization.

In determining the critical Rayleigh number R_{a_c} at the first transition of the Benard convection, the Rayleigh number at the onset of first appearance of the Benard convection cells, Gotoh and Yamada (1982), show that (detailed by numerical study) the parameter $K = B_0/H_0 (\mu_0 + \chi)$, the characteristic parameter of the nonlinearity of the fluid magnetization curve, plays an important role, and further show that in cases where $K \rightarrow \infty$ (sufficiently large K), the stability problem will become a conventional stability problem of a Benard convection, as derived in Eq. (8.3.28). Consequently the critical Rayleigh number $R_{a_c}^* = 1708$ is found to be applied for ordinary thermogravitational and thermomagnetic terms, which are written as

$$R_{a_c}^* = R_{a_c} + R_{m_c} = 1708 \tag{8.3.29}$$

The results obtained from a series of numerical work are also formulated by a linear relation

$$\frac{R_{a_c}}{R_{a_c}^*} = 1 - \frac{R_{m_c}}{R_{m_0}} \tag{8.3.30}$$

where R_{m_0} is the critical magnetic Rayleigh number in the absence of the gravitational effect, as $K \rightarrow \infty$, Blums et al. (1997).

The experimental evidence, Schwab et al. (1983), also supports the relationships found in Eqs. (8.3.24) and (8.3.28), as schematically shown in Fig. 8.10, where Nu is the Nusselt number (with reference to Fig. 6.2 for an ordinary natural convection). As seen in Fig. 8.10, the increase of the magnetic field H results in a lowering of the critical Rayleigh number, destabilizing the fluid state, and resultantly enhancing the heat transfer rate as thermal mixing increases by the convecting motion of the fluid.

The compatibility between $\rho\mathbf{g}$ and $M\nabla H$ is interesting, particularly in application to space engineering, where in the non-gravity condition a body force may be altered or controlled by means of $M\nabla H$. Widespread engineering applications or pure fluid science problems are found in space environments in conjunction with thermoconvective phenomena.

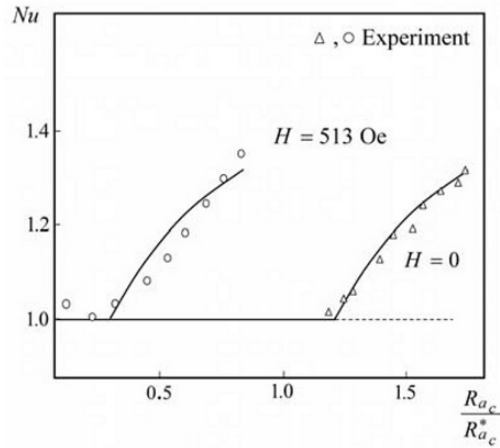


Fig. 8.10 Heat transfer characteristics in thermomagnetic convection (replotted after Schwab et al., 1983)

Exercise

Exercise 8.3.1 Magnetic Field Boundary Conditions and Pressure Jump

Give boundary conditions for a magnetic field when two magnetically permeable media are in contact, one of which is a magnetic fluid. Consider, taking account of the magnetic field boundary conditions, the pressure jump at the interface of a stationary media.

Ans.

The two magnetic field conditions given in Eqs. (8.2.38) and (8.2.39) can be applied to the boundary of magnetic fluids and magnetically permeable media. For the induction of \mathbf{B} , firstly according to the Gauss's divergence theorem, we can write the following relationship as

$$\int_V \nabla \cdot \mathbf{B} dV = \int_S \mathbf{B} \cdot d\mathbf{S} = (B_{1n} - B_{2n}) dS = 0 \quad (1)$$

Equation (1) yields the result that

$$B_{1n} = B_{2n} \quad \text{or} \quad (\mathbf{B}_1 - \mathbf{B}_2) \cdot \hat{\mathbf{n}} = 0 \quad (2)$$

It is mentioned that $\hat{\mathbf{n}}$ is the normal vector directed to medium 2 (supposing magnetically permeable medium) from medium 1 (supposing the magnetic fluid), as indicated in Fig. 8.11.

Equation (2) shows the continuity of the normal induction B_n , when \mathbf{B} passes through the interface of the media with different magnetization M_{1n} and M_{2n} . Equation (2) also gives a jump to the normal magnetic field intensity H_n , which is equal to the difference of a normal fluid magnetization M_n , so that

$$\mu_0 (H_{1n} - H_{2n}) = M_{2n} - M_{1n} \quad (3)$$

For the magnetic field \mathbf{H} , according to the Ampere's circulation law, we can write the relationship at the interface

$$\int_S (\nabla \times \mathbf{H}) \cdot d\mathbf{S} = \int_l \mathbf{H} \cdot d\mathbf{l} = (H_{1t} - H_{2t}) dl = 0 \quad (4)$$

Equation (4) yields the result that

$$H_{1t} = H_{2t} \quad \text{or} \quad (\mathbf{H}_1 - \mathbf{H}_2) \times \hat{\mathbf{n}} = 0 \quad (5)$$

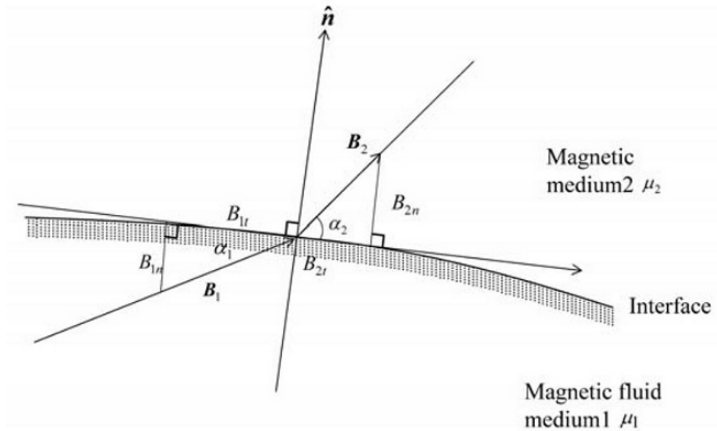


Fig. 8.11 Refraction at an interface

The conditions given in Eq. (5) involve the continuity of the tangential magnetic field intensity H_t at the interface. Altogether, Eqs. (2) and (5), give the conjugation of a magnetic field at an interface for an induction and magnetic field intensity. This conjugation gives an insight into the solution for a magnetic field at a boundary, such as a consideration of the refraction of magnetic flux lines of \mathbf{B}_1 and \mathbf{B}_2 at the interface of two media, as shown in Fig. 8.11. Denote that α is the angle between the magnetic flux line and the tangent to the interface, so that $\tan\alpha = B_n/B_t$, considering $\mathbf{B} = \mu_0\mathbf{H}$ for each medium at the interface, we may obtain the following relationship

$$\frac{\tan\alpha_1}{\tan\alpha_2} = \frac{B_{1n}/B_{1t}}{B_{2n}/B_{2t}} = \frac{B_{2t}}{B_{1t}} = \frac{\mu_2}{\mu_1} \quad (6)$$

where μ_1 and μ_2 are the magnetic permeability of medium 1 and medium 2 respectively. For example, as shown Fig. 8.11, in the case of $\mu_2 < \mu_1$, the magnetic flux line of medium 2 has a high refraction angle at the interface.

Now consider dynamic boundary conditions at the interface, simply assuming that the two media are thermally at equilibrium, i.e. isothermal and stationary, i.e. $\mathbf{u} = 0$ at the interface. The stress tensor for a magnetic fluid can be written as, according to Eqs. (8.2.9) and (8.2.13)

$$\mathbf{T} = (-p_0 - \frac{1}{2}\mu_0 H^2)\mathbf{I} + \mathbf{HB} \quad (7)$$

With the allowance of the conjugation of a magnetic field at an interface, the normal stress difference at the interface is balanced at the stationary condition so that

$$\begin{aligned} \mathbf{T}_2 \cdot \hat{\mathbf{n}} - \mathbf{T}_1 \cdot \hat{\mathbf{n}} &= (p_{01} - p_{02})\hat{\mathbf{n}} + \frac{1}{2}\mu_0(H_1^2 - H_2^2)\hat{\mathbf{n}} \\ &\quad - \sigma\left(\frac{1}{R_1} + \frac{1}{R_2}\right)\hat{\mathbf{n}} + (\mathbf{H}_2\mathbf{B}_2 - \mathbf{H}_1\mathbf{B}_1) \cdot \hat{\mathbf{n}} \\ &= \Delta p\hat{\mathbf{n}} - \sigma\left(\frac{1}{R_1} + \frac{1}{R_2}\right)\hat{\mathbf{n}} + \frac{1}{2}\mu_0[(\mathbf{M}_1 \cdot \hat{\mathbf{n}})^2 - (\mathbf{M}_2 \cdot \hat{\mathbf{n}})^2]\hat{\mathbf{n}} \end{aligned} \quad (8)$$

where the third term in the right hand side of equation is due to the surface tension where σ is the coefficient of the surface tension and R_1 and R_2 are the main surface curvature radii. With $\mathbf{T}_2 \cdot \hat{\mathbf{n}} - \mathbf{T}_1 \cdot \hat{\mathbf{n}} = 0$, we can obtain

$$\Delta p = \sigma \left(\frac{1}{R_1} + \frac{1}{R_2} \right) - \frac{1}{2} \mu_0 \left[(\mathbf{M}_1 \cdot \hat{\mathbf{n}})^2 - (\mathbf{M}_2 \cdot \hat{\mathbf{n}})^2 \right] \quad (9)$$

Thus, at the interface, a pressure jump may occur due to the effect of the surface tension and the difference of a squared magnetization (normal magnetization component) of the media.

Equation (9) gives the idea that for the magnetic fluid in contact with the atmosphere with the plane interface the pressure inside of the magnetic fluid is less than that of atmospheric pressure by $\mu_0 M_n^2 / 2$. Furthermore, in the case of only a tangential magnetic flux at the interface, there would not be a pressure jump due to the magnetization difference.

Exercise 8.3.2 Effect of Mass Concentration on Thermomagnetic Convection

In thermomagnetic convection, if the concentration of magnetic phase in a magnetic fluid has any space dependency, include the terms due to the non-uniformity of fluid components to the Rayleigh number Ra^* defined in Eq. (8.3.24).

Ans.

Let the density of the bulk magnetic fluid ρ be spatially non-uniform and define ρ_m as the density of the magnetic phase in a magnetic fluid. The concentration of the magnetic phase is thus written as

$$n_m = \rho_m / \rho \quad (1)$$

n_m is a function of spacial coordinates. ρ and M then have a functional relationship for independent parameters; T , H and n_m are as follows

$$\rho = \rho(T, n_m) \quad (2)$$

$$M = M(T, H, n_m) \quad (3)$$

so that, in differential forms

$$\nabla \rho = \left(\frac{\partial \rho}{\partial T} \right)_{n_m} \nabla T + \left(\frac{\partial \rho}{\partial n_m} \right)_T \nabla n_m \quad (4)$$

$$\nabla M = \left(\frac{\partial M}{\partial T} \right)_{n_m, T} \nabla T + \left(\frac{\partial M}{\partial H} \right)_{T, n_m} \nabla H + \left(\frac{\partial M}{\partial n_m} \right)_{T, H} \nabla n_m \quad (5)$$

The substitution of Eqs. (4) and (5) for Eq. (8.3.18) yields

$$\left(\frac{\partial \rho}{\partial T} \mathbf{g} + \frac{\partial M}{\partial T} \nabla H \right) \times \nabla T + \left(\frac{\partial \rho}{\partial n_m} \mathbf{g} + \frac{\partial M}{\partial n_m} \nabla H \right) \times \nabla n_m = 0 \quad (6)$$

For the existence of the critical phenomena, likewise discussed in Eq. (8.3.20), the following conditions are to be met

$$\frac{\partial \rho}{\partial T} \mathbf{g} = - \frac{\partial M}{\partial T} \nabla H \quad \text{and} \quad \frac{\partial \rho}{\partial n_m} \mathbf{g} = - \frac{\partial M}{\partial n_m} \nabla H \quad (7)$$

Therefore, when ∇T or ∇n_m are parallel to \mathbf{g} and ∇H , the convection may set up under definite conditions. By definition of the Rayleigh number, Ra^* given in Eq. (8.3.21), we can define the generalized Rayleigh number for magnetodiffusion convection, considering ∇n_m and writing the necessary condition on mechanical equilibrium similar to Eq. (8.3.20) as

$$\left(\frac{\partial \rho}{\partial n_m} \mathbf{g} + \frac{\partial M}{\partial n_m} \nabla H \right) \times \nabla n_m = 0 \quad (8)$$

Analogous to deriving Eq. (8.3.24), we can derive an expression for the generalized Rayleigh number Ra^* by writing

$$Ra^* = \left(\rho_0 g \beta_n - \beta_p M_0 \frac{dH}{dz} \right) \left(\frac{dn_m}{dz} \right) \frac{l^4}{\eta_a D} \quad (9)$$

where β_n and β_p are defined in such a way that $\beta_n = \frac{1}{\rho_0} \frac{\partial \rho}{\partial n_m}$ and

$$\beta_p = \frac{1}{M_0} \frac{\partial M}{\partial n_m}, \quad \text{Blums et al. (1997).}$$

Note that D is the diffusion coefficient of magnetic particles in a carrier liquid.

It is mentioned that under the non-isothermal conditions that the flow instability is largely dependent upon by a thermoconvective mechanism, rather than a mass transfer of colloidal particles. This is due to the reason that the thermal relaxation time is considerably shorter than the time required for colloidal particles to establish an equilibrium concentration field of ρ_m . This can be characterized by the Lewis number Le , which is defined as

$$Le = D\rho_0 c_p / k_c = \frac{D}{k_\alpha} \quad (10)$$

where k_α is the thermal diffusivity. The magnitude of D can be estimated by Einstein's formula for the diffusion coefficient

$$D = k_B T / 6\pi\eta_0 r \quad (11)$$

where $2r \approx 10\text{nm}$ is the diameter of a magnetic particle. For a water base magnetic fluid, Le may be calculated to give

$$Le = \frac{0.44 \times 10^{-11}}{1.5 \times 10^{-7}} = 0.3 \times 10^{-4} \quad (12)$$

Small Le shows that the mass diffusion is smaller than the thermal diffusion, indicating that the relaxation is considerably shorter than the mass diffusion time scale.

Problems

8.3-1 Consider a non-magnetic body of density ρ_s with a representative radius of R . If the density ρ of a magnetic fluid is $1.3 \times 10^3 \text{ kg/m}^3$, and $\bar{M} = 2.5 \times 10^{-2}$ Tesla and $\nabla H = -8 \times 10^5 \text{ A/m}^2$ are kept constant, what is the floating criterion of the nonmagnetic body when $R \approx 0.001 \text{ m}$ is considered?

$$\text{Ans. } \left[\begin{array}{l} \text{From Eq. (8.3.13)} \\ 0 = [(\rho - \rho_s)g - \bar{M}\nabla H] \frac{4}{5} \pi R^3 \\ \rho_s = 3.3 \text{ kg/m}^3 \end{array} \right]$$

8.3-2 Consider a single stage rotating shaft with a magnetic fluid seal, as in Fig. 8.8, when a strong magnetic field of $H_2 = 1.19 \times 10^3 \text{ kA/m}$ and $H_1 \approx 0$ is imposed at both sides of the seal. Estimate the seal pressure Δp if the mean corresponding magnetization \bar{M}_s is $\bar{M}_s \approx 4.02 \times 10^{-2}$ Tesla.

$$\text{Ans. } [4.78 \times 10^4 \text{ Pa}]$$

8.3-3 Considering the constitutive equation given in Eq. (8.2.9), derive Eq. (8.3.1) by describing the conditions to derive Eq. (8.3.1).

8.3-4 Give reasons why the curve for $H \neq 0$ in Fig. 8.10 shifts to left.

Nomenclature

\mathbf{A}	: Pseudovector, vector of tensor
\mathbf{B}	: magnetic induction vector
b	: heat generation per unit mass
\mathbf{c}	: couple stress tensor
D	: diffusion coefficient
d	: diameter
\mathbf{f}	: body couple per unit mass
f_0	: Larmor frequency
\mathbf{g}	: body force
\mathbf{g}	: gravity acceleration
Gr	: Grashof number
\mathbf{H}	: magnetic field vector
\mathbf{I}	: unit tensor
I	: moment of inertia
K	: Pyromagnetic coefficient, characteristic parameter of nonlinearity or anisotropy constant
k_c	: thermal conductivity
k_B	: Boltzmann constant
k_α	: thermal diffusivity
l	: characteristic length
Le	: Lewis number
\mathbf{M}	: magnetization vector
M_s	: saturation magnetization
m	: magnetic moment
N	: number of particle per unit volume
Nu	: Nusselt number
$\hat{\mathbf{n}}$: normal unit vector
p	: pressure
p^*	: total pressure
P_{em}	: electromagnetic energy per unit volume
p_0	: hydrostatic pressure

Pr	: Prandtl number
q	: heat transfer rate
\mathbf{q}	: heat flux vector
R, R_1, R_2	: representative radius
Ra	: Rayleigh number
Ra^*	: generalized Rayleigh number
R_m	: magnetic Rayleigh number
\mathbf{s}	: intrinsic angular momentum vector
s	: specific entropy, surfactant thickness
\mathbf{T}	: total stress tensor
T	: temperature
T_0	: reference temperature
\mathbf{u}	: velocity vector
u	: internal energy of system
u_m	: Internal energy of magnetic fluid
V	: volume
x, y, z	: Cartesian coordinates system
r, θ, z	: cylindrical coordinates system
r, θ, ϕ	: spherical coordinates system
α	: diffraction angle
β_m	: relative pyromagnetic coefficient
β_T	: coefficient of thermal expansion
$\boldsymbol{\varepsilon}$: polyadic alternator
ζ	: Langevin argument, vortex viscosity
η	: viscosity of bulk magnetic fluid
η_0	: base (carrier) liquid viscosity
η_a	: apparent viscosity
η_r	: rotational (additional) viscosity
η'	: shear coefficient of spin viscosity
ρ	: density of bulk magnetic fluid
ρ_s	: particle material density
μ_0	: permeability of free space
μ, μ_s, μ_1, μ_2	: magnetic permeability
λ'	: bulk coefficient of spin viscosity
ϕ	: void fraction
ϕ_c	: critical volume fraction
ϕ_m	: void fraction of magnetic material

ϕ_v	: void fraction of magnetic material with surfactant layer
σ	: (coefficient of) surface tension
τ	: stress tensor
τ_B	: Brownian diffusion time constant
τ_N	: Néel relaxation time
τ_s	: rotational relaxation time
$\tau_{ }, \tau_{\perp}$: characteristic relaxation time
ν	: kinematic viscosity $\nu = \eta/\rho$
χ	: magnetic susceptibility
m	: mass of a particle
ω	: vorticity vector
ω_p	: spin angular velocity
Ω	: fluid particle rotation rate vector, angular velocity

Bibliography

With the appearance of a magnetic fluid, the conceptual treatment of ferrohydrodynamics was first introduced by

1. J.L. Neuringer and R.E. Rosensweig, *Ferrohydrodynamics*, Phys. Fluid 7 (12), 1964.

An excellent and rather authoritative overview on ferrohydrodynamics is found in the text, of which students who wish to study this field of science should be aware.

2. R.E. Rosensweig, *Ferrohydrodynamics*, Cambridge University Press, Cambridge, MA, 1985. Republished from Dover Publications, Inc., 1997.
3. R.E. Rosensweig, An Introduction to Ferrohydrodynamics, Chemical Engineering Communication, 67, 1–18, 1988.
4. E. Blums, A. Cebers and M.M. Maiorov, *Magnetic Fluids*, Walter de Gruyter & Co., Berlin – New York, 416, 1997.

A great deal of thermodynamical treatment on the subject and its engineering applications are found in

5. V.G. Bashtovoy, B.M. Berkovsky and A.N. Vislovich, *Introduction to Thermodynamics of Magnetic Fluids*, Hemisphere Publication Corporation, New York, 1988.

6. B.M. Berkovsky, V.F. Medvedev and M.S. Krakov, *Magnetic Fluid, Engineering Application*, Oxford University Press, Oxford, 1993.

Recent developments in ferrohydrodynamics is well documented via various topics in the academic field of magnetic fluid, in

7. R.E. Rosensweig, Basic equations for magnetic fluids with internal rotations, *Ferrofluids* (Edited by S. Odenbach), Springer, 2002.
8. S. Odenbach (edited), *Magnetoviscous Effects in Ferrofluids*, Springer, New York, 2002.

Flow phenomena, specific data, correlations and approximations that are referred to in individual topics are presented in

9. W.F. Brown, Thermal fluctuation of single domain particle, *Phys. Rev.*, 130 (5), 1963.
10. L. Néel, Effect of thermal fluctuation on the magnetization of small particles, *C. R. Acad. Sci. Paris*, 1949.
11. A. Einstein, On the movement of small particles suspended in a stationary liquid demanded by the molecular kinetic theory of heat, *Annaler der physic* 17, 1906, which is also found in an English translation, R. Furth, *Einstein Investigation on the Theory of the Brownian Movement*, Dover, New York, 1956.
12. M.A. Martsenyuk, Yu. L. Raikher and M.I. Shliomis, On the kinetics of magnetization of suspensions of ferromagnetic particles, *Sov. Phys. JETP*, 38 (2), 1974.
13. L.D. Landau and E.M. Lifshitz, *Electrodynamics of Continuous Media*, (2nd Edition, 1984) Pergamon Press, Oxford, 1960.
14. M.I. Shliomis, Effective viscosity of magnetic fluid suspensions, *Soviet Phys. JETP*, 341 (6), 1972.
15. L.D. Landau and E.M. Lifshitz, *Fluid Mechanics*, (2nd Edition, 1987) Pergamon Press, 1959.
16. M.I. Shliomis, Convective instability of magnetized ferrofluid, *Lecture Notes in Physics*, Springer-Verlag, New York, 2001.
17. K. Gotoh and M. Yamada, Thermal convection in a horizontal layer of magnetic fluids, *J. Phys. Soc.*, 51 (9), 1982.
18. L. Schwab, U. Hildebrandt and K. Stierstadt, Magnetic Benard convection, *J. Magn. Magn. Mater.*, 39 (1–2), 1983.

19. G. Kronkalns, M. Maiorov and E. Blums, Preparation and Properties of Temperature-Sensitive Magnetic Fluids, *Magnetohydrodynamics*, 33, 92–96, 1997.
20. G.Z. Gershuni and E.M. Zhukhovitskii, *Convective Stability of Incompressible Fluids*, Kepter Publishing House Jerusalem Ltd. (translated from Russian), Jerusalem, 1976.

Appendix

Appendix A

Table A.1 Physical properties of water

$T[^\circ\text{C}]$	$\rho[\text{kg}/\text{m}^3]$	$\eta_0[\text{Pa}\cdot\text{s}]$	$\nu[\text{m}^2/\text{s}]$	$p_{\text{vapor}}[\text{kPa}]$	$\sigma[\text{N}/\text{m}]$	$K[\text{GPa}]$
0	1000	1.75×10^{-3}	1.75×10^{-6}	0.611	0.0756	2.02
10	1000	1.30×10^{-3}	1.30×10^{-6}	1.23	0.0742	2.10
20	998	1.02×10^{-3}	1.02×10^{-6}	2.34	0.0728	2.18
30	996	8.00×10^{-4}	8.03×10^{-6}	4.24	0.0712	2.25
40	992	6.51×10^{-4}	6.56×10^{-7}	7.38	0.0696	2.28
50	988	5.41×10^{-4}	5.48×10^{-7}	12.3	0.0679	2.29
60	984	4.60×10^{-4}	4.67×10^{-7}	19.9	0.0662	2.28
70	978	4.02×10^{-4}	4.11×10^{-7}	31.2	0.0644	2.25
80	971	3.50×10^{-4}	3.60×10^{-7}	47.4	0.0626	2.20
90	965	3.11×10^{-4}	3.22×10^{-7}	70.1	0.0608	2.14
100	958	2.82×10^{-4}	2.94×10^{-7}	101.3	0.0589	2.07

Table A.2 Typical physical Properties of some common liquids at 1atm and 20°C

Liquid	$\rho[\text{kg}/\text{m}^3]$	$\eta_0[\text{Pa} \cdot \text{s}]$	$p_{\text{vapor}}[\text{kPa}]$	$\sigma[\text{N}/\text{m}]$
Ammonia	829	2.20×10^{-4}	910	0.0213
Benzene	879	6.51×10^{-4}	10.1	0.0289
Ethanol	7887	1.20×10^{-3}	5.75	0.0228
Glycerine	1258	1.49	1.4×10^{-5}	0.0633
Kerosene	819	1.92×10^{-3}	3.11	0.0277
Methanol	788	5.98×10^{-4}	13.4	0.0226

Appendix B

Appendix B-1 Vector Tensor Operations

Write a vector \mathbf{u} as a sum $\sum_i \hat{\mathbf{e}}_i u_i$ and a tensor \mathbf{T} as a sum $\sum_i \hat{\mathbf{e}}_i \hat{\mathbf{e}}_j T_{ij}$, where $\hat{\mathbf{e}}_i \hat{\mathbf{e}}_j$ is the unit dyad. Note that the unit vectors $\hat{\mathbf{e}}_i$ are defined to give vectors and there are the scalar products $(\hat{\mathbf{e}}_i \cdot \hat{\mathbf{e}}_j)$ and vector products $(\hat{\mathbf{e}}_i \times \hat{\mathbf{e}}_j)$. A third kind of product can be formed with the unit vector, namely the dyadic product $\hat{\mathbf{e}}_i \hat{\mathbf{e}}_j$, where the products $\hat{\mathbf{e}}_i \hat{\mathbf{e}}_j$ are the second order tensor. $\hat{\mathbf{e}}_i$ and $\hat{\mathbf{e}}_j$ are of unit magnitude, so that the products $\hat{\mathbf{e}}_i \hat{\mathbf{e}}_j$ are treated as unit dyads.

Based upon the dot and cross products of unit vector, which are performed by the geometrical definitions, the analogous operations for the unit dyads are defined by relating them to the operations for unit vectors

$$\hat{\mathbf{e}}_i \hat{\mathbf{e}}_j \cdot \hat{\mathbf{e}}_k \hat{\mathbf{e}}_l = (\hat{\mathbf{e}}_j \cdot \hat{\mathbf{e}}_k)(\hat{\mathbf{e}}_i \cdot \hat{\mathbf{e}}_l) = \delta_{jk} \delta_{il} \quad (\text{B.1-1})$$

$$\hat{\mathbf{e}}_i \hat{\mathbf{e}}_j \cdot \hat{\mathbf{e}}_k = \hat{\mathbf{e}}_i (\hat{\mathbf{e}}_j \cdot \hat{\mathbf{e}}_k) = \hat{\mathbf{e}}_i \delta_{jk} \quad (\text{B.1-2})$$

$$\hat{\mathbf{e}}_i \cdot \hat{\mathbf{e}}_j \hat{\mathbf{e}}_k = (\hat{\mathbf{e}}_i \cdot \hat{\mathbf{e}}_j) \hat{\mathbf{e}}_k = \delta_{ij} \hat{\mathbf{e}}_k \quad (\text{B.1-3})$$

$$\hat{\mathbf{e}}_i \hat{\mathbf{e}}_j \cdot \hat{\mathbf{e}}_k \hat{\mathbf{e}}_l = \hat{\mathbf{e}}_i (\hat{\mathbf{e}}_j \cdot \hat{\mathbf{e}}_k) \hat{\mathbf{e}}_l = \delta_{jk} \hat{\mathbf{e}}_i \hat{\mathbf{e}}_l \quad (\text{B.1-4})$$

$$\hat{\mathbf{e}}_i \hat{\mathbf{e}}_j \times \hat{\mathbf{e}}_k = \hat{\mathbf{e}}_i (\hat{\mathbf{e}}_j \times \hat{\mathbf{e}}_k) = \epsilon_{jkl} \hat{\mathbf{e}}_i \hat{\mathbf{e}}_l \quad (\text{B.1-5})$$

$$\hat{\mathbf{e}}_i \times \hat{\mathbf{e}}_j \hat{\mathbf{e}}_k = (\hat{\mathbf{e}}_i \times \hat{\mathbf{e}}_j) \hat{\mathbf{e}}_k = \epsilon_{ijl} \hat{\mathbf{e}}_l \hat{\mathbf{e}}_k \quad (\text{B.1-6})$$

Appendix B-2 Representative Operations

$$\mathbf{I} \cdot \mathbf{u} = \mathbf{u} \cdot \mathbf{I} = \mathbf{u} \quad (\text{B.2-1})$$

$$\mathbf{uv} \cdot \mathbf{w} = \mathbf{u}(\mathbf{v} \cdot \mathbf{w}) \quad (\text{B.2-2})$$

$$\mathbf{w} \cdot \mathbf{uv} = (\mathbf{w} \cdot \mathbf{u})\mathbf{v} \quad (\text{B.2-3})$$

$$(\mathbf{uv} : \mathbf{wz}) = (\mathbf{uw} : \mathbf{vz}) = (\mathbf{w} \cdot \mathbf{v})(\mathbf{u} \cdot \mathbf{z}) \quad (\text{B.2-4})$$

$$\mathbf{T} : \mathbf{uv} = (\mathbf{T} \cdot \mathbf{u}) \cdot \mathbf{v} \quad (\text{B.2-5})$$

$$(\mathbf{uv} : \mathbf{T}) = (\mathbf{u} \cdot [\mathbf{v} \cdot \mathbf{T}]) \quad (\text{B.2-6})$$

Appendix B-3 Differential Operators

Cartesian Coordinates

$$\nabla = \hat{\mathbf{e}}_x \frac{\partial}{\partial x} + \hat{\mathbf{e}}_y \frac{\partial}{\partial y} + \hat{\mathbf{e}}_z \frac{\partial}{\partial z} \quad (\text{B.3-1})$$

Cylindrical Coordinates

$$\nabla = \hat{\mathbf{e}}_r \frac{\partial}{\partial r} + \hat{\mathbf{e}}_\theta \frac{1}{r} \frac{\partial}{\partial \theta} + \hat{\mathbf{e}}_z \frac{\partial}{\partial z} \quad (\text{B.3-2})$$

Spherical Coordinates

$$\nabla = \hat{\mathbf{e}}_r \frac{\partial}{\partial r} + \hat{\mathbf{e}}_\theta \frac{1}{r} \frac{\partial}{\partial \theta} + \hat{\mathbf{e}}_\phi \frac{1}{r \sin \theta} \frac{\partial}{\partial \phi} \quad (\text{B.3-3})$$

Appendix B-4 ∇ Operations

(i) Representative ∇ operations in Cartesian Coordinates (x, y, z)

$$\nabla \cdot \mathbf{u} = \frac{\partial u_x}{\partial x} + \frac{\partial u_y}{\partial y} + \frac{\partial u_z}{\partial z} \quad (\text{B.4-1})$$

$$\nabla^2 s = \frac{\partial^2 s}{\partial x^2} + \frac{\partial^2 s}{\partial y^2} + \frac{\partial^2 s}{\partial z^2} \quad (\text{B.4-2})$$

$$\begin{aligned} \mathbf{T} : \nabla \mathbf{u} = & T_{xx} \left(\frac{\partial u_x}{\partial x} \right) + T_{xy} \left(\frac{\partial u_x}{\partial y} \right) + T_{xz} \left(\frac{\partial u_x}{\partial z} \right) \\ & + T_{yx} \left(\frac{\partial u_y}{\partial x} \right) + T_{yy} \left(\frac{\partial u_y}{\partial y} \right) + T_{yz} \left(\frac{\partial u_y}{\partial z} \right) \\ & + T_{zx} \left(\frac{\partial u_z}{\partial x} \right) + T_{zy} \left(\frac{\partial u_z}{\partial y} \right) + T_{zz} \left(\frac{\partial u_z}{\partial z} \right) \end{aligned} \quad (\text{B.4-3})$$

(ii) Representative ∇ operations in Cylindrical Coordinates (r, θ, z)

$$\nabla \cdot \mathbf{u} = \frac{1}{r} \frac{\partial}{\partial r} (r u_r) + \frac{1}{r} \frac{\partial u_\theta}{\partial \theta} + \frac{\partial u_z}{\partial z} \quad (\text{B.4-4})$$

$$\nabla^2 s = \frac{1}{r} \frac{\partial}{\partial r} \left(r \frac{\partial s}{\partial r} \right) + \frac{1}{r^2} \frac{\partial^2 s}{\partial \theta^2} + \frac{\partial^2 s}{\partial z^2} \quad (\text{B.4-5})$$

$$\begin{aligned} (\mathbf{T} : \nabla \mathbf{u}) = & T_{rr} \left(\frac{\partial u_r}{\partial r} \right) + T_{r\theta} \left(\frac{1}{r} \frac{\partial u_r}{\partial \theta} - \frac{u_\theta}{r} \right) + T_{rz} \left(\frac{\partial u_r}{\partial z} \right) \\ & + T_{\theta r} \left(\frac{\partial u_\theta}{\partial r} \right) + T_{\theta\theta} \left(\frac{1}{r} \frac{\partial u_\theta}{\partial \theta} + \frac{u_r}{r} \right) + T_{\theta z} \left(\frac{\partial u_\theta}{\partial z} \right) \\ & + T_{zr} \left(\frac{\partial u_z}{\partial r} \right) + T_{z\theta} \left(\frac{1}{r} \frac{\partial u_z}{\partial \theta} \right) + T_{zz} \left(\frac{\partial u_z}{\partial z} \right) \end{aligned} \quad (\text{B.4-6})$$

(iii) Representative ∇ operations in Spherical Coordinates (r, θ, ϕ)

$$\nabla \cdot \mathbf{u} = \frac{1}{r^2} \frac{\partial}{\partial r} (r^2 u_r) + \frac{1}{r \sin \theta} \frac{\partial}{\partial \theta} (u_\theta \sin \theta) + \frac{1}{r \sin \theta} \frac{\partial u_\phi}{\partial \phi} \quad (\text{B.4-7})$$

$$\nabla^2 s = \frac{1}{r^2} \frac{\partial}{\partial r} \left(r^2 \frac{\partial s}{\partial r} \right) + \frac{1}{r^2 \sin \theta} \frac{\partial}{\partial \theta} \left(\sin \theta \frac{\partial s}{\partial \theta} \right) + \frac{1}{r^2 \sin^2 \theta} \frac{\partial^2 s}{\partial \phi^2} \quad (\text{B.4-8})$$

$$\begin{aligned} \mathbf{T} : \nabla \mathbf{u} = & T_{rr} \left(\frac{\partial u_r}{\partial r} \right) + T_{r\theta} \left(\frac{1}{r} \frac{\partial u_r}{\partial \theta} - \frac{u_\theta}{r} \right) + T_{r\phi} \left(\frac{1}{r \sin \theta} \frac{\partial u_r}{\partial \phi} - \frac{u_\phi}{r} \right) \\ & + T_{\theta r} \left(\frac{\partial u_\theta}{\partial r} \right) + T_{\theta\theta} \left(\frac{1}{r} \frac{\partial u_\theta}{\partial \theta} + \frac{u_r}{r} \right) + T_{\theta\phi} \left(\frac{1}{r \sin \theta} \frac{\partial u_\theta}{\partial \phi} - \frac{u_\phi}{r} \cot \theta \right) \\ & + T_{\phi r} \left(\frac{\partial u_\phi}{\partial r} \right) + T_{\phi\theta} \left(\frac{1}{r} \frac{\partial u_\phi}{\partial \theta} \right) \\ & + T_{\phi\phi} \left(\frac{1}{r \sin \theta} \frac{\partial u_\phi}{\partial \phi} + \frac{u_r}{r} + \frac{u_\theta}{r} \cot \theta \right) \end{aligned} \quad (\text{B.4-9})$$

Appendix B-5 Representative Differential Relations

$$\nabla \times \nabla s = 0 \quad (\text{B.5-1})$$

$$\nabla \cdot (\nabla \times \mathbf{u}) = 0 \quad (\text{B.5-2})$$

$$\nabla r s = r \nabla s + s \nabla r \quad (\text{B.5-3})$$

$$\nabla \cdot s \mathbf{u} = (\nabla s \cdot \mathbf{u}) + s (\nabla \cdot \mathbf{u}) \quad (\text{B.5-4})$$

$$\nabla \times s \mathbf{u} = \nabla s \times \mathbf{u} + s \nabla \times \mathbf{u} \quad (\text{B.5-5})$$

$$\begin{aligned} \nabla \cdot (\mathbf{u} \cdot \mathbf{w}) = & \mathbf{u} \cdot \nabla \mathbf{w} + \mathbf{w} \cdot \nabla \mathbf{u} \\ & + \mathbf{u} \times (\nabla \times \mathbf{w}) + \mathbf{w} \times (\nabla \times \mathbf{u}) \end{aligned} \quad (\text{B.5-6})$$

$$\nabla \cdot (\mathbf{u} \times \mathbf{w}) = \mathbf{w} \cdot (\nabla \times \mathbf{u}) - \mathbf{u} \cdot (\nabla \times \mathbf{w}) \quad (\text{B.5-7})$$

$$\begin{aligned} \nabla \times (\mathbf{u} \times \mathbf{w}) = & \mathbf{u} (\nabla \cdot \mathbf{w}) - \mathbf{w} (\nabla \cdot \mathbf{u}) \\ & + \mathbf{w} \cdot \nabla \mathbf{u} - \mathbf{u} \cdot \nabla \mathbf{w} \end{aligned} \quad (\text{B.5-8})$$

$$\nabla \times (\nabla \times \mathbf{u}) = \nabla (\nabla \cdot \mathbf{u}) - \nabla^2 \mathbf{u} \quad (\text{B.5-9})$$

$$\nabla \cdot \nabla \mathbf{u} = \nabla (\nabla \cdot \mathbf{u}) - \nabla \times (\nabla \times \mathbf{u}) \quad (\text{B.5-10})$$

$$\nabla \cdot (\nabla s \times \nabla r) = 0 \quad (\text{B.5-11})$$

$$\mathbf{u} \cdot \nabla \mathbf{u} = \frac{1}{2} \nabla (\mathbf{u} \cdot \mathbf{u}) - \mathbf{u} \times (\nabla \times \mathbf{u}) \quad (\text{B.5-12})$$

$$\nabla \cdot \mathbf{u} \mathbf{w} = \mathbf{u} \cdot \nabla \mathbf{w} + \mathbf{w} (\nabla \cdot \mathbf{u}) \quad (\text{B.5-13})$$

$$s \hat{\mathbf{e}} : \nabla \mathbf{u} = s (\nabla \cdot \mathbf{u}) \quad (\text{B.5-14})$$

$$\nabla \cdot s \hat{\mathbf{e}} = \nabla s \quad (\text{B.5-15})$$

$$\nabla \cdot s \mathbf{T} = \nabla s \cdot \mathbf{T} + s \nabla \cdot \mathbf{T} \quad (\text{B.5-16})$$

$$\nabla \cdot \mathbf{T}_a = -\frac{1}{2} \nabla \times \mathbf{A}, \quad \mathbf{A} = \text{vec } \mathbf{T} \quad (\text{B.5-17})$$

$$\text{where } \mathbf{T}_a = \frac{1}{2} (\mathbf{T} - \mathbf{T}^T)$$

Appendix B-6 Equation of Continuity

$$\frac{\partial \rho}{\partial t} + (\nabla \cdot \rho \mathbf{u}) = 0$$

Cartesian Coordinates (x, y, z)

$$\frac{\partial \rho}{\partial t} + \frac{\partial}{\partial x} (\rho u_x) + \frac{\partial}{\partial y} (\rho u_y) + \frac{\partial}{\partial z} (\rho u_z) = 0 \quad (\text{B.6-1})$$

Cylindrical Coordinates (r, θ, z)

$$\frac{\partial \rho}{\partial t} + \frac{1}{r} \frac{\partial}{\partial r} (\rho r u_r) + \frac{1}{r} \frac{\partial}{\partial \theta} (\rho u_\theta) + \frac{\partial}{\partial z} (\rho u_z) = 0 \quad (\text{B.6-2})$$

Spherical Coordinates (r, θ, ϕ)

$$\frac{\partial \rho}{\partial t} + \frac{1}{r^2} \frac{\partial}{\partial r} (\rho r^2 u_r) + \frac{1}{r \sin \theta} \frac{\partial}{\partial \theta} (\rho u_\theta \sin \theta) + \frac{1}{r \sin \theta} \frac{\partial}{\partial \phi} (\rho u_\phi) = 0 \quad (\text{B.6-3})$$

When the fluid is assumed to have constant mass density ρ , the equation simplifies to $\nabla \cdot \mathbf{u} = 0$

Appendix B-7 Equation of Motion in Terms of Stress Tensor τ

$$\rho \frac{D\mathbf{u}}{Dt} = -\nabla p + \nabla \cdot \boldsymbol{\tau} + \rho \mathbf{g}$$

(i) Cartesian Coordinates (x, y, z)

$$\begin{aligned} & \rho \left(\frac{\partial u_x}{\partial t} + u_x \frac{\partial u_x}{\partial x} + u_y \frac{\partial u_x}{\partial y} + u_z \frac{\partial u_x}{\partial z} \right) \\ &= -\frac{\partial p}{\partial x} + \left(\frac{\partial}{\partial x} \tau_{xx} + \frac{\partial}{\partial y} \tau_{yx} + \frac{\partial}{\partial z} \tau_{zx} \right) + \rho g_x \end{aligned} \quad (\text{B.7-1})$$

$$\begin{aligned} & \rho \left(\frac{\partial u_y}{\partial t} + u_x \frac{\partial u_y}{\partial x} + u_y \frac{\partial u_y}{\partial y} + u_z \frac{\partial u_y}{\partial z} \right) \\ &= -\frac{\partial p}{\partial y} + \left(\frac{\partial}{\partial x} \tau_{xy} + \frac{\partial}{\partial y} \tau_{yy} + \frac{\partial}{\partial z} \tau_{zy} \right) + \rho g_y \end{aligned} \quad (\text{B.7-2})$$

$$\begin{aligned} & \rho \left(\frac{\partial u_z}{\partial t} + u_x \frac{\partial u_z}{\partial x} + u_y \frac{\partial u_z}{\partial y} + u_z \frac{\partial u_z}{\partial z} \right) \\ &= -\frac{\partial p}{\partial z} + \left(\frac{\partial}{\partial x} \tau_{xz} + \frac{\partial}{\partial y} \tau_{yz} + \frac{\partial}{\partial z} \tau_{zz} \right) + \rho g_z \end{aligned} \quad (\text{B.7-3})$$

(ii) Cylindrical Coordinates (r, θ, z)

$$\begin{aligned} & \rho \left(\frac{\partial u_r}{\partial t} + u_r \frac{\partial u_r}{\partial r} + \frac{u_\theta}{r} \frac{\partial u_r}{\partial \theta} + u_z \frac{\partial u_r}{\partial z} - \frac{u_\theta^2}{r} \right) \\ &= -\frac{\partial p}{\partial r} + \left\{ \frac{1}{r} \frac{\partial}{\partial r} (r \tau_{rr}) + \frac{1}{r} \frac{\partial}{\partial \theta} \tau_{\theta r} + \frac{\partial}{\partial z} \tau_{zr} - \frac{\tau_{\theta\theta}}{r} \right\} + \rho g_r \end{aligned} \quad (\text{B.7-4})$$

$$\begin{aligned} & \rho \left(\frac{\partial u_\theta}{\partial t} + u_r \frac{\partial u_\theta}{\partial r} + \frac{u_\theta}{r} \frac{\partial u_\theta}{\partial \theta} + u_z \frac{\partial u_\theta}{\partial z} + \frac{u_r u_\theta}{r} \right) \\ &= -\frac{1}{r} \frac{\partial p}{\partial \theta} + \left\{ \frac{1}{r^2} \frac{\partial}{\partial r} (r^2 \tau_{r\theta}) + \frac{1}{r} \frac{\partial}{\partial \theta} \tau_{\theta\theta} + \frac{\partial}{\partial z} \tau_{z\theta} \right\} + \rho g_\theta \end{aligned} \quad (\text{B.7-5})$$

$$\begin{aligned}
& \rho \left(\frac{\partial u_z}{\partial t} + u_r \frac{\partial u_z}{\partial r} + \frac{u_\theta}{r} \frac{\partial u_z}{\partial \theta} + u_z \frac{\partial u_z}{\partial z} \right) \\
&= -\frac{\partial p}{\partial z} + \left\{ \frac{1}{r} \frac{\partial}{\partial r} (r \tau_{rz}) + \frac{1}{r} \frac{\partial}{\partial \theta} \tau_{\theta z} + \frac{\partial}{\partial z} \tau_{zz} \right\} + \rho g_z
\end{aligned} \tag{B.7-6}$$

(iii) Spherical Coordinates (r, θ, ϕ)

$$\begin{aligned}
& \rho \left(\frac{\partial u_r}{\partial t} + u_r \frac{\partial u_r}{\partial r} + \frac{u_\theta}{r} \frac{\partial u_r}{\partial \theta} + \frac{u_\phi}{r \sin \theta} \frac{\partial u_r}{\partial \phi} - \frac{u_\theta^2 + u_\phi^2}{r} \right) \\
&= -\frac{\partial p}{\partial r} + \left\{ \frac{1}{r^2} \frac{\partial}{\partial r} (r^2 \tau_{rr}) + \frac{1}{r \sin \theta} \frac{\partial}{\partial \theta} (\tau_{r\theta} \sin \theta) + \frac{1}{r \sin \theta} \frac{\partial}{\partial \phi} \tau_{r\phi} - \frac{\tau_{\theta\theta} + \tau_{\phi\phi}}{r} \right\} \\
&+ \rho g_r
\end{aligned} \tag{B.7-7}$$

$$\begin{aligned}
& \rho \left(\frac{\partial u_\theta}{\partial t} + u_r \frac{\partial u_\theta}{\partial r} + \frac{u_\theta}{r} \frac{\partial u_\theta}{\partial \theta} + \frac{u_\phi}{r \sin \theta} \frac{\partial u_\theta}{\partial \phi} + \frac{u_r u_\theta - u_\phi^2 \cot \theta}{r} \right) \\
&= -\frac{1}{r} \frac{\partial p}{\partial \theta} \\
&+ \left\{ \frac{1}{r^2} \frac{\partial}{\partial r} (r^2 \tau_{r\theta}) + \frac{1}{r \sin \theta} \frac{\partial}{\partial \theta} (\tau_{\theta\theta} \sin \theta) + \frac{1}{r \sin \theta} \frac{\partial}{\partial \phi} \tau_{\phi\theta} + \frac{\tau_{r\theta} - \tau_{\phi\phi} \cot \theta}{r} \right\} \\
&+ \rho g_\theta
\end{aligned} \tag{B.7-8}$$

$$\begin{aligned}
& \rho \left(\frac{\partial u_\phi}{\partial t} + u_r \frac{\partial u_\phi}{\partial r} + \frac{u_\theta}{r} \frac{\partial u_\phi}{\partial \theta} + \frac{u_\phi}{r \sin \theta} \frac{\partial u_\phi}{\partial \phi} + \frac{u_\phi u_r + u_\theta u_\phi \cot \theta}{r} \right) \\
&= -\frac{1}{r \sin \theta} \frac{\partial p}{\partial \phi} \\
&+ \left\{ \frac{1}{r^2} \frac{\partial}{\partial r} (r^2 \tau_{r\phi}) + \frac{1}{r} \frac{\partial}{\partial \theta} \tau_{\theta\phi} + \frac{1}{r \sin \theta} \frac{\partial}{\partial \phi} \tau_{\phi\phi} + \frac{(\tau_{r\phi} - \tau_{\phi r}) + 2\tau_{\theta\phi} \cot \theta}{r} \right\} \\
&+ \rho g_\phi
\end{aligned} \tag{B.7-9}$$

Appendix B-8 Equation of Motion for a Newtonian Fluid with Constant ρ and η_0

$$\rho \frac{D\mathbf{u}}{Dt} = -\nabla p + \eta_0 \nabla^2 \mathbf{u} + \rho \mathbf{g}$$

(i) Cartesian Coordinates (x, y, z)

$$\begin{aligned} & \rho \left(\frac{\partial u_x}{\partial t} + u_x \frac{\partial u_x}{\partial x} + u_y \frac{\partial u_x}{\partial y} + u_z \frac{\partial u_x}{\partial z} \right) \\ &= -\frac{\partial p}{\partial x} + \eta_0 \left(\frac{\partial^2 u_x}{\partial x^2} + \frac{\partial^2 u_x}{\partial y^2} + \frac{\partial^2 u_x}{\partial z^2} \right) + \rho g_x \end{aligned} \quad (\text{B.8-1})$$

$$\begin{aligned} & \rho \left(\frac{\partial u_y}{\partial t} + u_x \frac{\partial u_y}{\partial x} + u_y \frac{\partial u_y}{\partial y} + u_z \frac{\partial u_y}{\partial z} \right) \\ &= -\frac{\partial p}{\partial y} + \eta_0 \left(\frac{\partial^2 u_y}{\partial x^2} + \frac{\partial^2 u_y}{\partial y^2} + \frac{\partial^2 u_y}{\partial z^2} \right) + \rho g_y \end{aligned} \quad (\text{B.8-2})$$

$$\begin{aligned} & \rho \left(\frac{\partial u_z}{\partial t} + u_x \frac{\partial u_z}{\partial x} + u_y \frac{\partial u_z}{\partial y} + u_z \frac{\partial u_z}{\partial z} \right) \\ &= -\frac{\partial p}{\partial z} + \eta_0 \left(\frac{\partial^2 u_z}{\partial x^2} + \frac{\partial^2 u_z}{\partial y^2} + \frac{\partial^2 u_z}{\partial z^2} \right) + \rho g_z \end{aligned} \quad (\text{B.8-3})$$

(ii) Cylindrical Coordinates (r, θ, z)

$$\begin{aligned} & \rho \left(\frac{\partial u_r}{\partial t} + u_r \frac{\partial u_r}{\partial r} + \frac{u_\theta}{r} \frac{\partial u_r}{\partial \theta} + u_z \frac{\partial u_r}{\partial z} - \frac{u_\theta^2}{r} \right) \\ &= -\frac{\partial p}{\partial r} + \eta_0 \left\{ \frac{\partial}{\partial r} \left(\frac{1}{r} \frac{\partial}{\partial r} (ru_r) \right) + \frac{1}{r^2} \frac{\partial^2 u_r}{\partial \theta^2} + \frac{\partial^2 u_r}{\partial z^2} - \frac{2}{r^2} \frac{\partial u_\theta}{\partial \theta} \right\} + \rho g_r \end{aligned} \quad (\text{B.8-4})$$

$$\begin{aligned} & \rho \left(\frac{\partial u_\theta}{\partial t} + u_r \frac{\partial u_\theta}{\partial r} + \frac{u_\theta}{r} \frac{\partial u_\theta}{\partial \theta} + u_z \frac{\partial u_\theta}{\partial z} + \frac{u_r u_\theta}{r} \right) \\ &= -\frac{1}{r} \frac{\partial p}{\partial \theta} + \eta_0 \left\{ \frac{\partial}{\partial r} \left(\frac{1}{r} \frac{\partial}{\partial r} (ru_\theta) \right) + \frac{1}{r^2} \frac{\partial^2 u_\theta}{\partial \theta^2} + \frac{\partial^2 u_\theta}{\partial z^2} + \frac{2}{r^2} \frac{\partial u_r}{\partial \theta} \right\} + \rho g_\theta \end{aligned} \quad (\text{B.8-5})$$

$$\begin{aligned}
& \rho \left(\frac{\partial u_z}{\partial t} + u_r \frac{\partial u_z}{\partial r} + \frac{u_\theta}{r} \frac{\partial u_z}{\partial \theta} + u_z \frac{\partial u_z}{\partial z} \right) \\
&= -\frac{\partial p}{\partial z} + \eta_0 \left\{ \frac{1}{r} \frac{\partial}{\partial r} \left(r \frac{\partial u_z}{\partial r} \right) + \frac{1}{r^2} \frac{\partial^2 u_z}{\partial \theta^2} + \frac{\partial^2 u_z}{\partial z^2} \right\} + \rho g_z
\end{aligned} \tag{B.8-6}$$

(iii) Spherical Coordinates (r, θ, ϕ)

$$\begin{aligned}
& \rho \left(\frac{\partial u_r}{\partial t} + u_r \frac{\partial u_r}{\partial r} + \frac{u_\theta}{r} \frac{\partial u_r}{\partial \theta} + \frac{u_\phi}{r \sin \theta} \frac{\partial u_r}{\partial \phi} - \frac{u_\theta^2 + u_\phi^2}{r} \right) = -\frac{\partial p}{\partial r} \\
&+ \eta_0 \left\{ \frac{1}{r^2} \frac{\partial^2}{\partial r^2} (r^2 u_r) + \frac{1}{r^2 \sin \theta} \frac{\partial}{\partial \theta} \left(\sin \theta \frac{\partial u_r}{\partial \theta} \right) + \frac{1}{r^2 \sin^2 \theta} \frac{\partial^2 u_r}{\partial \phi^2} \right\} \\
&+ \rho g_r
\end{aligned} \tag{B.8-7}$$

$$\begin{aligned}
& \rho \left(\frac{\partial u_\theta}{\partial t} + u_r \frac{\partial u_\theta}{\partial r} + \frac{u_\theta}{r} \frac{\partial u_\theta}{\partial \theta} + \frac{u_\phi}{r \sin \theta} \frac{\partial u_\theta}{\partial \phi} + \frac{u_r u_\theta - u_\phi^2 \cot \theta}{r} \right) \\
&= -\frac{1}{r} \frac{\partial p}{\partial \theta} + \eta_0 \left\{ \frac{1}{r^2} \frac{\partial}{\partial r} \left(r^2 \frac{\partial u_\theta}{\partial r} \right) + \frac{1}{r^2} \frac{\partial}{\partial \theta} \left(\frac{1}{r \sin \theta} \frac{\partial}{\partial \theta} (u_\theta \sin \theta) \right) \right. \\
&\quad \left. + \frac{1}{r^2 \sin^2 \theta} \frac{\partial^2 u_\theta}{\partial \phi^2} + \frac{2}{r^2} \frac{\partial u_r}{\partial \theta} - \frac{2 \cot \theta}{r^2 \sin \theta} \frac{\partial u_\phi}{\partial \phi} \right\} + \rho g_\theta
\end{aligned} \tag{B.8-8}$$

$$\begin{aligned}
& \rho \left(\frac{\partial u_\phi}{\partial t} + u_r \frac{\partial u_\phi}{\partial r} + \frac{u_\theta}{r} \frac{\partial u_\phi}{\partial \theta} + \frac{u_\phi}{r \sin \theta} \frac{\partial u_\phi}{\partial \phi} + \frac{u_\phi u_r + u_\theta u_\phi \cot \theta}{r} \right) \\
&= -\frac{1}{r \sin \theta} \frac{\partial p}{\partial \phi} + \eta_0 \left\{ \frac{1}{r^2} \frac{\partial}{\partial r} \left(r^2 \frac{\partial u_\phi}{\partial r} \right) + \frac{1}{r^2} \frac{\partial}{\partial \theta} \left(\frac{1}{\sin \theta} \frac{\partial}{\partial \theta} (u_\phi \sin \theta) \right) \right. \\
&\quad \left. + \frac{1}{r^2 \sin^2 \theta} \frac{\partial^2 u_\phi}{\partial \phi^2} + \frac{2}{r^2 \sin \theta} \frac{\partial u_r}{\partial \phi} + \frac{2 \cot \theta}{r^2 \sin \theta} \frac{\partial u_\theta}{\partial \phi} \right\} + \rho g_\phi
\end{aligned} \tag{B.8-9}$$

Appendix B-9 Equation of Energy in Terms of q ($b=0$)

$$\rho c_p \frac{DT}{Dt} = -\nabla \cdot \mathbf{q} + \left(\frac{\partial \ln \frac{1}{\rho}}{\partial \ln T} \right)_p \frac{Dp}{Dt} + \boldsymbol{\tau} : \nabla \mathbf{u}$$

(i) Cartesian Coordinates (x, y, z)

$$\begin{aligned} & \rho c_p \left(\frac{\partial T}{\partial t} + u_x \frac{\partial T}{\partial x} + u_y \frac{\partial T}{\partial y} + u_z \frac{\partial T}{\partial z} \right) \\ &= - \left(\frac{\partial q_x}{\partial x} + \frac{\partial q_y}{\partial y} + \frac{\partial q_z}{\partial z} \right) + \left(\frac{\partial \ln \frac{1}{\rho}}{\partial \ln T} \right)_p \frac{Dp}{Dt} + \boldsymbol{\tau} : \nabla \mathbf{u} \end{aligned} \quad (\text{B.9-1})$$

(ii) Cylindrical Coordinates (r, θ, z)

$$\begin{aligned} & \rho c_p \left(\frac{\partial T}{\partial t} + u_r \frac{\partial T}{\partial r} + \frac{u_\theta}{r} \frac{\partial T}{\partial \theta} + u_z \frac{\partial T}{\partial z} \right) \\ &= - \left(\frac{1}{r} \frac{\partial}{\partial r} (r q_r) + \frac{1}{r} \frac{\partial q_\theta}{\partial \theta} + \frac{\partial q_z}{\partial z} \right) + \left(\frac{\partial \ln \frac{1}{\rho}}{\partial \ln T} \right)_p \frac{Dp}{Dt} + \boldsymbol{\tau} : \nabla \mathbf{u} \end{aligned} \quad (\text{B.9-2})$$

(iii) Spherical Coordinates (r, θ, ϕ)

$$\begin{aligned} & \rho c_p \left(\frac{\partial T}{\partial t} + u_r \frac{\partial T}{\partial r} + \frac{u_\theta}{r} \frac{\partial T}{\partial \theta} + \frac{u_\phi}{r \sin \theta} \frac{\partial T}{\partial \phi} \right) \\ &= - \left(\frac{1}{r^2} \frac{\partial}{\partial r} (r^2 q_r) + \frac{1}{r \sin \theta} \frac{\partial}{\partial \theta} (q_\theta \sin \theta) + \frac{1}{r \sin \theta} \frac{\partial q_\phi}{\partial \phi} \right) \\ & \quad + \left(\frac{\partial \ln \frac{1}{\rho}}{\partial \ln T} \right)_p \frac{Dp}{Dt} + \boldsymbol{\tau} : \nabla \mathbf{u} \end{aligned} \quad (\text{B.9-3})$$

Appendix C

Appendix C-1 Buckingham π -Theorem

The Buckingham π -theorem is used in the study of dimensional analysis and similitude, which is based on the notion of dimensional homogeneity. The theorem is examined in a given fluid system where variables of q_1, q_2, \dots, q_n are chosen so that they are pertinent to a physical phenomena. Then, we will express the phenomena by a functional form as

$$f(q_1, q_2, q_3, \dots, q_n) = 0 \quad (\text{C.1-1})$$

where n represents the total number of variables. If there are m basic dimensions involved in the variables of $q_1 \sim q_n$, the Buckingham π -theorem states that the same physical phenomena can be correlated by $(n-m)$ nondimensional numbers (independent from nondimensional groups), called π -parameters, which are given as a functional form

$$g(\pi_1, \pi_2, \pi_3, \dots, \pi_{n-m}) = 0 \quad (\text{C.1-2})$$

When a given fluid system contains a dependent variable, say q_1 , the physical phenomenon can be expressed similarly in the form

$$q_1 = h(q_2, q_3, \dots, q_n) \quad (\text{C.1-3})$$

and

$$\pi_1 = s(\pi_2, \pi_3, \dots, \pi_{n-m}) \quad (\text{C.1-4})$$

where π_1 includes the dependent variable and the remaining π -parameters include the rest of independent variables. The procedure adopted for determining the nondimensional π -parameters are as follows; Step (1) In having written the functional form of either Eq. (C.1-1) or Eq. (C.1-3), select m repeating the variables from n -independent variables in Eq. (C.1-1) or $(n-1)$ -independent variables in Eq. (C.1-3). The repeating variables must include all of the basic dimensions, but they must not form π -parameters by themselves. In order to obtain the most significant π -parameters, it is desirable to choose one variable with geometric characteristics, second variable with flow characteristics and another variable with fluid properties, such as l, U and ρ respectively, with reference to Table C.1. For example, writing Eq. (C.1-1)

$$f(q_1, q_2, q_3, \dots, q_n) = 0 \quad (\text{C.1-5})$$

we may choose m repeating variables, say if $m = 3$, select three variables to meet the criteria, say q_2, q_4 and q_5 among n variables.

Step (2) Write π -parameters of $\pi_1, \pi_2, \dots, \pi_{n-m}$ in the power form for the repeating variables, for example with q_2, q_4 and q_5 in Step (1) with each of the remaining variables as

$$\pi_1 = q_2^a q_4^b q_5^c q_1$$

$$\pi_2 = q_2^a q_4^b q_5^c q_3$$

$$\pi_3 = q_2^a q_4^b q_5^c q_6$$

$$\vdots$$

$$\pi_{n-m} = q_2^a q_4^b q_5^c q_n$$

Step (3) Apply the dimensional analysis to obtain the power constants for each π -parameter subjecting that the π -parameters are all dimensionless.

Step (4) Write the functional form using π -parameters to describe the physical phenomenon of the fluid system.

Step (5) In correlating experimental results, one dependent π -parameter (say π_1) can be expressed by a function likewise

$$\pi_1 = s(c_2 \pi_2^{\alpha_2}, c_3 \pi_3^{\alpha_3}, \dots, c_{n-m} \pi_{n-m}^{\alpha_{n-m}}) \quad (\text{C.1-6})$$

where c_2, c_3, \dots, c_{n-m} and $\alpha_2, \alpha_3, \dots, \alpha_{n-m}$ are constants determined from the results of experiments. Note that if some dimensionless variable, such as the length ratio l_1/l_2 , the roughness $\varepsilon \dots$ etc, are contained in the primary variables (q_1, q_2, \dots, q_n) , they are themselves treated as π -parameters and to be excluded from the procedure by simply adding as π -parameters in the resultant functional form, for example

$$f(q_1, q_2, \dots, q_n, \theta, l_1/l_2) = 0 \quad (\text{C.1-7})$$

$$s(\pi_1 \dots \pi_{n-m}, \varepsilon, l_1/l_2) = 0 \quad (\text{C.1-8})$$

Table C.1 Dimensions of quantities frequently used in fluid flow problems

Quantity	Symbol	Dimensions
Length	l	L
Time	t	T
Mass	m	M
Area	A	L^2
Volume	V	L^3
Force	F	ML/T^2
Velocity	U	L/T
Acceleration	a	L/T^2
Angular frequency	ω	$1/T$
Gravity	g	L/T^2
Flow rate	Q	L^3/T
Mass flux	\dot{m}	M/T
Pressure	p	M/LT^2
Stress	\mathbf{T}	M/LT^2
Work	W	ML^2/T^2
Power, heat flux	P, q	ML^2/T^3
Density	ρ	M/L^3
Specific weight	γ	M/L^2T^2
Viscosity	η_0	M/LT
Kinematic viscosity	ν	L^2/T
Surface tension	σ	M/T^2
Bulk modulus	K	M/LT^2

(*)Basic Dimensions; L (length), M (Mass), and T (Time), i.e. $m = 3$

Appendix C-2 Example of π -Analysis

In order to illustrate π -theorem, suppose that force F acting in a fluid system is supposed to be dependent on the velocity U , density ρ , gravity g , viscosity η_0 , surface tension σ , angular frequency (velocity) ω , bulk modulus K , surface roughness ε , characteristic length l and another representative linear dimension l_1 . For this fluid system a physical phenomena would be described with nondimensional numbers by applying π -theorem as demonstrated below.

(i) Functional form

$$f\left(F, l, U, \rho, \eta_0, g, \sigma, K, \omega, \frac{l_1}{l}, \varepsilon\right) = 0 \quad (\text{C.2-1})$$

We have eleven variables, i.e. $n = 11$, which contain three basic dimensions L , M and T , i.e. $m = 3$. According to π -theorem, we can find eight ($n - m = 11 - 3 = 8$) π -parameters, so that we have

$$g(\pi_1, \pi_2, \pi_3, \pi_4, \pi_5, \pi_6, \pi_7, \pi_8) = 0 \quad (\text{C.2-2})$$

(ii) Choice of repeating variables

Choose three repeating variables such as l, U and ρ , and set $\pi_7 = l_1/l$ and $\pi_8 = \varepsilon$, since they are two already dimensionless parameters. Thus we will find π_1 to π_6 , i.e. six π -parameters.

(iii) Conduct dimensional analysis

$$\pi_1 = l^a U^b \rho^c F \quad (\text{C.2-3})$$

$$\begin{aligned} [M^0 L^0 T^0] \pi_1 &= L^a (LT^{-1})^b (ML^{-3})^c MLT^{-2} \\ 0 &= c + 1, 0 = a + b - 3c + 1, 0 = -b - 2 \\ \therefore a &= -2, b = -2, c = -1 \end{aligned} \quad (\text{C.2-4})$$

$$\pi_1 = F / (\rho U^2 l^2) \quad (\text{C.2-5})$$

$$\begin{aligned} \pi_2 &= l^a U^b \rho^c \eta_0 \\ [M^0 L^0 T^0] \pi_2 &= L^a (LT^{-1})^b (ML^{-3})^c ML^{-1}T^{-1} \\ 0 &= c + 1, 0 = a + b - 3c - 1, 0 = -b - 1 \\ \therefore a &= -1, b = -1, c = -1 \end{aligned} \quad (\text{C.2-6})$$

$$\pi_2 = \frac{\eta_0 / \rho}{lU} \quad (\text{C.2-7})$$

Similarly for $\pi_3 \sim \pi_6$, we can obtain

$$\pi_3 = \frac{lg}{U^2}, \pi_4 = \frac{\sigma}{U^2 lg}, \pi_5 = \frac{K}{U^2 \rho} \text{ and } \pi_6 = \frac{l\omega}{U} \quad (\text{C.2-8})$$

(iv) Set functional form

Each of the π - parameters for $\pi_2 \sim \pi_6$ in this expression is a common nondimensional number, which is derived from similitude (Section 6.2), so that we have

$$f\left(\frac{F}{\rho U^2 l^2}, \frac{1}{Re}, \frac{1}{Fr^2}, \frac{1}{M^2}, St, \frac{l_1}{l}, \varepsilon\right) = 0 \quad (C.2-9)$$

and for the dependent variable F , the functional form is given where

$$c_f = \frac{F}{1/2 \rho U^2 l^2} = f\left(Re, Fr, M, St, \frac{l_1}{l}, \varepsilon\right) \quad (C.2-10)$$

Appendix D

Appendix D-1 Invariant of Second Order Tensor

The invariants of a tensor are scalar quantities, which remain unchanged for the coordinate transformation of rotation. There are three principal invariants for second order tensors.

Consider a second order tensor \mathbf{T} , whose components are a_{ij} for unit dyads $\hat{e}_i \hat{e}_j$, and b_{ij} for unit dyads $\hat{e}'_i \hat{e}'_j$ after the coordinate transformation. When λ is a scalar and is an eigenvalue of \mathbf{T} , we have the following relationship

$$\psi_B(\lambda) = |\lambda \delta_{ij} - a_{ij}| = |\lambda \delta_{ij} - b_{ij}| = \psi_A(\lambda) \quad (D.1-1)$$

where ψ_A and ψ_B are the characteristic equations of a_{ij} and b_{ij} . Eq. (D.1-1) shows that the characteristic equations are equal to both frames ($\hat{e}_i \hat{e}_j$ and $\hat{e}'_i \hat{e}'_j$), so that they are unaffected by the coordinate transformation. They are also given when

$$\psi(\lambda) = \psi_A(\lambda) = \psi_B(\lambda) = \lambda^3 - I_1 \lambda^2 + I_2 \lambda - I_3 \quad (D.1-2)$$

where I_1 , I_2 and I_3 are principal invariants, which are also unaffected by the coordinate transformation. They are respectively defined as

$$I_1 = a_{11} + a_{22} + a_{33} \quad (D.1-3)$$

$$I_2 = \begin{vmatrix} a_{22} & a_{23} \\ a_{32} & a_{33} \end{vmatrix} + \begin{vmatrix} a_{33} & a_{31} \\ a_{13} & a_{11} \end{vmatrix} + \begin{vmatrix} a_{11} & a_{12} \\ a_{21} & a_{22} \end{vmatrix} \quad (\text{D.1-4})$$

$$I_3 = \begin{vmatrix} a_{11} & a_{12} & a_{13} \\ a_{21} & a_{22} & a_{23} \\ a_{31} & a_{32} & a_{33} \end{vmatrix} \quad (\text{D.1-5})$$

and alternating, I_1 , I_2 and I_3 are written where

$$I_1 = t_r A, \quad I_2 = \frac{1}{2} (t_r^2 A - t_r A^2) \text{ and } I_3 = \det A \quad (\text{D.1-6})$$

where $t_r^2 A = (t_r A)^2$ and $t_r A^2 = t_r (AA)$. Another set of invariants is defined by the so-called moment, as follows

$$\bar{I}_k = t_r A^k \quad (\text{D.1-7})$$

With the moment, given by Eq. (D.1-7), the invariants are representatively given for $k=1,2$ and 3 as

$$\bar{I}_1 = t_r A = I_1 \quad (\text{D.1-8})$$

$$\bar{I}_2 = t_r A^2 = I_1^2 - 2I_2 \quad (\text{D.1-9})$$

$$\bar{I}_3 = t_r A^3 = \frac{1}{2} (6I_3 + 2I_1^3 - 6I_1 I_2) \quad (\text{D.1-10})$$

It is useful to note that there are relationships between two principal invariants I_k and the moments \bar{I}_k as follows

$$I_1 = \bar{I}_1 \quad (\text{D.1-11})$$

$$I_2 = \frac{1}{2} (\bar{I}_1^2 - \bar{I}_2) \quad (\text{D.1-12})$$

$$I_3 = \frac{1}{6} \bar{I}_1^3 - \frac{1}{2} \bar{I}_1 \bar{I}_2 + \frac{1}{3} \bar{I}_3 \quad (\text{D.1-13})$$

For a symmetric tensor \mathbf{T} , eigenvalues of \mathbf{T} are real and \mathbf{T} is diagonalizable. For example, if eigenvalues λ_1, λ_2 and λ_3 are of a symmetric tensor \mathbf{T} , \mathbf{T} can be transformed to a diagonal matrix

$$\mathbf{T}' = \begin{vmatrix} \lambda_1 & 0 & 0 \\ 0 & \lambda_2 & 0 \\ 0 & 0 & \lambda_3 \end{vmatrix} \quad (\text{D.1-14})$$

Then we have invariants

$$I_1 = \lambda_1 + \lambda_2 + \lambda_3 \quad (\text{D.1-15})$$

$$I_2 = \lambda_1\lambda_2 + \lambda_2\lambda_3 + \lambda_3\lambda_1 \quad (\text{D.1-16})$$

and

$$I_3 = \lambda_1\lambda_2\lambda_3 \quad (\text{D.1-17})$$

Index

A

Acceleration
 convective, 8
 Corioli's, 18
 local, 11, 12
 reference frame, 84–87
 Accelerometer, 111, 112, 524
 Acoustic velocity, 225
 Action angle, 98, 100
 Actuator-disk theory, 142
 Adiabatic process, 228, 233, 241, 258–264
 Adverse pressure gradient, 350–352
 Airfoils, aerofoils, 154, 188–194
 Alternating unit tensor (polymeric alternator), 14, 49
 Ampere's (circulation) law, 533
 Analytic function, 118, 159
 Angular
 momentum, 47–52, 127, 128, 183–188, 507, 509–513
 momentum conservation, 47–52, 128, 507, 512, 513
 velocity, 16, 18, 74
 Anisotropy of particles, 502
 Anti-symmetric, *see* Skew-symmetric tensor (anti-symmetric tensor)
 Apparent
 viscosity, 400, 502, 516–519
 wall shear rate, 443
 Archimedes' principle, 82, 524
 Atmospheric pressure, 76, 93–96, 110
 Attack angle, 155
 Axial flow pumps, 183, 189–194, 199
 Axisymmetric flows, 312, 323, 328, 330, 410–413

B

Barotropic, 152–154, 158
 Base liquid
 See also Carrier liquid
 Bearing
 journal, 310
 slipper-pad, 306–310
 thrust, 309
 with magnetostatic lubricant, 524
 Bell-mouth, 144
 Benard
 cell, 527, 531
 convection, 297, 527–532
 Bend, 140–149
 Bernoulli equation, 122–125, 521, 522
 ferrohydrodynamic, 521
 generalized, 521, 522
 surface, 122, 123
 Bessel's
 differential equation, 332
 functions, 332, 333
 Biaxial stretching flow, 422
 Bingham plastic (fluid), 403
 Blasius
 equation, 345, 346
 first theorem, 159
 second theorem, 159, 179
 solution, 345
 Blunt body, 254, 255
 Body
 couple, 49, 51, 52
 force, 26, 45, 74, 525
 Boltzmann
 constant, 282, 500
 superposition principle, 425
 Borda's mouth piece, 271, 272

Boundary conditions

- dynamic, 534
- free surface, 85–87
- inviscid flow, 115–129
- for a magnetic field, 532–535
- no-slip, 177, 336, 341, 472, 474
- for temperature, 292, 353–355
- for velocity, 301, 302, 324, 331, 335, 337, 375, 411

Boundary layer equations, 343, 344

Boundary layer flow, 177, 178, 340–364

Boundary layer separation, 350–353

Boundary layers on a flat plate, 177, 178, 340–350, 475–477

Boundary layer thickness, 341, 346, 360, 476

Bounding vortex, 155

Boussinesq approximation, 295–297

Brinkman number, 294

Broad-crested weir, 137–140, 175, 176

Brownian

- motion, 498, 511
- relaxation time, 502, 504–506, 515
- rotational diffusion, 501

Buckingham theorem, 196

Buffer layer, 372

Bulk modulus, 228

Bulk viscosity coefficient, 280

Buoyant force, 80, 82, 100–105, 312, 524

C

Camber line, 154

Capillary viscometer, 437

Carrier liquid, 498, 502

Cartesian coordinates, 11, 23, 82

Cauchy

- equation of motion, 46, 50, 52, 73, 407, 410, 413, 431, 438, 473, 507
- strain tensor, 23, 464
- theorem (stress), 26–30, 37, 38

Cauchy-Riemann conditions, 118

Cavitation

- critical, 206, 207, 217, 219
- number, 206
- in turbo-machines, 203–207

Cayley-Hamilton theorem, 464

Center

- of buoyancy, 101
- of pressure, 79, 96–100

Centrifugal force, 85

Centrifugal pump, 86, 211–213, 218, 219

Centripetal acceleration, 18, 74

Centroid, 78–80, 98

Characteristic equation, 37

Characteristic length, 290, 291, 350, 369, 488

Characteristic scale of velocity, 368, 488

Choked flow, 238–241, 262, 266

Chord

- length, 155
- line, 155

Circulation, 119, 155

Circumferential velocity, 129

Coefficients

- contraction, 134
- correction, 132
- pyromagnetic, 501
- of surface tension, 87, 534–537
- of thermal expansion, 60, 292, 529

Colloidal suspension, 497

Complex

- modulus, 424–427, 440
- potential, 118
- velocity, 118
- viscosity, 426

Compressibility, 131, 135, 225

Compressibility factor, 132, 255

Compressible flow, 131, 225

Compression, 249

Concentric cylinders (spheres), 299–306, 412, 414

Conduction (Heat), 61, 527

Cone and plate rheometer, 428–430

Configuration parameter (of turbulent flow), 374

Conformal mapping, 119, 160

Conservation

- of (linear) momentum, 44–47, 63, 64, 507
- of angular momentum, 47–52, 507, 510–513
- of energy, 52–56, 508
- of mass, 43, 44, 62, 63, 507

Constant of anisotropy, 502

-
- Constitutive equations, 23, 280, 405, 408, 508, 509
 - Contact angle, 104
 - Continuity equation, 44, 62, 64, 122, 133, 234, 421, 507
 - Continuum mechanics, 5, 6, 43, 507
 - Contraction coefficient, 134, 144
 - Contravariant, 21
 - Control volume, 26, 35, 36, 126, 129, 183, 189, 196
 - Convected generalized Maxwell model, 463
 - Convective
 - acceleration (term), 8
 - derivative, 19–22, 478
 - Converging
 - channel, 436, 437
 - nozzle, 238, 241
 - Converging-diverging nozzle, 273–274
 - Corioli's acceleration (force), 18, 125
 - Corotational
 - derivative, 21, 482
 - Jeffrey's equation, 460
 - Correction factor (constant), 134, 143, 144
 - Correlation length, 6
 - Correlations relating efficiency to size, 202, 203
 - Couette flow, 301, 302, 428, 437–439
 - Couple stress tensor, 51, 507, 512
 - Covariant, 21
 - Cox-Merz rule, 427
 - Creep, 452
 - Creeping flow, 323
 - Critical
 - area, 240
 - cavitation number, 206
 - pressure, 239–241
 - Rayleigh number, 297, 298, 531
 - Reynolds number, 366, 390
 - state, 234, 236
 - strain rate, 487
 - velocity, 249
 - volume fraction, 503
 - Curtiss-Bird constitutive equation, 465
 - Curvature, 87, 344
 - Curve
 - flow, 399, 400
 - of magnetization approximation, 501, 502
 - surface, 344, 350
 - Cylindrical gap flow, 302, 303, 415, 416, 437–439
- D**
- D'Alembert
 - paradox, 160
 - principle, 85
 - Dampers, 310, 524
 - Damping factor (of turbulent flow), 374
 - Darcy friction factor, 302, 326, 412
 - Darcy-Weisbach equation, 302, 326
 - Deborah number, 489
 - Debye relaxation equation, 514
 - Deflection angle, 168, 171, 252, 253
 - Deflectors
 - moving, 171, 172
 - stationary, 170
 - Delta function (Dirac), 453
 - Density, 5, 6
 - Derivative
 - substantial, 7, 8
 - time (material derivative), 25
 - Developed flow, 320–322
 - Deviatoric stress (tensor), 30, 47, 419
 - Diffuser efficiency, 144, 145
 - Diffusive transport, 51
 - Diffusivity (diffusion) coefficient, 285, 537, 538
 - Dilatant fluid, 403
 - Dilatation, 25
 - Dilatational viscosity, 281
 - Dimensional analysis
 - homogeneity, 294
 - turbomachinery, 195–203
 - Dipole moment, 504
 - Discharge, 137, 196, 215
 - Discharge coefficient, 135, 139, 140
 - Displacement
 - function, 480, 481
 - gradient tensor, 10, 22–23
 - thickness, 348–350

Dissipation
 energy, 369, 439, 440
 function, 293
 scale, 369
Divergence theorem, *see* Gauss's
 divergence (integral) theorem
Diverging nozzle, 273, 274
Doublet, 119
Draft tube, 204, 214
Drag
 on an airfoil, 155, 178
 on a cylinder, 317
 on a sphere, 312–318
Drag-lift ratio, 309
Dyad, Dyadic, 11, 28
Dynamic
 head loss, 205
 pressure, 130
 similarity, 288–290
 viscosity, 425

E

Eckert number, 293
Eddington symbol (notation), 15
Eddy
 diffusivity, 378, 390
 viscosity, 366, 369, 378, 382
Effective Prandtl number, 378
Effects
 magnetocaloric, 497, 514
 magnetoviscous, 498, 503
Efficiency
 hydraulic, 194, 195, 210, 219
 mechanical, 195, 209, 219
 optimum, 201
 overall (total), 194, 219
 pump, 194–203
 volumetric, 195, 209
Einstein's formula, 503, 537
Elongational
 flow, 11, 421–424, 428
 rheometer, 433–437
Energy
 cascade, 369
 conservation, 52–56
 equation, 56, 264

 free, 464
 internal, 57
Ensemble average, 365
Enthalpy, 59, 60, 233, 241–246, 256, 354
Enthalpy thickness, 355
Entrance flow
 laminar flow, 320–322
 length, 320–322
 turbulent flow, 320–322
Entropy, 58, 241–246, 265, 266
Equations
 of angular momentum, 47–52
 Bernoulli, 124, 138, 142, 146
 of continuity, 44
 of energy, 52–56
 heat transfer, 61
 of linear momentum, 44–47
 of motion, 45
 Rayleigh-Plesset, 149–152
 Rosensweig, 516–517
 of state, 56, 57, 227, 260
Equilibrium, 57, 73, 84–87, 227, 297, 369,
 497, 498, 504, 525
Equivalent thickness, 350
Ergodic hypothesis, 365
Euler
 differential equation, 314
 equation, 115, 124, 283
 head, 185
 number, 289, 290
 relation, 13, 31, 32
 turbine and pump, 129, 183
Eulerian (time) derivative, 8
Eulerian description (specification), 7, 26
Expansion waves, 237, 238
Extensional
 flow, 11, 12, 422, 423, 433
 strain, 11
 viscosity, 423
 See also elongational
External flow, 340

F

Fanning friction factor, 326
Fanno line (curve), 241–243, 258–264
Ferrohydrodynamic equations, 507–516

Fiber-spinning, 434
 Finger tensor, 40, 457, 458, 484
 First law of thermodynamics, 52, 53, 57
 First normal
 stress coefficient, 419, 427, 465–472
 stress difference, 419, 428–430, 484
 Flow
 coefficient, 135
 curve, 400–403, 444, 445
 instability, 305
 measurement, 129–140
 meters, 135
 separation, 155
 work, 265
 Flows
 of films, 310, 311
 of jet, 168, 176, 177, 208
 Fluid-fluid interface, 87–90
 Fluid particle, 7, 23, 26
 Fluid static, 73–77
 Flux, 36, 44, 46, 52, 55
 Forced vortex, 85
 Fourier's law, 61
 Francis turbine, 181, 185, 186
 Free surface, 85–87
 Friction
 factor (coefficient), 211, 259, 302,
 326–328, 399, 412
 velocity, 372, 389
 Froude number, 289, 290
 Fully developed flow, 321–330

G

Gas constant, 93, 227
 Gauge pressure, 76, 99
 Gauss's divergence (integral) theorem, 13,
 26, 45, 49, 55, 68, 122, 523, 532
 Generalized Bernoulli equation,
 521, 522
 Generalized Newtonian fluid, 400,
 406–408
 Generalized Reynolds number, 408
 Geometric similarity, 287, 288
 Giesekus model (equation), 461, 462,
 471, 472
 Glassy modulus, 427
 Goddard-Miller equation, 460

Grashof number (gravitational), 293
 Gravitational
 acceleration, 47, 283
 potential, 68, 92, 121, 295, 521
 Guide vanes, 189–191

H

Hagen-Poiseuille flow, 321, 323, 324,
 330–334
 Harmonic function, 116, 118
 Head
 coefficient, 197
 loss, 186, 205
 manometric, 185
 piezometric, 75
 potential, 124
 pressure, 124
 pump, 185–187
 theoretical, 185, 186, 218
 total, 124
 turbine, 189–195
 velocity, 124
 Heat
 conduction, 61, 297, 337–339
 flux vector, 55
 generated, 55
 input, 53
 transfer, 55, 61, 264–267, 295, 296,
 353, 355, 359–361,
 381–385, 388
 transfer coefficient, 296, 384
 Hele-Shaw flow, 311, 312
 Hencky strain, 435, 481
 Hook's law, 405
 Hydraulic
 efficiency, 194, 195
 radius, 320
 Hydrostatic
 paradox, 92, 93
 pressure, 73
 stress, 29, 73
 Hydrostatics, *see* Fluid static

I

Ideal gas law, 225, 227
 Immiscible fluid, 87, 90

Impeller

- radial flow, 181, 182
- of turbo-pump, 181, 182

Impulse

- function, 244
- turbine, 172, 209

Inclined tube manometer, 75, 76**Incompressible (fluid) flow, 30, 44, 280–283****Inertia damper, 524****Inertial reference frame, 16–19, 73, 74, 85****Initial conditions, 331, 354, 451, 473–475****Instability**

- dynamics of development, 303
- of thermal equilibrium, 297
- thermomagnetic, 527–532, 535

Interface, 73, 87–90**Internal**

- angular momentum, 51
- energy, 53, 57, 265, 508
- flow, 225, 230, 243, 527

Intrinsic

- angular momentum, 497, 510
- rotation, 510

Invariant of tensors, 37, 38, 406**Inviscid**

- core length, 319, 320
- flow, 115–122, 343, 344

Irrotational flows, 116**Isentropic**

- flow, 228, 255
- process, 237

Isotropic fluid (flow), 37, 44**J****Jacobian, 24, 25, 31, 32****Jaumann (time) derivative, 21, 459****Jeffreys**

- element, 449, 452, 453

Joukowski

- airfoil, 160–168
- transformation, 120, 161

Journal bearing, 310**K****Kaplan turbine, 214****Kàrmàn integral equation, 349****Kàrmàn-Trefftz airfoil, 164, 178****K-BKZ model (equation), 464, 465****Kelvin**

- circulation theorem, 152–160
- element, 449–451
- force density, 510, 521
- k- ϵ model, 378–380

Kinematic

- similarity, 286–288
- viscosity, 198, 277, 369, 476

Kinetic energy of turbulence, 370**Knudsen number, 6****Kolmogorov (micro) scales, 369, 370****Kronecker delta, 15****Kutta condition (hypothesis), 156****Kutta-Joukowski**

- hypothesis, 156
- theorem, 160

L**Lagrangian**

- derivative, 8
- specification, 7, 26

Laminar entrance flow, 320–322**Laminar flow**

- between concentric pipes, 339
- between parallel plates, 299
- between rotating cylinders, 302–306, 318
- in a pipe, 319–334

Langevin

- argument, 500, 501, 504
- function, 499

Laplace's equation, 116, 150, 312, 337**Lapse rate, 93, 96****Larmor frequency, 502****Laval tube (nozzle), 232****Law of wall, 372, 388, 389****Leading edge, 154, 155****Level meter, 524****Levitation of magnets, 497, 524**

Lewis number, 536
 Lift
 on an airfoil, 156, 160, 166, 192
 coefficient, 166, 192
 Limiting length, 262
 Linear
 elastic material (body), 405
 momentum conservation, 44–47
 momentum flux, 46
 sublayer, 372–375
 viscoelasticity, 425, 454
 Linearly accelerating containers, 86, 87, 108, 109
 Load-bearing capacity, 309
 Local
 heat transfer coefficient, 361, 384
 Nusselt number, 361, 385
 Lodge network (rubberlike) liquid (model), 457, 463
 Logarithmic velocity distribution, 374
 Loss coefficient, 143–145, 205
 Loss modulus, 425, 426, 440, 441
 Lower convective
 derivative, 21, 459
 Maxwell model, 459
 Lubrication
 equation, 306, 307
 rotating shaft, 305

M

Mach
 angle, 230
 corn, 230
 correction, 131
 number, 131, 230, 289, 290
 Magnetic
 boundary condition, 532–534
 dimension, 527
 force (Kelven force density), 497, 521, 530
 materials, 502, 503
 normal traction, 523
 particles, 498, 502
 permeability, 506, 508
 polarization, 508, 517
 pressure jump, 523, 525, 532–535

Rayleigh number, 531
 susceptibility, 501, 506
 Magnetic fluids, 2, 497
 dynamics, 507–514
 properties, 497–498
 shaft seals, 525
 Magnetite, 497
 Magnetization
 of saturation, 498, 499
 Magnetocaloric effect, 497, 514, 517
 Magnetostatic buoyant force, 524
 Magnetoviscous effect, 498, 503, 512
 Manometers, 90, 91, 130, 131
 Manometric head, 185
 Mapping function, 119, 120
 Mass
 conservation, 43, 44
 diffusion, 536
 flow rate, 123
 flux, 44, 241
 transfer, 532
 Material
 derivative, 7, 20, 152
 functions, 417, 422, 423, 425
 line (element), 9, 21, 23, 24
 objectivity, 19–22, 33–35, 459, 460
 Maxwell
 element, 448–453
 equation, 58, 516
 model of viscoelastic fluid, 447, 448
 model of viscosity, 280
 stress tensor, 507–509, 511
 Maxwell model (CRM), 455, 463–473
 Mean free path, 5
 Mechanical
 efficiency, 195
 loss angle, 425, 441
 Memory function, 455, 458, 463
 Metacenter, 101
 Metacentric height, 101
 Metric tensor, 23
 Micromanometer, 90, 91
 Minor losses, 140–145
 Mises airfoil, 164
 Mixed flow pumps, 202
 Mixing length, 371
 Mobility factor, 461

Modulus, 405, 425–427, 440, 441,
448–454, 463

Molecular Prandtl number, 383

Moment, 160

Moment of inertia (of surface), 79

Moment of momentum, 128, 183–188

Momentum

flux, 126, 243

thickness, 350–356, 386

N

Nappe, 137

Natural convection, 295, 297

Navier-Stokes equations, 282–285

Néel relaxation, 502, 505

Net positive suction head (NSPH), 206
coefficient, 205

Neumann energy equation, 56

Newton's law of viscosity, 279

Newton's second law, 43, 64, 126, 289

Newtonian fluid, 279, 280, 440

Non-Newtonian fluid, 399, 400

Normal

instability, 520

shock (wave), 236, 237, 246, 248

stress, 29, 88

No-slip condition, 311, 336, 337, 341,
358, 472

Nozzle, 176, 177

Numbers (nondimensional)

of Brinkman, 294

of Deborah, 489

of Eckert, 293

of Euler, 289

of Froude, 289

of Grashof, 293

of Lewis, 536

of Mach, 289

of Nusselt, 296

of Peclet, 294

of Prandtl, 294, 360, 378, 383

of Rayleigh, 297

of Reynolds, 289, 290, 302, 312, 408,
412, 415

of Stanton, 296, 362

of Strouhal, 292, 352, 408, 489

of Taylor, 305, 306

of Weber, 289

of Weissenberg, 489

Numerical solutions, 334, 474, 475

O

Oblique shock, 237, 251–255, 274

Oil feeding reservoir, 108–110

Oldroyd's equations, 460, 461, 485–487

One equation models, 370–377

Open channel flow, 137

broad-crested wire choked flow, 176

Orifice meter, 132–135

Oscillatory rheometric flow, 424–427

Outer layer, 372–374

Over-expanded condition, 237, 238

Overlap layer, 372

Overshooting, 475

P

Paraboloid of revolution, 108

Parallel plates, 299

Peclet number, 294

Pelton wheel, 172, 173, 208–211, 219

Perfect fluid, 30, 115, 154

Performance curves, 198, 199

Phan-Thien and Tanner model, 463

parameter, 196, 291

Phase-shift, 425, 441

Piezometric head, 75

Piezotropic (fluid), 152

Pitot probe (tube), 129–132, 255–258

Planar elongational flow, 422

Plane flow, 301, 334

Poiseuille

flow, 301, 321–325, 328–332

paraboloid, 324, 412

Polar (material) fluid, 48, 51, 52, 507

Polarization of magnetic fluid, 517

Polyadic (alternator), 15, 49

Polymeric fluid (solution), 2, 424,
460, 489

Polytropic change, 93–96

Potential

flow, 115–121

function, 92, 116

vortex, 119

Power

- coefficient, 197
- law fluid, 401–403, 412–414, 444, 445
- law profile, 329, 330, 387, 409

Prandtl

- boundary layer equation, 343
- number, 294, 360, 378, 382, 388
- relation, 250
- universal law of friction, 327

Pressure, 29

- (loss) coefficient, 142–146, 197, 321
- drop (loss), 145, 325, 409, 436
- dynamic, 130
- at elbow channel, 140, 141, 145
- equation, 124
- function, 122, 152, 233
- head, 124, 185, 192
- jump, 523, 525, 532–535
- recovery (factor), 144
- stagnation, 130
- total, 124, 322
- vessel, 106

Principal axes (of stress), 37, 38**Principal stress, 280****Principle of Archimedes, 82****Principle of frame invariance, 19, 20****Product of surface area (inertia), 79****Profile development region, 320, 321****Propeller, 142, 146**

- efficiency, 147–149

Pseudoplastic fluids, 401**Pseudovector, 14, 16, 33, 49, 128, 509, 513****Pump**

- efficiency, 194, 195
- head, 185

Pumps

- axial flow, 182, 183
- mixed flow, 182, 183, 213
- performance curve, 198, 199
- radial flow, 181

Pyromagnetic coefficient, 501, 530**Q****Quasi-linear, 457****Quasi-stationary, 497, 507, 516, 521****R****Rabinowitsch**

- correction, 444
- equation, 443
- procedure, 441–445

Radial flow pumps, 183, 188**Rankine-Hugoniot relationship, 248, 252****Rankine ovoid (oval), 173, 174****Rate of**

- deformation tensor, 10, 34
- heat transfer, 264, 265, 267
- strain tensor, 11, 280, 381, 406, 456, 478–483

Rayleigh line (curve), 241–246, 264–270**Rayleigh number, 297, 298, 527–532****Rayleigh-Plesset equation, 149–152****Reaction turbine, 208****Rectilinear acceleration, 18****Relative**

- acceleration, 74, 85
- strain tensors, 23, 453, 478–483
- velocity, 74

Relaxation

- model, 505
- modulus, 454
- time, 448–457, 502, 505, 506

Retardation time, 452, 453**Retarded elasticity, 452****Reversible, 228****Reynolds**

- decomposition, 365
- equation for lubrication, 307
- equation for turbulent flow, 368
- number, 289, 302, 312, 408, 412, 415
- stress, 367, 368, 372

Reynolds' analogy, 361, 362, 381–385**Reynolds' transport theorem, 23–26, 35, 36, 45, 48, 65, 68, 128****Rheometric flow, 418, 419, 424–427****Rheopectic fluid, Rheopexy, 404****Rigid body rotation, 16, 82****Rosensweig equation, 516–519****Rotating**

- blade, 140–142
- containers, 85, 108
- cylinders, 119, 299–306, 415

- reference frame, 16–19, 73, 85, 124, 125
- spheres, 412–415
- Rotational
 - Reynolds number, 305
 - viscosity, 517–519
- Rotation tensor, 16–35
- Roughness, 287, 298
- Runner, 185
- S**
- Saturation magnetization, 501
- Scale effect, 202, 203
- Shafts seals, 525
- Second
 - coefficient of viscosity, 291
 - moment of surface area (inertia), 79, 81, 103
 - normal stress coefficient, 419, 467
 - normal stress difference, 419, 484, 485
- Self-levitating effect, 524
- Semi-vertex angle, 251, 274
- Separated
 - point, 350
 - region, 350–353
- Shaft power, 195
- Sharp-crested weir, 137–140
- Shear
 - stress, 29, 418–421, 476
 - thickening fluid, 403
 - thinning fluid, 401
 - velocity, 421
 - work, 439, 440
- Shearfree flow, 421–424
- Shliomis magnetic relaxation
 - equation, 515
- Shock
 - strength, 249
 - wave, 241, 246–255, 281
- Shroud, 181
- Similarity rules, 194–203,
- Similarity solution, 344–346
- Similitude, 195, 196, 286–294
- Simple
 - (shearfree) extensional flow, 11, 12, 421–424, 478–483
 - shear flow, 11, 12, 415, 472–478
- Sink, 118, 119
- Siphon, 174, 423
- Skew-symmetric tensor (anti-symmetric tensor), 14, 15, 18, 49, 50, 52, 55, 509–511
- Skin friction coefficient, 326
- Slip factor, 188
- Slipper-pad bearing, 306–312, 318
- Slipstream, 142
- Soft magnet approximation, 529
- Solenoidal velocity field, 44
- Sonic
 - line, 255
 - velocity, 225
- Sound
 - velocity (speed), 131, 132, 225–230
 - wave, 229
- Source, 118, 119
- Specific
 - energy, 59, 185
 - gravity, 524
 - heat, 59
 - heat ratio, 131, 228
 - speed, 201, 202, 207
 - volume, 57, 227
- Speed
 - factor, 210
 - of sound, 225, 229
- Spherical gap flow, 412–415
- Spin
 - energy, 56
 - flux, 52
 - tensor, 10, 21, 55
 - viscosity, 512
- Sprinkler, 179, 180
- Squeeze film, 308, 423
- Stability of floating object, 100–104
- Stagnation
 - hole, 130, 131
 - point, 130, 155, 156
 - pressure, 130, 255
 - quantities, 232
- Stall, 167
- Standard
 - atmosphere, 76, 93–96
 - flow, 417, 418, 478–483
 - temperature, 93–96

Stanton number, 296, 362, 385
 Starting vortex, 155, 156
 Static hole, 130, 131
 Static pressure, 130, 151
 Steric repulsion, 498
 Stokes
 equation, 322, 323, 335
 flow, 310–316
 law, 316
 Stokes' hypothesis, 281, 282
 Stopping vortex, 156
 Storage module, 425, 426, 440, 441
 Stratosphere, 110
 Stream function, 116, 117, 312, 345
 Stream lines, 122, 125, 130, 138
 Stream tube, 122, 123, 125, 127, 128
 Stress
 of force, 27, 28
 ratio, 420, 421
 tensor, 26, 30, 279, 418
 vector, 27
 Strong shock, 249
 Strouhal number, 292, 352, 408, 489
 Sturm-Liouville problem, 338
 Submerged surface, body, 80–82,
 100–104
 Subsonic flow, 229, 236, 255, 269
 Substantial derivative, 7, 47
 Sudden
 contraction, 140, 141
 expansion, 140, 141, 272
 Supercritical, 520
 Superparamagnetism, 501, 502
 Supersonic
 flow, 230, 257
 nozzle, 232
 Surface
 couple, 49, 51, 512
 force, 26, 45
 shape, 344
 tension, 87, 104, 105, 151, 152, 499
 Surfactant, 88, 498
 System International, 2, 3

T

Tab-orifice, 136–140
 Tank-orifice, 136, 138

Taylor
 microscale, 369, 370
 number, 305, 306
 vortex, 305
 Theoretical specific energy, 185
 Thermal
 boundary layer, 351–353
 chocking, 268
 conductivity, 61, 62, 293
 diffusivity, 62, 360, 513, 537
 expansion, coefficient, 60, 61, 292, 529
 similarity, 293, 294
 Thermodynamic relations, 56–62
 first law, 52, 53
 Maxwell equation, 58
 pressure, 29, 57, 59, 73
 second law, 57, 58
 Thermomagnetic natural convection
 (Thermoconvective), 520, 527–532
 Thixotropic fluid, thixotropy, 404
 Thrust
 bearing, 309
 function, 244
 Time average, 364
 Torque, 65, 66, 128, 304, 305
 coefficient, 305, 414
 Torricelli's theorem, 138, 139
 Total
 drag force, 309
 efficiency, 194
 energy, 122
 enthalpy, 354
 head, 124
 pressure, 432, 510
 stress tensor, 37, 74, 87, 279, 280,
 418–420, 431, 438, 456,
 507, 509
 Trailing
 edge, 155, 156, 162
 vortex (stopping vortex), 156
 Transducer, 439
 Transport equation, 375
 Troposphere, 96, 110
 Trouton viscosity, 423
 Turbine
 axial flow, 183
 Francis, 185
 impulse, 172, 208

Kaplan, 189, 213–217
mixed flow, 182, 183
Pelton wheel, 208–211, 219
radial flow, 181
reaction, 208
Turbomachines, 180–183
 of efficiencies, 194, 195
Turbulent
 boundary layer, 346, 370–385
 diffusion, 287
 entrance flow, 320–322
 flow, 364–389
 heat flux coefficient, 382
 intensity (relative), 366
 models, 368, 370–380
 pipe flow, 327–328
 Prandtl number, 382, 383, 388
 transport, 281
 velocity profile, 328, 329, 373–375
Two equation models, 378–380

U

Uniaxially stretching, 422, 433, 466
Unidirectional flow, 299–306
Unitary matrix, 16
Units, 2, 3
Unit tensor, 14, 15
Upper convective
 derivative, 21, 33–35, 459, 478
 Maxwell model (UCM), 33, 457,
 465–478, 484–487
U-tube manometer, 75, 129

V

Vane, 189, 193
Velocimetry, 129–132, 255–258
Velocity
 coefficient, 134, 210
 defect (volume flow rate), 124
 diagram, 125, 183–188
 gradient tensor, 10, 13
 head, 124
 measurement, 257
 potential, 116, 118, 312
Vena contracta, 133, 271, 272
Venturi meter (tube), 135, 136

Viscoelastic
 boundary layer, 475–478
 fluid, 23, 405–406
 linear, 454
Viscometer, *see* Rheometric flow
Viscometric
 flow, 417, 418, 428–437
 function, 419, 420
 See also Rheometric flow
Viscoplastic fluid, 403
Viscosity
 definition, 279, 280
 of magnetic fluid, 499, 512–514
 rotational, 517–519
 second coefficient, 291
Viscous
 sublayer, 372–375
V-notch weir, 137–140
Voigt
 element, 449, 451
 model of viscoelasticity, 451
Volume
 flow, 132–140, 195, 197, 328, 339,
 406, 408, 434, 436, 437,
 445, 446
 flux, 126, 307
Volumetric efficiency, 195
Volute, 181
Von Kármán
 integral equation, 359
 street, 352
Vortex
 design, 194
 lines, 285
 shedding, 352, 353
 viscosity, 509, 510
Vorticity
 tensor, 16
 transport equation, 47, 284
 vector, 16, 47, 284

W

Wake, 351
Wall-function, 379
Wall region (law of wall), 372,
 388, 389
Wall shear rate, 437

Wave
 equation, 227
 function, 227
Weak shock, 253
Weber number, 289
Wedge angle (semi-vertex angle),
 253, 277
Weir
 broad-crested, 175
 sharp-crested, 137–140
 v-notch, 137–140
Weissenberg
 effect, 419, 446
 number, 489
Wetted perimeter, 320
White-Metzner model, 463, 487–489
Wilhelmy plate method, 105, 106

Wind turbine, 142–149
 efficiency, 148, 149
Work
 input, 56
 output, 53
 transfer, 196, 293

Y

Yield stress, 403
Young-Laplace relationship, 87

Z

Zero equation models, 370–375
Zero-shear (rate) viscosity, 402, 423, 427,
 457, 461, 488

Mechanics

FLUID MECHANICS AND ITS APPLICATIONS

Series Editor: R. Moreau

Aims and Scope of the Series

The purpose of this series is to focus on subjects in which fluid mechanics plays a fundamental role. As well as the more traditional applications of aeronautics, hydraulics, heat and mass transfer etc., books will be published dealing with topics which are currently in a state of rapid development, such as turbulence, suspensions and multiphase fluids, super and hypersonic flows and numerical modelling techniques. It is a widely held view that it is the interdisciplinary subjects that will receive intense scientific attention, bringing them to the forefront of technological advancement. Fluids have the ability to transport matter and its properties as well as transmit force, therefore fluid mechanics is a subject that is particularly open to cross fertilisation with other sciences and disciplines of engineering. The subject of fluid mechanics will be highly relevant in domains such as chemical, metallurgical, biological and ecological engineering. This series is particularly open to such new multidisciplinary domains.

1. M. Lesieur: *Turbulence in Fluids*. 2nd rev. ed., 1990 ISBN 0-7923-0645-7
2. O. Métais and M. Lesieur (eds.): *Turbulence and Coherent Structures*. 1991 ISBN 0-7923-0646-5
3. R. Moreau: *Magnetohydrodynamics*. 1990 ISBN 0-7923-0937-5
4. E. Coustols (ed.): *Turbulence Control by Passive Means*. 1990 ISBN 0-7923-1020-9
5. A.A. Borissov (ed.): *Dynamic Structure of Detonation in Gaseous and Dispersed Media*. 1991 ISBN 0-7923-1340-2
6. K.-S. Choi (ed.): *Recent Developments in Turbulence Management*. 1991 ISBN 0-7923-1477-8
7. E.P. Evans and B. Coulbeck (eds.): *Pipeline Systems*. 1992 ISBN 0-7923-1668-1
8. B. Nau (ed.): *Fluid Sealing*. 1992 ISBN 0-7923-1669-X
9. T.K.S. Murthy (ed.): *Computational Methods in Hypersonic Aerodynamics*. 1992 ISBN 0-7923-1673-8
10. R. King (ed.): *Fluid Mechanics of Mixing*. Modelling, Operations and Experimental Techniques. 1992 ISBN 0-7923-1720-3
11. Z. Han and X. Yin: *Shock Dynamics*. 1993 ISBN 0-7923-1746-7
12. L. Svarovsky and M.T. Thew (eds.): *Hydroclones*. Analysis and Applications. 1992 ISBN 0-7923-1876-5
13. A. Lichtarowicz (ed.): *Jet Cutting Technology*. 1992 ISBN 0-7923-1979-6
14. F.T.M. Nieuwstadt (ed.): *Flow Visualization and Image Analysis*. 1993 ISBN 0-7923-1994-X
15. A.J. Saul (ed.): *Floods and Flood Management*. 1992 ISBN 0-7923-2078-6
16. D.E. Ashpis, T.B. Gatski and R. Hirsh (eds.): *Instabilities and Turbulence in Engineering Flows*. 1993 ISBN 0-7923-2161-8
17. R.S. Azad: *The Atmospheric Boundary Layer for Engineers*. 1993 ISBN 0-7923-2187-1
18. F.T.M. Nieuwstadt (ed.): *Advances in Turbulence IV*. 1993 ISBN 0-7923-2282-7
19. K.K. Prasad (ed.): *Further Developments in Turbulence Management*. 1993 ISBN 0-7923-2291-6
20. Y.A. Tatarchenko: *Shaped Crystal Growth*. 1993 ISBN 0-7923-2419-6
21. J.P. Bonnet and M.N. Glauser (eds.): *Eddy Structure Identification in Free Turbulent Shear Flows*. 1993 ISBN 0-7923-2449-8
22. R.S. Srivastava: *Interaction of Shock Waves*. 1994 ISBN 0-7923-2920-1

Mechanics

FLUID MECHANICS AND ITS APPLICATIONS

Series Editor: R. Moreau

23. J.R. Blake, J.M. Boulton-Stone and N.H. Thomas (eds.): *Bubble Dynamics and Interface Phenomena*. 1994 ISBN 0-7923-3008-0
24. R. Benzi (ed.): *Advances in Turbulence V*. 1995 ISBN 0-7923-3032-3
25. B.I. Rabinovich, V.G. Lebedev and A.I. Mytarev: *Vortex Processes and Solid Body Dynamics*. The Dynamic Problems of Spacecrafts and Magnetic Levitation Systems. 1994 ISBN 0-7923-3092-7
26. P.R. Voke, L. Kleiser and J.-P. Chollet (eds.): *Direct and Large-Eddy Simulation I*. Selected papers from the First ERCOFTAC Workshop on Direct and Large-Eddy Simulation. 1994 ISBN 0-7923-3106-0
27. J.A. Sparenberg: *Hydrodynamic Propulsion and its Optimization*. Analytic Theory. 1995 ISBN 0-7923-3201-6
28. J.F. Dijksman and G.D.C. Kuiken (eds.): *IUTAM Symposium on Numerical Simulation of Non-Isothermal Flow of Viscoelastic Liquids*. Proceedings of an IUTAM Symposium held in Kerkrade, The Netherlands. 1995 ISBN 0-7923-3262-8
29. B.M. Boubnov and G.S. Golitsyn: *Convection in Rotating Fluids*. 1995 ISBN 0-7923-3371-3
30. S.I. Green (ed.): *Fluid Vortices*. 1995 ISBN 0-7923-3376-4
31. S. Morioka and L. van Wijngaarden (eds.): *IUTAM Symposium on Waves in Liquid/Gas and Liquid/Vapour Two-Phase Systems*. 1995 ISBN 0-7923-3424-8
32. A. Gyr and H.-W. Bewersdorff: *Drag Reduction of Turbulent Flows by Additives*. 1995 ISBN 0-7923-3485-X
33. Y.P. Golovachov: *Numerical Simulation of Viscous Shock Layer Flows*. 1995 ISBN 0-7923-3626-7
34. J. Grue, B. Gjevik and J.E. Weber (eds.): *Waves and Nonlinear Processes in Hydrodynamics*. 1996 ISBN 0-7923-4031-0
35. P.W. Duck and P. Hall (eds.): *IUTAM Symposium on Nonlinear Instability and Transition in Three-Dimensional Boundary Layers*. 1996 ISBN 0-7923-4079-5
36. S. Gavrilakis, L. Machiels and P.A. Monkewitz (eds.): *Advances in Turbulence VI*. Proceedings of the 6th European Turbulence Conference. 1996 ISBN 0-7923-4132-5
37. K. Gersten (ed.): *IUTAM Symposium on Asymptotic Methods for Turbulent Shear Flows at High Reynolds Numbers*. Proceedings of the IUTAM Symposium held in Bochum, Germany. 1996 ISBN 0-7923-4138-4
38. J. Verhás: *Thermodynamics and Rheology*. 1997 ISBN 0-7923-4251-8
39. M. Champion and B. Deshaies (eds.): *IUTAM Symposium on Combustion in Supersonic Flows*. Proceedings of the IUTAM Symposium held in Poitiers, France. 1997 ISBN 0-7923-4313-1
40. M. Lesieur: *Turbulence in Fluids*. Third Revised and Enlarged Edition. 1997 ISBN 0-7923-4415-4; Pb: 0-7923-4416-2
41. L. Fulachier, J.L. Lumley and F. Anselmet (eds.): *IUTAM Symposium on Variable Density Low-Speed Turbulent Flows*. Proceedings of the IUTAM Symposium held in Marseille, France. 1997 ISBN 0-7923-4602-5
42. B.K. Shivamoggi: *Nonlinear Dynamics and Chaotic Phenomena*. An Introduction. 1997 ISBN 0-7923-4772-2
43. H. Ramkissoon, *IUTAM Symposium on Lubricated Transport of Viscous Materials*. Proceedings of the IUTAM Symposium held in Tobago, West Indies. 1998 ISBN 0-7923-4897-4
44. E. Krause and K. Gersten, *IUTAM Symposium on Dynamics of Slender Vortices*. Proceedings of the IUTAM Symposium held in Aachen, Germany. 1998 ISBN 0-7923-5041-3

Mechanics

FLUID MECHANICS AND ITS APPLICATIONS

Series Editor: R. Moreau

45. A. Biesheuvel and G.J.F. van Heyst (eds.): *In Fascination of Fluid Dynamics*. A Symposium in honour of Leen van Wijngaarden. 1998 ISBN 0-7923-5078-2
46. U. Frisch (ed.): *Advances in Turbulence VII*. Proceedings of the Seventh European Turbulence Conference, held in Saint-Jean Cap Ferrat, 30 June–3 July 1998. 1998 ISBN 0-7923-5115-0
47. E.F. Toro and J.F. Clarke: *Numerical Methods for Wave Propagation*. Selected Contributions from the Workshop held in Manchester, UK. 1998 ISBN 0-7923-5125-8
48. A. Yoshizawa: *Hydrodynamic and Magnetohydrodynamic Turbulent Flows*. Modelling and Statistical Theory. 1998 ISBN 0-7923-5225-4
49. T.L. Geers (ed.): *IUTAM Symposium on Computational Methods for Unbounded Domains*. 1998 ISBN 0-7923-5266-1
50. Z. Zapryanov and S. Tabakova: *Dynamics of Bubbles, Drops and Rigid Particles*. 1999 ISBN 0-7923-5347-1
51. A. Alemany, Ph. Marty and J.P. Thibault (eds.): *Transfer Phenomena in Magnetohydrodynamic and Electroconducting Flows*. 1999 ISBN 0-7923-5532-6
52. J.N. Sørensen, E.J. Hopfinger and N. Aubry (eds.): *IUTAM Symposium on Simulation and Identification of Organized Structures in Flows*. 1999 ISBN 0-7923-5603-9
53. G.E.A. Meier and P.R. Viswanath (eds.): *IUTAM Symposium on Mechanics of Passive and Active Flow Control*. 1999 ISBN 0-7923-5928-3
54. D. Knight and L. Sakell (eds.): *Recent Advances in DNS and LES*. 1999 ISBN 0-7923-6004-4
55. P. Orlandi: *Fluid Flow Phenomena. A Numerical Toolkit*. 2000 ISBN 0-7923-6095-8
56. M. Stanislas, J. Kompenhans and J. Westerveel (eds.): *Particle Image Velocimetry*. Progress towards Industrial Application. 2000 ISBN 0-7923-6160-1
57. H.-C. Chang (ed.): *IUTAM Symposium on Nonlinear Waves in Multi-Phase Flow*. 2000 ISBN 0-7923-6454-6
58. R.M. Kerr and Y. Kimura (eds.): *IUTAM Symposium on Developments in Geophysical Turbulence* held at the National Center for Atmospheric Research, (Boulder, CO, June 16–19, 1998) 2000 ISBN 0-7923-6673-5
59. T. Kambe, T. Nakano and T. Miyauchi (eds.): *IUTAM Symposium on Geometry and Statistics of Turbulence*. Proceedings of the IUTAM Symposium held at the Shonan International Village Center, Hayama (Kanagawa-ken, Japan, November 2–5, 1999). 2001 ISBN 0-7923-6711-1
60. V.V. Aristov: *Direct Methods for Solving the Boltzmann Equation and Study of Nonequilibrium Flows*. 2001 ISBN 0-7923-6831-2
61. P.F. Hodnett (ed.): *IUTAM Symposium on Advances in Mathematical Modelling of Atmosphere and Ocean Dynamics*. Proceedings of the IUTAM Symposium held in Limerick, Ireland, 2–7 July 2000. 2001 ISBN 0-7923-7075-9
62. A.C. King and Y.D. Shikhmurzaev (eds.): *IUTAM Symposium on Free Surface Flows*. Proceedings of the IUTAM Symposium held in Birmingham, United Kingdom, 10–14 July 2000. 2001 ISBN 0-7923-7085-6
63. A. Tsinober: *An Informal Introduction to Turbulence*. 2001 ISBN 1-4020-0110-X; Pb: 1-4020-0166-5
64. R.Kh. Zeytounian: *Asymptotic Modelling of Fluid Flow Phenomena*. 2002 ISBN 1-4020-0432-X
65. R. Friedrich and W. Rodi (eds.): *Advances in LES of Complex Flows*. Proceedings of the EUROMECH Colloquium 412, held in Munich, Germany, 4–6 October 2000. 2002 ISBN 1-4020-0486-9

Mechanics

FLUID MECHANICS AND ITS APPLICATIONS

Series Editor: R. Moreau

66. D. Drikakis and B.J. Geurts (eds.): *Turbulent Flow Computation*. 2002 ISBN 1-4020-0523-7
67. B.O. Enflo and C.M. Hedberg: *Theory of Nonlinear Acoustics in Fluids*. 2002
ISBN 1-4020-0572-5
68. I.D. Abrahams, P.A. Martin and M.J. Simon (eds.): *IUTAM Symposium on Diffraction and Scattering in Fluid Mechanics and Elasticity*. Proceedings of the IUTAM Symposium held in Manchester, (UK, 16–20 July 2000). 2002 ISBN 1-4020-0590-3
69. P. Chassaing, R.A. Antonia, F. Anselmet, L. Joly and S. Sarkar: *Variable Density Fluid Turbulence*. 2002 ISBN 1-4020-0671-3
70. A. Pollard and S. Candel (eds.): *IUTAM Symposium on Turbulent Mixing and Combustion*. Proceedings of the IUTAM Symposium held in Kingston, Ontario, Canada, June 3–6, 2001. 2002 ISBN 1-4020-0747-7
71. K. Bajer and H.K. Moffatt (eds.): *Tubes, Sheets and Singularities in Fluid Dynamics*. 2002
ISBN 1-4020-0980-1
72. P.W. Carpenter and T.J. Pedley (eds.): *Flow Past Highly Compliant Boundaries and in Collapsible Tubes*. IUTAM Symposium held at the University of Warwick, Coventry, United Kingdom, 26–30 March 2001. 2003 ISBN 1-4020-1161-X
73. H. Sobieczky (ed.): *IUTAM Symposium Transsonicum IV*. Proceedings of the IUTAM Symposium held in Göttingen, Germany, 2–6 September 2002. 2003 ISBN 1-4020-1608-5
74. A.J. Smits (ed.): *IUTAM Symposium on Reynolds Number Scaling in Turbulent Flow*. Proceedings of the IUTAM Symposium held in Princeton, NJ, U.S.A., September 11–13, 2002. 2003 ISBN 1-4020-1775-8
75. H. Benaroya and T. Wei (eds.): *IUTAM Symposium on Integrated Modeling of Fully Coupled Fluid Structure Interactions Using Analysis, Computations and Experiments*. Proceedings of the IUTAM Symposium held in New Jersey, U.S.A., 2–6 June 2003. 2003
ISBN 1-4020-1806-1
76. J.-P. Franc and J.-M. Michel: *Fundamentals of Cavitation*. 2004 ISBN 1-4020-2232-8
77. T. Mullin and R. Kerswell (eds.): *IUTAM Symposium on Laminar-Turbulent Transition and Finite Amplitude Solutions*. 2005 ISBN 978-1-4020-4048-1
78. R. Govindarajan (ed.): *Sixth IUTAM Symposium on Laminar-Turbulent Transition*. Proceedings of the Sixth IUTAM Symposium on Laminar-Turbulent Transition, Bangalore, India, 2004. 2006 ISBN 978-1-4020-3459-6
79. S. Kida (ed.): *IUTAM Symposium on Elementary Vortices and Coherent Structures: Significance in Turbulence Dynamics*. Proceedings of the IUTAM Symposium held at Kyoto International Community House, Kyoto, Japan, 26–28 October 2004. 2006
ISBN 978-1-4020-4180-8
80. S. Molokov, R. Moreau and H.K. Moffatt (eds.): *Magnetohydrodynamics. Historical Evolution and Trends*. 2007 ISBN 978-1-4020-4832-6
81. S. Balachandar and A. Prosperetti (eds.): *IUTAM Symposium on Computational Approaches to Multiphase Flow*. Proceedings of an IUTAM Symposium held at Argonne National Laboratory, October 4–7, 2004 2006 ISBN 978-1-4020-4976-7
82. A. Gyr and K. Hoyer: *Sediment Transport. A Geophysical Phenomenon*. 2006
ISBN 978-1-4020-5015-2
83. I.N. Ivchenko, S.K. Loyalka and R.V. Thompson Jr.: *Analytical Methods for Problems of Molecular Transport*. 2007 ISBN 978-1-4020-5864-6

Mechanics

FLUID MECHANICS AND ITS APPLICATIONS

Series Editor: R. Moreau

84. M. Lesieur: *Turbulence in Fluids*, Fourth Revised and Enlarged Edition. 2008
ISBN 978-1-4020-6434-0
85. H. Yamaguchi: *Engineering Fluid Mechanics*. 2008
ISBN 978-1-4020-6741-9